GL01495

# ANEXOS

## CEBORUCO-DOMO DE SAN PEDRO
## MAGNETOTELLURIC SURVEY

NAYARIT, MEXICO

GL01495

# APPENDIX B

# A DESCRIPTION OF MAGNETOTELLURIC DATA AND A DEFINITION OF TERMS USED IN MAGNETOTELLURIC EXPLORATION

January 1985

By

ARNOLD S. ORANGE

ARNOLD ORANGE ASSOCIATES
8806 POINT WEST DRIVE
AUSTIN, TEXAS 78759

Note:

This apppendix contains material originally prepared by the author when he was a partner in Emerald Exploration Consultants, Inc. (EMEX). The appendix is used by joint agreement between EMEX and Arnold Orange Associates.

# APPENDIX B

# A DESCRIPTION OF MAGNETOTELLURIC DATA

# AND

# A DEFINITION OF TERMS USED IN MAGNETOTELLURIC EXPLORATION

## TABLE OF CONTENTS

# APPENDIX B

# A DESCRIPTION OF MAGNETOTELLURIC DATA

# AND

# A DEFINITION OF TERMS USED IN MAGNETOTELLURIC EXPLORATION

## LIST OF FIGURES

APPENDIX B

A DESCRIPTION OF MAGNETOTELLURIC DATA

AND

A DEFINITION OF TERMS USED IN MAGNETOTELLURIC EXPLORATION

LIST OF FIGURES
(Page 2)

Note:

This appendix was prepared in 1985 using as examples magnetotelluric data acquired and processed by Z-Axis Exploration (now AET Inc.). The PNG MT data were acquired and processed by Phoenix Geosciences, however. There will therefore be differences between the Z-Axis plots shown in this appendix and the Phoenix PNG data. These differences are primarily in the mode of presentation, the principals discussed regarding features observed in MT data apply to any data processed to result in a rotated tensor apparent resistivity and the functions associated with the rotated tensor. A full description of the Phoenix plotting conventions is included as part of Appendix F.

# APPENDIX B

# A DESCRIPTION OF MAGNETOTELLURIC DATA

# AND

# A DEFINITION OF TERMS USED IN MAGNETOTELLURIC EXPLORATION

## 1. Introduction

The purpose of this appendix is to provide a detailed description of the magnetotelluric (MT) data submitted by the acquisition and processing contractor. The MT data "package" consists of several parameters computed from the measured electric and magnetic fields. These parameters are used either in the MT interpretation or in assessing data quality. The discussion will use data examples obtained by Z-AXIS Exploration, Inc. Most MT contractors compute the same or very similar parameters, although presentation style may vary.

The description of MT data will be accomplished in three parts. First, in section 2 the data displays of the various parameters will be described, with no attention given to the interpretation or evaluation of the data. Second, in section 3 some of the effects of structural complexity on MT data and the terms used to describe this complexity will be discussed. Third, in section 4, data quality parameters will be discussed.

The appendix concludes with a glossary of terms used in MT exploration. In both the descriptions of data and the definitions the approach is as non-mathematical as possible.

2. MT Data

A. Apparent Resistivity - Fundamental Relationships

The fundamental information obtained in MT is the apparent resistivity, calculated as a function of frequency. The magnitude of the apparent resistivity* has the units of ohm-meters. Through the skin depth relationship, which describes the penetration of the electromagnetic wave into the earth as a function of frequency and resistivity, apparent resistivity as a function of frequency is related to resistivity as a function of depth, with lower frequencies relating to deeper penetration and resistivity values deeper within the earth.

The electromagnetic field from which the apparent resistivity is calculated is a vector quantity, and is measured by two sets of electric and magnetic field sensors orthogonal to one another. Placement of these sensors on the ground, i.e., the measurement coordinate system, is arbitrary. The fields are influenced by the resistivity structure of the earth (which is, of course, what makes MT useful in exploration), and the components of apparent resistivity parallel and perpendicular to strike can be identified mathematically in the course of MT data processing. The fact that there are two resistivities that are computed and that these are

*The apparent resistivity is actually a complex number, with an amplitude and a phase, the result of a Fourier transform operation on the measured electric and magnetic field time-series.

in general different is what makes MT interpretation possible in the presence of structure. The apparent resistivities parallel and perpendicular to strike are said to be the rotated resistivities, since they have been rotated mathematically from the measurement coordinate system into the coordinate system related to the strike and dip of the geologic structure in the vicinity of the site.

Stated mathematically, the relationship between the measured electric and magnetic fields and the calculated apparent resistivities is, in the measurement coordinate system:

$$\begin{aligned} Ex &= \rho_{xx}\, Hx + \rho_{xy}\, Hy \\ Ey &= \rho_{yx}\, Hx + \rho_{yy}\, Hy \end{aligned} \qquad (1)$$

where Ex, Ey, Hx, and Hy are the electric and magnetic field components measured in the arbitrarily oriented, orthogonal xy coordinate system.* The coordinate rotation, to coordinates parallel and perpendicular to strike in a two-dimensional situation (where there are little or no structural variations along strike) yields

$$\begin{aligned} Ex &= \rho_{xy}\, Hy \\ Ey &= \rho_{yx}\, Hx \end{aligned} \qquad (2)$$

In this equation, the $\rho_{xx}$ and $\rho_{yy}$ terms of (1) are equal

*Remember that all of the terms of (1) are functions of frequency, the E's and H's being the Fourier transforms (power series) of the measured time functions. Further, these are complex numbers with amplitude and phase, although here we are dealing with the amplitude as discussed earlier.

to zero. If there is no structure, i.e., if the only variations in earth resistivity are with depth (the one-dimensional, or plane-layered situation) then

$$\rho_{xy} = \rho_{yx} \qquad (3)$$

since there is not preferred orientation or coordinate system. When there are structural variations, as there usually are at prospects where MT is used as an exploration tool, then

$$\rho_{xy} \neq \rho_{yx} \qquad (4)$$

and the differencies between $\rho_{xy}$ and $\rho_{yx}$ become an interpretive tool, as well as the actual values of $\rho_{xy}$ and $\rho_{yx}$.

Since the world is rarely if ever completely two-dimensional, in forming (2) from (1), the so called "diagonal" terms. $\rho_{xx}$ and $\rho_{yy}$ will not go completely to zero. Departure of these terms from zero is a measure of structural complexity, of how well the approximation of two-dimensionality used in rotating from (1) to (2) has been met.

In summary, then, the results of processing MT data are two apparent resistivity functions at each measurement location, aligned parallel and perpendicular to strike, presented as a function of frequency. These functions are the fundamental tools of MT interpretation.

## B. Apparent Resistivity - Data Presentation

The apparent resistivity data are presented by Z-AXIS in the format shown in Figure B-1. The apparent resistivity values are calculated at discrete frequencies and presented

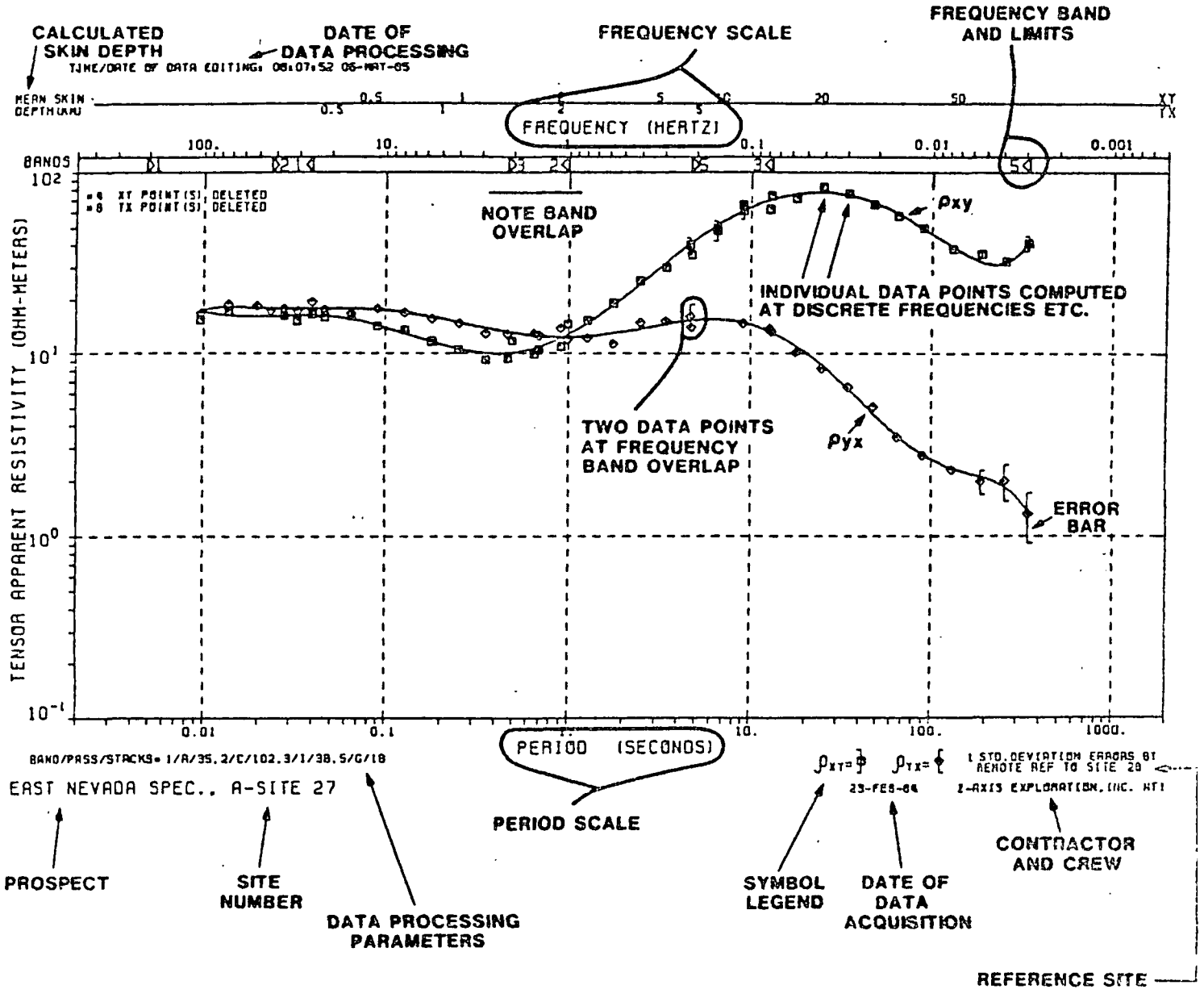


**APPARENT RESISTIVITY SCALE**

**(VERTICAL AXIS)**

$10^{1} = 0.1$

$10^{0} = 1.0$

$10^{1} = 10$

$10^{2} = 100$

ETC.

**FIGURE B - 1**

**APPARENT RESISTIVITY DATA**

as individual data points. These points are the basic data! Note that both resistivity and frequency scales are logarithmic. The smooth curves through the data points are mathematical fits to the data points. Z-AXIS uses a least squares polynomial fit, that may vary at the option of the processor from third to tenth orders. When the data are of high quality, as in the example, the polynomial fit is an accurate representation of the basic data points. As data quality deteriorates the smooth curve becomes more of an interpretive approximation to the data points. This will be discussed in detail in section 4 of this appendix.

The time series are recorded and digitized in several overlapping frequency "bands". These are noted.

Most of the information presented on the data plot is self evident. Note that the MT data processing sequence includes stacking of several time series "runs". The statistics of the stack are presented as "error bars", the resistivity range that encompasses a portion of the statistical distribution of the data that makes up the stack, in this case two standard deviations. The particular stack presented is noted for each recording band, in the lower left hand corner. For example, the notation "1/R/35" refers to band 1, stack R, which contained 35 time-series runs. This may be thought of as "35 fold" data.

The MT data is acquired at multiple sites simultaneously, with the signal-to-noise ratio improved by a

cross-correlation technique between sites. The particular "reference" site used in the calculation of the site being plotted is noted in the lower right hand corner.

Since the data may be reprocessed, the time and date of the data processing for the particular display is noted as well as the date of acquisition.

C. Inverted Resistivity

MT interpretation to be of a practical value requires that the apparent resistivity versus frequency described above be transformed into the form of resistivity versus depth, so that the MT data can be related to geology. The first step in this process* is the mathematical "inversion" of the <u>frequency</u> data shown in Figure B-1 into the <u>depth</u> data shown in Figure B-2. The mathematical computation of this inverse relationship was developed by Professor Francis X. Bostick of the University of Texas, and is thus termed the "Bostick" inverse. The equations utilized are

$$\rho = \rho_a^{\frac{(1-m)}{(1+m)}} \qquad (5)$$

where

$$d = \sqrt{2\frac{\rho_a}{\pi f u}}$$

$\rho$ = resistivity to be computed

d = depth to be computed

*Other steps include one-dimensional forward, one-dimensional layered (ridge-regression) inverse, two-dimensional, and three-dimensional models. All of these may be applied to a complex prospect. See Appendix C.

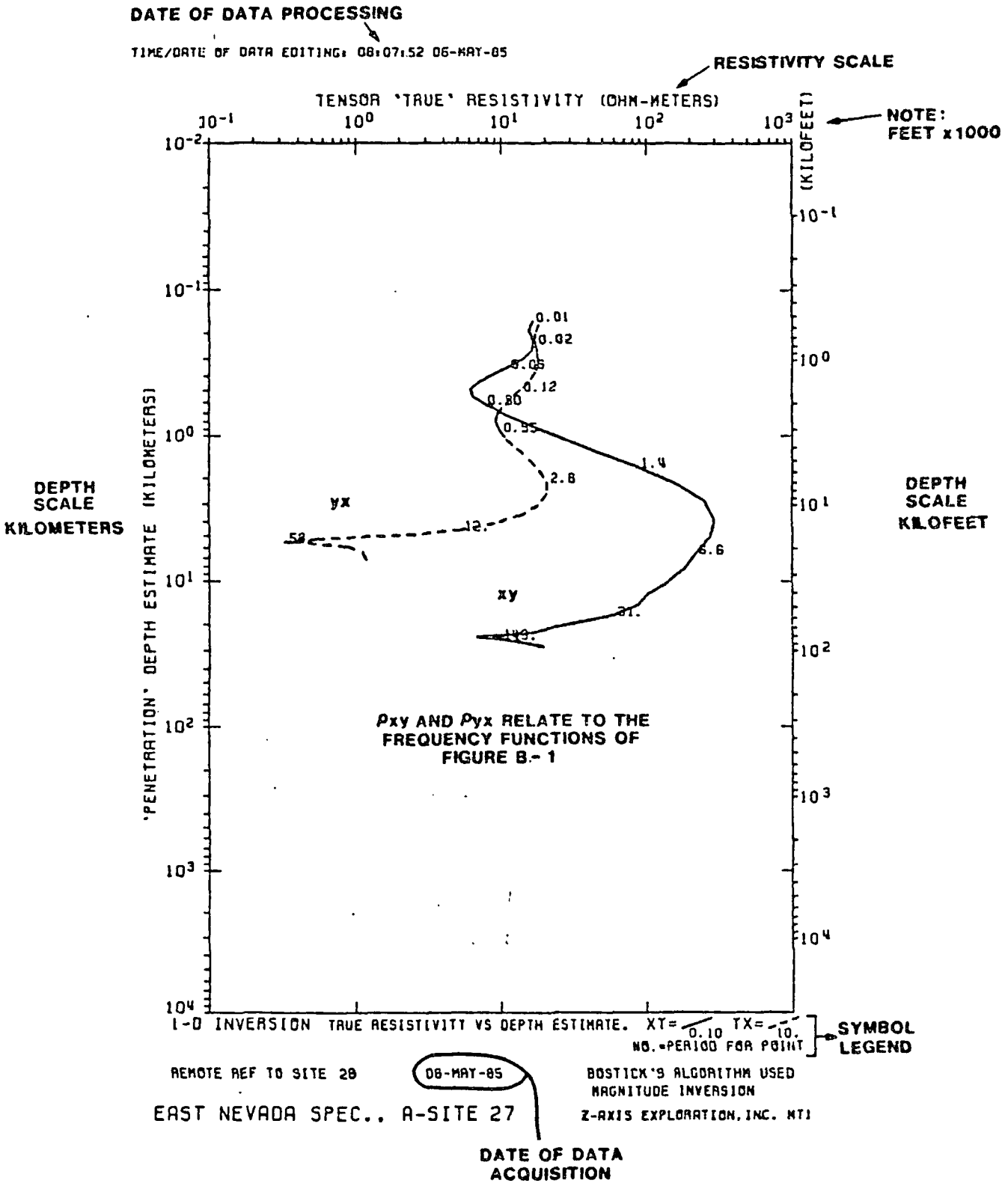


FIGURE B - 2

INVERTED RESISTIVITY DATA

$\rho a$ = apparent resistivity, at frequency f

f = frequency

m = slope of apparent resistivity function

u = magnetic parmeability

Since the apparent resistivity data (Figure B-1) used by Z-AXIS in the inversion calculation is the smoothed curves, the inverted resistivity is also a smooth curve, and is considered to be representative of an average, or bulk volume, resistivity of the subsurface. Note that since the inversion is of the smooth apparent resistivity function, it will only be as accurate a representation of the basic data as the smooth curve is an accurate representation of the basic data points.

On the data display, Figure B-2, the inversions for both $\rho xy$ and $\rho yx$ are shown. Resistivity and depth scales are both logarithmic. Much of the processing information contained on Figure B-1 is repeated on this and subsequent displays.

D. Apparent Resistivity Phase

It was mentioned earlier that the apparent resistivity is a complex function (in the mathematical sense) with an amplitude and phase. The phase of the apparent resistivity is related to the slope of the amplitude through a relationship such that if

slope of $\rho_a$ = 0; phase of $\rho_a$ = -45° (or 135°)

slope of $\rho_a$ positive; Phase <-45° (or >135°) (6)

slope of $\rho_a$ negative; Phase >-45° (or <135°)

where $\rho_a$ is the apparent resistivity amplitude function of Figure B-1. Note that the sign convention on the phase may vary between contractors, depending on the sign convention used at the field site in data acquisition. The ±45° relationship always holds, however.

The phase data are presented by Z-AXIS as shown in Figure B-3, on a page shared with other functions. Phase is plotted separately for $\rho_{xy}$ and $\rho_{yx}$, as a function of frequency. Phase is plotted in degrees linearly, as a logarithmic function of frequency. As with the amplitude function, a smooth polynomial-fit curve is passed through the basic data points.

In Figure B-4 the phase and amplitude data are shown together to illustrate the relationships of (6). Since the amplitude and phase curves are generated separately the agreement with (6) is a cross-check on data quality and the validity of data processing. Note that in the example at the highest frequencies the slope is negative but the phase is less than -45°, indicating a possible instrument or processing problem.

E. Coherency

Coherency is a measure of data quality. For the apparent resistivity data at an individual site (i.e., disregarding the reference of a simultaneously recorded site) the

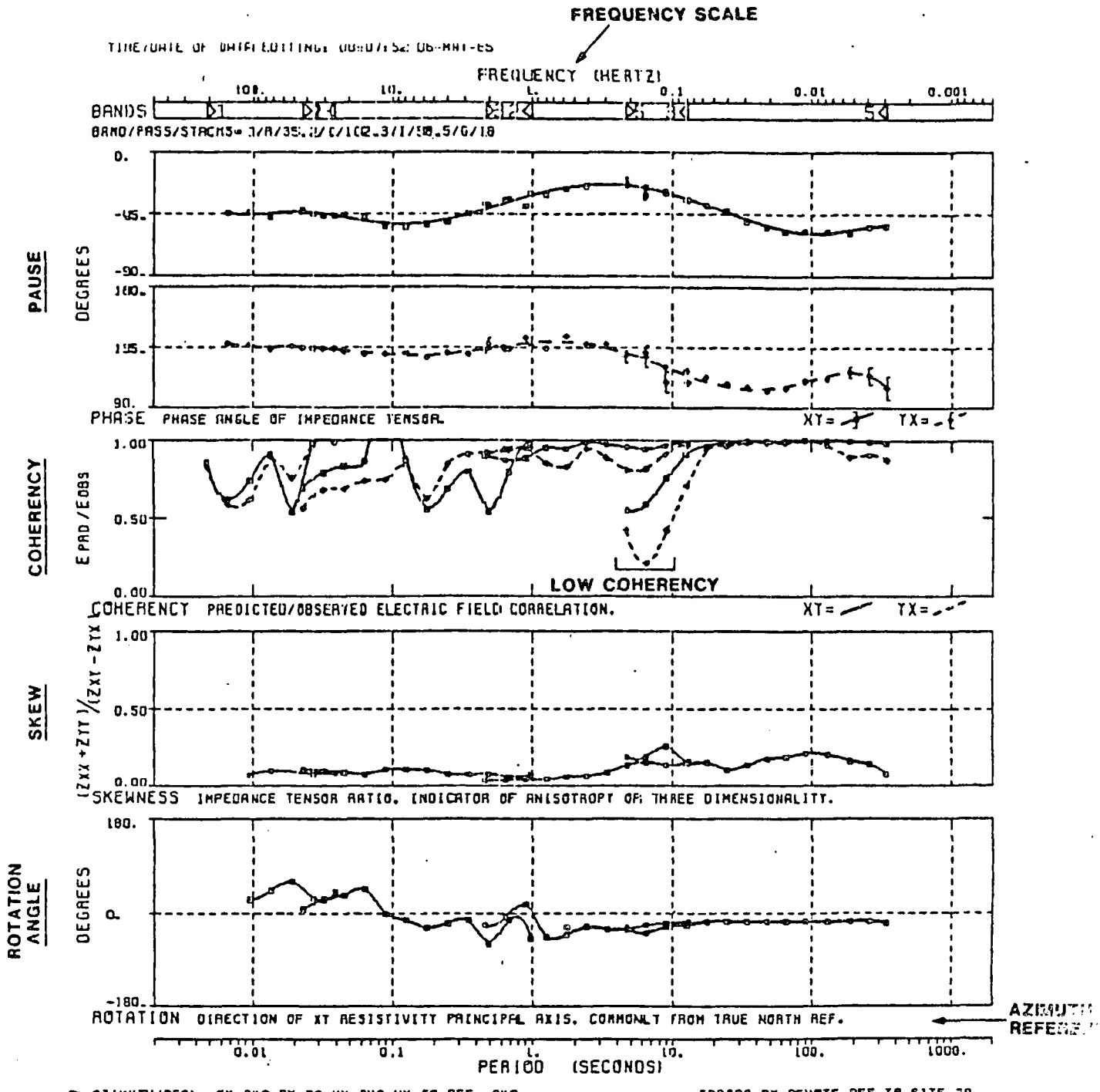


AZIMUTH OF MEASUREMENT COORDINATE SYSTEM, TRUE NORTH REFERENCE

**FIGURE B - 3**

**PHASE, COHERENCY, SKEW, AND ROTATION ANGLE DATA**

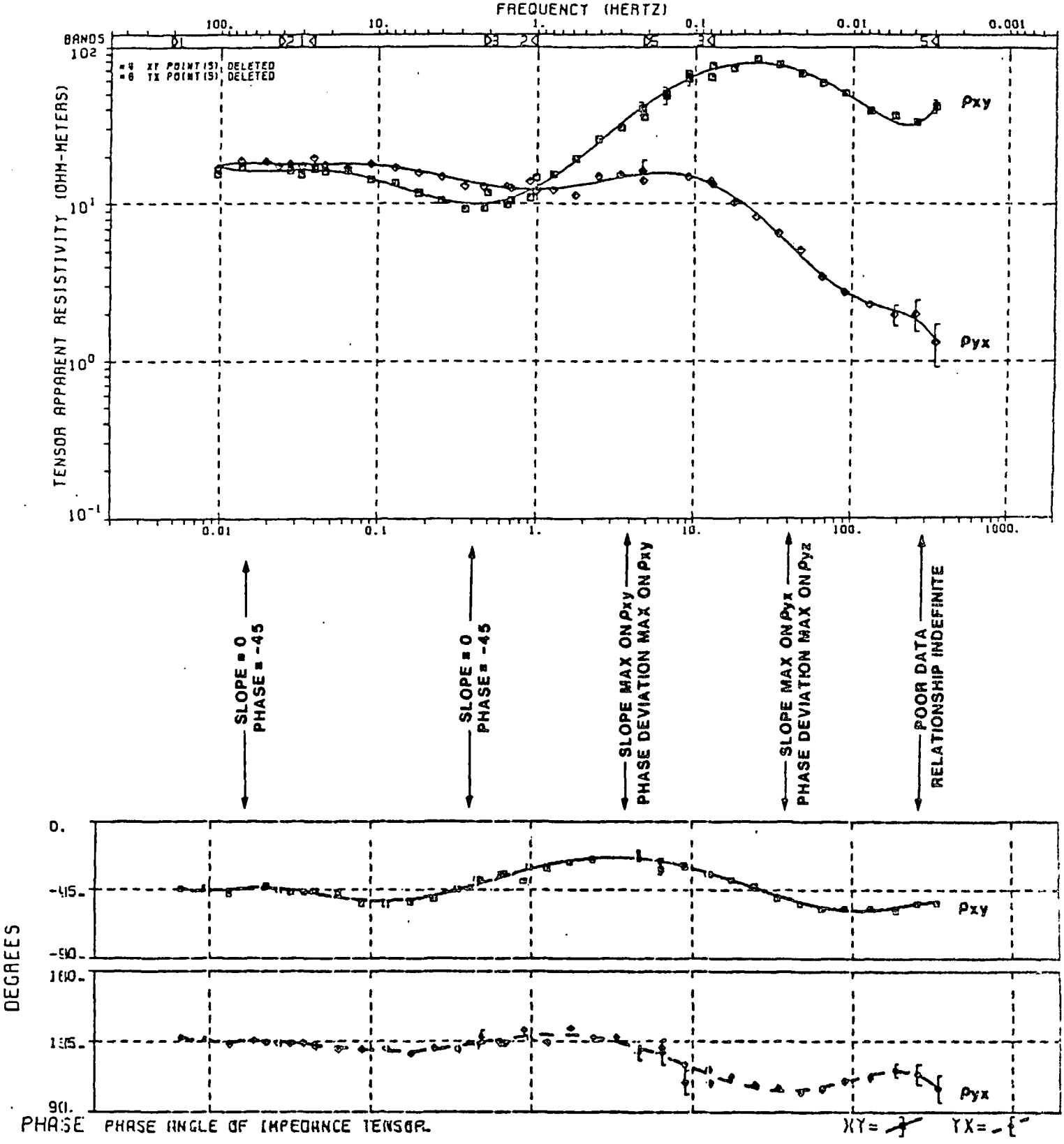


**FIGURE B - 4**

**AMPLITUDE-PHASE RELATIONSHIP (OF APPARENT RESISTIVITY)**

computed apparent resistivity is combined with the measured magnetic field to compute a predicted electric field. Expressed mathematically, first

$$\rho x_c = f \qquad (7)$$

where $\rho x_c$ is the calculated apparent resistivity and Exm and Hym are the measured fields. Then, $\rho x_c$ and $Hy_m$ are used to compute a predicted electric field

$$Ex_p = f' (Hy_m, \rho x_c). \qquad (8)$$

In other words, the quantities $Hy_m$ and $\rho x_c$ are used to recreate an electric field function, $Ex_p$. In the absence of noise or distortion

$$Ex_p = Ex_m \qquad (9)$$

The "recreated", or predicted, E will be exactly equal to the original measured E, since f' is just the inverse of f. To measure the noise and/or distortion of the real world, the coherency (in a statistical sense) between $Ex_p$ and $Ex_m$ is computed and presented.

The coherency is plotted by Z-AXIS on the same page as the phase, as shown in Figure B-3. The coherency function is normalized, so that a value of 1.0 is perfect coherency, while a value of zero implies a completely random relationship.

In the example, the coherency is low in the vicinity of 0.1 Hz (10 sec. period). Note that this is single site coherency, the use of the reference site can be expected in most cases to improve data quality. Using the reference

technique the coherency function snerves mainly to "flag" those portions of the frequency band where noise problems might occur.

F. Skew

Earlier it was pointed out that with a two-dimensional structure the relationship (2) could be established through a mathematic coordinate rotation. In practice the purity of (2) is not attained and after rotation (usually to locate the maximum of $\rho xy$, the "off-diagonal" or resistivity amplitude term) $\rho xx$ and/or $\rho xy$ do not reduce to zero. This can be expressed as

$$\begin{aligned} Ex' &= \rho xx' \; Hx' + \rho xy' \; Hy' \\ Ey' &= \rho yx' \; Hy' + \rho yy' \; Hy' \end{aligned} \qquad (10)$$

where the primes serve to differentiate the rotated relationship (10) from the unrotated (1). The departure of $\rho xx'$ and $\rho yy'$ from zero is a measure of how well the assumptions of two-dimensional structure are met. The skew is a measure of that departure, and is defined as

$$S = \frac{1(\rho xx + \rho yy)}{1(\rho xy - \rho yx)}. \qquad (11)$$

For skew to be low both $\rho xx$ and $\rho yy$ have to be small. Skews on the order of 0.25 or less are considered to indicate a probably primarily two-dimensional environment. Skews of 0.5 or greater are considered to indicate that three-dimensionality may be an important factor in the interpretation. Note that low skew is not a guarantee of two-dimensionality.

The skew as shown in Figure B-3 is plotted linearly in the range between zero and one, as a function of frequency.

G. Rotation Angle

The coordinate rotation from the arbitrary measurement coordinate system (the direction that the electric and magnetic field sensors are installed in at the site) to the "rotated" coordinate system that has been computed as the best mathematical fit to the assumptions of equation (2) is a critical step in MT data processing. The importance of the apparent resistivity terms, $\rho xy$ and $\rho yx$, and the "diagonal" terms, $\rho xx$ and $\rho yy$, have been discussed above. The rotation angle, defined as the azimuth* of the rotated coordinate system, is also important. This is the azimuth of the resitivity components related to the strike azimuth. The listed azimuth may be for the resistivity component parallel or perpendicular to strike, this is an interpretive decision.

The rotation angle is computed and displayed as a function of frequency. The Z-AXIS convention is that the angle plotted is the azimuth of the $\rho xy$ resistivity component,

*The azimuth, or rotation angle, is defined in MT parlance as the azimuth of either $\rho xy$ or $\rho yx$. It is assumed that the azimuth of the other component is orthogonal to the listed or plotted rotation angle. Thus, if the rotation angle of $\rho xy$ is 35° relative to true north, the angle of $\rho yx$ is 125°. Further, it is assumed that if $\rho xy$ (at 35°) is the maximum that $\rho xy$ will be at any rotation angle (the assumption of two-dimensionality) then $\rho yx$ (at 125°) will be the minimum.

as defined by the symbols in the resistivity display, Figure B-1.

The rotation angle is presented on the same page as the phase, coherency, and skew, Figure B-3. The angle is plotted referenced to true north. The azimuth of the measurement coordinate system, and the azimuth reference of the rotation angle, are shown. Note that through the skin depth relationship the rotation angle will be constant with frequency only if either the shallow and deeper structures have the same geologic strike or if a structure at one depth or distance from the site completely dominates other structural trends. The variation of rotation angle with frequency is an obvious indication of three-dimensional structural complexity, and an important interpretive tool.

The rotation angle is also displayed as part of the "polar plot" presentation. These will be discussed in section I below.

H. Tipper Functions

The term "Tipper" refers to the distortion caused by geologic structure of the electromagnetic wave from which the MT functions are computed. The electromagnetic source wave is an EM wave propagating vertically into the earth, with the electric (E) and magnetic (H) fields horizontal, at right angles to the direction of propagation. If the earth is electrically one-dimensional, with the resistivity

varying only with depth, then the EM field measured at the surface, the superposition of the source and reradiated waves*, behaves as above with the direction of the E and H components still horizontal. If there are lateral variations in resistivity, however, the resultant EM field (again, the superimposed source and reradiated) will be distorted such that the resultant direction of propagation is not vertical. In particular, the magnetic field is not horizontal and is said to be "tipped", out of the plane that is horizontal or parallel to the earth's surface.**

The tipped magnetic field is measured by a three-coordinate magnetic field sensor system, the x and y coordinates of all of the previous discussion plus the vertical, or Z, coordinate.*** The distortion of the magnetic field, as

---

*The reradiated wave is sometimes referred to as secondary radiation.

**If the structure is two-dimensional the magnetic field is "tipped" so that the strike of the geologic structure is perpendicular to the strike direction and parallel to the dip direction of the plane formed by the resultant magnetic field vectors. Thus, if the geologic strike is in the X direction, then Hx will remain horizontal while Hy will be tipped out of the horizontal. Since the measurement coordinate system is at an arbitrary azimuth, the aximuth of the tipped field must be computed mathematically. This calculation results in the "Tipper Direction", the azimuth of the dip of the tipped magnetic field (associated with the dip azimuth of the causitive structure), and in the "Tipper Strike", the azimuth of the strike of the tipped magnetic field (associated with the strike azimuth of the causitive structure).

***Because of the extreme contrast in resistivity between the air and the earth there is no vertical electric field on the surface.

presented in the "Tipper" functions is an indication of structural complexity. As such the Tipper can be a useful interpretive tool.

The Z-AXIS presentation of the Tipper functions is shown in Figure B-5. The Tipper magnitude is the ratio of vertical to horizontal magnetic field vectors, when the resultant "Tipped" magnetic field is resolved into its horizontal and vertical components. The magnitude is plotted linearly vertically while frequency is logarithmic.

Tipper coherency is a measure of vertical field data quality. In the example (Figure B-5) the higher frequencies, above about 5-10 Hz, vertical field data quality is poor, the result of low signal levels as evidenced by the magnitude plot.

In a two-dimensional setting the vertical field component of the tipped field will be a maximum in the dip direction and zero along strike. The Tipper skew, the ratio of vertical field maximum to minimum, is a measure of agreement of the actual data to the assumption of two-dimensionality.

The Tipper Direction and Strike are plotted as a function of frequency. The Reference angle is true north, as indicated in the discussion of rotation angle, and noted on Figure B-3.

I. Polar Plots

Polar plots of the apparent resistivity have become a useful interpretive and diagnostic tool in MT exploration.

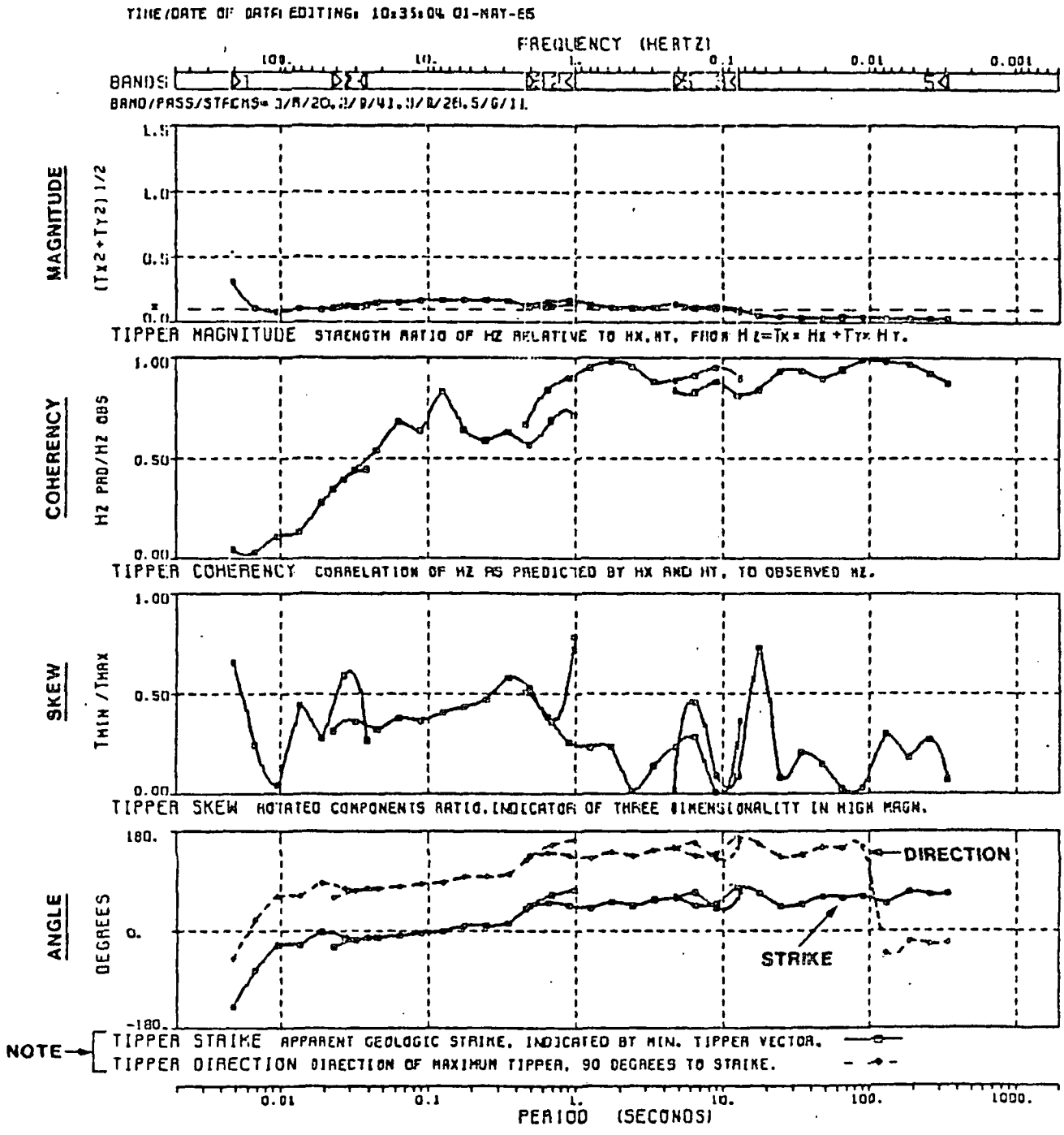


FIGURE 5-5
TIPPER DATA

Equation (1), the fundamental MT relationship, was discussed in section A above and is repeated here:

$$Ex = \rho xx\ Hx + \rho xy\ Hy$$
$$Ey = \rho yx\ Hx + \rho yy\ Hy \qquad (1)\ \text{(repeated)}$$

The technique for mathematically rotating the xy coordinate system of (1), the measurement coordinate system, to a new coordinate system parallel and perpendicular to strike (at each frequency) has also been described. The rotation of coordinates can also be made to <u>any</u> arbitrary coordinate azimuth, and the $\rho xy$, $\rho yx$, $\rho xx$, and $\rho yy$ terms computed for that coordinate system. This forms the basis for the polar plot.

The Z-AXIS presentation of the Polar Plot is shown in Figure B-6. To form the polar plot $\rho xy$ and $\rho xx$ are calculated as a function of azimuth (rotation angle), usually at increments of 2 to 4 degrees. The calculations are performed as a function of frequency, on the Z-AXIS plots at half of the frequency points calculated for the other data, Figures B-1 through B-5. The $\rho xy$ and $\rho yx$ data at each frequency are then plotted in polar form. At any angle $\theta$ the magnitude of $\rho xy$ is represented by the length of the vector $\rho xy$, and the magnitude of $\rho xx$ is represented by the vector $\rho xx$. The polar plot is the focus of the tip of each vector over $\theta$ between 0 and 360 degrees. The plots at each frequency for both $\rho xy$ <u>and</u> $\rho xx$ are normalized to the <u>maximum</u> <u>$\rho xy$</u>, as shown on the sketch. Thus, the magnitude of $\rho xx$ relative to that of $\rho xy$

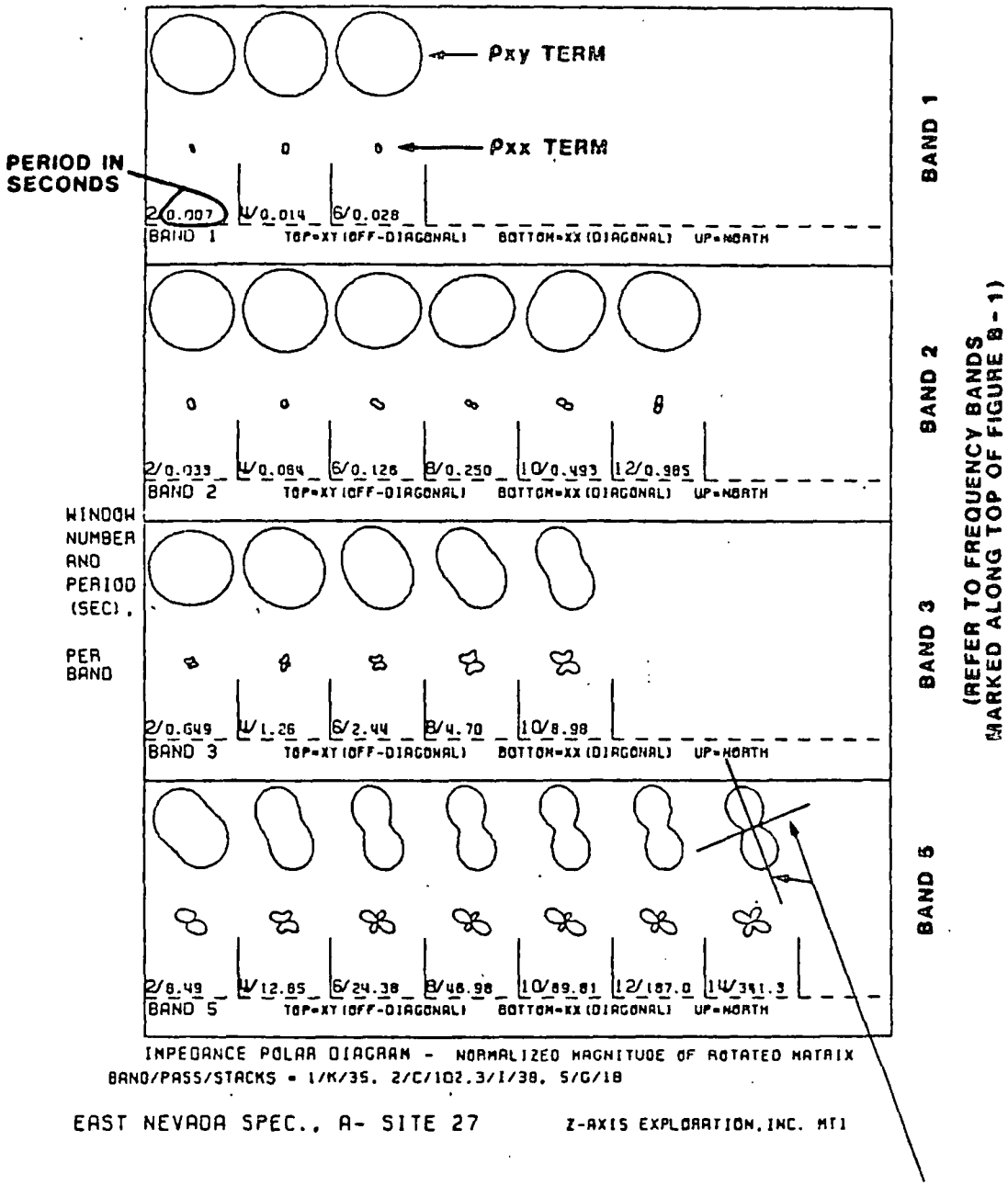


FIGURE B - 6
RESISTIVITY
POLAR PLOTS

can be assessed visually at each frequency. For relative magnitudes as a function of frequency reference must be made to Figure B-1. Note that the magnitudes are plotted linearly (as opposed to the logarithmic presentation of Figure B-1) accentuating the ellipticity of the plots.

## 3. Complex MT Data - Description and Definitions

### A. Introduction

The purpose of this section is to describe some of the more common effects of structural complexity observed in MT data, and to introduce the terminology employed in discussion of these types of data. The interpretation of complex data will not be covered here, reference is made to Appendix C for a discussion of interpretation.

### B. "Simple" MT Data

The least complex MT data is that acquired where the earth is one-dimensional, i.e., where the resistivity varies only with depth. In this case the MT apparent resistivity will be independent of azimuth, $\rho xy = \rho yx$ in equation (1), and the concept of rotation angle loses any meaning. In addition, the magnetic field will be horizontal, free of any distortion, and the Tipper magnitude will thus be zero (or reflect only sensor and instrument noise).

The MT apparent resistivity data that would be obtained at such a site is defined as "isotropic", or independent of azimuth, throughout the frequency range. The two resistivity curves would overlie one another, and appear as one (or close to one) on the apparent resistivity plot (Figure B-7). Note that the data in the figure is not entirely isotropic at the lower frequencies.

One-dimensional data, MT data that is isotropic throughout the frequency range, is exceedingly rare, especially

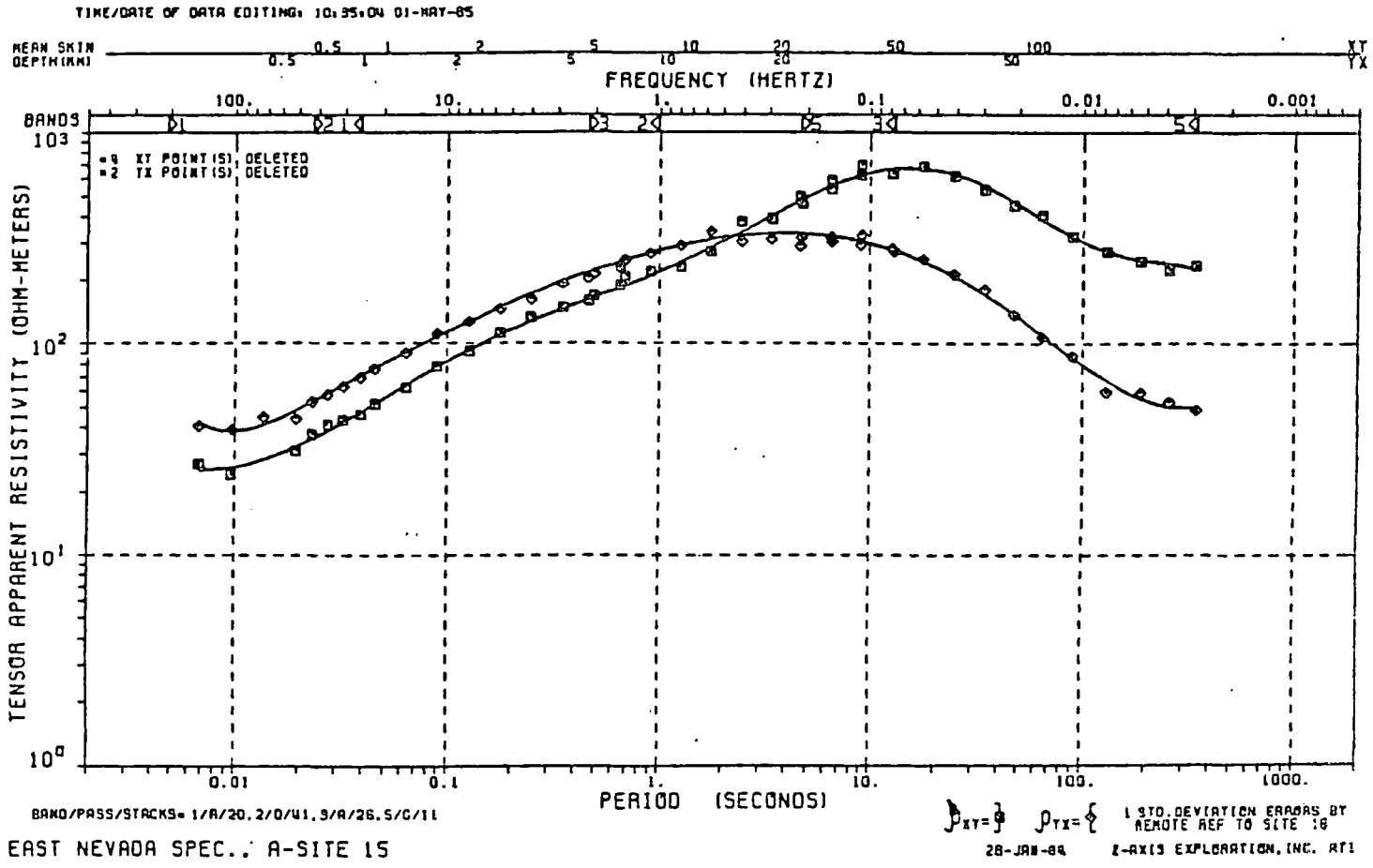


**FIGURE B - 7**

**EXAMPLE OF ISOTROPIC DATA**

in practical exploration where geologic structural complexity of some kind is almost always present. In practice, if the two apparent resistivity functions ($\rho_{xy}$ and $\rho_{yx}$ of the fundamental equations) differ by a factor of 1.2 or less the data is considered isotropic. The data shown in Figure B-7 comes close to this over the higher frequencies, above about 0.3 Hz. Note that for this site the vertical magnetic field (Tipper) magnitude as shown in Figure B-8 is also negligible over most of the frequency range, with only a low amplitude peak magnitude of about 0.20 at 4.0 Hz.

C. Statics Effects

Lateral variations in resistivity at or near the surface have an effect on MT data analogous to the effects of near-surface velocity variations on seismic data. These effects on MT data are thus termed "statics" effects in recognition of this analogy. The statics effect, discussed in detail in Appendix C, is illustrated in Figures B-9 and B-10. The statics effect is manifested by a parallel separation of the two resistivity curves, starting from the highest frequencies (left side of the data plot) and extending throughout the frequency range. The statics effect is dramatically shown in Figure B-10, where the data of Figure B-9 with large statics "shift" is compared with the data of Site B-45. The data of site B-45 exhibits a very small statics shift when compared with site B-43.

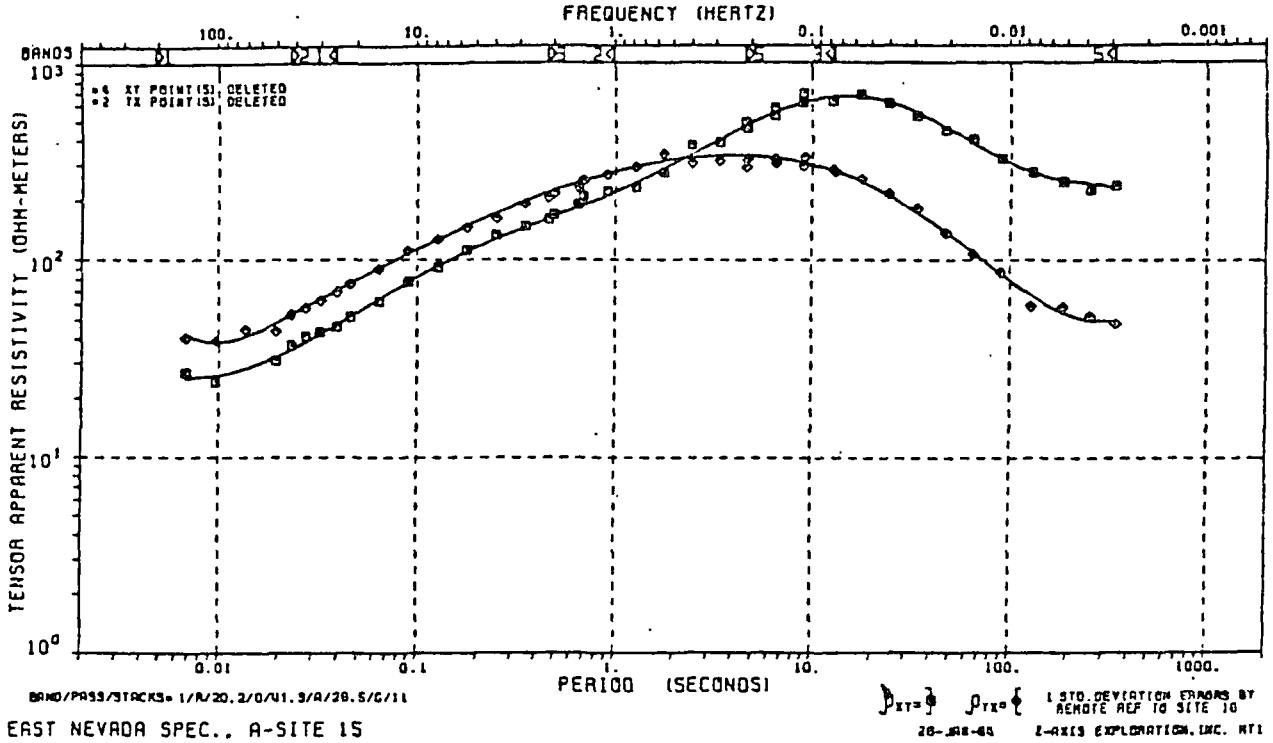


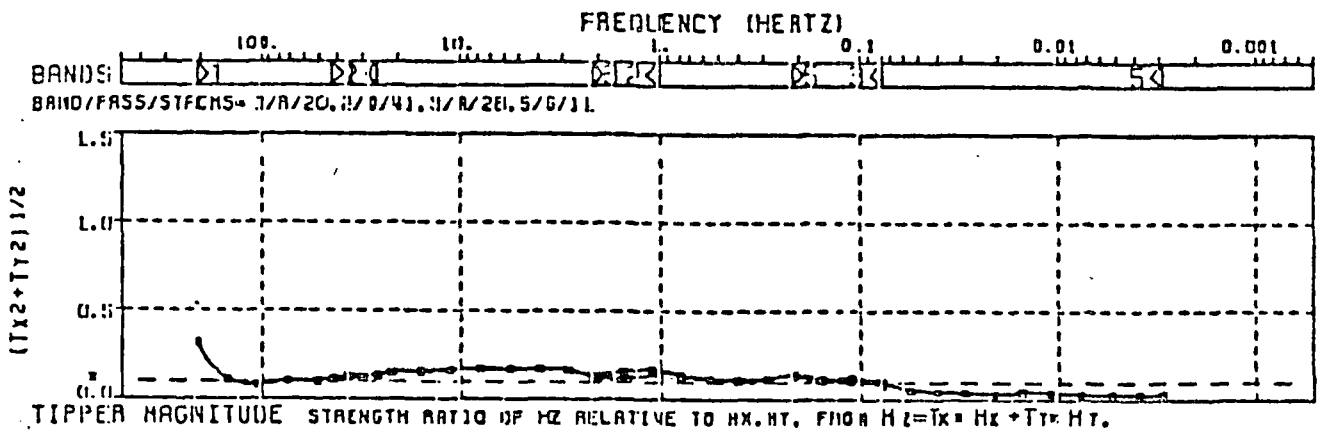


**FIGURE B - 8**

**EXAMPLE OF TIPPER MAGNITUDE AS RELATED TO ISOTROPIC DATA**

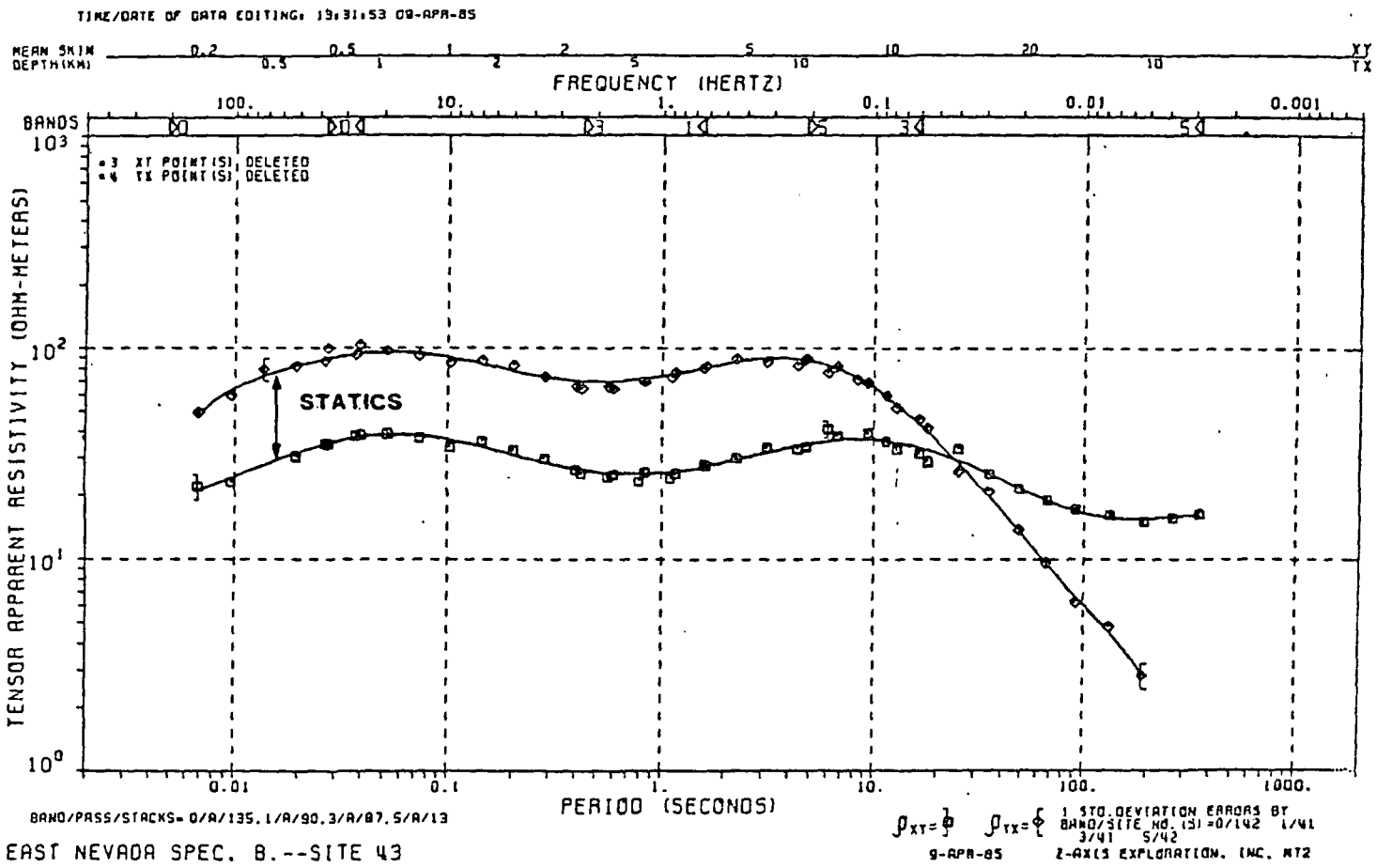


**STATICS EFFECT: PARALLEL SEPARATION OF THE TWO APPARENT RESISTIVITY CURVES, STARTING AT THE HIGHEST FREQUENCIES.**

**FIGURE B - 9**

**STATICS EFFECT**

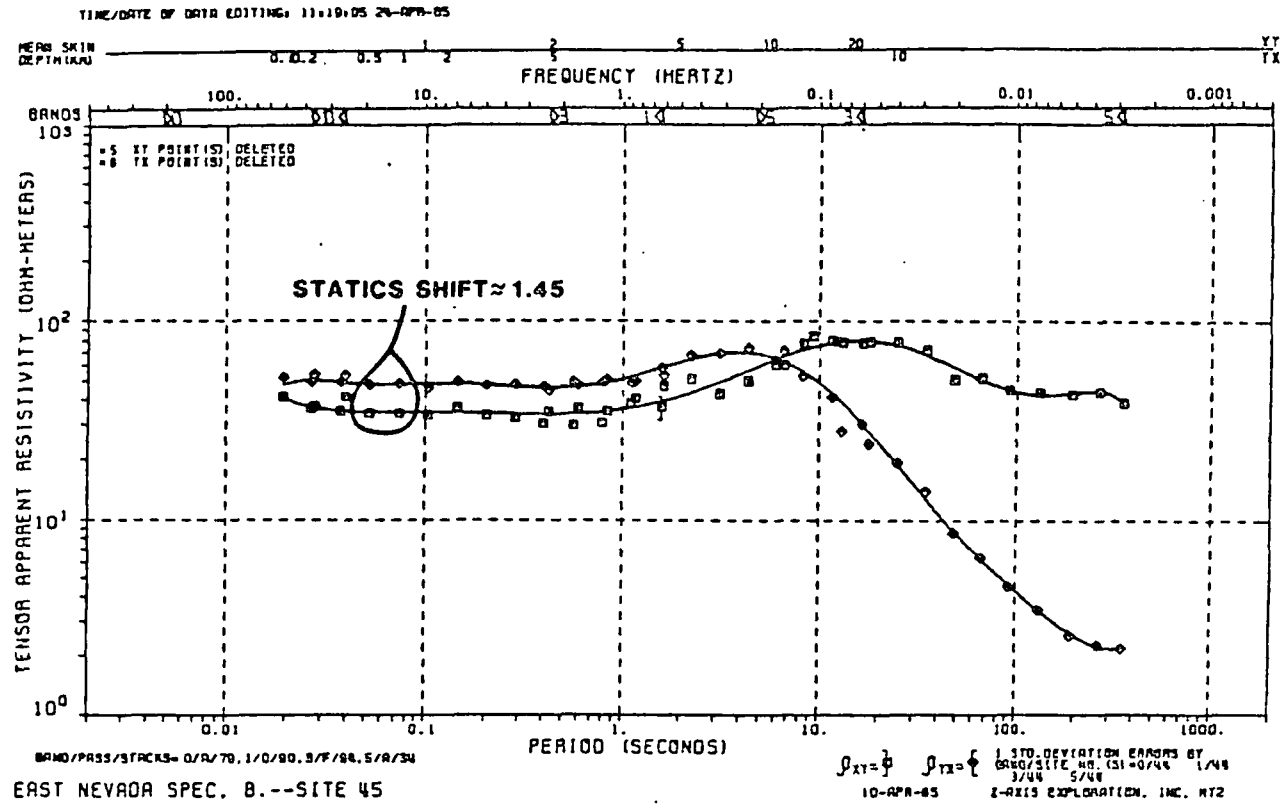


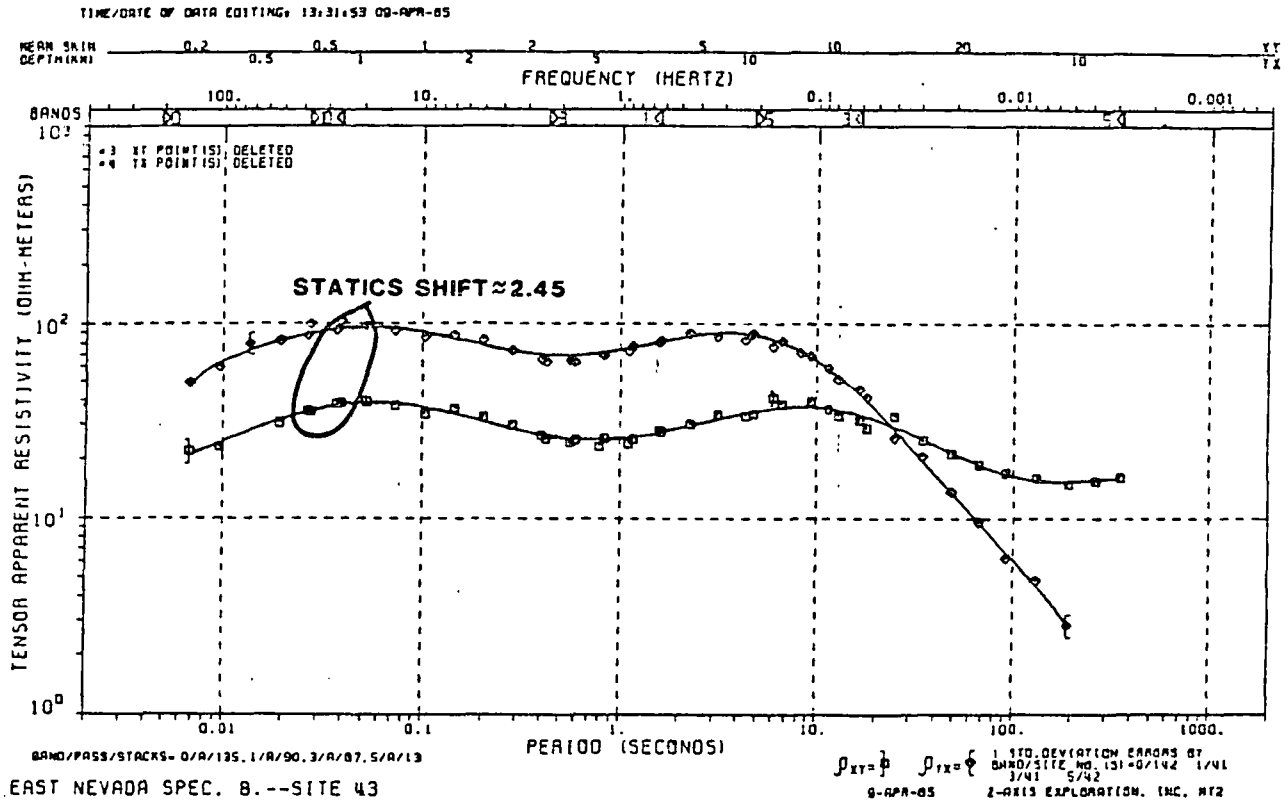


**FIGURE B - 10**

**STATICS EFFECT COMPARISON**

Statics effects are "corrected" by a linear shift of one (or both) of the apparent resistivity curves as shown in Figure B-11. The correction arrow shows the direction and magnitude of the correction applied by the interpreter. On Figure B-11 the shifted $\rho_{xy}$ curve has been sketched in to illustrate that after correction the two curves overlie one another at the high frequencies, revealing the complex relationship of the two curves below a frequency of about 1.0 Hz.

A statics shift of an apparent resistivity curve requires a corresponding shift in the inverted resistivity data for that curve. Since the depth varies as the square root of resitivity (equation (5), section 2.C above) on the logarithmic plot of resistivity versus depth the depth will vary as a factor of ½ of resistivity, when the length of line segments on the inversion plot are considered. Thus, on Figure B-12 if the vector $\Delta\rho$ is the resistivity correction factor (the same $\Delta\rho$ as in Figure B-11), the vector $\Delta D$, the depth correction, is one half the length of $\Delta\rho$. The $\rho_{yx}$ inversion curve has been in effect "slid" along the correction slope to a new position, where the distance slid is the length of the hypotenuse of the $\Delta D\ \Delta\rho$ triangle.

On Figure B-12 the correction factors $\Delta\rho$ and $\Delta D$ are shown graphically, as is the correction along the correction slope. Uncorrected depth "picks" are shown as solid lines, statics corrected picks as dashed lines. Statics corrected depth values are noted with the suffix "S", as in 2950S.

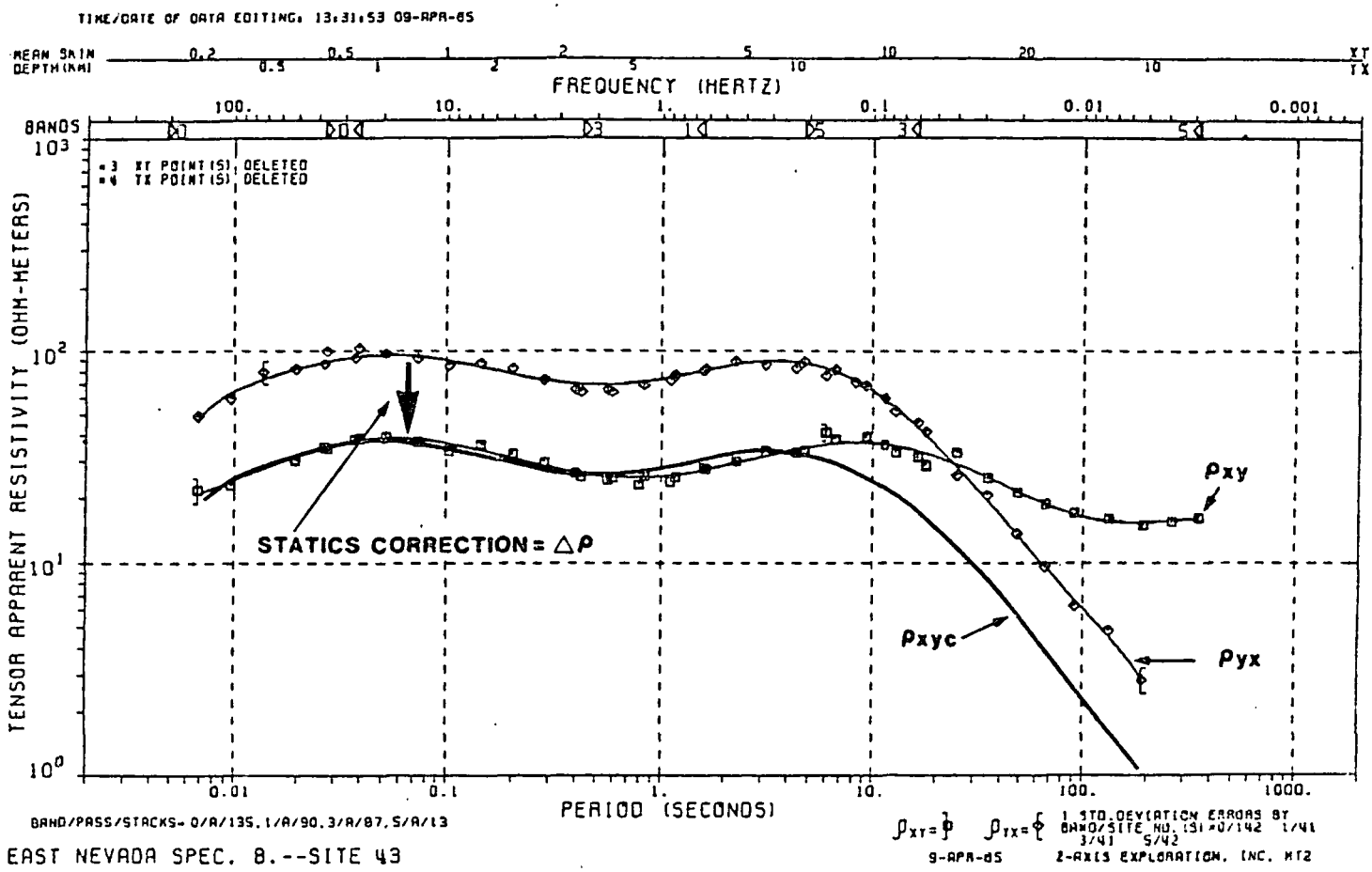


**STATICS CORRECTION: VERTICAL SHIFT ONE OR BOTH RESISTIVITY CURVES. IN THIS CASE ρyx HAS BEEN SHIFTED TO OVERLIE ρxy AT HIGH FREQUENCIES. △ρ IS THE CORRECTION FACTOR ρxyc = △ρ x ρyx**

**FIGURE B - 11**

**STATICS CORRECTION**

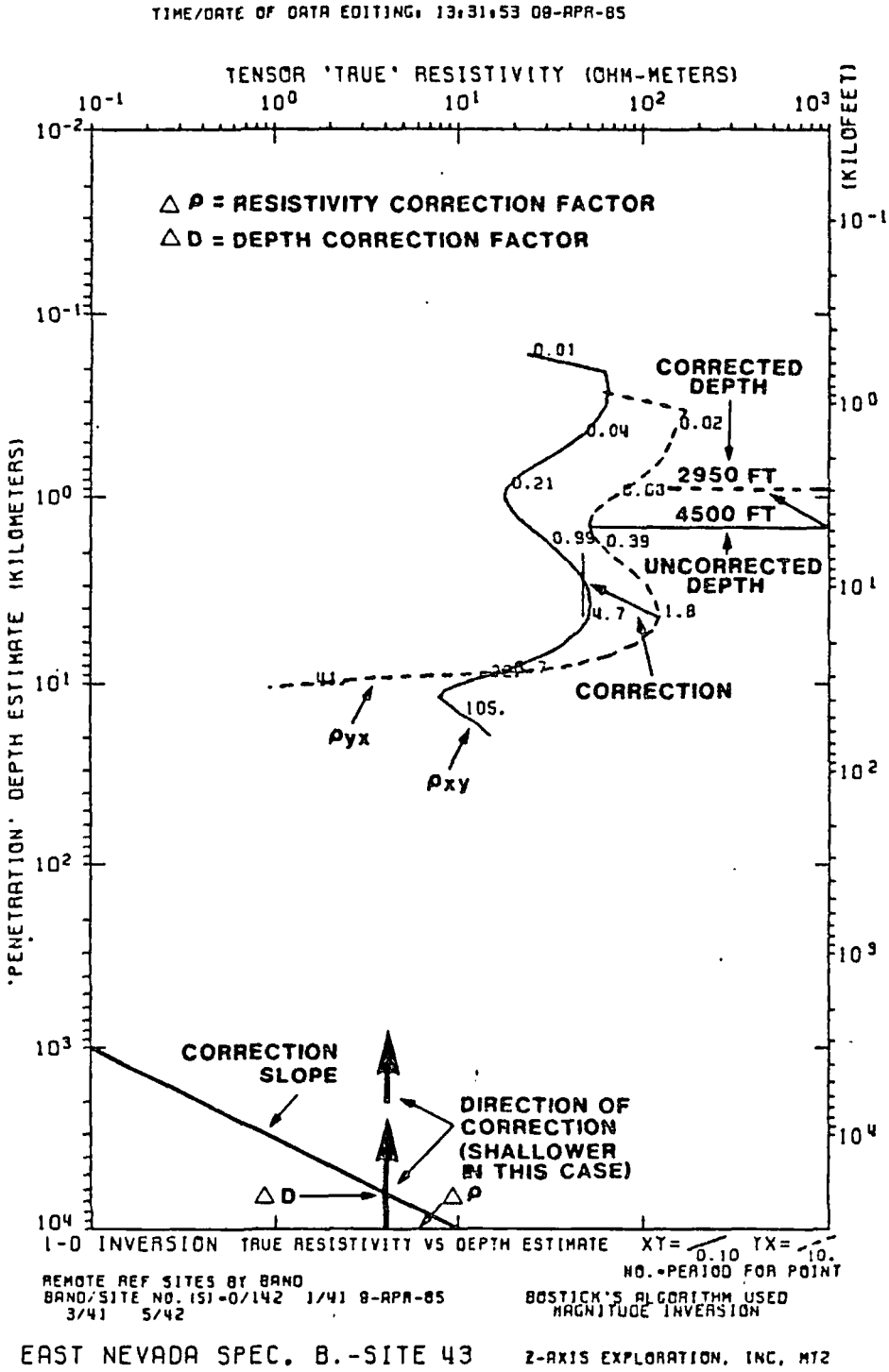


**FIGURE B - 12**
**STATICS CORRECTION, INVERTED RESISTIVITY**

D. Effects of Geologic Structure

MT data in the presence of geologic structure is anisotropic, which means that the apparent resistivity is a function of direction. As discussed earlier, this means that in the fundamental relationships of equations (1) and (2), $\rho_{xy}$ does not equal $\rho_{yx}$. The two resistivity curves are computed and presented as described in sections 2.A and 2.B above. The shape of the $\rho_{xy}$ and $\rho_{yx}$ curves, and the differences between them, forms the basis for the structural interpretation of MT data.

An example of anisotropic resistivity data, the result of structure, is shown in Figure B-13. This data is compared with more isotropic data in Figure B-14.

For a discussion of the interpretation of data such as this refer to Appendix C, in particular the sections on fault, horst, and graben geology.

E. Compound Data

Most MT data obtained in operational surveys exhibits a combination of statics and structural effects. An example is shown in Figures B-15 and B-16. In Figure B-16 the $\rho_{xy}$ curve is shown in its corrected position in the bottom plot. Another example is shown in Figure B-17. Note that after the statics shift in Figure B-17, the similarity between this site and that of site A-15 (the top graph in Figure B-7) is apparent, an observation not readily apparent in the uncorrected data.

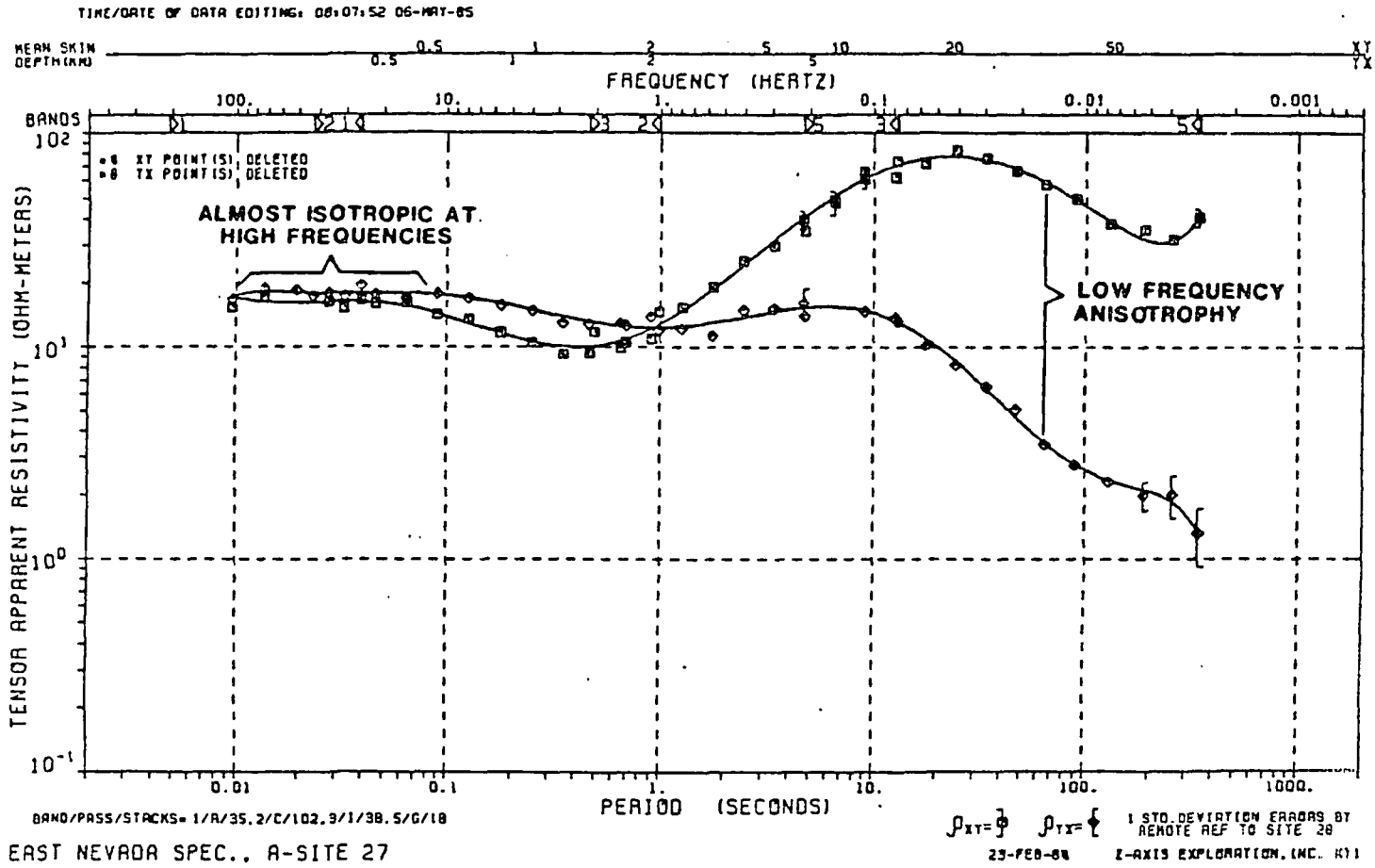


**FIGURE B - 13**

**EFFECT OF STRUCTURE, LOW FREQUENCY ANISOTROPHY**

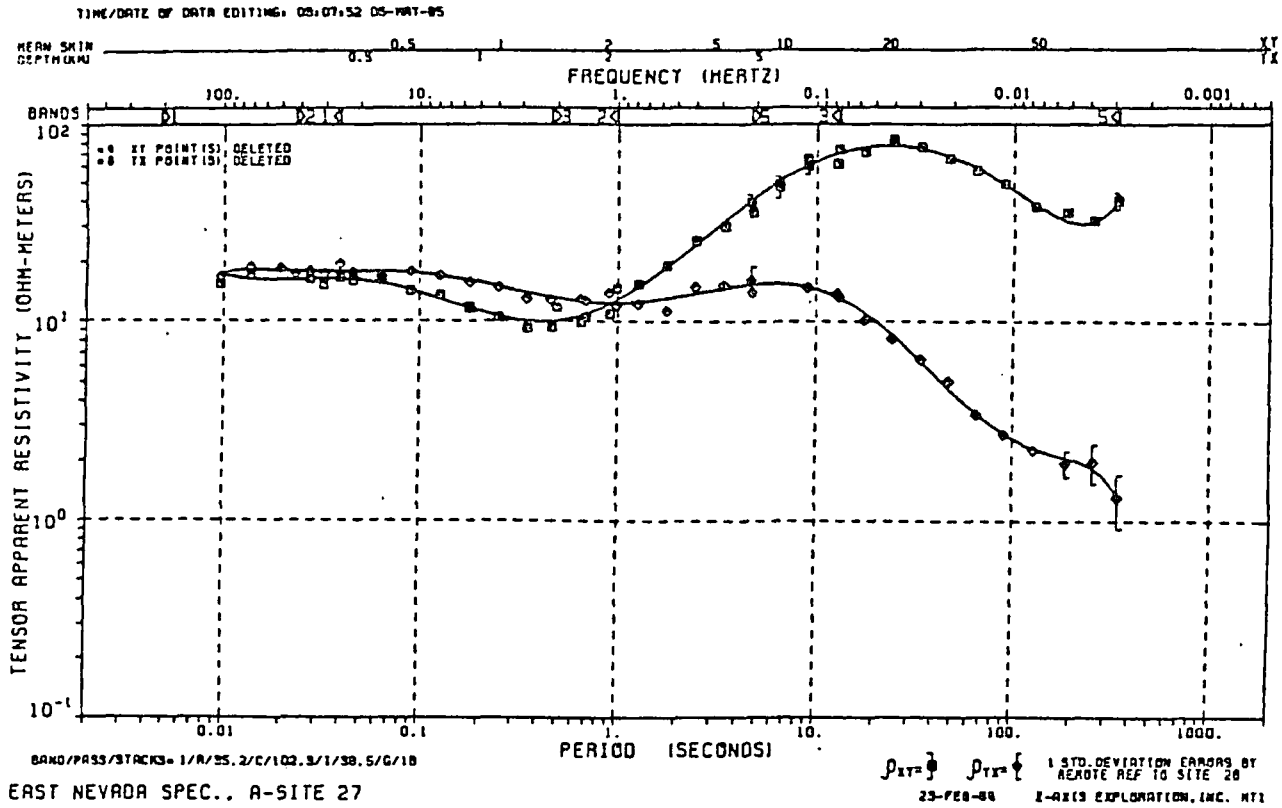


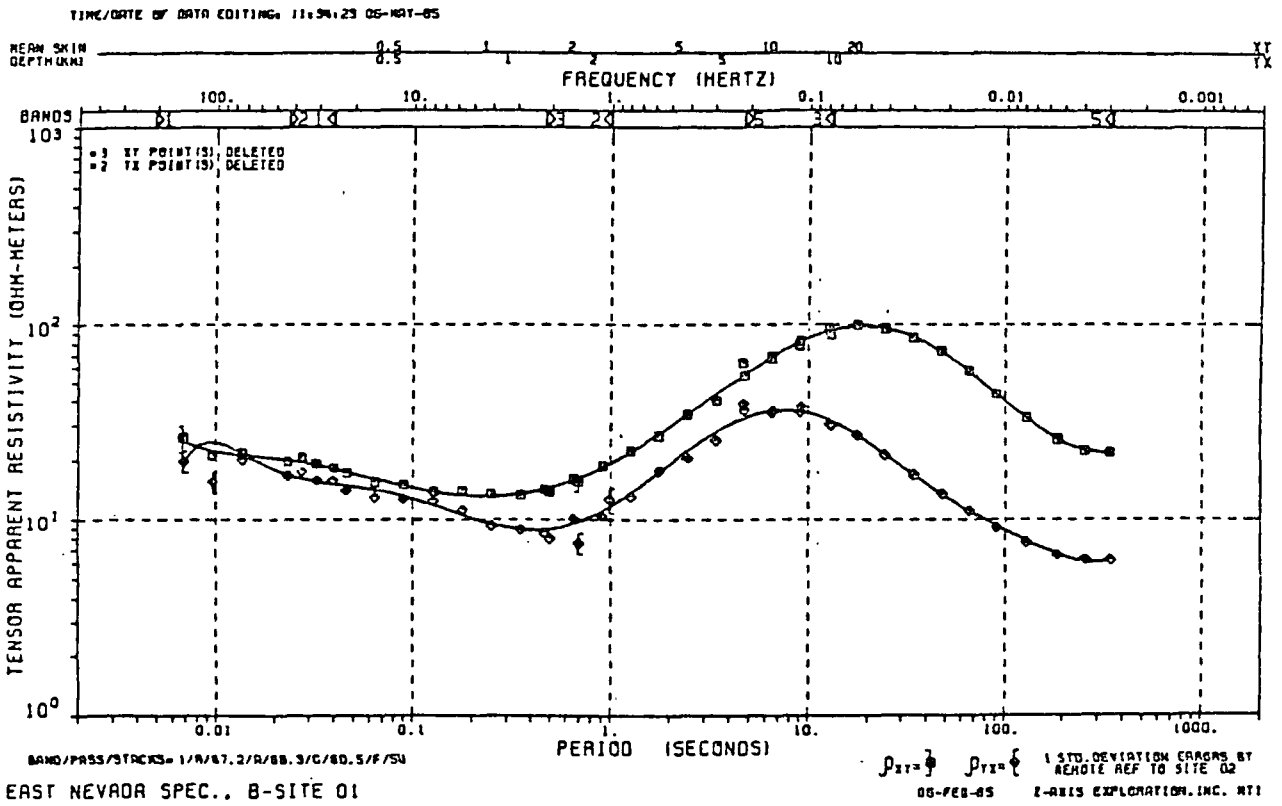


**FIGURE B - 14**
**ISOTROPIC VERSUS ANISOTROPIC DATA COMPARISON**

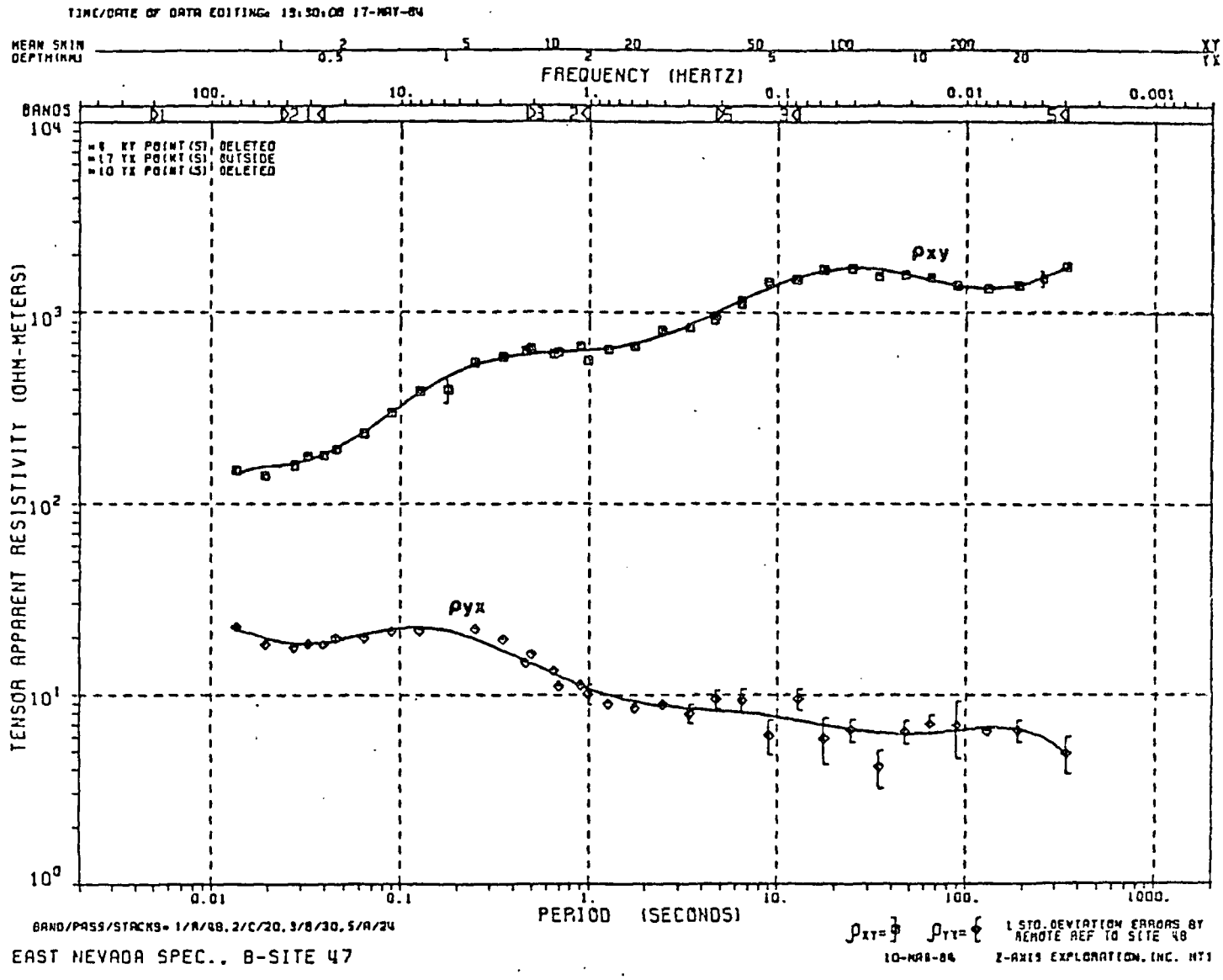


**SUPERPOSITION OF STATICS AND STRUCTURAL EFFECTS**

**FIGURE B - 15**
**COMPOUND DATA**

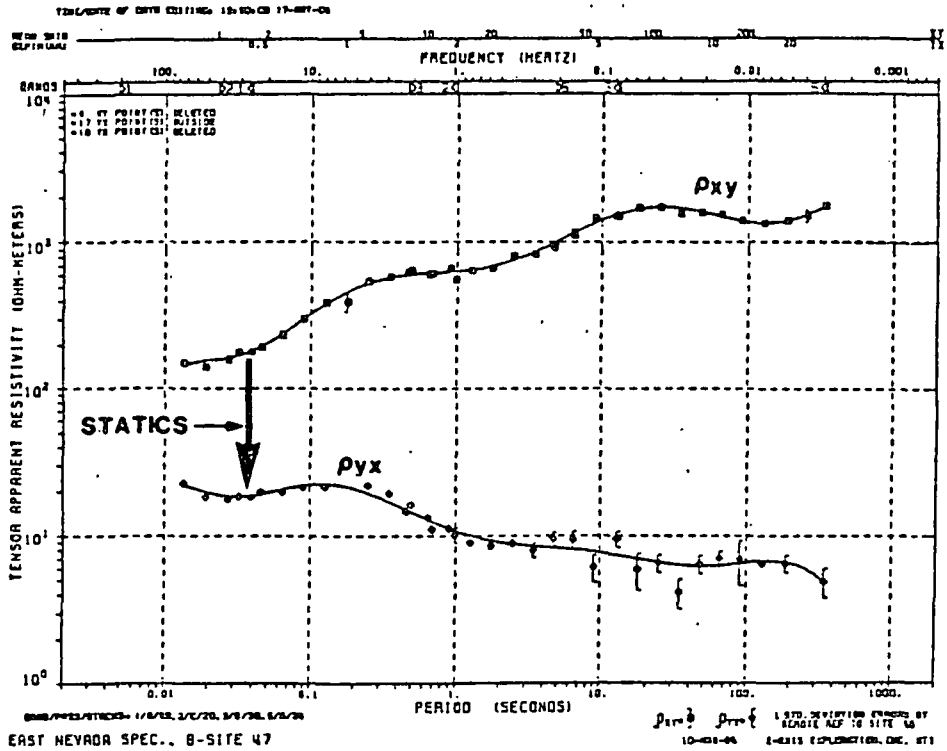


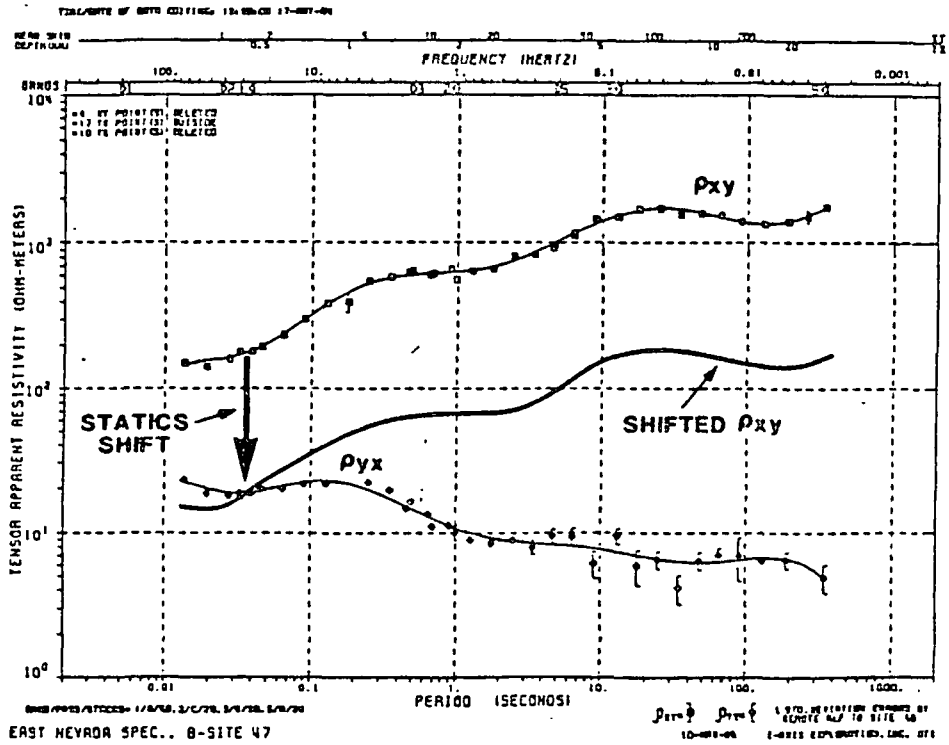


**FIGURE B - 16**

**COMPOUND DATA WITH CORRECTION**

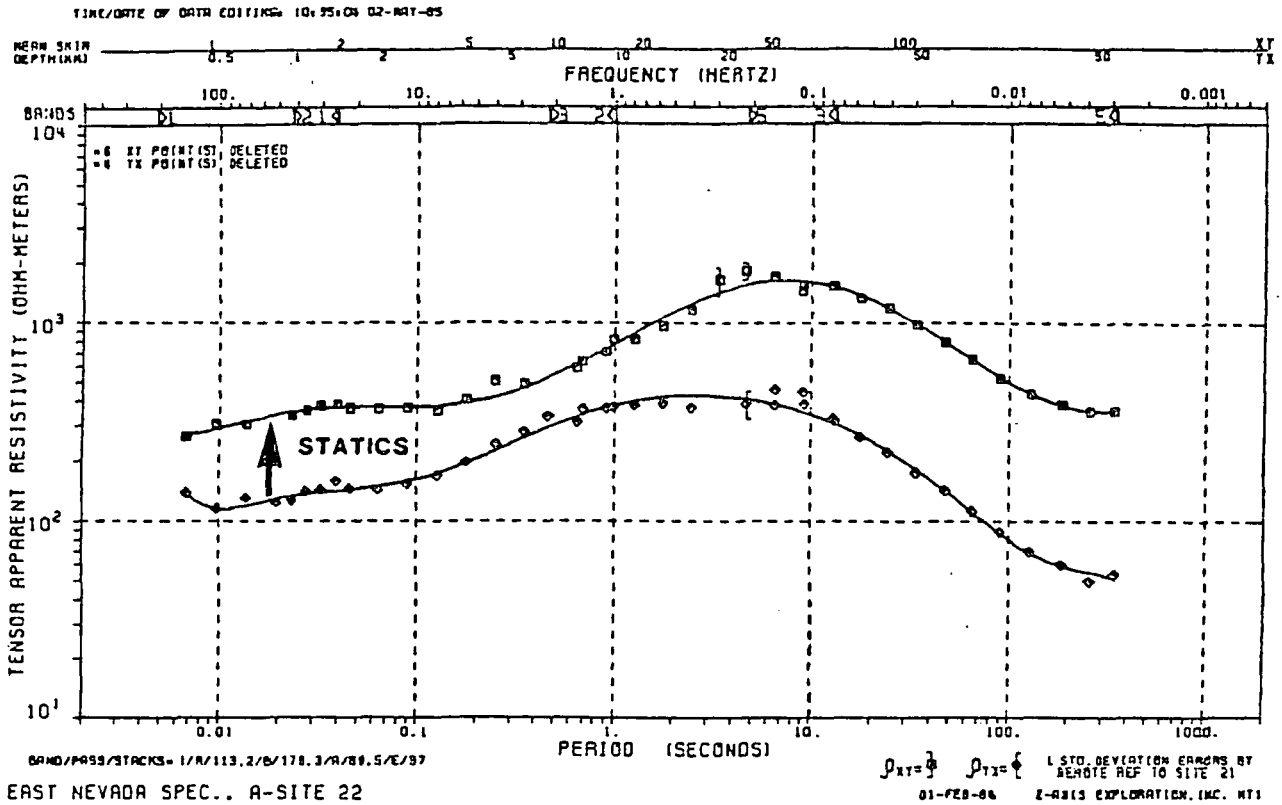


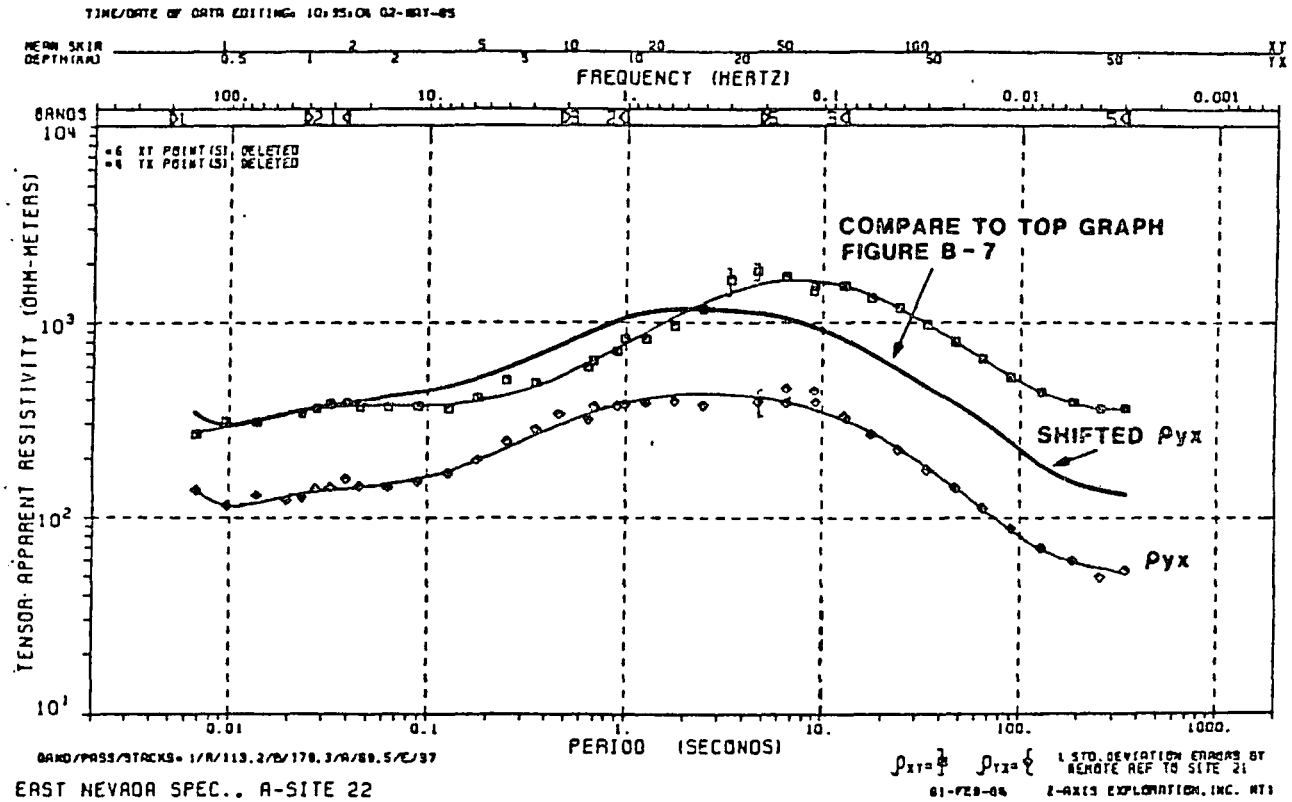


**FIGURE B - 17**

**COMPOUND DATA WITH CORRECTIO**

4. MT Data Quality

MT data quality is described in terms of the characteristics of the plotted parameters (Figures B-1 through B-5). In this section the apparent resistivity versus frequency data (Figure B-1) will be emphasized, with the purpose of the illustration of the terms used to describe MT data quality.

An example of good quality data is shown in Figure B-18. Examples of fair and poor quality data are shown in Figures B-19 and B-20, annotated to show the characteristics used in describing data quality. All these examples were acquired and processed by Z-AXIS using similar processing parameters.

Point-to-point consistency is the most important data quality criterion, especially in better quality data. The MT apparent resistivity function is smoothly varying, with a maximum theoretical slope of 1 (when plotted on a log-log scale). Since a small error bar is not in itself a guarantee of good data*, when the error bars are small the point-to-point alignment becomes critical. Compare the high frequency portions of Figures B-19 and B-20 with the data of Figure B-18. The data pointed out in Figures B-19 and B-20 have medium or large error bars, but exhibit poor point-to-point consistency.

While small error bars are not guarantee of good data, large error bars are an indication of poor data. Gaps in

*Since the number of data points stacked appears in the denominator of the determination of error bar length, an infinitely large stack of pure noise will have an infinitely small error bar.

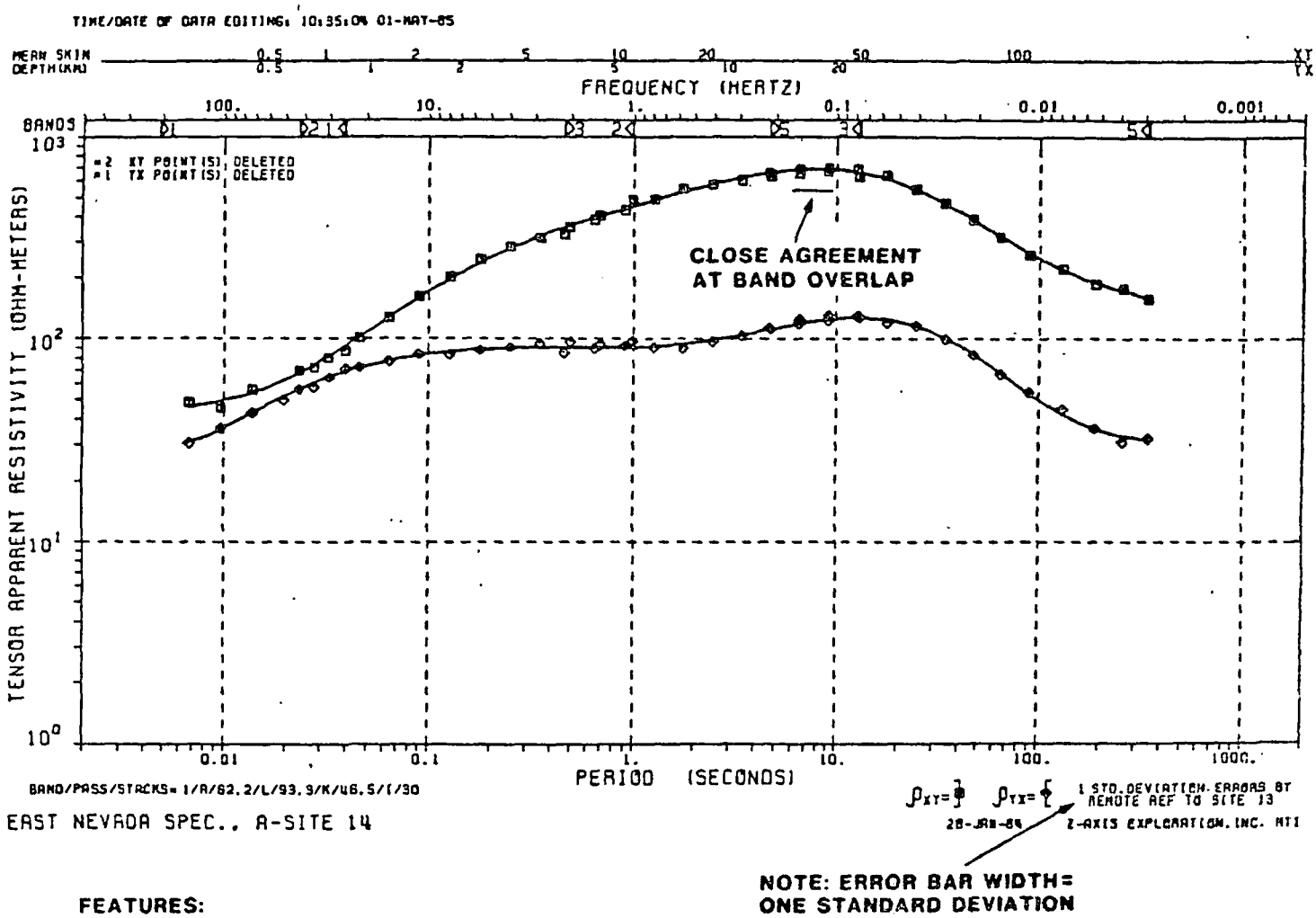


**FEATURES:**

- **POINT TO POINT CONSISTENCY**
- **NO ERROR BARS**
- **AGREEMENT AT FREQUENCY BAND OVERLAP (NOTED ON PLOT)**
- **FEW IF ANY GAPS IN DATA**

**FIGURE B - 18**

**GOOD QUALITY DATA**

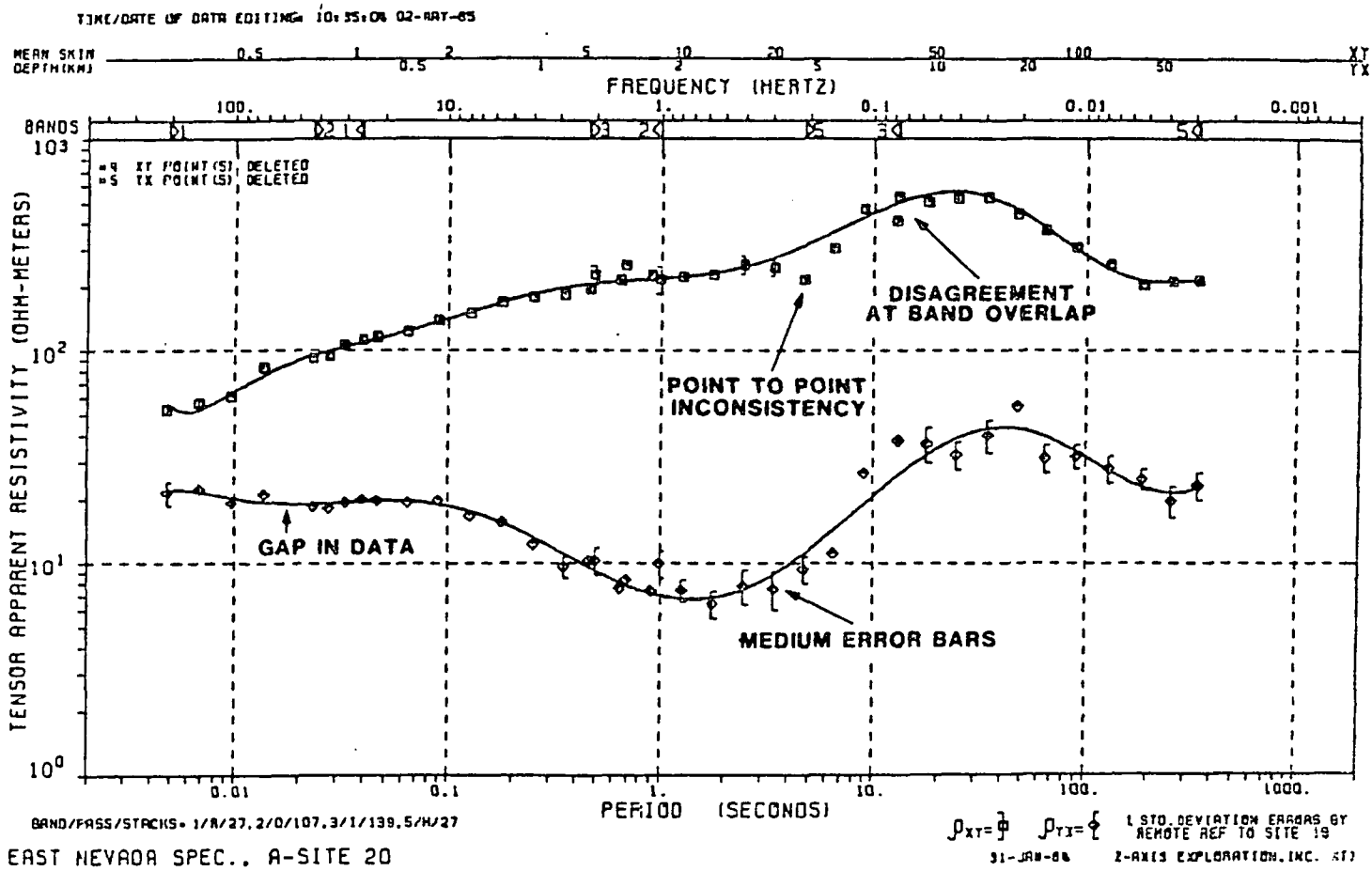


**FIGURE B - 19**
**FAIR QUALITY DATA**

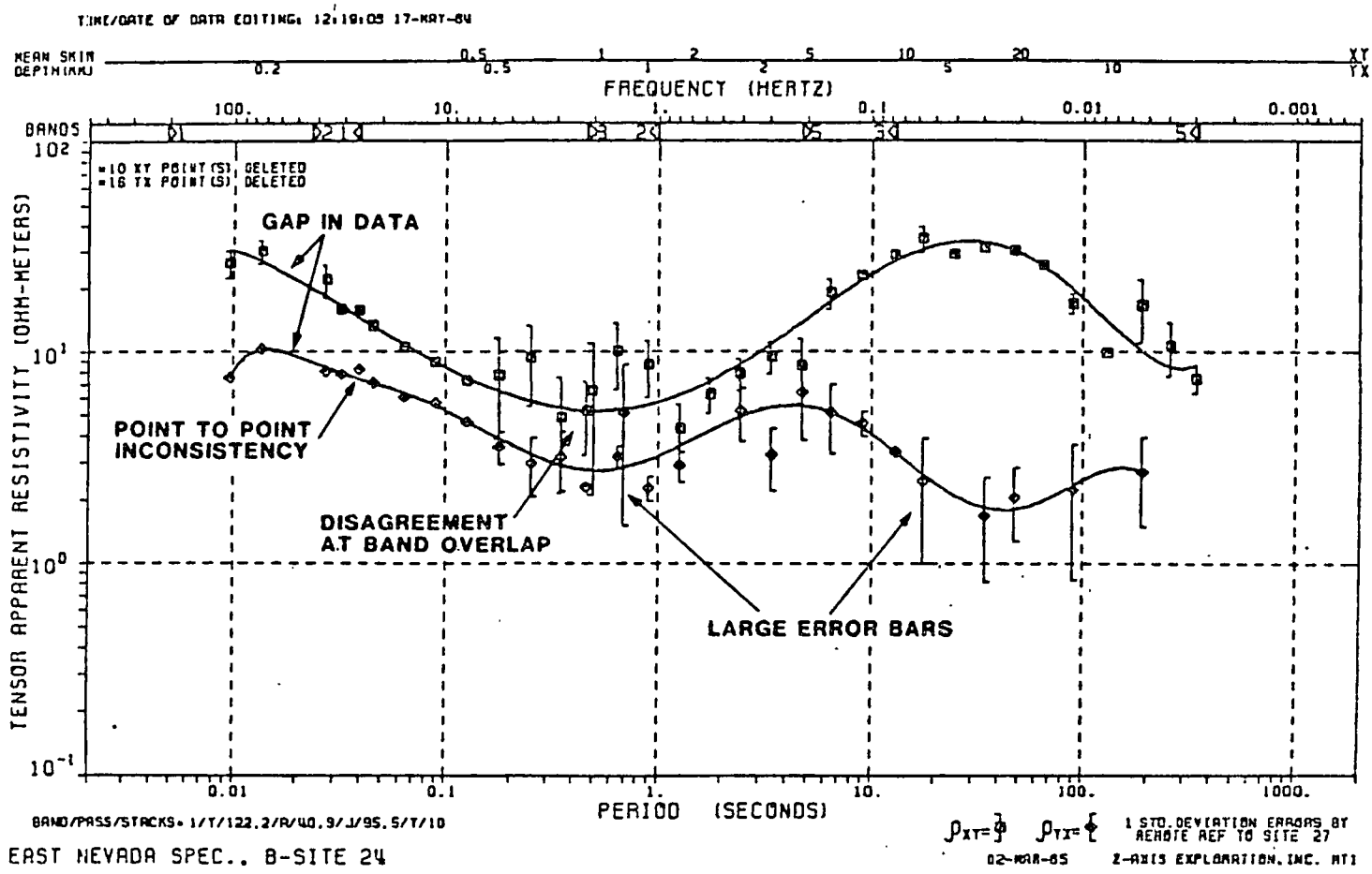


**FIGURE B - 20**

**POOR QUALITY DATA**

the data indicate that the missing points were rejected by the computer as not meeting some minimum quality criteria. Finally, since the frequency bands in which the data are recorded and processed overlap, the data from two overlapping bands should agree closely in the overlapping frequency range.

The Coherency has been discussed earlier in section 2.E above. This function must be used with caution. As discussed in section 2.E, the coherency is a single-site function. Data with poor coherency characteristics can be processed to yield high quality results using reference site techniques. On the other hand, data can exhibit excellent coherency characteristics yet contain "coherent", or bias, noise which will render results over all or part of the frequency range invalid. The reference technique may eliminate all or part of this noise, but in some instances detection will be difficult.

## 5. Glossary of Terms

The following is a glossary of some of the more common terms used in magnetotelluric (MT) exploration and in describing MT data. Some of these terms are used in other exploration contexts; these may have the same meaning as applied to MT, or the meaning as applied to MT may differ from that when used elsewhere.

Acquisition - the measurement and recording, usually in digital form, of the basic MT data, the time-varying electric and magnetic fields.

Anisotropic - the characteristic of a material whereby a property varies with the direction through the material that that property is measured. MT data is termed anisotropic if the apparent resistivity varies as a function of azimuth (on the surface). This variation may be determined by rotating the measurement axes, or more easily by measuring using an arbitrary coordinate system and then peforming the rotation mathematically (cf. isotropic).

Apparent Resistivity - the results of the basic MT processing, derived as a function of frequency from electric and magnetic field data. Related to depth and/or distance through the skin depth relationship. An average resistivity, from the surface to some depth, where the depth or distance of investigation is a function of actual earth resistivities and the discrete frequency under consideration (see skin depth).

Bostick inverse - a mathematical transformation of an apparent resistivity versus frequency curve into an "intrinsic" resistivity versus depth curve. The "intrinsic" resistivity is in units of ohm-meters and is a smooth curve, like the input frequency function.

Coherency - in MT terminology, a data quality criterion that relates the relationship between an electric or magnetic field component predicted mathematically with the actual component.

Compound data - MT data which exhibits two or more complicating features, such as a superposition of statics and deep-structure effects.

Compound structure - a structural situation where the MT data are influenced by two or more structural features, such as when a site is located on an overthrust plate, and also adjacent to a fault-to-surface feature.

Conductivity - the inverse of resistivity. Conductivity (mhos/meter) = 1/Resistivity (ohm-meters)

Contrast - usualy refers to resistivity contrast, the ratio of the resistivities of the rocks on either side of a boundary.

Diagonal components - the $\rho xx$ and $\rho yy$ components of the resistivity tensor, as defined by $Ex = \rho xx\ Hx + \rho xy\ Hy$ $Ey = \rho yx\ Hx + \rho yy\ Hy$

(See Resistivity tensor)

Electrical basement - in a vertical geologic section the deepest low-resistivity over high-resistivity interface which can be resolved, and which occurs at or above geologic basement. A point of confusion often arises when, for example, a high resistivity geologic basement (say Precambrian granite) is overlain by Paleozoic carbonates, which are in turn overlain by a low resistivity marine clastic section. If the carbonates are tight and roughly equivalent to the granite in resistivity so that there is little or no electrical contrast between them, then the electrical basement will be at the high resistivity-contrast, clastic-carbonate interface. Thus, electricl basement may be several thousand feet above what is normally considered geologic basement.

Ellipticity - an indicator of three-dimensionality of MT data, not displayed by Z-AXIS Exploration, Inc. Ellipticity is defined as

$$B = \frac{(\rho xx - \rho yy)}{(\rho xy \pm \rho yx)}$$

where the $\rho$ terms are after rotation, and are complex numbers.

Error bars - on MT data displays a graphical display of the statistical distribution of a stack of several data samples, usually expressed in standard deviations, or alternately the width of the distribution where the number of samples at that value is a percentage of the samples at the mean.

Forward model - a model where the input data is a geologic-derived geometry and the output is simulated geophysical, in this case MT, data.

In-Field processing - the capability to process MT data at the field site, usually refers to obtaining at a minimum the rotated tensor resistivities and tipper functions.

Inverted resistivity - a resistivity-depth function derived from the apparent resistivity-frequency functions using any one of several mathematical or modeling techniques.

Isotropic - the characteristic of a material whereby a property is independent of the direction through the material in which the property is measured. MT data is termed isotropic if the apparent resistivity is independent of measurement (or computed) horizontal azimuth (cf. anisotropic).

Lateral variations - are variations in resistivity that occur with horizontal distance away from an MT site.

Layered inverse - an inverse technique that, using as an input the MT apparent resistivity versus frequency data, yields a sequence of layers each with a discrete resistivity and thickness.

MT - short for magnetotelluric.

Noise - any unwanted signals that affect the quality and validity of MT data. Noise may occur within the data acquisition instrumentation, in processing, or from sources such as wind, powerlines, or other cultural sources outside of the MT instruments.

Off-diagonal components - the $\rho xy$ and $\rho yx$ components of the resistivity tensor, as defined by $Ex = \rho xx\ Hx + \rho xy\ Hy$, $Ey = \rho yx\ Hx + \rho yy\ Hy$ (see Resistivity Tensor)

Ohm-meters - the physical units of resistivity.

One-dimensional earth - in MT the geometry where resistivity varies only as a function of depth (cf. two-dimensional earth).

Period - the inverse of frequency, denoted by the letter T. $T = 1/f$.

Polar plot - the diagonal ($\rho xx$) or off-diagonal ($\rho xy$) resistivity terms computed and plotted as a function of horizontal azimuth, at a discrete frequency.

Processing - in MT the calculations of the fundamental MT parameters from the measured and digitized electric and magnetic field time series. These parameters include the resistivity tensor functions and Tipper functions.

Real-time processing - MT data processing performed in the field, at the field site, coincident with data acquisition.

Reference angle - the horizontal azimuth, usually true north, that is the reference for the resistivity tensor and tipper rotation angles. The reference angle may or may not be the same as the measurement angle, the angle that the sensors are installed at at the site.

Reference MT - the technique whereby MT data is acquired simultaneoulsy at two or more sites, with the data at each site processed using one or more of the other sites in an effort to improve the signal-to-noise ratio utilizing correlation techniques.

Resistivity - the electrical property of a material, measured in ohm-meters, that is determined by MT. (See also apparent resistivity and inverted resistivity.)

Resistivity contrast - see contrast.

Resistivity Tensor - the mathematical expression

$$\begin{vmatrix} \rho_{xx} & \rho_{xy} \\ \rho_{yx} & \rho_{yy} \end{vmatrix}$$

that relates the electric and magnetic fields at the surface of the earth.

Rotated Apparent Resistivity - the $\rho_{xy}$ and $\rho_{yx}$ terms of the relationship

$$E_x = \rho_{xx} H_x + \rho_{xy} H_y$$
$$E_Y = \rho_{yx} H_x + \rho_{yy} H_y$$

where the xy coordinate system has been rotated mathematically from the measurement coordinate system to an orientation where $\rho_{xy}$ or $\rho_{yx}$ is a maximum (and $\rho_{yx}$ and $\rho_{xy}$ is a minimum). An alternate approach is to minimize $\rho_{xx}$ and $\rho_{yy}$.

Rotation angle - the azimuth to which the resistivity tensor is rotated in the computation of rotated apparent resistivity.

Scaler resistivity - the apparent resistivity computed for an isotropic earth where there is no variation of apparent resistivity with measurement or calculation azimuth. Also the apparent resistivity(ies) calculated using the horthogonal electric and magnetic fields along the measurement axes. This latter are sometimes called the "Cagniard" resistivities, after the original MT paper in Geophysics in 1953.

Signal-to-Noise ratio - the ratio of that portion of the recorded, digitized and processed electric or magnetic field data that will produce valid MT results to that portion that will not. This is a particularly difficult factor to determine in MT as there are forms of noise that are very difficult to distinguish from the natural electromagnetic wave that will yield proper MT results.

Skew - a measure of the agreement of the computed resistivity tensor with the theoretical assumption of two-dimensional behavior, defined as

$$\frac{(\rho_{xx} + \rho_{xy})}{(\rho_{xy} - \rho_{yx})}$$

where the $\rho$ items are as defined for the Resistivity Tensors.

Skin depth - an electromagnetic wave propagating into the earth (or any material other than vacuum) is attenuated with distance. The skin depth is defined as that depth where the amplitude of the wave has been attenuated to 1/e of its original value.

Stacking - in MT data processing the combination of several discrete data samples. Stacking is usually performed in the frequency domain, after the Fourier Transform has been applied to the time series but before the tensor resistivity calculations have been performed. Stacking improves data quality in that coherent signal should add constructively in the combination process, while random noise should tend to cancel. MT stacking is analogous to Vibroseis sweep stacking in seismic exploration.

Statics - the effects on MT data of shallow lateral resistivity variations. Statics effects can influence MT data throughout the frequency range.

TE, TM - refer to Transverse Electric and Transverse Magnetic wave propagation nodes, terms borrowed from electrical engineering parlance. TE refers to electric field (and apparent resistivity) parallel to strike, while TM refers to electric field perpendicular to strike. Strictly speaking, TE and TM nodes are only defined for a two-dimensional geometry.

Tensor Resistivity - see Resistivity Tensor. The Tensor Resistivities are the $\rho_{xy}$ and $\rho_{yx}$ terms of the Resistivity Tensor.

Three-Dimensional Structures - structures where the resistivity may vary vertically and in any horizontal direction.

Time Series - the measurement and recording format of MT data, where the electric and magnetic fields are recorded as a function of time. These recordings are taken over a discrete time interval whose length is a function of the frequency band being recorded (lower frequencies require longer times).

Tipper - the term applied to the distortion of the magnetic field vector of the MT electromagnetic wave caused by two and three-dimensional structure. In the one-dimensional case the magnetic field vector will be horizontal with respect to the surface of the earth. In the presence of two and three-dimensional structure this will not be the case; the magnetic field vector will be "Tipped" out of the horizontal.*

Two-Dimensional structure - a structure where the resistivity varies with depth and only one horizontal direction, i.e., the structure extends with constant cross-section infinity along strike.

Vertical field (Vertical Magnetic Field) - the quantity measured to determine the Tipper. With a three axis magnetic field measurement system (x and y horizontal, parallel to the earth's surface, and z vertical) any departure of the magnetic field from horizontal will be manifested by a vertical field component, as the vector is resolved by the measurement sensors into its horizontal and vertical components.

*Except in certain cases where the MT site is at a point of symmetry with regard to the surrounding structure.

# APPENDIX C

# NOTES ON THE INTERPRETATION

# OF

# MAGNETOTELLURIC DATA IN COMPLEX AREAS

FOURTH EDITION

REVISED AND EXPANDED, MAY 1983

By

ARNOLD S. ORANGE

ARNOLD ORANGE ASSOCIATES
8806 POINT WEST DRIVE
AUSTIN, TEXAS 78759

APPENDIX C

# NOTES ON THE INTERPRETATION OF MAGNETOTELLURIC DATA IN COMPLEX AREAS

TABLE OF CONTENTS



Note:

This apppendix contains material originally prepared by the author when he was a partner in Emerald Exploration Consultants, Inc. (EMEX). The appendix is used here by joint agreement between EMEX and Arnold Orange Associates.

APPENDIX C

NOTES ON THE INTERPRETATION

OF

MAGNETOTELLURIC DATA IN COMPLEX AREAS

LIST OF FIGURES

APPENDIX C

NOTES ON THE INTERPRETATION

OF

MAGNETOTELLURIC DATA IN COMPLEX AREAS

LIST OF FIGURES
(Page 2)

APPENDIX C

NOTES ON THE INTERPRETATION

OF

MAGNETOTELLURIC DATA IN COMPLEX AREAS

LIST OF FIGURES
(Page 3)

# APPENDIX C

# NOTES ON THE INTERPRETATION OF MAGNETOTELLURIC DATA IN COMPLEX AREAS

## I. Introduction

These notes are intended to provide guidance as to the interpretation and understanding of magnetotelluric (MT) data obtained in geologically complex areas. The discussion will be non-mathematical, relying heavily on the use of computed models and analogies to other geophysical methods to explain interpretive concepts.

In the context of these notes, complexity is defined as any geologic situation where the MT data differs markedly from that which would be obtained over a homogeneous or plane-layered earth. Obviously, this encompasses a great many, if not most, prospects of current interest to explorationists. Therefore, MT will only be useful if meaningful interpretations can be obtained in these cases. We feel that such interpretations are routinely possible, but only when the effects of complex structure on the data are recognized and understood.

In the section that follows, the basis for MT exploration and a brief description of interpretive procedures will first be reviewed. Then, the MT effect as observed over representative structures will be discussed, with emphasis on potential interpretive "pitfalls" that await the unwary.

## II. Interpretive Concepts

### A. Definitions

In order to understand the material that follows, it is necessary to become familiar with the terminology that is used to describe magnetotelluric data. It is assumed that the reader possesses a general familiarity with MT and its utilization as an exploration tool. For a review, the paper by Vozoff (1972)[1] is recommended.

1. Apparent Resistivity - Apparent resistivity is the basic parameter computed from the MT field data. It is a function of the ratio of electric to magnetic field variations, and is computed as a complex function (amplitude and phase) of frequency. While not giving the resistivity-depth relationship directly, the apparent resistivity versus frequency is related to true resistivity versus depth in that the electromagnetic field obeys the skin depth relationship, i.e., the lower the frequency the deeper the depth of investigation. (It should be noted that the apparent resistivity is not an interpreted function, but is the results of straightforward computation of the field-recorded data.)

2. True, or Intrinsic, Resistivity - Sometimes termed inverted resistivity, this function is derived from the apparent

[1]Vozoff, K., 1972, The Magnetotelluric Method in the Exploration of Sedimentary Basins: Geophysics, v. 37, No. 1, p. 98-141.

resistivity (1. above) and is expressed as resistivity versus depth. True resistivity functions can be obtained by modeling, or through analytic inversion of the apparent resistivity-frequency function.

3. TE/TM Modes - In a one-dimensional setting (variation of resistivity with depth only) the apparent resistivity will be the same regardless of the azimuthal direction that the electromagnetic field is measured in. However, in a two-dimensional setting (variation of resistivity vertically with depth and horizontally in the dip direction, but with no variation along strike), due to the "channeling" of the flow of induced currents in the earth by the two-dimensional structure, the apparent resistivity will vary as a function of measurement direction. Borrowing from electrical engineering terminology, two "modes" are defined: TE (transverse electric), resistivity parallel to structural strike; and TM (transverse magnetic), resistivity perpendicular to structural strike. Note that the actual orientation of the field sensors is arbitrary, "rotation" to a coordinate system parallel and perpendicular to strike is an arithmetic step performed on the data in the computer processing step. Plots of apparent resistivity versus frequency thus have two curves shown, representing the two modes. In the case of a departure from the assumption of two-dimensionality (towards the normal three-dimensional structure wtih finite strike dimensions), two modes are still computed but can no longer be simply defined as parallel or perpendicular to strike.

4. Anisotropy - An anisotropic material is one in which the physical property under consideration is a function of the measurement direction within the material. In MT parlance, anisotropic data is data where the apparent resistivity varies with measurement azimuth, and two orthogonal resistivity functions (the TE and TM modes described in 3. above) which differ (or are separated when plotted) are computed. Note that the "anisotropic" data may be the result of structure involving intrinsically isotropic rocks.

5. Conductivity - Conductivity is the inverse of resistivity, i.e., high resistivity is low conductivity and vice versa. This is important as it is at times confusing when extremely low resistivity materials are referred to as "highly conductive".

6. Resistivity Contrast - The contrast between the resistivities of different materials, i.e., the resistivity contrast between a 100 ohm-meter carbonate and 10 ohm-meter shale is said to be 10:1. MT responds to contrast, and the ability to resolve an interface between two rock units is a function of the resistivity contrast and thicknesses involved.

7. Electrical Basement - In a vertical geologic section the depth of the deepest low-resistivity over high-resistivity interface which can be resolved, and which occurs at or above anticipated geologic basement. A point of confusion often arises when, for example, geologic basement (say Precambrian granite) is overlain by Paleozoic carbonates, which are in

turn overlain by a marine clastic section. If the carbonates are tight and roughly equivalent to the granite in resistivity so that there is little or no electrical contrast between them, then the electrical basement will be at the high resistivity contrast, clastic-carbonate interface. Thus, electrical basement may be several thousand feet above what is normally considered geologic basement.

B. Rock Resistivity

The interpretation of MT data requires a familiarity with the relationship between rock types and the resistivities inferred from MT data. While there is a correlation between rock resistivities as measured by well logs and those measured by MT, it must be borne in mind that the log investigates properties only in the immediate vicinity of the well bore while MT investigates bulk properties averaged over a considerable volume of rock. The resistivity of most rocks (including virtually all of the rocks of interest to hydrocarbon exploration) is determined by the fluids contained within the rock. This is because the dry rock matrix is a virtual insulator and for even the tightest of crystalline rocks electrical conduction can be considered entirely through the pore fluids. In sedimentary rocks the conduction is through the fluids which are present in the ordinary pore space in the rock. In very tight rocks; the igneous, metamorphic, and nonporous carbonate rocks where intrinsic porosity is very low, the fluids in joints,

cracks, and faulted zones become the primary conductors. Thus, the factors affecting resistivity are the porosity (bulk porosity including intergranular pores as well as micro and macro-joints) and the salinity of the pore fluids. Of lesser importance at oil exploration depths is the temperature of the formation; this becomes a strong factor in locating geothermal anomalies.

As an aid to the interpreter, the following table presents an approximate relationship between rock types and *in situ* bulk resistivity. As with most phenomena in nature there are important exceptions.

TABLE 1

Rock Resistivities

| Rock Type | Resistivity Range | |
|---|---|---|
| Clay | 1-5 | ohm-meters |
| Shale | 2-20 | ohm-meters |
| Sandstone | 10-80 | ohm-meters |
| Carbonate* | 50-500 | ohm-meters |
| Volcanics (volcaniclastic) | 5-50 | ohm-meters |
| Volcanics (flow)* | 200-4000 | ohm-meters |
| Igneous* | 1000-10,000 | ohm-meters |

*Unfractured; jointing, and fracturing especially if fault-related can drop resistivities in excess of an order of magnitude.

C. MT Interpretation Procedure

MT interpretation, as with other exploration techniques, consists of several steps, some of which are easily quantifiable and others which involve the complex interplay between the

interpreter and the character of the data base under consideration. An MT interpretation begins when the interpreter first sees the data for quality control purposes, which, in the case of data acquired utilizing an in-field processing system, occurs while data acquisition is still in process.

Probably the single most important interpretive step is the systematic examination of the apparent resistivity versus frequency data for the survey area. This step, roughly equivalent to the familiar seismic "brute stack", yields (a) the approximate vertical sequence of resistive and conductive units, (b) approximate location of faults and structural trends, and (c) most important, the structural complexity as evidenced in the data, which will indicate which modeling route to take for the continuation of the interpretation. The above procedures involve examining all of the MT data with an eye to the interrelation between sites, as impressions gained from an individual site by itself or even a single profile may be misleading. As will be seen from the examples that follow, it is most important to identify evidence of strong two and three-dimensional effects. While one is usually forewarned by preliminary geologic and regional geophysical (gravity, magnetics) studies, frequently the MT data will exhibit unanticipated effects. The qualitative examination step identifies these effects, and leads to the determination of the appropriate modeling procedures.

Prior to beginning the interpretation all available geological and geophysical data are accumulated and studied.

The formal steps in performing the interpretation may be summarized as follows, bearing in mind that in practice steps overlap and that the interpretation is an iterative process:

1. Prepare and examine montage. The montage made up of the apparent resistivity data is the display used most frequently by EMEX interpreters for the study of the basic apparent resistivity versus frequency data. The resistivity-frequency data for the entire survey are presented in the form of the data montage. The resistivity-frequency plots for each site are reduced and placed on the base map at their appropriate locations. Lines representing 10 ohm-meter horizontal axis and 1.0 Hz vertical axis are usually highlighted to facilitate comparison of one set of curves to an adjacent set. Comparison of each site with model examples from the case book and with the data from individual sites chosen as "representative" of the survey lead to a qualitative interpretation by grouping like sites together, locating zones of changes, etc. The form of the data at individual sites, and the site-to-site relationships are used to form a qualitative interpretation in which the gross features of the electrical section and structure are identified.

The montage is used as the basic data display for the following reasons: The study of MT apparent resistivity versus frequency data involves three primary considerations; first, the magnitude of the observed resistivities; second, the shape of the resistivity-frequency curves; and third, the

nature of the anisotropy, or difference between the two component resistivity curves. These three factors must be looked at together since they are interrelated. In particular, the fact that there are two resistivity curves at each site renders the common resistivity sections difficult to use, and at times misleading. This is especially true if component selection is in error, or if neither curve is representative of the subsurface. In addition, since most practical prospects are three-dimensional in nature, the montage, with the addition of the frequency axis, is essentially a three-dimensional display.

The use of the montage facilitates a qualitative interpretation by site-to-site comparison as well as by examination of the characteristics of individual sites. The montage provides a natural display for the interpretation of MT data in geologically complex areas, which starts with a study of curve shape and the comparison of field data with computed models.

2. Plot tensor rotation and magnetic field "tipper" strike directions. This information is useful in determining strike, in assessing the two and three-dimensional characteristics of an area, and in determining tensor resistivity components (as parallel or perpendicular to strike) in complex areas.

3. Compute two-dimensional models. Models, such as those discussed in the pages that follow, are computed to investigate specific structural questions. In addition, the

"case book" is perused to identify models computed in the past which are applicable to the project at hand. The models are used to identify the structural style of a prospect and to provide either a basis for the appropriate use of one-dimensional inversions, correction factors for the inversions, or an indication that the one-dimensional inversions will be inappropriate and that more exact two-dimensional models will be required. In the case of strongly three-dimensional situations, some sample models used as guides to interpretation have been computed. However, for some complex cases no currently available modeling procedures may be appropriate. The modeling stage is an iterative one, with models compared with the data and then modified to provide a better "fit".

4. "Pick" resistivity interfaces on the inverted data. This step, similar to picking seismic records, consists of examining the inversions for each site and then determining which curve (or if both curves) represent the subsurface resistivity configuration. The study of models and <u>inverted model data</u> are critical at this point. Interface depths are picked. Then, corrections are applied. These are necessary since the inversion algorithm assumes that each curve represents a one-dimensional layered earth. Any structural complexity results in a deviation from this assumption, and while in the presence of structure a one-dimensional inversion is strictly speaking invalid, experience plus the use of models allows the interpreter to confidently apply corrections so as to more closely approximate the actual resistivity section.

5. Post depths and prepare maps and sections. At this point the depth values are posted, structural forms contoured and faults and anticlinal and synclinal axis drawn in. The total geological and geophysical data base is called upon at this stage to complete the geologic interpretation. Various supporting MT information (phase, skew, coherency, etc.) are utilized either in data quality assessment or in examining in detail the departure of the data from assumptions of two and three-dimensionality.

It should be noted that resistivity sections are not prepared as a matter of course as part of the above sequence. There are several reasons for this. For complex prospects in many instances neither of the two resistivity curves computed for each site will be an accurate representation of the subsurface, both curves must be examined together and in relationship to surrounding sites. It follows that in these cases the one-dimensional, continuous (Bostick) or discrete layered inversions of neither curve will be an accurate representation of the subsurface resistivity section. The inversions are a starting point, and are corrected and modified based on computed models, prospect geology and experience. This is most important when considering the interpretation of deeper structure and electrical properties, since these inversions <u>always</u> computes resistivity as a function of depth, while the low frequency MT data (from which the "deeper" inverted data is computed)

is more often than not strongly affected by two and three-dimensional structure.

It should be pointed out that the interpretation of MT data as currently practiced by many if not most of the geophysicists active in the field relies heavily on one-dimensional inversions of the parallel to strike (TE) component of apparent resistivity. Two-dimensional models are used as an aid to interpretation but final resistivity and geologic sections are most frequently seen as contoured or "picked" sections with the one-dimensional (TE) inversions as the base. This technique is applicable in many instances, and excellent MT interpretations have been produced as a result. There are, however, important geologic structures where the TE based, one-dimensional inversion interpretation will be seriously in error. To avoid this the interpreter must learn to recognize those situations where the procedure is inappropriate, and to have available alternate procedures to follow in order to arrive at a successful interpretation.

## III. Model Studies

### A. Introduction

It is not possible within the confines of these notes to present an exhaustive compendium of MT "type" examples. The few cases presented are considered among those most important to practical exploration problems. Attention is drawn to the summary at the close of the section, where we endeavor to point out the concepts that it is felt are most critical.

The examples, as well as the rest of these notes for that matter, are not offered as an unbiased, academic treatise, but are the results of many years of active MT interpretation, and of watching other interpreters at work.

"Pitfalls" lie in wait of the unwary in each of the cases to be discussed. In many cases there would be no pitfall if perfect, noise-free data were available and if data were recorded at any and all points on the surface. However, noisy data, and more important, a finite sampling of the surface, lead to ambiguities and potential misinterpretations. For the examples the effects of noise and low site density will be pointed out.

NOTE: For each example the model results will be shown as plotted apparent resistivity versus frequency, in a manner identical to the presentation of the apparent resistivity computed from field data. The convention followed in plotting the resitivity data is <u>high frequencies to the right</u>. Among the MT contractors this is the convention used by Argonaut

Enterprises, Inc. and Geotronics Corporation. Both Phoenix Geophysics and Z-AXIS Exploration, Inc. use the opposite convention, high frequencies to the left. When studying reports and professional papers, it is necessary to determine which plotting convention is being employed, since both are in common use. TE refers to resistivity parallel to strike, TM to resistivity perpendicular to strike.

Each example contains a sketch of the model, and a sketch of the resistivity curve computed at one or more locations on the surface. Curves noted as "1-D" are the layered earth, forward model for the sequence of interfaces vertically beneath the indicated location. The sketch of the model geometry is a sectional view perpendicular to the strike of the structure. As a two-dimensional feature each structure is considered to extend to infinity into and out of the page.

B. Two-Dimensional Model Series - Shallow Feature Test (Figures 1 through 3)

Object. The object of this series of models is to examine the "statics" effect on MT data resulting from shallow resistivity anomalies. Such anomalies might be represented in nature by alluvial-filled depressions, stream beds, narrow valleys bounded by outcrop, etc. These shallow resistivity anomalies have the effect of shifting the MT apparent resistivity versus frequency and intrinsic resistivity versus depth sections in a manner completely analagous to the effect of shallow velocity anomalies on seismic data of shifting the time and depth sections.

TWO DIMENSIONAL MT MODEL

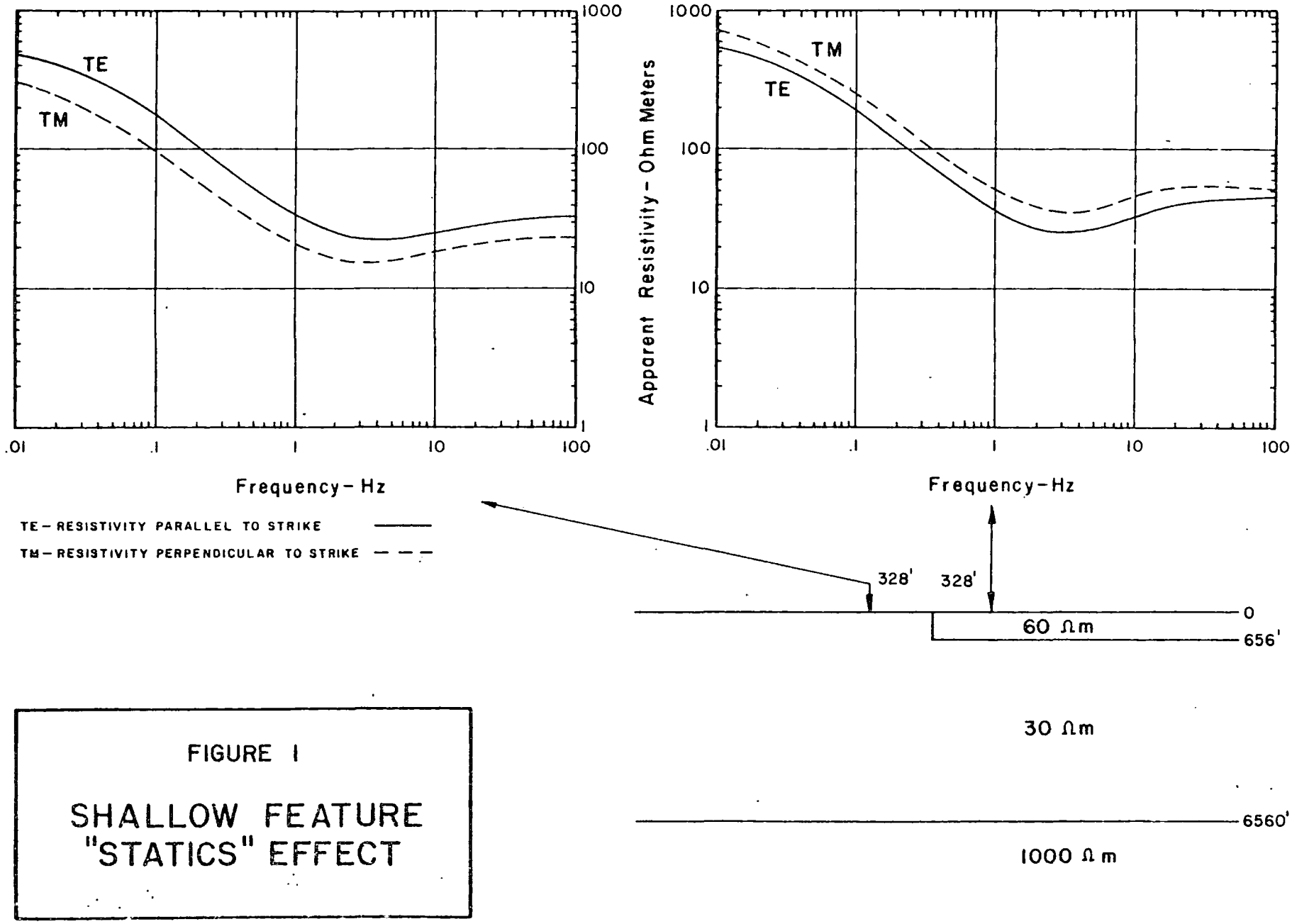


FIGURE 1

SHALLOW FEATURE
"STATICS" EFFECT

TWO DIMENSIONAL MT MODEL

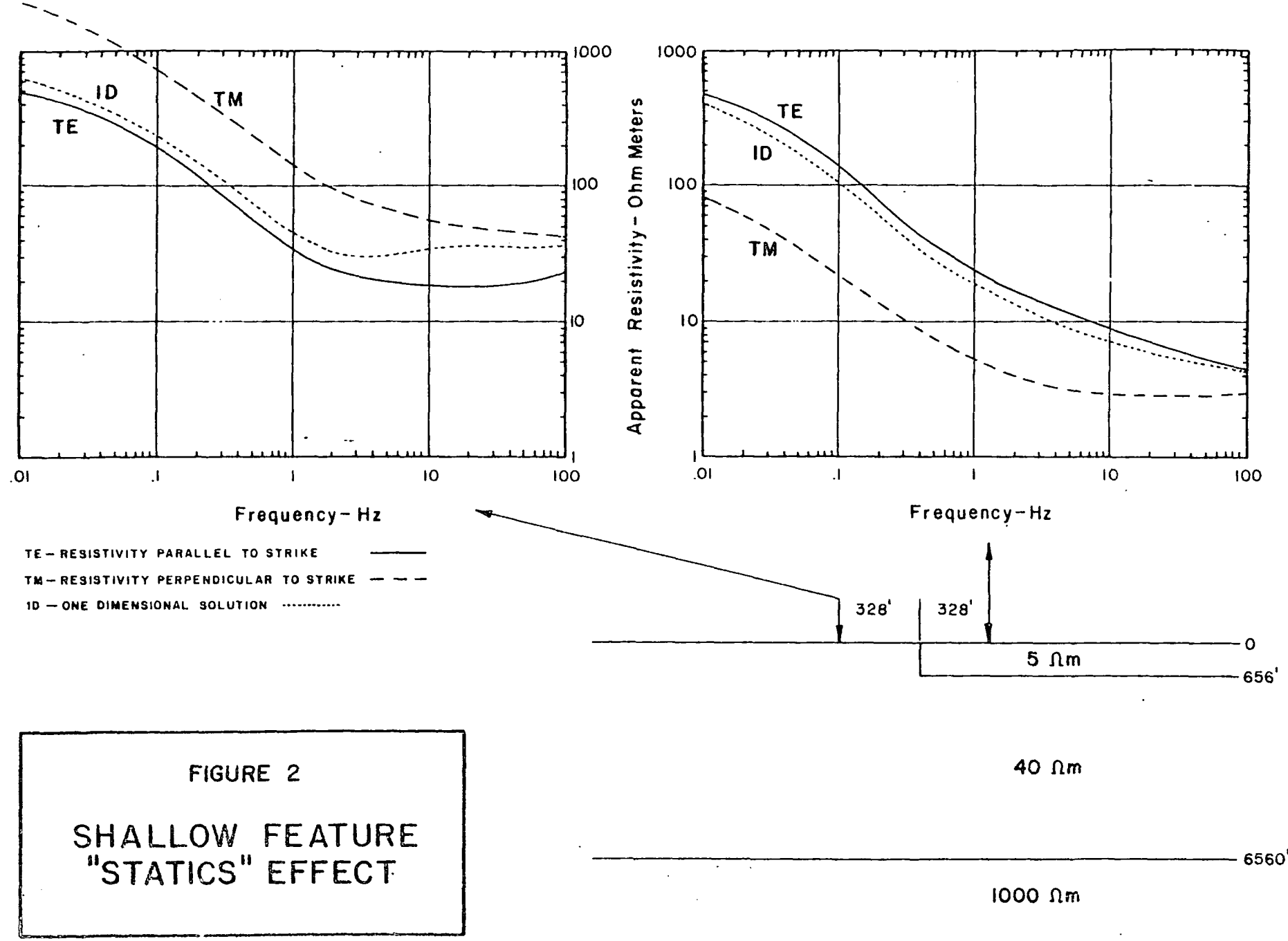


FIGURE 2

SHALLOW FEATURE
"STATICS" EFFECT

TWO DIMENSIONAL MT MODEL

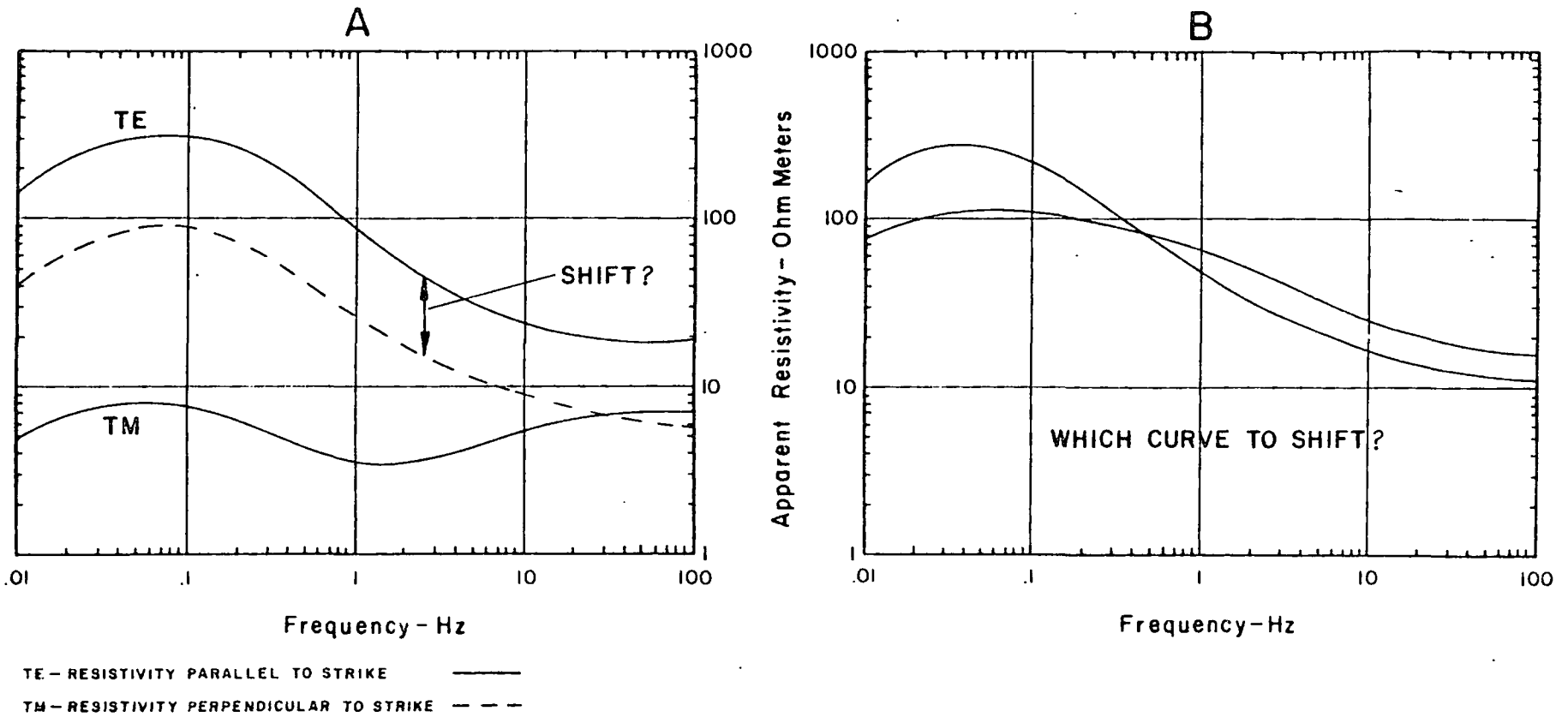


FIGURE 3

COMPLEX DATA WITH SURFACE EFFECT

Hence the term "statics correction" is used in an identical sense in both cases.

Determination of the statics correction is one of the most critical, and difficult, tests in an MT interpretation when accurate depth information is desired. The statics shift is frequently in excess of the vertical dimensions of the target structure, as is the case in many seismic prospects.

Description of Models. These models consist of a thin tabular layer on the surface in an otherwise plane-layered earth. The only two-dimensional complexity is the surface layer termination. Resistivity data is plotted for measurement locations on both the resistive and conductive sides of the boundary. The different models have been computed with various resistivity values to illustrate varying degrees of the statics effect.

Description of Results. The model for Figure 1 contains a low contrast (2:1) shallow resistive body. The tabular body may be thought of as a thin, discontinuous resistive volcanic or carbonate layer. The effect in the immediate vicinity of the contact is a shift of the TM curve over the full frequency range, a conductive shift on the conductive side, a resistive shift on the resistive side. The TE curves for the two cases are nearly identical except for the highest frequencies. The 1-D curve is virtually identical with the TE curve, thus inversion of the TE curve will give the best interpreted subsurface resistivity. The inversion of the TM mode curve on the

conductive (left) side will result in a computed depth to the electrical basement interface (actually at 6500 feet) as erroneously shallow, while on the resistive side the error will be towards a too deep pick. At a distance of 1000 feet from the boundary the effect has virtually disappeared, with TE and TM curves almost coincident.

The model of Figure 2 is the same geometry as that of Figure 1, but with a higher, 8:1, contrast. The conductive, 5 ohm-meter unit may be a saturated clay or alluvial unit. The effect again is a shift of the TM curves. The 1-D solution is not identical to the TE curve, but is close enough to make the TE solution a good approximation if the error at the high frequencies is corrected.

Discussion. The problem presented to the interpreter by this class of models is to insure that the mode selection is correct, since obviously it is the TE curve (relative to the shallow anomaly*) one wants to choose to invert. Mode selection is simple with closely spaced sites, but since the effect dies out significantly in a mile or less, if sites are two or more miles apart as in a normal reconnaissance survey then site-to-site correlation becomes difficult. The vertical field relationship, which one would like to utilize for mode selection, presents problems in two ways: First, the vertical

*Note that one of the apparent resistivity curves can exhibit the characteristics attributed to the parallel-to-strike component for a shallow feature, yet be the perpendicular-to-strike component for a deeper structure.

field for these features is relatively weak, the effect is easily dominated by a deep geologic structure which can be at some distance. Second, because the vertical fields are weak, noise presents a real problem. It is often difficult to record good vertical field data, especially at the higher frequencies which are needed here. Thus, in the case of simple, parallel curves such as shown in the examples, the interpreter must often rely heavily on topographic and surficial geologic maps to decide which curve to utilize. If all else fails an alternative is to minimize the possible error by drawing an "average" curve between the two plotted curves.

A potentially more serious problem exists in the case of data exhibiting complexity due to deep, significant structures with the effects of a shallow feature superimposed. Consider the examples shown on Figure 3. Assume that the interpreter wishes to rely heavily on the curve identified as TE in Figure 3A. The separation of the curves at 100 Hz indicates that the curves are affected by a near-surface feature, in addition to the deeper feature causing the further split below 10 Hz. If the curve marked "TE" is TE also with respect to the near-surface feature, then it can be safely inverted and interpreted "as is". If, on the other hand, the marked TE curve is in reality the TM curve with respect to the near-surface feature, then it must be shifted as shown to eliminate the "statics", or near-surface feature, effect. In a case such as that illustrated the vertical field is usually of little

help, since the effect of the deep feature will tend to dominate that of the shallow feature so that the determination of which curve to adjust must again be based on geologic and topographic evidence.

Of even more concern is the hypothetical case shown in Figure 3B. Here, with the effect more subtle, the interpreter may not know which curve to shift, and in all likelihood will need to test an interpretation using both curves. The shift shown, although of low amplitude, will nevertheless significantly affect the interpretation of a structure of exploration interest. Thus, the examination of each site and a determination of the correct shift can be of crucial importance.

In cases where application of the statics correction is not straightforward (which probably includes most real prospects) EMEX interpreters have developed the following procedure: First, a site-consistent statics correction is applied, where one or both apparent resistivity versus frequency curves are shifted so that they coincide at the high frequency portion of the data, such as the shift of the dashed curve for the left-hand sketch of Figure 3. The results are frequently displayed as an overlay to the data montage described earlier. Use of the site-specific statics display facilitates examination of the data, especially in complex areas since the confusing effects of unimportant, shallow features are eliminated, or at least minimized, and the effects of deeper (and possibly more subtle in an MT sense) structures can be recognized.

The second step is the application of a survey-consistent statics correction. Here, the shift at each site affected with a statics problem is examined in the light of all available information, and the best estimate of the actual position of the curves made. The final "fine tuning" of the statics correction is frequently made, as in seismic interpretation, when the structures and isopach maps are being prepared.

C. Two-Dimensional Model Series - Fault and Graben Geology (Figures 4 through 6)

Object. The object of this series of models is to examine the MT effect caused by large scale faulting, especially that which comes near or to the surface. Such features dominate MT data acquired in the basin and range provinces, and are a major factor in the interpretation of many mountainous prospects. The effect on the MT data is a marked anisotropy, or difference between the two MT curves. The anisotropy is not as simple as for the shallow features discussed in the previous section, and can be much more extreme. In the previous section the effect was a "shift" or offset in one or both curves. In the models to be presented here often the two curves bear little or no similarity to one another, or to the one-dimensional solution at the location in question.

Description of Models. The models consist of simple fault or graben situation, with the faults or bounding faults brought to or near the surface. A high 100:1 resistivity

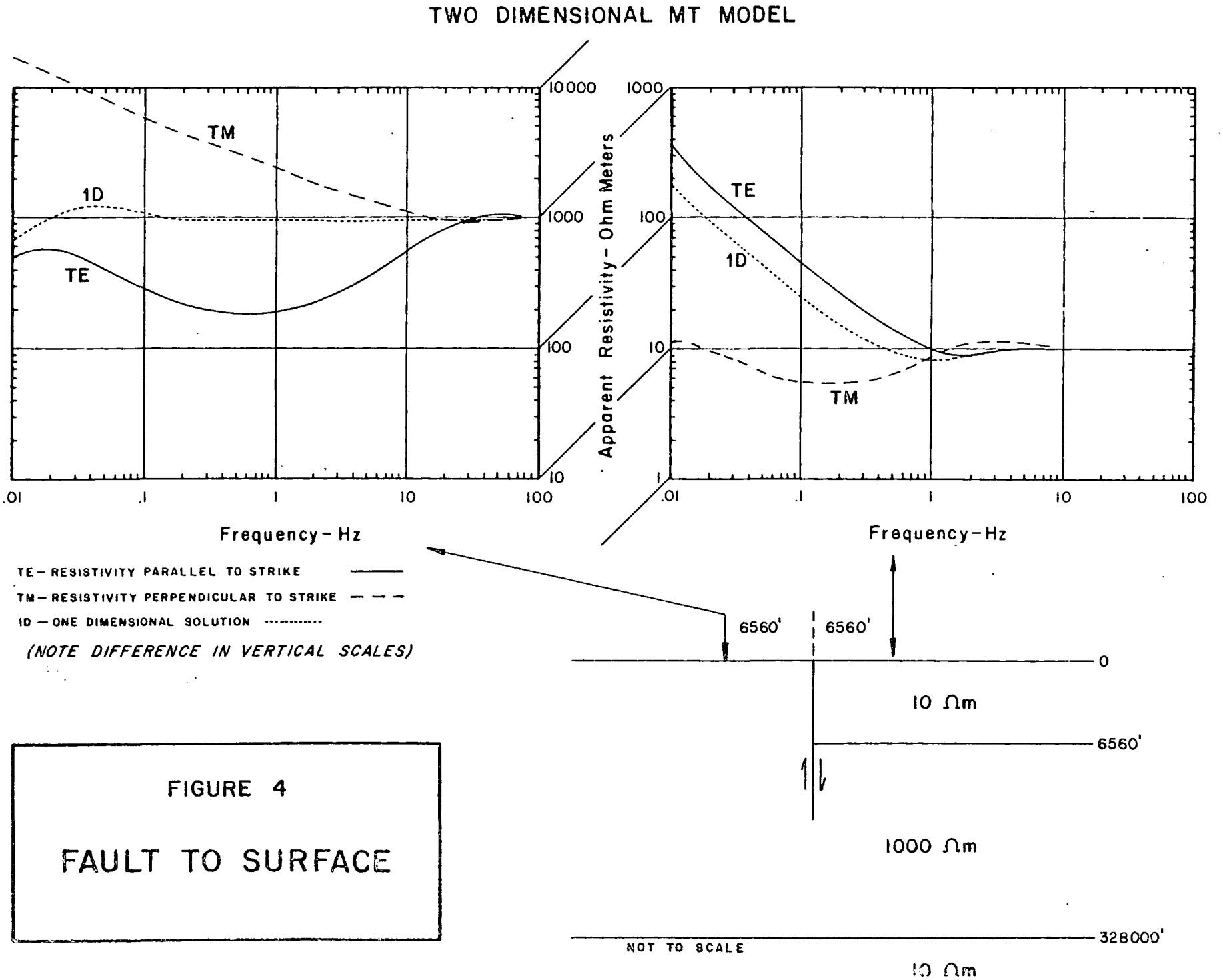


FIGURE 4

FAULT TO SURFACE

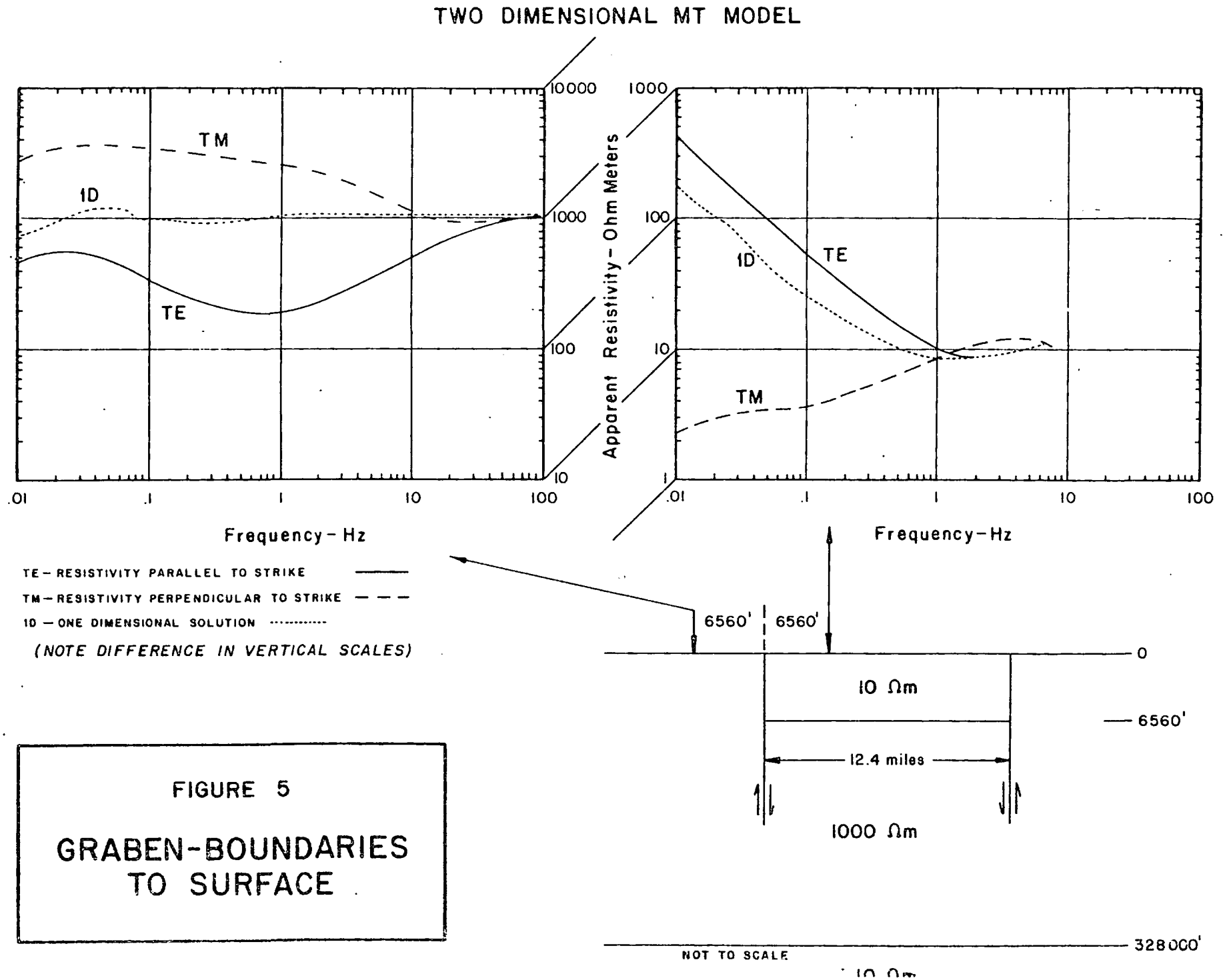


FIGURE 5

GRABEN-BOUNDARIES TO SURFACE

# TWO DIMENSIONAL MT MODEL

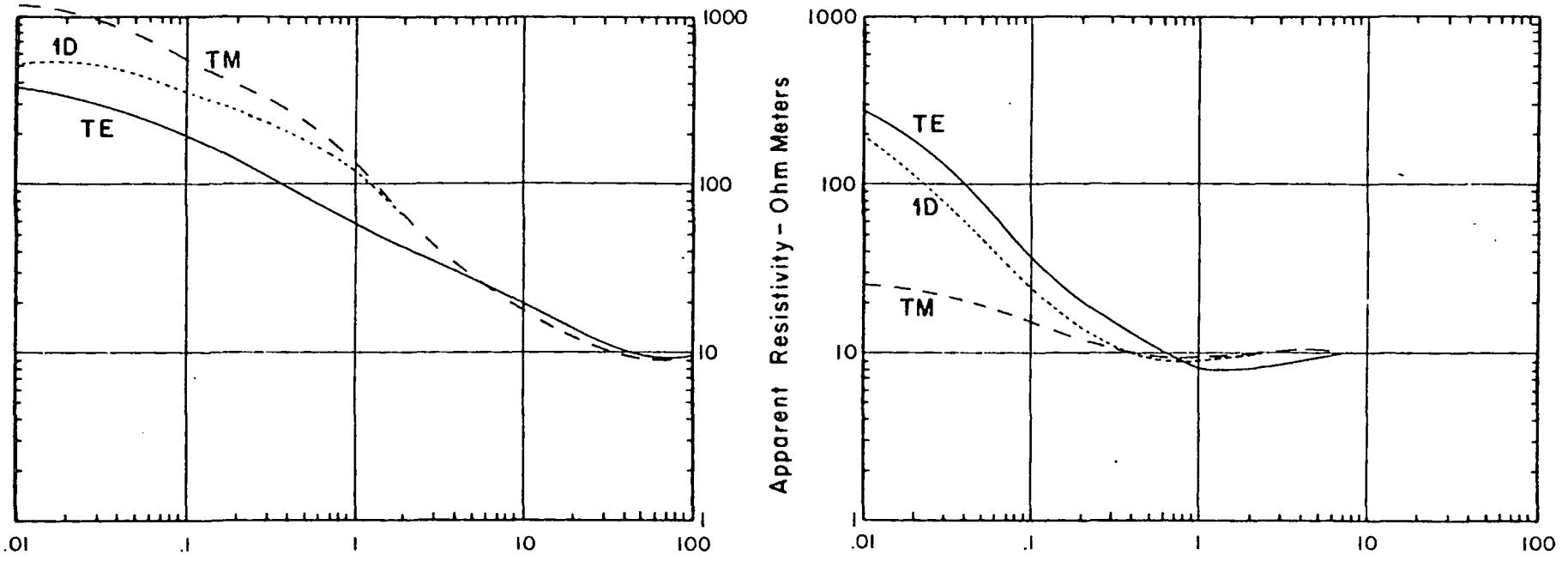


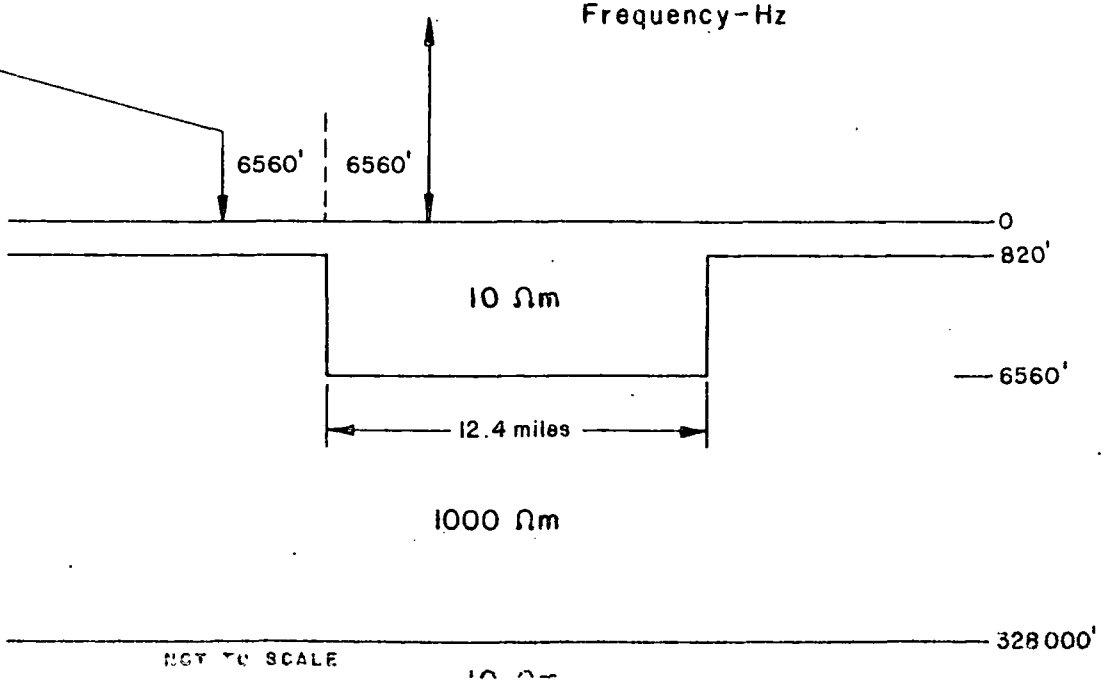


FIGURE 6

BURIED GRABEN

contrast is used to illustrate the effects, with the conductive clastics and/or recent fill modeled by 10 ohm-meter materials and the resistive carbonate and crystalline rocks modeled by 1000 ohm-meters. The extremely deep, hot lower crust is modeled by 10 ohm-meters.

For each model the computed MT data is shown for two cases, one on either side of the fault or bounding fault. Both TE and TM curves are shown, as well as the one-dimensional, layered earth solutions. Note that it is the 1-D solution that, if it could be measured or computed would, when inverted, lead to the most accurate interpretation of the subsurface immediately beneath that one site alone.

Description of Results. The model of Figure 4 contains a fault to the surface with a throw of 6560 feet, with a 10 ohm-meter conductive section terminating against the fault. The computed apparent resistivity is shown for "sites" 6560 feet on either side of the fault. Note the vertical scale difference between the two plots.

The data illustrates the important features of this class of models. On the conductive (right) side of the fault the TE curve is of the same form as the 1-D solution, but exhibits a shift to the right. The TM curve, on the other hand, bears no relationship to the 1-D solution, showing a strong "undershoot" at the frequency where the resistive electrical basement becomes evident on the TE.

On the resistive (left) side of the fault neither curve is a good approximation to the 1-D solution, although the TM curve is probably least misleading. The TE curve is strongly affected by the 10 ohm-meter material across the fault, a phenomenon similar to the "side shot" in seismic data. If the TE curve were inverted and used alone as the base for an interpretation, a non-existent conductor would be the result.

Clearly both sites together are needed to arrive at a correct solution since, except for the resistivity shift crossing the fault, certain similarities in curve character exist when comparing the two. This would be expected to be even more of a problem with field data where noise and more complicated geology combine to make the data less clear cut. If the geology is clearly two-dimensional, the vertical field can be used to good advantage to arrive at the strike direction, and then the resistivity magnitude used to determine which is the upthrown, resistive side of the fault.

The model of Figure 5 is a 10 ohm-meter material filled graben with the bounding faults brought to the surface. The results are similar to the previous model, except that the TM curve on the graben shows an even more extreme undershoot than for the simple fault model of Figure 4. Also note that on the upthrown (resistive) side, the TM curve is clearly a better approximation to the 1-D solution than the TE curve.

The model of Figure 6 is the same structure of Figure 5, but with the graben bounding faults terminating

820 ft below the surface, and the 10 ohm-meter graben materials acting as a cover over the shallow 1000 ohm-meter electrical basement off of the graben. Examination of the resistivity curves shows that there is a substantial change in curve shape, in particular the extent of anisotropy, when the resistive contact does not reach the surface. The TE mode remains the best approximation to the 1-D solution on the graben, while the TM is marginally better on the resistive side.

The accurate determination of the depth of electrical basement is often of prime importance in situations such as represented by Figures 4 through 6. While the shape of the TE curve on the conductive side of the bounding faults will yield an accurate qualitative interpretation of low resistivity rocks over a more resistive basement, a depth calculation will yield results that are erroneously shallow (because the transition from low to higher apparent resistivity values occurs at an erroneously high frequency). One approach to obtain more nearly correct depth values is to compute the inversion for the 2-D model results and compare with the depths of the input model. Then, correction factors can be applied to the inverted field data. As an example, for extreme anisotropy such as that of Figure 5 (right hand data), a correction of roughly 30% would be applied to basement depths obtained from the inverted TE curve. With widely spaced sites the correction becomes less accurate as the field data-model comparison becomes more difficult.

D. Two-Dimensional Model Series - Horst and Unrooted Block Geology (Figures 7 through 10)

Object. The object of this series of models is to examine the difference in MT response between rooted horst and unrooted "horst-like" structures. The question is frequently posed as to whether an outcrop, often Precambrian, is autochthonous (rooted) or allochthonous (unrooted, or thrust from elsewhere). MT, with its capability to detect conductive rocks beneath surface crystalline masses, is a natural tool to provide the answer.

Description of Models. The models consist of a simple horst block with vertical bounding faults brought to the surface. The horst is 12.4 miles wide and electrical basement on the downthrown sides is at 6560 ft. Material bounding the horst is 10 ohm-meters while the horst and basement is 1000 ohm-meters. A 10 ohm-meter conductive lower crust is placed at 100,000 ft.

The model of Figure 7 is the simple horst, with the 1000 ohm-meter material extending to depth. For the models of Figures 8 and 9, the surface 1000 ohm-meter block is 4920 ft thick and rests on conductive material of 100 and 10 ohm-meters respectively. In both of these cases electrical basement beneath the block is at 6560 ft.

Description of Results. For the rooted horst, Figure 7, the results are similar in form to those of the graben, Figure 5. On the resistive side, on the horst, the TM curve "overshoots" while the TE curve is strongly influenced by the conductive

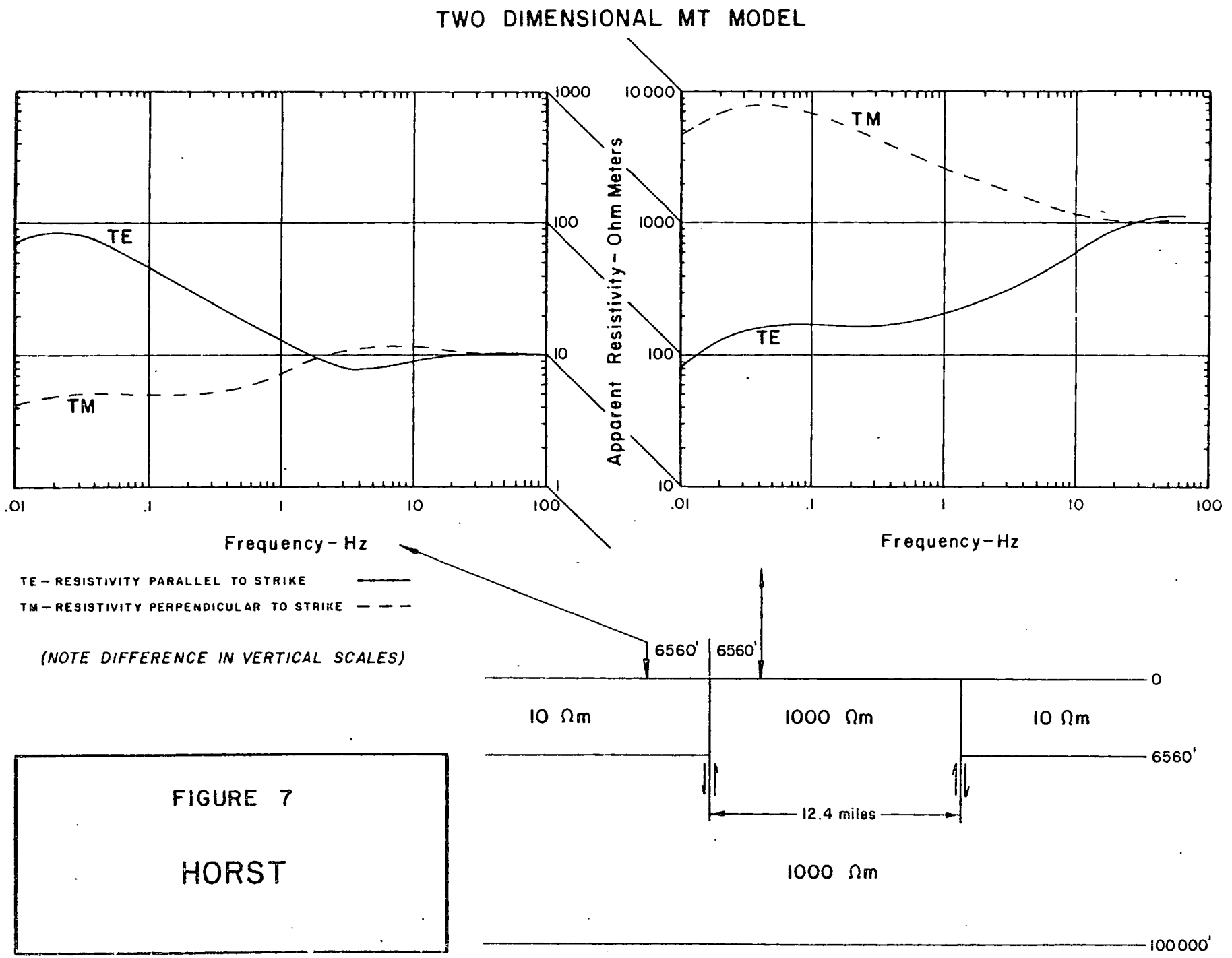


FIGURE 7

HORST

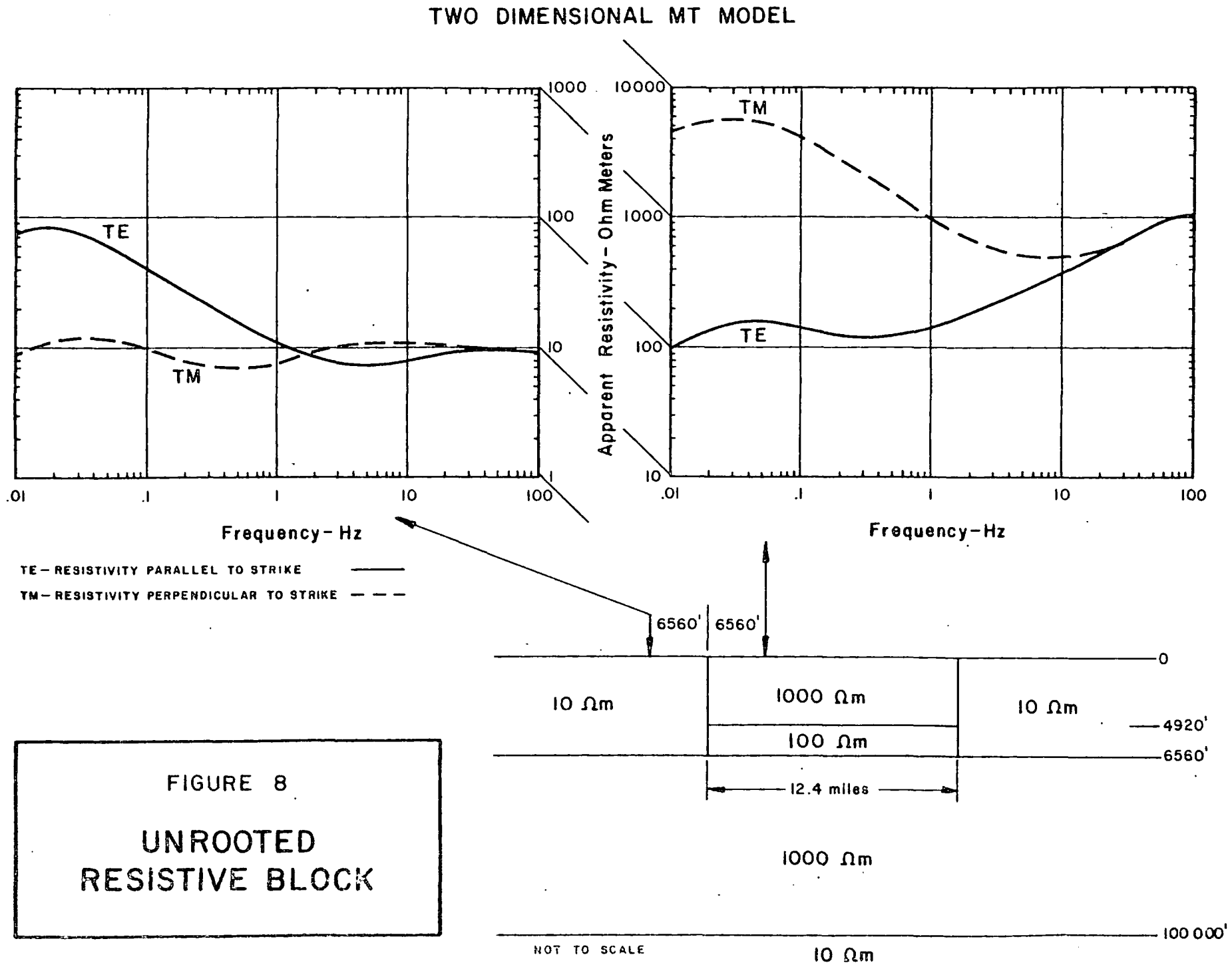


FIGURE 8

UNROOTED
RESISTIVE BLOCK

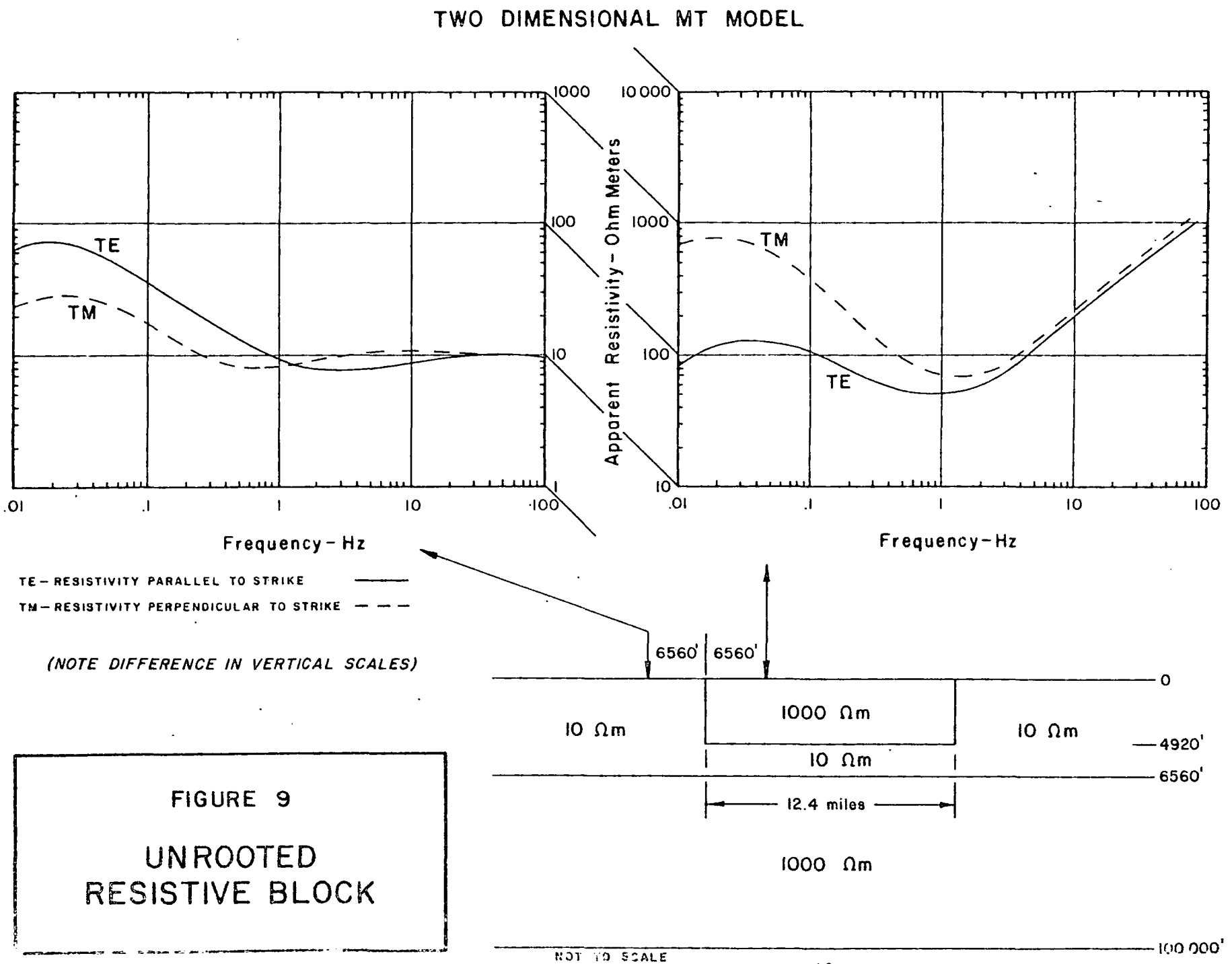


FIGURE 9

UNROOTED
RESISTIVE BLOCK

TWO DIMENSIONAL MT MODEL

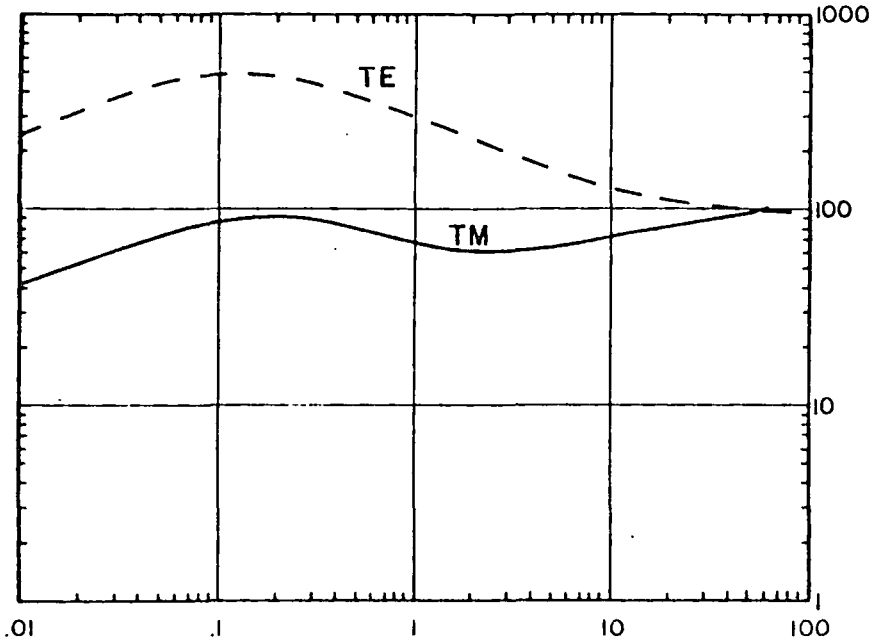


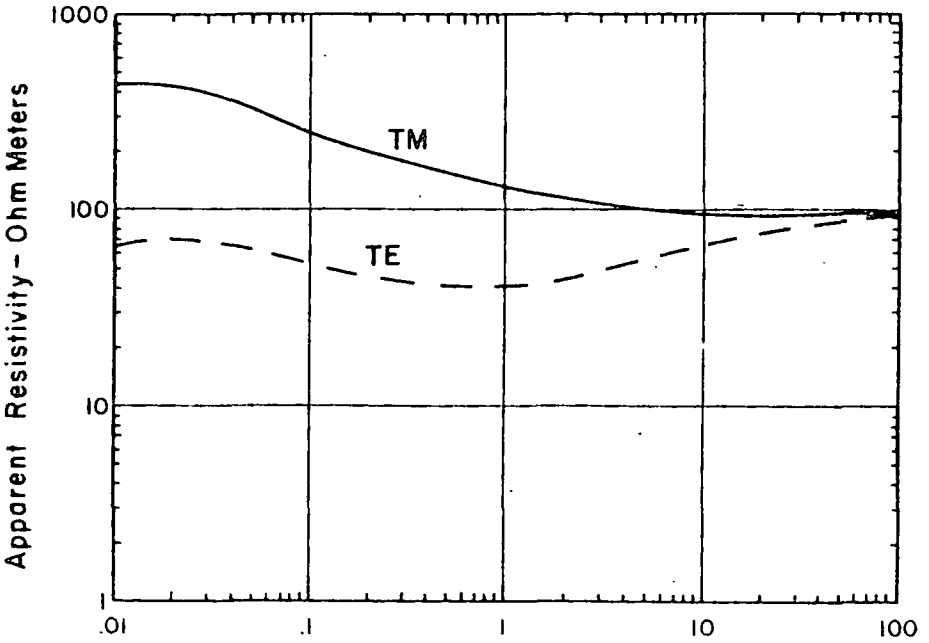


TE - RESISTIVITY PARALLEL TO STRIKE ——

TM - RESISTIVITY PERPENDICULAR TO STRIKE — — —

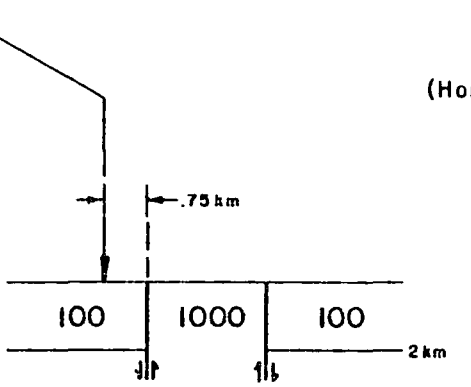


(Horst 20km wide)

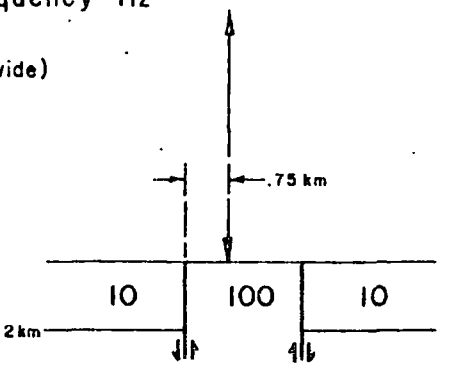


←10 Ωm at 30km→

FIGURE 10

HORST COMPARISON

material across the fault. Off of the horst to the left the now familiar extreme anisotropy is seen, with the TM curve undershooting and the TE component most faithful to the 1-D solution.

The effect of conductive material beneath the horst is to depress both TE and TM components on the horst, and off of the horst to soften the effect on the TM component by bringing it close to the TE component. With 100 ohm-meter materials beneath, Figure 8, the effect is less extreme than for the 10 ohm-meter case, but unmistakable.

To continue with the discussion of the rooted horst structure, Figure 10 illustrates an extremely important interpretive point. Two models are shown, both of a horst. The left hand horst involves a resistivity contrast of 10 to 1, with the 1000 ohm-meter material possibly respresenting crystalline rock and the 100 ohm-meter material a carbonate or very tight sand. The right hand horst also involves a resistivity contrast of 10 to 1, with the 100 ohm-meter materials possibly as above and the 10 ohm-meter materials a porous sand or shale. Data is plotted for a site on the 100 ohm-meter material for both models, which is the off-horst material on the left hand model and the horst material to the right. The scales for the two plots are identical. The form of the data including both curves is very similar for the two cases, and in the presence of noise they would be virtually indistinguishable. The consequences inferred by this model are as follows:

a. Closely spaced sites on either side of the bounding fault will clearly and unambiguously identify the structure.

b. Reliable vertical magnetic field data will identify the TM mode, and also lead to an unambiguous solution <u>if the area is truly two-dimensional</u>. It cannot be overemphasized that the vertical field data, either through noise or the presence of three-dimensional structural features, is frequently ambiguous or misleading. Bear in mind that a vertical magnetic field null occurs at the center of the horst, so that any structural complications along horst strike may easily result in mode misidentification if the vertical field is relied upon. (The vertical field will point or "tip" towards or away from the along-strike structure rather than to the horst-bounding faults, since the effects of the latter cancel in the center of the horst.)

c. The data at adjacent sites are interrelated, more so as complexity increases. No data may be "taken for granted" but must be examined in light of all available information.

E. Two-Dimensional Model Series - Overthrust Geology (Figures 11 through 19)

<u>Object</u>. The object of this series of models is to examine in detail the MT response in exploration situations involving overthrust geology. This application, related to the allochthonous horst studies earlier (page C-24), is a natural one for MT since most frequently the older rocks thrust over the younger strata are more resistive than those beneath. This

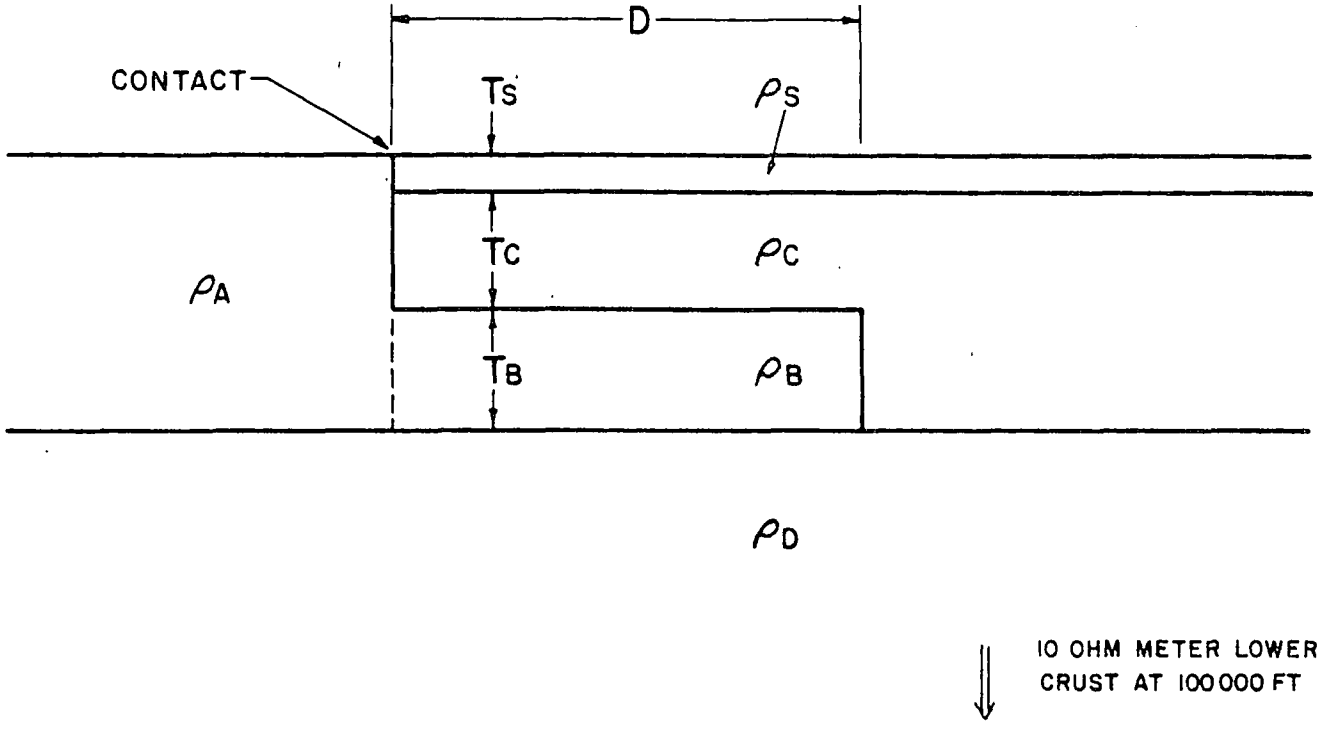


MODEL SERIES — THICKNESS OF OVERTHRUST

NOTATION: OT X, Tc / TB

SUBTHRUST CONDUCTOR THICKNESS

| MODEL | SERIES | $\rho_A$ | $\rho_B$ | $\rho_C$ | $\rho_D$ | $\rho_C/\rho_B$ | D | $\rho_S$ | Ts |
|---|---|---|---|---|---|---|---|---|---|
| OT | 1 | 10 | 10 | 1000 | 1000 | 100:1 | 12 km | – | – |
| OT | 2 | 10 | 10 | 1000 | 1000 | 100:1 | 4 km | – | – |
| OT | 3 | 10 | 100 | 1000 | 1000 | 10:1 | 12 km | – | – |
| OT | 4 | 10 | 10 | 100 | 1000 | 10:1 | 12 km | – | – |
| OT | 6 | 10 | 10 | 100 | 100 | 10:1 | 12 km | – | – |
| OT | 5 | 10 | 10 | 1000 | 1000 | 100:1 | 12 km | 10 | .08km |

(OT-5C SERIES HAS SURFACE LAYER, $\rho_s$, TERMINATED)

(RESISTIVITIES IN OHM METERS)

FIGURE 11

OVERTHRUST MODEL GEOMETRY AND NOTATION

## TWO DIMENSIONAL MT MODEL

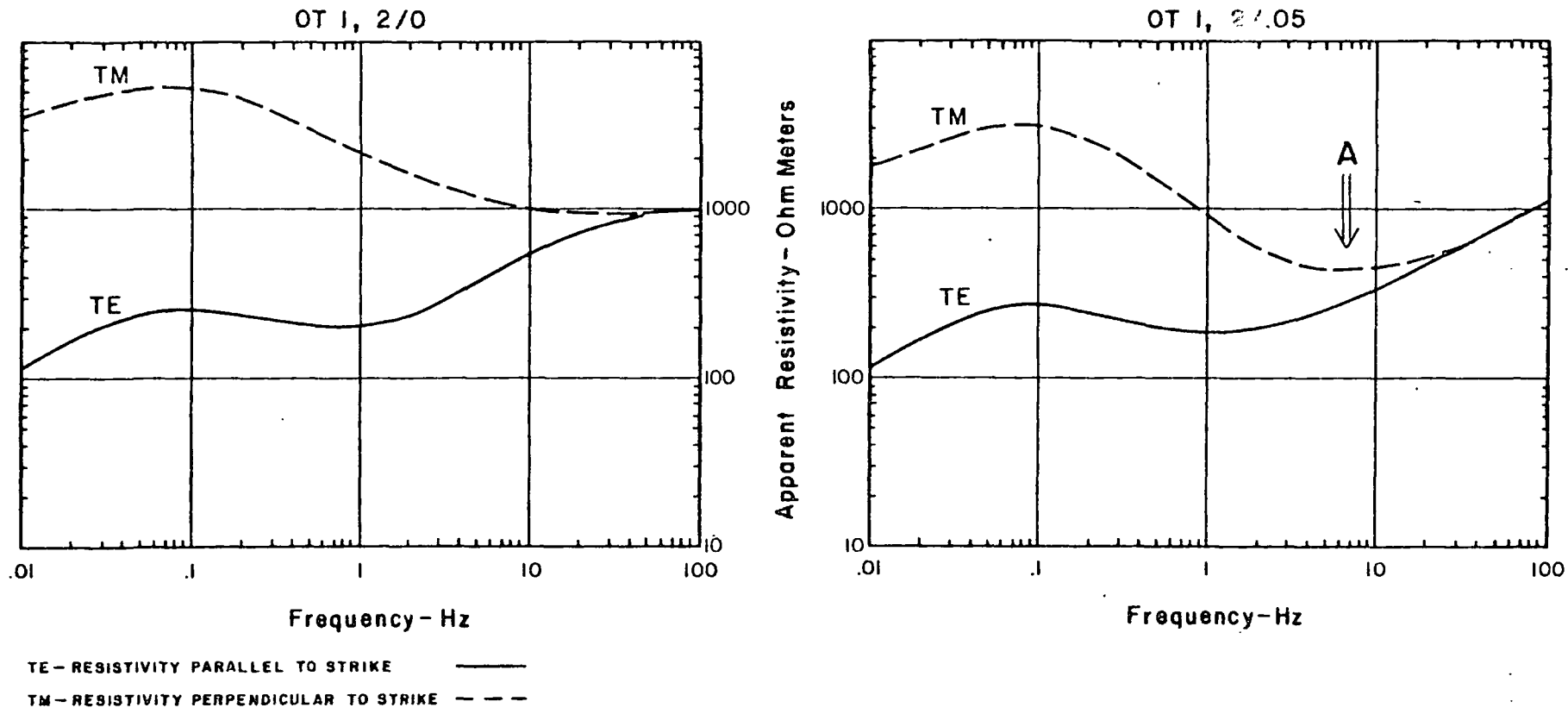


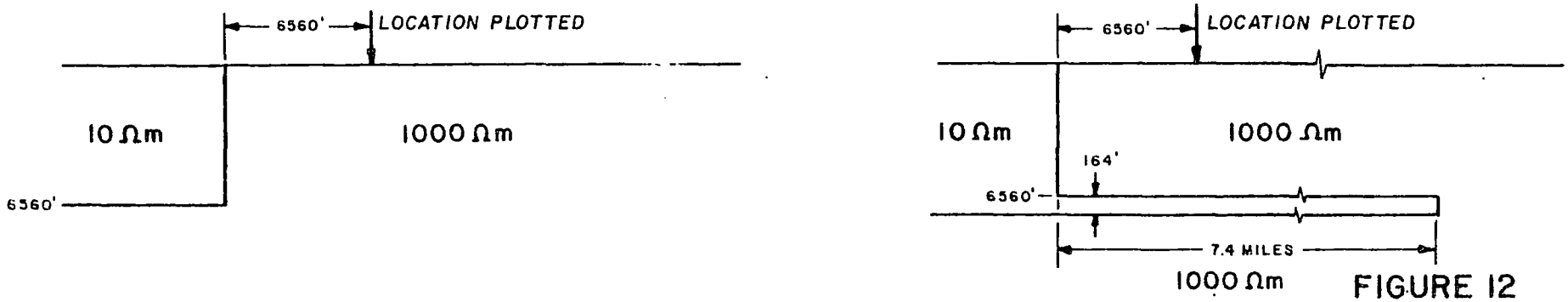


FIGURE 12
EFFECT OF THRUST
OVER THIN CONDUCTOR

(10 Ωm LOWER CRUST AT 100,000 FEET, SKETCH NOT TO SCALE)

## TWO DIMENSIONAL MT MODEL

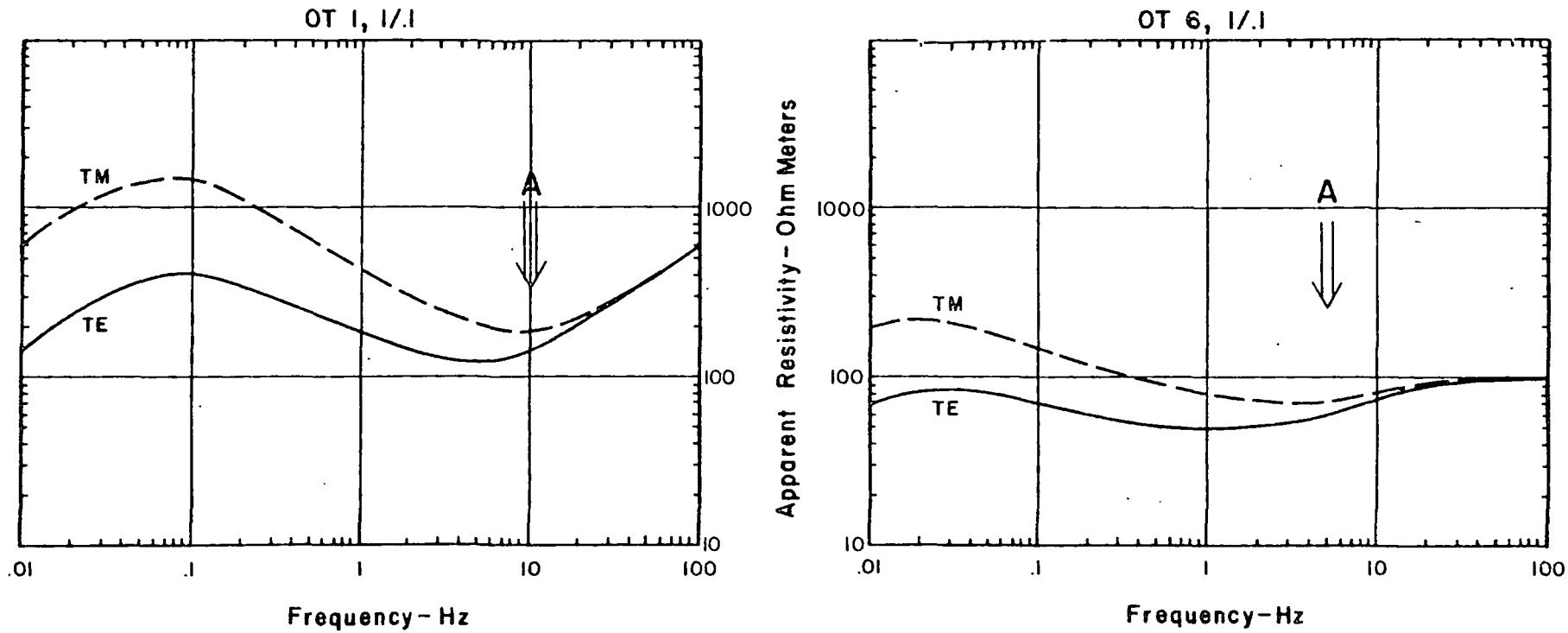


FIGURE 13

EFFECT OF VARIATION OF CONTRAST ON THRUST RESPONSE

(10 Ωm LOWER CRUST AT 100,000 FEET, SKETCH NOT TO SCALE)

## TWO DIMENSIONAL MT MODEL

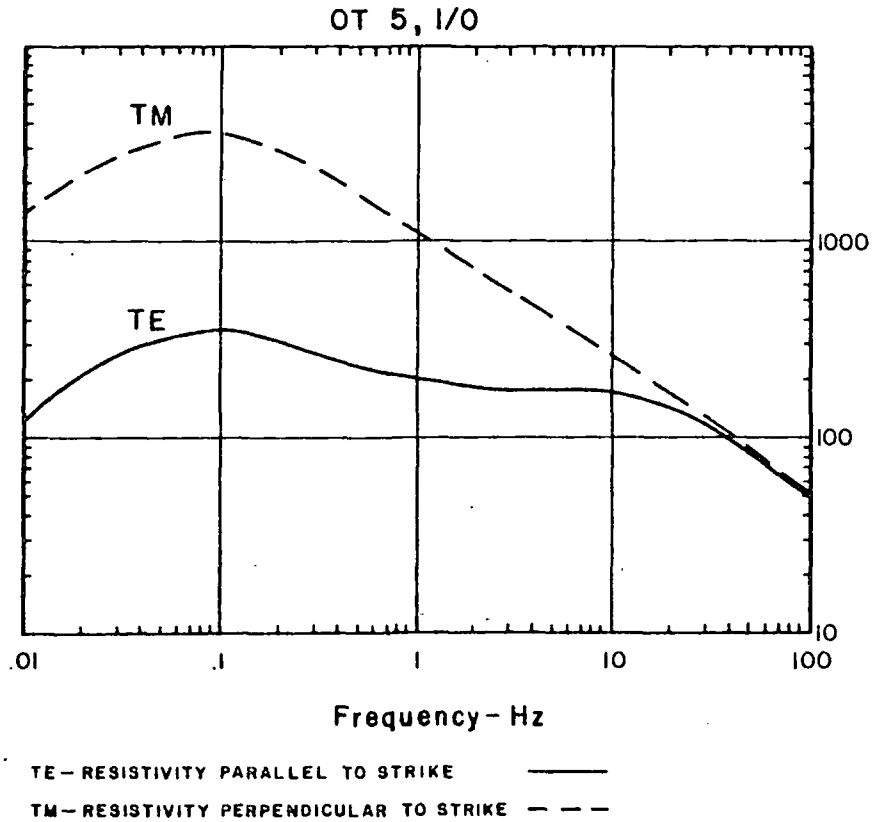


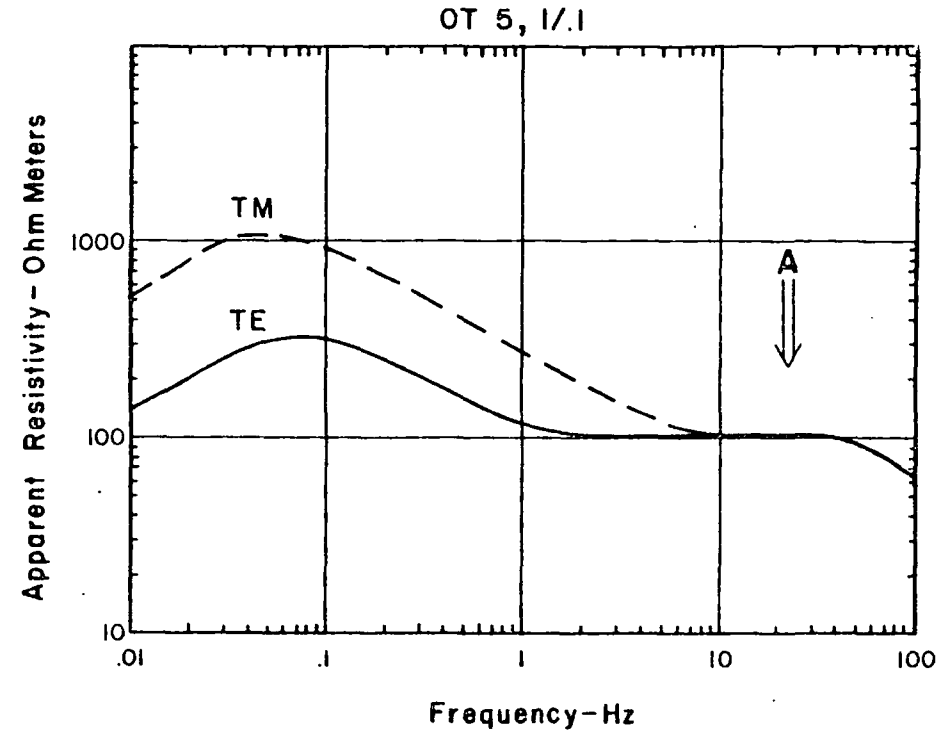


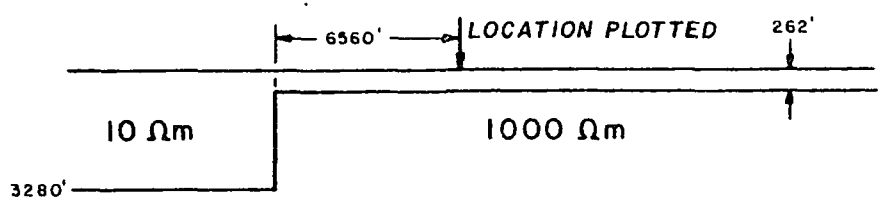


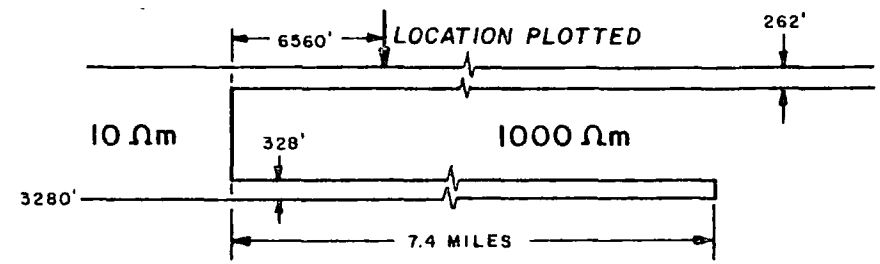


(10 Ωm LOWER CRUST AT 100,000 FEET, SKETCH NOT TO SCALE)

FIGURE 14
EFFECT OF THIN SURFACE CONDUCTOR ON THRUST RESPONSE

## TWO DIMENSIONAL MT MODEL

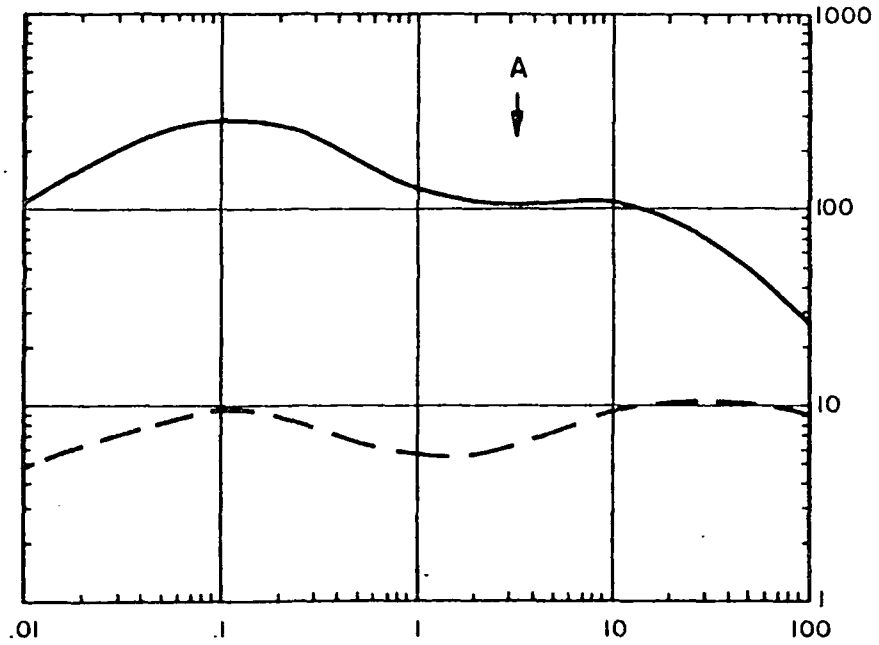


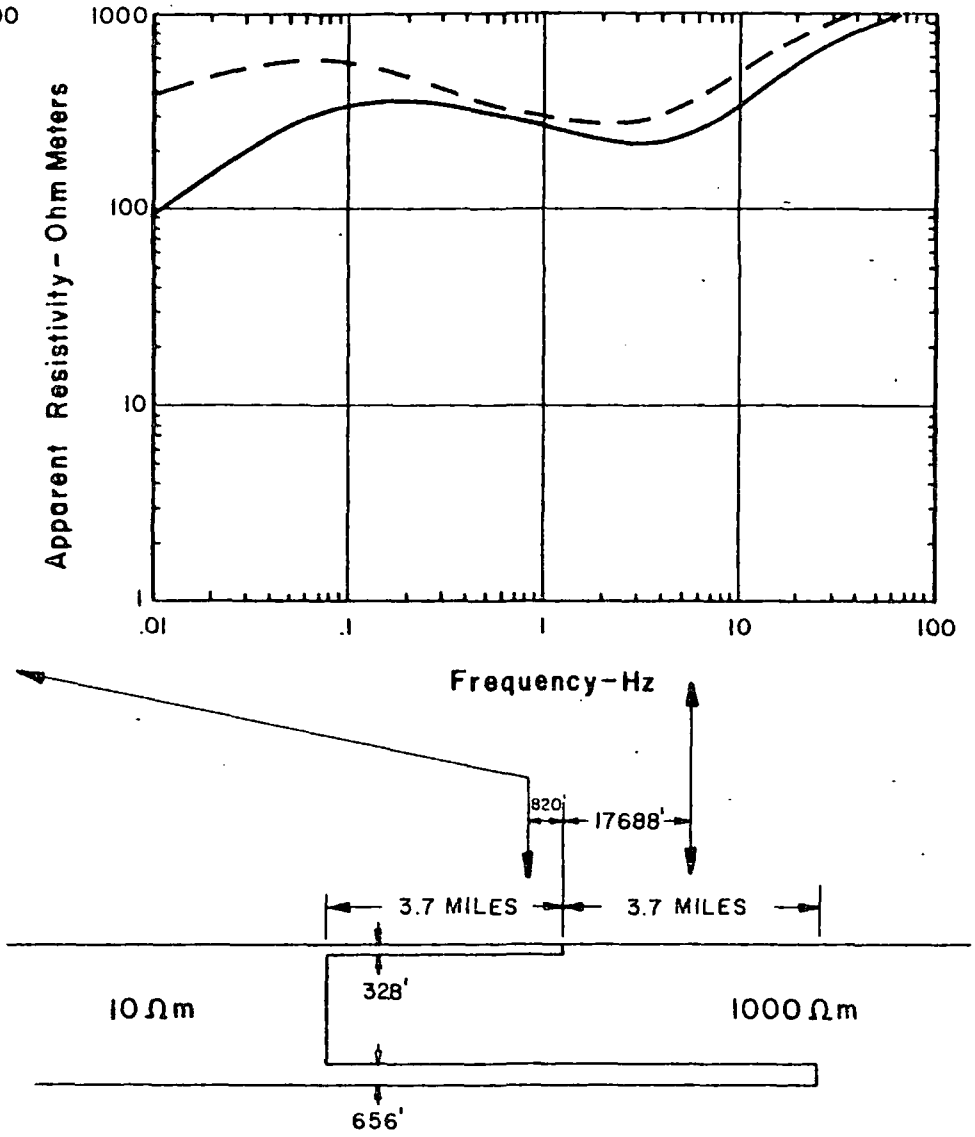


FIGURE 15

EFFECT OF TERMINATED THIN SURFACE CONDUCTOR ON THRUST RESPONSE

## TWO DIMENSIONAL MT MODEL

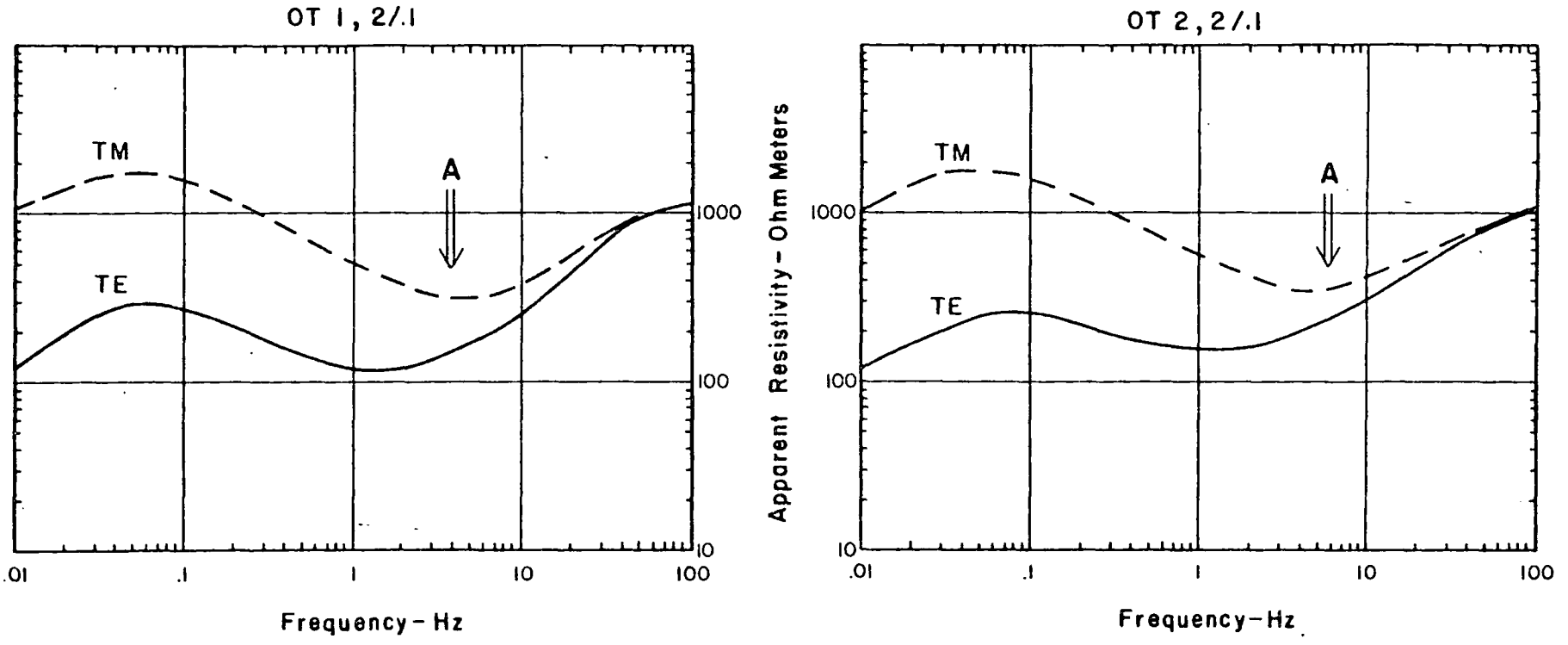


(10 Ωm LOWER CRUST AT 100,000 FEET, SKETCH NOT TO SCALE)

FIGURE 16
EFFECT OF
SHORTENED THRUST

## TWO DIMENSIONAL MT MODEL

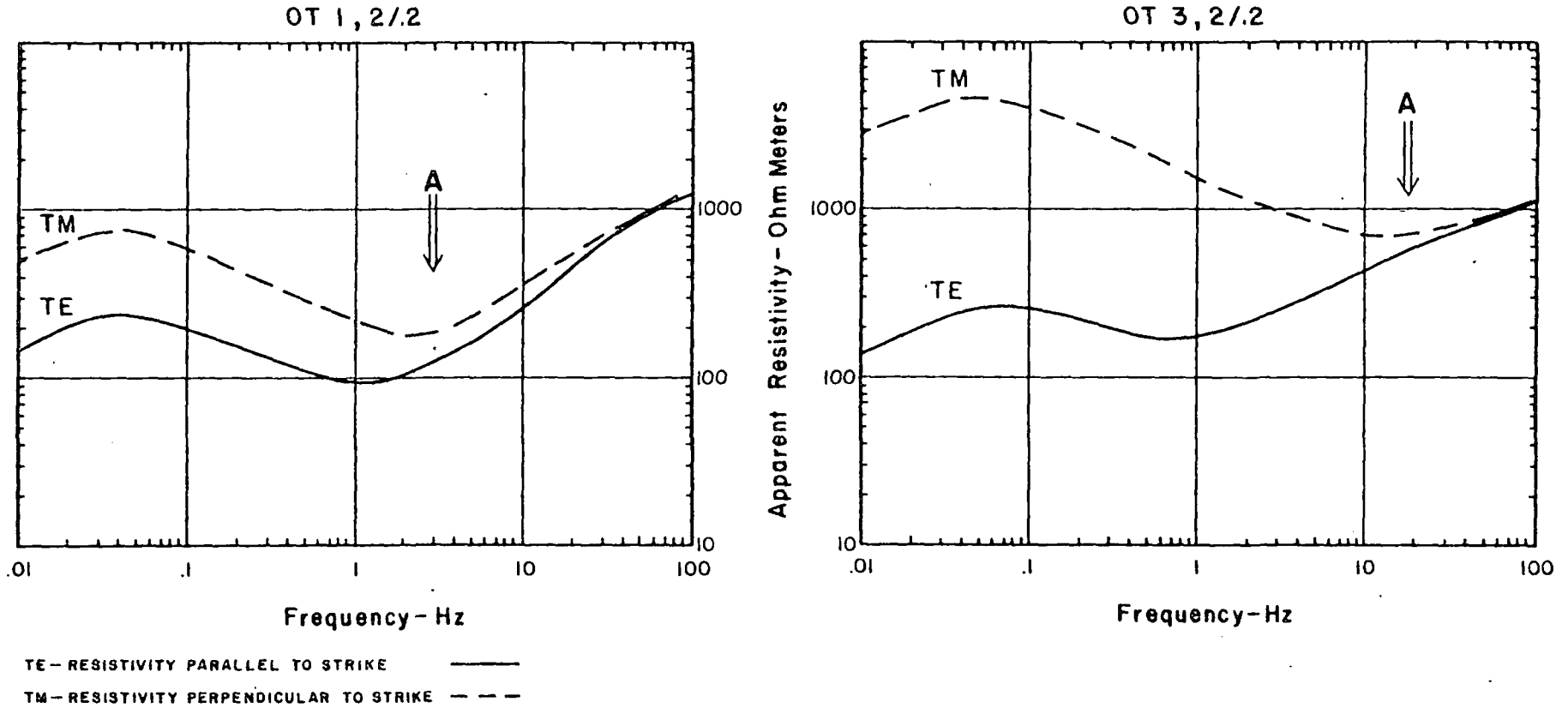


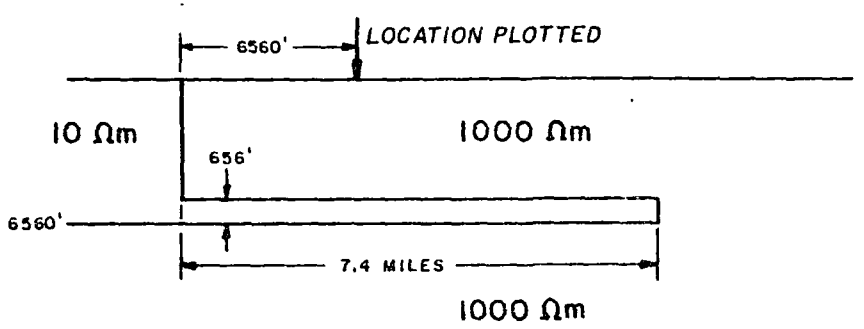


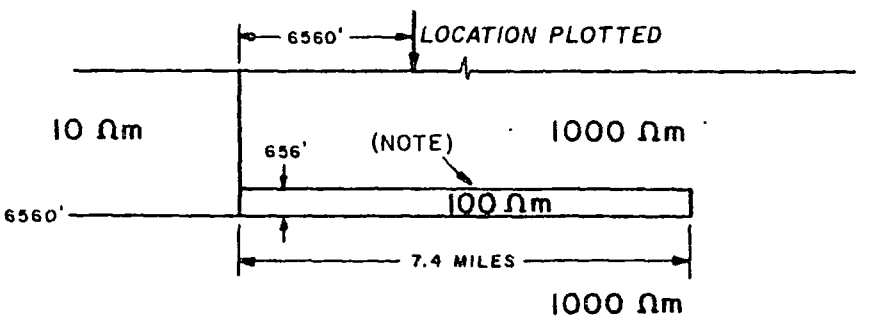


(10 Ωm LOWER CRUST AT 100,000 FEET, SKETCH NOT TO SCALE)

FIGURE 17
COMPLEX THRUST

# TWO DIMENSIONAL MT MODEL

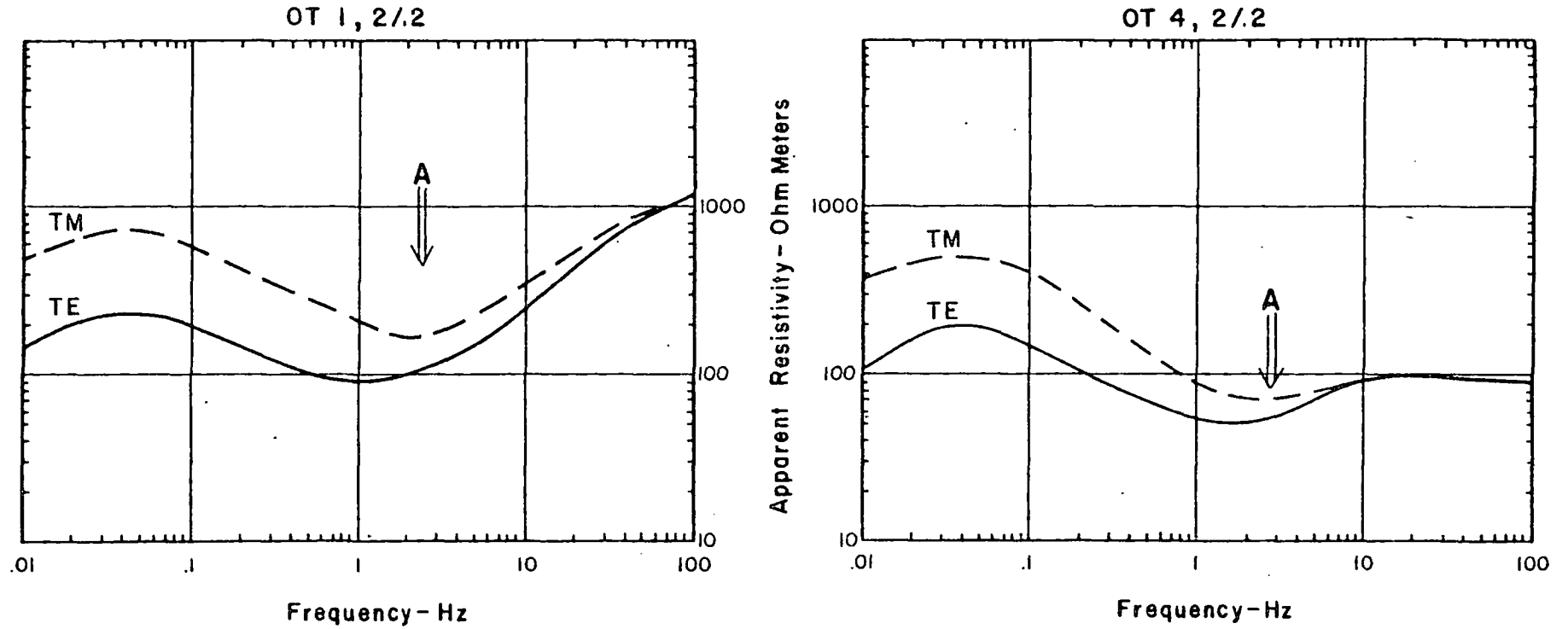


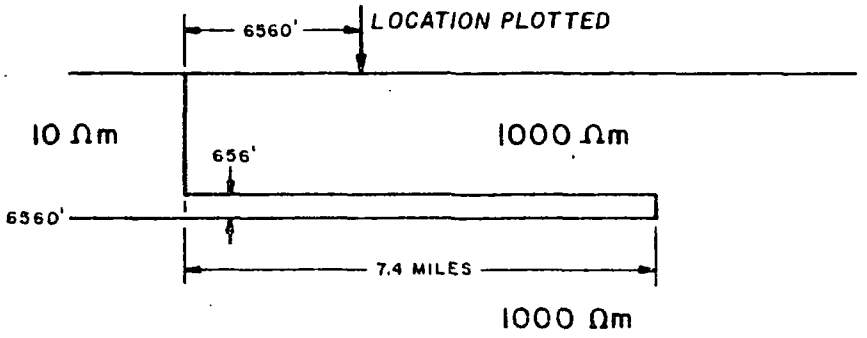


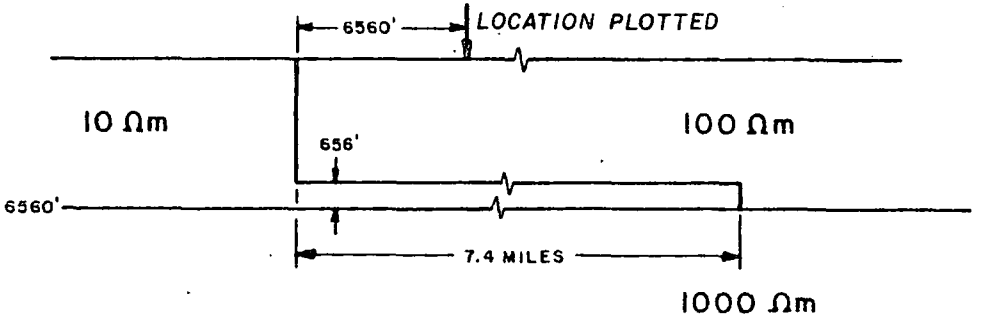


(10 Ωm LOWER CRUST AT 100,000 FEET, SKETCH NOT TO SCALE)

FIGURE 18
COMPLEX THRUST

## TWO DIMENSIONAL MT MODEL

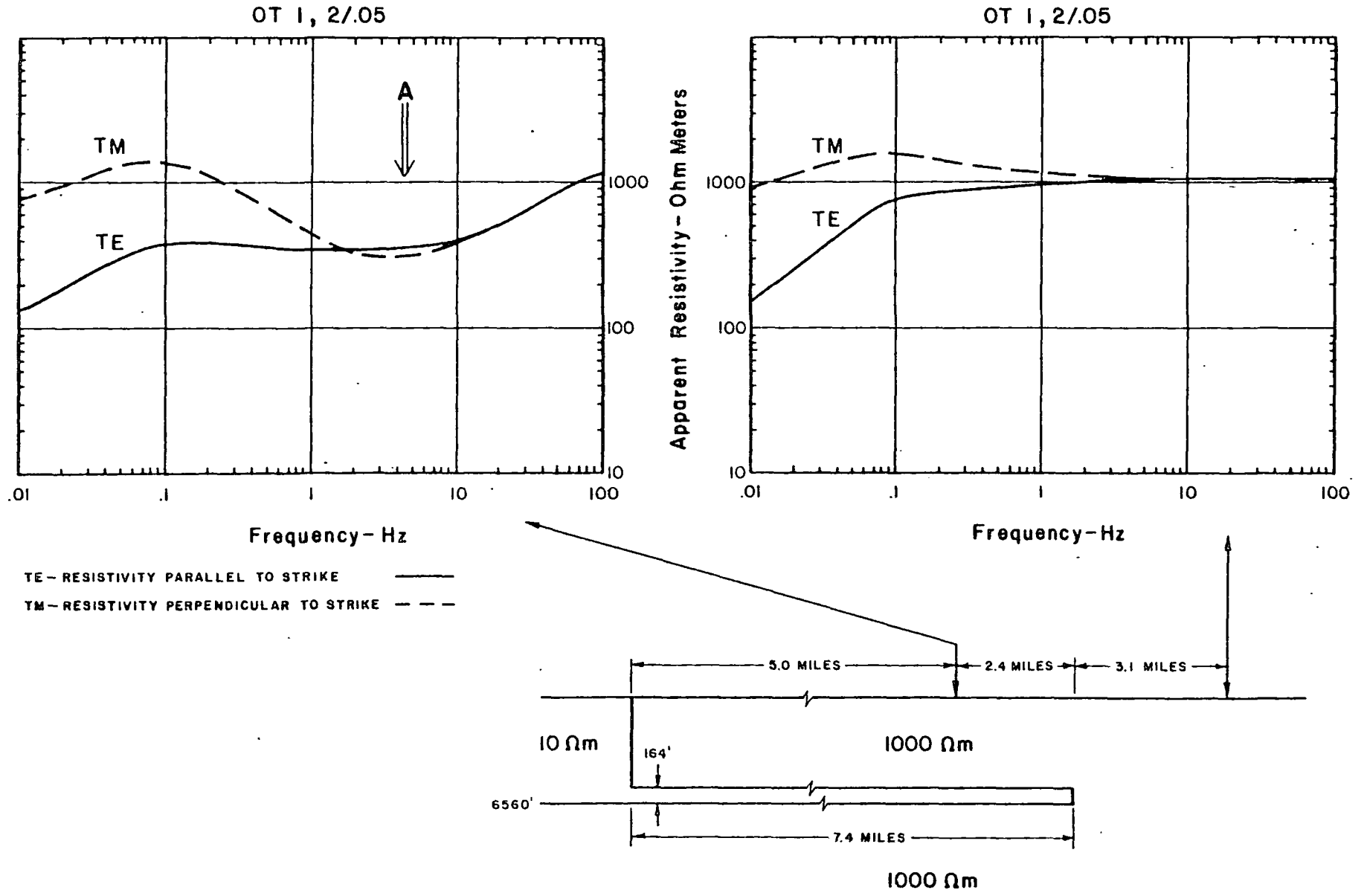


(10 Ωm LOWER CRUST AT 100,000 FEET, SKETCH NOT TO SCALE)

FIGURE 19
OVERTHRUST

contrast leads one to intuitively believe that the presence or absence of the subthrust lower resistivity materials can be determined through examination of the MT response. Adding to the importance of this MT application is the frequent inability to obtain satisfactory geophysical data with other methods in overthrust areas, especially when crystalline rocks are involved.

Description of Models. A large number of models were computed in the course of this overthrust study. To facilitate comparison a common geometry was utilized and a notation developed for ease of reference. These are illustrated on Figure 11. The rock strata $\rho_C$ has been thrust over $\rho_B$. $_A$ lies in front of the thrust while $_D$ forms the basement. A surface layer of thickness $T_S$ and resistivity $\rho_S$ may also be present. For most of the computed models the subthrust ($\rho_B$) and forethrust ($\rho_A$) materials are the same, as are the overthrust ($\rho_C$) and basement ($\rho_D$) materials. The model notation is self-explanatory as is the tabulation of the model series. Note that, in the notation, unit thicknesses are given in kilometers.

Description of Results. The results are presented as a series of comparisons between various thrust situations. In all cases the "site" for which the data is shown is on the overthrust or suspected overthrust. Data format, apparent resistivity as a function of frequency, is as utilized for the previous models with both TM, resistivity perpendicular to strike, and TE, resistivity parallel to strike, curves shown.

Figure 12 introduces the overthrust study. Two cases are shown, one with and one without the subthrust unit. A high, 100:1, contrast has been used, with the 1000 ohm-meter overthrust and basement materials simulating crystalline or extremely tight carbonate rocks and the 10 ohm-meter subthrust and forethrust materials simulating conductive sedimentary units. The overthrust extends 12 km (7.4 miles) past the contact, which comes to the surface. For the model on the right with subthrust materials present, the subthrust unit is .05 km (164 ft) thick while the overthrust plate is 2 km (6560 ft) thick. The model on the left is a simple normal fault to the surface with a vertical throw of 6560 ft. In both cases a 10 ohm-meter lower crust has been placed at roughly 100,000 ft. This model is the same (except for the depth to the deep [100,000 ft] conductor) as the "Fault to Surface" model discussed earlier and illustrated in Figure 4.

Data has been plotted for a location 2 km (6560 ft) from the contact. The introduction of the subthrust conductor has a striking effect on the TM curve, the minima at A, while the TE curve is virtually unchanged. Further onto the thrust, away from the contact, an effect on the TE curve, similar to that on the TM, is noted. This will be discussed later and shown on Figure 19. Data for locations in front of (to the left of) the contact and to the right beyond the extent of the thrust have been computed, but are not shown here. Little variation is noted at these locations between the thrust and

the normal fault cases shown in Figures 4 through 6. As the thickness of the subthrust unit is increased, the effect on the TM component is a deepening minima, with also some lowering of the TE values.

This model illustrates the key observation that the presence of the subthrust materials is evidenced by changes in the TM curve characteristics. The TE curve, while it may be affected by the thrust, is not by itself diagnostic. As with the fault, horst, and graben models (Figures 4 through 7), on the resistive side of the contact the TE curve is largely influenced by the conductive materials in front of the contact, and, especially near the contact, exhibits a minima <u>whether there are subthrust conductors or not</u>.

The case of lower resistivity contrast subthrust materials is examined in Figure 13. The two models shown are identical with regard to geometry but the one illustrated at the right involves a 10:1 contrast (10 ohm-meter subthrust, 100 ohm-meter thrust and basement) while the one on the left involves a 100:1 contrast as in Figure 12. The thickness of the thrust plate is 1 km (3280 ft) while the subthrust unit is .1 km (328 ft).

The difference is striking, the decrease in contrast softening the effect to a very marked degree. The presence of the subthrust materials is still noted by a minima ("A") in the TM component, with the TE curve virtually unchanged from the "no subthrust" case (not shown). Again, the important

observation is that the identification of the thrust requires that the minima be present on both components.

With high contrast there is no mistaking the presence of the thrust. For the lower contrast, 10:1 case model computations the subthrust is still clearly visible. However, the effect is dampened, so that poor data or additional geologic complication may make interpretation difficult. For relatively thinner subthrust sections, at the lower contrast the difference (between presence and absence of subthrust materials) becomes increasingly marginal.

Comparison of the left hand, 100:1, model of Figure 13 with the right hand model of Figure 12 illustrates the effect of the relatively thicker subthrust section of Figure 12. While a deepening minima on the TE curve is noted, the most striking effect is observed on the TM.

The additional complexity of a thin surface conductor is illustrated in Figure 14. An 80 meter (262 ft) 10 ohm-meter surface layer has been added to the thrust geometry discussed in the previous figures. A 100:1 thrust-subthrust contrast is used, with the thicknesses as shown. The thrust case (right hand model) is compared to that of the simple normal fault (left hand model), both with the surface conductor.

Again, the primary difference is a minima, or change in slope at A in the TM component. The TE curve does exhibit a difference, but minor compared to the change in the TM case. As the subthrust section becomes relatively thinner, the effect

of the subthrust becomes overshadowed by that of the surface conductor, and identification becomes marginal.

If the surface low resistivity layer terminates, as is often the case in the field where surface alluvium terminates against outcrop, the effect becomes more complex. In the example of Figure 15 the thin surface layer has been terminated over the subthrust. To the right of the termination the results are similar to those observed in earlier examples. To the left of the termination, on the low resistivity surface materials the effect of the subthrust rocks is visible at "A" but the anisotropy caused by the nearby termination is extreme. The results at the two sites differ far more markedly than would be expected from the addition of such a thin layer. As the surface layer becomes thicker interpretation in the vicinity of the termination becomes more difficult.

The remaining examples of this overthrust series, Figures 16 through 19, illustrate but a few of the large number of possibilities. Figure 16, comparing a less extensive thrust (2.5 miles as opposed to 7.4 miles), shows that the effect is relatively unchanged. When the location is over the conductive subthrust units, the principal factor is the proximity to the forethrust contact.

Figure 17 illustrates the effect where for the right hand model the contrast with the subthrust materials is 10:1 with 100 ohm-meter materials beneath the 1000 ohm-meter thrust, while the forethrust materials remain 10 ohm-meters. The

comparison is with the 100:1 contrast "simple" thrust with identical geometry shown to the left. The effect is striking. With the lower contrast (right hand model) while a minima in TM at A is still observed it is much more subtle than with the 10 ohm-meter subthrust of the left hand model. A key observation is again the minimal difference in characteristics of the TE component, which should also be compared with the TE component of the no-thrust case, Figure 12 left hand model.

In Figure 18, subthrust 10 ohm-meter materials are overlain by 100 ohm-meter rocks, all over a 1000 ohm-meter basement. Again, as in the previous thrust cases, the effect is a minima noted on the TM curve.

Figure 19 completes the examples with a return to the overthrust model first examined earlier in Figure 12. In Figure 19 a location well back on the 7.4 mile thrust, 5 miles from the leading edge and 2.4 miles from its termination, and a location 3.1 miles back from the termination on the entirely resistive section, are shown. On the thrust (left hand model) the presence of the thrust is clearly visible on both components. Here, well away from the influence of the low resistivity forethrust environment the TE component as well as the TM shows the effect of the subthrust materials.

Back from the thrust (right hand model, Figure 19) the data is that expected on an entirely resistive body, with a lateral conductive contact in the vicinity as evidenced by the low frequency anisotropy. In the absence of any thrust

(the model of Figure 12, left hand), data 5 miles back from the contact is very similar to that 12.5 miles back shown on Figure 19.

Interpretation. The interpretation of data where a thrust is expected (or suspected) should begin with examination of models such as those presented here. If the resistivity contrast (as deduced from logs and geologic data) and/or the geometry differs markedly from the "case" studies, models specific to the prospect must be computed. The presence of subthrust conductive materials should be observed directly on the data. Note that if no anomaly is noted, the presence of a thrust is not disproved. The thrust may involve resistivity contrasts and/or a geometry that places the thrust beyond the resolving power of the tool.

Once the presence of a thrust has been interpreted qualitatively, the qualitative interpretation is best pursued through one-dimensional inversion of the TM component data. Inversion of 2-D model data will give the interpreter insight into the inaccuracies inherent in a particular case.

Summary. The results of the overthrust model study may be summarized as follows, referring to Figure 11:

a. In every case, the presence of the thrust is indicated by a two component conductive anomaly. On the resistive side of a lateral contact, the TE curve normally has a minimum, with characteristics that are a function of resistivity contrast and geometry, in particular the proximity of

the site to the contact. This minimum will be present to some extent with or without a thrust. When the presence of a thrust is distinguishable from the no-thrust case, it is by observing a minima also in the TM curve.

b. For the 100:1 contrast thrust (OT1 series) the presence of the subthrust materials is clearly indicated when the thickness of the conductive subthrust is less than 2% of the thickness of the resistive overthrust.

c. Electrical contrast is critical. For the 10:1 thrust (OT6 series) a subthrust-to-thrust thickness ratio on the order of 5 to 10% is required for identification. Additional complexity, such as in the OT3, OT4, and OT5 series, makes identification more difficult, especially when the thickness ratio is less than 10%.

d. The effect of shortening the extent of the thrust is minimal.

The interpreter is advised when faced with known or suspected overthrust geology to perform a model study specific to the case in hand. As with all other cases, supporting data should be used whenever applicable.

F. Two-Dimensional Model Series - Buried Low Resistivity Formation (Figures 20 through 23)

Object. The object of this series of models is to examine in detail the MT response for the geologic situation where a low resistivity formation is buried within an otherwise

TWO DIMENSIONAL MT MODEL

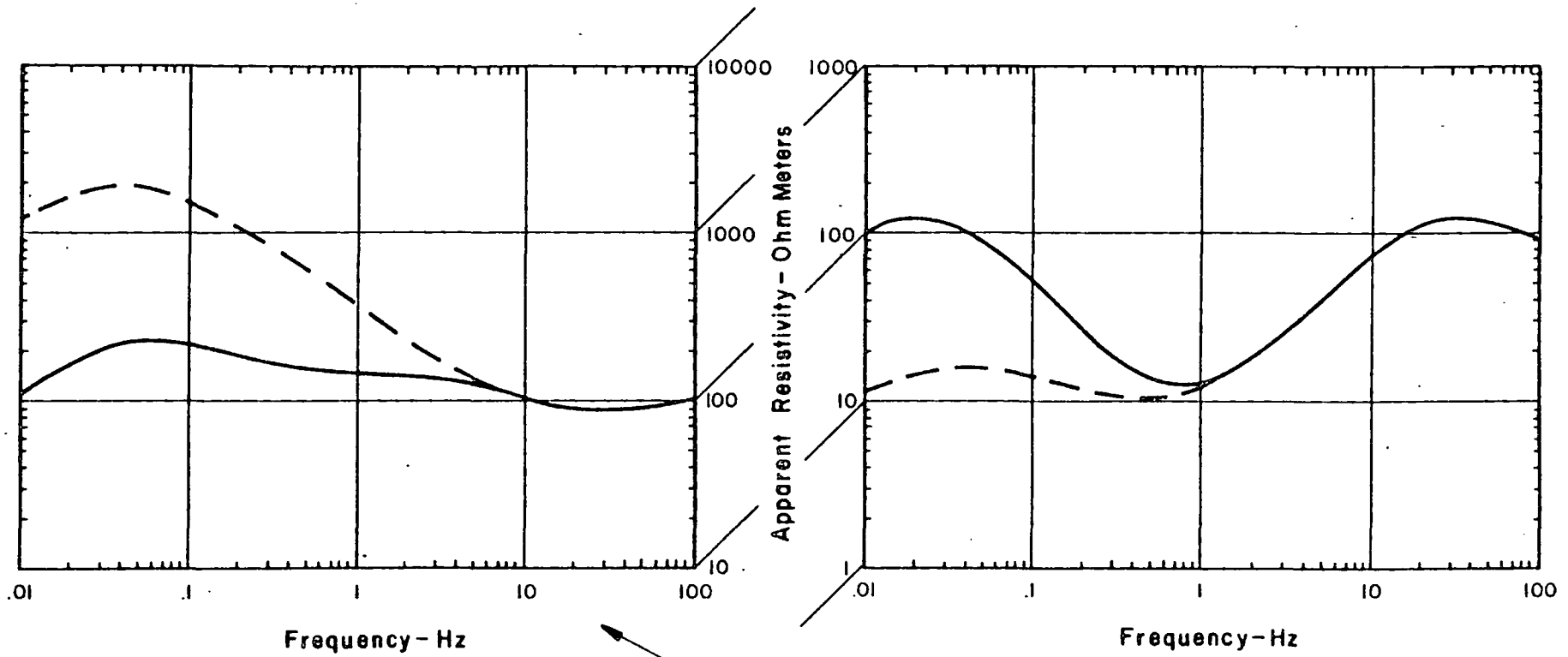


TE - RESISTIVITY PARALLEL TO STRIKE ——

TM - RESISTIVITY PERPENDICULAR TO STRIKE — — —

(NOTE DIFFERENCE IN VERTICAL SCALE)

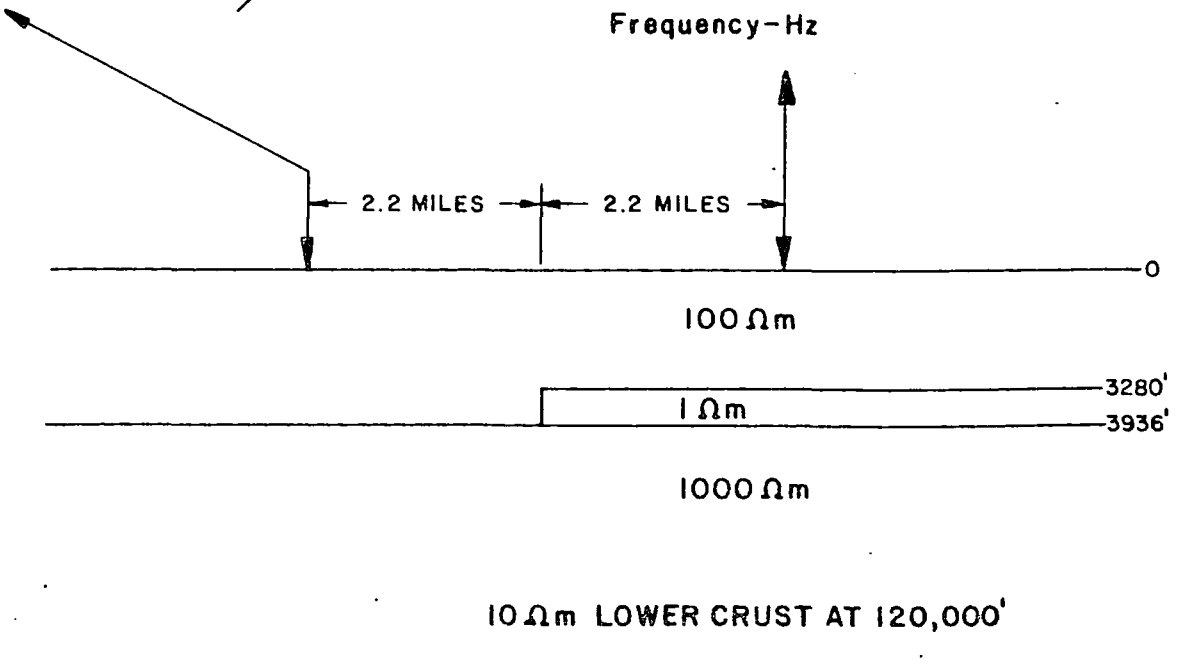


FIGURE 20

TERMINATED BURIED CONDUCTOR

## TWO DIMENSIONAL MT MODEL

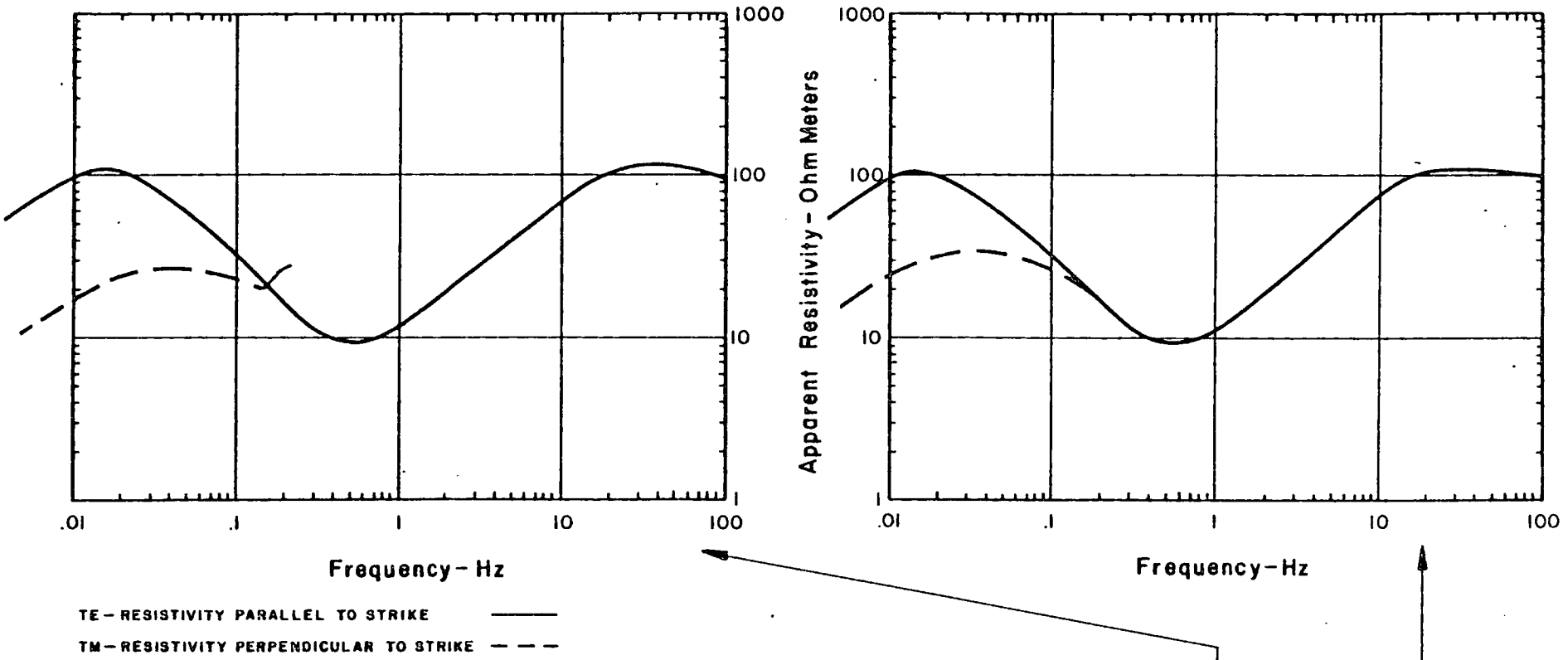


FIGURE 21

TERMINATED BURIED CONDUCTOR

## TWO DIMENSIONAL MT MODEL

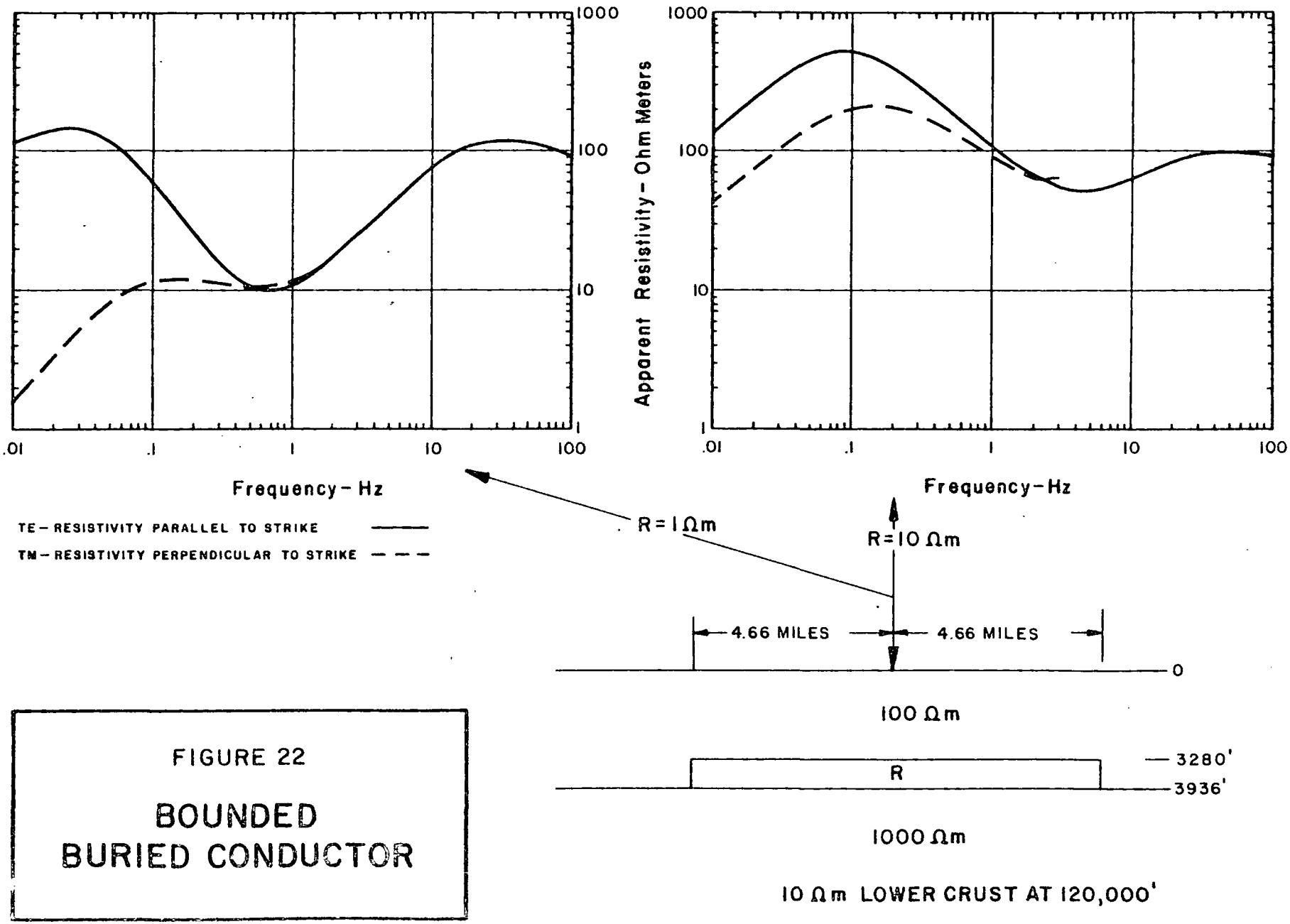


FIGURE 22

**BOUNDED BURIED CONDUCTOR**

TWO DIMENSIONAL MT MODEL

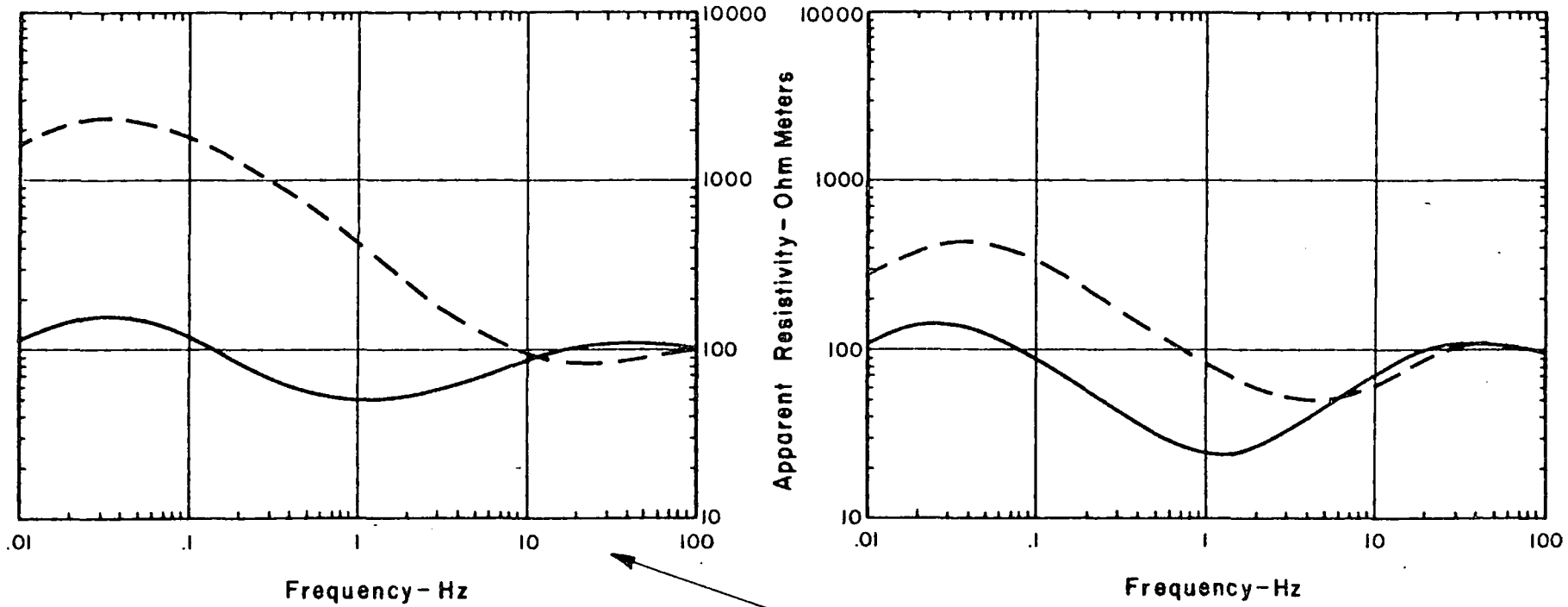


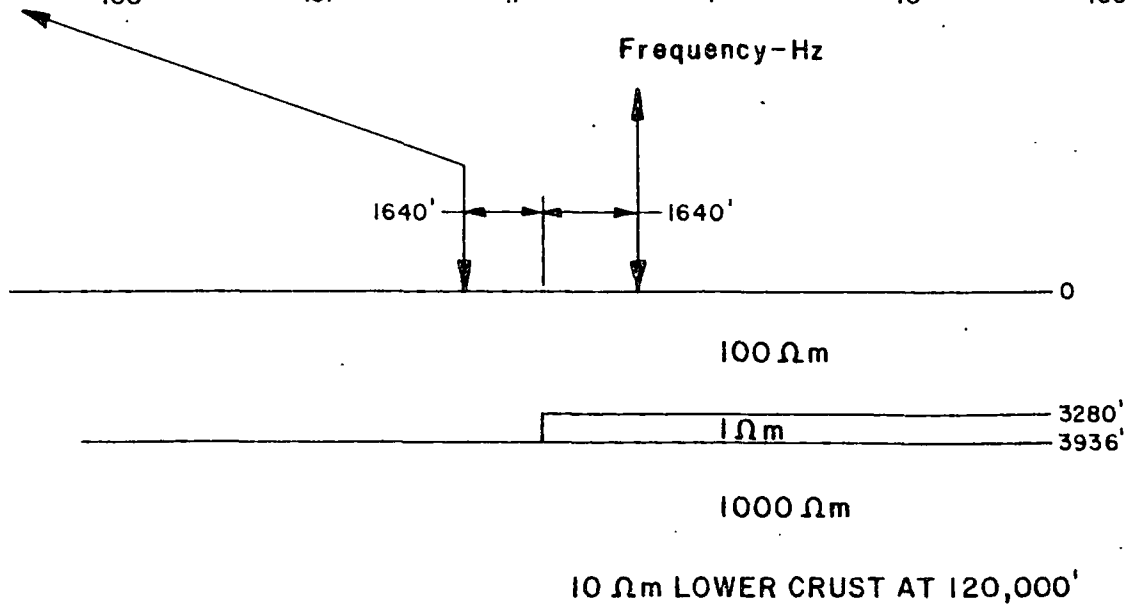


FIGURE 23

TERMINATED BURIED CONDUCTOR

more resistive section. This case is important in many prospective areas that are covered with volcanic rocks, where highly resistive basaltic or andesitic flows cover or are interbedded with very low resistivity volcaniclastics or marine or continental sediments, all over a more resistive electrical basement. The two-dimensional effect occurs when the low resistivity formation terminates abruptly, as with a fault or intruded igneous dike, or stratigraphic pinch-out.

Description of Models. The models consists of a surface 100 ohm-meter layer over a 1000 ohm-meter electrical basement. At the interface between these two units a terminated low resistivity formation unit is inserted. Resistivity, thickness, and depth of burial of the low resistivity unit are varied. The low resistivity unit is modeled as extending to infinity away from the termination, or as bounded on two sides.

Description of Results. The fundamentals of this class of models are shown on Figure 20. The model is of a 1 ohm-meter formation 656 ft thick at a depth of 3280 ft. The MT results over the low resistivity formation are typical of much MT data obtained in volcanic covered areas; high resistivities at high frequencies, low resistivities at somewhat lower frequencies, and moderate to extreme anisotropy at the lowest frequencies. To the left, off of the low resistivity formation, apparent resistivities are high, but considerable anisotropy is still apparent. Figure 21 is data from the same model, but at locations further removed from the termination.

The key point here is that, due to the high resistivity of the surface and basement layers and the high contrast, the effect persists for a considerable distance away from the termination. This leads to the persistent nature of this MT signature, at times over an entire prospect.

Figure 22 is similar to that of the previous models, but the low resistivity formation terminated on two sides. The data, measured at the center of the 9.3 mile wide feature, is shown for two resistivity values, 1 and 10 ohm-meters. In the 1 ohm-meter case the low frequency anisotropy is extreme, with the TM component showing virtually no evidence of the electrical basement.

Figure 23 is data for the model of Figures 20 and 21, for data acquired in the immediate vicinity of the termination. At the site over the low resistivity formation, just at the termination, the low resistivity "null" occurs at different frequencies for the two components, an observation that has proven diagnostic for field data. Also note that the data at this location are unusual in that, while the site is on the conductive side of the contact, the TM curve is higher resistivity than the TE. Further onto the conductive side the TE curve becomes the higher resistivity, as illustrated in Figure 20. The data at the site to the right, 1640 ft from the termination, is anomalous in that the anisotropy is less than that observed at the site in Figure 20, further from the termination.

Interpretation. Once the data has been recognized as the result of this class of geologic feature, the interpretation is straightforward if data are available over a sufficient geographic area. The location of the termination(s) can be inferred from the variation of the low frequency anisotropy with site location. Depth of burial and thickness of the low resistivity formation can be inferred at sites over the formation and not in the immediate vicinity of the termination from inversion of the maximum apparent resistivity curve, as this component most accurately represents the subsurface geometry.

G. Two-Dimensional Models - Topographic Effect (Figures 24 through 27)

Object. The object of this series of models is to examine the effect of topographic relief on MT data. When considering topographic effects it is helpful to think of a steep ridge or hill as a structure similar to the fault and graben models discussed earlier. The sketch in Figure 24 illustrates the concept. The topographic feature sketched in Figure 24A may be approximated by the model of Figure B, where the air in the "valley" has been simulated by an extremely high resistivity material. From the earlier models, anomalous MT data would be expected in the vicinity of the contact between the two materials. In particular, in 24B on the "low resistivity" side of the contact, on the "hill" as opposed to on the adjacent "air", the TM component would be expected to be anomalously depressed in the fault and graben models.

A. TOPOGRAPHIC MODEL

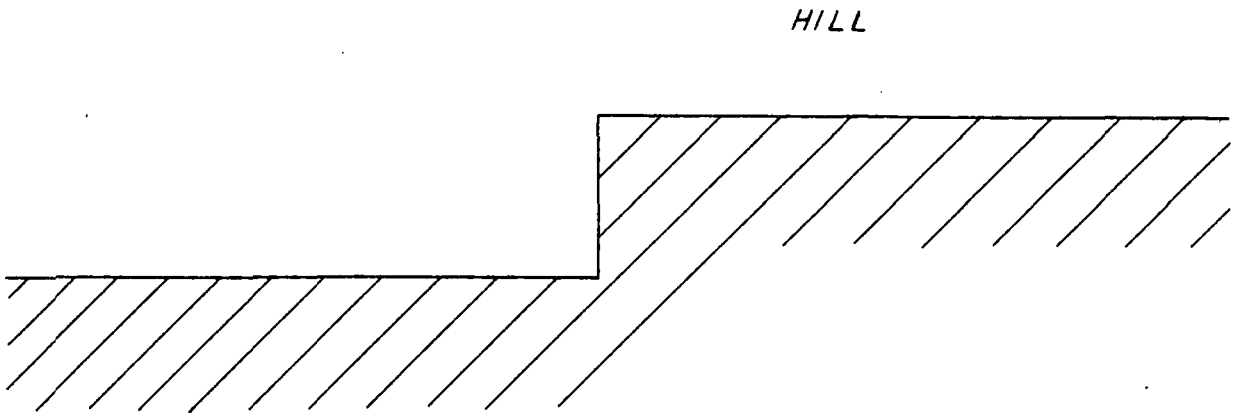


B. INTERPRETIVE CONCEPT

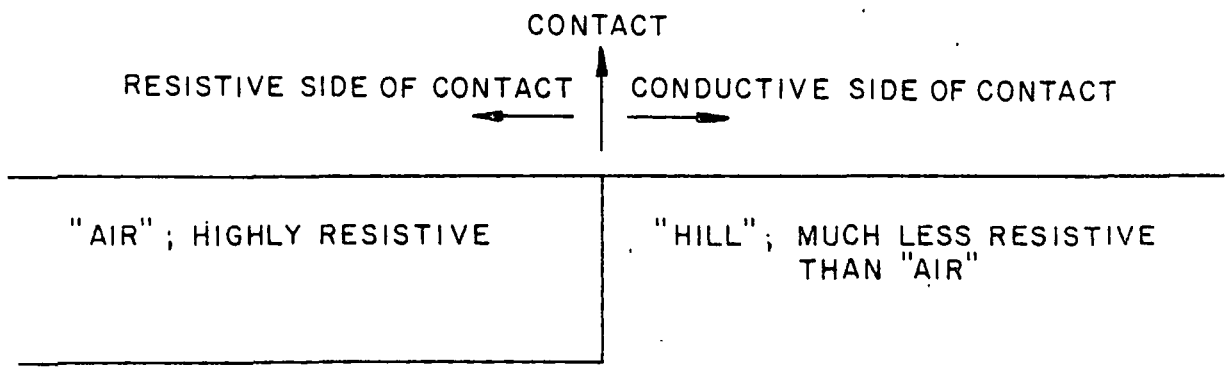


COMPARE WITH MODEL OF FIGURE 4

FIGURE 24
INTERPRETIVE CONCEPT
TOPOGRAPHIC MODELS

## TWO DIMENSIONAL MT MODEL

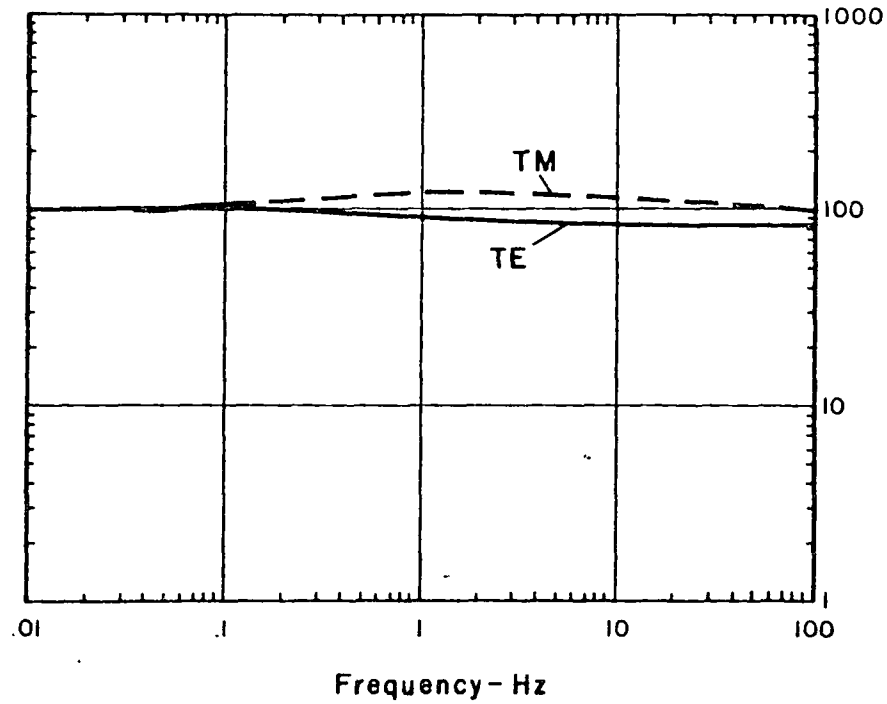


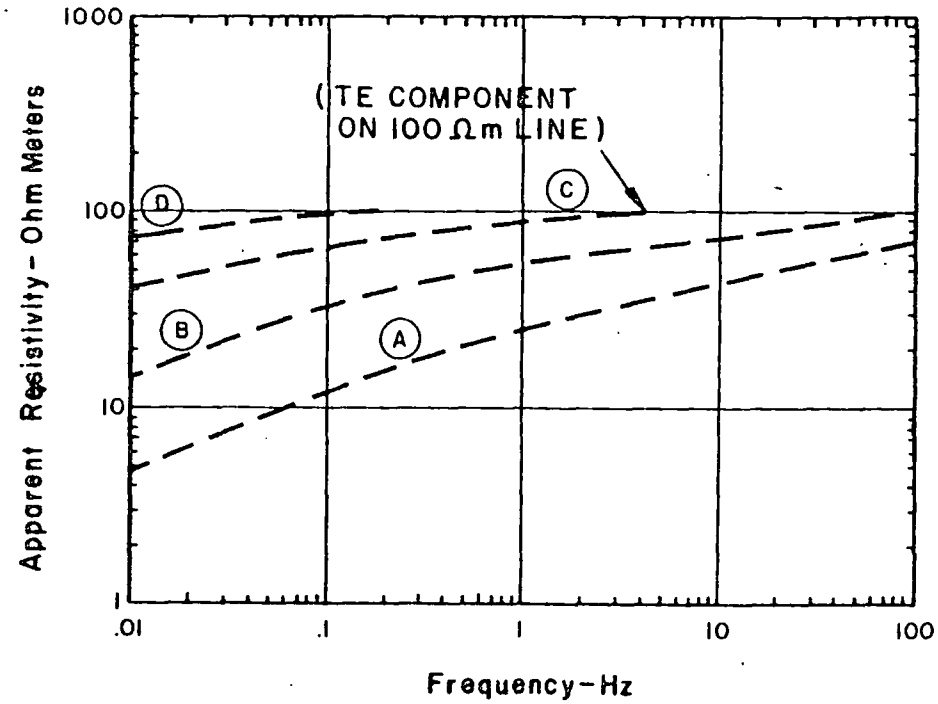


TE – RESISTIVITY PARALLEL TO STRIKE ———

TM – RESISTIVITY PERPENDICULAR TO STRIKE – – –

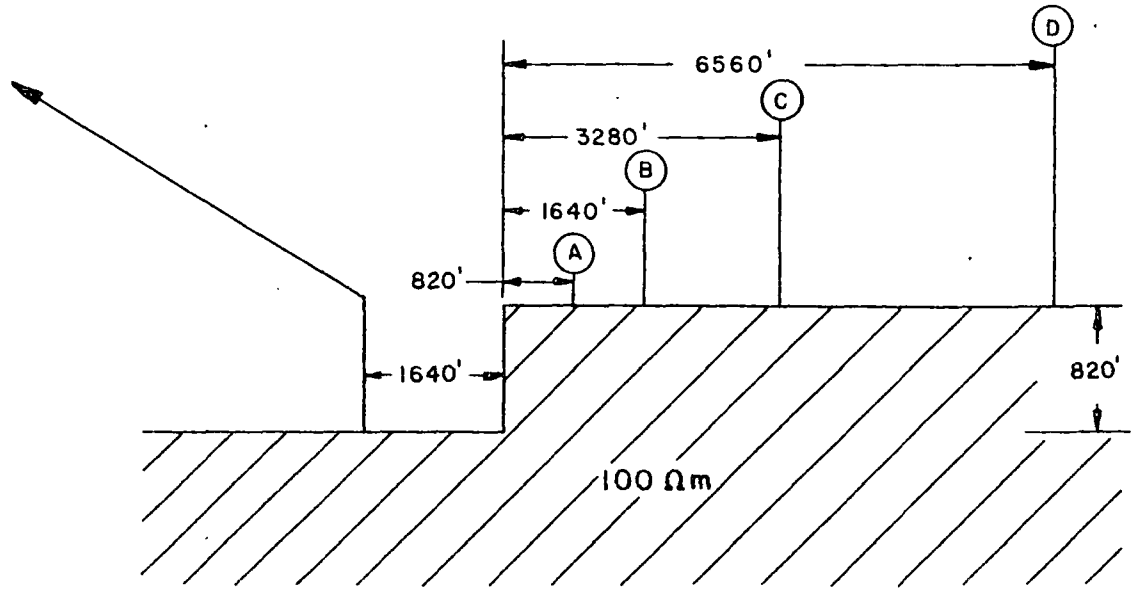


FIGURE 25

TOPOGRAPHIC MODEL
SIMPLE HILL

TWO DIMENSIONAL MT MODEL

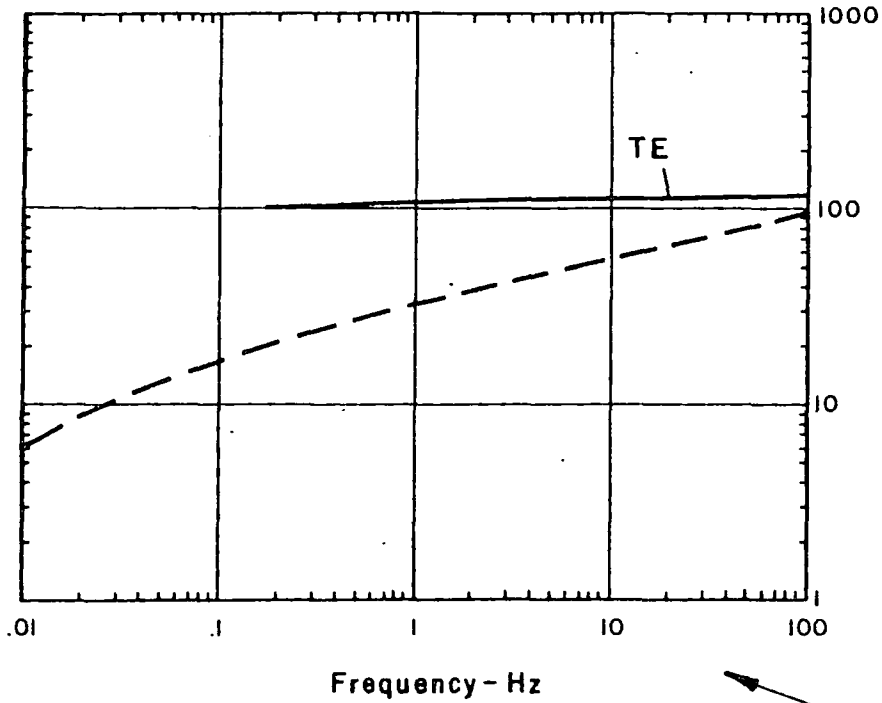


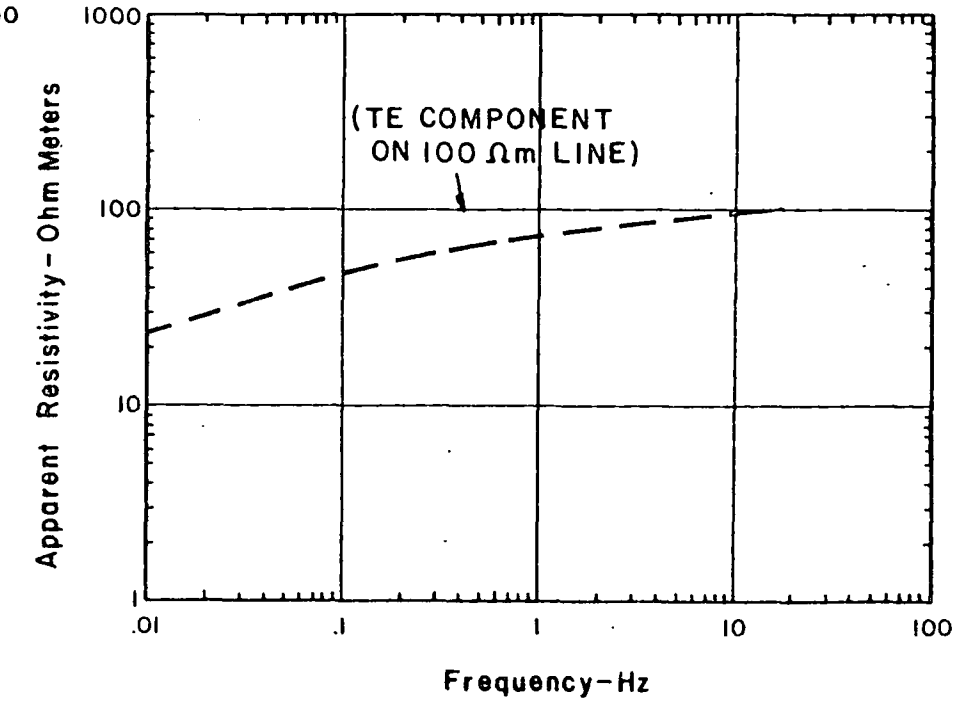


TE - RESISTIVITY PARALLEL TO STRIKE ——

TM - RESISTIVITY PERPENDICULAR TO STRIKE — — —

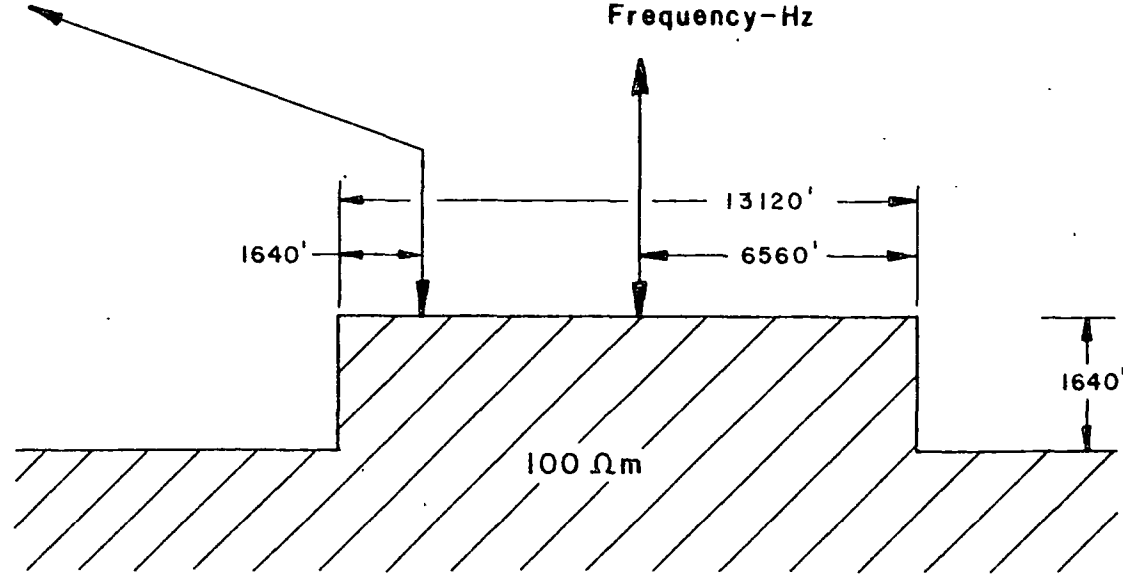


FIGURE 26

TOPOGRAPHIC MODEL
RIDGE

TWO DIMENSIONAL MT MODEL

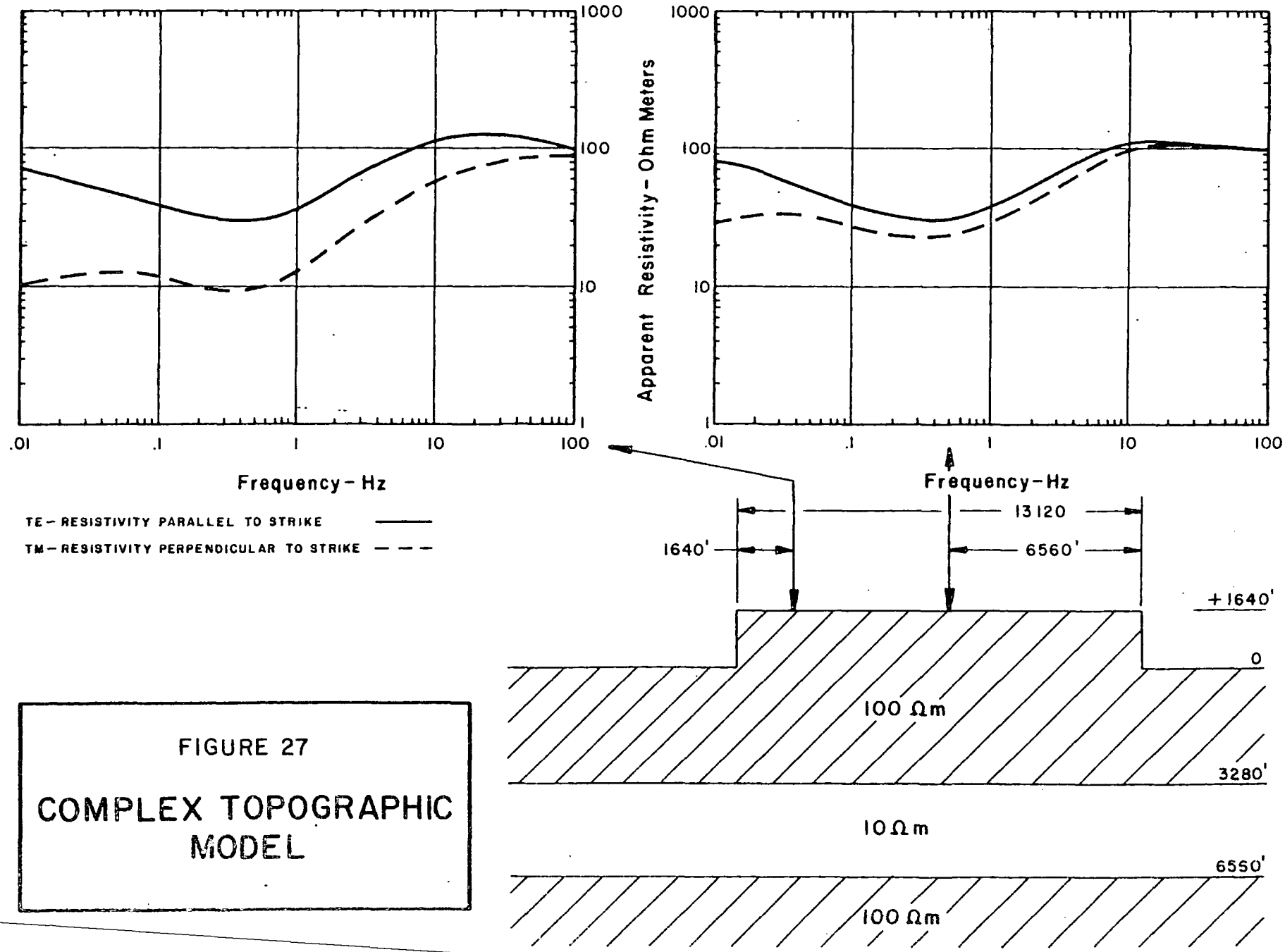


FIGURE 27

COMPLEX TOPOGRAPHIC MODEL

Description of Models. The basic topographic models consist of an earth of uniform resistivity with a hill or ridge. Vertical relief and width of the ridge are varied. Models have also been computed for a more complex subsurface.

Description of Results. Figure 25 presents the results for a simple "hill" 825 ft high in an otherwise uniform 100 ohm-meter earth. Virtually no effect is seen at the foot of the hill. On the hill, however, the behavior of the TM resistivity component is high anomalous, with the effect increasing at lower frequencies. Figure 26 presents the results at two locations on a 2.5 mile wide, 1640 ft high ridge, 1640 ft from the edge and in the ridge center. This model is a good approximation of many MT site locations in hilly or mountainous terrain. Near the edge of the ridge the effect is extreme, and is still such as to be of concern to the interpreter in the center of the feature.

Figure 27 presents the results for a slightly more complex topographic model, a ridge similar to that shown in Figure 26 but with a low resistivity formation at depth. The results are similar to those shown above, an anomalous depression of the TM curve and very little effect on the TE curve.

Interpretation. The results of the model series indicate that there will be topographic effects in MT data obtained in hilly terrain. While in many cases these effects will not obstruct a qualitative interpretation, it should be clear that the effect on the TM curve (relative to the

topographic feature, see footnote to page 17) if not identified would cause an erroneous interpretation of depth and thickness of subsurface formations. The features modeled above involve considerable topographic relief, more subtle features will result in more subtle MT effects which will be more difficult to discern, especially in the presence of more complex subsurface structure.

The interpretive technique starts with an examination of the topography in the vicinity of each MT site in any survey where terrain effects might be a factor, utlizing large scale topographic maps. Corrections are applied based on the model studies unless it is determined that the TE (relative to the topography) curve will provide the needed depth and thickness data. The models indicate that the TE component is virtually unaffected by topography. The great concern here, however, is the effect of three-dimensional topographic features, which are of course much more common than true two-dimensional features. The effects of three-dimensional features are the subject of ongoing studies at the time of the writing of these notes (May 1983).

H. Three-Dimensional Considerations

While it has long been realized that three-dimensional structure will have an affect on MT data, it is only recently that modeling results have become available to provide quantitative analysis and insight into exploration problems. The

data discussed here are the results of studies conducted at the Massachusetts Institute of Technology Department of Earth Sciences and at the University of Utah Department of Geology and Geophysics.

The preliminary results of the MIT three-dimensional modeling studies have been published as a USGS report[2] and at the time of this writing have been accepted by Geophysics for publication in the October 1983 issue. The following is a summary of that paper:[3]

Recent model studies at MIT have shown that significant errors may result when applying one-dimensional or two-dimensional interpretation methods to magnetotelluric data collected in three-dimensional (3-D) environments. Both depths and resistivities can be grossly incorrect if 1-D or 2-D methods are applied in a 3-D setting. Examples will be presented of MT sounding curves generated using a 3-D modeling program (Madden, et al, 1982)[2] that illustrate some interpretation pitfalls if 3-D effects are not considered. The 3-D effects discussed herein are simple ones, and can be readily identified in MT data from a well designed MT survey.

---

[2]Madden, T.R., and Park, S., 1982, Magnetotelluric Modeling for a Crustal Environment; Final Report, USGS Contract 14-08-001-G-G43: MIT Dept. Earth Sciences.

[3]Park, S.K., Orange, A.S., and Madden, T.R., 1983, Evidence of Three-Dimensional Structure in Magnetotelluric Sounding Curves: Geophysics (in press).

The sounding curves shown here were generated for the model shown in Figure 28. The model is of an "L" shaped valley one kilometer thick filled with 10 ohm-meter, conductive sediments and surrounded by 400 ohm-meter, resistive mountains. The valley is 50 km wide at the narrow end, 100 km wide at the wide end, and 150 km long, so it is typical of basins in the Basin and Range Province of the western United States.

The maximum and minimum apparent resistivities have been computed for sites A, B, C, and D (see Figure 28 for site locations) and the results plotted in Figures 29 through 32, respectively. One-dimensional MT sounding curves for both inside and outside the valley were generated assuming the top layer resistivity was uniformly 10 ohm-meters and 400 ohm-meters, respectively. These 1-D curves are superimposed upon the sounding curves in Figures 29 through 32.

Two important effects manifest themselves in Figures 29 through 32. The first is the insensitivity of electric fields to heterogeneities more than a few electromagnetic skin depths away. This insensitivity is only seen at the higher frequencies where the thickness of the heterogeneous region is larger than the skin depth. The second effect is the ability of the conductive heterogeneity to gather currents from its sides and up from the mantle. This effect is seen at low frequencies where the skin depth is much greater than the thickness of the heterogeneity.

## MAP VIEW

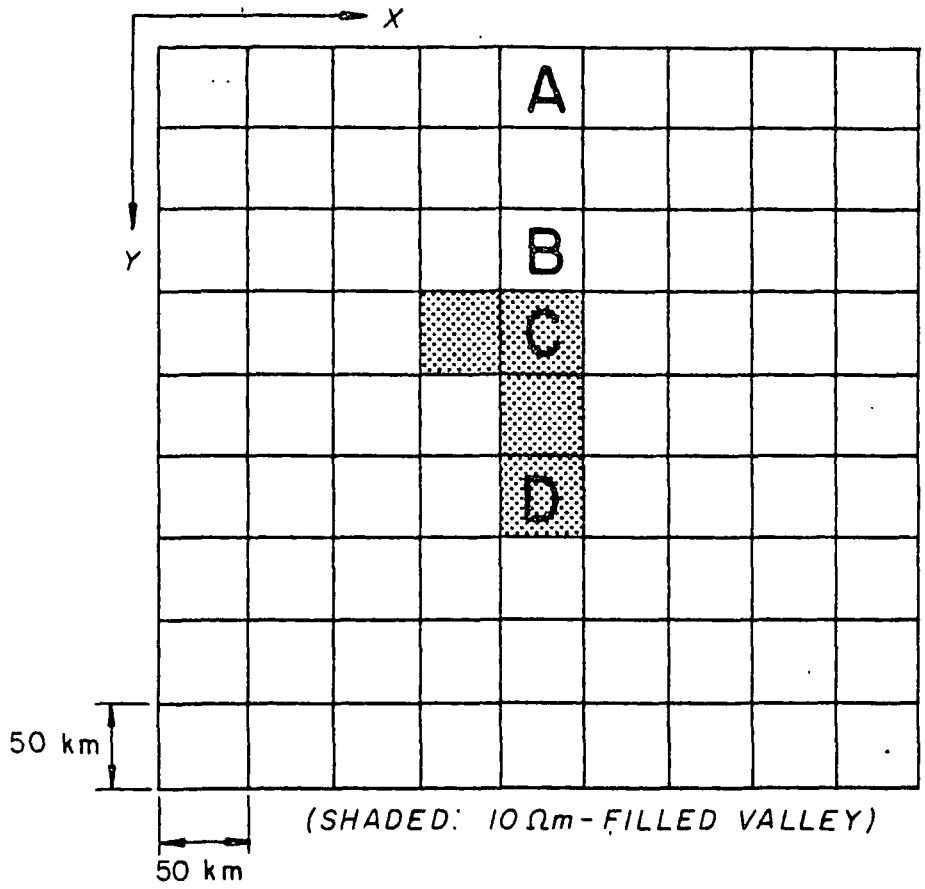


## CROSS SECTION

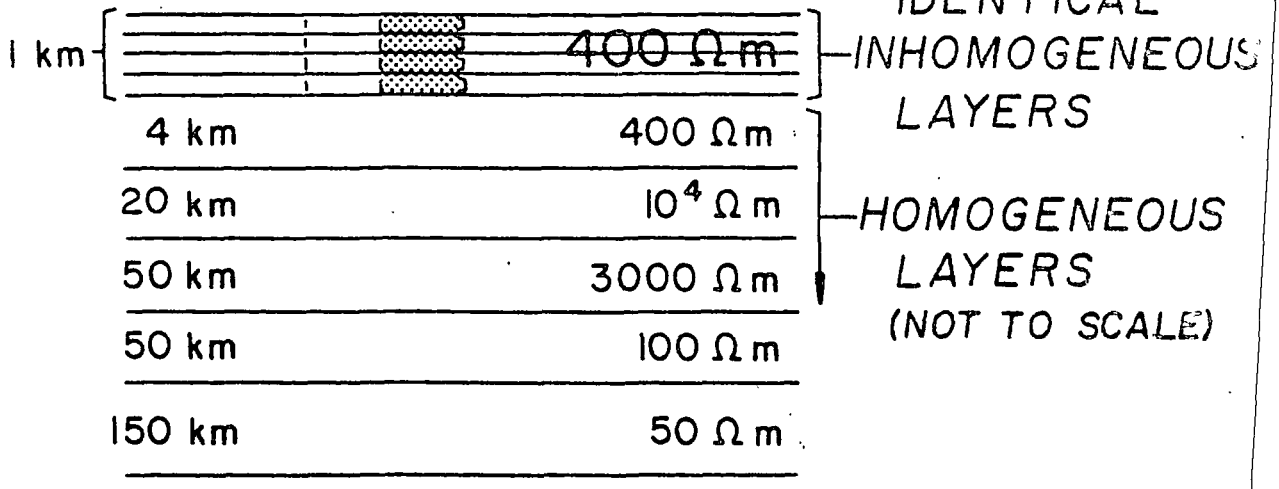

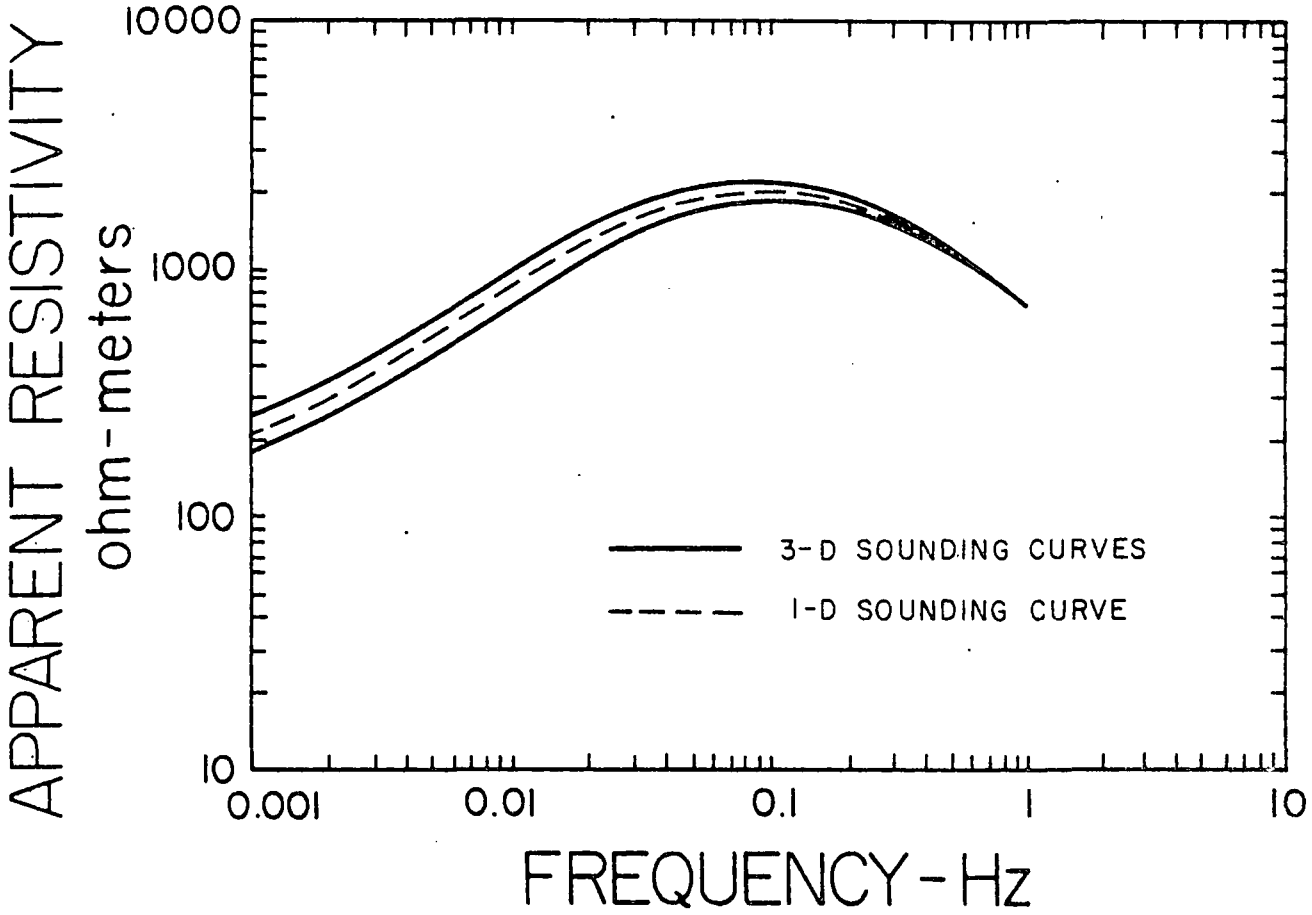


FIGURE 29
3-D MODEL RESULTS
MT SOUNDING FOR SITE A

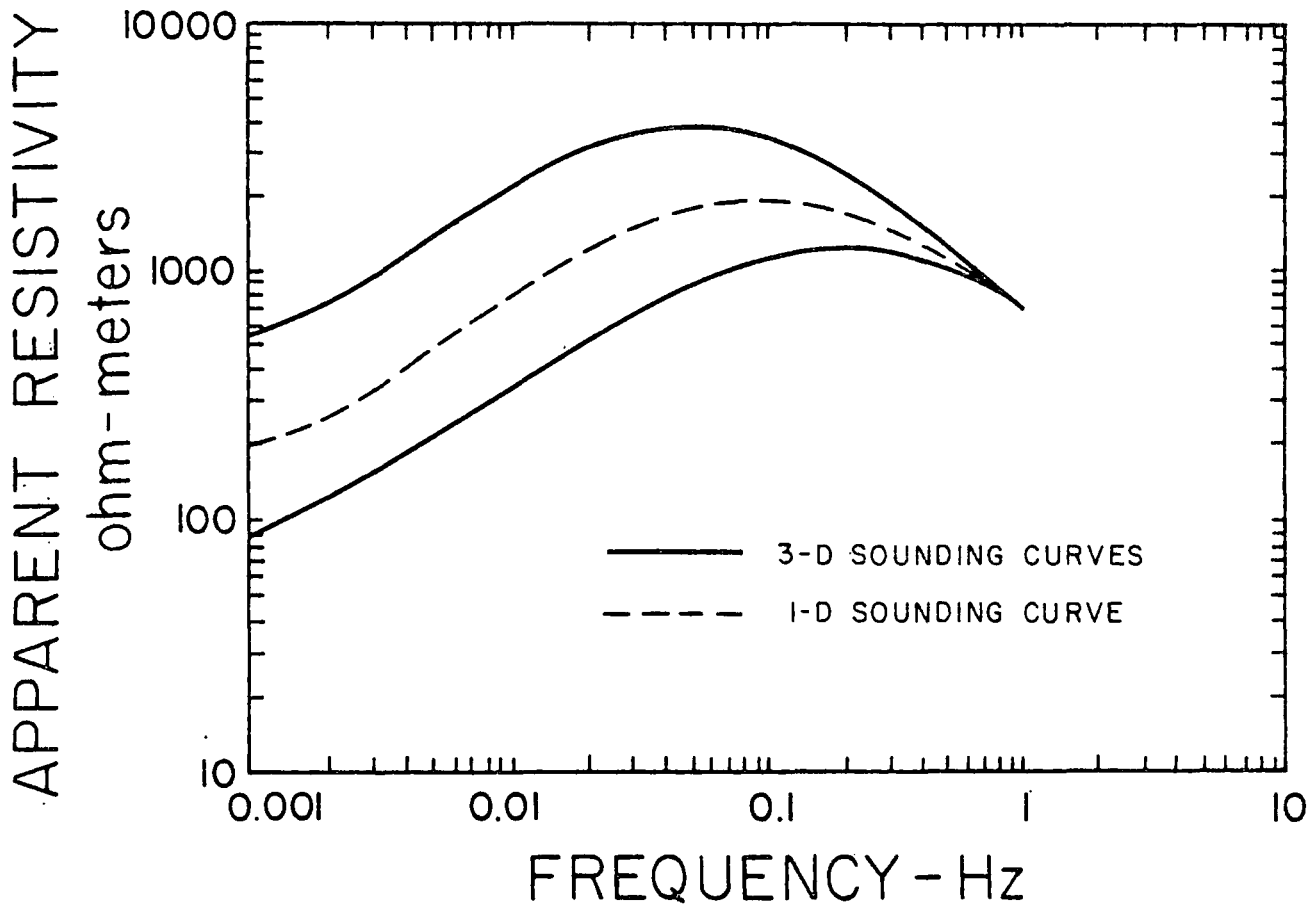


FIGURE 30
3-D MODEL RESULTS
MT SOUNDING FOR SITE 3

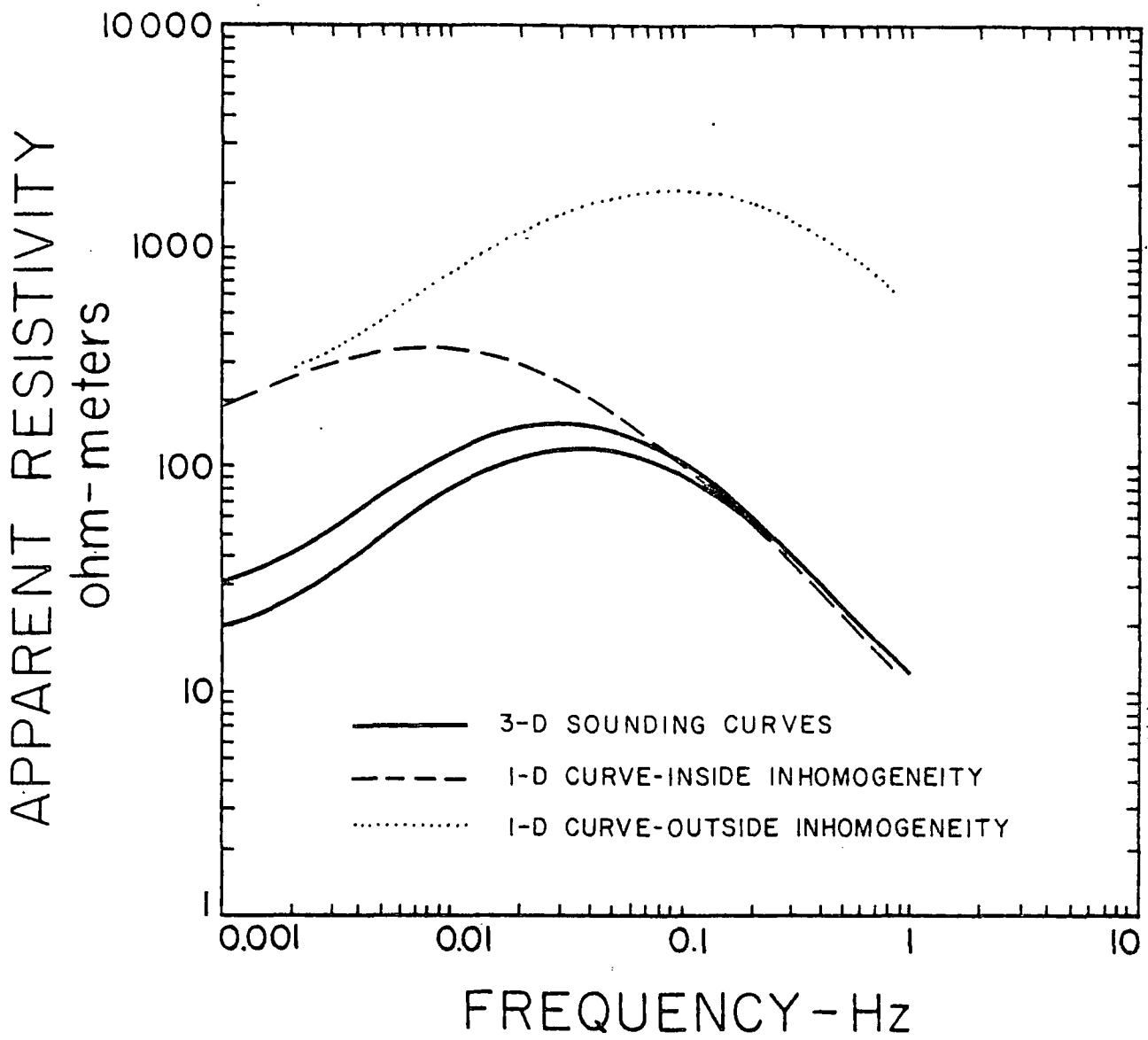


FIGURE 31
3-D MODEL RESULTS
MT SOUNDING FOR SITE C

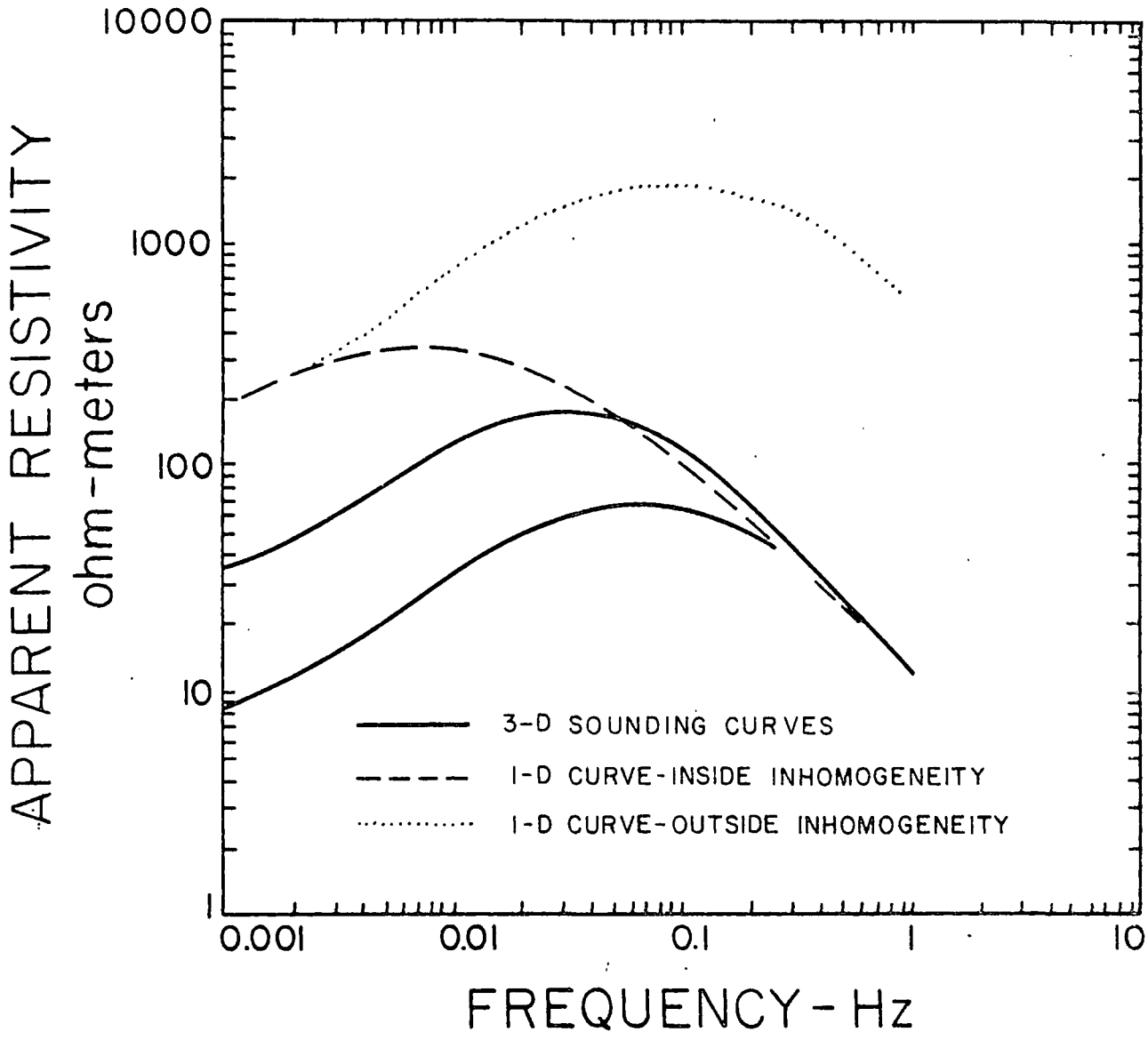


FIGURE 32
3-D MODEL RESULTS
MT SOUNDING FOR SITE D

The first effect can be seen at all sites. At the sites within the heterogeneity, Figures 31 and 32, the MT sounding curves and the local 1-D sounding curves merge at frequencies above 0.1 Hz. The nearest boundary is 25 km, or 5 skin depths, from the MT sites. The secondary fields due to interactions at the boundary have decayed to a negligible fraction of the primary 1-D fields at these sites, so the structure is essentially one-dimensional above 0.1 Hz. This same effect can be seen in Figures 29 and 30 or sites outside the heterogeneity, but the merging occurs above 0.5 Hz. The skin depth at 0.5 Hz outside the heterogeneity is 14 km, and the nearest boundary is thus about 1.5 skin depths away.

The current gathering effect is seen at low frequencies. The effect is frequency-independent when the thickness of the heterogeneous surface layer is much smaller than the electromagnetic skin depth. We see this effect as a parallel shift of the low frequency 1-D curve. This shift is present in Figures 29 through 32 for frequencies below 0.1 Hz. The electromagnetic skin depths inside and outside the heterogeneity at this frequency are 16 km and 100 km, respectively.

The conductive feature attracts current both horizontally and vertically. The 'adjustment distance' is compared to the horizontal dimensions of the conductive feature to discriminate between effects from current attracted laterally and current drawn up from the mantle. The 'adjustment distance' is a function of the resistivities and layer thicknesses

involved and is a measure of the lateral distance over which currents re-equilibrate to their 1-D values because the conductor is pulling current up from the mantle. The model shown here has an 'adjustment distance' inside the heterogeneity of 187 km. The conductive valley is only 150 km by 50 km so very little current has been drawn up from the mantle. Most of the excess current that <u>is</u> present has thus been attracted laterally.

Figures 29 and 30 show sounding curves for sites outside the heterogeneity. The maximum apparent resistivity curves, which generally represent electric fields perpendicular to the local contact between the conductive valley and the resistive surroundings, are shifted up compared to the local 1-D curve because current is being attracted towards the heterogeneity. The minimum curves, which generally represent electric fields parallel to the contact, are depressed compared to the 1-D curve because less current is flowing parallel to the conductor's boundary. Both the maximum and minimum sounding curves outside the heterogeneity resemble the local 1-D curves, but are just shifted up or down.

The conductive heterogeneity attracts insufficient current to raise the fields inside to their 1-D values, and both the maximum and minimum apparent resistivity curves inside the heterogeneity are depressed relative to the local 1-D curve. However, the sounding curves inside the heterogeneity are similar in <u>shape</u> to the <u>outside</u> 1-D curve at low frequencies, not the inside 1-D curve. The inflection points seen on the MT sounding

curves in Figures 31 and 32 are not longer due to deep structure as in the 1-D case, but are due rather to surface heterogeneities. The resistivity, thickness and lateral extent of surface heterogeneities control both the amount of shift and at what frequency the curves begin to merge with the inside 1-D curve. The net result is a set of sounding curves which resemble the local 1-D curve at high frequencies and a shifted version of the outside 1-D curve at low frequencies.

Site C, shown in Figure 31, is of particular interest because we would infer from the sounding curves that the site is isotropic. The usual interpretation approach would be to use a 1-D inversion on one of the sounding curves to deduce the resistivity structure beneath the site. Comparison of these sounding curves to the inside 1-D curve shows that the above structure would be wrong in its estimates of intermediate depth resistivity structure.

It is important to note that a detailed examination of the computed 3-D results reveal that the maximum skew and elipticity, the conventional indicators of 3-D geology in MT survey data, are on the order of .006 and .118, respectively, for site C. These values are lower than typically observed in real field data in simple settings, and would not call attention to a 3-D problem. Nowhere within the valley were skews higher than .15 and elipticities higher than .21 observed.

Two-dimensional MT soundings were computed as a further comparison with the 3-D data. Maximum and minimum apparent

resistivity curves for the 2-D and 3-D cases are shown for sites B, C, and D, in Figures 33, 34, and 35, respectively. The model, as sketched on each figure, is a two-dimensional cross-section through the long axis of the valley of Figure 28, extended to infinity away from the plane of the section.

Outside of the valley at site B (Figure 33), the 2-D data bears a close resemblance to the 3-D. Inside the valley, the strong anisotropy in the 2-D sounding curves is very different from the isotropic nature of the 3-D data at site C (Figure 34). The 3-D data at site D (Figure 35) resemble that of the 2-D case, but with about a factor of two decrease in anisotropy. The implication is that for sites B and D an interpretation of the 3-D curves based on 2-D models would resemble an actual cross-section through these two sites, but with inaccurate depth and resistivity values. Clearly, if the profile includes the 3-D data for site C and a 2-D based interpretation is then attempted, the results will be seriously in error (if a 2-D solution can be found at all).

The University of Utah work has been reported recently by P. E. Wannamaker, et al (1980)[4]; and by Sam C. Ting and G. W. Hohmann (1981)[5]. As with the MIT work, the principal

[4]Magnetotelluric Models of the Roosevelt Hot Springs Thermal Area, Utah: Report N. DOE/ET/17002-8, University of Utah, September, 1980.

[5]Integral Equation Modeling of Three-Dimensional Magnetotelluric Response: Geophysics, v. 46, no. 2, February 1981, p. 182-197.

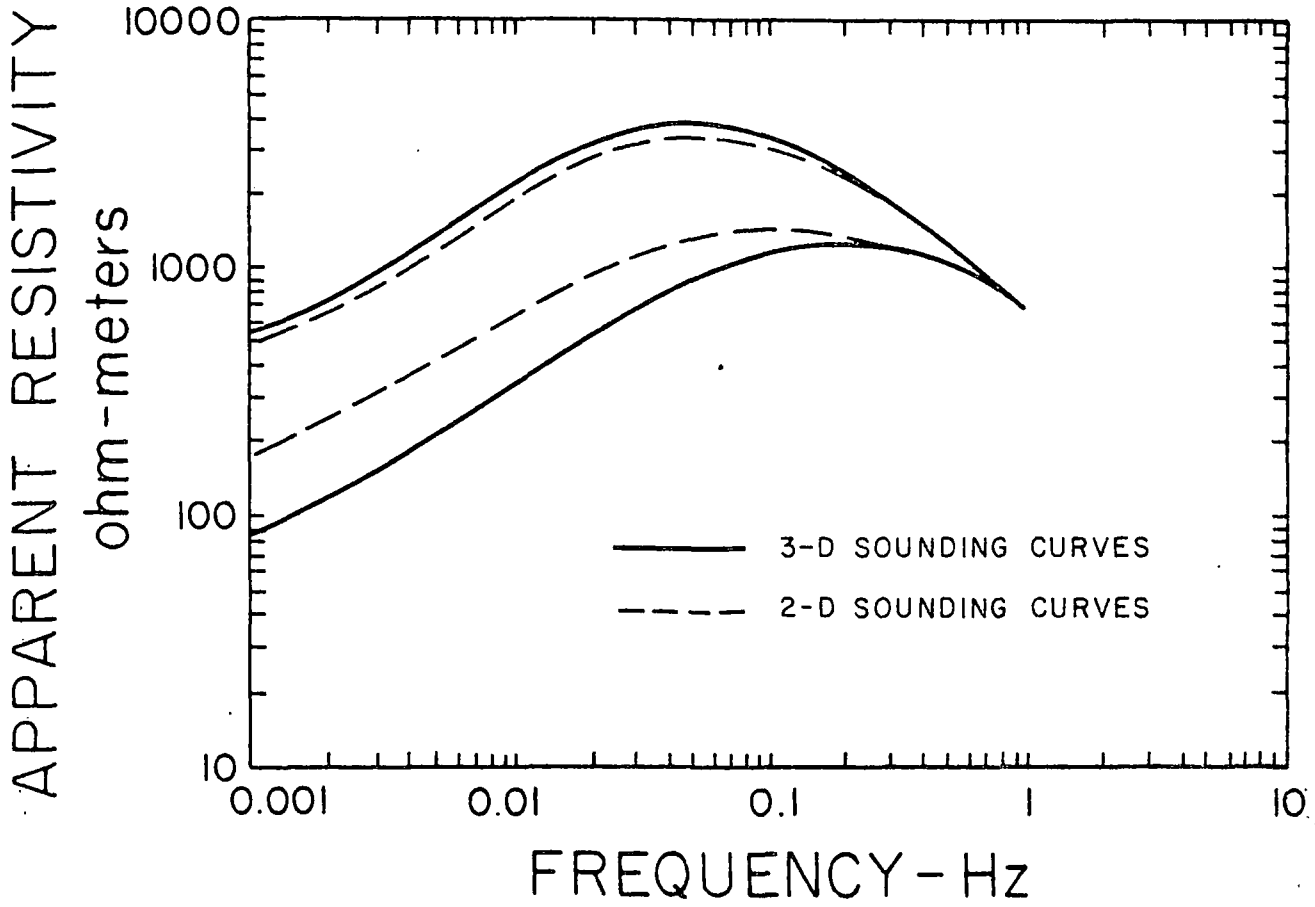


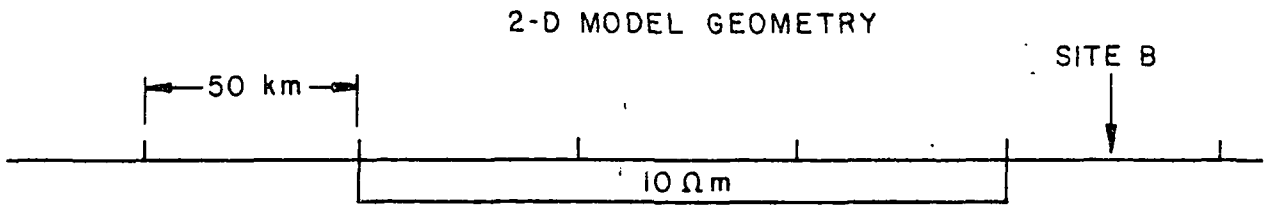


VERTICAL PROFILE AS IN MODEL OF FIGURE 1

FIGURE 33
2-D AND 3-D MODEL RESULTS
FOR SITE B

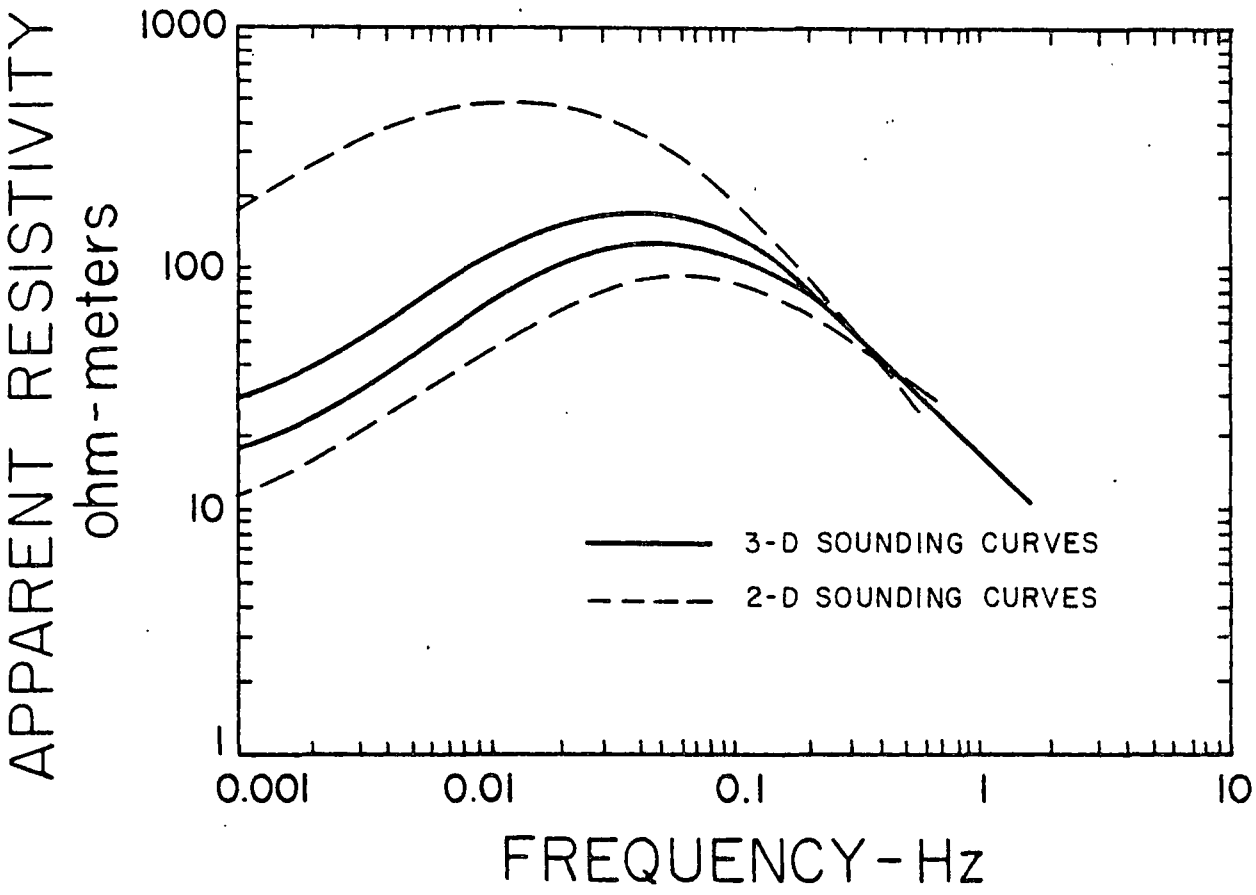


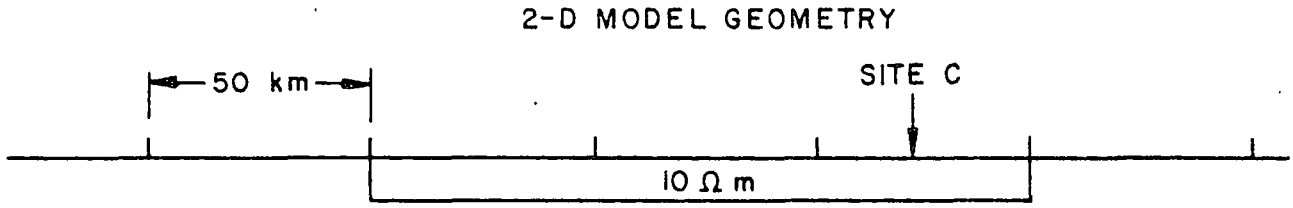


VERTICAL PROFILE AS IN MODEL OF FIGURE 1

FIGURE 34
2-D AND 3-D MODEL RESULTS
FOR SITE C

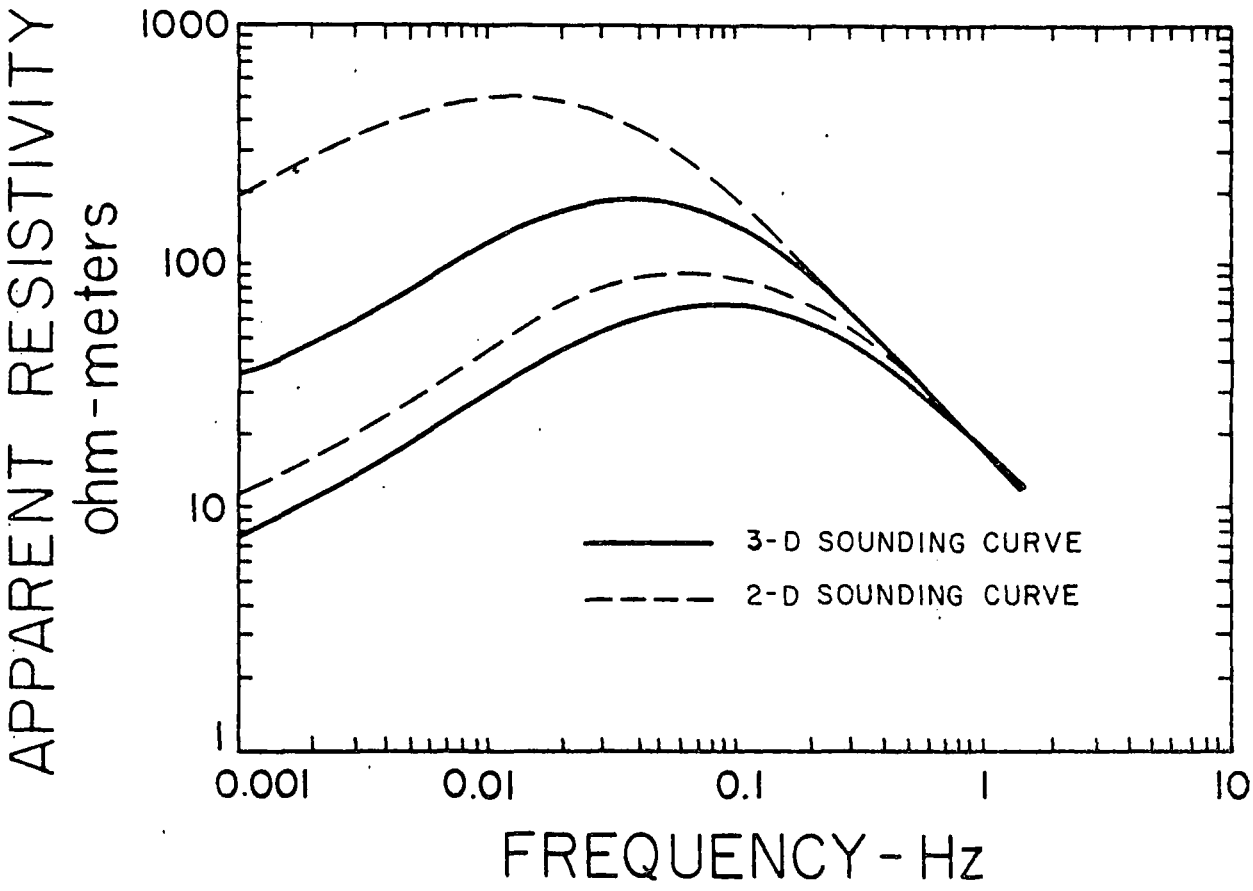


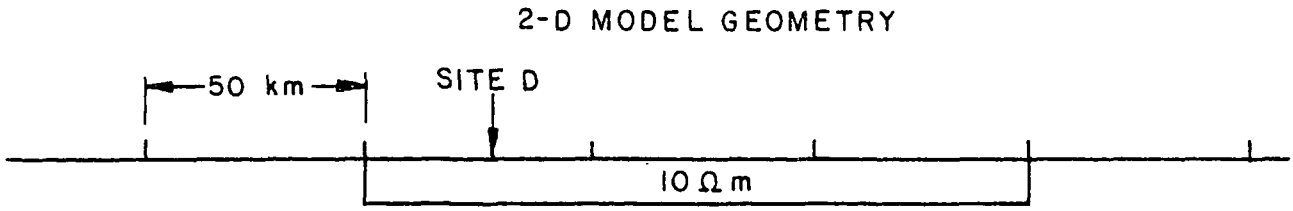


VERTICAL PROFILE AS IN MODEL OF FIGURE 1

FIGURE 35
2-D AND 3-D MODEL RESULTS
FOR SITE D

conclusion resulting from their model studies is that, for three-dimensional structures, interpretations based on one-dimensional inversions do not apply. Further, in many cases the TM two-dimensional interpretation will provide an acceptable interpretation.

Consider the example in Figure 36, which has been taken from the referenced report.[4] The model geometry shown on Figure 36 (designed around the constraints of the modeling program) consists of a 14 km wide by 1 km thick low resistivity (2 ohm-meter) body buried 1 km in 400 ohm-meter country rocks. The feature is shown in cross-section on the figure, and extends for 36 km along strike perpendicular to the plane of the section, as shown on the plan view. Apparent resistivities were computed for only three frequencies due to the lengthy calculation (20 hours per frequency) required.

Computed apparent resistivity curves are shown on Figure 37 for positions on and off the slab. Also shown are the "TE" and "TM" curves for a hypothetical two-dimensional model calculation assuming the slab to be infinitely long (in the 36 km direction). The similarity of the 3-D "TM" curves to the 2-D "TM" curve is apparent. It is also apparent that the 3-D "TE" curve does not agree with the 2-D "TE" curve, especially for site B on the conductive slab.

The utility of the TM 2-D solution in 3-D situations is a mixed blessing. On the one hand it allows the interpreter to relate field data to models that can be computed economically

conclusion resulting from their model studies is that, for three-dimensional structures, interpretations based on one-dimensional inversions do not apply. Further, in many cases the TM two-dimensional interpretation will provide an acceptable interpretation.

Consider the example in Figure 36, which has been taken from the referenced report.[4] The model geometry shown on Figure 36 (designed around the constraints of the modeling program) consists of a 14 km wide by 1 km thick low resistivity (2 ohm-meter) body buried 1 km in 400 ohm-meter country rocks. The feature is shown in cross-section on the figure, and extends for 36 km along strike perpendicular to the plane of the section, as shown on the plan view. Apparent resistivities were computed for only three frequencies due to the lengthy calculation (20 hours per frequency) required.

Computed apparent resistivity curves are shown on Figure 37 for positions on and off the slab. Also shown are the "TE" and "TM" curves for a hypothetical two-dimensional model calculation assuming the slab to be infinitely long (in the 36 km direction). The similarity of the 3-D "TM" curves to the 2-D "TM" curve is apparent. It is also apparent that the 3-D "TE" curve does not agree with the 2-D "TE" curve, especially for site B on the conductive slab.

The utility of the TM 2-D solution in 3-D situations is a mixed blessing. On the one hand it allows the interpreter to relate field data to models that can be computed economically

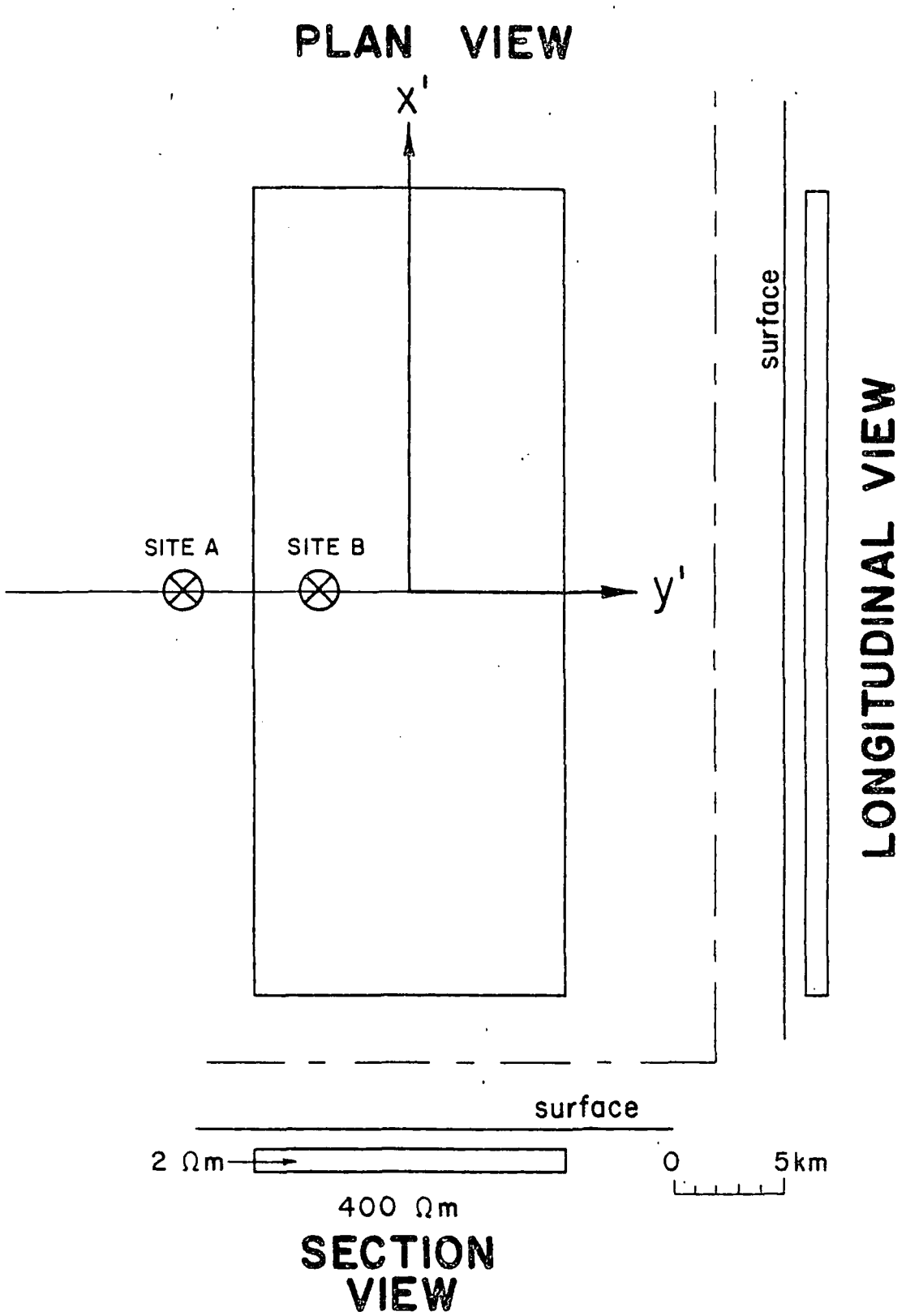


FIGURE 36. PLATE-LIKE CONDUCTIVE PRISM IN A CONDUCTING HALF-SPACE USED TO REPRESENT THE MILFORD VALLEY SEDIMENTARY FILL. DIMENSIONS MAY BE INFERRED FROM THE SCALE PROVIDED OR TAKEN FROM MAIN TEXT.

(FROM: "MT MODELS OF THE ROOSEVELT HOT SPRINGS THERMAL AREA, UTAH", Univ. OF UTAH REPORT No. DOE/ET/27002-8)

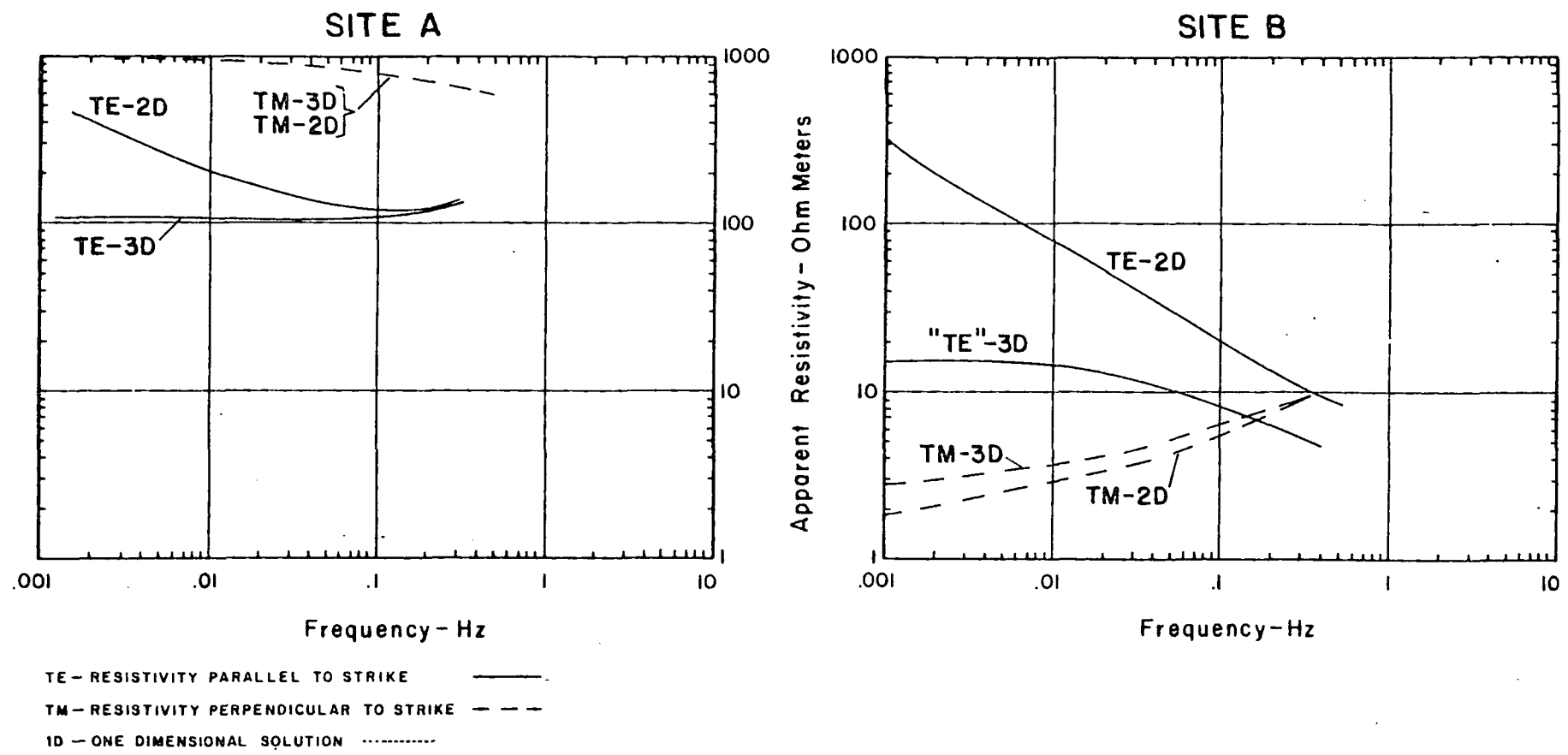


*(SEE FIGURE 10 FOR MODEL SKETCH)*

FIGURE 37

# THREE DIMENSIONAL MODEL

(the Utah three-dimensional MT models currently consume hours of large computer CPU time. The MIT program is more economical, but has limitations as to model geometry and resistivity values that can be accomodated). On the other hand, the TM solution can be extremely insensitive to structure. For the example of Figure 36, on the slab the TM (and 3-D) solution do not reflect the underlying 400 ohm-meter basement, and structure on the basement surface or intrabasement will be very difficult to locate.

As the three-dimensional structure elongates and begins to approximate the two-dimensional case, the "TE" component (electric field parallel to strike) begins to approximate the 2-D model TE component. This is a frequency dependent effect, with the higher frequencies reacting first as the along-strike dimension increases. To turn the previous statement around, the lower frequencies will continue to reflect the 3-D phenomena as the structure elongates long after the high frequencies approach the 2-D model curves. (This agrees with the MIT results discussed earlier.) Thus, extra caution is required at all times in interpreting the deeper events, especially where structural complexity is known to exist.

The severe effect of three-dimensional structures places additional constraints on the interpreter. Not only must the resistivity components be identified correctly, but the presence and nature of three-dimensional structure must be evaluated. Since an MT grid of sites capable of this

evaluation will rarely be economically possible, then geologic studies and gravity and magnetic data will have to play a large part in the interpretation.

In summary, magnetotelluric sounding curves generated by the MIT modeling program have shown how 3-D structures influence fields measured at the surface. Application of 1-D and 2-D modeling to data collected near 3-D structures can result in errors in the inferred structures. These errors can be severe in some instances. It is stressed again that an important observation based on our 3-D models is the occurrence of isotropic, 1-D <u>appearing</u> resistivity data near points of approximate symmetry of complex 3-D structures.

## IV. Summary

These notes have touched on a variety of potential problems facing the MT interpreter. The individual interpreter is encouraged to build a "case book" of two-dimensional models in order to be able to recognize gross structure through matching field data with "type" model curves. In the case of three-dimensional structure, the MT data can be strongly affected, and the recognition of these effects should be the first chore for the interpreter.

The necessity for a grid of closely spaced recording stations in complex areas should be apparent. The resolution of the "statics" problem and the recognition of two and three-dimensional effects all require data acquired more than just widely spaced along a single profile. Site density will be a function of economics and of the availability of other reconnaissance exploration data. The most economical site layout results from survey planning based on all available information and guided by reference to computed "case" models.

The models presented provide an insight into the MT interpretation process. In the case of simple "statics", the MT curves are separated but parallel and the interpretive problem is one of choosing the right curve to correct. The problem becomes more difficult when additional structural complexity is present on top of the statics shift, and selecting the curve or curves to correct will in most cases involve study of data in addition to the MT.

It has been shown that faults at or near the surface can result in extreme anisotropy, as do the related horsts and grabens. Interpretation in these cases is a two-dimensional process and relies heavily on mode identification. When approximating the true resistivity section by use of one-dimensional inversions, a good rule of thumb is "TE mode on the conductive side, TM on the resistive".

The above rule of thumb is also valid when considering overthrust models. For positive identification the interpretation of subthrust conductive units requires a resistivity minimum on the TM mode as well as on the TE, as a minimum on TE alone can be the result of solely a normal or high angle fault to the surface.

Three-dimensional effects can be severe, in many 3-D cases the TE mode as defined for the 2-D case does not exist and interpretations relying on TE inversions will be seriously in error. In other cases isotropic, one-dimensional appearing MT data may be present in the vicinity of complex, two-dimensional structure. With 3-D modeling in its infancy, the interpreter in 3-D situations may be able to rely on proper use of a TM-mode based interpretation or on application of corrections to both curves if the effect can be identified. For surveys where 3-D effects are anticipated, the interpretation will be aided by planning as high a site density as possible, and by utilizing all of the ancillary geologic geophysical data available.

# CONDUCTIVE DIKE SERIES: CEBORUCO MODEL 2A

# PLATE M-1

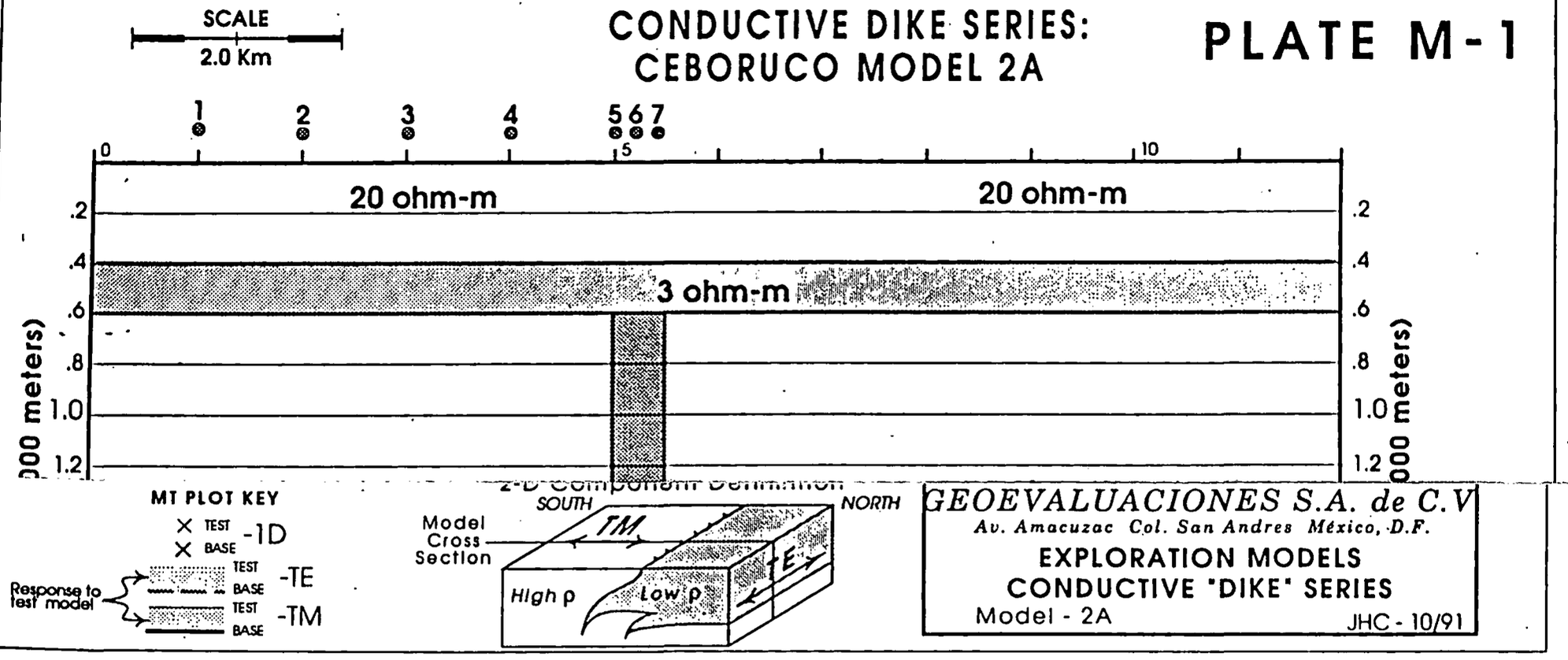


GEOEVALUACIONES S.A. de C.V
Av. Amacuzac Col. San Andres México, D.F.

EXPLORATION MODELS
CONDUCTIVE "DIKE" SERIES
Model - 2A

JHC - 10/91

# CONDUCTIVE DIKE SERIES: CEBORUCO MODEL 3A

# PLATE M-2

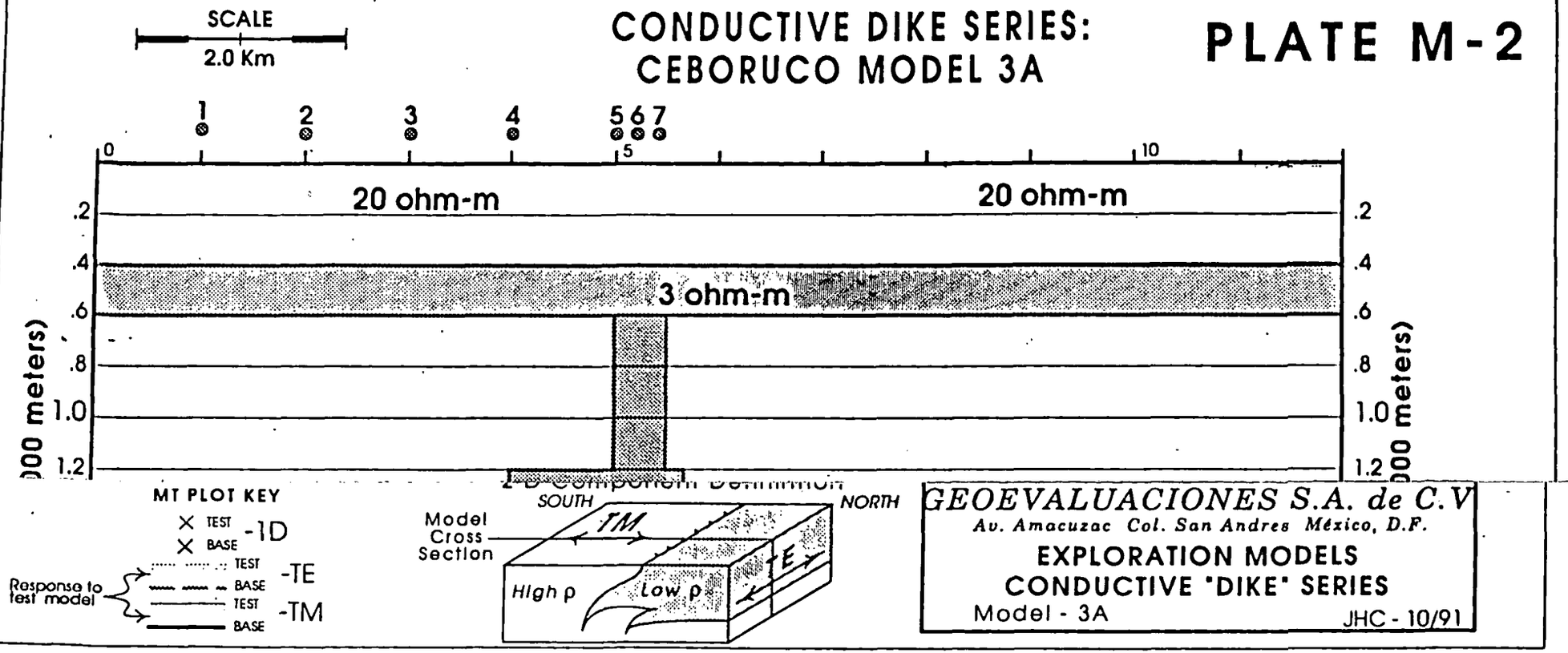


GEOEVALUACIONES S.A. de C.V
Av. Amacuzac Col. San Andres México, D.F.

EXPLORATION MODELS
CONDUCTIVE "DIKE" SERIES
Model - 3A

JHC - 10/91

# CONDUCTIVE DIKE SERIES: CEBORUCO MODEL 4A

# PLATE M-3

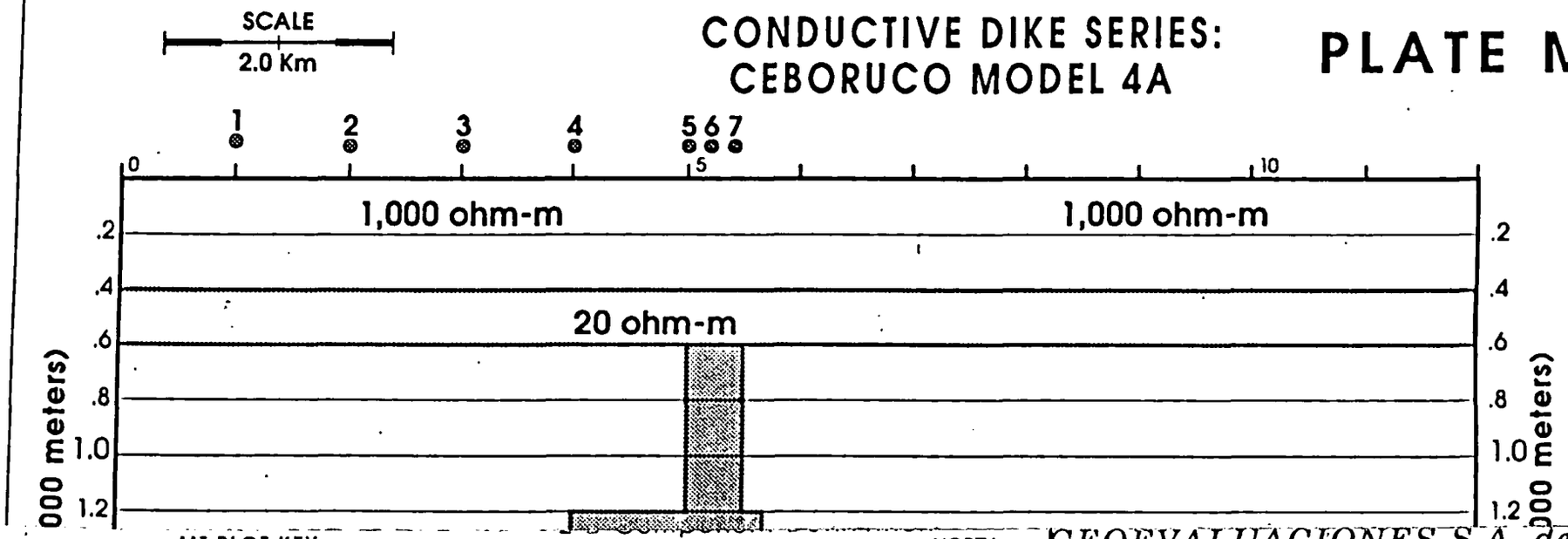


MT PLOT KEY

× TEST
× BASE
-1D

Response to test model

TEST
BASE
-TE

TEST
BASE
-TM

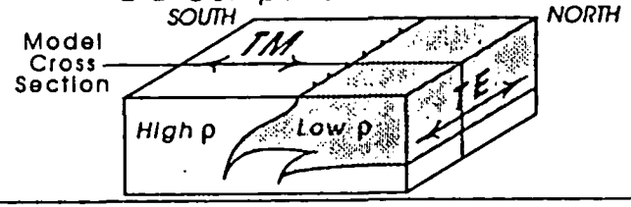



*GEOEVALUACIONES S.A. de C.V*

*Av. Amacuzac Col. San Andres México, D.F.*


EXPLORATION MODELS
CONDUCTIVE "DIKE" SERIES

Model - 4A

JHC - 10/91

# CONDUCTIVE DIKE SERIES: CEBORUCO MODEL 5A

# PLATE M-4

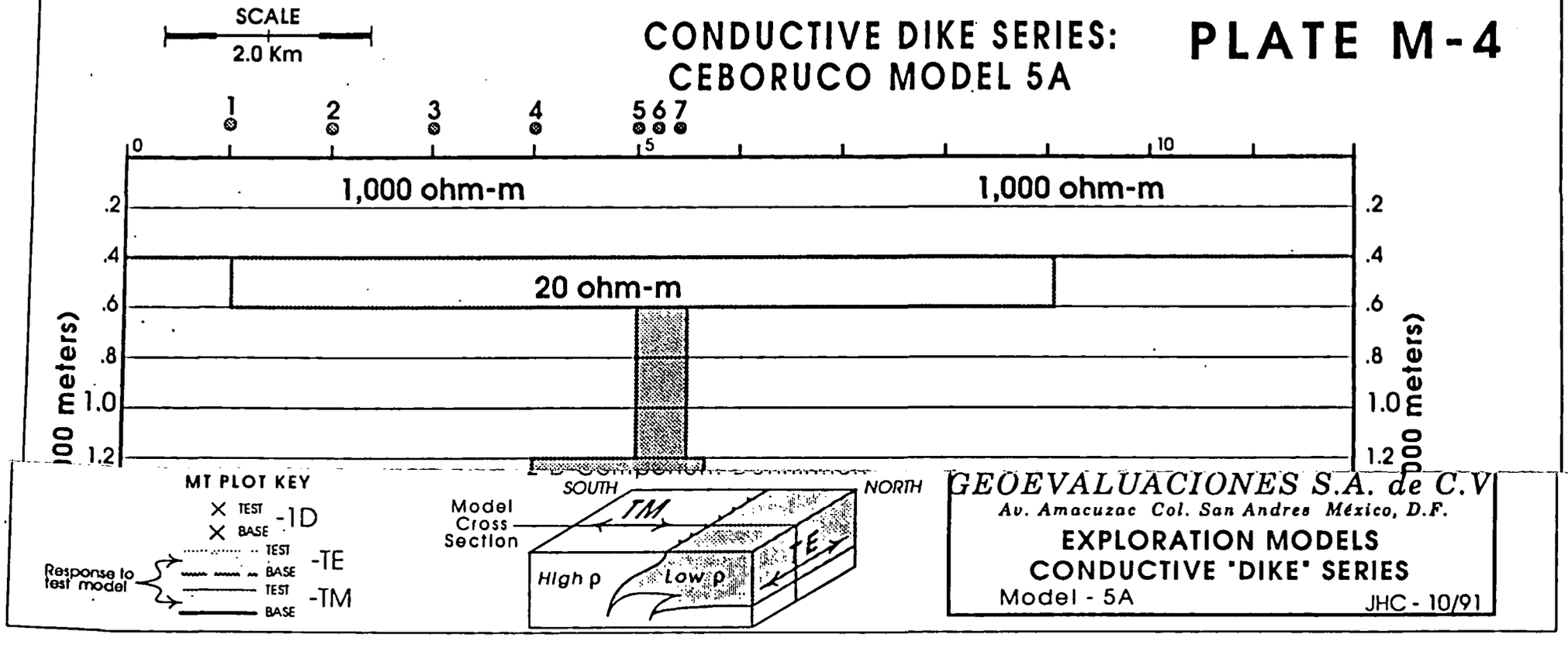



GEOEVALUACIONES S.A. de C.V
Av. Amacuzac Col. San Andres México, D.F.


EXPLORATION MODELS
CONDUCTIVE "DIKE" SERIES
Model - 5A

JHC - 10/91

# CONDUCTIVE DIKE SERIES: CEBORUCO MODEL 6A

# PLATE M-5

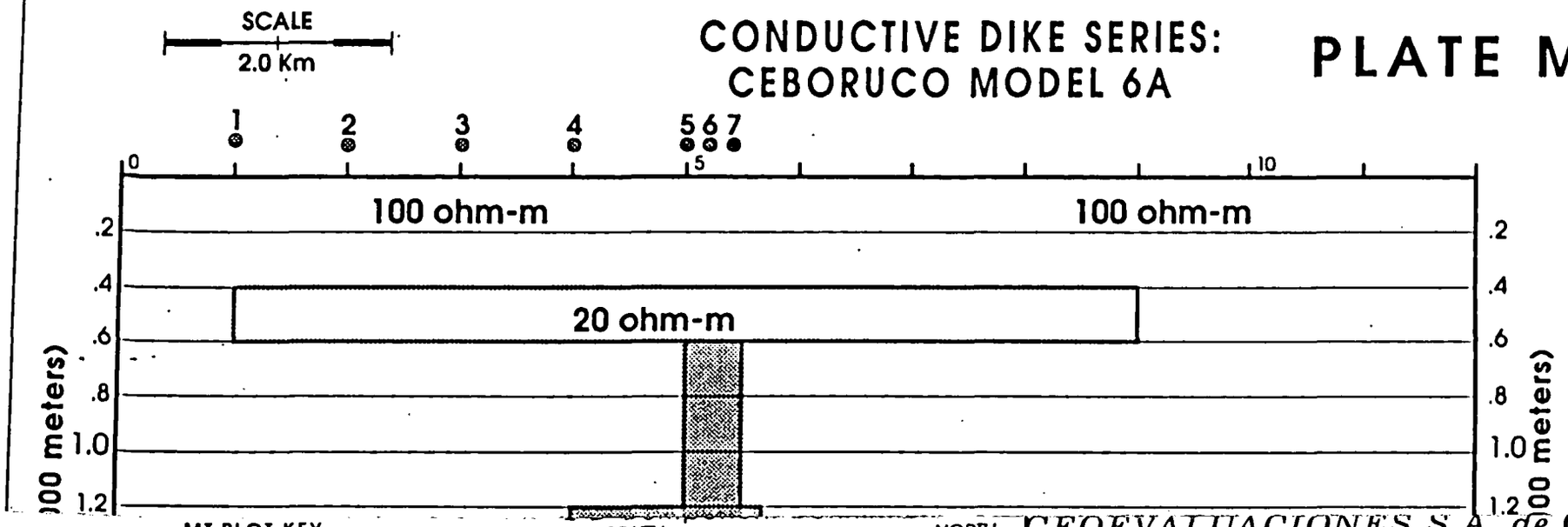


MT PLOT KEY

× TEST
× BASE
-1D

Response to test model

TEST
BASE
-TE

TEST
BASE
-TM

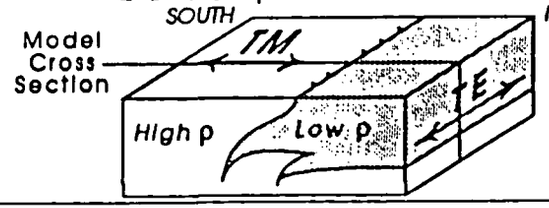



GEOEVALUACIONES S.A. de C.V
Av. Amacuzac Col. San Andres México, D.F.


EXPLORATION MODELS
CONDUCTIVE "DIKE" SERIES

Model - 6A

JHC - 10/91

# CONDUCTIVE DIKE SERIES: CEBORUCO MODEL 7A

# PLATE M-6

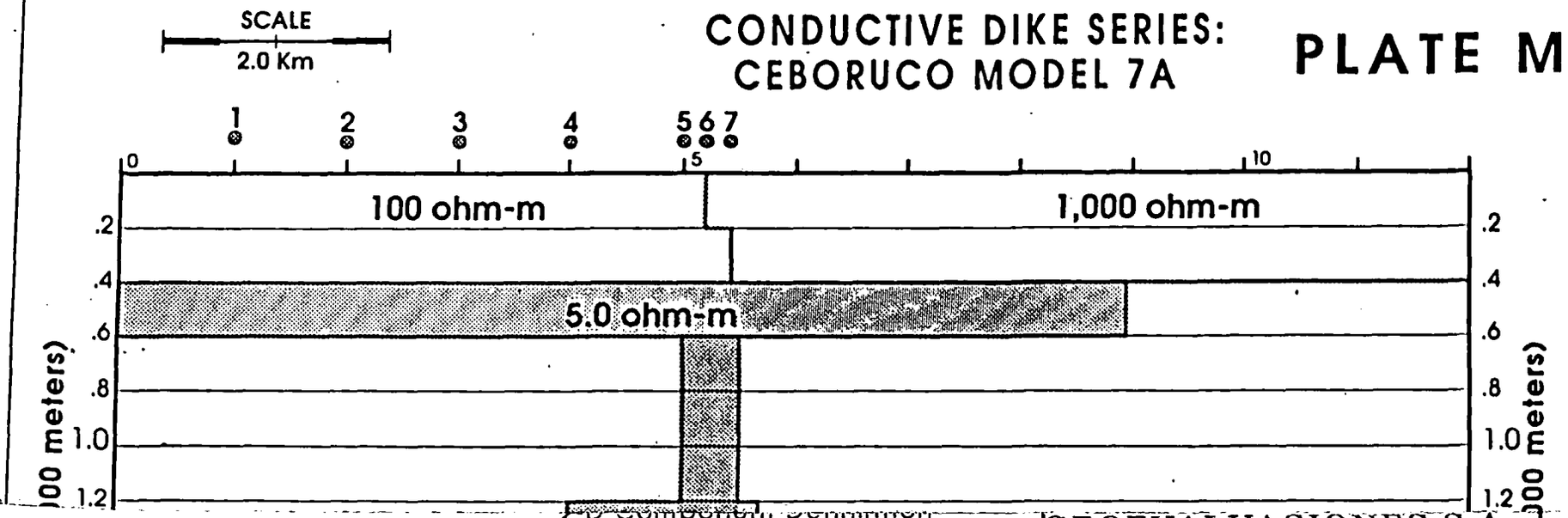


MT PLOT KEY

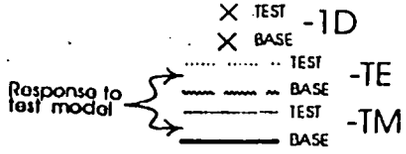


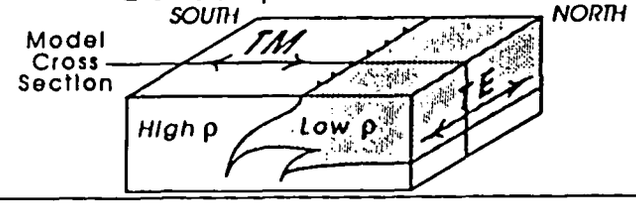



*GEOEVALUACIONES S.A. de C.V*

*Av. Amacuzac Col. San Andres México, D.F.*


**EXPLORATION MODELS**
**CONDUCTIVE "DIKE" SERIES**

Model - 7A

JHC - 10/91

# CONDUCTIVE DIKE SERIES: CEBORUCO MODEL 8A

# PLATE M-7

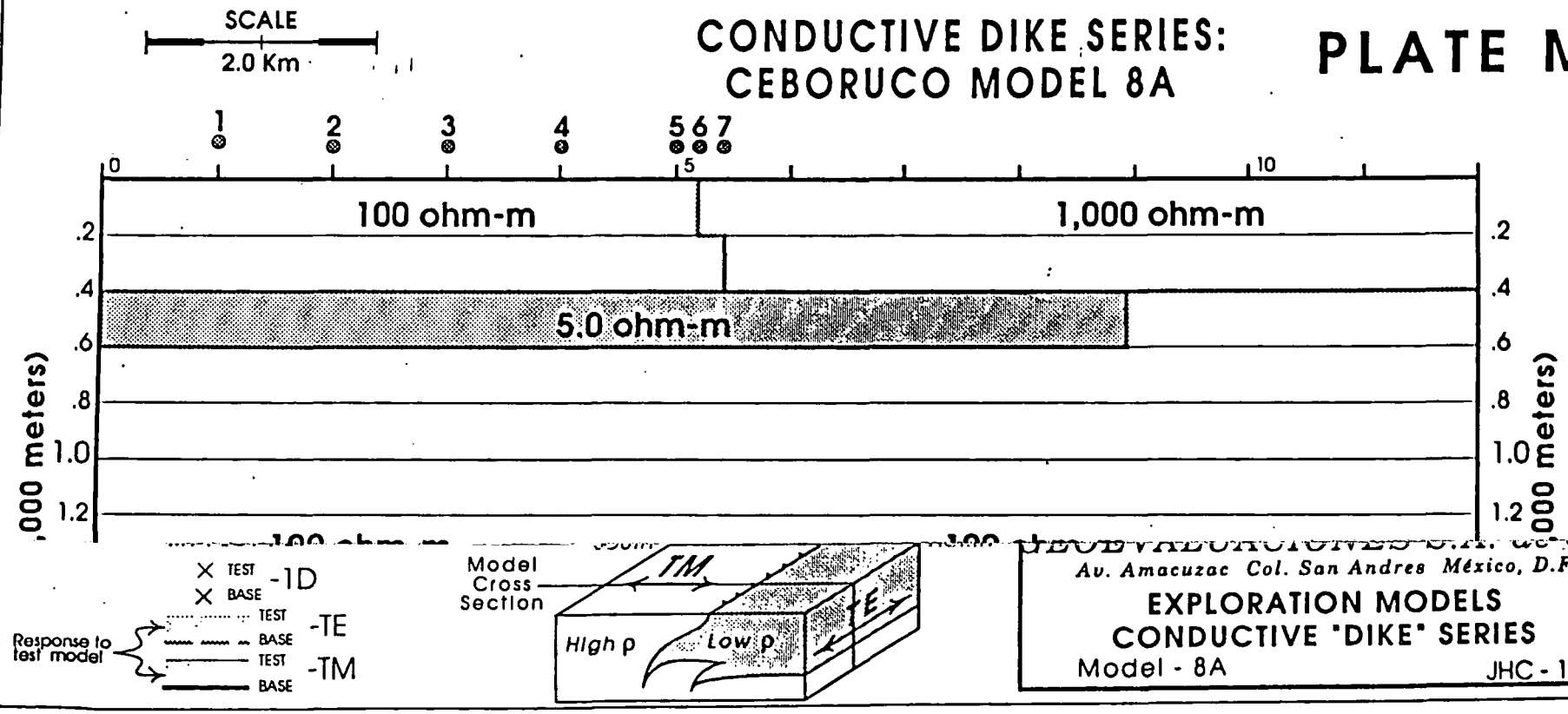



Av. Amacuzac Col. San Andres México, D.F.


**EXPLORATION MODELS**
**CONDUCTIVE "DIKE" SERIES**

Model - 8A

JHC - 10/91

# CONDUCTIVE DIKE SERIES: CEBORUCO MODEL 9A

# PLATE M-8

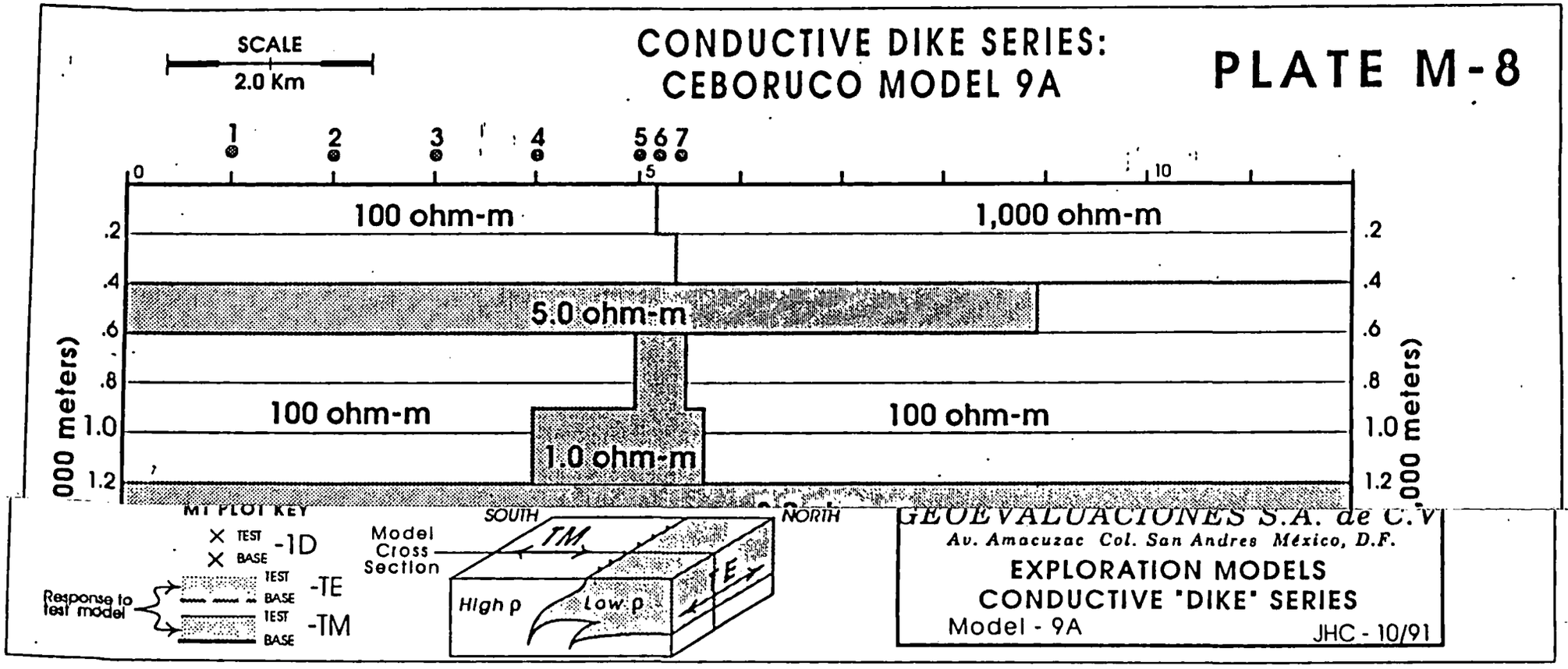


GEOEVALUACIONES S.A. de C.V
Av. Amacuzac Col. San Andres México, D.F.

EXPLORATION MODELS
CONDUCTIVE "DIKE" SERIES
Model - 9A

JHC - 10/91

# CONDUCTIVE DIKE SERIES: CEBORUCO MODEL 10A

# PLATE M-9

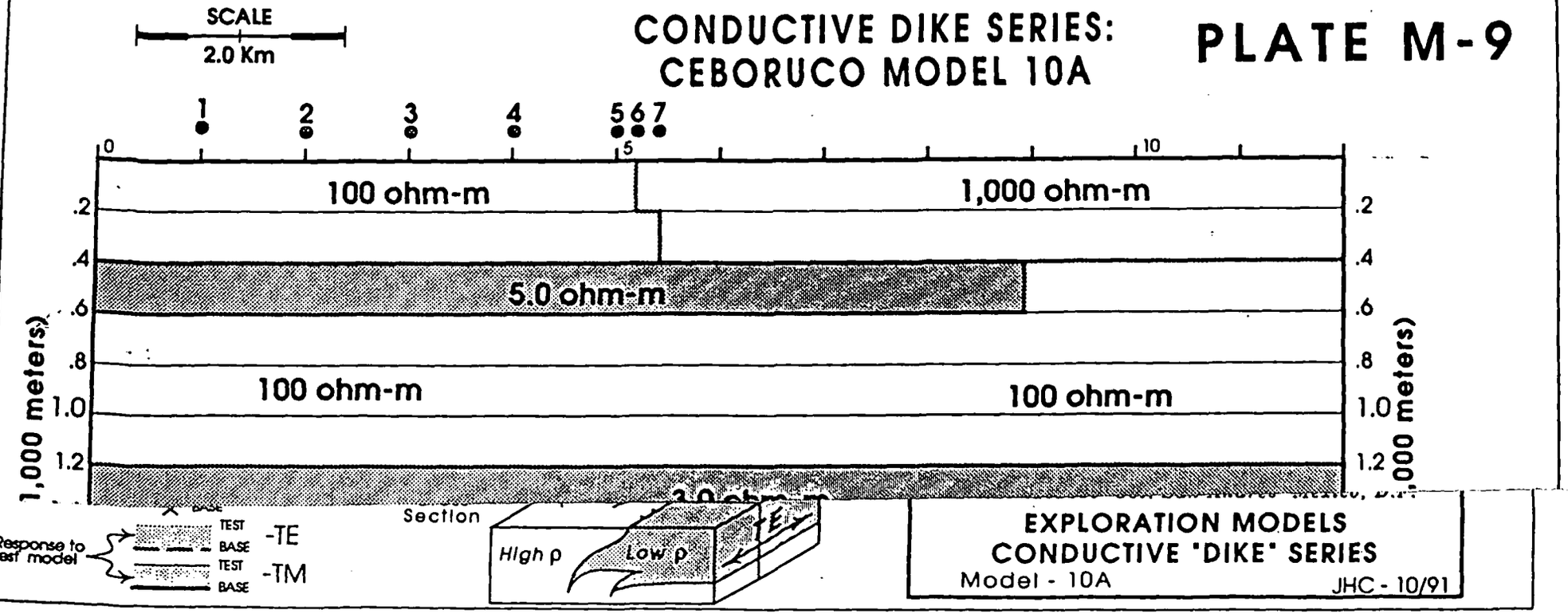


**EXPLORATION MODELS**
**CONDUCTIVE "DIKE" SERIES**
Model - 10A
JHC - 10/91

# PLATE M-10

## CONDUCTIVE DIKE SERIES: CEBORUCO MODEL 11A

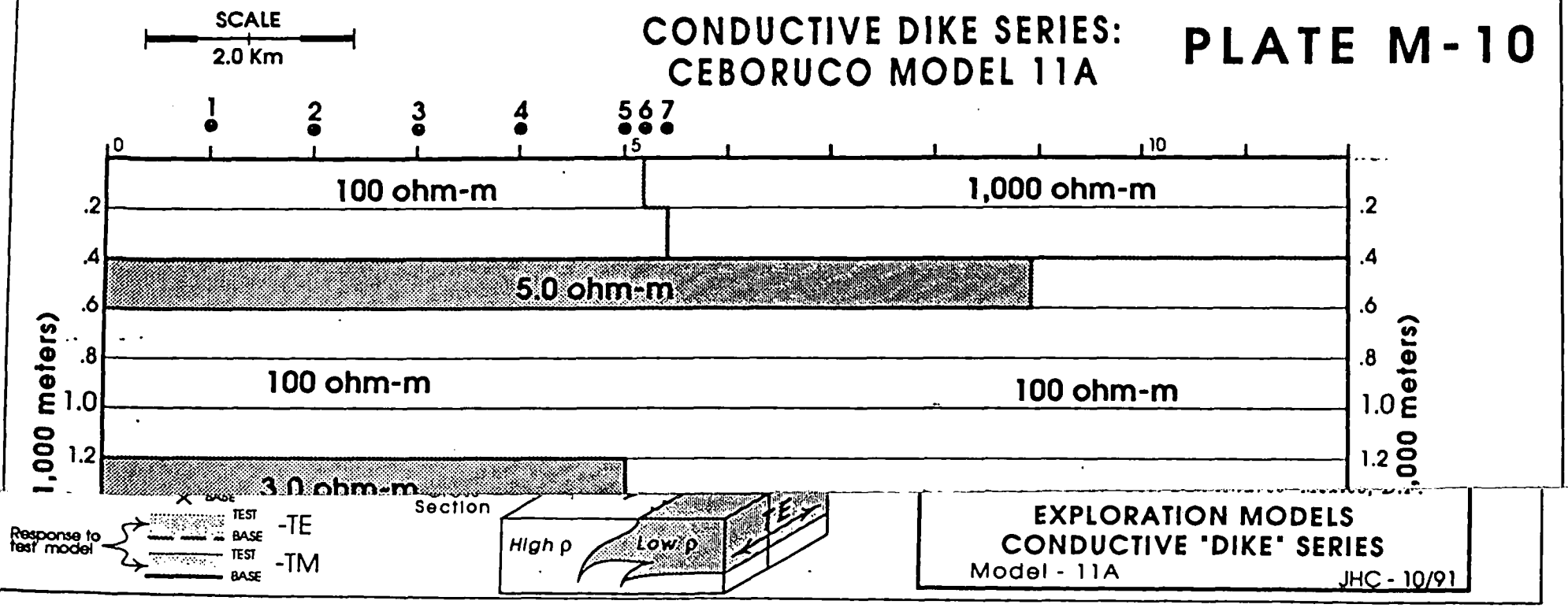


**EXPLORATION MODELS**
**CONDUCTIVE "DIKE" SERIES**
Model - 11A

JHC - 10/91

# CONDUCTIVE DIKE SERIES: CEBORUCO MODEL 11B

# PLATE M-11

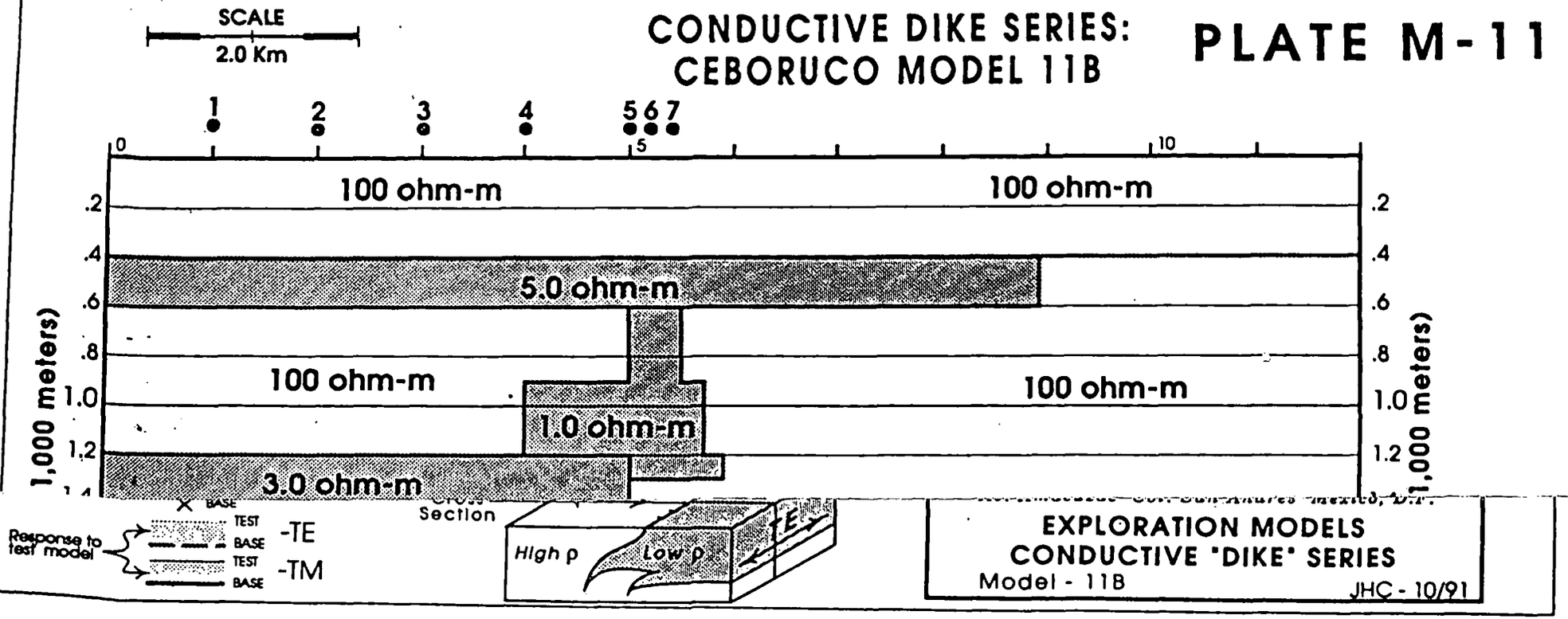


**EXPLORATION MODELS**
**CONDUCTIVE "DIKE" SERIES**
Model - 11B

JHC - 10/91

# CONDUCTIVE DIKE SERIES: CEBORUCO MODEL 11C

# PLATE M-12

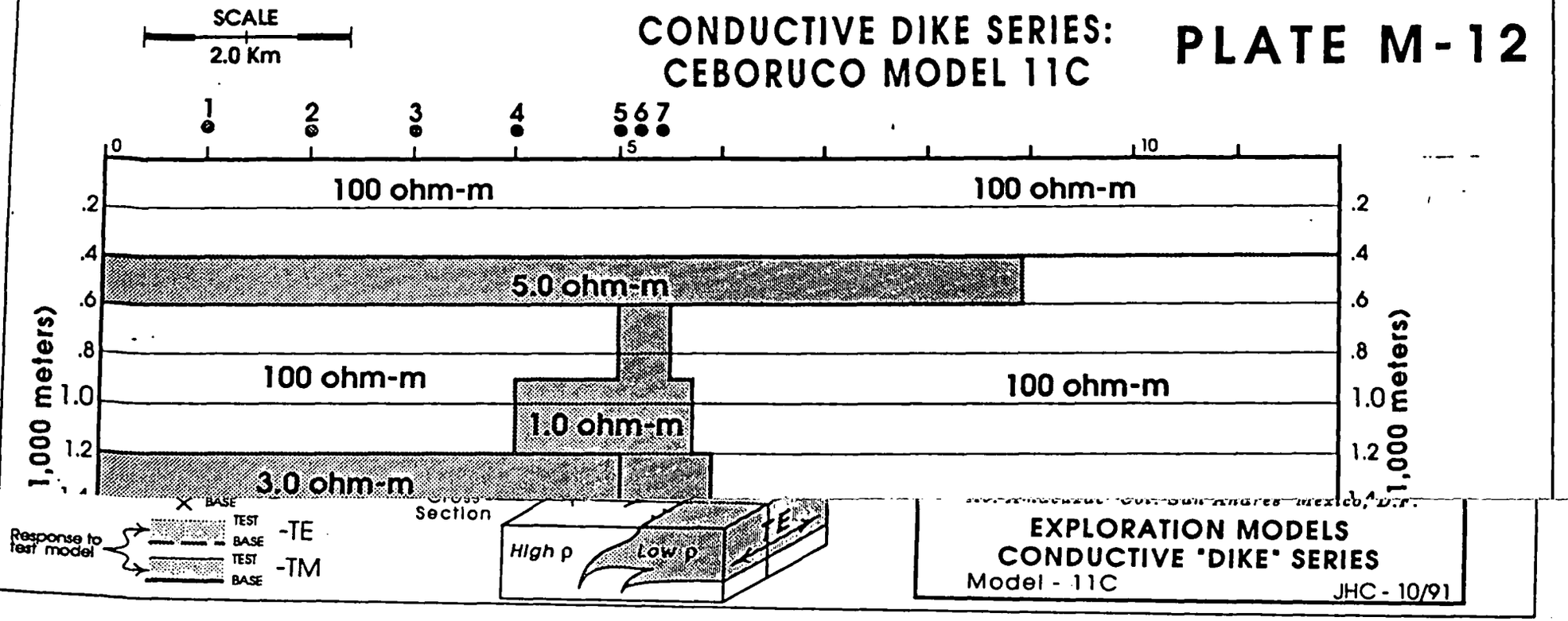


EXPLORATION MODELS
CONDUCTIVE "DIKE" SERIES
Model - 11C

JHC - 10/91

# PLATE M-14

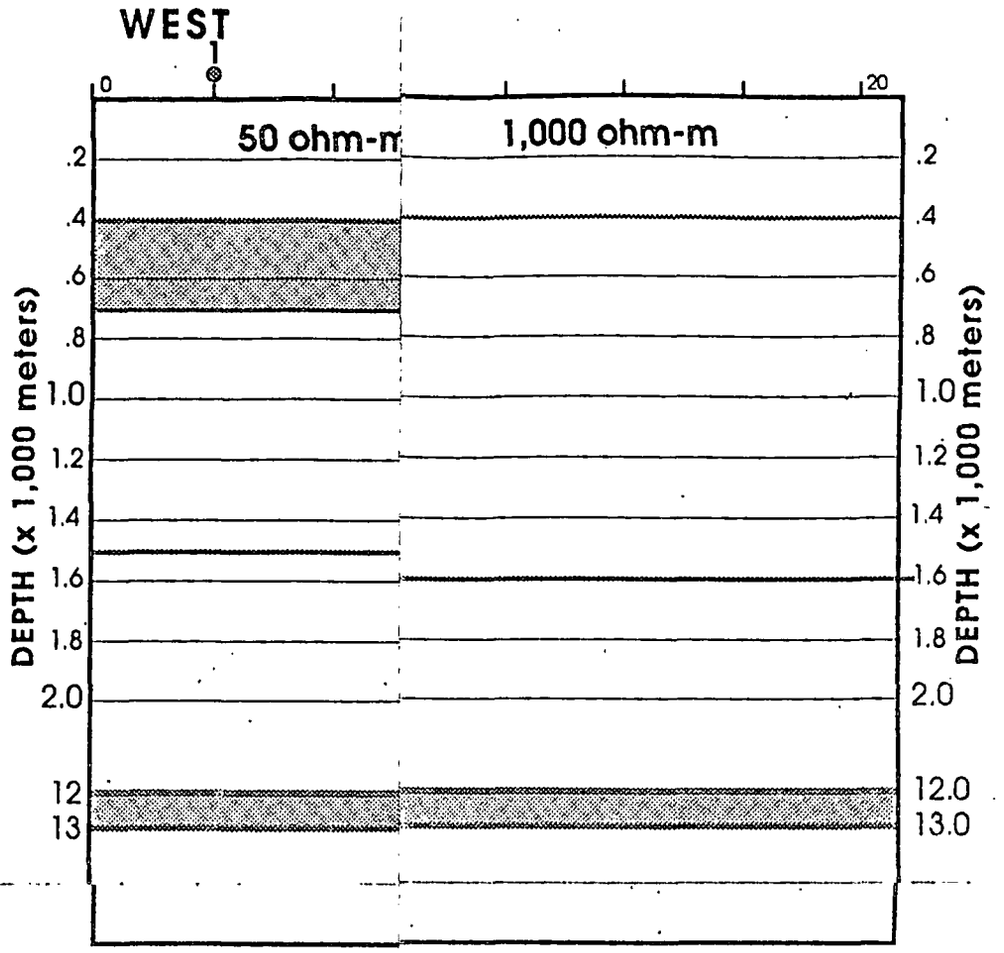


**CALCULATED RESPONSE:**
**Ceboruco Model 13**

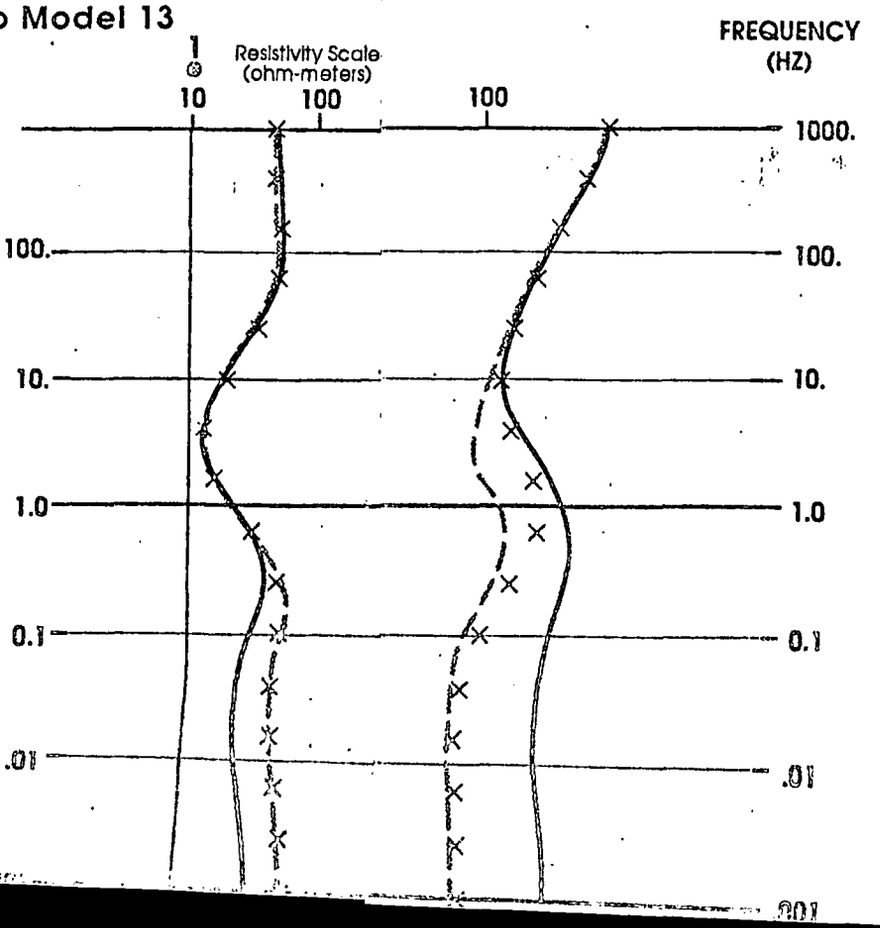

# PLATE M-15

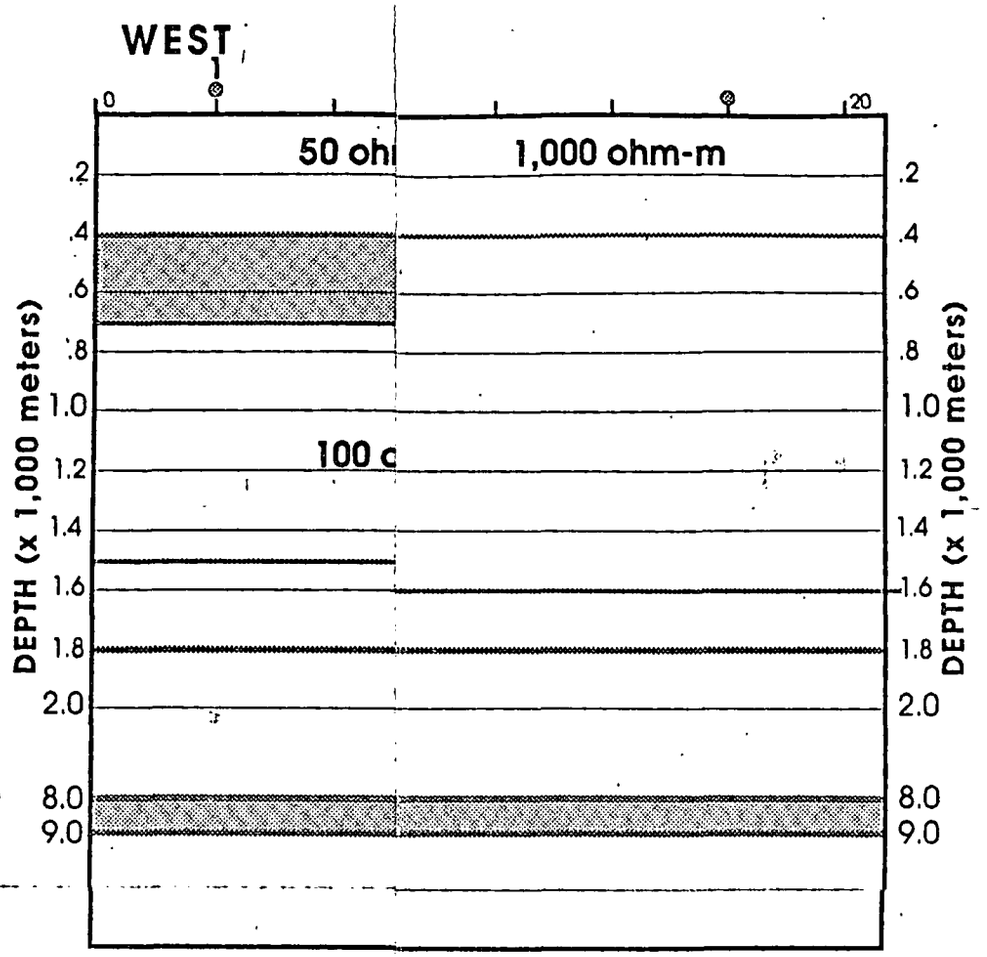


**CALCULATED RESPONSE:**
**Ceboruco Model 14**

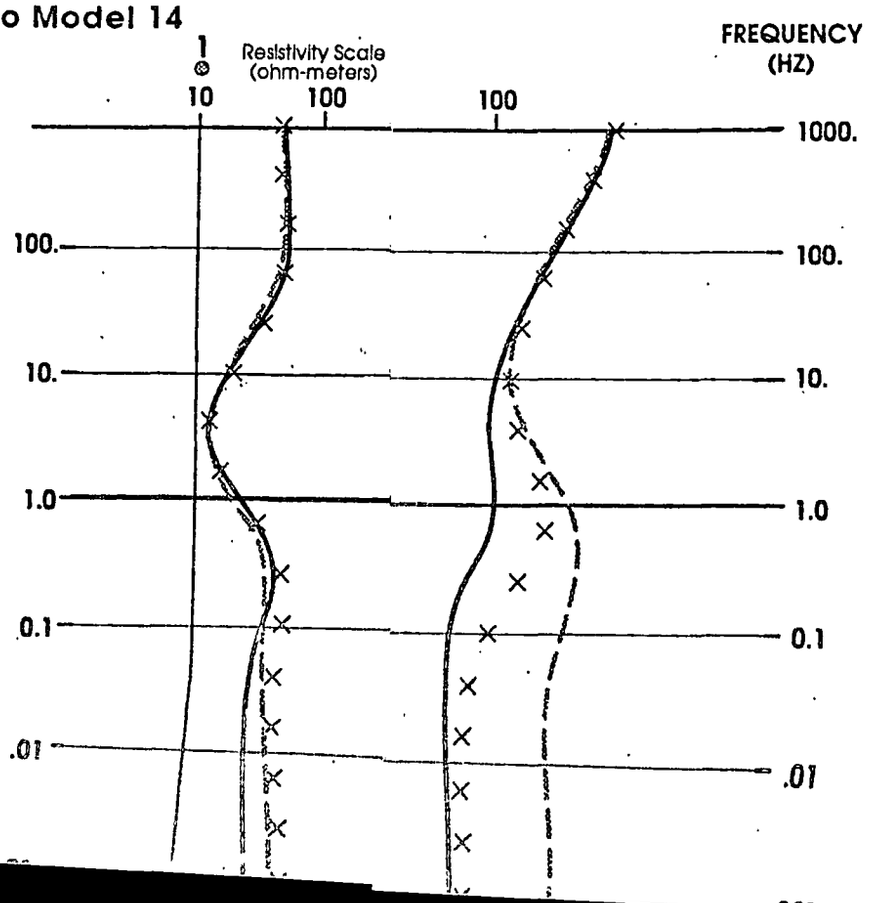

# PLATE M-16

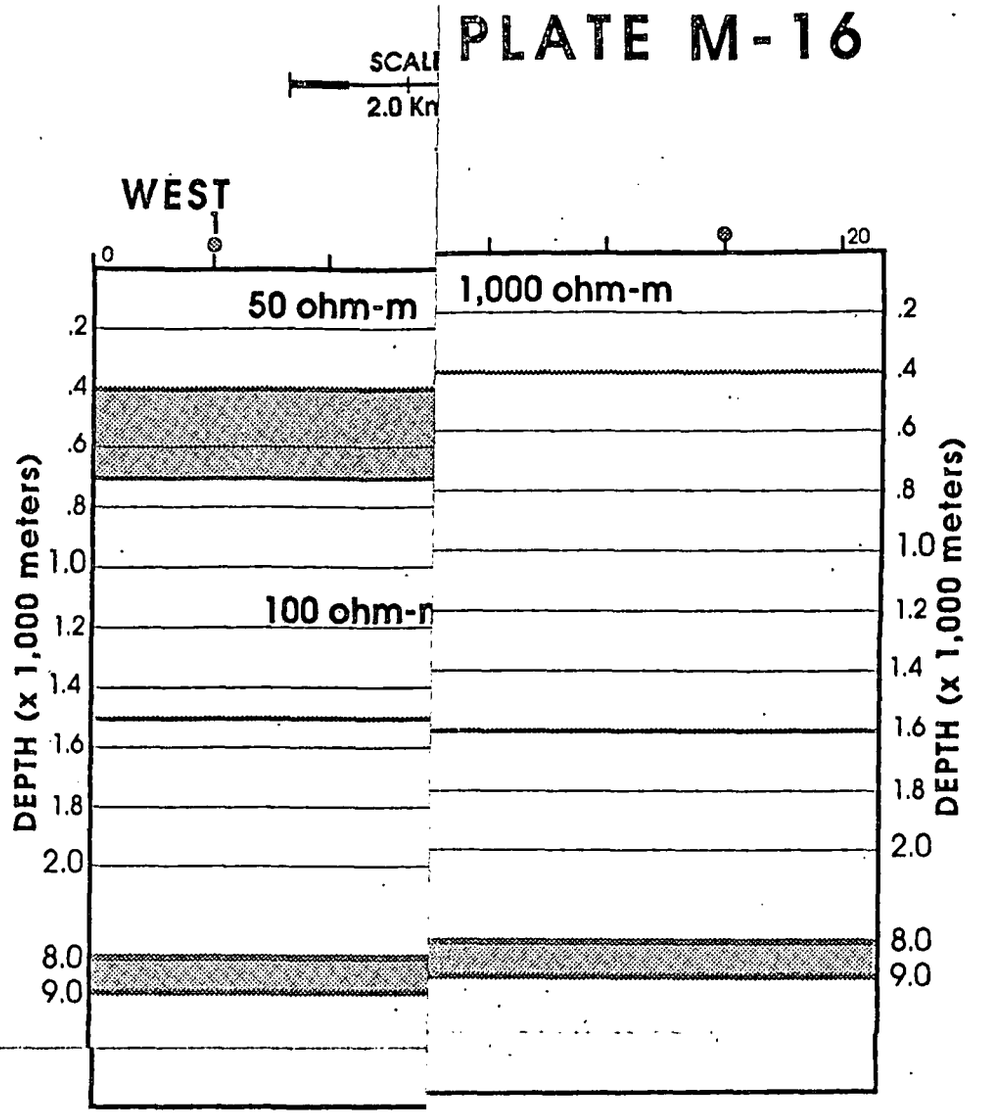


**CALCULATED RESPONSE:**
**Ceboruco Model 15**

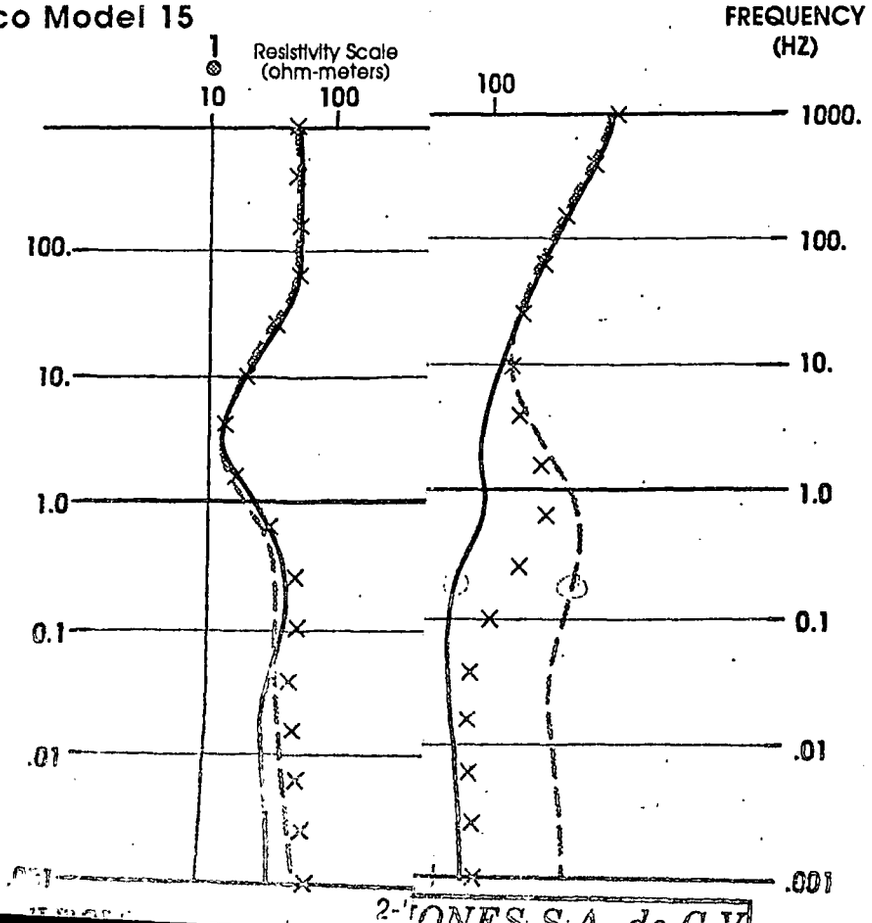

# PLATE M-17

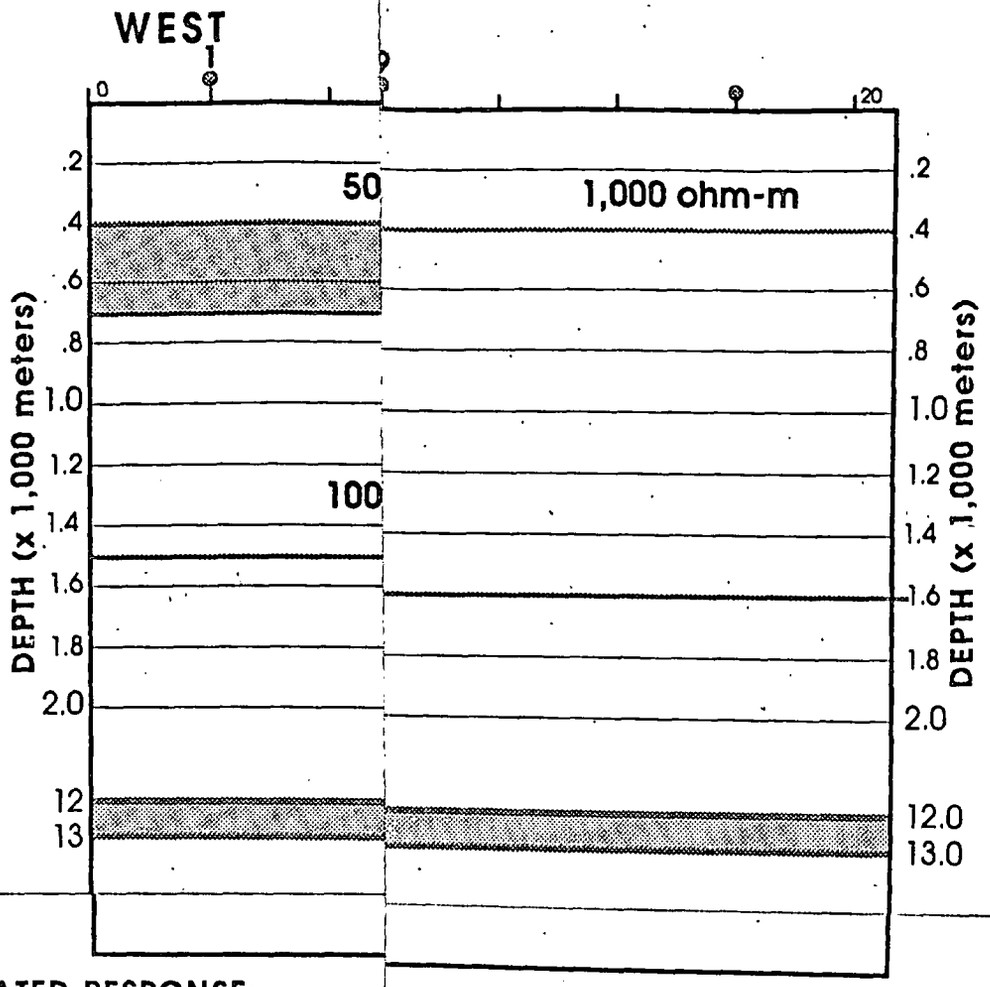


**CALCULATED RESPONSE:**
**Ceboruco Model 16**

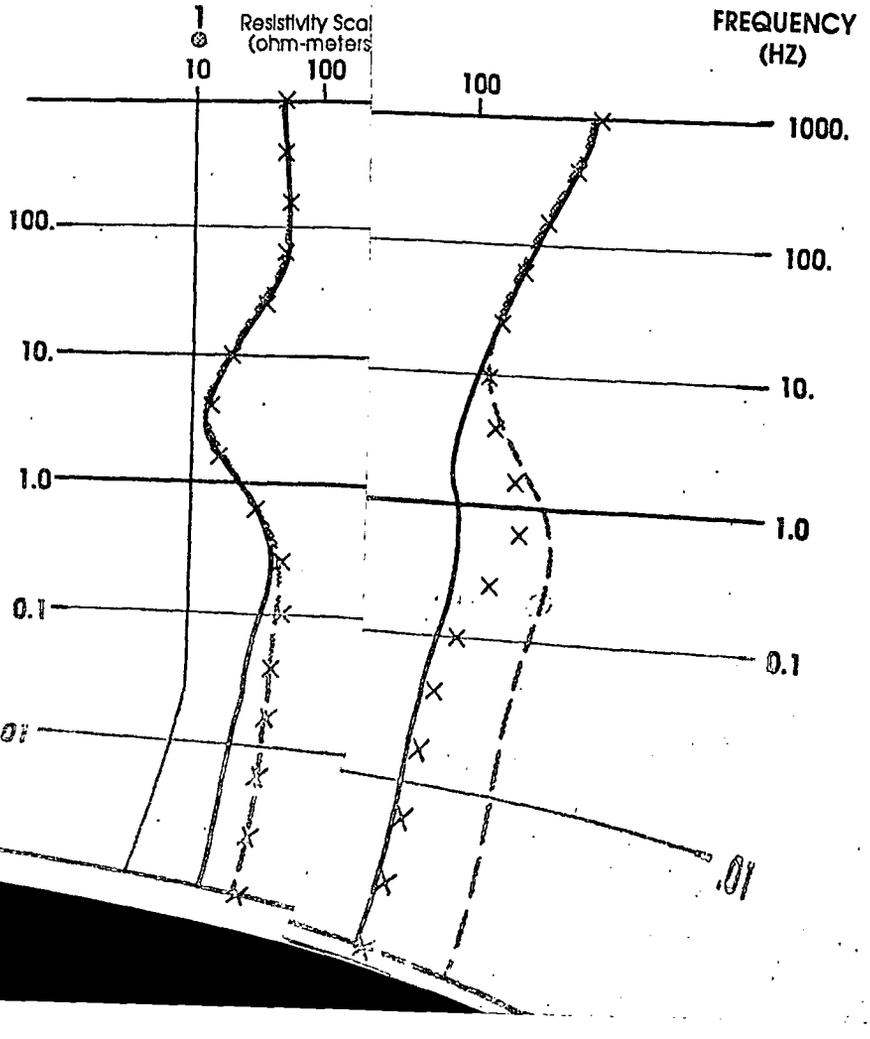

# PLATE M-18

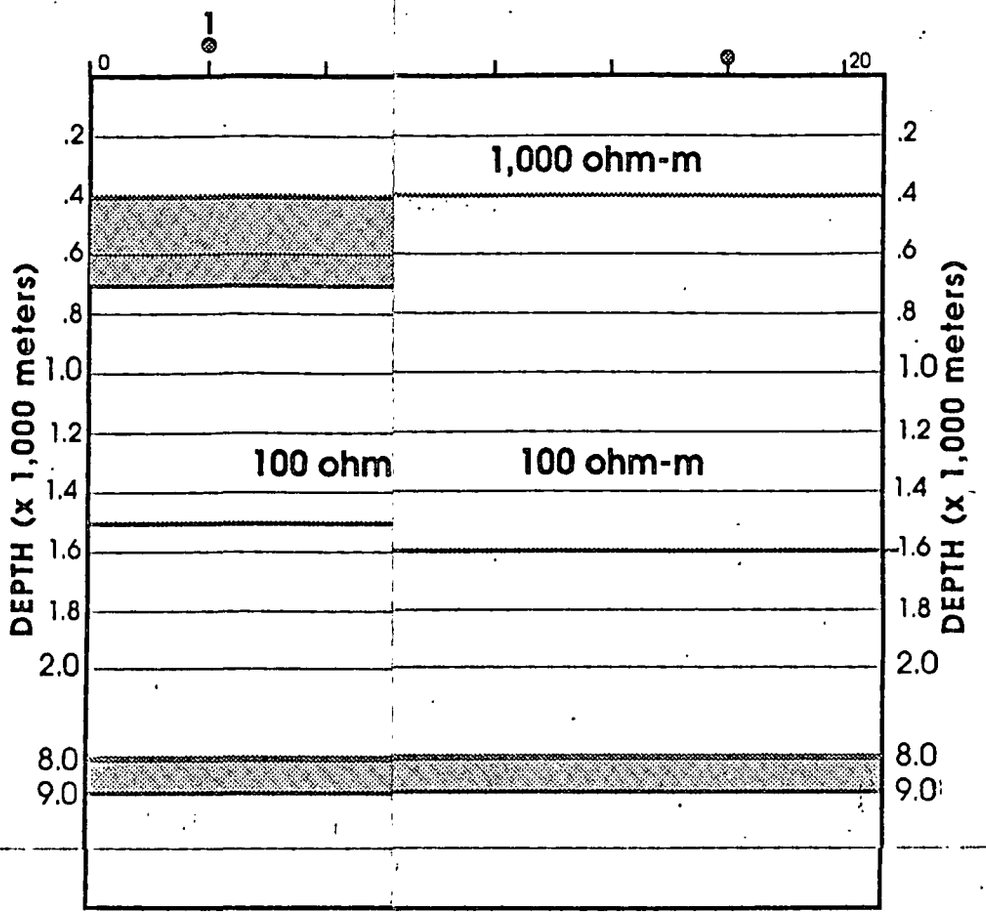


**CALCULATED RESPONSE:**
**Ceboruco Model 17**

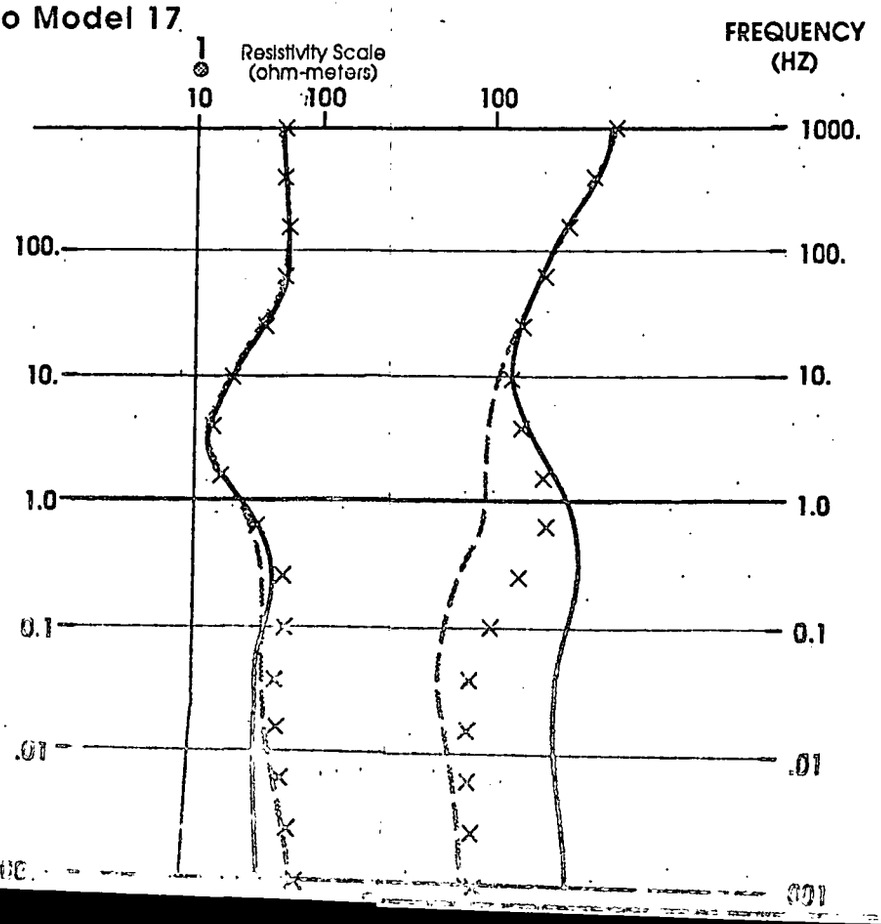

SC
2.0

# PLATE M-19

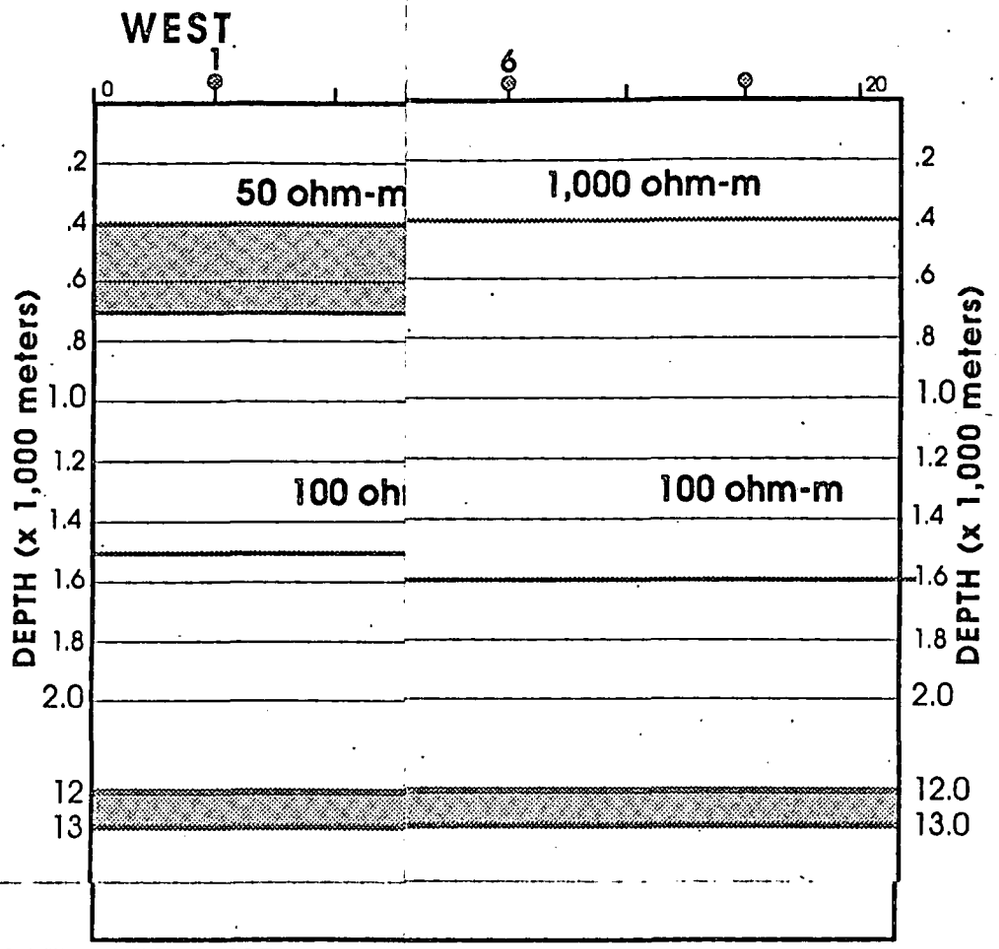


**CALCULATED RESPONSE:**
**Ceboruco Model 18**

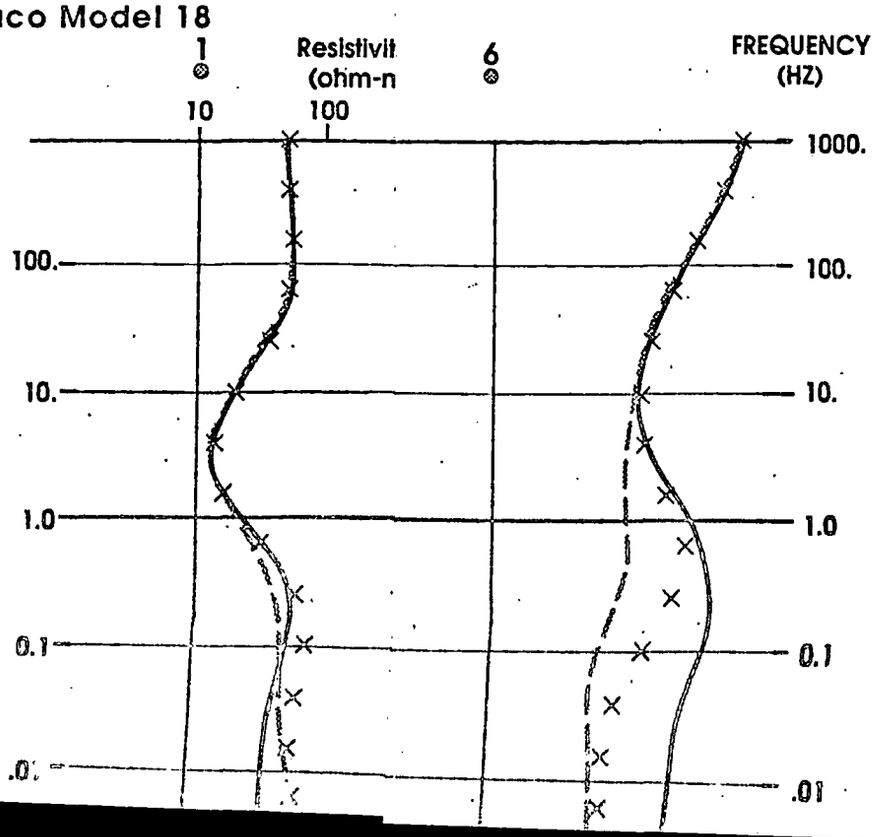

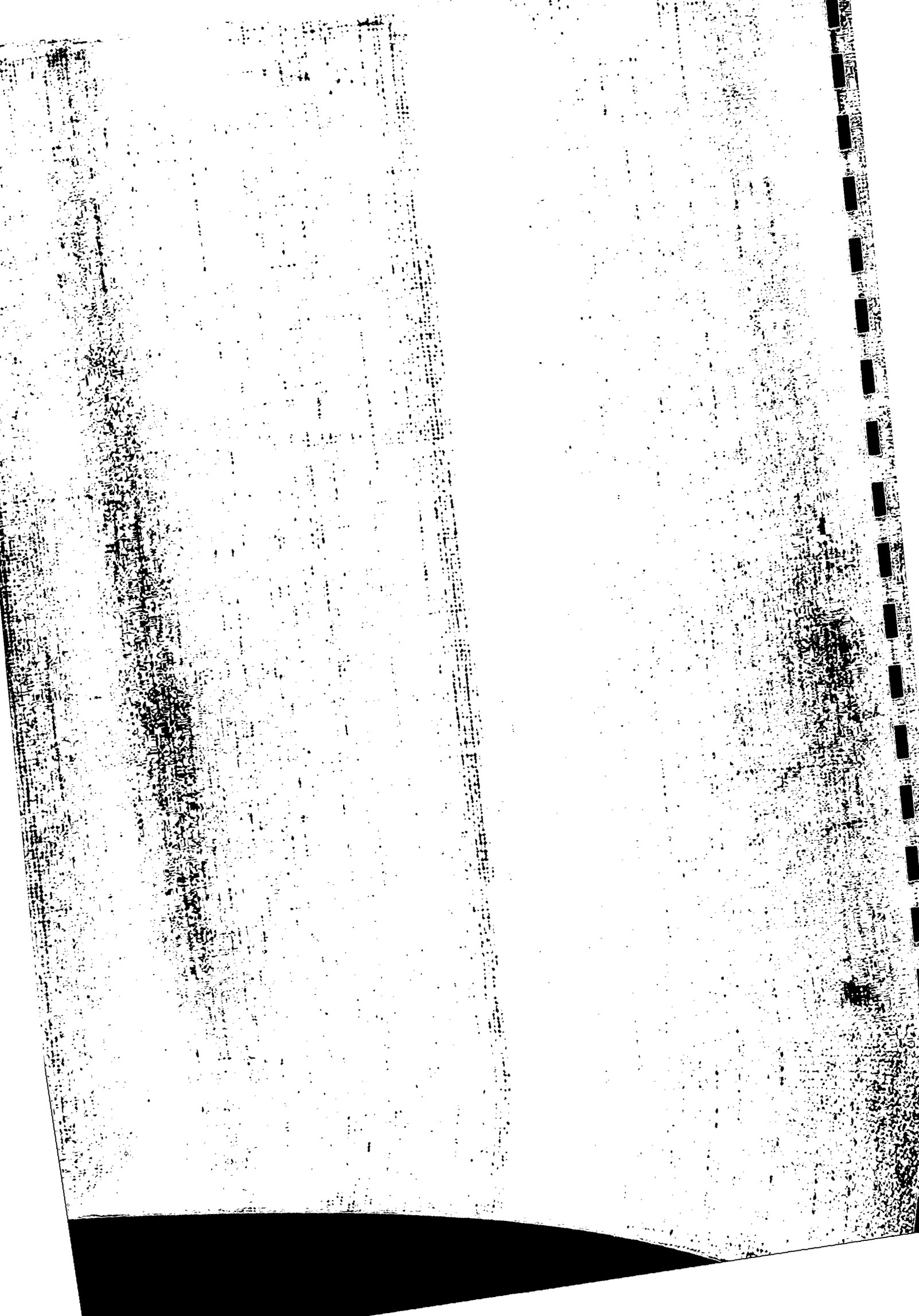

# FINAL REPORT
# CEBORUCO-DOMO DE SAN PEDRO
# MAGNETOTELLURIC SURVEY
# NAYARIT, MEXICO

by:
JEFFREY H. COPLEY
ARNOLD S. ORANGE

# FINAL REPORT

# CEBORUCO - DOMO de SAN PEDRO MAGNETOTELLURIC SURVEY

# NAYARIT, MÉXICO

Prepared For

COMISION FÉDERAL de ELECTRICIDAD
MORELIA, MICHOACAN

NOVEMBER 1991

by:
JEFFREY H. COPLEY
ARNOLD S. ORANGE

GEOEVALUACIONES S.A. de C.V.
Av. Amacuzac 615
Col. San Andrés Tetepilco
México, D.F.

# CEBORUCO - DOMO de SAN PEDRO MAGNETOTELLURIC SURVEY

## ABSTRACT - SUMMARY OF THE PROJECT AND RESULTS

A magnetotelluric (MT) survey was performed during July through September, 1991 for the Comision Federal de Electricidad (CFE) in the Ceboruco-Domo de San Pedro area of Nyarit, México (Figure 1). The MT acquisition program was initiated as part of a regional exploration program for geothermal reservoirs by CFE. A 90 site program was planned and data acquisition initiated at the end of June, 1991. MT data were actually acquired at 93 locations (Plate 1). Preliminary model studies and industry experience indicated that low resistivity zones characteristic of geothermal reservoirs would be detected by the MT method. A DC resistivity study using the Schlumberger method was performed by CFE prior to the decision to employ MT in this area and the areas of lower resistivity identified by the DC resistivity program selected as the initial areas of interest for the MT program.

MT data were acquired using the remote reference technique of data acquisition. Data acquisition and processing followed accepted industry practice for geothermal exploration. Time domain electromagnetic (TDEM) data were acquired at the MT site locations to assist in providing MT statics corrections. The data interpretation utilized one-, two-, and three-dimensional analysis techniques. The results are presented in a series of maps and cross-sections, and described in this report.

The interpretation of the MT data identifies three major areas where anomalous low resistivity zones possibly related to geothermal zones may exist. These primary areas of interest identified in the MT data are A) North Ceboruco, B) Amado Nervo, and C) San Pedro. The anomalous zones are relatively shallow, with the top probably less than 1 km subsurface, and with a vertical extent probably of the order of one to three kilometers. The vertical extent of the anomalies is poorly resolved by the MT data. Each of these areas was

identified by a characteristic response predicted by a series of two-dimensional MT models. The models were designed based on the assumption that a geothermal reservoir within the geologic context of the survey area will be characterized by a low resistivity zone with a strong resistivity contrast between it and the surrounding, more resistive, units. The identification of these "anomalous" areas is an observation from the processed data. The interpretation of the anomalous areas as being related to a geothermal zone is a subjective judgement based on detailed model studies and experience.

There are no indications in the MT results of any significant intra-basement low resistivity anomalies that might be related to a magma chamber or other deep feature of importance to the interpretation.

In addition to the anomalous areas, the MT data define a subsurface low resistivity body about 35 km long by 15 km wide extending from the Jala/Ahuacatlan area west to San Pedro and Cerro Pelon. The zone has an average thickness of 200-400 meters and a depth to the base of the unit of about 1 km. The low resistivities are representative of a primarily volcaniclastic and mixed-continental sedimentary section, although other lithologies such as alteration and erosional products will exhibit similar resistivities. A high resistivity basement is observed beneath the low resistivity body at all locations. The electrical basement is probably a complex assemblage of very low porosity volcanic and metamorphic rocks. In the area surrounding the low resistivity body, where there is no evidence in the MT response of such a low resistivity body, the MT data show a moderate resistivity layer (50-100 ohm-meters) above a high resistivity (more than 1,000 ohm-meters) electrical basement.

Recommendations for future work include one or more test wells both for calibration of the MT interpretation and for temperature measurement. Depending on these results an additional detailed MT program may be valuable to further investigate the complex response of the three areas of interest and to provide a higher resolution definition of the anomalous areas.

TABLE OF CONTENTS

APPENDICES

A. Data plots and listings

B. Glossary of MT Terms and Definitions

C. Interpretation of Complex MT Data

D. 2-D Model listings

# FIGURES

## PLATES



Model Study Plates:

# GEOEVALUACIONES, S.A. de C.V.

## ARNOLD ORANGE ASSOCIATES

## COMISION FEDERAL DE ELECTRICIDAD

GERENCIA DE PROYECTO GEOTERMOELECTRICA
SUBGERENCIA DE EXPLORACION
DEPARTAMENTO DE EXPLORACION

# PLANO DE LOCALIZACION

# PROYECTO MT CEBORUCO

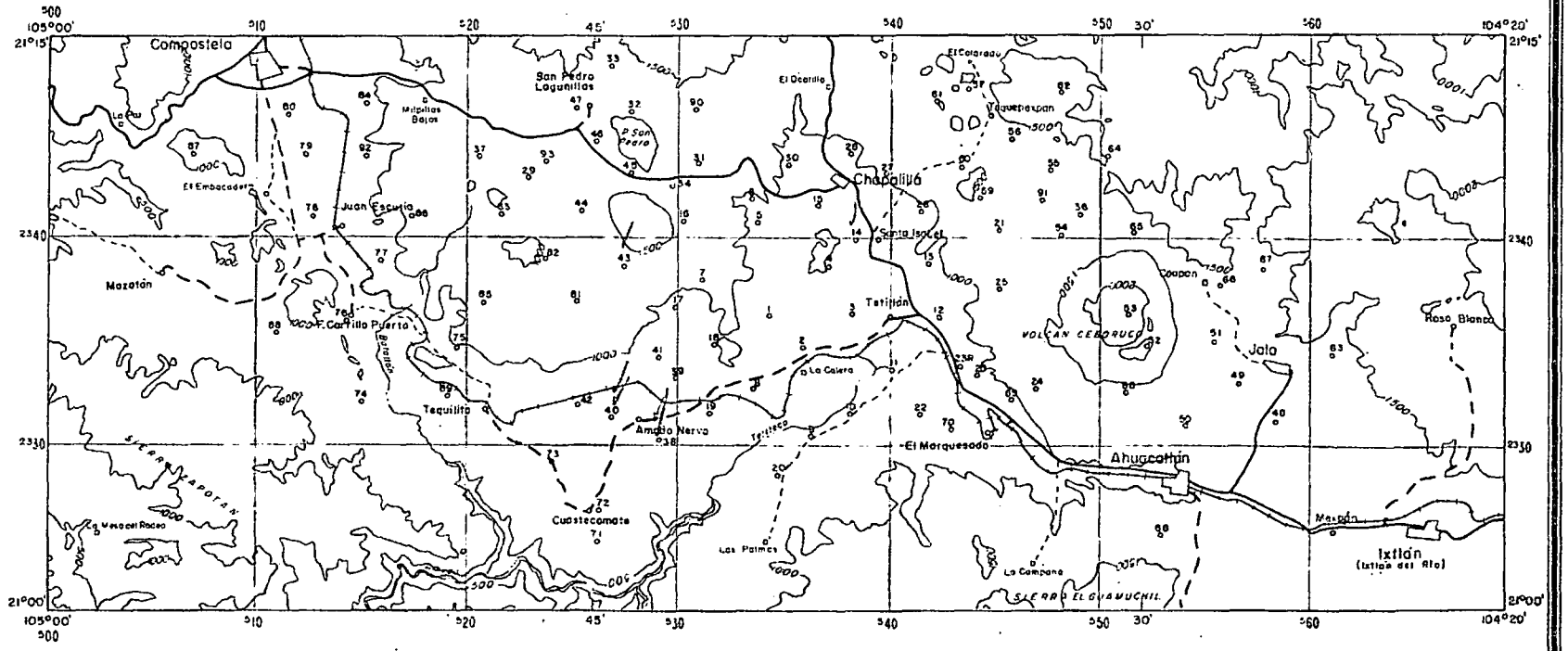


ESCALA 1 : 250 000

0 5 10 15 25

# FINAL REPORT
# CEBORUCO - DOMO de SAN PEDRO MAGNETOTELLURIC SURVEY
# NAYARIT, MÉXICO

## I. Introduction

### A. History and general location

A magnetotelluric (MT) survey was performed during July through September, 1991 for the Comision Federal de Electricidad (CFE) in the Ceboruco-Domo de San Pedro area of Nyarit, México (Figure 1). The MT acquisition program was initiated as part of a regional exploration program for geothermal reservoirs by CFE. A 90 site program was planned and acquisition initiated at the end of June, 1991 and MT data were actually acquired at 93 locations (Plate 1). Preliminary model studies indicated that low resistivity zones characteristic of geothermal reservoirs would be detected by the MT method. A DC resistivity study using the Schlumberger method was performed by CFE prior to the decision to employ MT in this area. Areas of lower resistivity identified by the DC resistivity program were the initial areas of interest for the MT program.

The Ceboruco-Domo de San Pedro area is of interest to CFE for geothermal exploration as it is part of a regional system of extensional and transverse tectonics with associated recent volcanism (less than 4.5 MA). Large scale geologic and geophysical studies suggest that the study area is part of a regional tectonic system which forms the northern boundary of the Jalisco tectonic block.

### B. Objectives

The MT program was designed as a reconnaissance investigation to locate potential geothermal zones, which were thought to be represented by vertical, "dike like" zones of low resistivity. MT data were acquired to determine the electrical resistivity of the subsurface at the locations selected. Subsurface resistivity data determined through application of MT may be interpreted in terms of rock characteristics important to geothermal exploration, in particular relative porosity, selected zones of alteration, and an indication of the presence of anomalous pore fluids. Major stratigraphic units may be identified on the basis of their characteristic average resistivity. MT data are also utilized to

interpret geologic structure, where geologic characteristics and MT site placement and/or density permit.

C. Project Organization and Management

This project was accomplished in cooperation with the exploration staff of the Comision Federal de Electricidad. The initial program proposed by the CFE exploration staff was reviewed by project geophysicists from Geoevaluaciones and final site locations agreed upon. The MT data were acquired and processed by an MT crew owned and operated by Geoevaluaciones, S.A. of Mexico, D.F. Data acquisition operations were continually review by CFE staff; daily operational reports were provided verbally as requested by CFE representatives in Ahuacatlan. Weekly reports were provided to note acquisition progress. Included in these reports were preliminary presentations (plots and listings) of the MT data. Updates to the location map were made by the Geoevaluaciones crew chief as required.

D. Report organization and deliverables

This report begins with a general introduction to the MT method and the specific acquisition operation as conducted by Geoevaluaciones. This will include a review of the acquisition hardware, typical site setup, recording procedures and processing software. It is intended to provide a general understanding of MT data acquisition as conducted in the Ceboruco-Domo de San Pedro MT Project. A complete discussion of the interpretation is presented in Sections VII and VIII of the report. Several tabulations of site information, such as location, data quality and inversion results, are included for reference at the conclusion of Section IX.

Data volumes are included that contain paper copies of the plots and listings of all of the computed MT functions for each site (Appendix A). Tables which summarize the site location information, frequency range of the individual recording bands, a summary of the layered inversion results, and an MT data review are also included.

Appendices are included as support for the material included in the body of the report that cover in detail aspects of MT technology. These appendices include: An explanation of MT data displays and a glossary of terms used in MT exploration (Appendix

B), and A discussion of MT interpretation in complex areas (Appendix C). Appendix D contains listings of all computed two-dimensional models.

In addition to this report and its accompanying plates and appendices, project deliverables include the MT data on digital magnetic tape prepared by Geoevaluaciones. The data include auto- and cross-powers, edited data, and computed functions. An accompanying document describes the storage format for this data. Included as part of this report is the database created for the GEOTOOLS® workstation, this information is stored on magnetic tape and can be used by CFE for supplemental interpretation in the future by the CFE exploration staff.

II. Data acquisition - overview

A. MT - An introduction

A.1. Objectives of applying MT to a geologic exploration program

Magnetotellurics is an electrical method which makes use of naturally occurring electromagnetic phenomena to determine the electrical resistivity of the subsurface. A knowledge of the resistivity is important since rock types important to a determination of subsurface geology and to geothermal exploration can be differentiated on the basis of resistivity value. Thus, a resistivity versus depth cross-section of the earth can be broadly interpreted in terms of rock type, and spatial variations in the resistivity-depth relationship observed at closely spaced locations on the surface can be interpreted in terms of subsurface geologic structure. As used for geothermal exploration the MT method cannot detect high temperature water or steam directly, but can be used to locate zones of low resistivity which may be related to aquifers and geothermal reservoirs.

MT data are acquired where the exploration objectives involve geologic units of contrasting resistivity. The method has probably been used most commonly for exploration in volcanic, carbonate, and overthrust areas around the world, where the targets are lower resistivity clastic sediments within and beneath more resistive formations. Seismic data quality is often poor under such conditions, and the MT data can form an important part of the geophysical data base. The method is also useful under difficult terrain conditions where seismic data quality is expected to be good, but seismic data acquisition is so expensive that it pays to perform an MT survey to demonstrate the validity of a geologic concept and/or assist in laying out a cost-effective seismic program limited to the actual target. In general, detailing such as locating a structural location to drill is not an MT application except in special circumstances. Recent international projects where MT has been employed have included large scale basin evaluations, overthrust geology, and poor seismic areas. MT used with gravity and magnetics is a powerful reconnaissance approach which has been used successfully throughout the world.

Of particular importance in the MT method is the measurement and presentation of a tensor resistivity measurement. This is a unique property of the method and is of particular importance in complex geologic areas or situations where the exploration target may have

specific properties (geometry or resistivity) not resolved by other electrical methods. A particular unit is not simply defined as having a relatively high or low resistivity, rather the behavior of the electrical field within the unit is detected. This is very different from other electrical methods which as commonly used provide a more one-dimensional sounding of resistivity.

A.2 Measured quantities

The fundamental quantities measured in MT are naturally occurring low frequency electromagnetic signals. Both electric field and magnetic field variations are measured at the surface of the earth. The complete vector electromagnetic field is measured; the magnetic field by measuring three orthogonal components, usually two horizontal and one vertical, and the electric field by measuring two orthogonal horizontal components (there is no vertical electric field at the surface).

MT analysis over the depths of interest to geothermal or hydrocarbon exploration requires naturally occurring source signals over a frequency range of roughly 0.0005 - 500.0 Hz. Two primary energy sources are responsible for providing this almost 6 decade bandwidth. At the lower frequencies, below approximately 1.0 Hz, the source (or sources) is energy originating in the upper ionosphere and magnetosphere. These variations of the earth's electromagnetic field, which include micropulsations, storms, and substorms, are related to the interaction of the solar wind, the stream of charged particles emanating from the sun, and the plasma layers that form the magnetosphere and ionosphere.

At the higher frequencies, above approximately 1.0 Hz, the energy source is the ever-present world wide lighting activity (spherics), propagating in and exciting the earth-ionosphere cavity. The first, or Schumann, resonance of this cavity occurs at roughly 8.0 Hz; the signals are attenuated rapidly below this frequency. The "high" and "low" frequency energy bands do not quite overlap, and there is an energy "hole" or minimum in the frequency range of roughly 0.1-2.0 Hz. It is within this band that it is typically most difficult to obtain high quality MT data.

In addition to covering a broad frequency range, the MT source energy also encompasses an extremely broad dynamic range; often more than nine decades range in the

magnetic field energy density, and seven decades in the electric field. The broad frequency band and wide dynamic range strongly influence both data acquisition and processing.

A.3 Computed functions

Several functions are computed from the measured electric and magnetic field fluctuations. These functions are defined and explained in this section:

Apparent resistivity and rotation angle - The fundamental function computed from the measured electromagnetic field data is the apparent resistivity, calculated as a function of frequency. The magnitude of the apparent resistivity has the units of ohm-meters. Through the skin depth relationship, which describes the penetration of the electromagnetic wave into the earth as a function of frequency and resistivity, apparent resistivity as a function of frequency is related to resistivity as a function of depth, with lower frequencies relating to deeper penetration and resistivity values deeper within the earth.

The electromagnetic field from which the apparent resistivity is calculated is a vector quantity as described in the preceding paragraph, measured by sets of orthogonal electric and magnetic field sensor. Placement of these sensors on the ground, i.e., the measurement coordinate systems, is arbitrary. The fields are influenced by the resistivity structure of the earth (which is, of course, what makes MT useful in exploration), and the components of apparent resistivity parallel and perpendicular to strike can be identified mathematically in the course of MT data processing, where the strike direction is usually different from that of the measurement azimuth. The fact that there are two resistivities that are computed and that these are in general different from one another is what makes MT interpretation possible in the presence of structure. The apparent resistivities parallel and perpendicular to strike are said to be the rotated resistivities, since they have been rotated mathematically from the measurement coordinate system into the coordinate system related to the strike and dip of the geologic structure in the vicinity of the site. The rotation angle is presented as one of the computed and plotted MT functions.

Apparent resistivity phase - The apparent resistivity is a complex function (in the mathematical sense) with an amplitude and phase. The magnitude is the apparent resistivity described above. The phase of the apparent resistivity is related to the slope of the apparent resistivity under all conditions of one- and two-dimensional structure, and most three-

dimensional cases. The phase is important as a diagnostic of instrument performance as well as an indicator of extreme structural complexity.

Skew - The skew is one indicator of possible three-dimensional complexity structural complexity. The skew value is calculated as a ratio of the sum of the diagonal components (zero for 1-D and 2-D cases) to the difference of the off-diagonal components. In general, high skew, of the order of approximately 0.2 or greater, is an indication that the structure is likely to be three-dimensional, and that one- and two-dimensional interpretation approaches may be inadequate. Low skew is an indication that the structure may be one- or two-dimensional. Note that low skew is not a positive indication of structural simplicity. Lower signal to noise ratios can also result in noise-induced high skew values.

Coherency - Coherency is a measure of data quality. For the apparent resistivity data at an individual site (i.e., disregarding the reference of a simultaneously recorded site) the computed apparent resistivity is combined with the measured magnetic field to compute a predicted electric field E. In the absence of noise or distortion the "recreated" or predicted, E will be exactly equal to the original measured E. The coherency is an attempt to quantify the noise and/or distortion of the real world MT response. The coherency (in a statistical sense) between predicted and measured E is computed and presented, for each of the two resistivity components.

Tipper (vertical magnetic field) - The term "Tipper" refers to the distortion of the electromagnetic wave from which the MT functions are computed caused by geologic structure. The electromagnetic source wave is an EM wave propagating vertically into the earth, with the electric (E) and magnetic (H) fields horizontal, at right angles to the direction of propagation. If the earth is electrically one dimensional, with the resistivity varying only with depth, then the EM field measured at the surface,the superposition of the source and re-radiated waves, behaves as above with the direction of the E and H components still horizontal. If there are lateral variations in resistivity, however, the resultant EM field (again, the superimposed source and re-radiated fields) will be distorted such that the resultant direction of propagation is not vertical. In particular, the magnetic field is not horizontal and is said to be "tipped" out of the plane that is horizontal or parallel to the earth's surface.

The tipped magnetic field is measured by a three-coordinate magnetic field sensor system, and horizontal X and Y coordinates plus the vertical, or Z, coordinate. The distortion of the magnetic field, as presented in the "Tipper" functions is an indication of structural complexity. As such the Tipper can be a useful interpretive tool. The Tipper magnitude is the ratio of vertical to horizontal magnetic field vectors, when the resultant "Tipped" magnetic field is resolved into its horizontal and vertical components. The magnitude is usually plotted linearly vertically while frequency is logarithmic.

The Tipper coherency is a measure of vertical field data quality. In a two dimensional setting the vertical field component of the tipped field will be a maximum in the dip direction and zero along strike. The Tipper Direction and Strike are plotted as a function of frequency. The Reference angle is true north.

Polar plots - The polar plots are plots of the impedance magnitude versus azimuth. To form the polar plot, at a specific frequency each of the impedance terms, the diagonal and off-diagonal of the impedance "tensor", are computed as a function of azimuth and displayed in polar form. The off-diagonal term is the familiar apparent resistivity, without constants and the frequency term. This display not only reveals the strike direction (as a function of frequency when a family of polar plots are prepared) but also graphically displays the extent to which three dimensional distortion is present. This distortion is identified, for example, by observing the behavior of the diagonal XX term which should approach zero at the maxima and minima of the off-diagonal XY term.

A.4 Remote reference

Remote reference MT is a technique used to deal with the effects of noise on the MT measurement. In general noise is defined as that part of the measured time series which is not correlated between the electric and magnetic fields. Noise in this context can consist of internal instrument noise, noise caused by sensor and cable motion, spurious electromagnetic radiation, spurious currents flowing in the earth, and moving metallic objects that are detected by the magnetometers. There are several methods employed to improve the signal-to-noise characteristics of the processed data. (It is assumed here that appropriate steps have been taken in site selection and installation to provide the best possible data under the constraints of survey objectives.) The methods that are available

are editing procedures, stacking, and the use of a remote reference. All three of these procedures were employed in the Ceboruco data acquisition.

Remote reference MT utilizes MT data acquired simultaneously at two locations, which may be separated by a few hundred meters to more than several tens of kilometers depending on the particular characteristics of the local noise. This technique assumes that the MT "signal" of interest (magnetic field) is coherent over large distances over the earth's surface while "noise" sources tend to be confined in areal extent. This assumption is a good one and has been verified for frequencies over 1,000 hertz.

Comparison of signals at two locations may allow separation of the signals into a coherent portion, the "signal", and an incoherent portion, the "noise". The data at the "base" site are usually analyzed using the magnetic fields at the other site as a "remote reference". When two MT sites are acquired simultaneously each site may be used as the reference for the other. The equations relating the Fourier components of the electric and magnetic fields are multiplied by a component of the magnetic field of the remote reference. By averaging the various cross-products, estimates of the impedance tensor not biased by noise are obtained, assuming that there is no correlation between the noise at the two locations. In practice, this assumption is normally correct if a separation appropriate to the particular noise environment is chosen. Remote reference acquisition is now a standard feature of exploration MT.

The key to effective reference processing is the choice of an appropriate separation between base and remote sites. In practice this is a variable depending upon the noise environment and operational considerations. Separations of one to tens of kilometers are common. If only sensor and instrument noise is a factor, the base-reference separation can be only meters. In the case of wind noise, separations of the order of a hundred meters,will suffice. In the case of local power lines and moving metal, separations of the order of several hundred meters or up to 1-3 km will provide sufficient separation.

The common choice for the reference field is the use of the magnetic signal. The two primary reasons for this are the reduction of bias in the calculated value of apparent resistivity due to electrical field noise and the relatively simpler field logistics for site setup. In cases where localized electrical field noise is not a problem, it is also possible to utilize the electrical field as the reference. This can be useful where distant lightning strikes create

a problem with magnetic field noise. Processing tests conducted during the Ceboruco survey demonstrate that except for sites located near high power transmission lines, the results of the two reference methods are virtually identical.

A.5 Interpretation overview - General Comments

The specific interpretation of the acquired MT data is presented beginning in section VII, this section presents a general description of the interpretation process. MT interpretation, as with other geophysical exploration techniques, consists of several steps, some of which are easily quantifiable and others which involve a complex interplay between the interpreter and the character of the data base under consideration. An MT interpretation begins when the interpreter first sees the data for quality control purposes, which, in the case of data acquired utilizing an in-field processing system, may occur while data acquisition is still in progress.

Probably the single most important interpretive step is the systematic examination of the apparent resistivity versus frequency data for the survey area, accompanied by referral to supporting data such as the electrical strike and vertical magnetic field information. This step, yields (a) the approximate vertical sequence of resistive and conductive units based on the frequency-depth penetration relationship, (b) the approximate location of faults and structural trends based on site-to-site relationships, and (c) most important, the structural complexity as evidenced in the data, which will indicate which modeling route to take for the continuation of the interpretation. The above procedures involve examining all of the MT data with an eye to the inter-relation between sites, as impressions gained from an individual site by itself or even a single profile may be misleading. At this stage, it is most important to identify evidence of strong two and three-dimensional effects. While the interpreter is usually forewarned by preliminary geologic and regional geophysical (gravity, magnetics) studies, frequently the MT data will exhibit unanticipated effects. The qualitative examination step identifies these effects, and leads to the determination of the appropriate modeling procedures.

Prior to beginning the interpretation all available geological and geophysical data are accumulated and studied. Each interpretation is an individual problem, the result of the great diversity found in nature. The interpretation steps summarized below are intended to provide the reader with insight into the process for a typical interpretation

The first formal step is to prepare and examine the basic data. The data may be examined as individual data sets from each site, or in montage, profile, or map form as described earlier. Comparison of the data with model examples (from the interpreter's case book, for example) and with the data from individual sites chosen as "representative" of the survey, leads to a qualitative interpretation where the site-to-site relationships are used to identify the gross features of the electrical section and structure.

Next, the interpreter might examine carefully and plot tensor rotation and magnetic field "tipper" strike directions, described above. This information is useful in determining electrical strike, in assessing the two and three dimensional characteristics of an area, and in determining tensor resistivity components (as parallel or perpendicular to strike) in complex areas.

Once the qualitative examination is well under way, the interpreter will begin the quantitative interpretation, utilizing various computer procedures to invert and model the data. Inversion programs that accommodate one- and two-dimensional geometries are available, as are one-, two-, and three-dimensional forward modelling programs. Forward models are computed to study general interpretive problems and to investigate specific structural questions. In addition, a "case book" may be studied to identify models computed in the past which are applicable to the project at hand. The models are used to identify the structural style of a prospect, and to provide either a basis and the initial parameters for the appropriate use of one dimensional inversions, correction factors for the inversions, or an indication that one-dimensional inversions will be inappropriate and that more exact two and three-dimensional models will be required. In the case of strongly three dimensional situations, some sample models used as guides to interpretation have been published. However, for some complex cases no currently available modeling procedures may be able to model the data and/or the interpreter may not be able to develop a satisfactory model that fits all of the characteristics of the data. The inversion and modeling stage is an iterative one, with models compared with the data and then modified to provide a better "fit".

Once the interpreter has "picked" vertical and lateral resistivity interfaces based on the inverted and modelled data, the interpretive maps and sections are prepared. At this point the depth values are posted, structural forms contoured, and faults and anticlinal and synclinal axes drawn in. The total geological and geophysical data base is called upon at

this stage to complete the geologic interpretation. The various supporting MT information (phase, skew, coherency, etc.) are utilized continuously either in data quality assessment or in examining in detail the departure of the data from assumptions of one and two dimensionality.

A.6 Statics considerations

Lateral variations in resistivity at or near the surface have an effect on MT data. Such variations might be represented in nature by alluvial-filled depressions, stream beds, narrow valleys bounded by rock outcrop, etc. The MT effects are analogous to the effects of near-surface velocity variations on seismic data which have been historically termed "statics" effects, hence the usage in MT. The MT statics effect may be manifested by a parallel or near-parallel separation of the two resistivity curves, with one or both of the curves shifted from its "correct position", or by more severe distortion than a mere shifting of the curves. Since analysis of the MT resistivity-depth relationship requires knowledge of the magnitude of the apparent resistivity function, any statics shift or distortion will result in errors in estimated depths and resistivities unless appropriate corrections are applied.

A variety of techniques have been suggested for the correction of statics distortion. The two of these favored by the authors of this report are the determination of the shallow resistivity, and modeling of statics effects. For the Ceboruco project the shallow resistivity structure was measured a shallow penetration time domain electromagnetic (TDEM) sounding. In addition the Schlumberger data provide an independent DC measurement of the same geologic section. In most cases the Schlumberger data are in good agreement with those MT sites where no static shift is evident. A summary of the near-surface resistivity for each site as measured by the three techniques will be found in Table II.

B. Primary considerations in data acquisition

In this section some of the considerations that must be taken into account when planning an MT survey will be discussed. This includes the pre-survey project planning as well as the site to site consideration required to assure that the data is useful for the exploration target. Consideration of many factors relating to the acquisition program are necessary for an efficient operation.

B.1 Effect of target characteristics on acquisition parameters

A critical step in planning an MT exploration program is the determination of the suitability of applying MT to the problem under consideration. Once this has been determined through a combination of experience and pre-survey modeling than the details of the data acquisition program are addressed.

The characteristics of the target primarily affect the data acquisition frequency range and the data quality that is deemed acceptable. Deep targets overlain by low resistivity sediments will require recording to lower frequencies, and hence over a longer time period, than will more shallow targets with more resistive rocks in the section. Subtle targets, or targets where the most accurate quantitative interpretation is desired will require much higher quality data and care in processing than will a target where a straight forward "yes" or "no" answer to the question of the presence of a specific unit is required.

The determination of a suitable frequency range, and the data quality required, are determined largely through pre-survey modeling. The range of target geometries and resistivities anticipated are used as inputs to one-, two, or three-dimensional models as appropriate, and the results evaluated. The evaluation should take into consideration the real world conditions of noise and unforeseen geologic complexity.

B.2 Data quality; noise environment

The quality of the basic data is of paramount importance in any geophysical study. This is especially true for MT, where subtle changes in the data may result in large variations in the interpretation. The basic MT data are the frequency domain functions computed from the electromagnetic field variations measured at each site. Of particular importance are the apparent resistivity magnitude and apparent resistivity phase data. Since the MT functions are computed from the measured naturally-occurring electric and magnetic field variations, any factors that affect the quality of the measured fields will affect the quality of the computed functions. Factors that affect the quality of the data are termed "noise". Noise may be thought of as any spurious signals from whatever cause that are present at the input to the data processing algorithm that are not part of the electromagnetic signal from which the MT functions will be computed.

Data quality throughout the Ceboruco program was consistently good to excellent with very few sites affected by large amplitude noise. The primary noise source affecting the data at the sites that did exhibit noise contamination was the almost continual lightning storms experienced during the data acquisition period. Cultural noise and other noise sources, although present, presented relatively minor problems.

The most common MT noise sources are summarized in the following paragraphs:

- Lightning - Nearby lightning was a major factor at many times during the course of this survey due to nearby thunderstorm activity. Recording time was limited at many sites due to constant storms. Throughout July and August these storms occurred at all times of the day with little predictability.

  Lightning has multiple effects on the MT data and operation: First, while the signal from a lightning stroke is an electromagnetic wave, if the stroke is nearby then the site may be in the near field of the source rather than the far field and the far field assumptions necessary to normally compute the MT functions may not hold, resulting in distortion of the computed functions. Second, even if the site is in the far field the lightning signal may be so strong that when the system gain is set such that these signals do not saturate the input amplifiers, the background, non-lightning signal may be so weak that the overall signal-to-instrument-noise ratio may be unacceptable. Third, if the lightning signals saturate the amplifiers, or if the signals exceed the dynamic range of the system and are "clipped", the results are severe distortion of the computed functions. Finally, when the lightning approaches the site the sensors must be disconnected and the instruments turned off, to avoid injury to the operator and instrument damage.

- Cultural noise - In general, cultural noise may be the result of spurious electromagnetic signals radiated by power lines, electric railroads, electrical machinery, electric fences, etc. Moving metal such as vehicles or nearby machinery will introduce spurious signals on the magnetic field sensors, the coils. People or other large animals walking near the coils will introduce vibrations that appear as noise. With the exception of just a few sites cultural noise was not a significant problem for this survey. Power lines and irrigation pumps are not generally present in the largely rural and agricultural project area.

- Proximity to streams and moving ground water - This is an uncommon source of MT noise, but one possibly present here due. Spurious currents arise from self potential and streaming potential effects, and the spurious electromagnetic fields that are generated from the movement of a conductor (the conductive water, in this case) in the main magnetic field of the earth. Running water, if sufficiently vigorous, may also cause seismic vibrations which will affect the magnetic field sensors.

- Wind noise - Wind has the effect of shaking or vibrating the magnetic field sensors, and the electric field dipole wire. Even a small amount of wind in trees and brush causes movement that is transmitted to the buried sensors via the root system. Wind also can vibrate the electric field antenna wires, causing induced currents as the wires are moved in the main magnetic field of the earth. Wind was only an occasional factor during this survey.

- Instrument and sensor noise - Instrument noise was a negligible factor in this survey. The instrument noise was checked before and after the survey, and found to be within specifications. Sensor noise results primarily from improperly installed electrodes. The electrodes are always reinstalled at any time that this problem was suspected. The system electrodes are specifically designed to have excellent, low noise characteristics. The usual procedure was to install them the day before acquisition to allow to become electrically stabilized.

B.3 Data Quality Evaluation Criteria

In order to provide an indication of data quality, each site is evaluated both in relation to the other sites in the survey and in relation to experience in similar areas. The following data quality evaluation criteria as used in this report: Four ratings have been assigned to MT data; Good, Fair, Poor, and Unusable. The criteria may be applied to a portion of the frequency range recorded:

Good - Good data allow accurate determination of the resistivity section and, if site density permits, structural style through an unambiguous evaluation of the MT functions computed at the site. Of particular importance are the two apparent resistivity and phase versus frequency curves. Data point scatter must be small. Gaps in the data are acceptable if they do not affect preparation of the smooth curve, or do not occur in a portion of the

frequency band of maximum interest. A Good site for this survey is one where low resistivity units (if such are present) and electrical basement may be unambiguously characterized . The resistivity value and anisotropy at the higher frequencies are clearly evident. The frequency of the resistivity minima or curve slope changes caused by the the low resistivity rocks and the value of the resistivity at the minima must be evident, since these parameters are critical to the determination of the thickness of the low resistivity section and the depth to electrical basement.

Fair - Fair data allow accurate determination of the gross characteristics of the resistivity curves and identification of the structural style, and are adequate for a fair determination of formation depths and thicknesses. The deteriorat. n from "Good" is usually the result of scatter in the data points at key portions of the frequency range.

Poor - Poor data is the most difficult to define. With Poor data it is possible to discern the general configuration of the subsurface with a degree of certainty, but the data are not adequate for a reliable relative depth and thickness interpretation. It is possible to calculate the depths and thicknesses as discussed above under Good and Fair, but without higher quality data at adjacent sites these value are unreliable and not adequate for preparation of a cross-section or map without qualifications. A Poor site, in the quantitative sense defined here, will yield depth and thickness estimates which may have a margin of error in excess of 50 to 100 percent.

Unusable - The data are not usable for calculation of depths and thicknesses. Curve characteristics may be discerned with difficulty, if at all.

B.4 Data quality - site-by-site evaluation

The data quality summary for each site will be found in Table II.

B.5 Instrument and data processing capabilities

Once the exploration objectives and data acquisition requirements have been evaluated it is necessary to ensure that the acquisition instrumentation and data processing capabilities are compatible with these requirements. Of particular concern are the data recording frequency range, instrument noise characteristics, and the reliability of the instruments. In areas of difficult terrain instrument portability is a concern. The data

processing capability should include the computation and display of all of the MT functions that will ultimately be used in the interpretation.

B.6 Interpretation tools - data transfer compatibility

The MT interpreter may have available a wide range of data analysis and forward and inverse modeling tools, installed on a range of computers. The data acquisition and processing output must provide the interpreter with the functions and data quality necessary to utilize all of the capabilities of these tools. The data processing output should be recorded on media compatible with the input required by the various data analysis and interpretation programs. Compatibility is meant to mean data content and format as well as the media itself.

## III. Instruments

### A. Overview and block diagram

The MT data were acquired by Geoevaluaciones utilizing MT instruments manufactured by ElectroMagnetic Instruments, Inc (EMI). The data were acquired using the remote reference technique, described in Section II.A.4 of this report. A simplified block diagram of the EMI acquisition system is shown in Figure 2. All aspects of system operation are controlled by the operator through keyboard input to the IBM-compatible laptop computer. In addition to controlling data acquisition and recording, the computer also is used for in-field processing, whereby the MT functions can be computed and displayed in real time during the recording procedure. The ability of a recording system to provide the operator with a display in real-time of referenced data is an important feature of any modern system.

An important feature of the instrumentation was the simultaneous recording of an operational site and a remote reference consisting of orthogonal horizontal or electric field sensors. At several locations two operational sites were recorded simultaneously, with each acting as the reference for the other. The site and its reference or the two operational sites were connected to a single set of recording instruments by a communications cable. The instruments were frequently located adjacent to one of the operational sites. Figure 3 is a sketch of the data acquisition configuration, including the reference site.

### B. The EMI system - detailed description and specifications

The components of the EMI data acquisition system will be discussed using as a guide the block diagram, Figure 2, and the site layout sketch of Figure 3.

- Electric field (telluric) sensors - The electric field sensors are grounded dipole antennas. For the Ceboruco project, dipole length was generally 100-150 meters, although there were some variations where field conditions dictated otherwise. The dipoles consisted of insulated copper wire, laid on the surface. The dipoles were installed in an "L" configuration, with a common electrode at the apex of the "L". The grounds at the dipole ends for the normal, low frequency data were provided by lead-lead chloride electrolyte-filled electrodes.

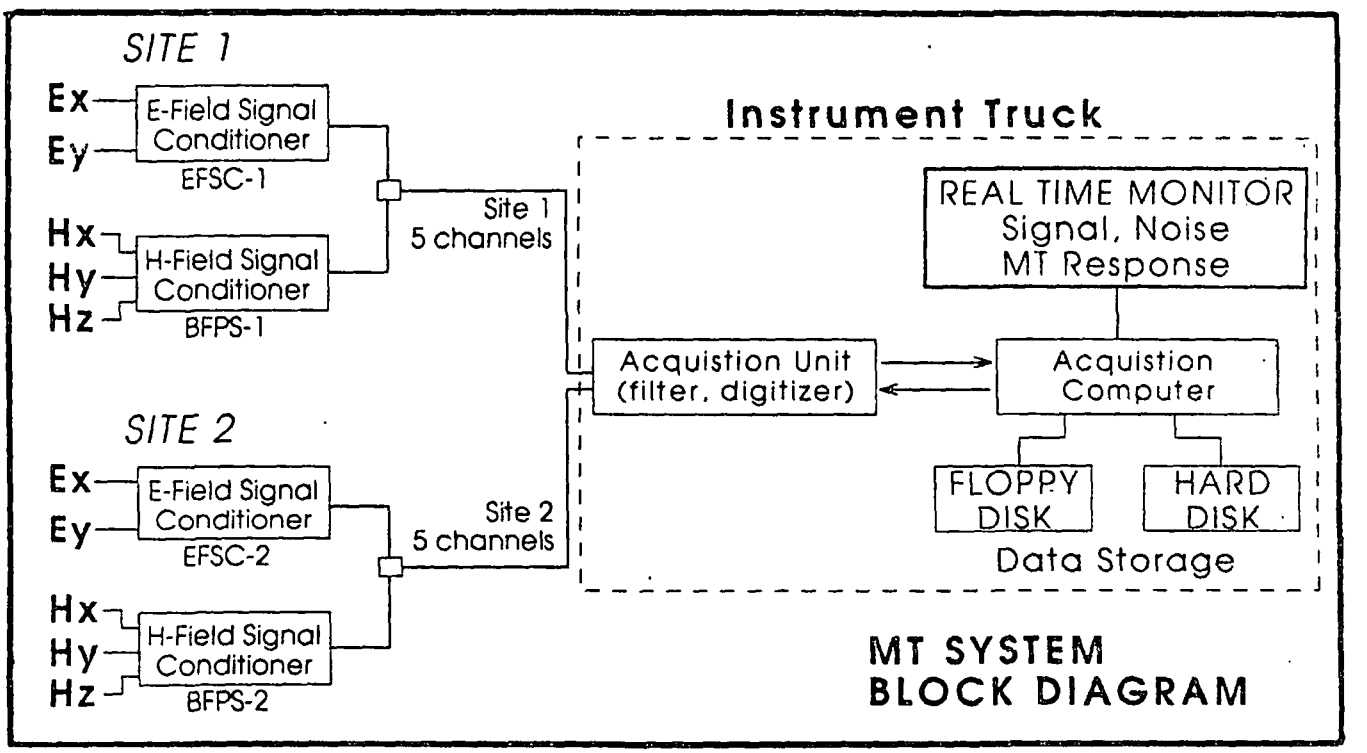
SITE 1
Ex
Ey
E-Field Signal Conditioner
EFSC-1
Hx
Hy
Hz
H-Field Signal Conditioner
BFPS-1
Site 1
5 channels
SITE 2
Ex
Ey
E-Field Signal Conditioner
EFSC-2
Hx
Hy
Hz
H-Field Signal Conditioner
BFPS-2
Site 2
5 channels
Instrument Truck
REAL TIME MONITOR
Signal, Noise
MT Response
Acquistion Unit
(filter, digitizer)
Acquistion Computer
FLOPPY DISK
HARD DISK
Data Storage
MT SYSTEM
BLOCK DIAGRAM

Figure 2

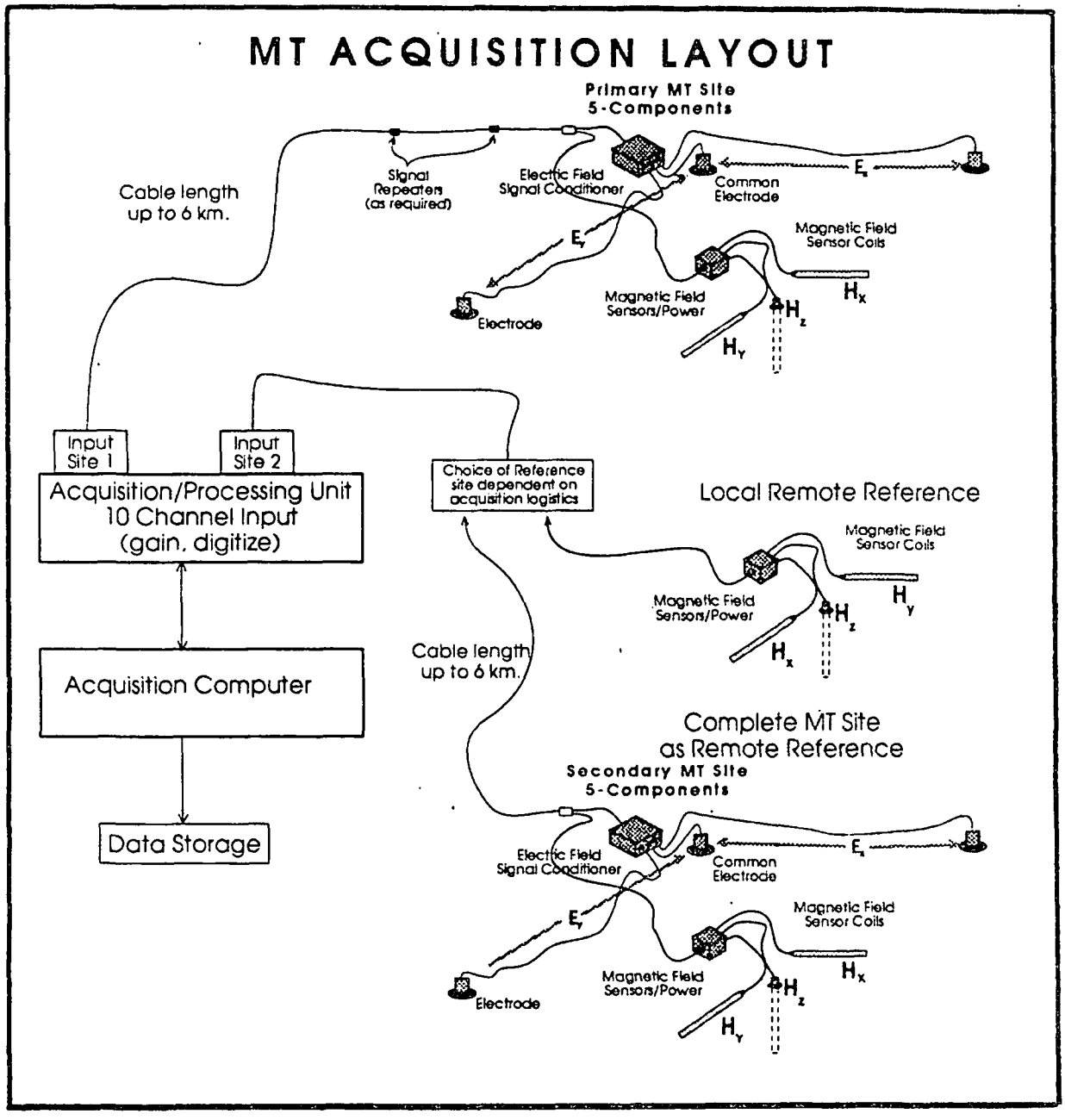
MT ACQUISITION LAYOUT
Primary MT Site
5-Components
Cable length
up to 6 km.
Signal
Repeaters
(as required)
Electric Field
Signal Conditioner
Common
Electrode
Magnetic Field
Sensor Coils
Electrode
Magnetic Field
Sensors/Power
Input
Site 1
Input
Site 2
Acquisition/Processing Unit
10 Channel Input
(gain, digitize)
Acquisition Computer
Data Storage
Choice of Reference
site dependent on
acquisition logistics
Local Remote Reference
Cable length
up to 6 km.
Complete MT Site
as Remote Reference
Secondary MT Site
5-Components

Figure 3

- Magnetic field sensors - The magnetic field is sensed using multi-turn iron-core coils. The horizontal magnetic field (Hx and Hy) coils for the low frequencies are installed in a weather-proof aluminum-fiberglass pipe roughly 6 cm in diameter and 1.3 meters long. The normal frequency vertical field sensor (Hz) is a similar iron core coil, but a few cm shorter than the vertical coil. All horizontal and vertical field coils include integral broad-band low-noise preamplifiers, powered by an external rechargeable battery connected to the sensor by a short cable.

- Electric field signal conditioner unit - The electric field signal conditioner unit is located at each sensor site and contains broad-band low-noise amplifiers to prepare the electric field signals for transmission to the digitizer. Optical coupling is employed to isolate the dipoles and input preamplifiers from the output amplifier-line driver section. The signal conditioner units are battery operated, with separate internal batteries for the input and output circuits to avoid any coupling or ground-loops across the optical interface.

- Communication cable - The cable transmits the signals from the sensor sites to the digitizer and computer in the instrument enclosure. The cable is made up into 100 to 300 meter long sections for ease of carrying into the field, with waterproof connectors for connecting the cable sections together. Repeaters are available for insertion into the cable for transmission over long separations or for transmission of data at frequencies above approximately 1 KHz where the impedance of the cable is a factor.

- Acquisition and processing unit - The acquisition and processing unit (APU) includes input amplifiers and power line rejection filters, programmable anti-alias, low- and high-pass filters, and a 10 channel, 16 bit analog-digital (A-D) converter. Filter and gain setting is either by front panel switches or by computer keyboard entry. Data acquisition by the APU is controlled by the laptop computer described below. The APU is a small portable unit which in Italy was placed, along with the computer, clock, and batteries, on the work bench in the back of the recording truck.

- Computer - The IBM-compatible laptop computer controls operation of the programmable amplifiers, filters and digitizer; formats the data; and controls the

recording on to the internal hard disk. The computer also computes the auto and cross-powers. In-field data editing and processing can be performed in the computer. The operator controls acquisition, processing, display, and recording parameters through computer keyboard input. The electric and magnetic field time series and all computed functions may be displayed on the computer screen. The computer is also used to control system calibration.

- Recorded functions and recording media - The in-field processed digital data are recorded on the laptop computer's hard disk, and on floppy disks as backup and for transfer of data to the base-camp computer. The disks contain the time series and the cross-and auto-power spectra, as described below. The results of the in-field processing, if such is performed, are also recorded on floppy disks.

- Base-camp processing center - The base camp processing center utilized an IBM-compatible desk-top computer with an operating system and software identical to that used for data acquisition and on-site processing, with the addition of a printer for hard-copy output.

C. In-field communications

In-field communications were required between the operator and installation personnel during site installation and check-out. In-field communications between the operator and site installation personnel was by hand-held VHF FM radios. The instrument truck had a more powerful mobile radio installed. Although limited to line-of-site, these radios proved to be effective in most instances.

IV. Field procedures

A. Site selection

Initial planning for specific site locations along the profiles was performed by the Geoevaluaciones staff prior to departure of the crew for the field, based upon the preliminary evaluation of access and surface characteristics as obtained from topographic maps. After this initial planning the Geoevaluaciones party chief and/or surveyor scouted each area to evaluate access, topography, and noise sources in the field. At this time exact site locations were specified. Then, at the time of site installation minor adjustments were made to the site locations based on the requirements for sensor installation and site separation of the two cable-connected sites.

B. Site preparation and sensor installation

Site preparation consisted of, if necessary, first any brush clearing required for the sensors and sensor cables as described above; and then the installation of the sensors and instruments. Since virtually all of the sites were located in cleared or partially cleared areas very little in the way of brush cutting or line clearing was required.

Electric field sensor installation consisted of laying the dipole wire and installing the electrodes in shallow, 10-30 cm. deep, holes containing a mud or bentonite and water slurry. The horizontal magnetic field sensors (coils) were installed in shallow, 15-30 cm deep trenches and buried to minimize vibration and wind noise. The vertical magnetic field sensor was installed in a vertical hole.. The battery box for the coils was placed on the ground near the coils. The electric field signal conditioner unit was placed on the ground near the common electrode. The common electrode served as the electrical ground for the input section of the unit.

The digitizer, computer, and the communications radio and any test equipment taken to the field were located on the workbench installed in the vehicles used as recording trucks. The individual components were connected by short, easily attached cables. Power to all instruments was provided by batteries. A local electrical ground was installed close to the instruments. The communications cable was laid out between the sensor site and the instrument truck and repeaters installed between cable sections as necessary.

Connecting the ends of the communications cable to the electric field signal conditioner unit and coil battery box at the sensor site and to the APU at the recording truck completed the installation.

C. Instrument check-out

Instrument performance was checked upon arrival in México and then whenever the operator or quality control supervisor felt a concern about instrument performance. The initial check-out consisted of first verifying that all functions of the APU and computer were being performed correctly. The electric and magnetic field sensors were then installed in parallel to check total system operation. Four parallel electric dipoles and six magnetic field sensors could be checked simultaneously with the EMI ten channel data acquisition system. When operating properly, and when there was no wind to induce uncorrelated sensor noise, the output on the parallel dipoles should be virtually identical, as should the output on the parallel magnetic field sensors.

D. Recording procedure

The following is a brief review of the recording procedure followed at all sites. An understanding of the in-field processing performed by the EMI system, to be discussed in Section V of this report, is helpful in understanding the recording procedure.

After the installation of the sensors and instruments was completed at the two sites to be recorded simultaneously, all components and computer functions were checked for proper operation. The site parameters were then entered into the computer. The key parameters entered were electric field dipole length and azimuth, coil azimuth (if different from dipole azimuth); and the serial number of the coils, electric field signal conditioner unit, and digitizer (to ensure that the proper calibration function was used in processing).

MT data were recorded with the EMI system in multiple overlapping frequency bands, which were later combined to provide continuous frequency coverage. Five separate bands were recorded in the field as shown in Table 3. The lowest frequency data was calculated after decimation of the band 1 data. Multiple data segments were recorded in each band. Later in the course of data processing the segments were added together (stacked) for signal-to-noise improvement. The amount of data required to provide acceptable data quality is primarily a function of the characteristics of the signal and the

noise at the site at the time of recording. A discussion of noise and signal character for this survey will be found in a following section.

The typical recording sequence consisted of a mixture of the several frequency bands. Since acquisition of the lowest frequency band took four to six hours or more as opposed to the 20-90 minutes required for the higher frequency bands, the preferred procedure was to first acquire data at the higher [frequency] bands, then the time consuming low band, and then more of the higher band data if necessary. This sequence was repeated at the sites with high noise either until satisfactory data were acquired or until the operator thought that additional recording would provide no improvement. During data acquisition the time series were continuously monitored on the computer screen. In addition, from time to time during the acquisition of a run the operator was able to compute the MT functions for the stack up to that time, as a check on system performance and signal quality.

At a typical site, installation and instrument check out were completed by early afternoon and recording initiated. In many cases excellent data was acquired within 5-6 hours. In the event of storm activity (a very common occurrence) recording was suspended until the early morning (1-4 AM). At a few sites recording was suspended for up to several hours due to nearby thunderstorm activity which had a severe effect on data quality as well as presenting a danger to the recording instruments. Upon completion of the recording the instruments and sensors were packed for transport to the next site. At a few sites data were recorded over a period of more than one day because of storms and high noise conditions.

E. In-field processing - quality control

Quality control was accomplished first by observing the electric and magnetic field time series on the computer display screen and then through computation and display of the signal parameters and MT functions during data acquisition or, in the case of the highest frequency bands, immediately following completion of a data run. The time series were examined to determine the appropriate amplifier gain settings, and to detect obvious noise contamination.

With regard to examination of processed data for quality control purposes, since the data processing programs used for the "real time" processing were identical to those used for the final processing, all of the signal parameters and functions were available. Primary signal characteristics used for quality control were the transfer impedances and phases for the equivalent electric and magnetic channels at the two sites, and the coherencies between the various electric and magnetic field channels. Primary MT functions examined were the apparent resistivity magnitude, resistivity phase, and the coherency between orthogonal electric and magnetic field channels.

In-field quality control consisted of examination for correct sensor installation and operation, appropriate amplifier gain settings, noise contamination, frequency band-to-band overlap and for resistivity values consistent with the known or postulated geology. The latter provided a check on the accuracy of the entry of the sensor geometry parameters and the preamplifier gains not read automatically by the computer.

V. Data processing and editing

A. Processing overview

The recorded MT data must be processed to compute the apparent resistivity tensor and associated frequency domain functions from the measured time series, the fluctuations of the natural electric and magnetic fields. Two approaches are used by the EMI processing programs; fast Fourier transform (FFT) and synchronous detection (SD).

In the FFT technique, the electric and magnetic field data are digitally recorded in short samples or data segments, typically for the Ceboruco survey consisting of 512 points. The fast Fourier algorithm is then applied to the time series, the time domain functions, to compute auto and cross power estimates, the frequency domain functions. After averaging to obtain constant percentage bandwidth "windows" and removal or deconvolution of the sensor and instrument transfer functions, the tensor apparent resistivity and associated MT functions are computed. The FFTs of individual segments are added together, or "stacked", to improve the signal to noise ratio by suppressing uncorrelated noise.

In the synchronous detection mode the incoming time series are multiplied in real time by sine and cosine wave forms of preselected frequencies to yield running estimates of the Fourier coefficients. These values are then sampled and averaged in the system computer in exactly the same way as the FFT data. This method is used to record the highest frequency data (band 6) as shown in Table 3.

Reference MT processing can be performed for each of the two operational sites recorded simultaneously using each as the reference for the other (local reference mode), or for each of the two operational sites using the remote reference. For processing using only the operational sites (local reference), only the data from these sites is required. In this mode processing can be from the time series, or from the auto and cross-power spectra as computed in the field in real time.

For data processing using the remote reference the time series data from the operational (base) sites and the reference site are copied onto the processing computer's hard disk. The processing program then uses all of the data when computing auto- and

cross-spectra and the MT functions. Note that all of the MT functions can be computed for the remote reference site, using as a reference signal the data acquired at the "primary" site. In addition, the data processor may process the data without a reference , even though the remote reference data are available. In cases where there is little or no noise the results will be identical.

The lowest frequency band is usually sampled (digitized) at a sampling rate of the order of 0.2-0.5 Hz. In order to economically process data to very low frequencies, to frequencies of 0.001 or less, the low band data are decimated, or resampled at a lower sampling rate. This is first accomplished through application of a digital anti-aliasing filter and resampling at the lower frequency. The result is a time series that can be processed in a manner identical to the normal time series but yielding a separate lower frequency band.

B. Processing programs - block diagram and data flow

A block diagram of the data processing programs illustrating the flow of data from acquisition to final output is shown in Figure 4. The processing flow will be described through a description of the individual programs. Note that only generic program names are given here; in practice different specific names will be encountered although the function of the programs will be unchanged.

A word about nomenclature: It was noted above that the time series data are acquired in 512 sample point segments (the choice of 512 points is arbitrary and selectable by factors of 2 by the operator). Several of these segments may be combined (stacked) to form a block. The elapse time for each segment will range from about 30 seconds for band 4 (20 hertz sample rate) to 17 minutes for band 1 (0.5 hertz sample rate). Decimation by a factor of 8 which resamples band 1 data at a rate of 0.0625 hertz results in a segment length of about 2.5 hours. The number of segments per block is operator-selectable. A number of blocks are recorded sequentially to form a run. When the FFT mode is chosen during data acquisition the results of the real-time FFT calculation are stored for each block and for the stacked average of all blocks if desired by the operator.

Program description:

MTACQ - This is the data acquisition program, installed on the laptop or PC computer used in the field to acquire and field-process the data. This program controls the

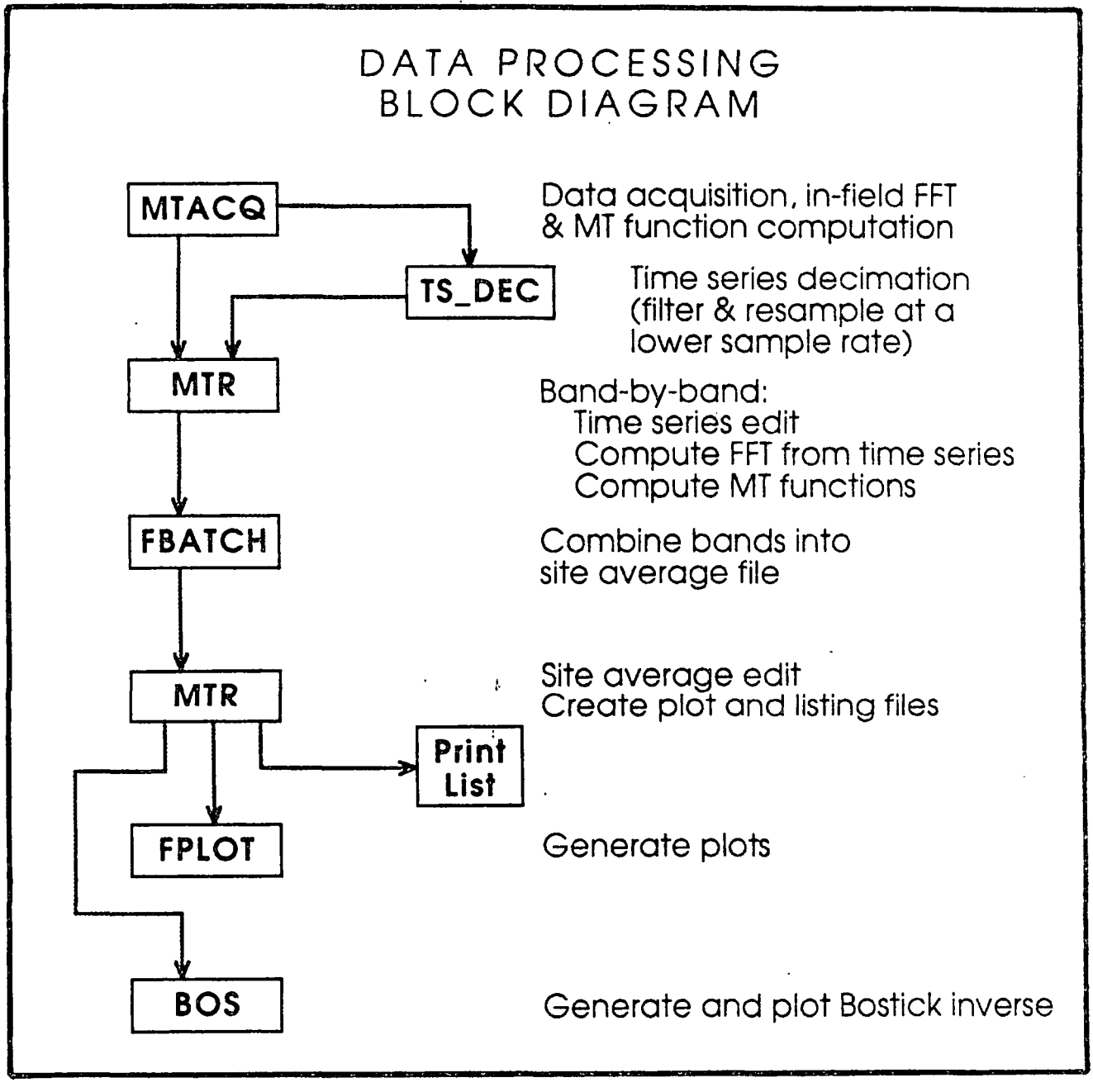
DATA PROCESSING
BLOCK DIAGRAM
MTACQ
TS_DEC
MTR
FBATCH
MTR
Print List
FPLOT
BOS
Data acquisition, in-field FFT & MT function computation
Time series decimation (filter & resample at a lower sample rate)
Band-by-band:
Time series edit
Compute FFT from time series
Compute MT functions
Combine bands into site average file
Site average edit
Create plot and listing files
Generate plots
Generate and plot Bostick inverse

Figure 4

operation of the APU; the acquisition, filtering, amplification, digitization, formatting, and storage of the data. The output are the digitized time series for the electric and magnetic field channels. As an option the operator can choose to have the auto-and cross-spectra computed, displayed, and stored using subroutines within MTACQ that are identical to those employed in MTR.

TS_DEC - This is the program that will resample (decimate) a time series run. Anti-alias filtering is applied automatically when the processor chooses a new sampling rate. Decimation factors available are factors of two; 1/2, 1/4, 1/8, 1/16, etc. The resampled time series is treated by MTR as any other time series.

TS_SHIFT - This program is used when the clock-synchronized remote reference is employed, and a data acquisition run is not started simultaneously at the base and remote locations. TS_SHIFT is applied to the time series that started first, shifting the start time by omitting the data recorded prior to the start at the other site, so that the start times at the two locations are now simultaneous.

MTR - This is the main processing program. Note that this program appears twice in the data flow, here and after the program COMBINE. Here, the input may be either time series (recorded at either just the two operational sites (base) or the operational sites and the remote reference site), or the in-field processed auto- and cross-power functions. When the input to MTR is either the time series or spectra for individual runs, the output is the stacked cross-power files for these runs, for those time series segments or FFT blocks selected by the processor.

COMBINE - This program combines selected runs into one averaged auto-and cross-spectra site-average file. Runs at different recording bands are combined into one site-average file that covers the complete frequency range. If there is more than one run at a frequency band these are stacked. In regions of frequency band overlap points at the same frequency are stacked.

MTR - Appearing here for the second time, the input of MTR is be the output of the program COMBINE described above. The combined processed data are edited and prepared for final presentation to the interpreter. The output is the edited plot and

listing files ready for final printing. The various features of MTR will be described in detail in the following section.

FPLOT - This program uses as input the plot files generated by MTR and generates the final plots of all of the signal parameters and MT functions. The program and the two that follow have provisions for driving several different printers, including laser printers.

POLAR - This program uses as input the plot files generated by MTR and generates plots of the tensor impedance polar diagrams (polar plots).

BOS - This program uses as input the plot files generated by MTR and generates plots of the Bostick one-dimensional inverse function.

C. Processing procedure

All processing was performed at the base camp or office from the time series recorded at the operational sites, and the remote reference site. Some of the final processing and the generation of the final data listings and plots was performed after the conclusion of the survey at one of the Geoevaluaciones office in México City. All processing used software supplied by EMI, the equipment manufacturer.

The data processing consisted of six steps, summarized as follows:

1. Time series preparation - After acquisition the time series required no further preparation prior to processing with the following exceptions: First, the low frequency data, the data recorded in the lowest frequency band, required decimation in order to allow processing to frequencies of the order of 0.001 Hz or below. Both base and reference data were decimated. Second, in the event that the start times of one or more runs at the base and reference sites did not coincide either due to an operator error or operational problems, the start times had to be synchronized through use of the TS_SHIFT program described above.

2. Time series editing and spectra generation - Time series were displayed 512 sample point segment-by-segment as a 10 channel suite (two operational sites with 5 channels each, or an operational site and a reference with two active reference channels and three

inactive channels) for each run. Segments with visible noise contamination were rejected, and spectra computed automatically for the acceptable spectra. The acceptable spectra were grouped into multi-segment blocks, and into an average spectra for the run.

2A. Spectral block editing (high frequency, synchronous detection, band 6, data only) - For that part of the frequency range where time series were not recorded, the high frequency synchronous detection data, each run was acquired as a series of spectra equivalent to time blocks. The results for each block were displayed and blocks selected or rejected on the basis of data quality. The acceptable spectra were grouped into an average spectra for the run.

3. Analysis of MT functions and selection of individual runs for the final site-average file - The MT and spectral functions for each run were examined both for geophysical content and data quality. The runs were ranked as to data quality and runs rejected in the few cases where there appear to be input errors rendering the results inconsistent with the rest of the dat for that site. After ranking the runs to be combined into the site-average file were selected.

4. Preparation and editing of the site-average file and preparation of plot files - The selected run files were combined into the site-average file, the file containing the auto- and cross-power data for the complete frequency range for either the normal or high frequency data. The MT functions computed using this file were examined and edited as described in the following section. After editing plot and listing files were generated.

5. Generation of the data plots and listings - The plot program allows the addition of title and legend information to the basic data, as well as a final check on data quality. The suite of plots and data listings were generated after this material was added. At the time of the processing of the Italian data, the polar plots and plots of the Bostick inverse were generated separately from the rest of the data.

6. Geotools® workstation processing - Additional processing was performed on this workstation prior to detailed examination of the data and inversion. The data were first reformatted into the SEG standard for MT data (EDI standard). A data base was then

created that included the site location as well as the auto- and cross-power spectra. The MT functions were then recalculated and reedited as a check on the original processing.

D. Data editing procedures

The data editing contained in the above processing procedures consisted of time series editing, selection of the band-average run files prior to combing the separate run files into the broadband site-average file, and editing of the site-average files prior to creation of plot files. All editing consisted of the deletion of segments, runs, or data points that were considered to be contaminated by noise or erroneous or questionable for any reason. The EMI software does not support the creation of data points or the shifting of data points for any reason other than input gain errors.

Time series editing - Time series editing consisted of rejecting (i.e., not including in the stacked data for the run) time series segments containing obvious noise contamination or sensor problems. In the case of sites in high noise environments, segments with the least noise contamination are selected.

Run-file selection - This process, described in paragraph D.3 above, involved only the selection of the highest quality runs for inclusion into the final site-average "stack". Runs were rejected on the basis of data point scatter, relatively large error bars, and if there was a suspicion of erroneous gain setting or other input parameters such as sensor polarity.

Site-average file editing - At this stage data covering the complete low or high frequency range were displayed, and data points rejected as necessary. Data points were rejected on the basis of data point scatter, relatively large error bars, anomalous phase, or anomalous skew. Note that at this stage all of the MT functions were examined in detail to ensure that only the most valid points were retained for plotting and eventual inversion. The results of this editing can be observed by examining the plotted data for any site. The apparent resistivity versus frequency data are presented twice; first with all of the points in the site-average file displayed and second after site-average file editing.

E. The effect of severe noise on acquisition, processing, and editing procedures

The data at many of the sites were affected more or less by lightning noise. The noise had the following effect on the survey:

Data acquisition:

- Amplifier gains were sometimes set low to avoid continuous saturation (and the lengthy amplifier recovery times) in the presence of extreme noise, to the extent that during those brief periods with lower noise levels, signal to instrument-noise levels were lower than optimum.

- Recording time was significantly increased in an attempt to record the occasional low noise periods and to provide as much data for examination and stacking as possible.

Data processing and Editing:

- Data processing was affected by noise primarily in the time required to process and edit the amount of data acquired under severe noise conditions, in particular the time series. Processing was frequently an iterative process as different combinations of time series segments or spectra blocks were selected for stacking in an attempt to yield at least some acceptable data points from a run.

F. Effects of processing and editing on the data

The processing of MT data is a relatively simple procedure when compared to other geophysical methods such as seismic data. There is no filtering of time series data or any other mathematical modification applied to the recorded data. Basically the only modification made to the original recording is the rejection of noise contaminated data segments.

The objective of data processing and editing is to present accurate and reliable MT functions for interpretation. To meet this objective the processing and editing procedures were first used to ensure that the data values were valid and that there were no operator or site set-up errors. Then, only data that was considered contaminated or biased by noise was rejected. The intent was that there be no effect on the data other than an improvement in reliability. The principal criteria used to determine whether an improvement has been made is the statistical analysis represented by the error bars displayed for each data point. These represent a one standard deviation range in values around the mean point.

The effects of processing and editing on the data under severe noise conditions are summarized as follows:

- Severe noise drastically affected the amount of data available for computation of spectra at those sites where a majority of time series segments were rejected.

- Severe noise affected the amount of acceptable data remaining after site-average file editing. Severe editing also resulted in data gaps as the result of the deletion of data points.

- Great care was taken to eliminate noise bias in the accepted data, primarily the close examination of phase as well as the magnitude of the resistivity.

G. Data presentation - description of plots and listings

The results of the survey are presented as a series of data plots and listings for each site. This material is found in a series of data volumes attached to this report as appendix A. In addition the recorded and processed data have been provided on magnetic disk and tape, a description of the storage format is found in appendix E. Both listings and plots are provided for all functions except the polar plots. The following is a summary and brief description of these results in the order that they appear in the plot package for each site. The functions have been described in section II.A.4. The references should be consulted for a more detailed explanation. All functions are plotted as a function of frequency, with high frequencies plotted to the left on the figure:

- Apparent resistivity (unedited) - The apparent resistivity is presented as apparent resistivity in ohm meters. The error bars encompass plus and minus one standard deviation. This plot contains all of the data that were compiled into the site-average file, as described in sections V.B and C. The legend on this and all plots includes the remote reference site used for the computation and the rotation algorithm chosen, plus the site-average file (the xxx.AVG file indicated under Filename in the legend). The date plotted refers to the date that the plot file was created, rather than the date the plot was generated.

- Apparent resistivity magnitude (edited) - This plot contains the apparent resistivity data edited as described in section V.D. The data are presented in the same format as the unedited data.

- Apparent resistivity phase (this and all of the remaining MT functions are edited) - The apparent resistivity phase is plotted as degrees phase shift between the orthogonal electric and magnetic field components. The Rho XY phase is plotted with -135° as the base line. The Rho YX phase is plotted with +45° as the base line.

- MT strike - The apparent resistivity, or MT, strike is plotted in degrees. The strike is defined here as the azimuth in degrees relative to true north of the Rho XY component, when the impedance tensor has been rotated using the algorithm noted in the legend. This strike may be parallel or perpendicular to geoelectric strike, depending upon where the Rho XY component is the parallel (TE) or perpendicular (TM) to strike resistivity component.

- Impedance skew - The skew , an indicator of possible three-dimensional complexity normally ranges between zero and one, with skews larger than approximately 0.2 indicative of either noise contamination or possible three-dimensional structural complexity.

- E multiple coherency - The E multiple (predicted) coherency ranges between zero and one, with values of one indicating perfect coherency. The predicted coherency does not completely take into account the effect of the reference processing, so is only an estimate of ultimate data quality.

- Tipper magnitude - The tipper magnitude is the ratio of vertical to horizontal magnetic field signal strength, with the horizontal magnetic field rotated to an axis with the maximum amplitude ratio using a rather complex equation [see reference (39), p.113 for a detailed discussion of this and the other tipper functions].

- Tipper phase - This is the phase of the tipper transfer function.

- Tipper strike - This is the azimuth in degrees relative to north of the horizontal magnetic field in the direction with the maximum H(vertical) to H(horizontal) coherency. In a strictly two-dimensional geologic setting this angle will be ±90° to geologic strike.

- HZ multiple coherency - This is a tipper data quality function based on a relationship between the vertical and magnetic field data similar to the electric field predicted coherency in that the tipper function and horizontal magnetic field components are combined to form a "predicted" vertical field, and this predicted field compared with the actual vertical magnetic field.

- Resistivity (impedance) polar diagrams - The polar diagrams contain the normalized magnitude versus azimuth data for the diagonal (solid line) and off-diagonal (dashed line) terms of the impedance tensor. The off-diagonal term is the familiar apparent resistivity (with appropriate constants). The polar plots are presented for 12 frequencies spaced across the frequency band. At each frequency the magnitude of the apparent resistivity (off-diagonal) is scaled for a maximum amplitude = 1.0, and the same scaling factor applied to the diagonal term. For an explanation of polar plots see reference (A), page 303.

- Electric and magnetic field field spectra - The electric field spectra are presented as millivolts per kilometer per square root of frequency. The magnetic field spectra are presented as milligammas per square root of frequency. Spectra and noise are given for each horizontal component and the vertical magnetic field.

- Electric and magnetic field estimated noise - This function is estimated from the coherency of the two channels under consideration. When to electric or magnetic field channels are used, as in the data presented here, the function is only a very crude estimate of noise power.

## VI. Operations

### A. Crew and supervision

The MT data were acquired and processed by a field crew operated by Geoevaluaciones S.A. de C.V., a Mexican owned geophysical contractor based in México, D.F. The crew consisted of the party chief, observers (instrument operators), a site installation foreman, laborers hired locally, and a field administrative assistant.

The day-to-day supervision, logistical planning, and data quality control were the responsibility of the crew chief, Mr. Thomas Garcia. Project management, interpretation, and planning were the responsibility of Mr. Arnold Orange and Mr. Jeffrey Copley. At Geoevaluaciones, Mr. Orange has overall responsibility for MT technology while Mr. Mario Romero has overall responsibility for operations.

### B. Logistics

The data acquisition operation was based out of Ahuacatlan, Nyarit. Since the local CFE office was also located in Ahuacatlan communication with the CFE project personnel was possible on a daily basis. Periodic communication with Geoevaluaciones project supervision personnel was primarily by facsimile (FAX), although telephone communications were used when necessary. The preliminary observations and interpretation were reviewed with CFE staff members from Ahuacatlan and Morelia as these were developed in the field during data acquisition.

The two primary logistical considerations for the project were site access and weather. Although almost all sites were accessible by four-wheel drive truck, most of the "roads" were very bad. Distances from the base of operations at Ahuacatlan to the western portion of the area, near Amado Nervo, were less than 70 kilometers, but the driving time was in excess of 2.5 hours. The sites south of Tequepexpan were only 15 kilometers (direct distance) from Ahuacatlan but travel time was at least two hours on very rough roads.

Weather was the largest factor affecting the progress of the survey. During the worst period lightning storms would begin building over Ceboruco in the morning and

thunder would be audible by early afternoon. Apart from the obvious physical danger to crew members of nearby lightning, recording would become impossible often before 2-3 PM due to amplifier saturation and severe noise (non-plane-wave propagation). Future operations should avoid the July to September period if at all possible if efficient field operations are desired.

Local agriculture presented a minor problem during this period and was a factor in logistic planning. Local farmers would begin operations soon after sunrise and continue into the afternoon. This required some consideration for those sites located near access roads or near fields where farm machinery was in operation.

C. Surveying

The MT sites were originally located by reference to the 1:50,000 topographic maps of the area. Once a site was established, the exact location was determined through use of the satellite-based global positioning system (GPS). A hand-held Magellan GPS receiver and data processor was used. Site locations were recorded in both UTM and polar coordinates. Site locations are listed in Table I, which will be found following Section IX of this report. Site elevations were also obtained from the GPS receiver, although elevations obtained in the non-differential GPS mode exhibit variable reliability. Permanent monuments were installed at each site.

Where tested, repeatability of the GPS information was within 20-50 meters, and was often better than 10 meters.

At the MT site, sensor orientation and electric field line length were determined using a measuring tape and hand-held Brunton compass, an industry-standard approach to site installation.

D. Schedule

Data acquisition began at the end of June 1991 with system checks and calibration, and was completed at the end of September. This was a somewhat longer period than originally planned, primarily due to weather-related problems. During the data acquisition phase the day-to-day schedule was planned in cooperation with the local CFE staff based in Ahuacatlan.

Field operations were conducted to take advantage of the relative brief intervals between lightning storms, which occurred almost constantly during most of July and August. Storms as far from the survey area as 10-20 kilometers from the recording station had the potential to shut down operations if the lightning was especially severe. Storms were found to occur at any time of the day or night. Many times it was possible to begin recording by 2-3 AM and complete acquisition before mid-day. In these cases the afternoon could be used to relocate the recording instruments and begin acquisition at the next location. In a number of cases it was possible to record a complete site during the night and make the move in the early morning, allowing a second recording to start before the storms became too severe.

## VII. Interpretation - Description of Results

### A. Introduction - Overview

An overview of the MT interpretation is presented on Plate 2, the Interpretation Summary Map. The interpretation identifies three major areas where anomalous low resistivity zones possibly related to geothermal zones may exist. These primary areas of interest identified in the MT data are A) north Ceboruco, B) Amado Nervo, and C) San Pedro. The anomalous zones are relatively shallow, with the top probably less than 1 km subsurface, and with a vertical extent of the order of one to three kilometers. Each of these areas were identified by a characteristic response predicted by a series of two-dimensional MT models. The models were designed based on the assumption that a geothermal reservoir within the geologic context of the survey area will be characterized by a low resistivity zone with a strong resistivity contrast between it and the surrounding, more resistive, units. The identification of these "anomalous" areas is an observation from the processed data. The interpretation of the anomalous areas as being related to a geothermal zone is a subjective judgement based on detailed model studies and experience.

In addition to the anomalous zones, the MT data delineate an elongate low resistivity layer 200-400 meters thick extending from Jala/Ahuacatlan to San Pedro and Amado Nervo. In each case the potential geothermal anomalous zones are located more or less along the boundary of this layer.

The detailed discussion and supporting information for the interpretation is presented in detail in Section VIII.

### B. Introduction, Correlation of Resistivity Units

After processing, MT data are interpreted in terms of the depth, thickness, and resistivity of rock resistivity units. Lithology and geologic structure are then inferred from these resistivities and from lateral and vertical variations in resistivity. Rock resistivity is largely a function of fluid content and pore geometry. Resistivity is related closely to the porosity and salinity of the pore fluids, and to a lesser extent to the formation temperature. Formation resistivity is also related to the surface to volume ratio of the pore spaces, where once a critical value is surpassed, the greater the surface to volume ratio the lower the

resistivity. This comes as a result of the effect on electric conduction, and thus resistivity, of the adsorbed layer of charged ions that occurs at the fluid-grain boundary. This is a primary cause of the very low resistivities and induced polarization effects associated with clay mineralization (and shales). Thus, in volcanic areas of interest to geothermal exploration lithology, the degree of alteration (as it relates to the creation or intensification of clay mineralization), and formation temperature are important parameters that will have an effect on resistivity.

It should be emphasized that MT provides an estimate of average or bulk resistivity over a volume of rock. Thus, within any of the resistivity units as defined in the following paragraph, the resistivity of individual members may be expected to differ from the average.

It is not possible to directly calibrate the subsurface geologic section with the interpreted resistivity units derived from the MT data because there are no deep wells with resistivity logs available for the area. In general the higher resistivity values (100 00 ohm-meters) observed in the near-surface were observed in areas on or adjacent to massive basalt or andesite flows in outcrop. Lower resistivity values in the shallow subsurface appear to be the result of recent fluvial and lacustrine sediments or the alteration of volcanic tuffs and ash units. In the subsurface it is expected that alteration products of the volcanic units, specifically clays, will result in a large decrease in the apparent resistivity. This alteration would be expected to be more extensive in the presence of high temperature geothermal zones.

The MT electrical basement is defined as the deepest low resistivity-higher resistivity interface that can be resolved. Electrical basement may not necessarily be related to what would be normally referred to as either geologic or economic basement. The nature of electrical basement in this area is not known with certainty. The higher resistivity zone identified as electrical basement on the maps and cross-sections is probably a complex assemblage of volcanic and metamorphic rocks.

The interpretation as presented on the maps and cross-sections is therefore expressed in terms of four primary subsurface resistivity units. Note that indications of all four units are not present at every location. The resistivity units are, from the surface, summarized as follows:

1) Relatively high resistivity, 30-1000 ohm meter materials. These probably represent a wide variety of materials, ranging from the highly resistive volcanics to the continental sediments mentioned above. Higher resistivities are related to the more massive basalt or andesite flows.

2) Low resistivity, 2-5 ohm meter materials. These low resistivities are representative of a primarily volcaniclastic and mixed-continental sedimentary section, although other lithologies such as alteration and erosional products will exhibit similar resistivities. In some parts of the survey area there are two low resistivity zones, referred to as the shallow and deep zones, separated by higher resistivity formations of varying thickness. For the sake of consistency, these units have been assigned resistivities of 3 and 5 ohm meters for inversion calculations.

3) A higher resistivity electrical basement as described above.

4) Anomalous low resistivity zones. The anomalous zones, interpreted using as a guide a large suite of two-dimensional models, are interpreted as dike-like zones of low resistivities extending from a depth of the order of less than one kilometer down into the subsurface. The low resistivities are probably related to alteration zones. Model studies indicate that the resistivities within the zones must be of lower resistivity than the widespread low resistivity zone, unit 2, described above. A minimum contrast of 1:3 is anticipated, yielding resistivities for the anomalous zones of the order of 1 ohm meter or less. Elevated temperatures may accompany these zones, although temperatures cannot be interpreted directly from the MT data.

C. Results - Regional Reconnaissance

The regional interpretation of the MT data is presented on the interpretation summary map, Plate 2; the electrical basement structure map, Plate 3; the map of the elevation of the top of the low resistivity unit, Plate 4; the isopach of the deep low resistivity unit, Plate 5; the thickness of the near surface higher resistivity unit, Plate 6; and the regional cross-sections, Plates 7-12. Note that all of the cross-section plates include the apparent resistivity versus frequency data for each site along that cross-section.

The anomalous areas defined by the MT data have been discussed in Paragraph A above. The models upon which the interpretation of the anomalies has been based are discussed in Section VIII.F. In addition to the anomalous areas, the MT data define a subsurface low resistivity body about 35 km long by 15 km wide extending from the Jala/Ahuacatlan area west to San Pedro and Cerro Pelon. The zone has an average thickness of 200-400 meters and a depth to the base of the unit of about 1 km. A high resistivity basement is observed beneath the low resistivity body at all locations. In the area surrounding the low resistivity body, where there is no evidence in the MT response of such a low resistivity body, the MT data show a moderate resistivity layer (50-100 ohm-meters) above a high resistivity (more than 1,000 ohm-meters) electrical basement. There are no indications in the MT results of any significant intra-basement low resistivity anomalies that might be related to a magma chamber or other deep feature of importance to the interpretation.

To the extent of the resolution possible with the MT method the low resistivity zone appears to be a single layer throughout most of the study area. In the eastern and southern portions of the body, however, the data appear to define a shallower and somewhat thinner zone of similar low resistivity. It is very likely that the low resistivity zone defined by the MT data is in fact composed of multiple layers of variable resistivity. The existing interpretation of Schlumberger resistivity data indicated the presence of a much smaller low resistivity zone, confined to the central portion of the survey area. It can be clearly observed from the MT response (data montage, Plate 13) that the low resistivity zone extends much farther to the east and west than previously interpreted. In fact the zone is observed to extend continuously from beneath Ceboruco to the east to beneath Domo de San Pedro to the west.

As shown on the cross sections and structure map, the depth of the low resistivity layer generally becomes shallower to the north and to the west. The interpreted depth to the top of the conductive layer is somewhat greater than previously thought. It may be that the Schlumberger method has mapped a somewhat thinner and shallower zone which could be the upper portion of the layer identified by the MT data. Depth to electrical basement is relatively consistent, on the scale of the MT response, with few abrupt changes in elevation. The margins of the low resistivity layer appear to be the result of non-deposition

rather than structural termination, as the isopach shows a consistent thinning at the boundary of the layer.

The details of the interpretation are presented in Section VIII.

D. Accuracy and resolution - General comments

Magnetotellurics, in common with other geophysical techniques, provides only an estimate of the physical properties of the subsurface and the geometry of geologic structure. The accuracy, or anticipated resolution, of these estimates is influenced by data quality, geologic complexity, and the validity of the underlying assumptions. Of principal concern in this as well as most MT surveys is the accuracy of the depth estimates, in particular the estimate of depth to electrical basement.

The accuracy of the depth estimates anticipated for this interpretation is of the order of minus 10 per cent and plus 15 percent of depth. That is to say, if the interpreted depth of electrical basement at a location as shown on Plate 3 and a cross-section is 700 meters, it is anticipated that the actual depth will fall probably within the range 630-840 meters. This range as a function of depth is shown graphically by the Resolution Analysis figure on the left side of each cross-section. The asymmetry in depth resolution is a result of the tendency of structural complexity, as evidenced by apparent resistivity anisotropy, to influence depth estimates so as to be biased to shallower depths upon inversion.

The primary factors that influence MT resolution are 1) the inherent volume averaging of the method, 2) the effects of two- and three-dimensional complexity upon the data, 3) the non-uniqueness present in any geophysical inversion, and 4) the quality of the data. For this project complexity of the data is not observed to be a significant factor as there appear to be no sites where the interpretation is affected by the type of complex three-dimensional distortion which has been observed in other projects. The MT response is observed to be one- or two-dimensional at most sites, or to involve a form of three-dimensional distortion that does not affect either the qualitative or quantitative interpretation of the low resistivity body or geothermal anomalies. Similarly data quality is also not a limiting factor in the interpretation as only a few sites are observed to have less than good quality data throughout the frequency range of importance.

Of course the other limiting factors, non-uniqueness and volume averaging will be a part of every MT interpretation. As more subsurface information is obtained in the project area, particularly resistivity logs or sample logs from deeper wells, the existing interpretation can be improved and more detailed information provided. The non-uniqueness problem for the inversion process is minimized by constraining the range of allowed solutions to a set of parameters that can be defined geologically with independent information.

## VIII. Interpretation - Details

### A. Interpretation Procedure - Qualitative Interpretation

This section of the report begins with a general introduction to the interpretation process beginning with a qualitative evaluation of the data acquired. Subsequent portions discuss the model studies required to understand the observed response, and finally the analysis of the data. An interpretation of MT data, as with other geophysical methods, is the result of an iterative process where each step has an influence on the others,combined with the professional experience of the people involved.

A qualitative interpretation begins with the first examination of the apparent resistivity versus frequency data. In this step the interpreter makes use of the frequency-depth relationship to identify major resistivity units. The frequency-depth, or "skin depth", relationship states that the lower the frequency under consideration, the greater the depth of investigation. Thus, the behavior of apparent resistivity as a function of frequency can be related to actual resistivity as a function of depth, bearing in mind that the resistivity measured by MT is a volume-average resistivity and that lateral effects can also be frequency dependent. The qualitative interpretation also includes a detailed analysis of data quality, as discussed in Section II.B.2 through II.B.4 of this report.

The qualitative interpretation continues in an iterative fashion with the computation of two-dimensional (2-D) models. The MT functions computed for each site, based on an analysis of the complete electromagnetic field as a function of frequency, contain information concerning the structural complexity for a volume surrounding that site. This is a key point; that MT data from individual sites can be interpreted in terms of structure in the volume of rock surrounding the site, and not just the resistivity section beneath the site. The volume of investigation can be large, extending many kilometers away from the site in many cases.

A primary indication of the 2-D (and possibly 3-D as well) nature of MT data is indicated by the difference between the two apparent resistivity versus frequency functions computed for each site, termed the "anisotropy". The vertical magnetic field component (Tipper) is also an indication of both 2-D and 3-D structural complexity, although it is not unusual to have a minimal or variable Tipper in the presence of complex structure. The

skew and ellipticity functions are 3-D structure indicators, although again it is possible to be in a 3-D setting and have low skew and/or ellipticity. Probably the most straightforward indicators of non-2-D behavior are the polar plots of apparent resistivity, where the departure from two-dimensionality is observed as variations in the behavior of the tensor components as a function of horizontal azimuth. Polar plots and the other functions mentioned in this paragraph are discussed with illustrations in Appendix B.

In the qualitative interpretation phase two-dimensional, and possibly three-dimensional, models are computed to determine the "form" of the resistivity model that fits the data. Since in many cases the solutions are non-unique, geologic constraints based on all available information are utilized in model design. The rotation angle data are utilized to determine the electrical strike of the structure, aided in many instances by the vertical magnetic field (Tipper) data. Two-dimensional models are discussed in more detail, accompanied by illustrative examples from this survey, in Section VIII.E below.

As an example of the qualitative interpretation consider the apparent resistivity data from Site 01, shown in Figure 5. The data are displayed in a standard format with the resistivity on the vertical axis and frequency decreasing to the right. The data have been annotated to point out the important characteristics such as the relative position in frequency of electrical basement. The indication of primarily moderate resistivity materials (20-30 ohm-meters) in the near surface portion of the geologic section is a direct observation from the high frequency portion of the curves. Similarly, the presence of the buried low resistivity section is a direct observation based on the resistivity minimum in the central portion of the response curves. This point cannot be stressed strongly enough; that in this survey area the presence of the low resistivity materials in the subsurface is a direct observation from the basic data. The "key curve" noted on the figure, is the resistivity component determined to be most representative of the subsurface based on the two-dimensional models, yields a positive indication of electrical basement as the apparent resistivity exhibits an abrupt increase at about 1 Hz. The model reviews to be presented in following sections discuss the fact that in most situations one of the components is approximately equal to the one dimensional solution (often this is the maximum component) and this is the component which should be used in the one-dimensional inversion process. The low frequency anisotropy (the difference between the two orthogonal apparent resistivity components noted on the figure) is indicative of a lateral

APPARENT RESISTIVITY SITIO 1

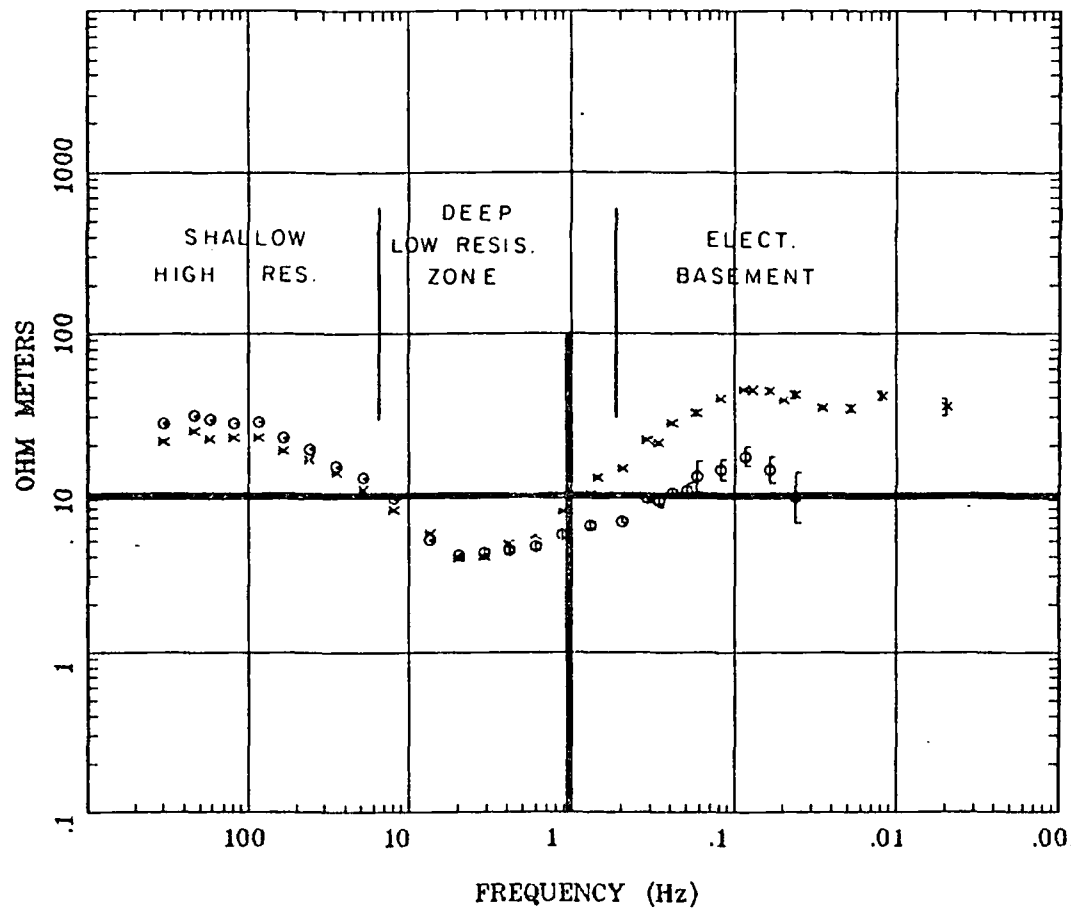


PROSPECTO MT CEBORUCO
Remote: SITIO 2
Rotation: ANALITICA
Acquired: 12:12 Oct 12, 1991
Client: C. F. E.

Filename: C0102AF.AVG
Ex1 Ey1 Hx1 Hy1 Hz1 Hx2 Hy2
GEOEVALUACIONES S.A. DE C.V.
Plotted: 13:46 Oct 31, 1991
< EMI Inc. >

FIGURE 5
APPARENT RESISTIVITY
SITE 1

change in rock resistivity or geometry. Anisotropy is discussed in detail in Appendix B. Much of the data from the central portion of the survey area is more or less similar to the data from site 01.

Now consider the data from Site 73, shown in Figure 6, as a comparison to the data from site 01 shown in Figure 5. At Site 73 the indication of higher resistivity electrical basement occurs at a frequency of approximately 12 Hz, a considerably higher frequency than at Site 01. More important, the low resistivity layer apparent at Site 01 and most of the sites in the survey area is notably absent at this location. The important differences between the data of Sites 01 and 73 are obvious. There is no doubt, that the basement is deeper at Site 01 than at Site 73 and that at site 01 there is a layer of low resistivity material in the subsurface that is either not present or too thin to be resolved at Site 73. Basement at both locations is high resistivity with the "apparent" resistivity of the basement at site 01 reduced because of the overlying section of lower resistivity which causes the average resistivity of the measured volume to be reduced.

The qualitative interpretation is facilitated by use of the Data Montage, Plate 13, which displays representative apparent resistivity data for all sites in the survey area. Resistivity data are also included on each of the cross-sections, Plates 7-12. The characteristics of the individual sites can be studied, and the site-to-site comparison made to evaluate changes in the subsurface across the survey area. The use of the data montage is discussed in Appendix C, page C-8.

B. Interpretation Procedure - Quantitative Interpretation

The quantitative interpretation begins with an evaluation of the continuous "Bostick" inverse for each site. The Bostick inverse is a mathematical formulation that transforms apparent resistivity versus frequency data to an intrinsic resistivity versus depth relationship. Each of the two apparent resistivity curves is inverted assuming that the earth is one-dimensional, with resistivity varying only with depth. If the two apparent resistivity curves computed for a site differ, the inverse functions computed from these curves will also differ. Thus, the Bostick inverse will provide the most straightforward interpretation and be most reliable if the stratigraphy in the vicinity of an MT site is one-dimensional, and will often become more difficult to evaluate and be less reliable as the structural setting becomes more complex. When there is evidence of structural complexity, two- or thee-

APPARENT RESISTIVITY SITIO 73

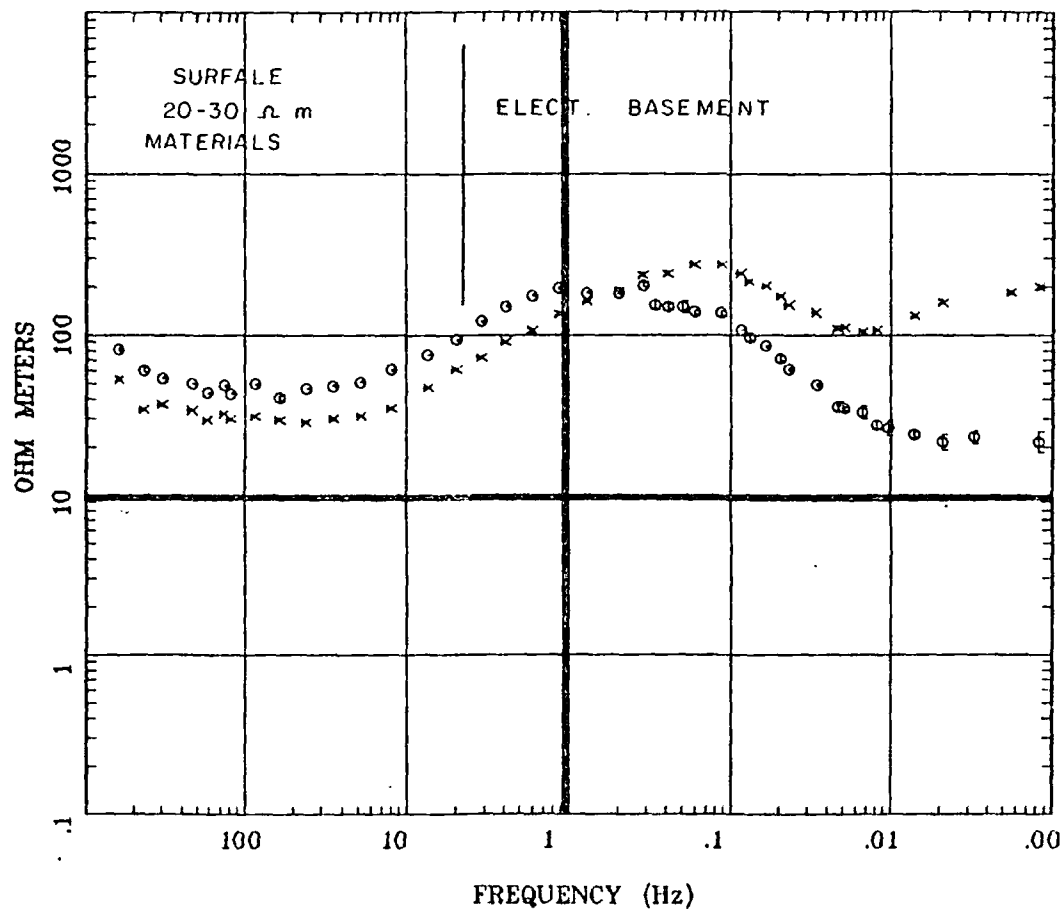


PROSPECTO MT CEBORUCO
Remote: R.L
Rotation: ANALITICA
Acquired: 09:58 Aug 31, 1991
Client: C. F. E.

Filename: c73lraf.avg
Ex1 Ey1 Hx1 Hy1 Hz1 Ex2 Ey2
GEOEVALUACIONES S.A. DE C.V.
Plotted: 11:40 Oct 24, 1991
< EMI Inc. >

FIGURE 6
APPARENT RESISTIVITY
SITE 73

dimensional models are used to predict whether either of the apparent resistivity components can be used as an approximation of the 1-D stratigraphy immediately beneath the site. A Bostick inversion is provided for all sites and this display is part of the site data package.

The Bostick inverse for the key curves of Site 01 and 73 are shown together on Figure 7. Note that both resistivity and depth are plotted with logarithmic scales. The difference between these two sites is readily apparent. Note that the Bostick inverse relates to a volumetric resistivity, a resistivity averaged over a volume of rock, and that no allowance for the non-one-dimensional behavior has been made. A layered inverse and/or 2-D model approach is required to interpret the data in terms of the discrete resistivity units that can be related to geologic formations. The layered inversions for the two sites are also shown on the figure for comparison with the conventional Bostick solution. Although the Bostick provides a useful initial model for the layered inversion, the layered solution allows the interpreter to constrain the solution to a more consistent result. The Bostick inverse data for all sites are contained in the data volumes submitted by Geoevaluaciones. A summary of results for the layered inversion of the key curves is found in Table IV. Plots of the layered inversion and a comparison of the "fit" to the field data will be found in Appendix A.

An expanded collection of forward two-dimensional and related one-dimensional models were computed as the next step in the quantitative interpretation. In addition to modeling the data directly, these models were used to evaluate the structural complexity observed in the data to determine the reliability to be placed on the one-dimensional inverse results, and to determine any corrections to be applied to the inversions to take into account the effects of structural complexity. More than 20 two-dimensional models were computed specifically for this survey. Models computed in the course of other related MT projects were also used to evaluate the two and three-dimensional effects noted in the data. Examples of modelled data are discussed in Section VIII.E below.

It was determined from the model studies that the one-dimensional results could be used at most sites as a first estimate of the resistivity and thickness of formations above electrical basement. Correction factors were required at some sites, however, to account for the two and three-dimensional nature of the data, as evidenced by the anisotropy

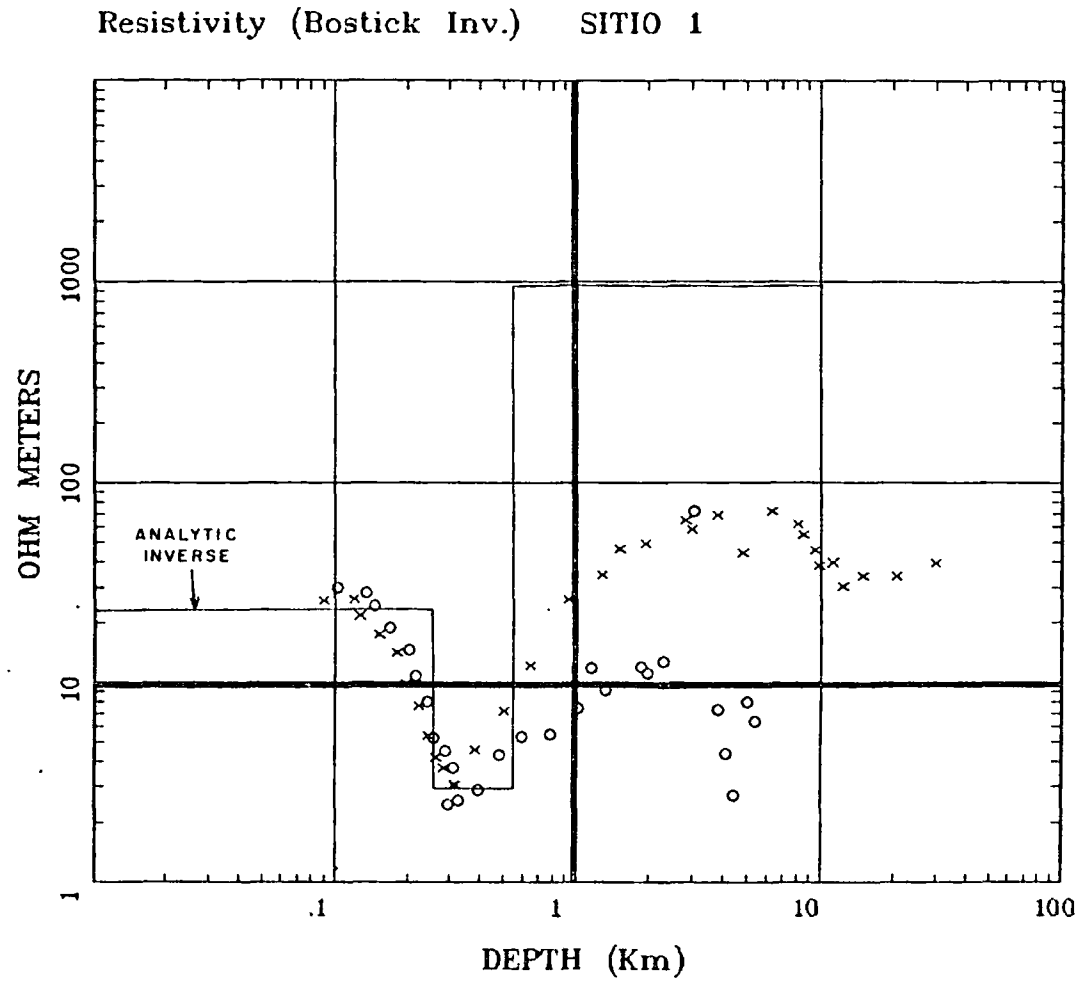


MT CEBORUCO
Client: C.F.E
Remote: SITIO 2
Acquired: 12:12 Oct 12, 1991
Survey Co: GEOEVALUACIONES S.A DE EMI - ElectroMagnetic Instruments

Rotation: ANALITICA
Filename: C0102AF.AVG
Channels: Ex1 Ey1 Hx1 Hy1 Hz1 Hx2 Hy
Plotted: 13:46 Oct 31, 1991

FIGURE 7A
BOSTICK INVERSE
SITE 1

Resistivity (Bostick Inv.) SITIO 73

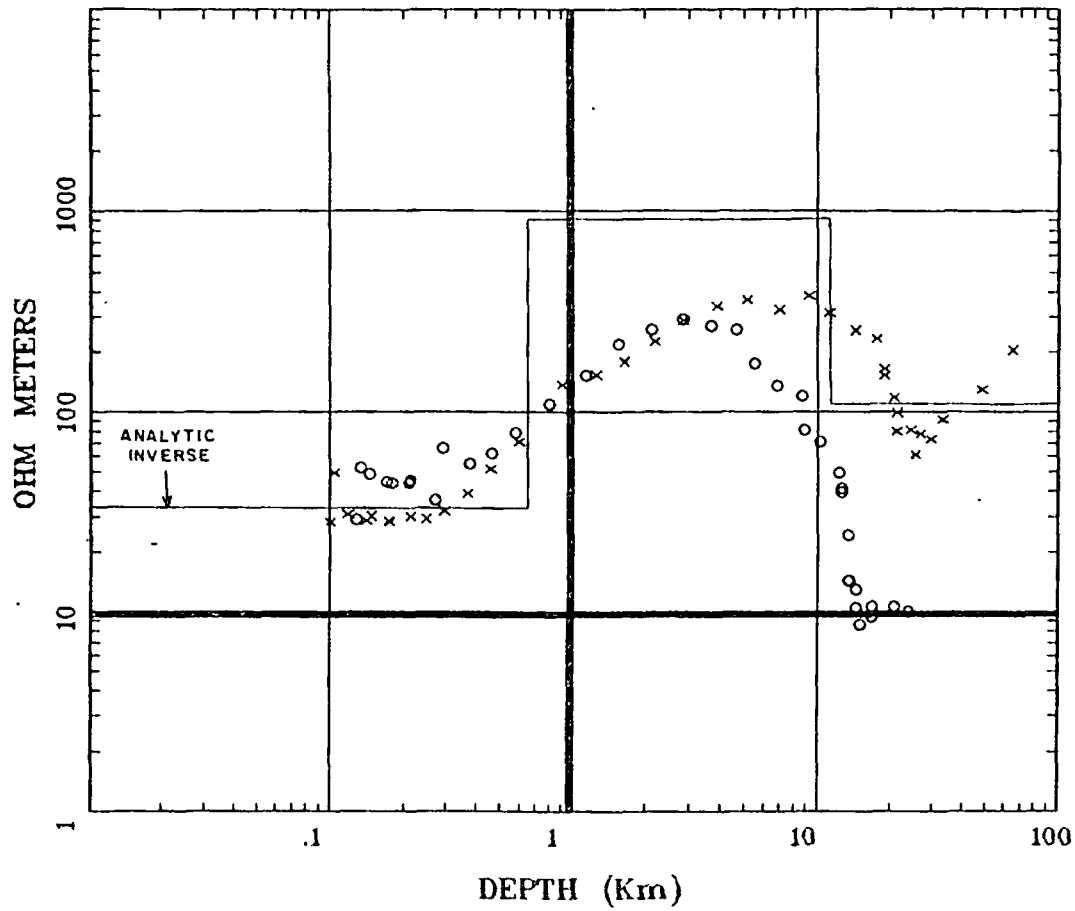


MT CEBORUCO
Client: C.F.E
Remote: R.L
Acquired: 09:58 Aug 31, 1991
Survey Co: GEOEVALUACIONES S.A DE C.V. - ElectroMagnetic Instruments

Rotation: ANALITICA
Filename: c73lraf.avg
Channels: Ex1 Ey1 Hx1 Hy1 Hz1 Ex2 Ey2
Plotted: 11:40 Oct 24, 1991

FIGURE 7B
BOSTICK INVERSE
SITE 73

observed at these sites. The correction factors were arrived at through analysis of two-dimensional models, as discussed in the previous paragraph.

The primary quantitative interpretive tool at those locations which were evaluated as being one-dimensional or near one-dimensi · al was the application of a one-dimensional layered earth inversion program to the apparent resistivity versus frequency data for each such site, corrected for any minor two-dimensional effects. The results of the inversion were a computed resistivity versus depth section for each site.

With regard to the examples presented earlier in this section, 2-D model studies indicated that the key curves for sites 01 and 73, shown above in Figures 5 and 6, provide an acceptable approximation to the 1-D response at those locations. The analytic layered inverse for these curves are shown in Figures 8 and 9. The computed fit to the field data is shown as the solid curve and the individual data points are displayed on a frequency-by-frequency basis. The depths to electrical basement obtained from these results is shown on the figure. The analytic layered inversion procedure is described in more detail, with additional examples, in Paragraph VIII.F below.

The interpretation presented is thus based on the resistivity inversions utilizing, or modified by evaluation of, two-dimensional models where appropriate. To reiterate, the steps in the interpretation procedure are summarized as follows:

1. Qualitative evaluation of the data, including all MT functions and displays. Initial 2-D model computations to evaluate the "form of the solution";

2. Initial quantitative evaluation utilizing the Bostick inverse;

3. Detailed 2-D model study to evaluate structural complexity, model the data as profiles and/or 3-D structures in detail where appropriate, and to determine correction factors to be applied to 1-D inversions at those sites where such an inversion of one or both of the apparent resistivity curves could be demonstrated to be reliable;

4. Computation of analytic 1-D inverse for those sites where appropriate; and

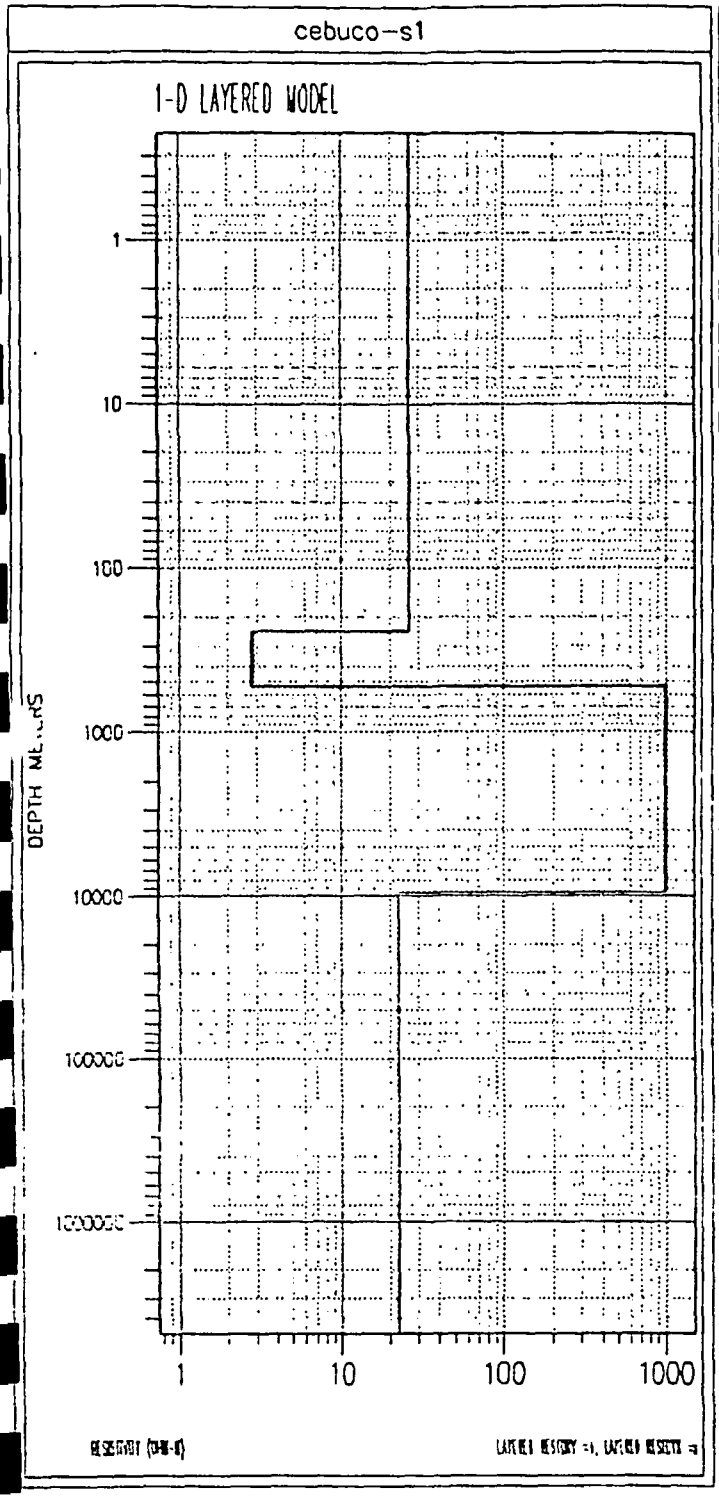


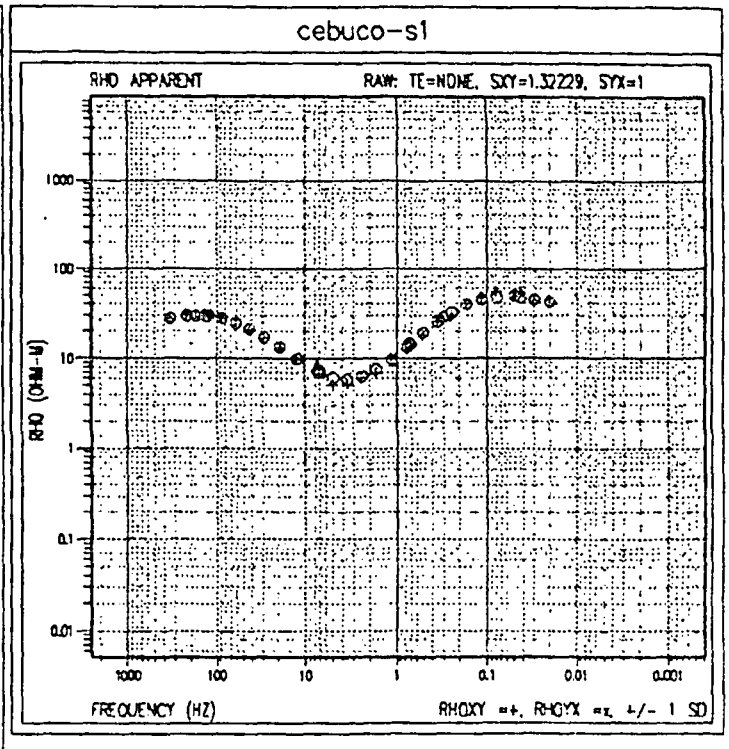


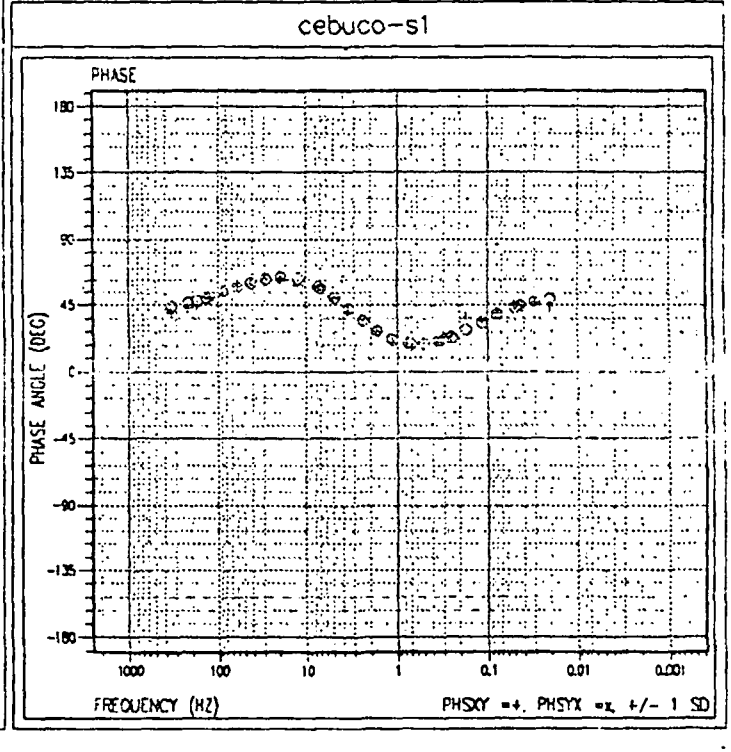


FIGURE 8

ANALYTIC INVERSE

SITE 1

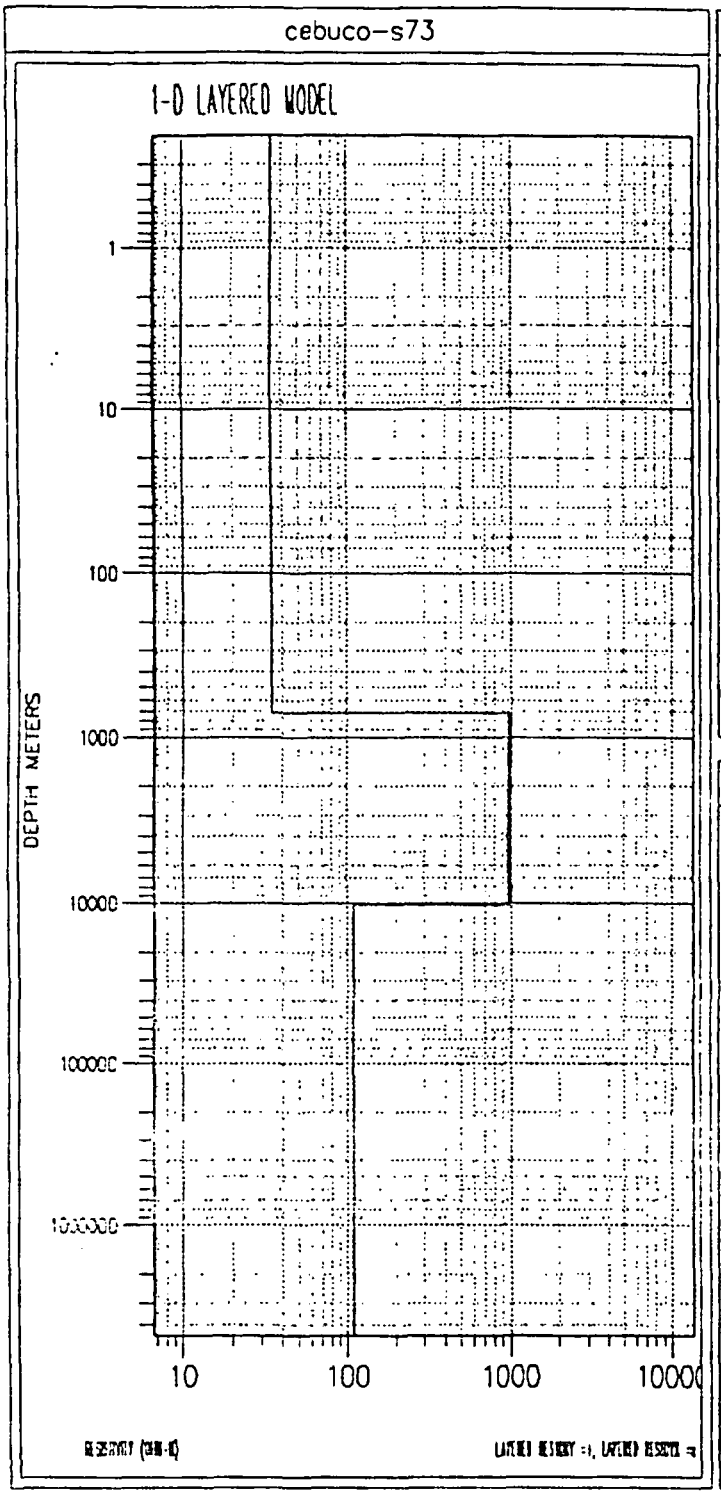


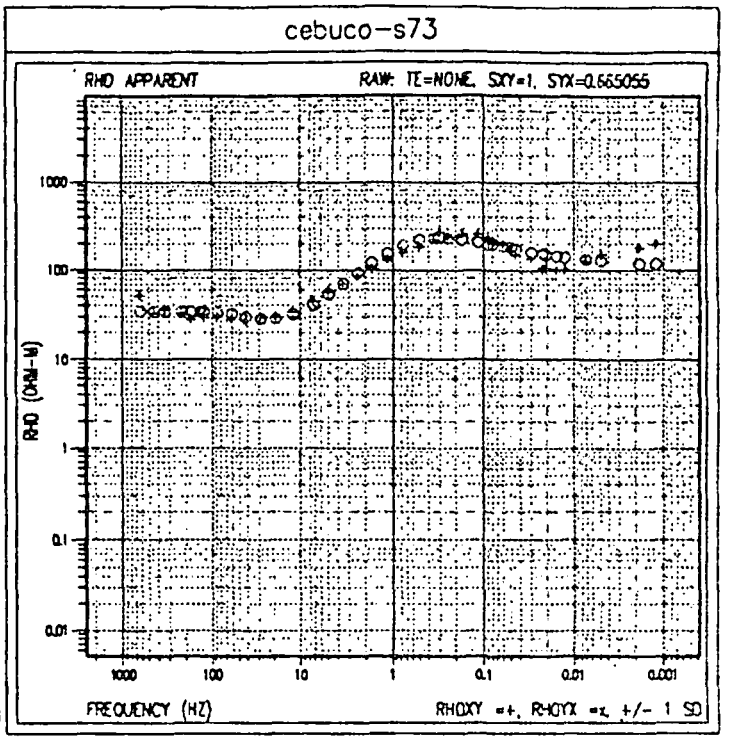


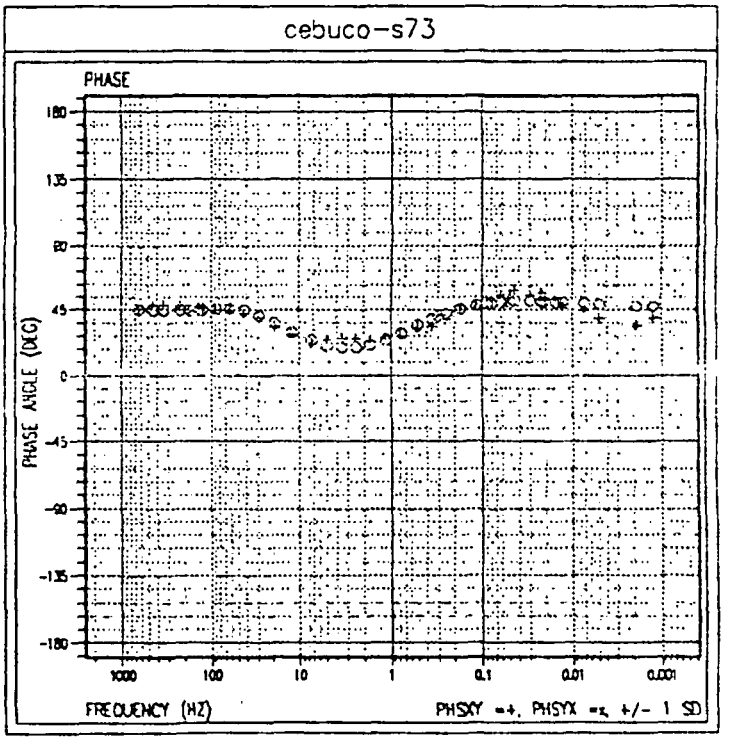


FIGURE 9

ANALYTIC INVERSE

SITE 73

5. Final MT interpretation based on the analytic inverse and 2-D models and the supporting MT functions such as the vertical magnetic field (Tipper), and the integration of the MT results with other available data such as well data and surface and regional geology.

C. MT and Geologic Assumptions Important to the Interpretation

Several assumptions are inherent in the MT interpretation presented in this report. These assumptions, and the rationale involved in their application, are summarized as follows:

MT assumptions:

1. One-dimensional (1-D) assumption - The use of the 1-D analytic inversions at most of the sites in the course of the quantitative interpretation assumes that at least one of the two apparent resistivity versus frequency components approximates the 1-D response to that section. It is assumed that the 2-D model upon which this interpretive decision is based is representative of the subsurface. The use of 1-D inversions in an interpretation is discussed in detail in Section VIII.G of this report.

2. Two-dimensional (2-D) assumption - The interpretation is strongly based on the use of 2-D models. It is assumed that much of the survey area can be approximated by 2-D geologic structure, and that 2-D models can be developed that yield results that are identical to or closely approximate complex field data. The design and use of 2-D models are discussed in detail in Section VII.E of this report. At the sites where 2-D models are employed this assumption is based on; a) confidence that the 2-D model selected is representative of the subsurface, c) the magnitude of the skew and ellipticity functions (indicators of 3-D complexity) are low at the frequencies of importance to the interpretation, and d) there is minimum distortion evident in the impedance polar plots through the frequency range of interest to the interpretation of the upper 10-15 km. Skew and polar plots are discussed in Appendix B, on pages B-10 and B-14 respectively.

3. Correction for two-dimensional (2-D) effects - The interpretation assumes that appropriate 2-D models were used to either directly model the data or to determine corrections to the depths and thicknesses obtained using the 1-D analytic

inversions. Two-dimensional effects are ...scussed in Appendix B, page B-20, and in Appendix C.

4. Interpretation of three-dimensional effects - The interpretation assumes that 3-D effects are minimal at most sites, and will not affect the interpretation. This assumption is based on an analysis of the resistivity data, the impedance polar plots, and on the skew and ellipticity data.

5. Undetected complex structure - It is assumed based upon experience and the model studies performed in support of this project that there are no undetected 2 or 3-D effects that affect the validity of the interpretation.

6. Modelling and Inversion constants - In this area of sparse subsurface control it was assumed that the resistivity of the major subsurface units varies slowly. Thus, the deep low resistivity unit observed at many sites was modeled using 3 ohm meters, in order to yield a consistent and reproducible interpretation. Where present, a value of 5 ohm meters was used for the more shallow low resistivity unit. This point is discussed further below in Section VIII.G.

7. Statics shifts - A statics effect in MT data occurs when the apparent resistivity versus frequency data are distorted due to shallow lateral variations in resistivity. The statics effects must be recognized, and corrections determined to account for the distortion. This may be a difficult step; the analogy is attempting to apply a statics shift to a seismic trace, where the nearest adjacent trace is a kilometer or more distant. Statics corrections were necessary at several sites in the survey area. The corrections were determined after analyzing the TDEM data, the results of the Schlumberger survey conducted previously by CFE, and the MT data itself. In this regard the presence of closely spaced sites materially helped in determining the appropriate correction by comparing the apparent resistivity at the site in question with the average resistivities observed at nearby sites. MT statics are discussed in more detail below and in Appendix B, page B-18.

Geologic assumptions:

1. Resistivity related to porosity and pore fluid characteristics - A basic assumption in evaluating the results of this survey is that the average resistivity of a volume of

rock is a function of average porosity; the greater the porosity the lower the resistivity. Note that this makes no statement about formation age or lithology. Lithology can be estimated based upon experience and upon the rocks observed on the surface and in any wells that penetrate a section that is anticipated to be similar to that of the survey area

2. Resistivity related to pore geometry - Formation resistivity is related to the surface to volume ratio of the pore spaces as well as total porosity. Once a critical value is surpassed, the higher the surface to volume ratio the lower the resistivity. This comes as a result of the effect on electric conduction (and thus resistivity) of the adsorbed layer of ions that occurs at the fluid-grain boundary. This layer has the effect of drastically reducing the resistivity of the pore fluid at the boundary. This is a primary cause of the very low resistivities and induced polarization effects associated with clay mineralization and some shales.

3. Representative section - The limited subsurface geologic information available for this interpretation makes the relationship between the identified resistivity sequence and a "representative" geologic section very difficult. Previous experience in analogous volcanic units in the Azufres-Araro area would indicate that the higher resistivity units are generally comprised of more massive basaltic or andesitic zones while the lower resistivity sections are composed of volcaniclastics and mixed continental erosional produces and sediments.

4. Absence of mineralogical effects - It is assumed that there is no unusual mineralogy in the area that would yield low resistivities other than the clay mineralization discussed in (2) above. Such effects are rare, and where observed in the course of other MT surveys, have been readily identified in the course of model studies.

D. Model design - General comments

The primary purpose of the model studies was to determine the expected MT response to the type of geothermal zone which is the object of this exploration project. The goal was not necessarily to provide an exact "match" to the field data, but rather to provide a guide to the character of the expected response and a framework for the interpretation of the survey data. The starting point, of course, is the experience of the interpreter under

similar geologic conditions and reference to model "case books", models computed earlier. The first one-dimensional (1-D) and two-dimensional (2-D) models for a survey are computed to confirm the intuition of the interpreter. Once these initial models have been evaluated, modeling proceeds in an iterative fashion, with 1-D and 2-D models computed to examine all of the features of the data. Geologic constraints are applied in the form of limits to the resistivities and geometry used in model design. The model parameters must be realistic and be physically realizable within the known or anticipated geologic framework of the area.

E. 1-D Sensitivity Models

As part of any interpretation or acquisition project it is useful to determine the relative sensitivity of the MT response to a variety of changes in the geologic parameters expected in the project area. The first step in this process is the calculation of a series of one-dimensional (1-D) models where the thickness or resistivity of a given layer is given a range of values covering the variations expected in the data. A review of the data montage on Plate 13 indicates that the majority of the MT data from the Ceboruco project can be described rather simply as having a resistive layer near the surface, a conductive (low resistivity) layer beneath the surface layer, and a more resistive electrical basement to great depth. This section of the report presents those 1-D models calculated for the Ceboruco project area which demonstrate the relative effect of changes in near surface resistivity, thickness or resistivity of the conductive layer, resistivity or thickness of the crustal layer and the resistivity of the deep half space. Also presented are models showing the effect of changing various parameters in the case of multiple low resistivity layers.

The first series of 1-D sensitivity models, in Figure 10, shows the effect of changes in the resistivity of the near surface layer with its thickness and other model parameters held constant. Results are computed for a first layer resistivity of 10, 20,50, 100 and 1,000 ohm-meters, with a constant thickness of 250 meters which is a typical value for many of the sites in the project area. The comparison clearly shows that the only difference between the response of all the models is in the high frequency portion of the curves. All of the responses converge at about 10 Hz and are effectively equivalent below about 1 Hz. Also shown on the figure is the frequency of the skin depth for the first layer, to provide an indication of the transition response to the conductive layer. The skin depth is defined as the depth at which the amplitude of an electromagnetic wave propagating into a lossy media

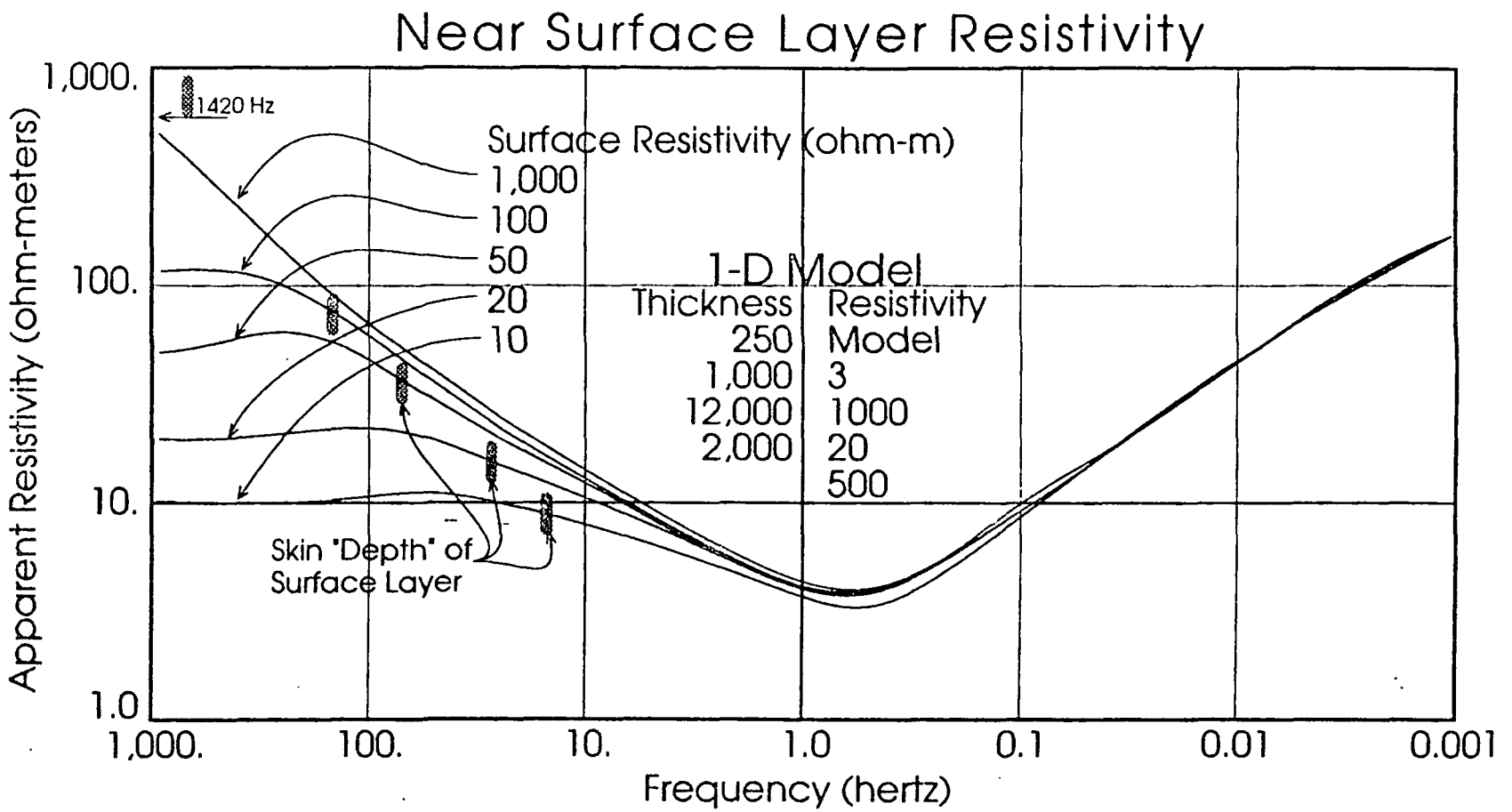


Figure 10
Effect of Surface Resistivity
on MT Response

will be attenuated to 1/e of its initial value. The value of the skin depth is directly related to resistivity and inversely related to frequency.

The next group of models, tests the relative MT response for changes in the thickness and resistivity of the low resistivity zone. In Figure 11, the thickness values are varied from 100 to 2,000 meters with a constant resistivity of 3 ohm meters. In Figure 12 the resistivity values of the zone are varied from 3 to 50 ohm-meters with a constant thickness of 1000 meters. In general as the resistivity of the layer is decreased or the thickness is increased, the result is that the minimum portion of the curve moves to lower frequency and lower apparent resistivity. Both of these changes represent an increase in the conductance of the layer.

The effect of changes in basement resistivity and thickness on the observed MT response is the parameter of interest in the next model series illustrated in Figures 13 and 14. The term basement resistivity refers to the effective average resistivity of the resistive geologic section below electrical basement. Electrical basement, not necessarily the same as geologic basement, is usually defined as the base of the deepest low resistivity zone that can be resolved by MT. The resistive electrical basement extends to a depth where the resistivity decreases due to high lower crustal temperatures. In general the Ceboruco area is found to have a relatively high apparent resistivity for the basement. The values of basement resistivity in Figure 13 are varied from 100 to 2,000 ohm-meters, with a constant basement thickness of 10 Km.. The response is observed to be basically the same for basement resistivities above 500 ohm-meters.

The effect of changes in basement thickness is illustrated in figure 14 where the thickness is varied from 5 to 50 kilometers for a 1,000 ohm-meter section. A comparison of the varied basement resistivity example (Figure 13) with this figure shows that the MT response is more sensitive to basement thickness than the resistivity, once the resistivity is greater than ~500 ohm-meters. It can be observed from this figure that the observed effect of an increase in basement resistivity is an increase in the observed apparent resistivity along the low frequency portion of the curve.

The final model series is intended to demonstrate an important concept for the interpretation of the data in terms of resistivity and thickness. It is important to understand that as a geophysical measurement the MT response has a certain amount of ambiguity

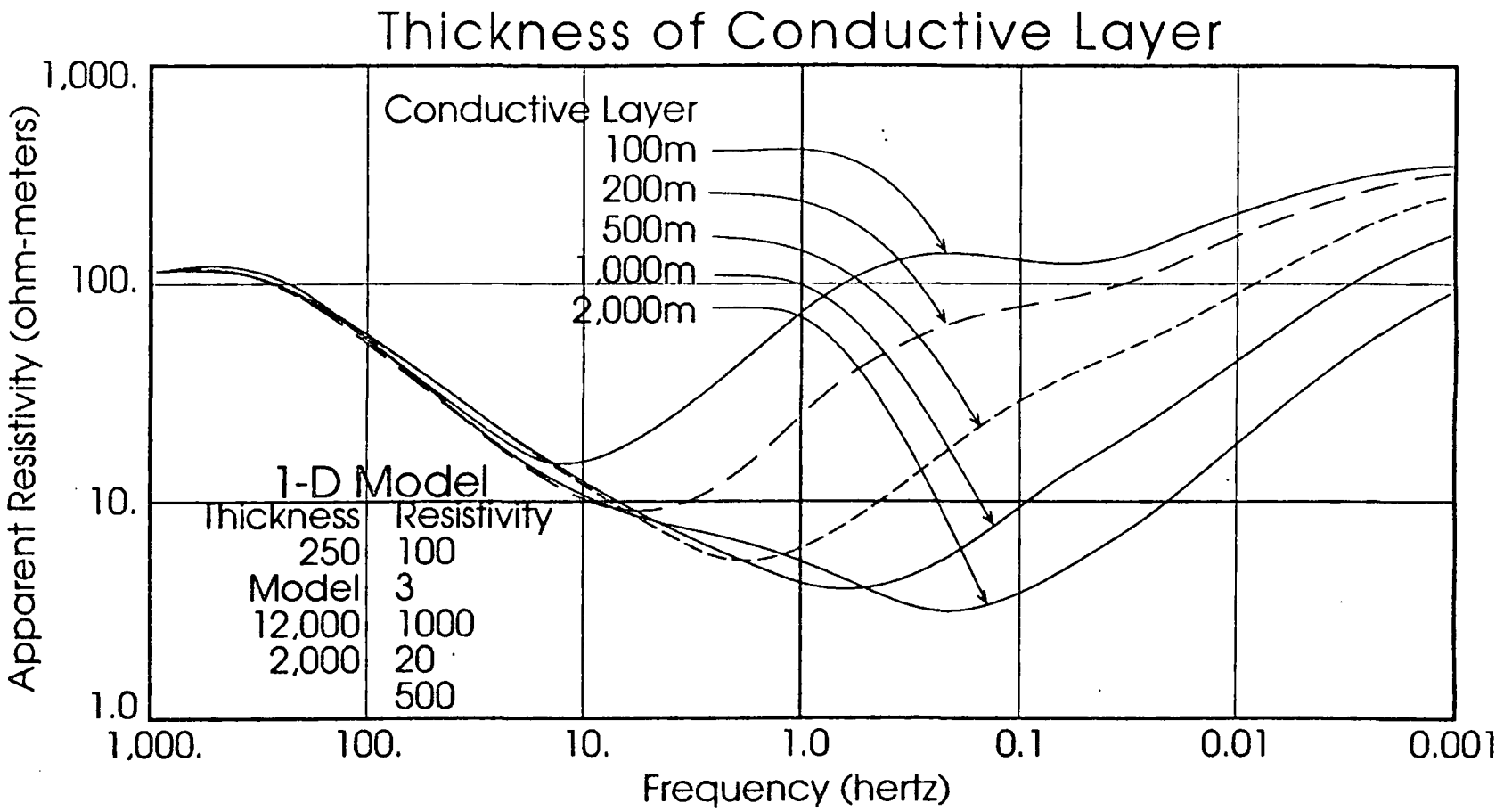


Figure 11
Effect of Conductive Layer
Thickness on MT Response

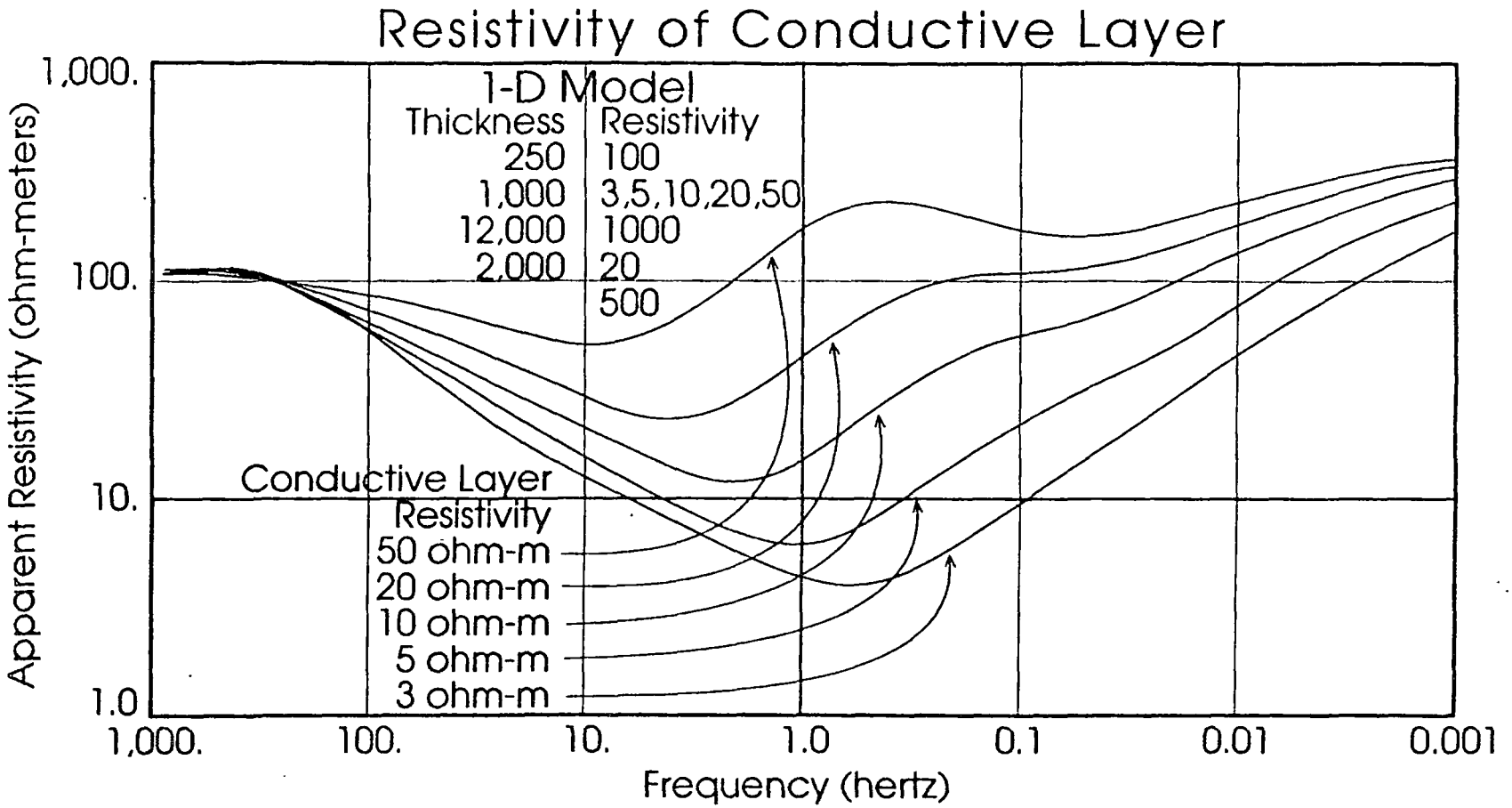


Figure 12
Effect of Conductive Layer
Resistivity on MT Response

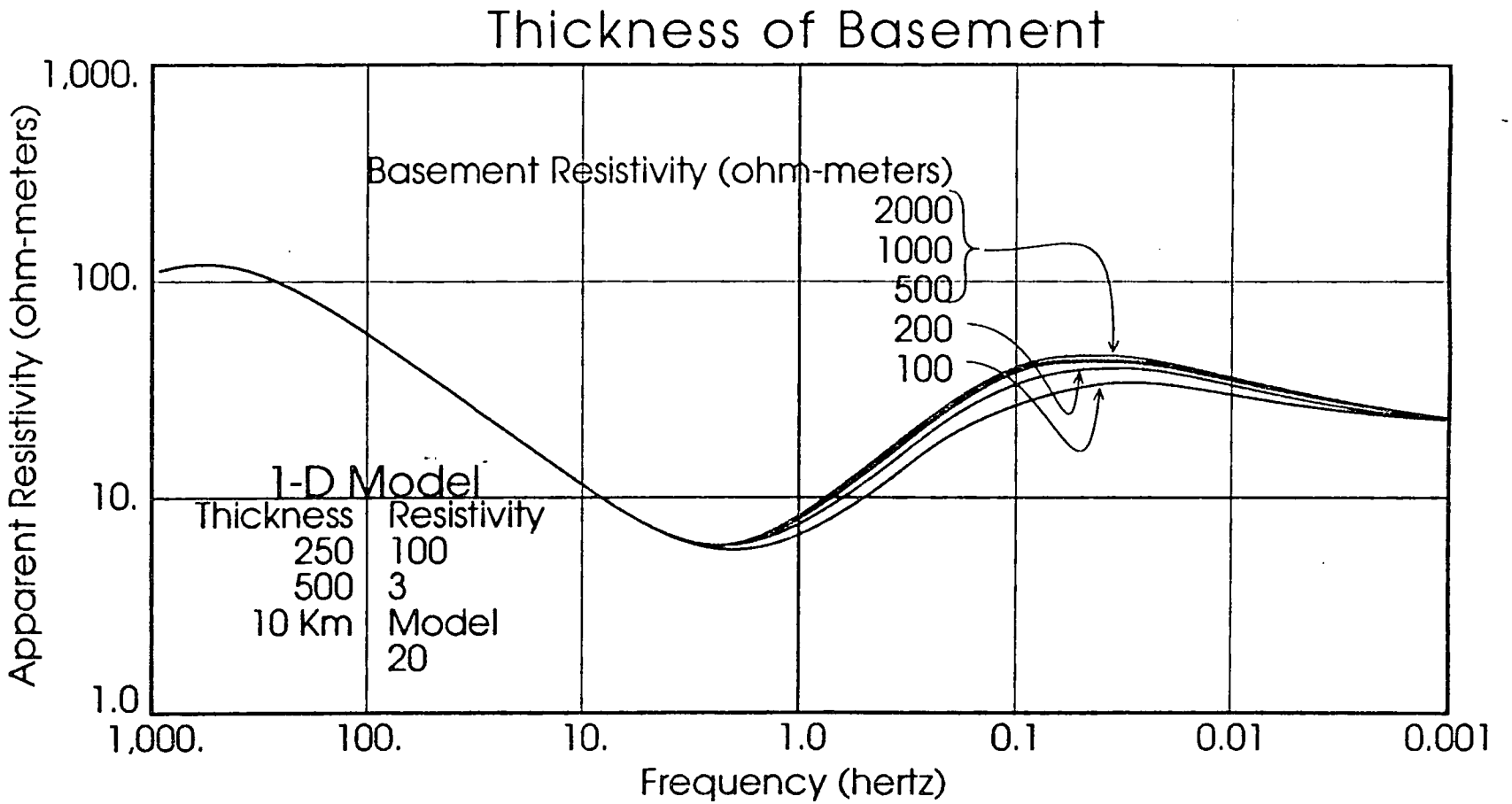


Figure 13
Effect of Basement Resistivity
on MT Response

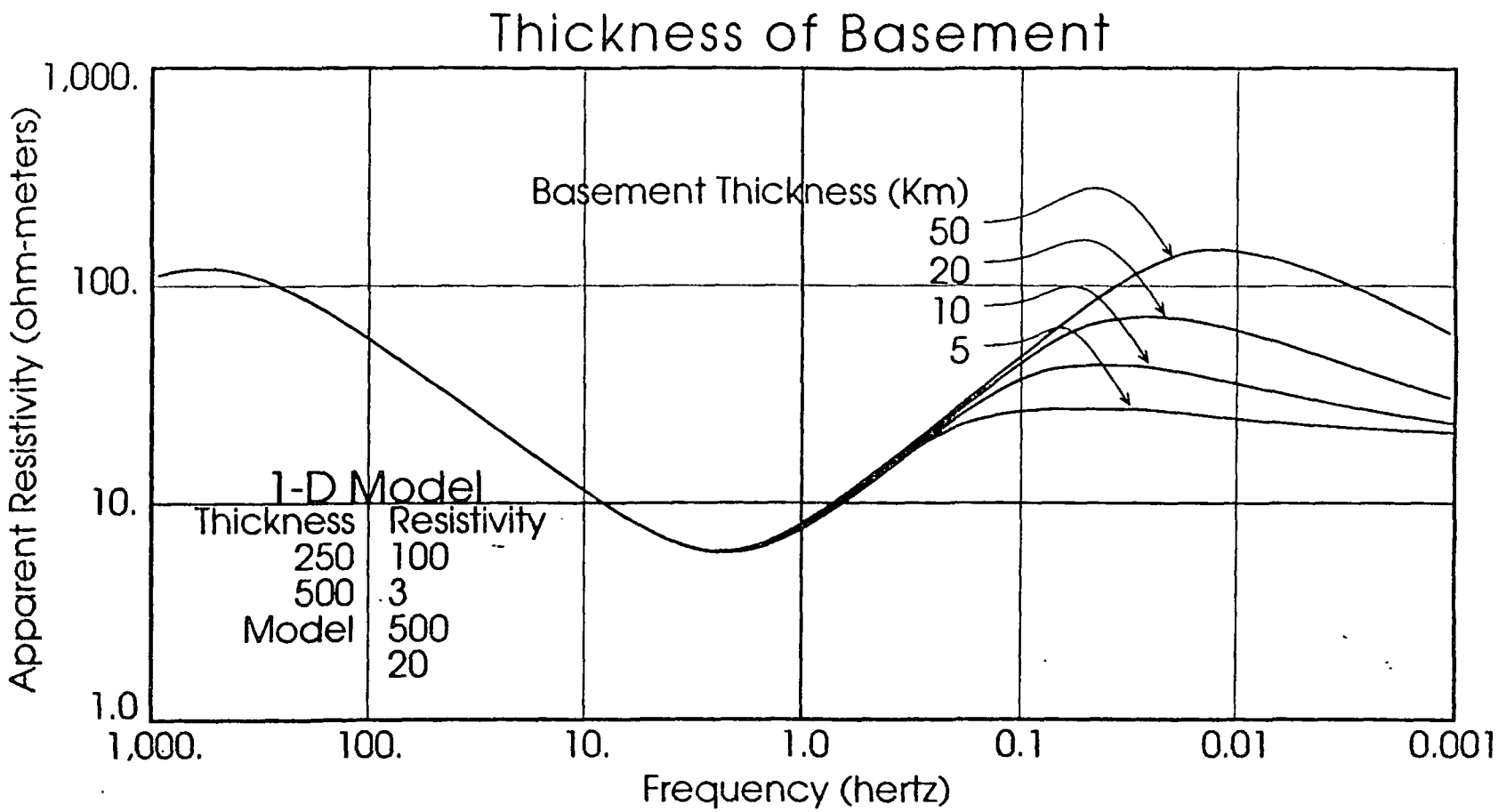


Figure 14
Effect of Basement Thickness
on MT Response

associated with the interpreted results. As mentioned above the response to a particular unit is related more to the conductance of that unit that to the specific thickness or resistivity, where conductance is defined as the thickness of a zone divided by its resistivity (or the equivalent, thickness times conductivity). Except for the first layer, the parameters determined for any layer will have a wide range of equivalent solutions, therefore it will be important to limit this range by using whatever other independent geologic or geophysical information which may exist. Also when comparing the response at one site to another site it is important to constrain either the thickness or resistivity to understand the difference.

The example shown in Figure 15 considers the MT response for two cases; first, the case of a thin low resistivity layer, case A, and then a thicker layer, case B. For case A the results for a 3 ohm meter layer 200 meters thick are compared with those for a 6 ohm meter layer 400 meters thick. For case B the results for a 3 ohm meter layer 1000 meters thick are compared with those for a 4.5 ohm meter layer 1,500 meters thick. For both case A and case B, the results for the two models computed for each case are very similar. The small differences are due to the changes in depths to the center of conductance. In each case, if one were to consider real data the inversion results would be difficult to differentiate.

F. Modelling - Two-dimensional Models

Two-dimensional models for this project were computed using a standard finite difference modelling approach, as described in the paper by Jupp and Vozoff (1977, see reference [30] at end of report). To design a model, the interpreter describes the desired structure in terms of rectangular blocks, and specifies the number and dimensions of the horizontal layers and vertical columns, and the resistivity of each block. The MT response for the input model is then calculated and the results plotted in the form of apparent resistivity versus frequency for selected MT "sites" located on the surface, using the same plotting conventions used in plotting field data. The input model is shown as a psuedo-cross-section. The AOA two-dimensional modelling program allows the calculation of models with topographic relief, with the "air" modelled by a $10^5$ ohm meter zone.

The previous discussion of 1-D analysis is useful for understanding the relative affect on the MT response of changes in the thickness or resistivity of a given geologic unit. In the case where these layers have a limited lateral extent or where the exploration

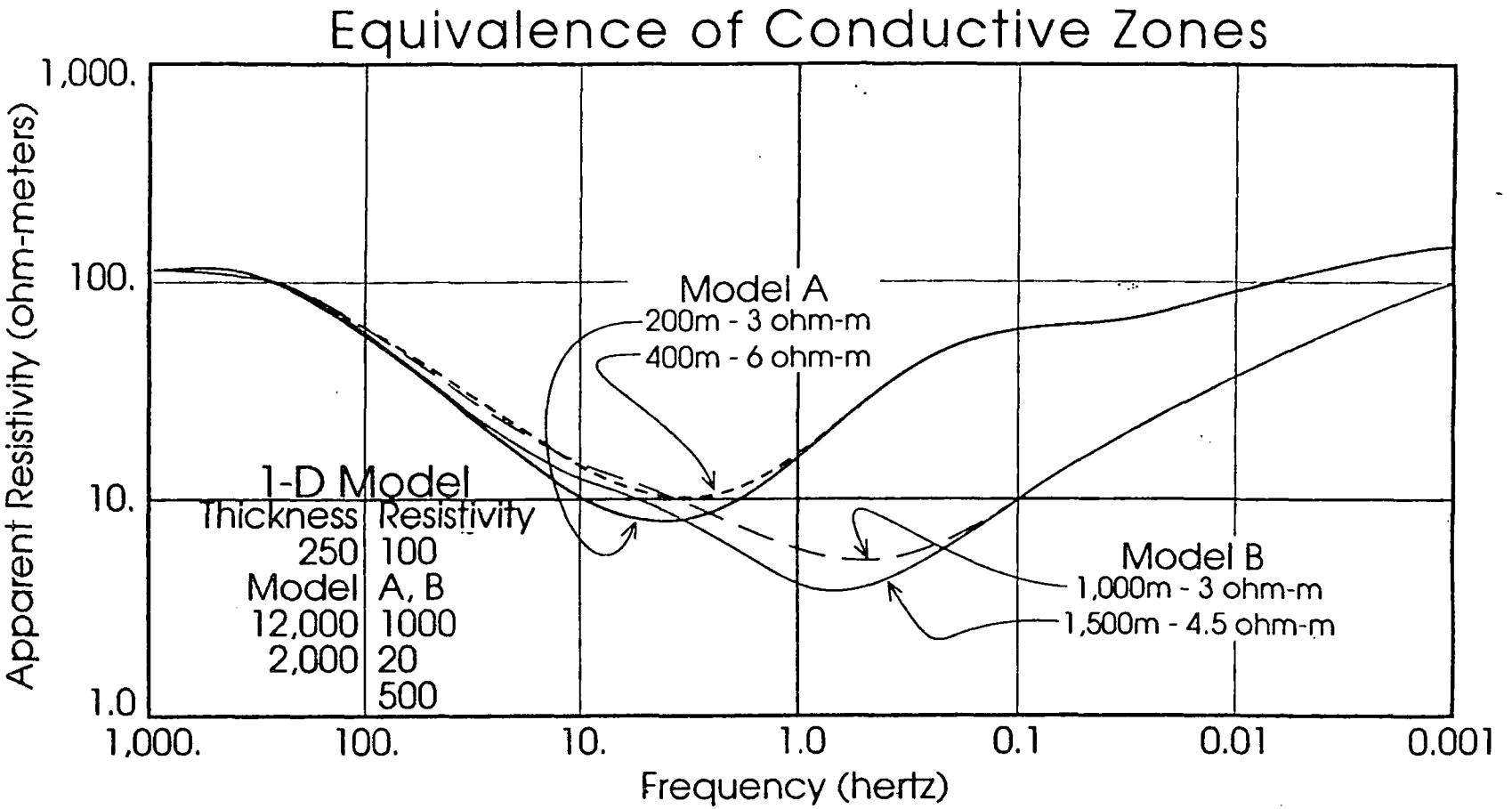


Figure 15
Effect of Thickness/Resistivity
on MT Response

target is limited in both the X and Y dimensions the problem of data interpretation becomes somewhat more complicated. This section presents a series of 2-D models which illustrate a portion of the range of geometries expected for the exploration problem which is the target of this project; the location of potential geothermal reservoirs.

A total of 20 2-D models (Plates M-1 through M-19) are presented as examples to show a range of possibilities for the exploration target of the project. This information is also summarized for particular models in several figures found in this section. Each model is presented on a summary plate, showing at the top a sketch of the input geometry and resistivities with the calculated MT response at specific locations beneath. For the model calculation, it is possible to determine the component parallel to strike (TE or transverse electric, with the electric field polarized parallel to strike) and the perpendicular to strike component (TM or transverse magnetic, with the electric field polarized perpendicular to strike). The model displays retain this distinction using a coded line pattern. However, it should be noted that it is generally difficult if not impossible to make a clear distinction when data from the real world is considered. Therefore, although the terminology of TE and TM is used for discussion of the model results it is not emphasized in the interpretation of the MT field data.

Base Case 2-D Models:

In the first major group of models (2A-11C), Plates M1-M12, the MT response as a function of distance from a single, low resistivity "dike" is tested for a variety of electrical structural conditions. The "geothermal" zone is shown in the models as a low resistivity zone (1 ohm-meter) which is more or less vertically oriented and 500-1,500 meters wide. For all model cross sections zones with resistivity less than 10 ohm-meters are shaded.

Models 2A and 3A, Plates M-1 and M-2, compare the effect of the width of the low resistivity zone on the MT response. The results are summarized in Figures 16 and 17. Except for the anomalous body the model has a layered, essentially 1-D geometry. In Figures 16 and 17 the TE field and TM results are summarized in separate plots on each figure. As might be expected the general character of the effect is similar between the two examples, but the magnitude of the distortion is greater for the larger low resistivity body.

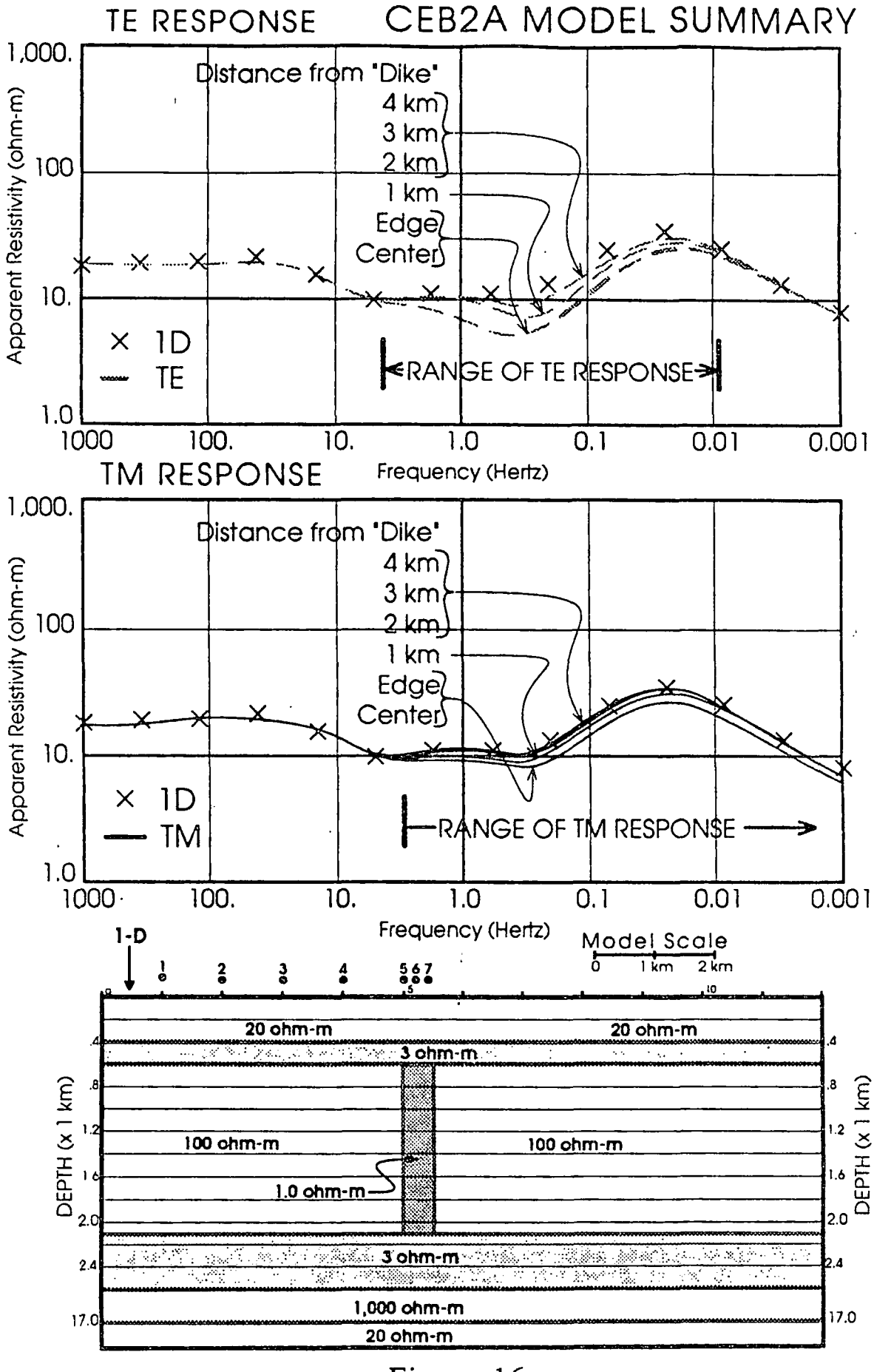


Figure 16
Summary of Model Response: CEB2A

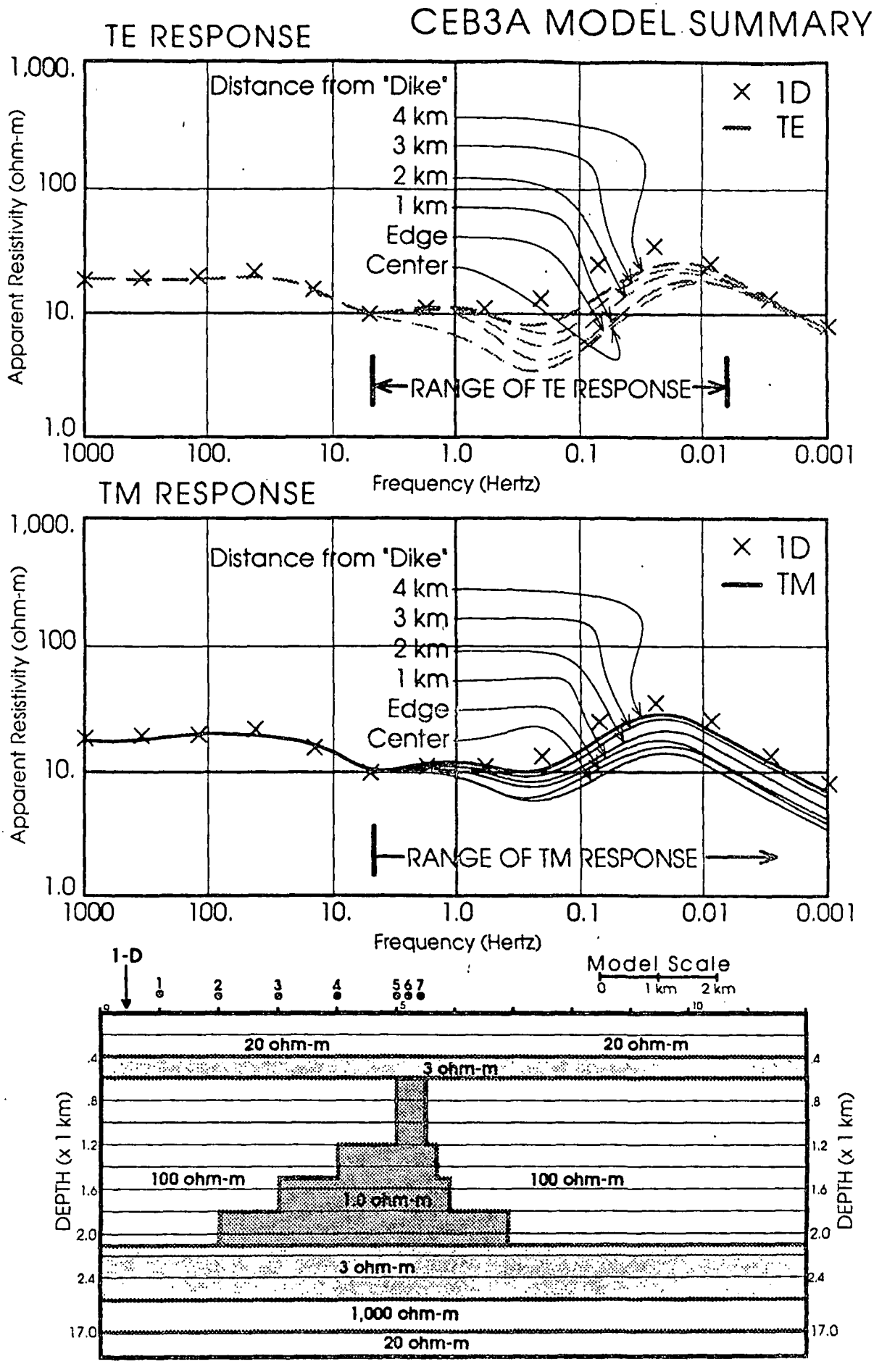


Figure 17
Summary of Model Response: CEB3A

An important conclusion from this model study is the difference in response for the TE and TM components. This difference is summarized in Figure 17 for the results of model CEB3A (Plate M-2). Results for the TE solution at each site are shown in the upper plot separately from the TM response in the lower plot. The calculation "sites" are shown on the model sketch at the bottom of the figure. The basic difference between the responses is that the effect of the conductive body is only observed over a limited range of frequencies in the TE solution, but the TM response shows a continuous response to low frequency. In other words the TE solutions at all sites are equal above and below the "range of response". In this case this range is from ~5-0.005 hertz. The TM solution shows a constant level of distortion at frequencies lower than a certain "threshold" frequency equal to the high frequency portion of the TE response. The 1-D solution for a location outside of the anomalous body is shown by the "X" on the model plot. The difference between the component displayed and the 1-D solution is a measure of the distortion created in the MT response by the anomalous body.

The magnitude of the distortion created by the low resistivity anomaly can be increased by removing the deep 3 ohm-meter layer and increasing the resistivity of the shallow layers. This in effect makes the anomalous body the dominant low resistivity feature, concentrating the induced current flow which in turn causes the "distortion" of the otherwise simple MT response. Figure 18 is a summary of the MT response for model 4A (plate M-3). Although the frequency range of the TE response is the same as the previous example the new model shows that the distortion (both TE and TM) is greatly increased by the greater contrast between the anomalous body and the resistivity structure of the surrounding units. In addition the higher near surface resistivity causes the anomaly to be detected at a greater lateral distance.

Models 5A and 6A (Plates M-4 and M-5) reduce the lateral extent of the shallow low resistivity layer in the presence of a 100 ohm-meter (model 5) and 1,000 ohm-meter (model 6) first layer, similar to models 4a and 5A respectively. The results, summarized in Figures 19 and 20, are quite similar for the two with an allowance made for the relatively simple effect of the change in near surface resistivity as shown in the previous 1-D examples (figure 10). The boundary in the shallow low resistivity zone creates only a minor difference in the response, primarily for the TM component, when compared with

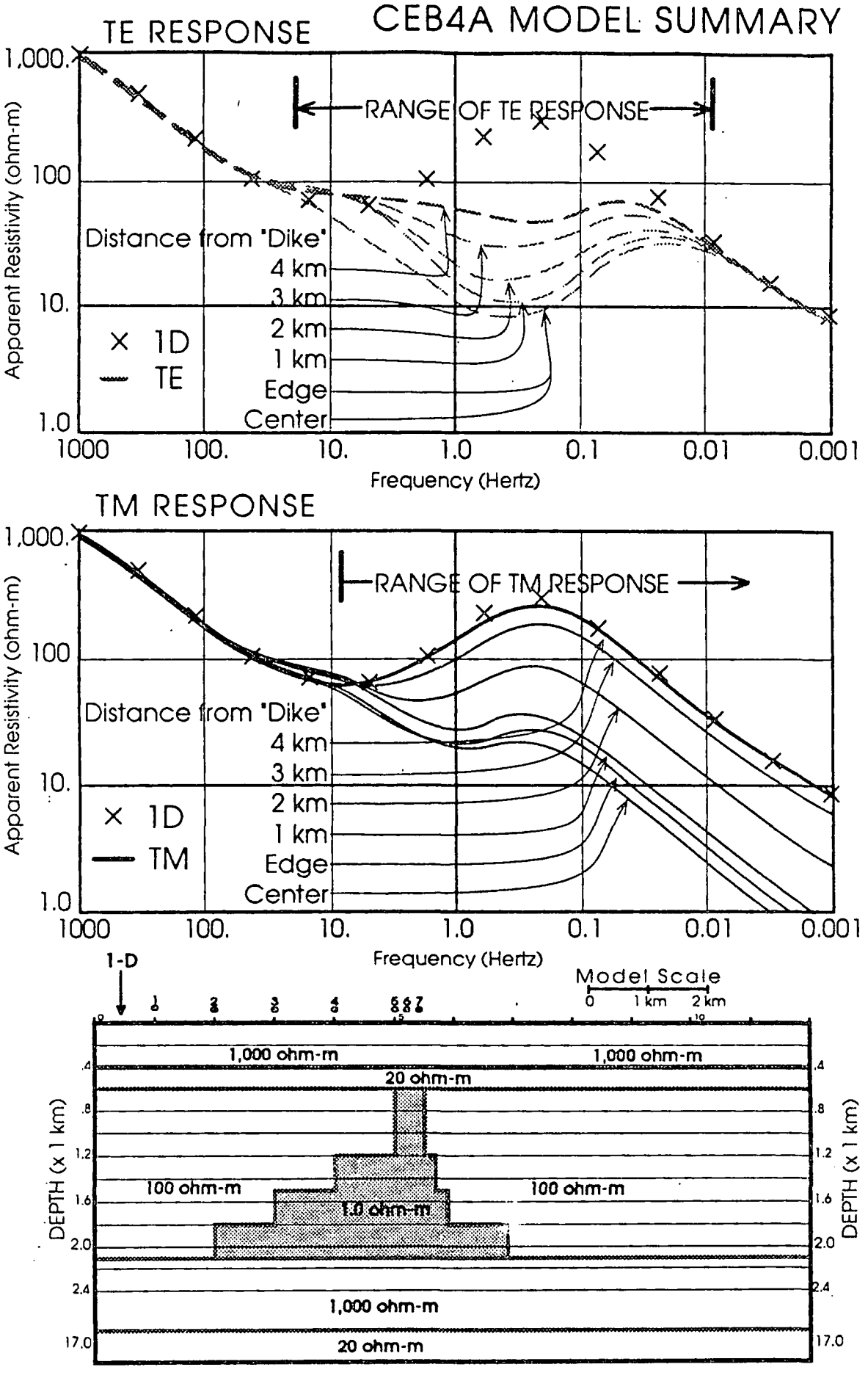


Figure 18
Summary of Model Response: CEB4A

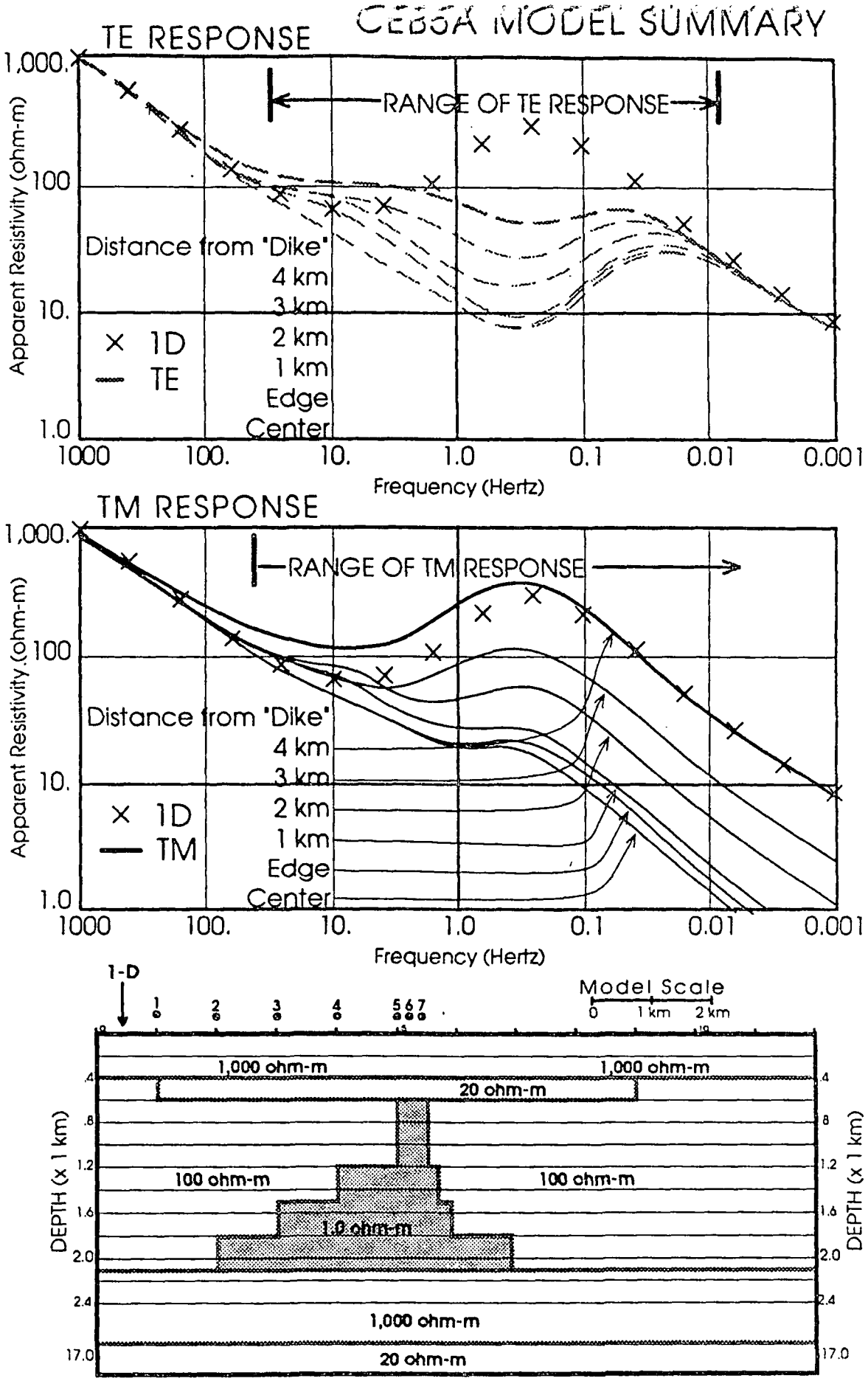


Figure 19
Summary of Model Response: CEB5A

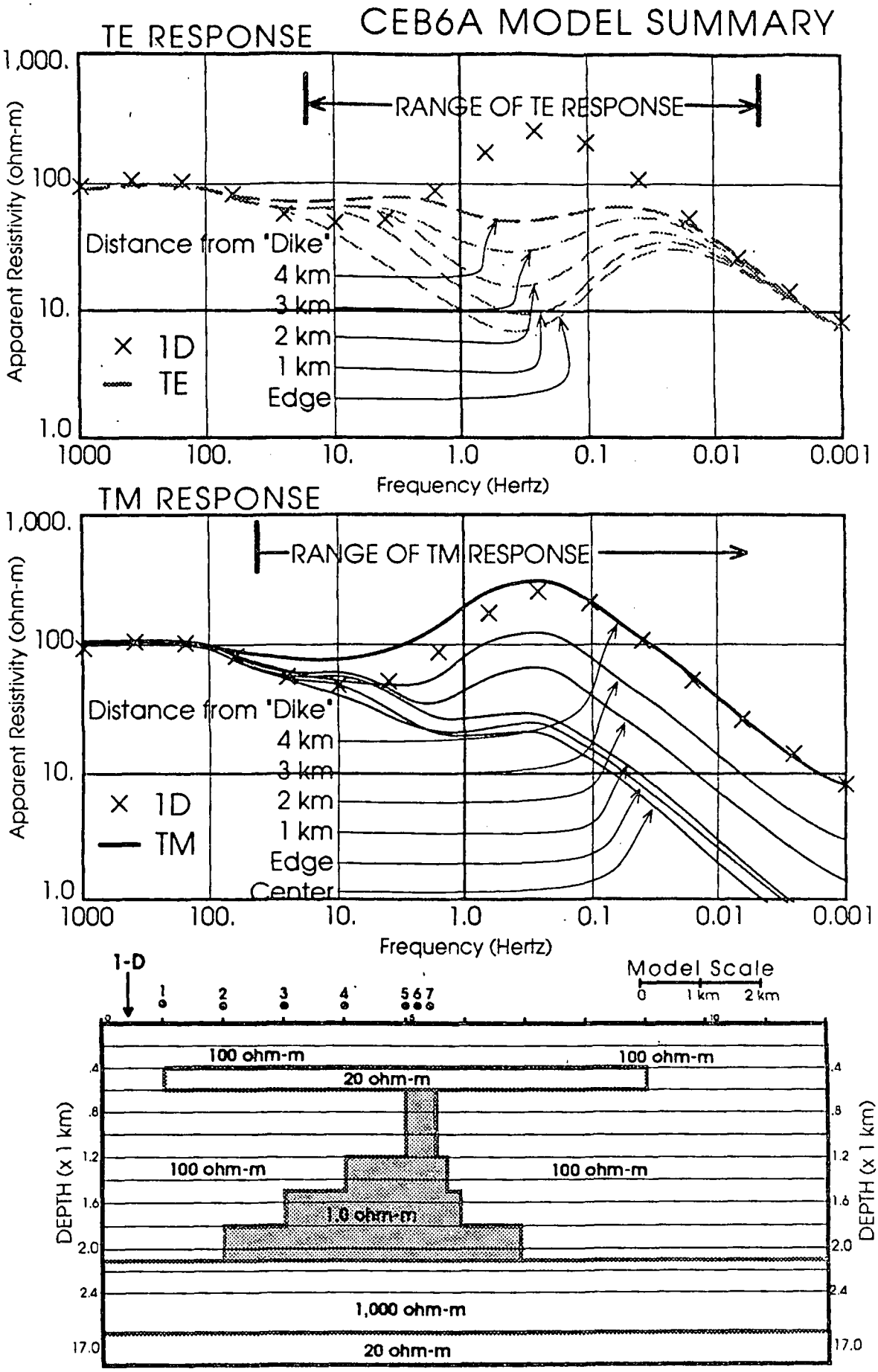


Figure 20
Summary of Model Response: CEB6A

the laterally continuous layer. At 20 ohm-meters the layer is relatively "resistive" when compared to the much lower resistivity of the anomalous body.

Model 7A and 8A (Plates M-6 and M-7, no summary figure) have two low resistivity layers in the subsurface, similar to models 2A and 3A, but also have a lateral termination in one or both of these layers. The surface layer has a lateral boundary where the resistivity changes from 100 to 1,000 ohm-meters. A review of the examples will show that the basic response is similar to that predicted by model 3A with the addition of a minor static shift at sites 5-7 due to the change in resistivity at the near surface.

This series of relatively simple models is concluded with models 9A-11C (Plates M-8 through M-12, no summary figure). In this group of examples the deep low resistivity zone is moved shallower for the base cases and the low resistivity "anomaly" is tested with different thicknesses. Models 9A and 10A retain the near surface boundary which provides a minor static shift for sites 5-7; models 11B and 11C have a constant resistivity near-surface layer (100 ohm-meters) and do not have this minor effect. There are primarily two significant results for these models. First, it is only the lateral termination of the deeper low resistivity layer which causes a significant amount of low frequency anisotropy, and this anisotropy increases with decreasing frequency (see sites 3 and 4 for model 11A). Secondly, since the anomalous low resistivity body primarily affects the TE component, in the vicinity of the low resistivity zone the TE component is the minimum curve through the frequency range responding to the anomaly. At very low frequencies the TE component is the maximum. This relationship causes the TE and TM components to cross as they change in relative amplitude (see sites 5 through 7, models 11B and 11C). This is a key feature which can be used to recognize a low resistivity zone of limited width oriented parallel to strike. However there are other 2-D effects which can be superimposed on this response.

The lateral extent for which these distortions can be observed is very limited and depends on a few factors. The major factor is the total conductance of the anomalous body, or at a constant resistivity its volume relative to the other low resistivity features. The second important factor is the average resistivity of the "host", or surrounding medium. In the case where the conductive body is enclosed in a higher resistivity structure the effects may be observed 2-4 km away, but in the presence of other conductive layers of a similar resistivity the distortion will attenuate rapidly and may not be observed 2 km

away. This observation should be considered in the design of exploration MT programs and in the more detailed follow-up program.

Contoured pseudo-sections of apparent resistivity (phase adds no information in a 2-D model) are shown for a series of three models to illustrate several more general observations from this model study. The sections are contoured more or less logarithmically at values of 100, 50, 25, 12, and 6 ohm-meters. These pseudo-sections are constructed from the model listings provided in Appendix D. Models CEB11X, 11B, and 11C show the effect of the addition of a conductive body to the termination of a low resistivity zone as discussed above. The contoured values of apparent resistivity are interesting in that they do not outline the anomalous body by themselves. It is the relative magnitude of TE and TM which is important in order to locate these anomalous conductive bodies.

The tipper magnitude is also contoured for the same group of models. The examples show that high tipper values are caused by lateral boundaries as would be expected. It is the lateral gradient of the transition in tipper magnitude which is observed to be an important characteristic related to the subsurface resistivity structure. In model 11A the termination of the deep low resistivity layer results in a transition in tipper values which occurs over a large distance, with significant values (more than 0.2) observed 4 km from the boundary. The addition of the conductive body in models 11B and 11C causes the tipper magnitude to attenuate rapidly to the conductive side of the model, with values of less than 0.1 observed within 1 km of the body.

Complex 2-D Model Series:

The objective for the second major series of models was to incorporate the observations of the first series into a model with a geometry designed to yield anomalies such as those observed in the project area. Model plates M-14 through M-19, which present these results in the same format as in the previous discussion, should be studied in detail as these illustrate many of the data characteristics used to identify the anomalous zones from the field data.

It has been shown with the previous models that a single low resistivity anomaly will create an MT response distortion observed only for those sites within 3-4 km of the

causative body, using the type of depths and resistivities observed in the field data. However in the interpretation discussed below the anomalous areas are observed to extend for a much larger distance. It has also been shown that a relatively narrow low resistivity body is required to create the type of change in maximum component observed in the field data. In addition, as a single body becomes wider it begins to create the type of response observed from a layer; a frequency dependent anisotropy, increasing with lower frequency.

Models 13 and 16 (Plates M-14 and 17) are base case models without the anomalous low resistivity "geothermal" body. The difference between the two is the resistivity of the deep layer (model 13 - 20 Ω-m, model 16 - 5 Ω-m). In both cases this layer has a limited lateral extent (10 km). The termination of the deep layer causes the majority of the observed low frequency anisotropy and the anisotropy is increased in the example with the lowest resistivity (model 16). Two individual low resistivity bodies, separated by about 5 km, are added to these base models and the results shown in models 14 and 15, and 17 and 18 (Plates M-15, M-16, M-18, and M-19).

The characteristic response to the low resistivity "dike", used as the basis for identification of the anomalous zones in the field data, is illustrated in Figure 21. In this figure the TE and TM components are plotted together, as in the field data, for two models, one with the anomalous "dike" (model 15) and one without (model 16). The differences between the two cases, the curve crossing and deep minimum in the parallel (TE) component when the dike is present, are striking.

Field examples that exhibit a characteristic response similar to the above model data are shown in Figure 22. The upper data, for sites 59 and 60, exhibit the anomaly. The lower data without the anomaly, sites 77 and 80, are shown as a comparison. The field data of Figure 22 should be compared with the model data, Figure 21. These data are shown with statics corrections applied.

G. Modelling - Inversion and One-dimensional Forward Models

The analytic inverse used for this survey is a computer-based approach whereby a layered earth is sought that yields a "best fit" MT response to the measured apparent resistivity versus frequency data. The interpreter specifies the number of layers and provides a starting point for the inversion. The interpreter may let the computer determine

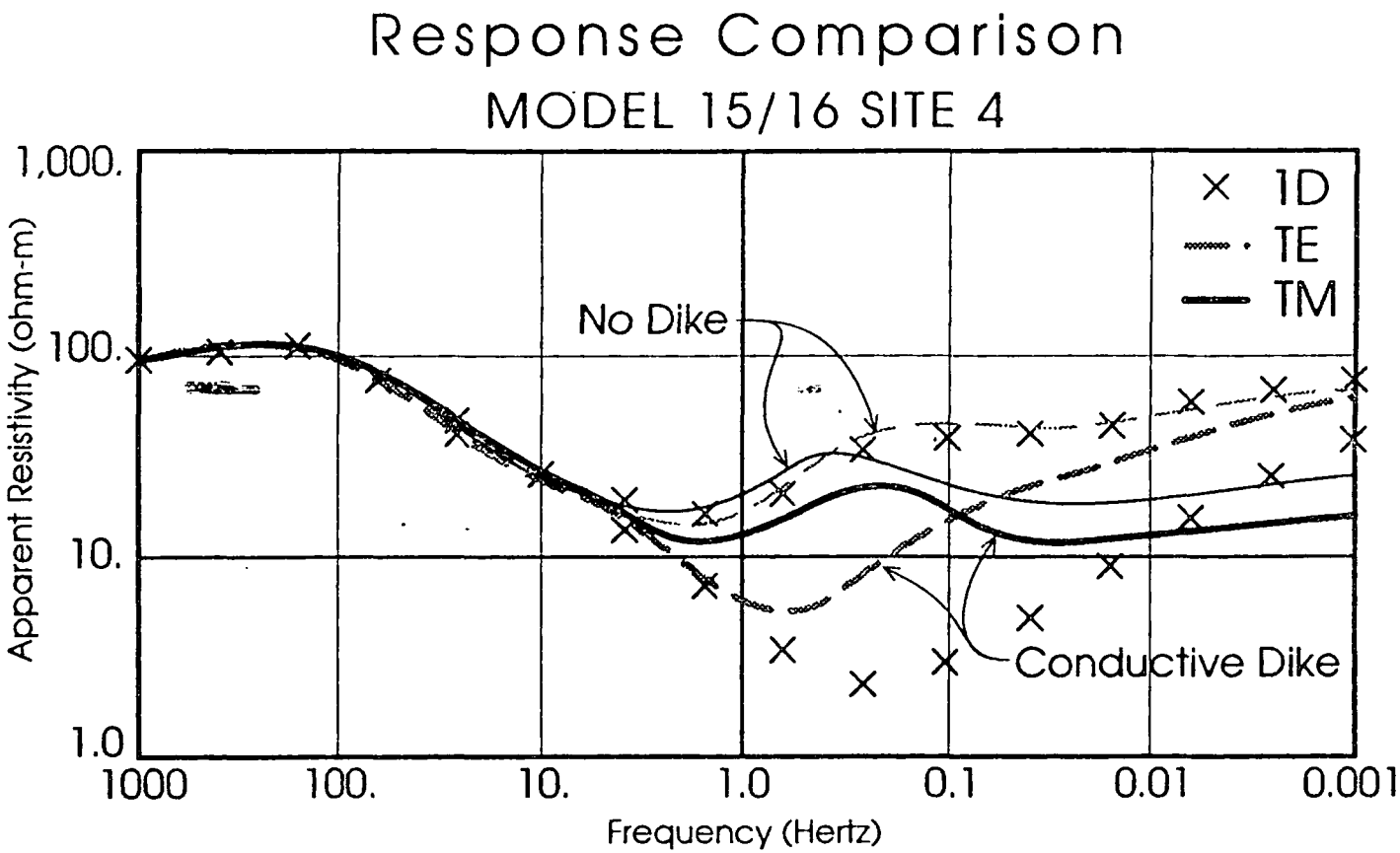


Figure 21
Characteristic Response
of Conductive Dike

Upper data: Sites 59 and 60 with anomalous response

Lower data: Sites 77 and 80 without anomalous response

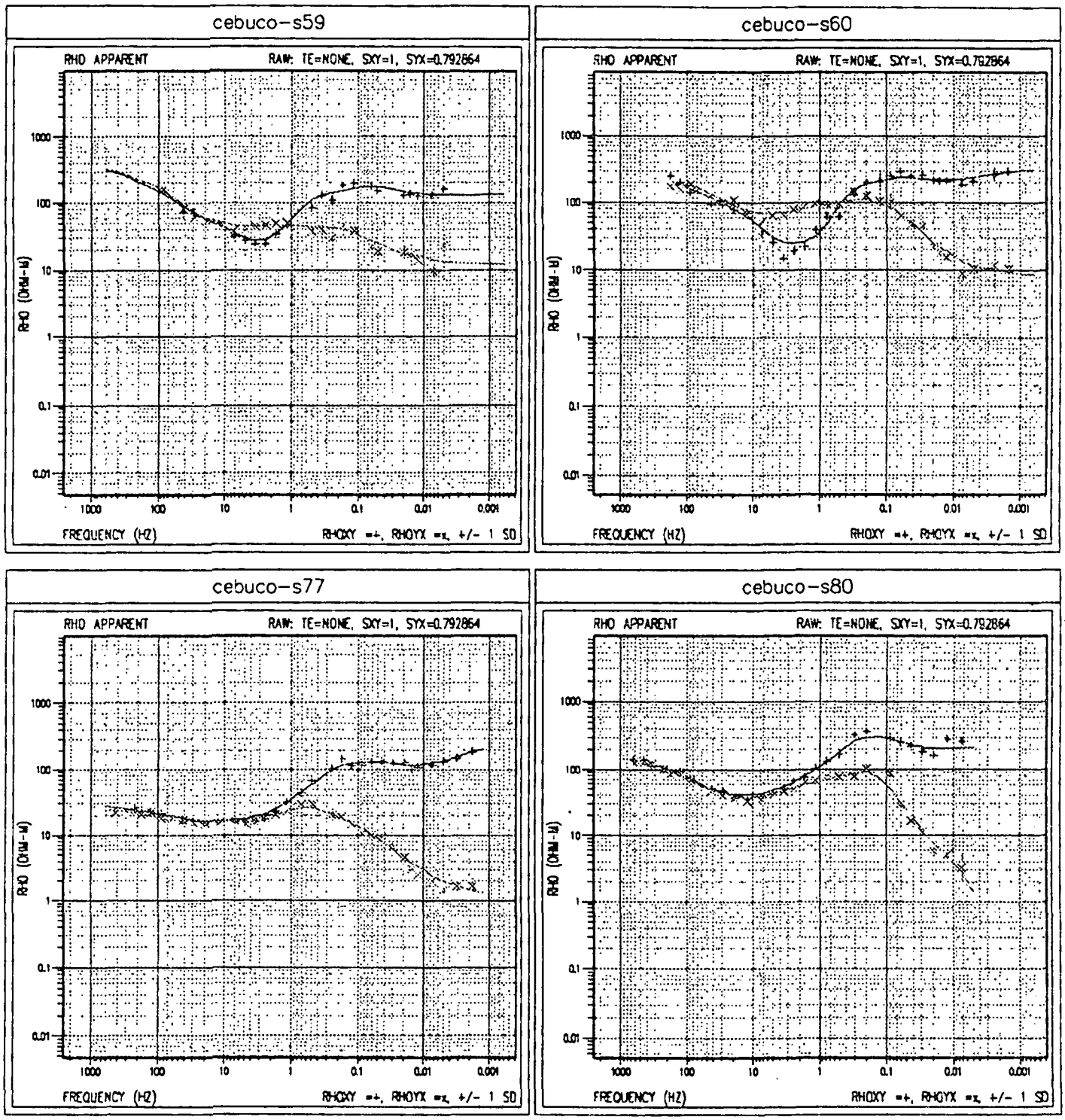


FIGURE 22

FIELD DATA COMPARISON

all of the resistivity and thickness values, or may "fix" the resistivity and/or thickness of one or more layers. This latter technique was used for the interpretation of the data for this survey to provide site-to-site continuity. The resistivity range of the three primary units was determined through an iterative approach and then employed consistently in the course of computing the final inverse solutions. The final layered inversions for all sites are included with this report as Appendix A.

In applying the inversion program to a given site, the interpreter investigated different layer sequences to ensure that an optimum solution was reached. Solutions with two to six layers were computed. The inversions were computed unrestrained, and then with key parameters fixed. When parameters were fixed, the computation was made for a range of values for the fixed parameter.

The inversions were computed using the Geotools™ work station operating on a Sun computer. The edited data, with statics corrections applied, were used for the inversion.

H. Correction of Static Shifts

Statics effects were not a major problem for this survey. The relatively close site spacing, the consistency of shallow resistivities over broad areas, and the largely two-dimensional geologic structural effects combined to assist the interpreter in this regard. The statics corrections were arrived at using the following techniques, listed in approximate order of importance:

- Near surface resistivity as observed on the MT data - The presence of almost isotropic (one-dimensional) high frequency MT data at key sites coupled with the apparent consistency of the surface over several kilometers led to the successful assignment of statics corrections using the MT data itself. This approach was cross-checked during the structural interpretation, and through use of the TDEM and Schlumberger data.

- Structural consistency - The primary requirement for a statics correction is that the subsurface interpretation make sense geologically, and be consistent from site to site. The statics corrections were applied prior to inversion, and then refined in an iterative way if in the opinion of the interpreter the correction resulted in an unrealistic or not physically realizable structural configuration or resistivity values.

- TDEM data - TDEM data were acquired at all sites using either a Geonics EM-47 or EM-37 transmitter and receiver. The central loop method was employed exclusively, using transmitter loops of 20 to 40 meters side-length. The TDEM data were inverted using the Interpex Timex software. The primary information used for the MT correction was the resistivity of the near-surface layers, and no attempt was made to interpret the TDEM data beyond this. The TDEM data were used primarily as a check on the corrections derived using the above methods. When a conflict existed between the correction suggested by the TDEM results and the MT data (points 1 and 2 above), the MT data were usually honored. The TDEM results are the subject of a separate memorandum.

- Schlumberger data - The Schlumberger resistivities were found to be reasonably consistent, and were used primarily as a guide to the gross resistivity of the shallow section. The Schlumberger resistivities were in general consistent with the MT data, and provided a starting point in many cases for assigning statics corrections. As with the TDEM data, when a conflict existed between the correction suggested by the Schlumberger results and the MT data (points 1 and 2), the MT data were usually honored. The Schlumberger data are available for review at the CFE offices.

The statics corrections were made on the edited data in the Geotools data base. A copy of this data base has been submitted to CFE on a Sun-compatible cassette tape.

The statics corrections used on the inverted data are noted on each layered inversion contained in Appendix A. The corrections are noted in the upper right hand corner of the apparent resistivity plot (the upper right window) of each inversion display.

I. Complex Structure - Three-dimensional Modelling

Three-dimensional (3-D) models are utilized when the MT data exhibit characteristics such as high skew, high ellipticity and/or distorted polar plots, or appear to be 2-D but require geologically unrealistic geometries or resistivities in order to fit the data with a 2-D model. Three-dimensional models are computed at AOA using one of two algorithms, that developed by Dr. S. Park while at MIT and in the public domain, and that developed by the industry-supported MIT consortium under the direction of Professor T. Madden. References are included at the end of this report that describe both the Park and Madden modelling approaches.

For the Ceboruco project 3-D effects were evaluated through the study of models computed in the course of past MT projects involving complex geology. This study led to the observation that 3-D effects that could influence the interpretation objectives of this project are minimal at most sites. There are no sites in the project area which exhibit the type of complex 3-D response which would require a 3-D model for explanation.

There are examples in the Ceboruco data of sites that exhibit current gathering, an important three-dimensional phenomenon. The effects are described in Appendix C, pages C-38-48, and in references [10], [11], [17] and others. The effect on the data is noted as a suppression of the basement apparent resistivity for both components. An example, which can be seen on the data montage Plate 13, is site 34. The interpretation of the important low resistivity zone is unaffected, but a one- or two-dimensional interpretation of the basement would be in serious error. The existence of current gathering is confirmed by the strong basement response at all surrounding sites. It is physically impossible to have an actual deep low resistivity body with the required limited extent result in these data.

## J. Final Interpretation - Discussion

### J.1. Introduction

One difficulty in the interpretation of this particular MT survey is the lack of available subsurface resistivity or lithologic information. Until this information becomes available the MT data can only be used to describe the general character of the subsurface from an electrical perspective. Some of the interpretive conclusions may be somewhat more qualified or general in nature without the ability to "calibrate" the response at one or more locations with independent information.

The model studies indicate that even with the best MT data the location of geothermal zones as represented by localized low resistivity bodies will require closely spaced MT data in the anomalous area. The models identify a characteristic response which is related to the geometry of the low resistivity zone, identification of these characteristics in the acquired data is an observation. The interpretation of these anomalies as geothermal zones assumes that the presence of such a zone will result in anomalously low resistivities (1-3 ohm-meters) as has been observed in other geothermal areas such as Las Azufres and Araro.

J.2. Discussion of Inversion Results - Regional Interpretation

The inversion procedures applied to the data resulted in specific depth information which was used to generate structure and isopach maps of the various resistivity units important to the interpretation. The inversion process is described in the previous section on procedures (section VIII. G). The primary feature of the MT response at nearly all of the locations is the prominent low resistivity zone with a minimum in the apparent resistivity versus frequency response at 1-5 Hz. In order to provide consistent and comparable inversion results the resistivity used in the inversion for this layer was constrained to 3 ohm-meters, which was found to provide the best fit at a majority of sites. Of course the actual average resistivity of the geologic units represented by this zone may change somewhat from site to site within the survey area. With no independent subsurface information there is no way to take this factor into account. For the case where the actual resistivity of the geologic units changes while the resistivity used for the inversion remains constant there will be an error in the predicted thickness. For those locations where the actual resistivity is greater than the inversion resistivity the thickness value from the inversion will be proportionally less than the actual thickness. Conversely, where the actual value is less than the inversion resistivity, the predicted thickness will be greater than the actual thickness. Changes in the actual average resistivity may account for some of the variation in predicted thickness observed on the cross-sections and maps.

J.3. Isopach of Low Resistivity Layer - Plate 5

A summary of the thickness values for the principle low resistivity zone is shown in Plate 5. The MT data define an elongate body (~15km x ~35km) of low resistivity averaging 200-400 meters thick, which extends from Jala/Ahuacatlan on the east to San Pedro and Cerro Pelon on the west. There appear to be two thicker areas within this overall area. The first extends from Ceboruco more or less to Santa Isabel, while the second extends from Amado Nervo north to Domo de San Pedro. Surrounding the area containing the low resistivity layer the MT data clearly shows moderately resistive units on high resistivity basement to great depth. Although there is some level of expected "error" in the thickness values due to the assumption of a consistent resistivity value for a zone which probably has some amount of variation, the results are generally consistent and deserve a high degree of confidence.

The MT results are somewhat in conflict with the results of the previous Schlumberger resistivity interpretation. This is probably due to the greater depth of penetration of the MT method and its greater sensitivity to low resistivity units. The Schlumberger data, at the larger spacing, show the major low resistivity zone extending north-south between Tetitlan/Chapalilla and Domo de San Pedro. The MT data does show the near surface layer to have a much lower resistivity in this area, but the major low resistivity unit extends much farther to the east and west than had been previously interpreted.

J.4. Structure at Electrical Basement - Plate 3

In a vertical geologic section the depth of the deepest low-resistivity over high-resistivity interface which can be resolved is termed the electrical basement. In a sedimentary geologic section this boundary can occur at or above "geologic" basement depending upon the resistivity contrasts involved. In a volcanic section, such as Ceboruco, the term basement becomes somewhat more difficult to define and the electrical characteristics of the overlying section are much more variable. In addition to this difficulty, the determination of a depth to a particular interface using the MT response has a degree of error associated with it. That is to say predicted depths and resistivities could be changed ±10-15% or more and forward models could be calculated that provide an acceptable fit to real-world field data. This level of error is a fact of the MT response and is unavoidable, regardless of the inversion algorithm used. For this reason, depth determinations from MT data when unconstrained by any subsurface data are of value only for a regional interpretation and some amount of variation is allowed in the contouring of the structural values.

The elevation of electrical basement (sea level datum) is shown on Plate 3. For the purposes of this interpretation, "electrical basement", is the interface at the base of the primary low resistivity zone (isopach of Plate 5). Values of structural elevation range from less than -200 meters to more than 900 meters. In general the depth of electrical basement is greater to the south becoming shallower to the north. The apparent depth is greatest in two areas; 1) south of Uzeta, and 2) the Amado Nervo area. It is interesting that there appears to be no abrupt change in structure at the top of the electrical basement associated with Ceboruco volcano, which is the most prominent surface feature in the project area.

J.5. Rotation Angle and Tipper Strike - Plate 14

In the MT response shown in the model study the orientation of the two MT components was defined by convention, with one component parallel to strike (TE) and the other perpendicular to it (TM). Of course in the real world the definition of "electrical strike" may be much more difficult to determine than "electrical basement". In fact electrical strike is often dependent on frequency, with the high frequency data responding to the near surface geologic structure or topography and the low frequency data affected by a completely different electrical structure independently oriented. The orientation of the impedance tensor is an important part of the interpretation.

The tipper magnitude and strike provide information regarding the proximity to vertical boundaries. As shown in the model data large tipper values do result from the type of 2-D structures expected in the project area. For an MT response with a large tipper magnitude (more than 0.3), tipper strike (defined as the azimuth of maximum vertical magnetic field to horizontal magnetic field ratio) should be more or less perpendicular to geologic strike. The vertical field data provides another indication of the boundary orientation of the subsurface electrical structure. It should be remembered that large tipper magnitudes can be created by many different types of electrical boundaries completely independent of the exploration objective and the information should be considered in the context of the other data from the particular site and from other sites in close proximity to make sure that the conclusions are consistent.

Plate 14 is a presentation of the rotation angle of the maximum component of apparent resistivity at about 1 Hz, and the tipper strike. A review of the data montage (Plate 13) shows that the anomalous response of interest occurs in a frequency range of about 0.5-10 hertz. Tipper strike and rotation angle data were selected for display to illustrate the electrical orientation of this part of the MT response, generally about 1 Hz. The majority of sites have tipper magnitudes less than 0.1 and the MT components at those locations are basically 1-D to below 1 hertz, with a modest anisotropy at lower frequency. There are no sites with an "anomalous" MT response and low tipper magnitudes (less than 0.1). Although the tipper response may not be directly related or caused by the anomalous body, it is a contributing factor in the identification of the anomalous areas.

Sites with large tipper magnitudes, 0.2 or greater, are found in three areas (outlined on the plate), which generally correspond to the outlines of the areas as defined by the anomalous component characteristics. The model studies indicate that large tipper values are related to the termination of a very conductive body. It can also be observed from the models that the simple termination of a regional low resistivity zone; 1) does not cause large tipper values (greater than 0.3), and 2) locations with large tipper values are restricted to a narrow zone in proximity to the causative body. The simple observation that large tipper values are observed in a few restricted locations and that much of the perimeter of the low resistivity zone (Plate 5) has no significant tipper response, is another indication of the anomalous nature of the high tipper values.

J.6. Cross-Sections - Plates 7-12

Each of the cross-section plates includes the apparent resistivity versus frequency data for each site along that cross-section. The MT data display is oriented with frequency on the vertical axis and resistivity horizontal, both plotted logarithmically. The location for each site is the 10 ohm-meter axis of the plot, with the resistivity scale shown on the sites at either end of the respective cross section. In the case where one of the components is shifted to correct for statics the shifted curve is shown as dashed.

The depth section is shown with an approximate surface profile, drawn as a smooth curve through the MT site elevation. The surface trace is intended to represent the approximate change in elevation between site locations. The horizontal scale is 1:50,000, the same as the interpretation maps. The vertical scale is shown on the sections. There is a vertical exaggeration of 6.4:1. Depths are the results of the 1-D layered inversion (see Table IV for summary of results), based on the analysis of the 2-D models as discussed earlier. Resistivity values are shown in parentheses. The sections are annotated with interpretive comments.

The six regional cross sections present much of the data acquired and are located to show the regional MT interpretation as well as the areas with an anomalous response. Locations for each section are shown on the Interpretation Summary map, Plate 2. For the depth section associated with each cross section site locations are shown with the appropriate vertical elevation. Depth values from the layered inversion are shown with error bars indicating the effective range of equivalent solutions (~±15%).

Cross-section A-A' Plate 7

This northwest-southeast trending cross-section crosses the central portion of the survey area, from the vicinity of El Marquesado northwest to a point east of San Pedro. Electrical basement is deepest at the southeast, becoming shallower to the northwest. Basement resistivity is high, more than 1,000 ohm-meters, across the whole section. At the northwest end the shallow portion (1 km) of the basement appears to be more moderate (~100 ohm-meters). The primary features of this section are the San Pedro resistivity anomaly to the northwest and the low resistivity layer (3-5 ohm-meters). This layer becomes thinner and shallower to the northwest. The near surface resistivity is much higher at the northwest end of the profile (100-300 ohm-meters) than to the southeast, indicating the probably presence of massive volcanics here.

Cross Section B-B' Plate 8

This profile is an east-west section across the northern portion of the survey area, crossing two anomaly areas: North Ceboruco and San Pedro. The distortion of the MT response by the anomalous bodies makes a direct interpretation of the 1-D inversion for those sites unreliable. In general the type of distortion present creates an apparent increase in the thickness of the low resistivity layer and depth to electrical basement. These zones of distortion are annotated on the cross section.

A high resistivity electrical basement is observed for the whole profile. In the central portion of the section, sites 28-60, the nature of the low resistivity zone changes and becomes the result of two distinct zones separated by a more moderate resistivity layer (100-500 ohm-meters). It is possible that fracturing and alteration of this intermediate layer creates the low resistivity anomaly observed in the North Ceboruco area.

At the west end of the profile the termination of the low resistivity layer is observed between sites 92 and 87. The 3-5 ohm-meter layer has actually terminated to the west of site 37, becoming a 10-25 ohm-meter layer between sites 37 and 92. The MT response is again distorted by an anomalous low resistivity body

Cross Section C-C' Plate 9

Profile C-C' provides a correlation from site 70 on the southeast side of the survey area, north through the North Ceboruco low resistivity anomaly. High resistivity units (100-500 ohm-meters) are observed in the near surface along the northern portion of the profile and are related the recent surface flows primarily from Ceboruco volcano. To the south the near surface resistivities are somewhat reduced (50-100 ohm-meters) indicating a greater proportion of continental sediments and volcaniclastic units. A deep low resistivity zone is observed to the south, to the north this zone appears to become shallower, but the MT response becomes distorted by the conductive anomaly so the structural interpretation becomes more questionable.

Cross Section D-D' Plate 10

Profile D-D' is drawn from the conductivity anomaly near Amado Nervo, in the southwest part of the project area, northeast to the North Ceboruco anomaly area. At the northeast end of the profile an alternative section (D-D1) from site 26 to 64 is presented to further illustrate the anomaly area. The structural information within the area of the conductive anomaly is not accurate due to the MT response distortion caused by the anomaly. However, the identification of the anomaly is a reliable observation of the data. Similarly the structural information from the San Pedro area (sites 31, 37, 47) will be misleading. The inversions show that the low resistivity zone (3 ohm-meters) has thinned or disappeared west of site 37. There is a zone of moderate resistivity (15-30 ohm-meters) above electrical basement which can be identified at sites 37 and 92. At the western boundary of the profile only higher resistivity units are observed above electrical basement.

Cross Section E-E' Plate 11

This is a north-south profile drawn through the Amado Nervo and San Pedro conductive anomalies. As in the other cross sections the inversion results are distorted in the area of the anomaly. Surface layer resistivity is observed to be moderate to the south (50-100 ohm-meters) and greater to the north (100-500 ohm meters). High resistivity basement is observed across most of the profile with an greater thickness of the shallow, moderate resistivity (100-200 ohm-meters) basement unit at the northern end. Depth to electrical basement is greatest at the southern portion of the profile.

Cross Section F-F' Plate 12

This section is drawn east-west across the southern part of the project area. The deep, low resistivity zone is observed across most of the profile terminating to the west between sites 42 and 89. Depth to electrical basement are generally greater to the east. The apparent increase in depth at sites 19, 39 and 40 is the result of response distortion from the Amado Nervo conductive anomaly. The dashed lines in this area show the probable depth of the low resistivity layer at this point.

J.7. Discussion of the Interpretation

The regional interpretation of the MT data is presented on the interpretation summary map, Plate 2; the basement structure map, Plate 3; the isopach of the deep low resistivity unit, Plate 5; and the regional cross-sections, Plates 7-12.

The interpretation concentrates on the three areas identified with an anomalous response generally similar to the model examples. The interpretation summary map, Plate 2, highlights the anomalous areas. Note that each of the anomalous areas appears to be at, or related to, a boundary of the widespread low resistivity body observed through much of the survey area. This relation may prove to be significant in future exploration. The anomalous areas are discussed in more detail individually below.

Northern Ceboruco:

The area identified as "Northern Ceboruco" is defined by roughly 20 MT sites of which 10 are within the anomalous area. Sites 59, 60 and 91 (see Data Montage, Plate 13) are all excellent examples with nearly identical characteristics of the type of anomalous MT response demonstrated by the model studies to be of exploration interest for this project. At each of these sites the high frequency response (greater than 10 Hz) is one-dimensional, after static correction. It is the change in relative magnitude or "curve crossing" which is apparent between the mid-range (~0.5-10 Hz) and low-range (0.5 Hz and lower) that is the clearest indicator of an anomalous electrical structure in the subsurface. Also consistent with the anomalous MT component relation is the pattern of large tipper values (see Plate 14). The model calculations indicate that the effect of the conductive anomaly will be to concentrate the large tipper values in the vicinity of the anomalous zone. The observation that tipper strike, defined in the literature [9] as perpendicular to geologic strike for two-

dimensional structure, is generally in the same direction as the maximum component further supports the interpretation that this direction is perpendicular to electrical strike at this frequency.

Average electrical azimuth for the maximum apparent resistivity component at about 1 Hz throughout the area as shown on the interpretation summary map (Plate 2) is more or less east-west. The model calculations show that this component should be perpendicular to the local geologic strike. This means that the anomalous low resistivity zone is expected to be oriented more or less north-south (±20°).

The boundary of this area is marked by a transition in the east to an MT response which is generally one-dimensional to ~0.5-1.0 Hz. The anisotropy observed at low frequency is characteristic of the simple termination of low resistivity layers. Electrical strike at ~1.0 Hz is at a high angle to the orientation observed in the anomalous area. On the north and east sides the MT response shows that the subsurface low resistivity zones are no longer present.

Amado Nervo:

The MT response in the vicinity of Amado Nervo is clearly distorted although the area affected is substantially less than the North Ceboruco area. Many of the comments and observation made above are applicable to the fewer sites in this anomalous area. This area is characterized by relatively higher tipper values and a similar type of curve crossing at sites 39 and 40. Electrical strike is not consistently defined, probably due to the smaller areal extent of the anomaly. The apparent increase in thickness of the low resistivity zone is interpreted to be largely a result of 2-D distortion caused by the anomalous body. As the electrical azimuth of the maximum apparent resistivity component appears to be generally southeast-northwest this anomalous zone should have an orientation roughly northeast-southwest. It is also interesting that surface manifestation of the possible thermal anomaly is found about 1 km northwest of site 19, which may be related to the anomalous zone.

San Pedro:

The San Pedro anomaly is similar to each of the other areas in that several sites are observed to exhibit more or less the same type of MT response. A dominant electrical azimuth is not well defined for this area, which is probably indicative of a complex

geometry for the conductive body and a somewhat more complex electrical structure in the surrounding area. At a few sites (sites 45, 16, and 31) the MT response is similar to the other anomalous areas with a component crossing at about 0.5 Hz. At a few other sites, such as site 34, a somewhat different response is observed. In this case the components do not cross but the portion of the curve related to electrical basement is offset to a lower frequency and lower resistivity.

The anomalous area is extends generally from the town of San Pedro south along the east side of Domo de San Pedro to a point south of site 16. Sites 01 and 05 are nearly one-dimensional and are not part of the anomalous area.

K. Description of the Observed MT Data

Most of the MT data represent a relatively simple sequence of resistive-conductive-resistive units with lateral changes in thickness and depth. Data from these locations generally exhibit 1-D characteristics to the frequency where electrical basement begins to influence the data (possibly with a small static shift), and have a modest amount of 2-D anisotropy in the low frequency portion of the curves.

A careful review of the data montage (Plate 13) shows that there are a small number of sites which exhibit the type of MT response shown by the models to be related to localized low resistivity bodies, possibly related to geothermal zones, as discussed earlier in section VIII.F and shown in Figure 22. This "anomalous" response is typified by data from sites 60 (north Ceboruco) and 40 (Amado Nervo), shown in Figure 23. Of particular significance for these examples is the change in relation between the two components from the high frequency portion of the curves where they are basically 1-D, to the mid-range (~10-0.5 Hz) and low range where the components change their relative magnitudes. The high frequency portion which appears to be 1-D (except for static shifts) shows that the shallow section is layered and relatively uniform laterally. This is much different from the electrical structure at depth, where the two components become significantly different. This anisotropy is complex in that for the mid-range data the YX component is maximum, but at low frequency XY becomes the maximum. It is this change in maximum component which is indicative of the type of conductive body of interest to this exploration program.

APPARENT RESISTIVITY SITIO 40

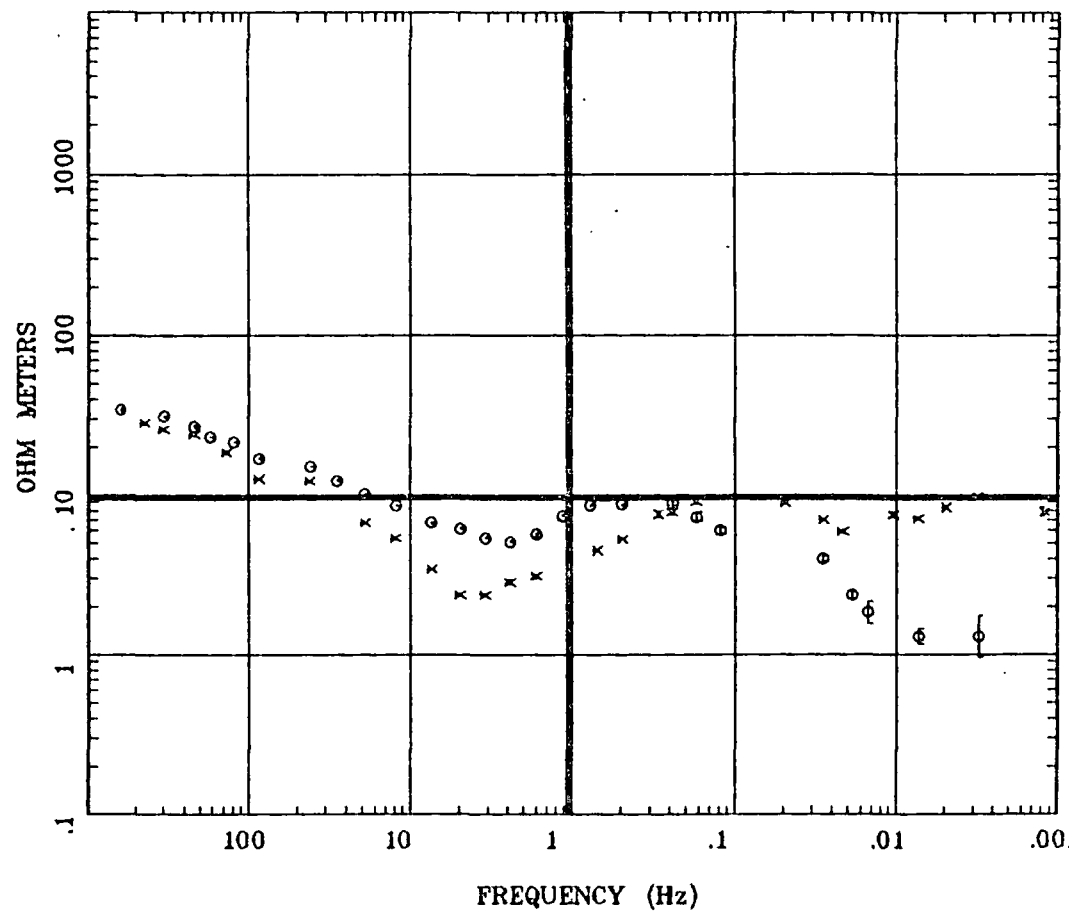


PROSPECTO MT CEBORUCO
Remote: R.L
Rotation: ANALITICA
Acquired: 14:37 Jul 31, 1991
Client: C. F. E.

Filename: C40LRA.AVG
Ex1 Ey1 Hx1 Hy1 Hz1 Hx2 Hy2
GEOEVALUACIONES S.A. DE C.V.
Plotted: 09:17 Oct 26, 1991
< EMI Inc. >

FIGURE 23A
APPARENT RESISTIVITY
SITE 40

APPARENT RESISTIVITY SITIO 60

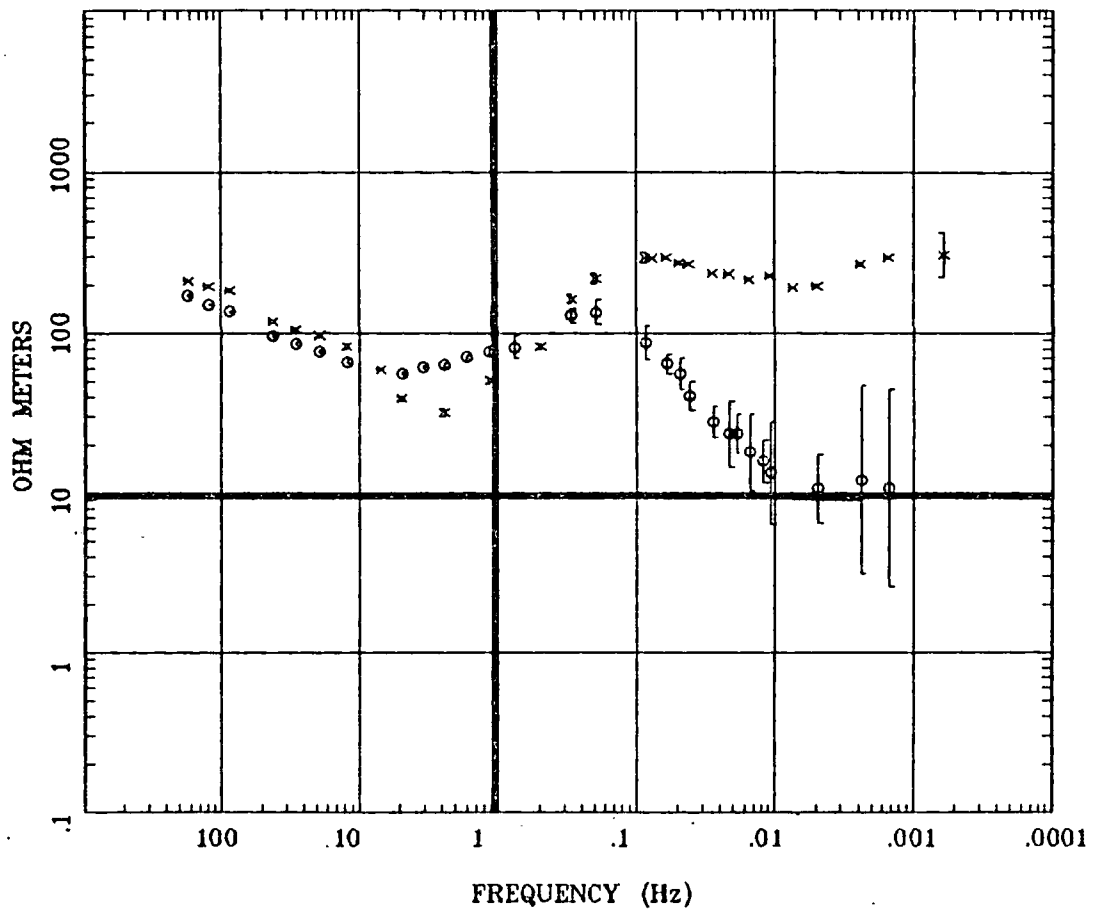


PROSPECTO MT CEBORUCO
Remote: SITIO 56
Rotation: ANALITICA
Acquired: 16:06 Oct 15, 1991
Client: C. F. E.

Filename: C5660A.AVG
Ex2 Ey2 Hx2 Hy2 Hz2 Hx1 Hy1
GEOEVALUACIONES S.A. DE C.V.
Plotted: 16:39 Oct 15, 1991
< EMI Inc. >

FIGURE 23B
APPARENT RESISTIVITY
SITE 60

A related response observed at several locations such as sites 34 and 39 (figure 24) is characterized by an apparent "offset" rather than a component change through the mid-frequency range. This can be created by the interaction between multiple conductive zones at a site in the central portions of these areas.

The model studies demonstrate that these responses are typically created by a low resistivity body of limited extent in the dip direction with a significant vertical dimension (a "dike" like structure). A layer or slab with similarly low resistivity has a different characteristic response. Examples of the anomalous data such as shown in Figure 19 are found in three areas: North of Ceboruco, the area near Amado Nervo, and south of San Pedro.

A more "1-D" type of response is observed at many sites in the central portion of the project area. For this data, such as sites 26 and 05 (Figure 25) the two components are coincident from high frequency to below 1 Hz, at which point some lateral structural complexity causes the components to separate. This low frequency anisotropy is a relatively simple 2-D response to the regional electrical structure, in this case interpreted the contrast between the lower resistivity sediments of the Ceboruco-Domo de San Pedro "graben" and the surrounding higher resistivity units of the mountains to the north and south.

APPARENT RESISTIVITY SITIO 34

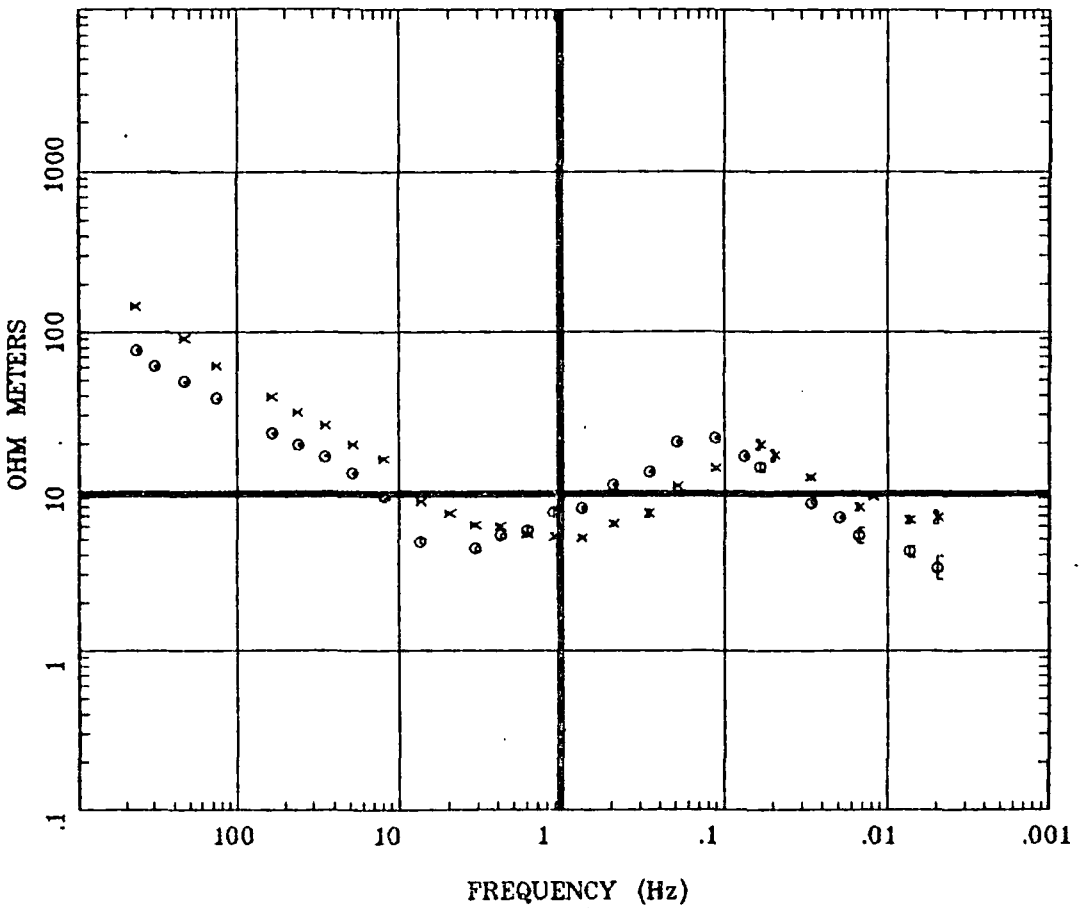


PROSPECTO MT CEBORUCO
Remote: R.L
Rotation: ANALITICA
Acquired: 09:51 Sep 16, 1991
Client: C. F. E.

Filename: C34LRA.AVG
Ex1 Ey1 Hx1 Hy1 Hz1 Hx2 Hy2
GEOEVALUACIONES S.A. DE C.V.
Plotted: 10:09 Nov 01, 1991
< EMI Inc. >

FIGURE 24A
APPARENT RESISTIVITY
SITE 34

APPARENT RESISTIVITY SITIO 39

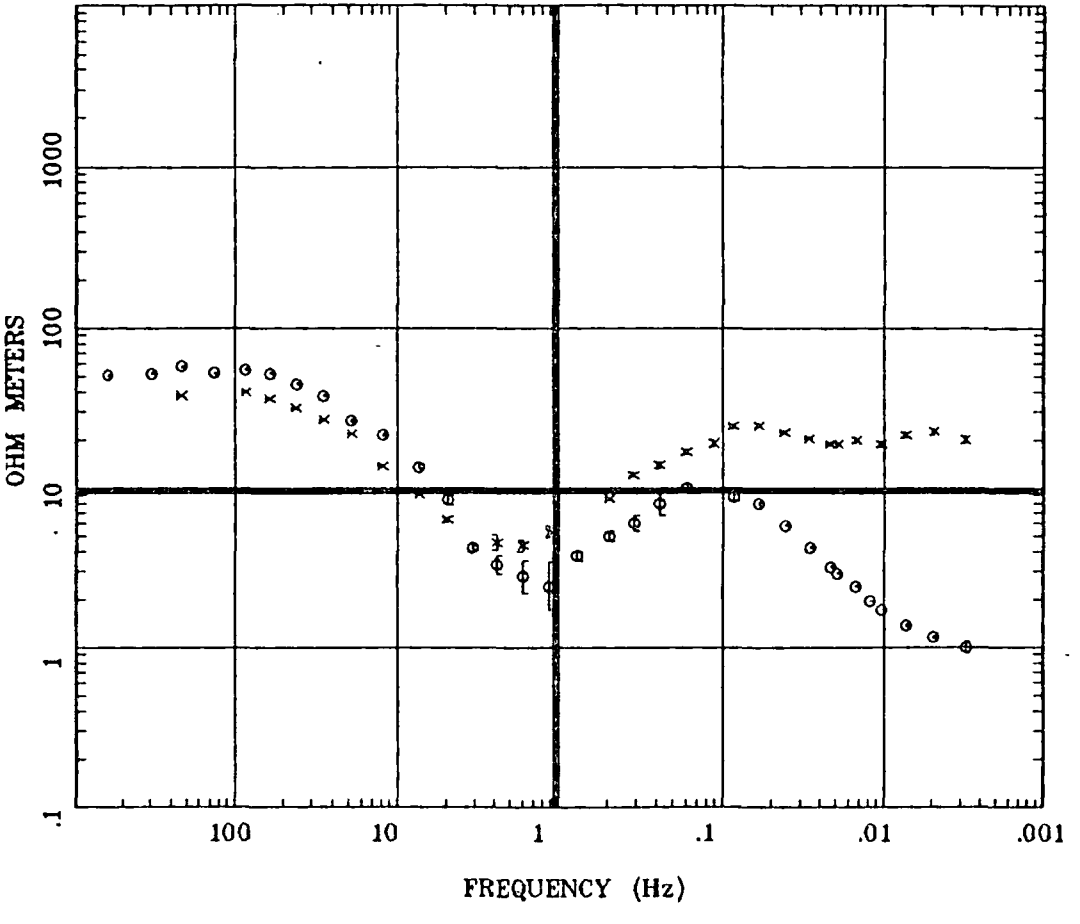


PROSPECTO MT CEBORUCO
Remote: SITIO 41
Rotation: ANALITICA
Acquired: 12:20 Jul 28, 1991
Client: C. F. E.

Filename: c3941d.avg
Ex1 Ey1 Hx1 Hy1 Hz1 Hx2 Hy2
GEOEVALUACIONES S.A. DE C.V.
Plotted: 09:41 Oct 13, 1991
< EMI Inc. >

FIGURE 24B
APPARENT RESISTIVITY
SITE 39

APPARENT RESISTIVITY SITIO 5

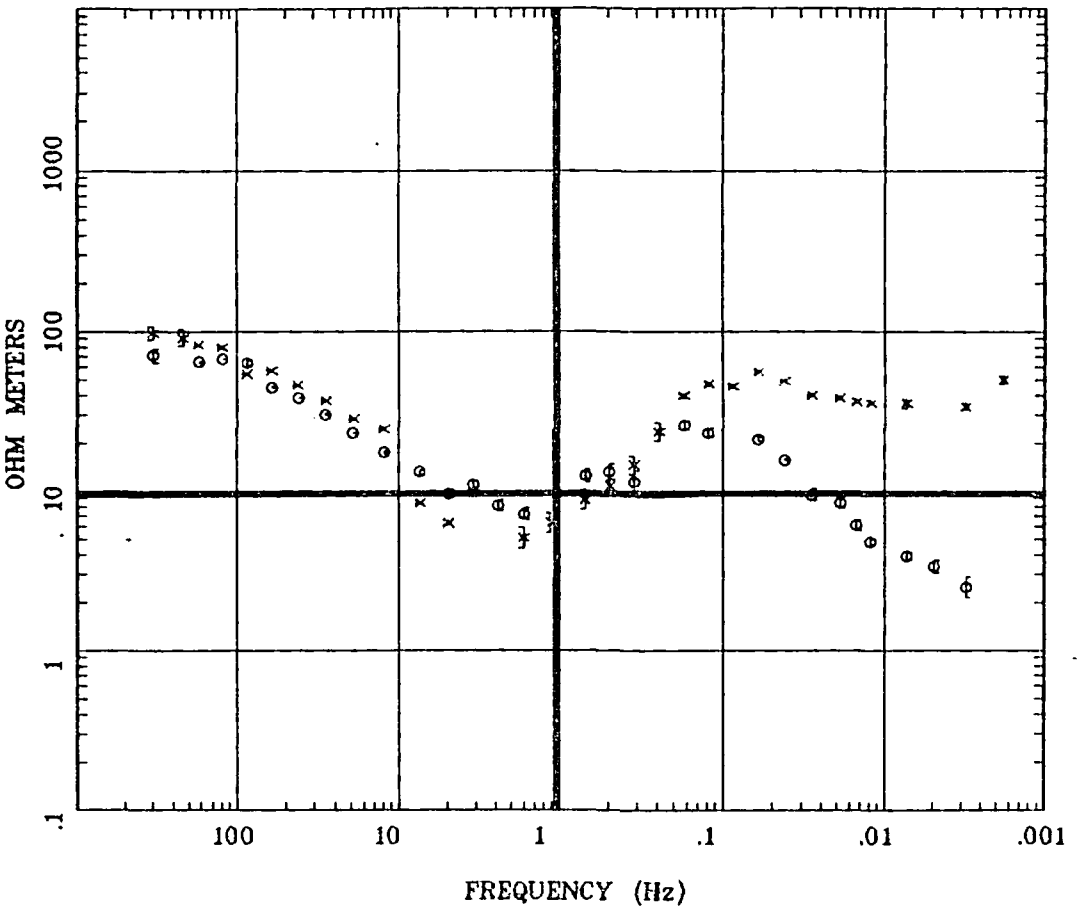


PROSPECTO MT CEBORUCO
Remote: SITIO 6
Rotation: ANALITICA
Acquired: 15:23 Oct 07, 1991
Client: C. F. E.

Filename: C0506AF.AVG
Ex1 Ey1 Hx1 Hy1 Hz1 Hx2 Hy2
GEOEVALUACIONES S.A. DE C.V.
Plotted: 16:47 Oct 30, 1991
< EMI Inc. >

FIGURE 25A
APPARENT RESISTIVITY
SITE 5

APPARENT RESISTIVITY SITIO 26

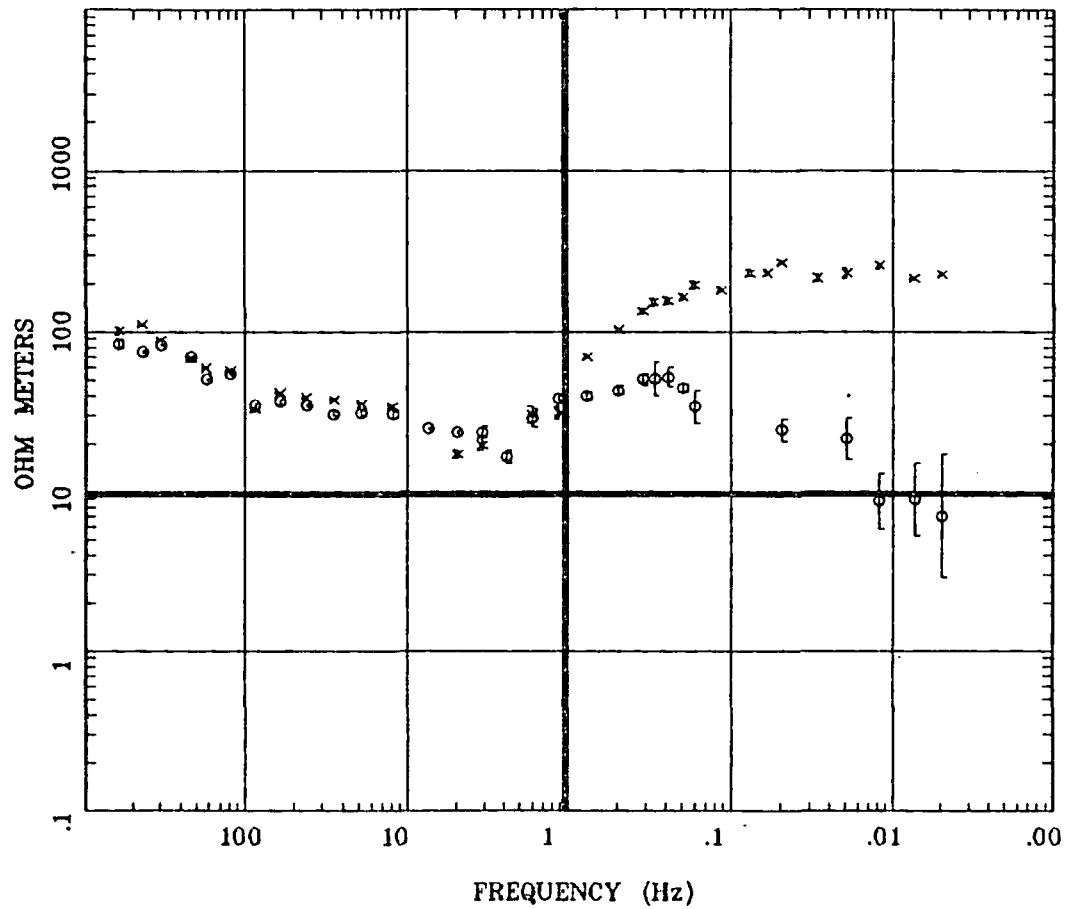


PROSPECTO MT CEBORUCO
Remote: R.L
Rotation: ANALITICA
Acquired: 10:46 Oct 11, 1991
Client: C. F. E.

Filename: C26LRAF.AVG
Ex1 Ey1 Hx1 Hy1 Hz1 Hx2 Hy2
GEOEVALUACIONES S.A. DE C.V.
Plotted: 10:55 Oct 11, 1991
< EMI Inc. >

FIGURE 25B
APPARENT RESISTIVITY
SITE 26

## IX. Recommendations

In general the program was well run on the part of both CFE and Geoevaluaciones. The extensive cooperation between the representatives in the field allowed a number of difficult problems to be solved efficiently. The location of the operational base for data acquisition in Ahuacatlan was also an advantage which allowed direct communication with the CFE technical staff whose office was in the same town. Subsequent MT projects in the Ceboruco area will probably not encounter many of the operational difficulties experienced in the present program because future surveys will probably be more concentrated or detailed type of programs rather than spread out to the extent here. The comments which follow are general suggestions based on the experience in the Ceboruco project.

### A. Data acquisition strategy

The most important improvement in acquisition strategy would be an attempt to avoid the severe weather periods of the year (late June to September). These storms affect data acquisition in many ways and constant, unpredictable delays are unpleasant for both the contractor and the client. In addition to the obvious logistical problems, data quality would be improve by recording at a time with fewer storms. Occasional bad weather is not a problem and the rain itself is also not a problem; it is the season of constant severe lightning storms that should be avoided if at all possible.

The site location planning should allow for a number of sites to be used as detail or fill-in locations in areas with interesting responses or where difficult access create a variable site spacing. It can often be extremely valuable for the interpreter to have available information from a location 1 or 2 km away from a difficult or interesting site.

### B. Processing and editing strategy

Future MT acquisition programs should continue with real-time recording systems where referenced MT data can be observed in the field during acquisition, as it was in the course of this project. This is an important factor in assuring that the data is high quality. It allows the operator to make better quality control decisions, and allows the interpretation to begin as soon as the data is recorded. Noise sources are more easily identified and equipment problems can be more efficiently isolated using this technique.

Similarly, the editing and processing of the data at the field base of operations provides the contractor and client with validated results as soon as possible. Generally the preliminary edit of a site was available for review within 24-48 hours of acquisition. The unedited data is of course available in the field immediately after acquisition. This is the advantage of a real-time data acquisition system. If a follow-up program is planned for the Ceboruco area it will probably be designed to provide detailed information regarding the character of the identified anomalous areas. This type of program will require presentation of preliminary data following acquisition in order to modify subsequent site locations based on the results.

C. Additional Data Acquisition

A detailed MT program could help delineate the electrical structure in each of the three areas identified. This type of program would be very useful to define the geometry of the anomalous low resistivity bodies possibly related to geothermal reservoirs. A total of 30-40 sites distributed between North Ceboruco, Amado Nervo and San Pedro would provide significant additional information and verify and provide added confidence for the existing interpretation.

TABLE I SITE LOCATIONS AND ELEVATIONS

| Site | U T M GRID LOCATION X | Y | Elevation | POLAR COORDINATES Latitude | Longitude |
|---|---|---|---|---|---|
| C 01 | 534 084 | 2 336 384 | 853 | 21° 07' 42" | 104° 40' 18" |
| C 02 | 535 084 | 2 334 649 | 737 | 21° 06' 45" | 104° 39' 24" |
| C 03 | 538 118 | 2 336 418 | 733 | 21° 07' 43" | 104° 37' 58" |
| C 04 | 536 944 | 2 338 748 | 993 | 21° 08' 59" | 104° 38' 39" |
| C 05 | 53 490 | 2 341 044 | 1,038 | 21° 10' 14" | 104° 40' 39" |
| C 06 | 533 317 | 2 342 189 | 1,050 | 21° 10' 51" | 104° 40' 48" |
| C 07 | 531 117 | 2 338 050 | 1,156 | 21° 08' 36" | 104° 42' 01" |
| C 08 | 533 606 | 2 332 540 | 812 | 21° 05' 37" | 104° 40' 35" |
| C 09 | 536 001 | 2 330 391 | 747 | 21° 04' 27" | 104° 39' 12" |
| C 10 | 538 896 | 2 331 508 | 811 | 21° 05' 03" | 104° 37' 32" |
| C11 | 540 021 | 2 333 590 | 706 | 21° 06' 11" | 104° 36' 53" |
| C12 | 542 404 | 2 336 293 | 918 | 21° 07' 45" | 104° 35' 30" |
| C13 | 541 836 | 2 338 993 | 853 | 21° 09' 06" | 104° 35' 49" |
| C 14 | 538 270 | 2 339 932 | 892 | 21° 09' 37" | 104° 7' 53" |
| C 15 | 536 405 | 2 341 938 | 873 | 21° 10' 42" | 104° 38' 57" |
| C 16 | 530 244 | 2 341 010 | 1,362 | 21°10' 13" | 104° 42' 31" |
| C 17 | 530 079 | 2 335 757 | 936 | 21°07' 22" | 104° 42' 37" |
| C 18 | 531 481 | 2 335 184 | 1,036 | 21° 07' 03" | 104° 41' 49" |
| C 19 | 531 755 | 2 331 030 | 741 | 21° 04' 48" | 104° 41' 39" |
| C 20 | 534 361 | 2 328 338 | 750 | 21° 03' 20" | 104° 40' 09" |
| C 21 | 545 226 | 2 340 865 | 1,234 | 21° 10' 07" | 104° 33' 52" |
| C 22 | 541 433 | 2 331 324 | 849 | 21° 04' 57" | 104° 36' 04" |
| C 23 | 544 110 | 2 333 367 | 897 | 21° 06' 03" | 104° 34' 31" |
| C 23R | 543 394 | 2 333 740 | 857 | 21° 06' 15" | 104° 34' 56" |
| C 24 | 547 042 | 2 332 741 | 1,092 | 21° 05' 42" | 104° 32' 49" |
| C 25 | 545 265 | 2 337 765 | 1,113 | 21° 08' 26" | 104° 33' 51" |
| C 26 | 541 404 | 2 341 548 | 919 | 21° 10' 29" | 104° 36' 04" |
| C 27 | 539 053 | 2 344 553 | 1,129 | 21° 11' 34" | 104° 36' 58" |
| C 28 | 538 053 | 2 344 553 | 951 | 21° 28' 07" | 104° 38' 00" |

| Site | U T M GRID LOCATION X | Y | Elevation | POLAR COORDINATES Latitude | Longitude |
|---|---|---|---|---|---|
| C 29 | 523 904 | 2 344 150 | 1,326 | 21° 11' 55" | 104° 46' 11" |
| C 30 | 534 994 | 2 343 948 | 877 | 21° 11' 48" | 104° 39' 46" |
| C 31 | 530 992 | 2 344 012 | 1,282 | 21° 11' 50" | 104° 42' 05" |
| C 32 | 527 763 | 2 346 611 | 1,291 | 21° 13' 15" | 104° 43' 57" |
| C 33 | 526 750 | 2 348 900 | 1,430 | 21° 14' 29" | 104° 44' 32" |
| C 34 | 529 618 | 2 349 906 | 1,290 | 21° 11' 14" | 104° 42' 53" |
| C 36 | 549 624 | 2 341 554 | 1,284 | 21° 10' 29" | 104° 31' 19" |
| C 37 | 520 629 | 2 344 364 | 1,286 | 21° 12' 02" | 104° 48' 04" |
| C 38 | 529 177 | 2 330 291 | 793 | 21° 04' 24" | 104°43' 09" |
| C 39 | 529 894 | 2 333 189 | 877 | 21° 05' 58" | 104° 42' 44" |
| C 40 | 527 065 | 2 31 128 | (559) | 21° 04' 51" | 104° 44' 22" |
| C 41 | 529 071 | 2 334 147 | 908 | 21° 06' 29" | 104° 43' 12" |
| C 42 | 525 342 | 2 331 975 | 862 | 21° 05' 19" | 104° 45' 22" |
| C 43 | 527 381 | 2 338 734 | 1,260 | 21°08' 59" | 104° 44' 11" |
| C 44 | 525 674 | 2 341 630 | 1,338 | 21° 10' 33" | 104° 45' 10" |
| C 45 | 527 782 | 2 343 357 | 1,303 | 21° 11' 29" | 104° 43' 56" |
| C 46 | 526 103 | 2 345 076 | 1,274 | 21° 12' 25" | 104° 44' 55" |
| C 47 | 525 147 | 2 346 742 | 1,361 | 21° 13' 19" | 104° 45' 28" |
| C 48 | 558 390 | 2 330 835 | 1,105 | 21° 04' 39" | 104° 26' 16" |
| C 49 | 556 738 | 2 332 798 | 1,120 | 21° 05' 43" | 104° 27' 14" |
| C 50 | 553 951 | 2 330 914 | 1,078 | 21° 04' 42" | 104° 28' 50" |
| C 51 | 555 386 | 2 334 936 | 1,209 | 21° 06' 53" | 104° 28' 00" |
| C 52 | 551 664 | 2 334 953 | 1,924 | 21° 06' 54" | 104° 30' 09" |
| C 53 | 551 444 | 2 356 334 | 2,018 | 21° 07' 39" | 104° 30' 17" |
| C 54 | 548 101 | 2 340 120 | 1,372 | 21° 09' 42" | 104° 32' 12" |
| C 55 | 547 828 | 2 343 386 | 1,264 | 21° 11' 29" | 104° 32' 21" |
| C 56 | 545 693 | 2 345 310 | 1,420 | 21° 12' 31" | 104° 33' 35" |
| C 57 | 543 814 | 2 347 898 | 1,513 | 21° 13' 56" | 104° 34' 40" |
| C 58 | 551 266 | 2 332 326 | 1,303 | 21° 05' 29" | 104° 30' 23" |
| C 59 | 544 365 | 2 342 348 | 1,350 | 21° 10' 55" | 104° 34' 21" |
| C 60 | 543 456 | 2 343 851 | 1,321 | 21° 11' 44" | 104° 34' 53" |
| C 61 | 542 351 | 2 347 190 | 1,417 | 21° 13' 33" | 104° 35' 31" |
| C 62 | 548 113 | 2 347 757 | 1,590 | 21° 13' 51" | 104° 32' 11" |

| Site | U T M GRID LOCATION X | Y | Elevation | POLAR COORDINATES Latitude | Longitude |
|---|---|---|---|---|---|
| C 63 | 561 144 | 2 334 372 | 1,110 | 21° 06' 34" | 104° 24' 40" |
| C 64 | 550 303 | 2 344 425 | 1,550 | 21° 12' 02" | 104° 30' 55" |
| C 65 | 551 687 | 2 340 619 | 1,423 | 21° 09' 58" | 104° 30' 08" |
| C 66 | 555 624 | 2 337 815 | 1,273 | 21° 08' 27" | 104° 27' 51" |
| C 67 | 557 761 | 2 338 726 | 1,168 | 21° 08' 56" | 104° 26' 37" |
| C 68 | 553 945 | 2 326 482 | 1,132 | 21° 02' 18" | 104° 28' 51" |
| C 69 | 545 822 | 2 332 112 | 998 | 21° 05' 28" | 104° 33' 32" |
| C 70 | 542 936 | 2 330 590 | 839 | 21° 04' 33" | 104° 35' 12" |
| C 71 | 526 303 | 2 324 822 | 711 | 21° 01' 28" | 104° 44' 49" |
| C 72 | 526 329 | 2 326 783 | 780 | 21° 02' 30" | 104° 44' 48" |
| C 73 | 524 111 | 2 328 933 | 776 | 21° 03' 40" | 104° 46' 04" |
| C 74 | 514 825 | 2 331 955 | 872 | 21° 05' 19" | 104° 51' 26" |
| C 75 | 519 897 | 2 334 426 | 989 | 21°06' 39" | 104° 48' 30" |
| C 76 | 514 413 | 2 335 911 | 875 | 21° 07' 27" | 104° 51' 40" |
| C 77 | 515 787 | 2 339 091 | 887 | 21° 09' 11" | 104° 50' 53" |
| C 78 | 512 787 | 2 341 050 | 879 | 21°10' 15" | 104° 52' 31" |
| C 79 | 511 923 | 2 345 196 | 1,132 | 21° 12' 13" | 104° 53' 06" |
| C 80 | 511 666 | 2 346 196 | 930 | 21° 13' 02" | 104° 53' 15" |
| C 81 | 525 473 | 2 337 058 | 1,478 | 21° 08' 04" | 104° 45' 17" |
| C 82 | 523 772 | 2 339 233 | 1,416 | 21° 09' 15" | 104° 46' 16" |
| C 83 | 521 749 | 2 341 427 | 1,449 | 21° 10' 27" | 104° 47' 26" |
| C 84 | 515 095 | 2 347 065 | 959 | 21° 13' 30" | 104° 51' 16" |
| C 85 | 520 838 | 2 336 341 | 1,024 | 21° 07' 41" | 104° 47' 58" |
| C 86 | 517 242 | 2 341 535 | 1.132 | 21° 10' 30" | 104° 50' 02" |
| C 87 | 506 853 | 2 344 199 | 65 | 21° 11' 57" | 104° 56' 02" |
| C 88 | 510 848 | 2 335 178 | 873 | 21° 07' 04" | 104° 53' 44" |
| C 89 | 519 051 | 2 332 235 | 887 | 21° 05' 28" | 104° 49' 00" |
| C 90 | 520 886 | 2 346 743 | 1,270 | 21° 13' 19" | 104° 42' 09" |
| C 91 | 547 202 | 2 342 246 | 1,309 | 21° 10' 52" | 104° 32' 43" |
| C 92 | 515 068 | 2 344 355 | 909 | 21° 12' 02" | 104° 51' 17" |
| C 93 | 523 058 | 2 343 315 | 1,282 | 21° 11' 28" | 104° 46' 40" |

TABLE II DATA QUALITY AND NEAR-SURFACE RESISTIVITY

| Site | Data Quality | Near Surface Resistivity, ohm-meters MT(XY) | MT(YX) | Schlumberger |
|---|---|---|---|---|
| C 01 | VG | 30 | 25 | 50 |
| C 02 | VG | 20 | 12 | 30 |
| C 03 | VG | 30 | 30 | 50 |
| C 04 | VG | 350 | 100 | 300 |
| C 05 | G | 150 | 100 | 100 |
| C 06 | VG | 100 | 30 | 100 |
| C 07 | VG | 30 | 20 | 50 |
| C 08 | VG | 25 | 15 | 100 |
| C 09 | VG | 20 | 15 | 22 |
| C 10 | VG | 15 | 10 | 25 |
| C 11 | VG | 20 | 12 | 20 |
| C 12 | VG | 30 | 20 | 20 |
| C 13 | VG | 300 | 100 | 2000 |
| C 14 | G | 50 | 30 | |
| C 15 | VG | 100 | 100 | |
| C 16 | VG | 200 | 80 | |
| C 17 | G | 60 | 10 | 35 |
| C 18 | VG | 140 | 80 | |
| C 19 | G | 100 | 70 | 50 |
| C 20 | VG | 10 | 10 | 35 |
| C 21 | VG | 400 | 300 | |
| C 22 | VG | 40 | 30 | 45 |
| C 23 | VG | 200 | 100 | 2000 |
| C 24 | F | 300 | 150 | 2000 |
| C 25 | F | 80 | 100 | 3000 |
| C 26 | F | 100 | 100 | |
| C 27 | VG | 80 | 30 | 1000 |
| C 28 | G | 50 | 30 | 300 |
| C 29 | G | 200 | 150 | |
| C 30 | G | 250 | 250 | 110 |

| Site | Data Quality | Near Surface Resistivity, ohm-meters MT(XY) | MT(YX) | Schlumberger |
|---|---|---|---|---|
| C 31 | F | 300 | 100 | 450 |
| C 32 | F | 20 | 10 | 450 |
| C 33 | G | 70 | 40 | 400 |
| C 34 | G | 200 | 100 | 500 |
| C 36 | F | 200 | 120 | 300 |
| C 37 | G | 350 | 200 | |
| C 38 | VG | 32 | 20 | 60 |
| C 39 | VG | 50 | 40 | 100 |
| C 40 | F | 35 | 35 | 50 |
| C 41 | G | 50 | 40 | 150 |
| C 42 | VG | 50 | 30 | 50 |
| C 43 | F | 200 | 150 | |
| C 44 | F | 300 | 60 | 450 |
| C 45 | F | 100 | 50 | 300 |
| C 46 | G | 45 | 30 | |
| C 47 | G | 200 | 80 | 300 |
| C 48 | VG | 100 | 70 | 130 |
| C 49 | F | 600 | 200 | 200 |
| C 50 | VG | 200 | 200 | 1800 |
| C 51 | F | 200 | 150 | 450 |
| C 52 | F | 500 | 200 | 3000 |
| C 53 | U | - | - | 3000 |
| C 54 | F | 300 | 100 | 2500 |
| C 55 | F | 23 | 35 | 200 |
| C 56 | G | 300 | 110 | 300 |
| C 57 | G | 200 | 100 | |
| C 58 | F | 500 | 250 | 3000 |
| C 59 | VG | 1000 | 1000 | |
| C 60 | G | 250 | 200 | 3000 |
| C 61 | G | 60 | 20 | |
| C 62 | G | 50 | 5 | |
| C 63 | VG | 200 | | 180 |
| C 64 | VG | 80 | 40 | 40 |

| | | Near Surface Resistivity, ohm-meters | | |
|---|---|---|---|---|
| Site | Data Quality | MT(XY) | MT(YX) | Schlumberger |
| C 65 | F | 200 | 150 | 20 |
| C 66 | VG | 200 | 100 | 180 |
| C 67 | F | 1000 | 100 | |
| C 68 | VG | 60 | 30 | |
| C 69 | F | 120 | 100 | |
| C 70 | G | 50 | 30 | 20 |
| C 71 | G | 70 | 100 | |
| C 72 | v | 100 | 80 | 200 |
| C 73 | VG | 60 | 40 | 60 |
| C 74 | VG | 25 | 20 | 45 |
| C 75 | VG | 300 | 100 | 100 |
| C 76 | G | 50 | 18 | 35 |
| C 77 | VG | 22 | 12 | 40 |
| C 78 | VG | 40 | 20 | 120 |
| C 79 | VG | 500 | 400 | 70 |
| C 80 | VG | 220 | 120 | 70 |
| C 81 | VG | 1000 | 800 | 550 |
| C 82 | F | 2000 | 400 | 450 |
| C 83 | G | 500 | 450 | 400 |
| C 84 | F | 40 | 30 | |
| C 85 | VG | 250 | 100 | 300 |
| C 86 | G | 100 | 90 | 200 |
| C 87 | VG | 20 | 30 | |
| C 88 | VG | 10 | 4 | 38 |
| C 89 | VG | 20 | 35 | |
| C 90 | VG | 200 | 300+ | |
| C 91 | G | 200 | 70 | |
| C 92 | G | 250 | - | |
| C 93 | F | 100 | 80 | |

* See section II.B.3 for a definition of the data quality criteria: VG (very good), G (good), F (fair), P (poor), and U (unusable). MT near surface values are of apparent resistivity. Schlumberger and TDEM values shown where available.

TABLE III RECORDING BANDS

| Freq no. | Frequency (hertz) | Period (seconds) | Recording Band Nomenclature | | |
|---|---|---|---|---|---|
| 1 | 620 | .002 | | | 6 |
| 2 | 430 | .002 | | | 6 |
| 3 | 330 | .003 | | | 6 |
| 4 | 215 | .005 | | | 6 |
| 5 | 172 | .006 | | 4 | |
| 6 | 135 | .007 | | | 6 |
| 7 | 122 | .008 | | 4 | |
| 8 | 85.9 | .012 | | 4 | |
| 9 | 85 | .012 | | | 6 |
| 10 | 60 | .017 | | 4 | |
| 11 | 41 | .024 | | 4 | |
| 12 | 28 | .035 | | 4 | |
| 13 | 19 | .053 | | 4 | |
| 14 | 12 | .082 | | 4 | |
| 15 | 7.32 | .137 | | 4 | |
| 16 | 6.90 | .145 | 3 | | |
| 17 | 4.88 | .205 | | 4 | |
| 18 | 4.88 | .205 | 3 | | |
| 19 | 3.44 | .291 | 3 | | |
| 20 | 2.40 | .416 | 3 | | |
| 21 | 1.66 | .602 | 3 | | |
| 22 | 1.13 | .883 | 3 | | |
| 23 | .762 | 1.31 | 3 | | |
| 24 | .689 | 1.45 | 2 | | |
| 25 | .488 | 2.05 | 3 | | |
| 26 | .488 | 2.05 | 2 | | |
| 27 | .344 | 2.91 | 2 | | |
| 28 | .293 | 3.41 | 3 | | |
| 29 | .24 | 4.16 | 2 | | |
| 30 | .195 | 5.12 | 3 | | |

| No. | Frequency (hertz) | Period (seconds) | Recording Band Definition | | |
|---|---|---|---|---|---|
| 31 | .172 | 5.80 | | | 1 |
| 32 | .166 | 6.02 | 2 | | |
| 33 | .122 | 8.19 | | | 1 |
| 34 | .113 | 8.83 | 2 | | |
| 35 | .086 | 11.64 | | | 1 |
| 36 | .076 | 13.12 | 2 | | |
| 37 | .060 | 16.64 | | | 1 |
| 38 | .049 | 20.49 | 2 | | |
| 39 | .042 | 24.10 | | | 1 |
| 40 | .029 | 34.13 | 2 | | |
| 41 | .028 | 35.34 | | | 1 |
| 42 | .021 | 46.51 | | D08 | |
| 43 | .019 | 51.28 | 2 | | |
| 44 | .019 | 52.63 | | | 1 |
| 45 | .015 | 65.36 | | D08 | |
| 46 | .012 | 81.97 | | | 1 |
| 47 | .011 | 93.46 | | D08 | |
| 48 | .008 | 133.3 | | D08 | |
| 49 | .007 | 137.0 | | | 1 |
| 50 | .005 | 192.3 | | D08 | |
| 51 | .005 | 204.1 | | | 1 |
| 52 | .003 | 285.7 | | D08 | |
| 53 | .002 | 416.7 | | D08 | |
| 54 | .0015 | 666.7 | | D08 | |
| 55 | .0009 | 1110. | | D08 | |
| 56 | .0006 | 1667. | | D08 | |

## TABLE IV SUMMARY OF LAYERED INVERSION RESULTS

| | Static Shift | | Resistivity Values (ohm-meters) | | | | | Thickness Values (Meters) | | | | |
|---|---|---|---|---|---|---|---|---|---|---|---|---|
| Site | XY | YX | R-1 | R-2 | R-3 | R-4 | R-5 | T-1 | T-2 | T-3 | T-4 | T-5 |
| C 01 | 1.32 | 1 | 26 | 3F | 1000 | 22 | | 242 | 289 | 9000 | | |
| C 02 | 1 | 1.3 | 16 | 3F | 26 | 1000 | | 190 | 297 | 184 | 7500 | |
| C 03 | 1 | 1 | 24 | 3F | 1000 | 32 | | 122 | 490 | 7870 | | |
| C 04 | 2.6 | 1 | 367 | 3 | 1000 | 36 | | 453 | 433 | 12500 | | |
| C 05 | 1 | .78 | 71 | 3 | 1000 | 29 | | 250 | 390 | 8620 | | |
| C 06 | 1 | 3.38 | 87 | 3 | 1000 | 26 | | 216 | 310 | 8200 | | |
| C 07 | 1 | 1.5 | 24 | 3 | 20 | 1000 | 42 | 100 | 93 | 1000 | 11580 | |
| C 08 | 2.35 | 1 | 30 | 3 | 1000 | 80F | 550 | 250 | 143 | 20400 | 29800 | |
| C 09 | 1 | 1.58 | 20 | 3 | 85 | 1000 | 25 | 75 | 100 | 3570 | 2150 | |
| C 10 | .78 | 1 | 10 | 3 | 1000 | 30 | | 305 | 200 | 5750 | | |
| C 11 | 1.9 | 1 | 45 | 4 | 30F | 3 | 1000 | 68 | 153 | 460 | 117 | 13200 |
| C 12 | 1 | .74 | 142 | 3 | 1000 | 48F | 250 | 260 | 340 | 15800 | 23200 | |
| C 13 | .62 | 1 | 91 | 3 | 1000 | 40f | 208 | 234 | 342 | 7160 | 33400 | |
| C 14 | .67 | 1 | 91 | 2f | 1000 | 40 | | 91 | 240 | 1400 | | |
| C 15 | 1 | 1 | 200F | 11 | 3 | 1000 | 47 | 150 | 370 | 125 | 11000 | |
| C 16 | 2.12 | 1 | 217 | 10 | 2F | 1000 | 3 | 282 | 127 | 388 | 4347 | |
| C 17 | .27 | 1 | 16 | 3 | 35 | 1000 | 5.4 | 121 | 170 | 2636 | 3143 | |
| C 18 | 1 | .36 | 48 | 5F | 16 | 3 | 1000 | 205 | 148 | 336 | 175 | 7300 |
| C 19 | .57 | 1 | 487 | 3 | 1000 | 53 | | 276 | 304 | 9100 | | |
| C 20 | 1 | 1.15 | 8 | 18 | 1000 | 121 | | 24 | 520 | 16500 | | |
| C 21 | 1 | 1 | 315 | 5F | 30 | 3 | 1000 | 370 | 92 | 609 | 94 | 8430 |
| C 22 | 1 | 1 | 47 | 27 | 3 | 1000 | 45 | 24 | 612 | 242 | 10260 | |
| C 23 | .85 | 2 | 187 | 5F | 20 | 3 | 1000 | 227 | 90 | 505 | 305 | 8740 |
| C 24 | 1 | 1.4 | 176 | 3 | 1000 | 1 | | 402 | 790 | 7475 | | |
| C 25 | 1.5 | 1 | 500 | 37 | 3 | 1000 | 20 | 260 | 48 | 616 | 6740 | |
| C 26 | 1 | 1 | 101 | 5F | 100F | 3 | 1000 | 210 | 65 | 419 | 83 | 22000 |
| C 27 | 2.6 | 1 | 500F | 20 | 3 | 1000 | 62 | 95 | 208 | 176 | 14000 | |
| C 28 | 1 | 1 | 49 | 5 | 195F | 3 | 1000 | 152 | 96 | 190 | 135 | 21000 |
| C 29 | 2.45 | 1 | 140 | 5 | 1000 | 160 | | 574 | 183 | 9225 | | |
| C 30 | 1 | 1 | 260 | 53 | 22 | 2500 | 168 | 175 | 570 | 100 | 36700 | |

| Site | Static Shift XY | YX | Resistivity Values (ohm-meters) R-1 | R-2 | R-3 | R-4 | R-5 | Thickness Values (Meters) T-1 | T-2 | T-3 | T-4 | T-5 |
|---|---|---|---|---|---|---|---|---|---|---|---|---|
| C 31 | 1 | 2.96 | 911 | 149 | 3 | 1000 | 5 | 66 | 166 | 240 | 5600 | |
| C 32 | 1 | 1.97 | 44 | 5F | 81 | 1000 | 88 | 95 | 70 | 3670 | 7100 | |
| C 33 | 1 | 2.16 | 200F | 21 | 170 | 1000 | 6.7 | 56 | 135 | 1727 | 10700 | |
| C 34 | 1.5 | 1 | 311 | 5F | 40F | 3 | 1000 | 181 | 162 | 6 | 264 | 5700 |
| C 36 | 1.46 | 1 | 236 | 10.3 | 1.6F | 1000 | 37 | 377 | 165 | 106 | 5100 | |
| C 37 | 1 | .57 | 356 | 3 | 28 | 260 | | 339 | 8.6 | 929 | | |
| C 38 | 1.37 | 1 | 84 | 13 | 3 | 1000 | 4.3 | 47 | 172 | 610 | 3230 | |
| C 39 | 1.32 | 1 | 92 | 30 | 3 | 1000 | 26 | 79 | 242 | 417 | 5080 | |
| C 40 | 1.17 | 1 | 50 | 3 | 1000 | 8.8 | | 100 | 573 | 2670 | | |
| C 41 | 1 | 1 | 100 | 3 | 1000 | 15 | | 218 | 637 | 4272 | | |
| C 42 | 1 | 1.75 | 52 | 5F | 1000 | 120 | | 207 | 116 | 7426 | | |
| C 43 | 1 | 1.46 | 225 | 2 | 1000 | 18 | | 488 | 522 | 3290 | | |
| C 44 | 5.4 | 1 | 495 | 46 | 3 | 1000 | 120 | 418 | 372 | 169 | 14700 | |
| C 45 | 1 | 1.39 | 377 | 45 | 3 | 1000 | 62 | 87 | 566 | 159 | 10400 | |
| C 46 | 1.39 | 1 | 100 | 13 | 79 | 272 | 1000 | 72 | 99 | 1590 | 6895 | 5050 |
| C 47 | .47 | 1 | 92 | 1000 | 185 | | | 4470 | 10575 | | | |
| C 48 | 1 | .59 | 53 | 3 | 5000 | 555 | | 520 | 98 | 30500 | | |
| C 49 | 1 | .45 | 250 | 23 | 3 | 1000 | 170 | 168 | 415 | 143 | 21300 | |
| C 50 | 1 | 1 | 500 | 13 | 3 | 1000 | 100 | 256 | 428 | 198 | 16900 | |
| C 51 | 1 | .75 | 225 | 20 | 3 | 1000 | 39 | 337 | 382 | 221 | 14000 | |
| C 52 | 3.1 | 1 | 677 | 230 | 40 | 3 | 77 | 173 | 275 | 496 | 1036 | 4313 |
| C 53 | | | (poor data) | | | | | | | | | |
| C 54 | 1 | .19 | 150 | 3 | 1000 | 71 | | 362 | 217 | 7890 | | |
| C 55 | 1.52 | 1 | 125 | 5 | 30 | 3 | 1000 | 146 | 37 | 286 | 242 | 7465 |
| C 56 | .42 | 1 | 113 | 10 | 2500 | 280 | | 2650 | 41 | 15700 | | |
| C 57 | . | 1 | 96 | 5 | 1000 | 211 | | 1665 | 98 | 17000 | | |
| C 58 | 1.76 | 1 | 980 | 3 | 10 | 3 | 1000 | 413 | 4.7 | 360 | 418 | 10440 |
| C 59 | 1 | .78 | 202 | 5 | 1000 | 116 | | 535 | 204 | 11133 | | |
| C 60 | 1 | 1 | 563 | 5 | 533 | 3 | 1000 | 369 | 38 | 422 | 126 | 21300 |
| C 61 | 1 | 2.2 | 103 | 207 | 1000 | 133 | | 449 | 1800 | 44000 | | |
| C 62 | 1 | 5.7 | 48 | 112 | 21 | 1000 | 92 | 477 | 188 | 406 | 16000 | |
| C 63 | 1 | 1 | 197 | 5000 | 1348 | | | 1870 | 54000 | | | |
| C 64 | 1 | 1.7 | 155 | 3 | 1000 | 44 | | 443 | 112 | 12000 | | |

| Site | Static Shift XY | YX | Resistivity Values (ohm-meters) R-1 | R-2 | R-3 | R-4 | R-5 | Thickness Values (Meters) T-1 | T-2 | T-3 | T-4 | T-5 |
|---|---|---|---|---|---|---|---|---|---|---|---|---|
| C 65 | .72 | 1 | 1000 | 3 | 1000 | 6 | | 500 | 298 | 12100 | | |
| C 66 | 1 | 1.8 | 120 | 19 | 3 | 1000 | 21 | 305 | 360 | 282 | 9100 | |
| C 67 | .056 | 1 | 56 | 5 | 1000 | 90 | | 714 | 140 | 11000 | | |
| C 68 | 1.39 | .68 | 39 | 126 | 1000 | 170 | | 385 | 2952 | 28000 | | |

| Site | Static Shift XY | YX | Resistivity Values (ohm-meters) R-1 | R-2 | R-3 | R-4 | R-5 | Thickness Values (Meters) T-1 | T-2 | T-3 | T-4 | T-5 |
|---|---|---|---|---|---|---|---|---|---|---|---|---|
| C 69 | 1 | 1 | 165 | 5 | 56 | 3 | 1000 | 213 | 100 | 421 | 340 | 5200 |
| C 70 | 1.27 | 1 | 68 | 20 | 3 | 1000 | 6 | 117 | 653 | 303 | 8500 | 12500 |
| C 71 | 1 | 1 | 243 | 38 | 5 | 1000 | | 6 | 117 | 546 | 98 | 15000 |
| C 72 | .66 | 1 | 73 | 5000 | 91 | | | 1036 | 32000 | | | |
| C 73 | 1 | .66 | 34 | 1000 | 108 | | | 707 | 9492 | | | |
| C 74 | 1 | 1.44 | 10 | 48 | 1000 | 84 | 1000 | 20 | 1097 | 16900 | 31300 | |
| C 75 | .5 | 1 | 141 | 21 | 1000 | 193 | | 150 | 584 | 16240 | | |
| C 76 | 2.16 | .88 | 22 | 177 | 5000 | 750 | 4000 | 42 | 1254 | 46500 | 72000 | |
| C 77 | 1.89 | 1 | 26 | 16 | 1000 | 142 | | 79 | 840 | 8322 | | |
| C 78 | 1.8 | . | 49 | 320 | 5 | 1000 | 177 | 187 | 214 | 112 | 17600 | |
| C 79 | 1 | 1 | 393 | 139 | 2730 | 647 | | 365 | 2434 | 35400 | | |
| C 80 | .6 | 1 | 135 | 61 | 5 | 1000 | 198 | 140 | 297 | 90 | 13300 | |
| C 81 | .74 | 1 | 1000 | 102 | 3 | 90 | 11 | 346 | 474 | 226 | 5760 | |
| C 82 | .34 | 1 | 1000 | 285 | 3 | 1000 | 85 | 132 | 763 | 243 | 7203 | |
| C 83 | .77 | 1 | 366 | 34 | 3 | 1000 | 125 | 535 | 294 | 192 | 13000 | |
| C 84 | 1.36 | 1 | 51 | 20 | 156 | 1000 | 147 | 121 | 478 | 5402 | 7386 | |
| C 85 | 2.5 | 1 | 204 | 10 | 1000 | 1800 | | 533 | 171 | 10200 | | |
| C 86 | 1.27 | 1 | 229 | 35 | 3 | 1000 | 235 | 235 | 683 | 64 | 17800 | |
| C 87 | 1.97 | 1 | 17 | 142 | 5000 | 600 | 5700 | 24 | 1734 | 26000 | 83000 | |
| C 88 | 1 | 2.03 | 13 | 94 | 1000 | 262 | | 132 | 1389 | 14900 | | |
| C 89 | 1.93 | 1 | 34 | 213 | 5000 | 331 | 5600 | 107 | 1684 | 30850 | 75200 | |
| C 90 | 1 | .46 | 121 | 5 | 23 | 905 | 42 | 200 | 101 | 533 | 13800 | |
| C 91 | 1 | .37 | 60 | 5 | 931 | 53 | | 458 | 140 | 9367 | | |
| C 92 | 1 | 1 | 506 | 28 | 1000 | 129 | 1000 | 227 | 762 | 31500 | 16700 | |
| C 93 | 1 | .66 | 74 | 5 | 1000 | 151 | | 448 | 99 | 4544 | | |

References

The following is only a limited sampling of the technical literature available concerning the magnetotelluric method. Reference [7] is recommended as a compendium volume that includes papers covering all aspects of MT technology. Annotation has been added to aid the reader.

This list of references has been extracted from the paper by A. S. Orange, *"Magnetotelluric Exploration for Hydrocarbons"*, published in the February 1988 issue of the Proceedings of the IEEE (reference "A").


[A] A.S. Orange, *"Magnetotelluric Exploration for Hydrocarbons"*, Proc. IEEE, vol 77, 2, pp. 287-317, 1988. (A survey paper covering all aspects of MT, including field examples)

[1] A.N. Tikhonov, *"Determination of the electrical characteristics of the deep strata of the earth's crust,"* Dok. Akad. Nauk, USSR , vol. 73, 2, pp. 295-297, 1950. (With Cagniard, the first of the papers on MT as an exploration tool)

[2] L. Cagniard, *"Basic theory of the magnetotelluric method of geophysical prospecting,"* Geophysics, vol. 18, pp. 605-635, 1953. (With Cagniard, the first of the papers on MT as an exploration tool)

[3] G.E. Archie, *"The electrical resistivity log as an aid in determining some reservoir characteristics,"* Trans. AIME, Petrol. Br., vol. 146, pp. 54-62, 1942. (The papers by Archie are essential to an understanding of the relationship between porosity and resistivity, and the electrical properties of rocks)

[4] G.E. Archie, *"Electrical resistivity-an aid in core analysis interpretation,"* Bull. Am. Assoc. Petrol. Geologists, vol. 31, no. 2, 1947.

[5] G.E. Archie, *"Classification of carbonate reservoir rocks and petrophysical considerations,"* Bull. Am. Assoc. Petrol. Geologists, vol. 36, no. 2, 1951.

[6] E. I. Parkhomenko, *"Electrical properties of rocks,"* New York, N.Y: Plenum Press, 1967, pp. 276-278. ( A basic text on the subject)

[7] K. Vozoff, ed., "*Magnetotelluric methods*, ," Tulsa, OK: Geophysics Reprint Series, Society of Exploration Geophysicists, 1986, 763 p. (Note: This volume contains 55 papers, including many of those referenced here.)

[8] J.A. Stratton, "*Electromagnetic Theory*", New York and London: McGraw-Hill, 1941. (A basic EM theory text)

[9] K. Vozoff, "*The magnetotelluric method in the exploration of sedimentary basins*," Geophysics, vol. 37, pp. 98-114, 1972. (An excellent review of applied MT theory, and the early use of MT as an exploration tool)

[10] S.K. Park, A. Orange, T. Madden, "***Effects** of three-dimensional structure on magnetotelluric sounding curves*," Geophysics, vol. 48, pp. 1402-1405,1983. (One of the first papers to discuss current gathering, an important 3-D MT effect)

[11] S.K. Park, "*Distortion of magnetotelluric sounding curves by three-dimensional structures*," Geophysics, vol. 50, no. 5, pp. 785-797, 1985. (A more in-depth discussion of various 3-D effects)

[12] D. W. Eggers, "*An eigenstate formulation of the magnetotelluric impedance tensor*," Geophysics, vol. 47, no. 8, pp. 1204-1214, 1982. (Important to the understanding of the effects of 3-D structure on MT data)

[13] G.W. Hohmann, "*Three-dimensional induced polarization and electromagnetic modeling*," Geophysics, vol. 40, pp. 309-324, 1975. (A valuable discussion of 3-D modeling techniques developed at the University of Utah)

[14] M.E. Best, P. Duncan, F.J. Jacobs, and W.L. Scheen, "*Numerical modeling of the electromagnetic response of three-dimensional conductors in a layered earth*," Geophysics, vol.50, pp. 665-676, 1985. (This paper contains some of the basics of 3-D modeling)

[15] G.A. La Torraca, T.R. Madden, and J. Korringa,"*An analysis of the magnetotelluric impedance for three-dimensional conductivity structures*", Geophysics, vol. 51, pp. 1819-1829, 1986. (Like Eggers [12] important to the understanding of the effects of 3-D structure on MT data)

[16] R. P. Ranganayaki, T. R. Madden, "*Generalized thin sheet analysis in magnetotellurics, an extension of Price's analysis*," Geophys. J. Roy. Astr. Soc., vol. 60, pp. 445-457. 1980. (This paper is basic to an understanding of the work of Park, et. al . [10], [11], [17])

[17] T. R. Madden and S. K. Park, "*Magnetotelluric modeling for a crustal environment*," Final Report, U.S.G.S. contract no. 14-08-0001-G-643, 74 p., 1982. (The initial report on the work of the group at MIT; contains a listing of the first Park 3-D code)

[18] J. Clarke and N.E. Goldstein, "*Magnetotelluric measurements*," in *SQUID applications to geophysics*, H. Winestock and W.C. Overton, Jr., Eds., Tulsa, OK: Society of Exploration Geophysicists, pp. 49-60 , 1982. (MT field procedures and data processing)

[19] J. Clarke, et al, "*Remote reference magnetotellurics*," Equipment and Procedure, Geophysical Prospecting, vol. 31, pp. 149-170, 1983. (With [23], the fundamental work on the remote reference MT technique)

[20] D.E. Wight and F.X. Bostick, "*Cascade decimation - a technique for real time estimation of power spectra*", in *1980 Proceedings IEEE international conference on acoustic speech and signal processing, April 9-11, 1980, Denver, CO,* Institute of Electrical and Electronics Engineers, pp. 626-620, 1980. (Data acquisition and processing techniques, in particular cascade decimation, a widely used technique))

[21] W. E. Sims, F. X. Bostick, Jr., and H. W. Smith, "*Estimation of magnetotelluric impedance tensor elements from measured data*," Geophysics, vol 36, pp. 938-942, 1971. (One of the fundamental papers, contains a rigorous discussion of MT processing algorithms)

[22] G. Kunetz, "*Processing and interpretation of magnetotelluric soundings*," Geophysics, vol. 37, pp. 1005-1021, 1972. (One of the fundamental papers with a discussion of MT processing algorithms)

[23] T. D. Gamble, W. M. Goubau, and J. Clarke, "*Magnetotellurics with a remote magnetic reference*," Geophysics, vol. 44, pp. 53-68, 1978. (With [19], the fundamental work on the remote reference MT technique)

[23] T.D. Gamble, W. M. Goubau, and J. Clarke, "*Error analysis for remote reference magnetotellurics*,", Geophysics, vol. 44, pp. 959-968. (Further analysis of remote reference MT)

[25] D.R., Word, H.W. Smith, and F.X. Bostick, Jr., "*An investigation of the magnetotelluric tensor impedance method*," EERL Tech. Rept. No. 82, U. of Texas at Austin, 1969. (An excellent and detailed discussion of the foundations of MT data analysis and processing)

[26] J. W. Cooley and J.W. Tukey, "*An algorithm for machine calculation of complex Fourier series*," *Math Computation*, vol. 19, pp. 297-301, April 1965. (An early discussion of the fast Fourier transform [FFT])

[27] F.X. Bostick, "*A simple almost exact method of MT analysis*", *Workshop on electrical methods in geothermal exploration*," U.S. Geol.Surv., Contract No. 14080001-8-359, 1977. (A simple but elegant approximation of the 1-D resistivity structure derived from the MT apparent resistivity)

[28] W. R. Petrick, W. H. Pelton and S. H. Ward, "*Ridge regression Inversion applied to crustal resistivity sounding data from South Africa,* " Geophysics, vol. 42, pp. 995-1005, 1977. (Analytic 1-D layered earth modeling, widely used in MT interpretation)

[29] C.M. Swift, Jr., "*A magnetotelluric investigation of an electrical conductivity anomaly in the southwestern United States*," in *Magnetotelluric Methods*, K. Vozoff, Ed. Tulsa, OK: Geophysics Reprint Series, Society of Exploration Geophysicists, 1986, pp. 156-166. (also: Ph. D. thesis, Massachusetts Institute of Technology, 211 p., 1967. (The fundamental paper on 2-D MT modeling)

[30] D. Jupp, and K. Vozoff, 1977, "*Two-dimensional magnetotelluric inversion*," Geophys. J.R. Astr. Soc., vol. 50, pp. 333. (An extension of the work of Swift; the 2-D program used most frequently by Arnold Orange Associates, coauthor of this report [29])

[31] P.E. Wannamaker, G.W. Hohmann, and W.A. San Filipo, "*Electromagnetic modeling of three-dimensional bodies in layered earth using integral equations*, "

Geophysics, vol. 49, no. 1, pp. 60-74, 1984. (A discussion of a widely used 3-D modeling program)

[32] P. Weidelt, "*Inversion of two-dimensional conductivity structures*," Phys. Earth Planet. Int., vol. 10, pp. 282-291, 1975. (A discussion of 2-D inversion technique)

[33] S. C. Ting, G. W. Hohmann, "*Integral equation modeling of three-dimensional magnetotelluric response*," Geophysics, vol. 46, pp. 182-197, 1981. (Discussion of an approach to 3-D MT modeling developed at the University of Utah)

[34] I.K. Reddy, D. Rankin, and R.J. Phillips, "*Three-dimensional magnetotelluric and magnetic variational sounding*," Geophys. J. Roy. Astr.Soc., vol. 51, pp. 313-325, 1977. (With the following paper, a discussion of an approach to 3-D MT modeling developed at the University of Edmonton)

[35] I.K. Reddy, D. Rankin, and R.J. Phillips, "*Three-dimensional modeling in magnetotelluric and magnetic variational sounding*," Geophys. J.R. Astr., vol. 51, pp. 313, 1977.

[36] T.R. Madden, R.L. Mackie, "*Three-dimensional magnetotelluric modelling and inversion*," Proc. IEEE, vol.77, pp. 318-333, 1989. (A discussion of 3-D modeling algorithm developed at MIT; currently in use by Arnold Orange Associates, coauthor of this report)

[37] C. Torres-Verdun and F.X. Bostick, "*Properties of EMAP in two-dimensional environments*" (expanded abstract), Proc. Soc. Expl. Geophys. 60th An.l Int. Mtg., San Francisco, pp. 520-523, 1990. (A discussion of one approach to MT spatial filtering)

[38] C.L. Shoemaker, Y. Shoham, and R.L. Hockey, "*Calibration case study of natural source electromagnetic array data recorded over a well in Oregon*," Proc. IEEE, vol.77, pp. 334-337, 1989. (A field example of MT spatial filtering)

# APPENDIX A

## DATA PLOTS AND LISTINGS

January 1992

By
ARNOLD S. ORANGE

ARNOLD ORANGE ASSOCIATES
8806 POINT WEST DRIVE
AUSTIN, TEXAS 78759

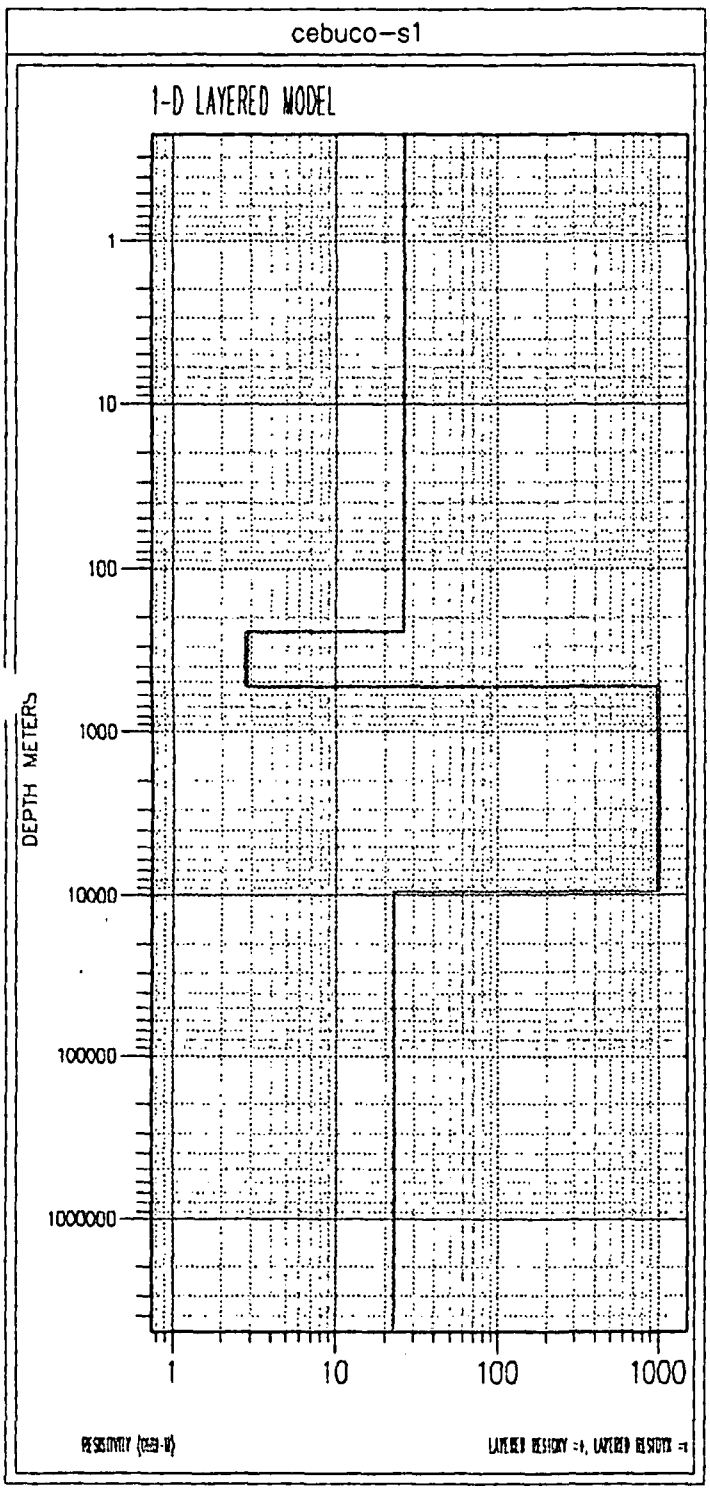
cebuco–s1
1-D LAYERED MODEL
DEPTH METERS
1
10
100
1000
10000
100000
1000000
1
10
100
1000

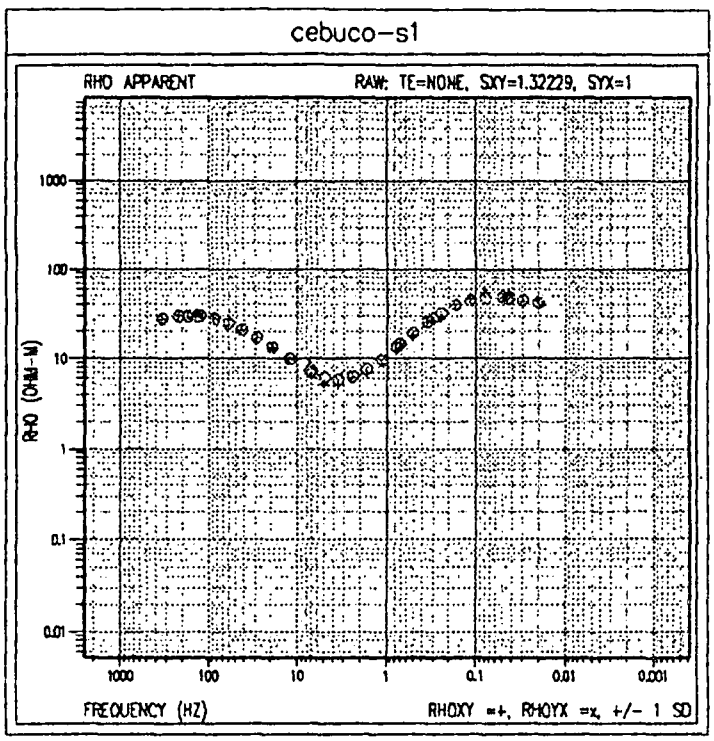
cebuco–s1
RHO APPARENT
RAW: TE=NONE, SXY=1.32229, SYX=1
RHO (OHM-M)
1000
100
10
1
0.1
0.01
1000
100
10
1
0.1
0.01
0.001
FREQUENCY (HZ)
RHOXY =+, RHOYX =x, +/- 1 SD

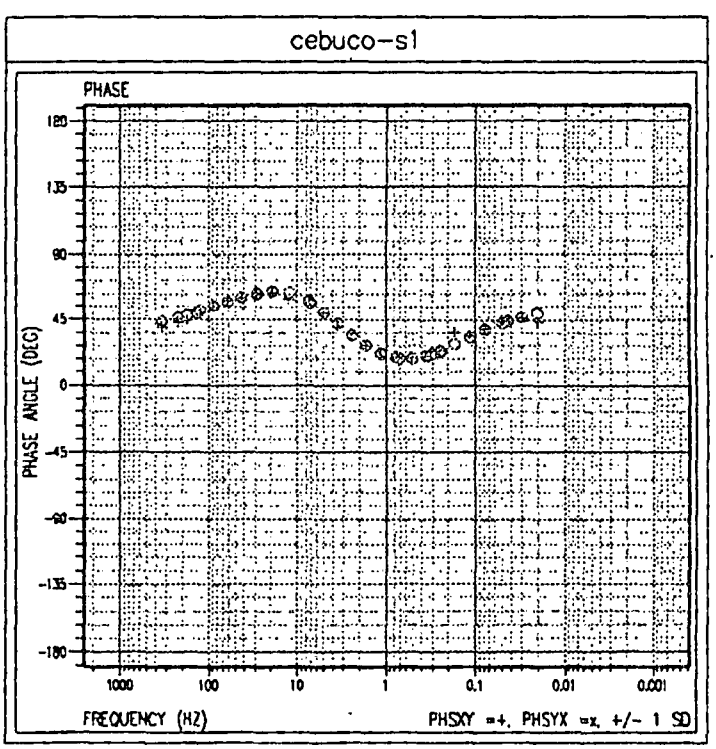
cebuco–s1
PHASE
PHASE ANGLE (DEG)
120
135
90
45
0
-45
-90
-135
-180
1000
100
10
1
0.1
0.01
0.001
FREQUENCY (HZ)
PHSXY =+, PHSYX =x, +/- 1 SD

cebuco–s2

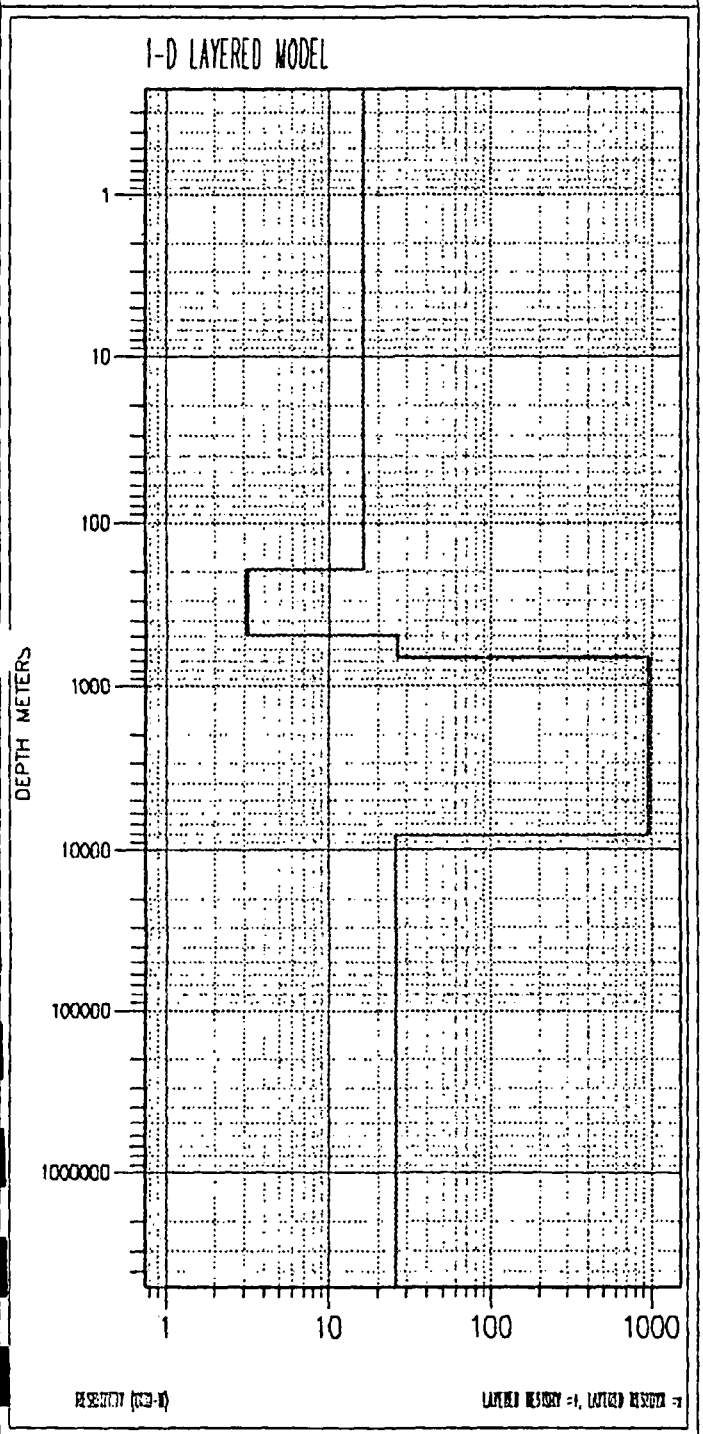


cebuco–s2

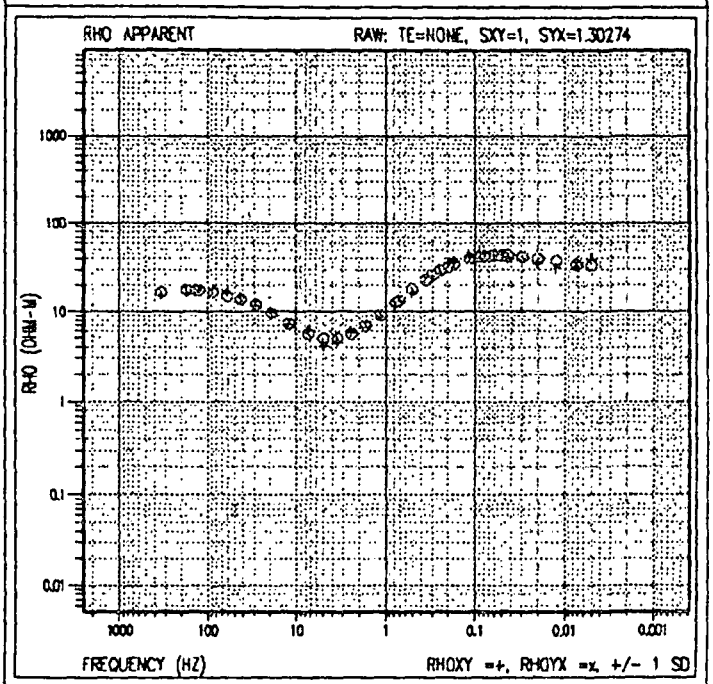


cebuco–s2

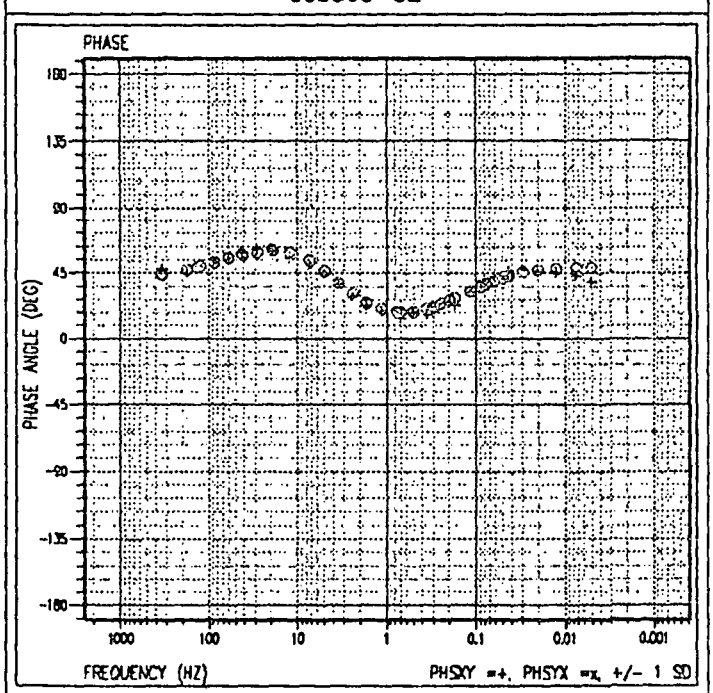

cebuco–s3

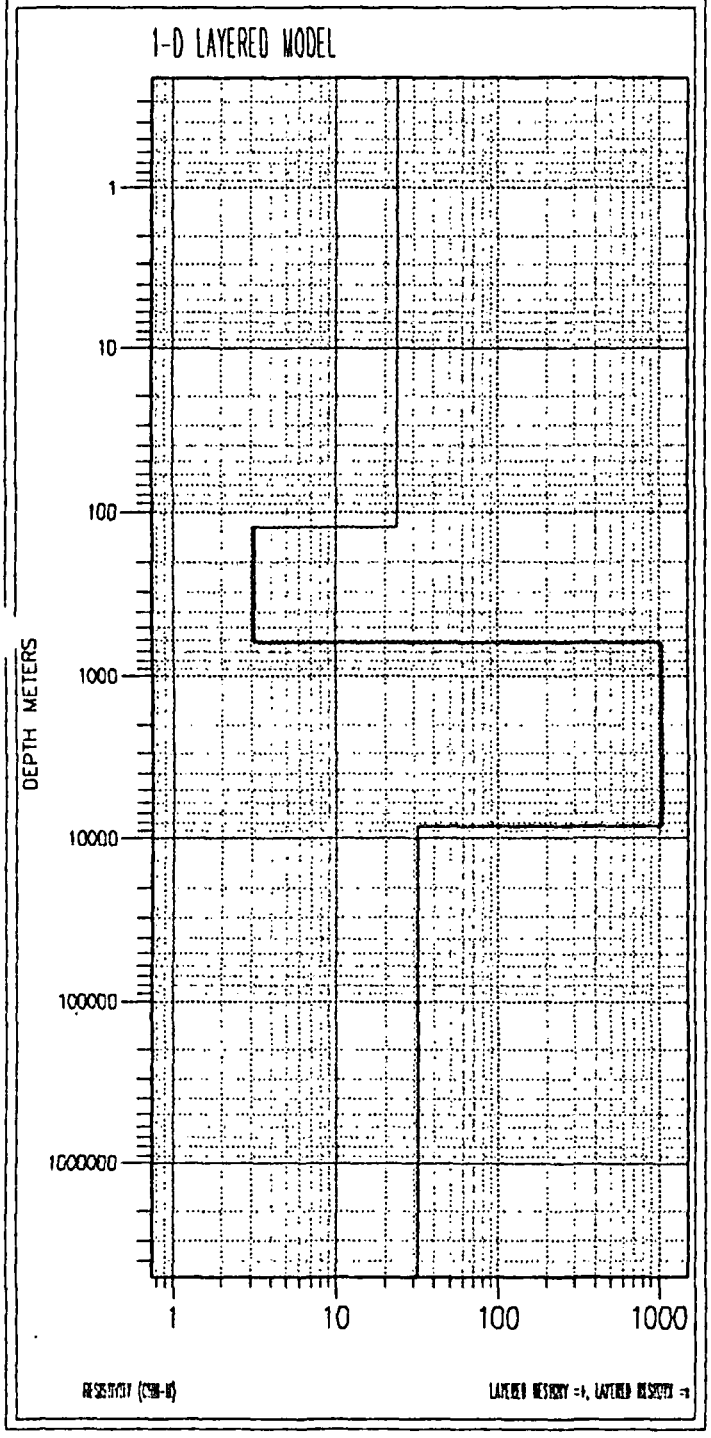


cebuco–s3

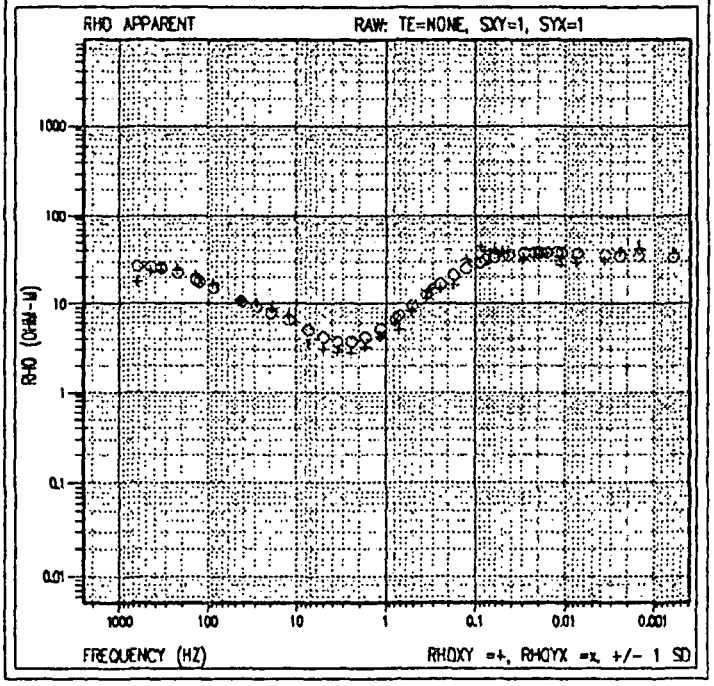


cebuco–s3

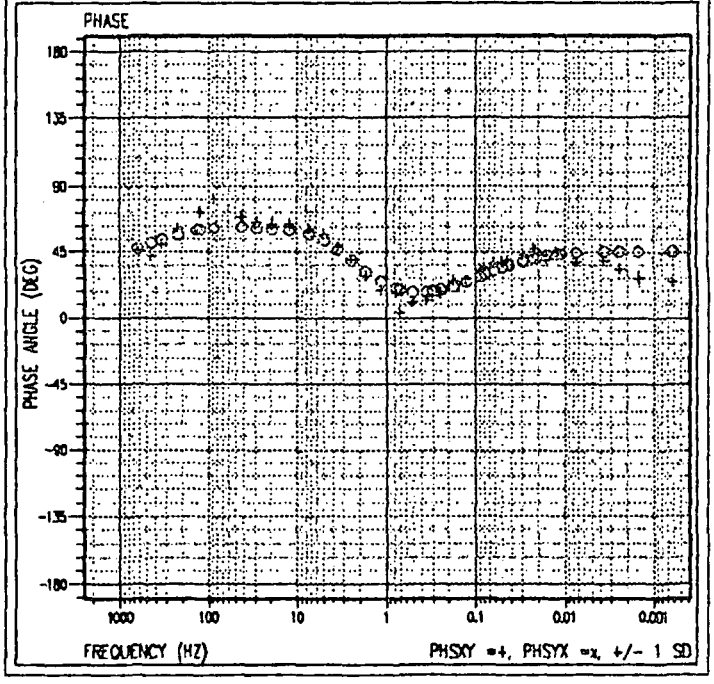

cebuco-s4

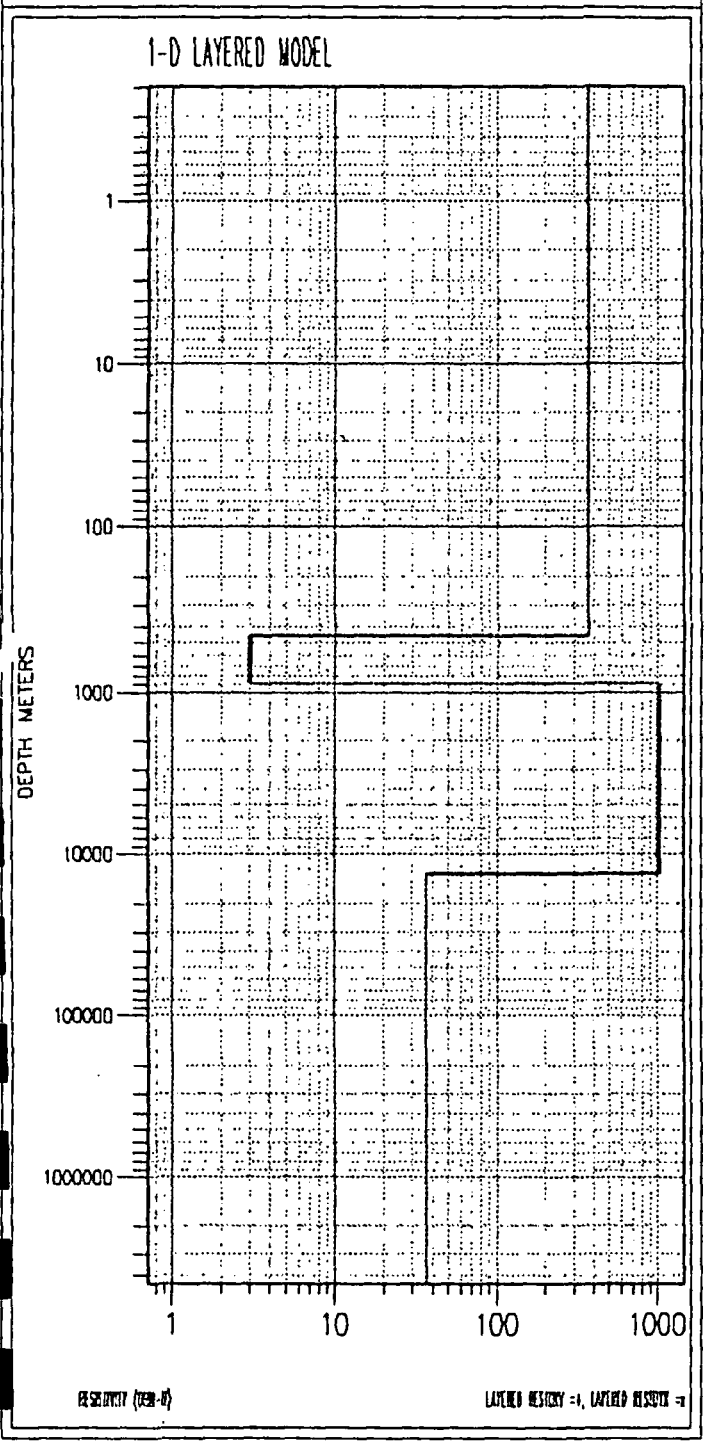


cebuco-s4

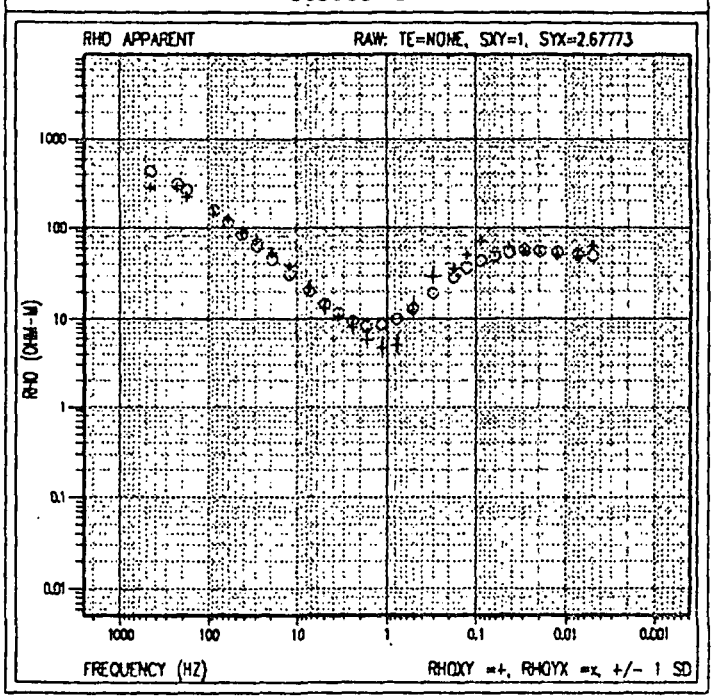


cebuco-s4

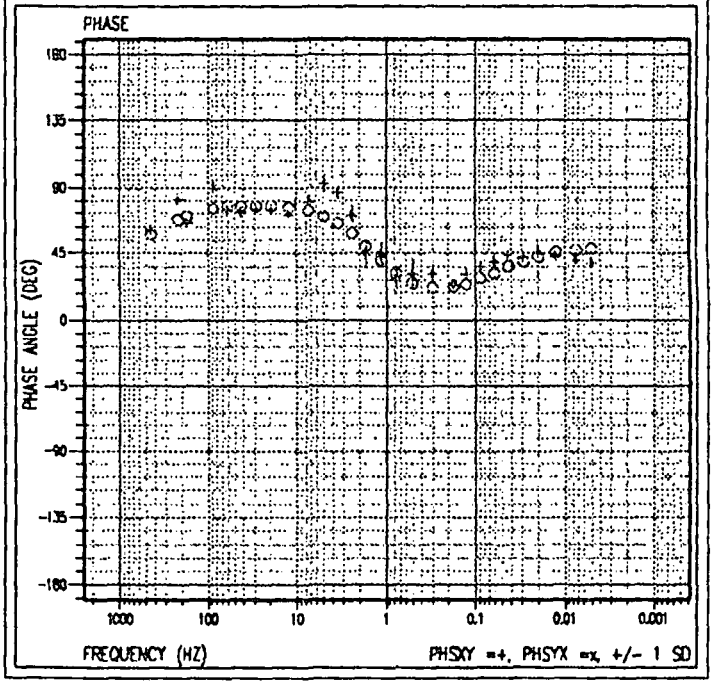

cebuco-s5

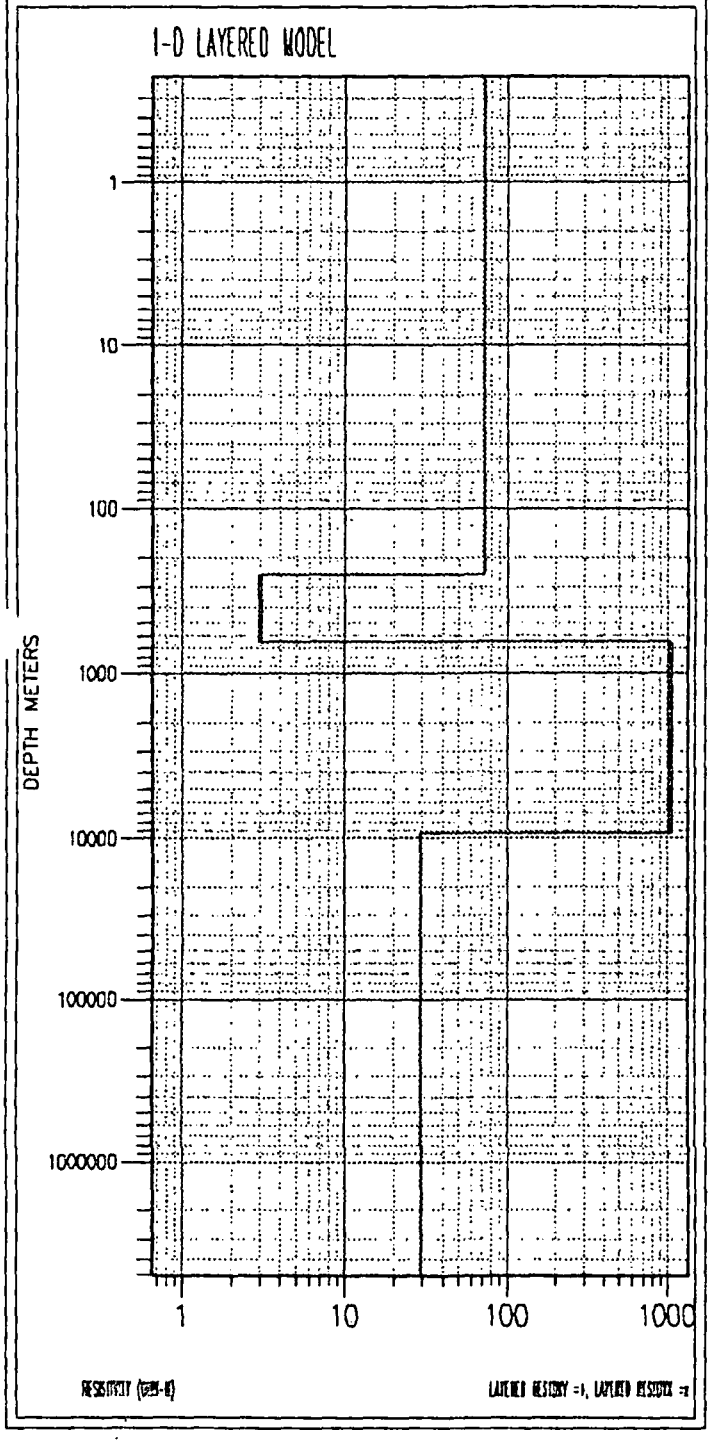


cebuco-s5

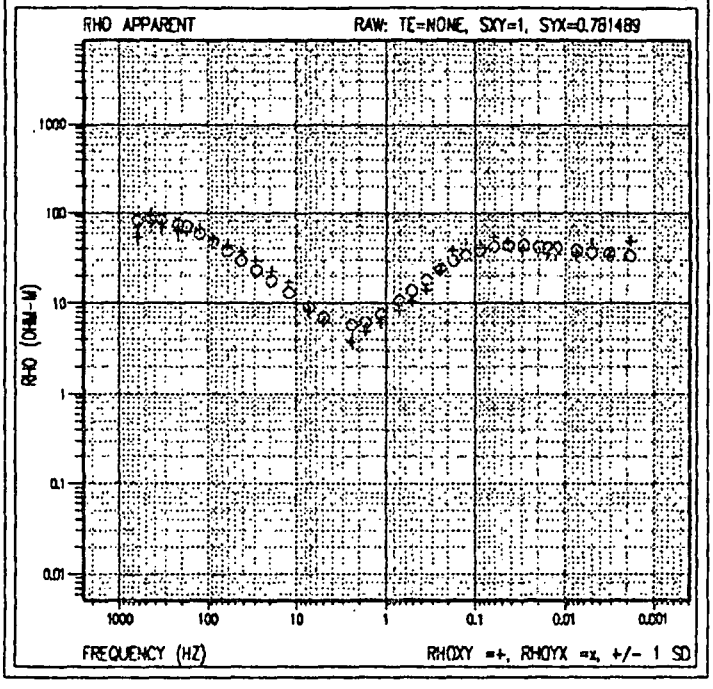


cebuco-s5

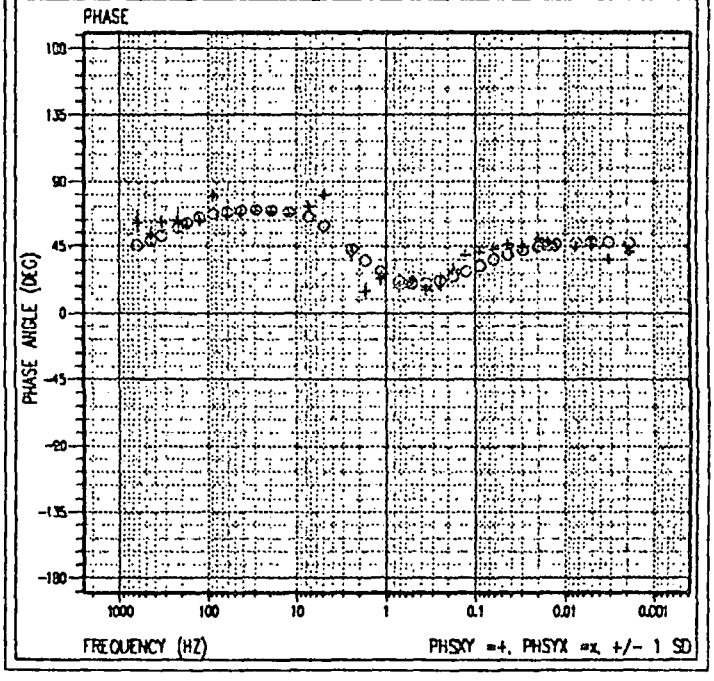

cebuco–s6

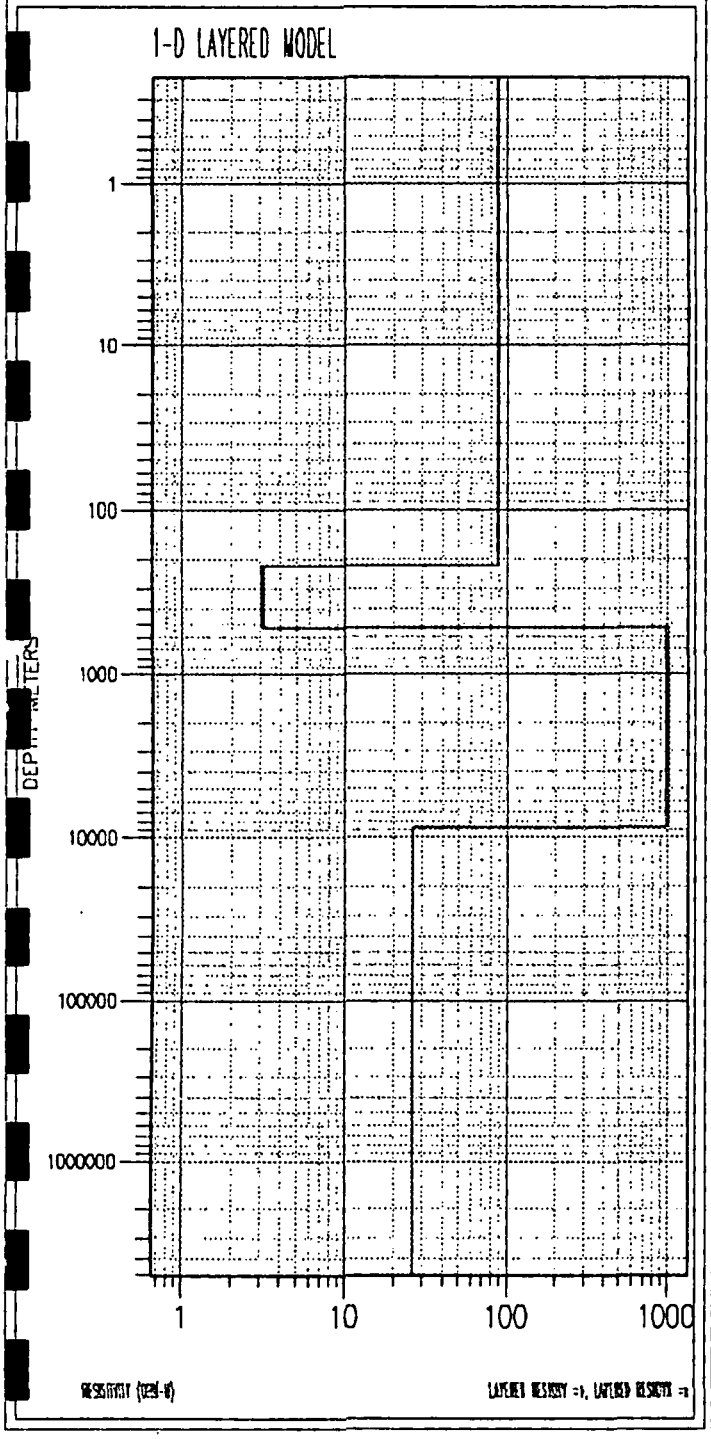


cebuco–s6

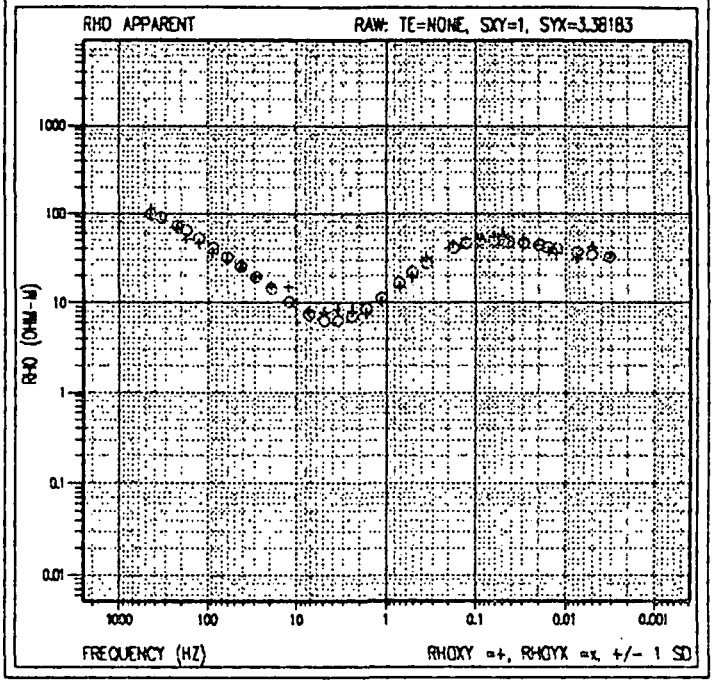


cebuco–s6

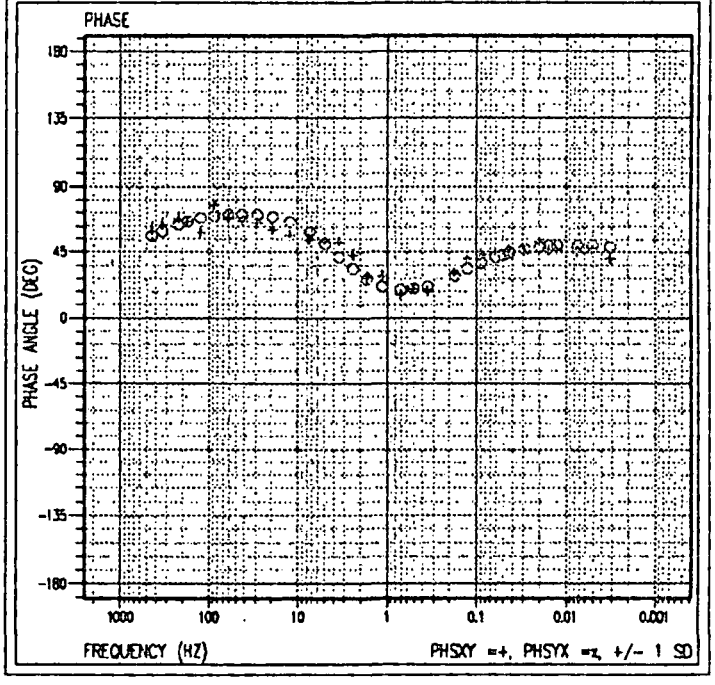

cebuco–s7

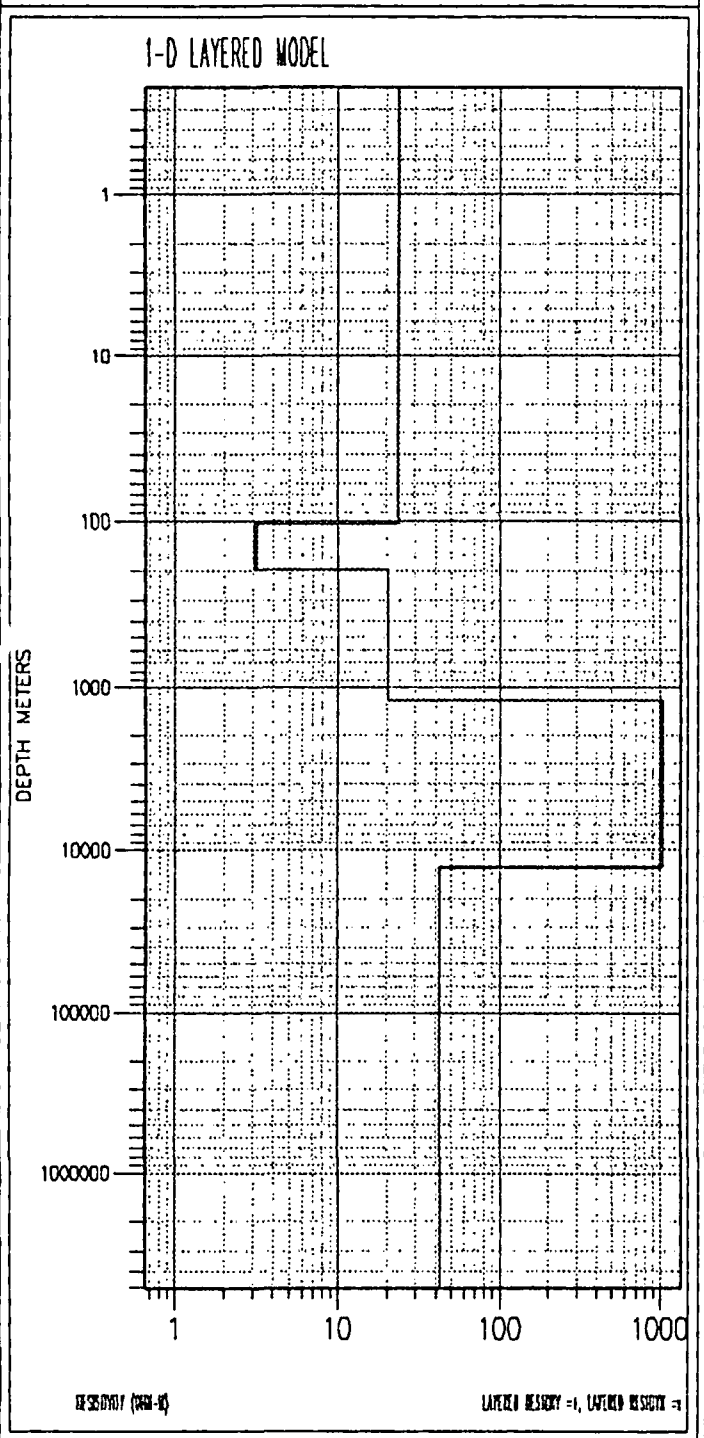


cebuco–s7

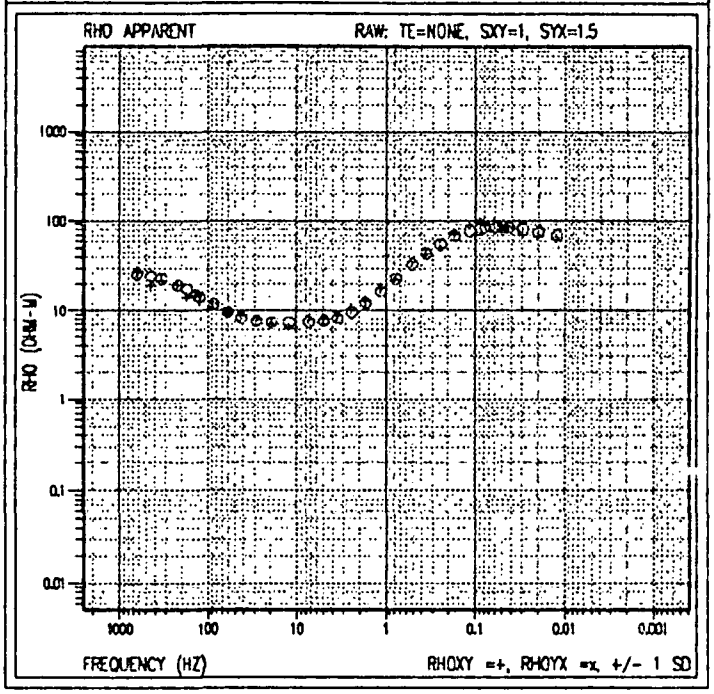


cebuco–s7

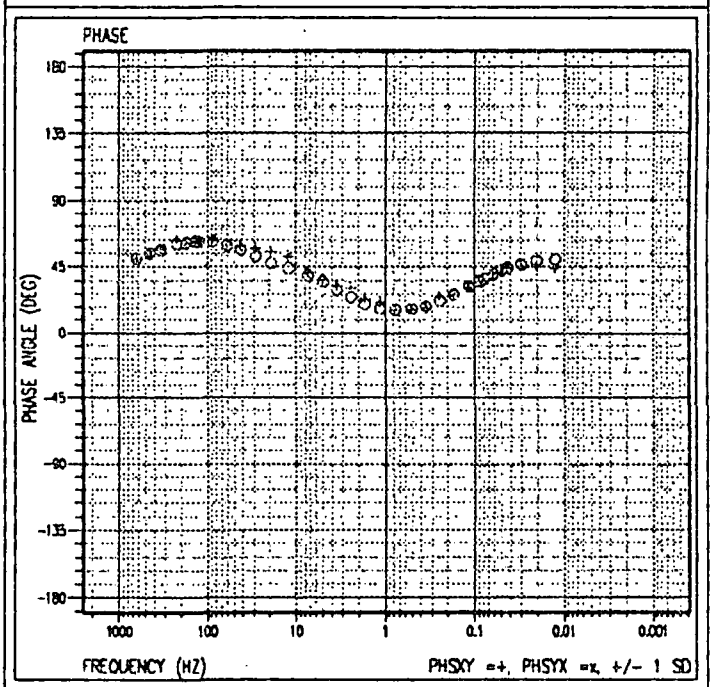

cebuco-s8

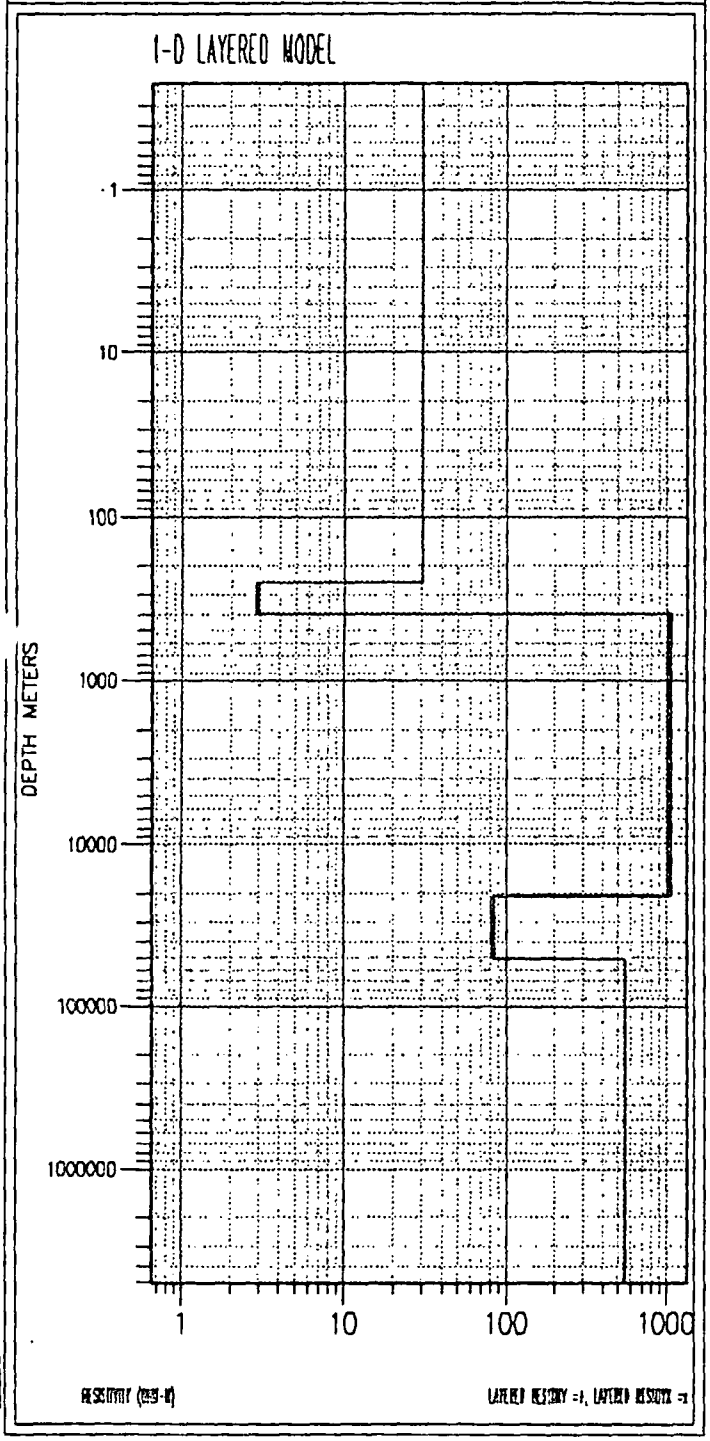


cebuco-s8

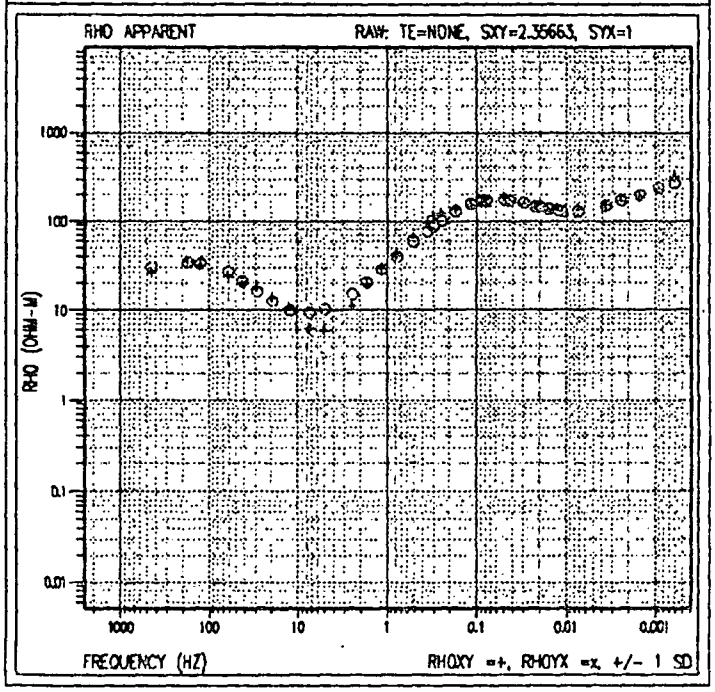


cebuco-s8

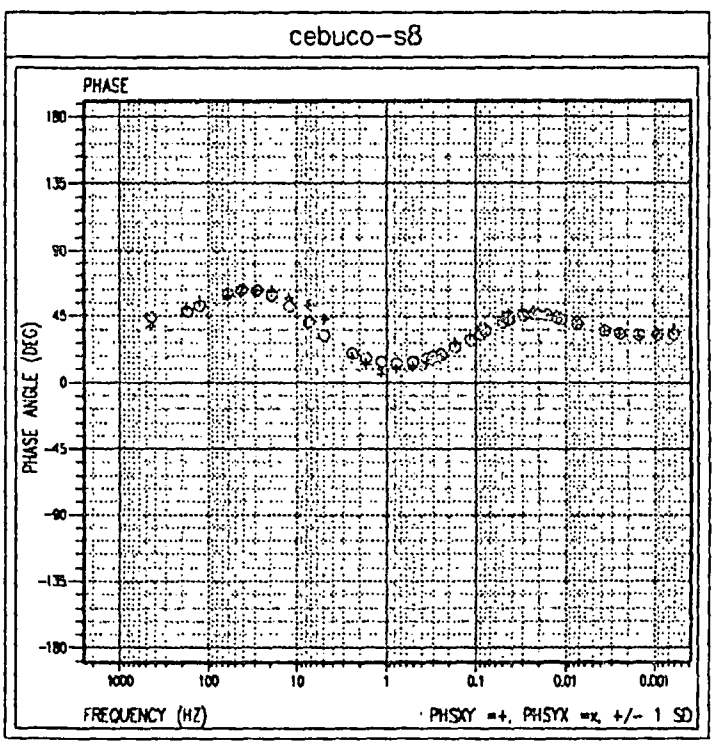

cebuco-s9

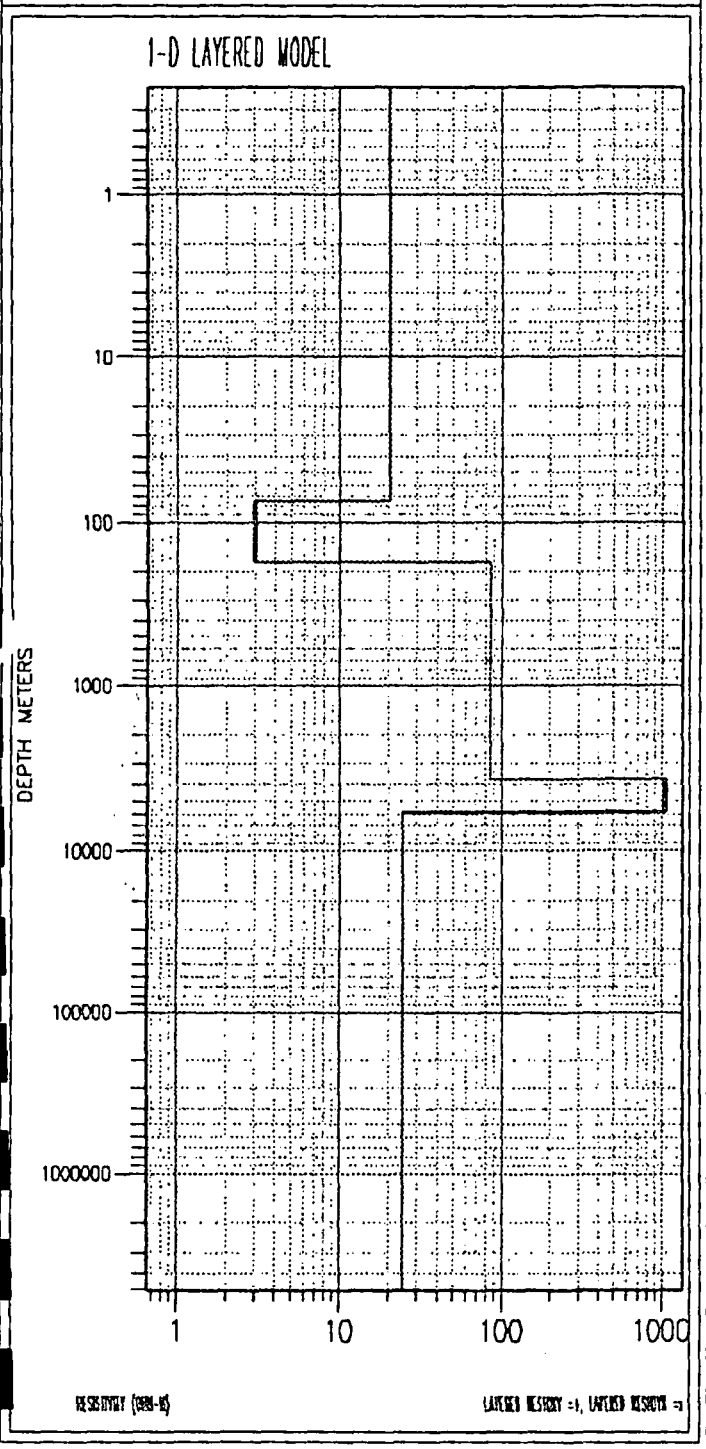


cebuco-s9

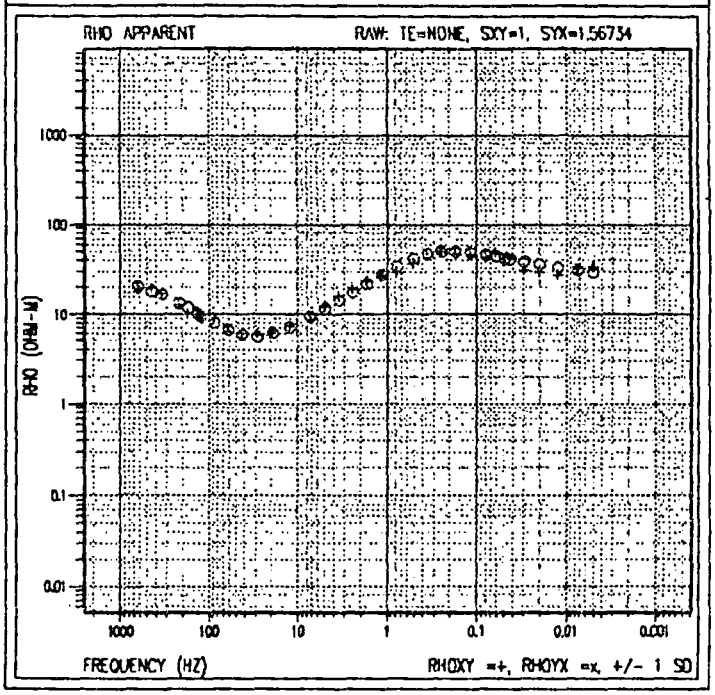


cebuco-s9

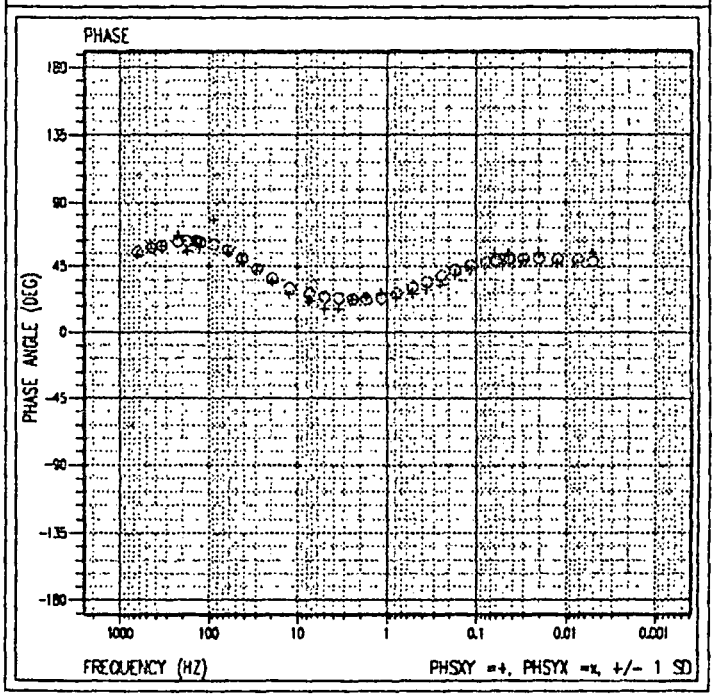

cebuco-s10

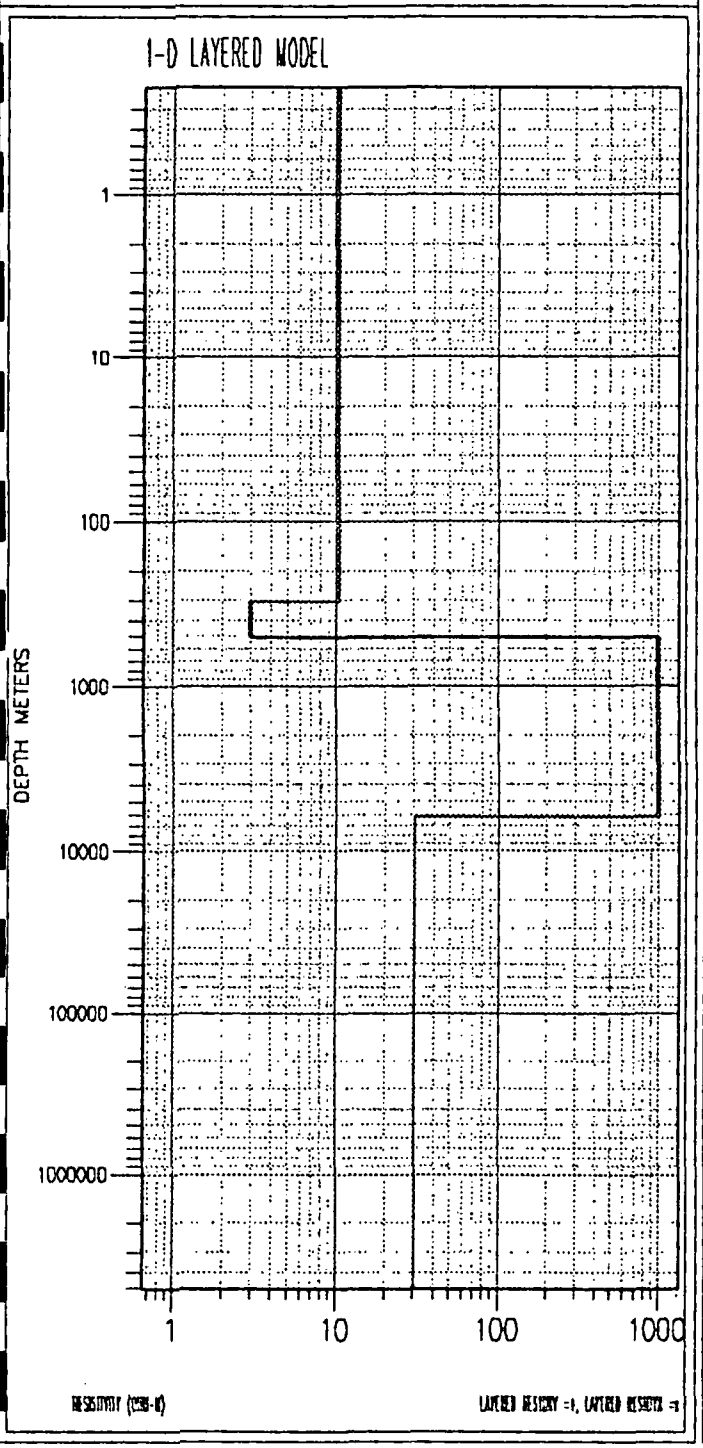


cebuco-s10

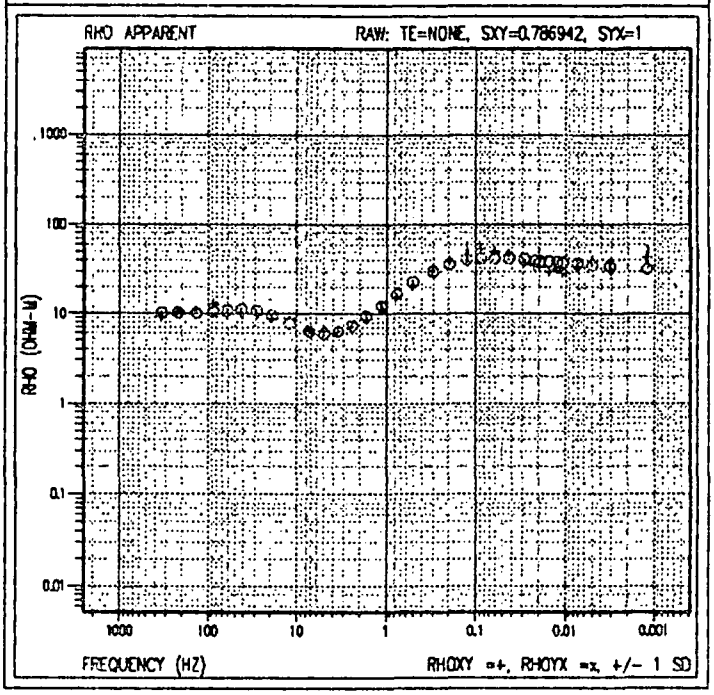


cebuco-s10

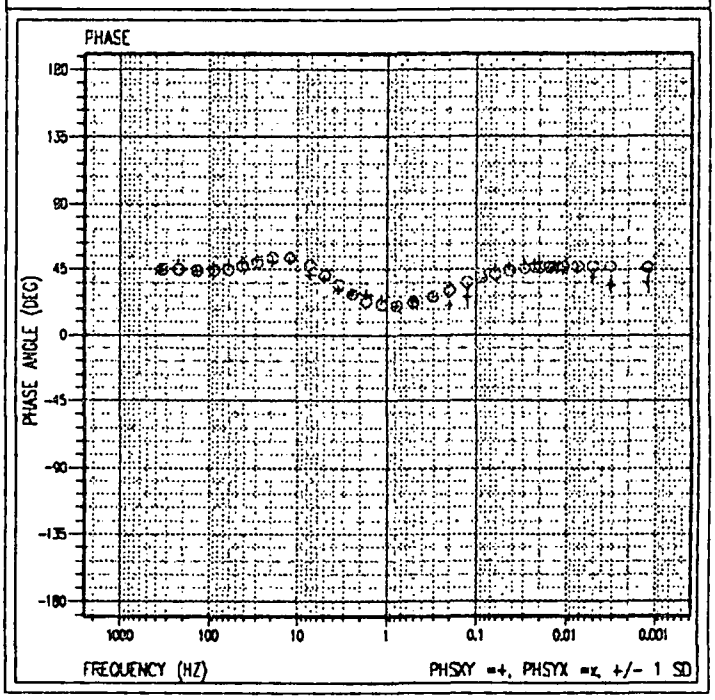

cebuco-s11

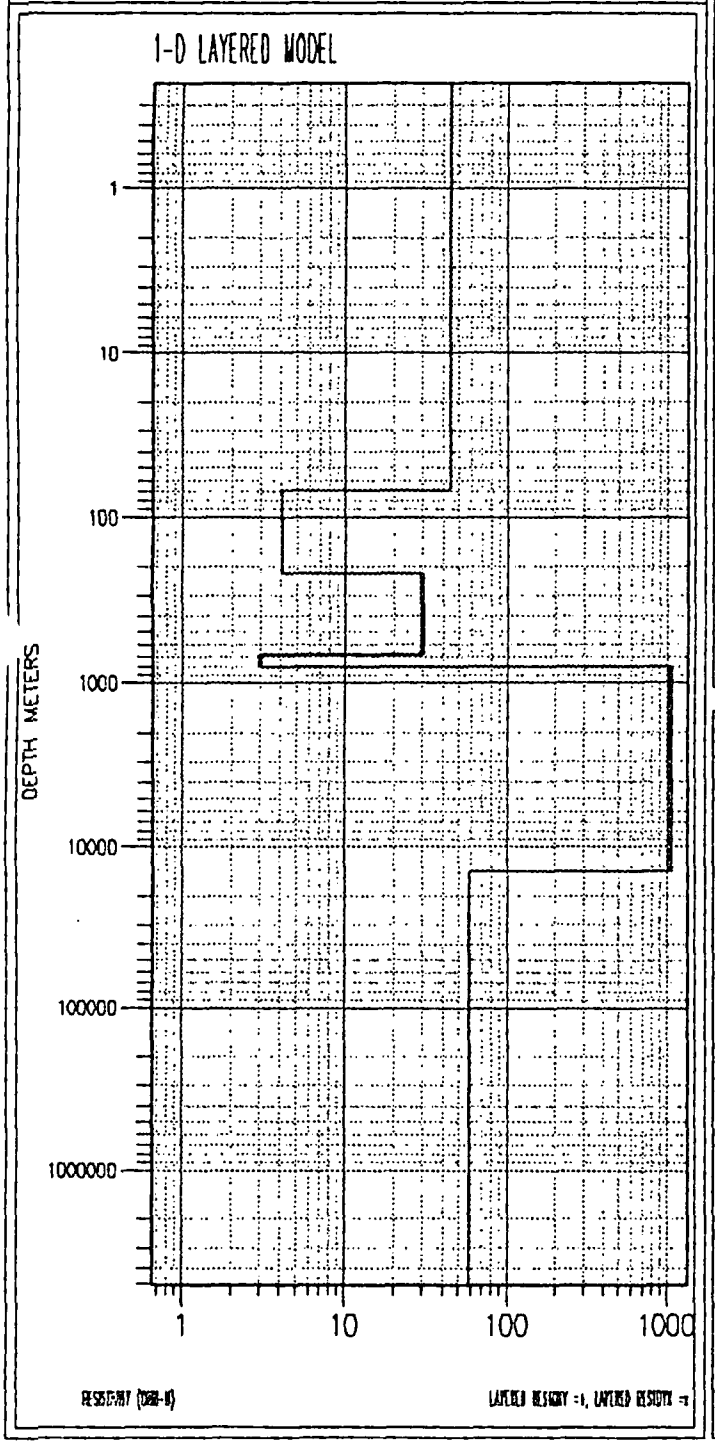


cebuco-s11

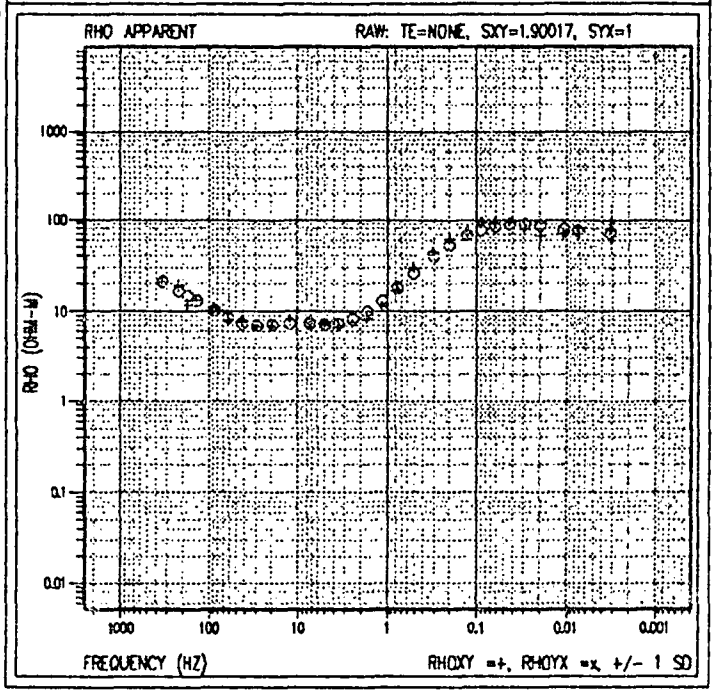


cebuco-s11

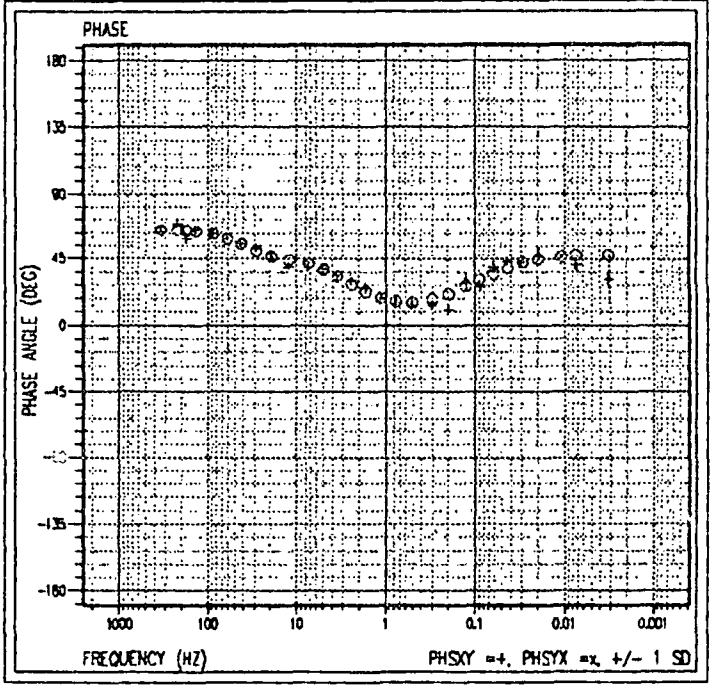

cebuco-s12

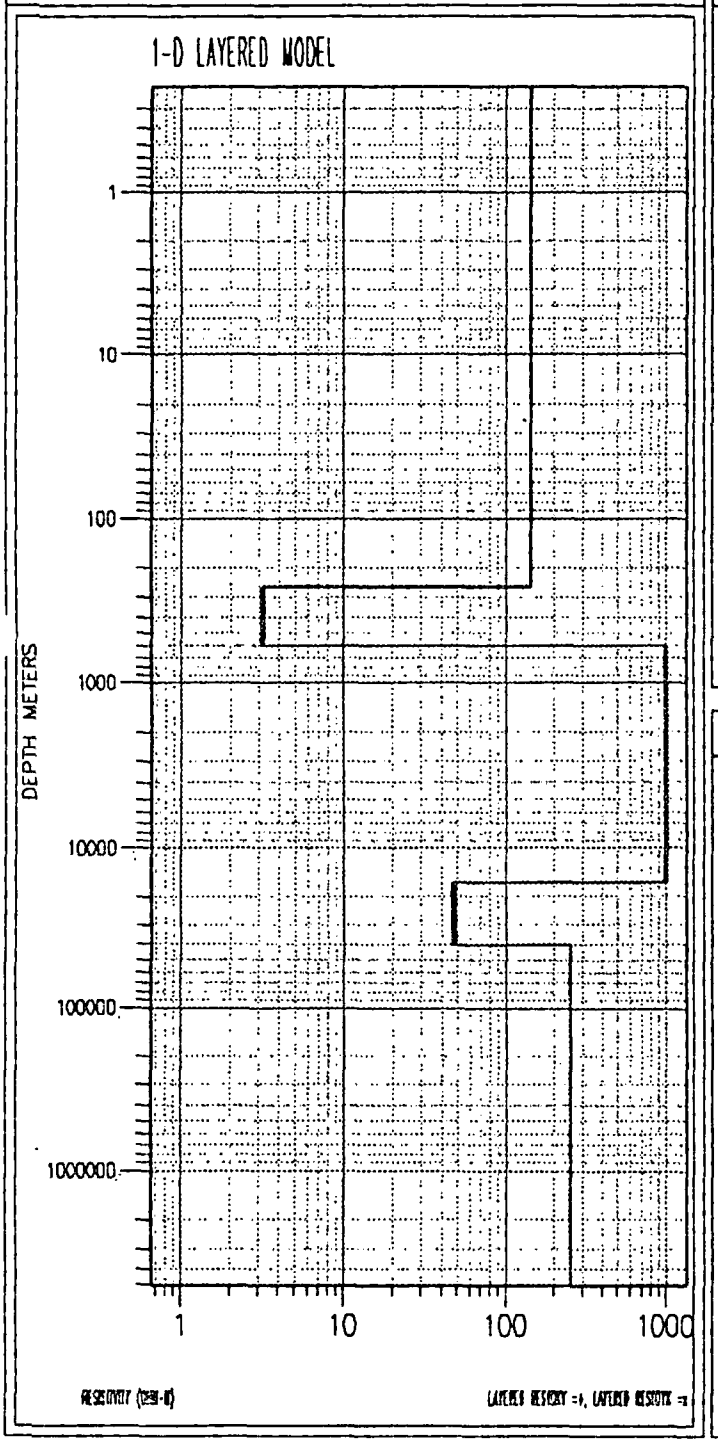


cebuco-s12

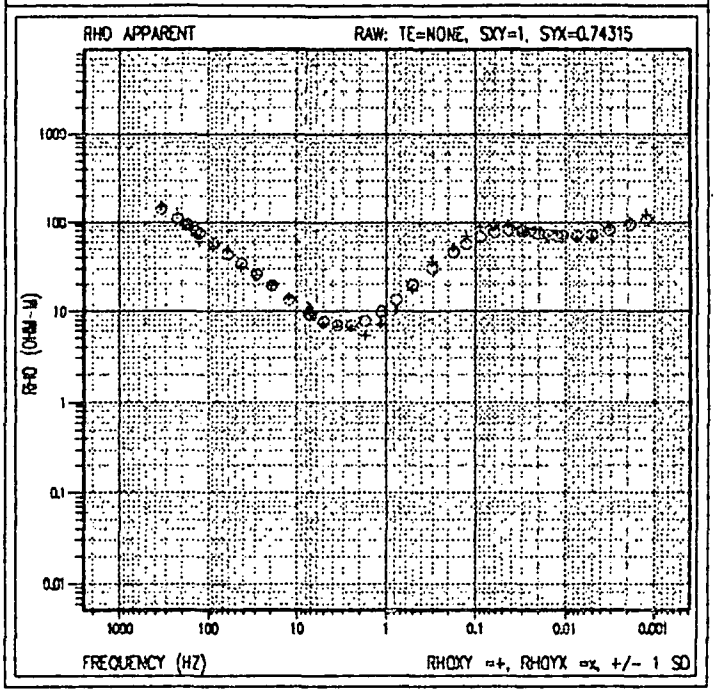


cebuco-s12

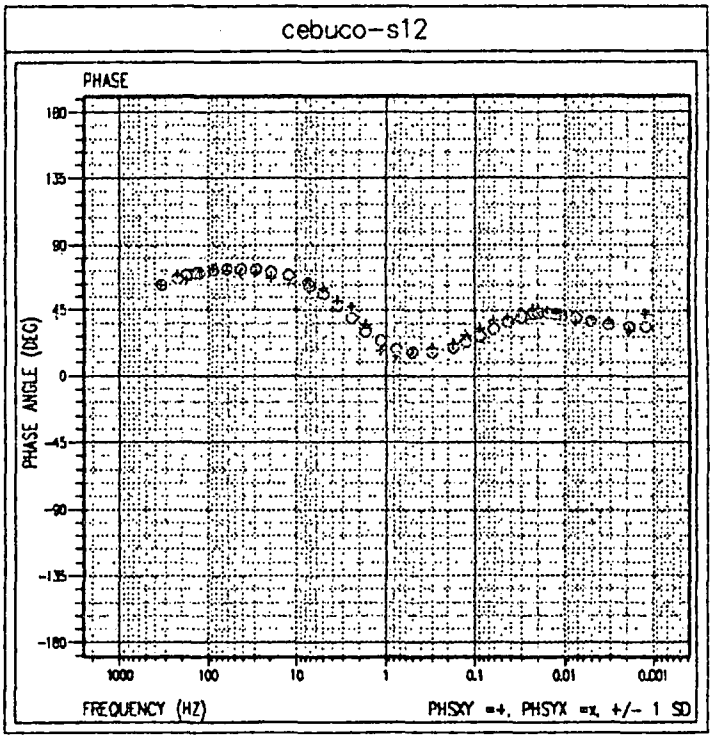

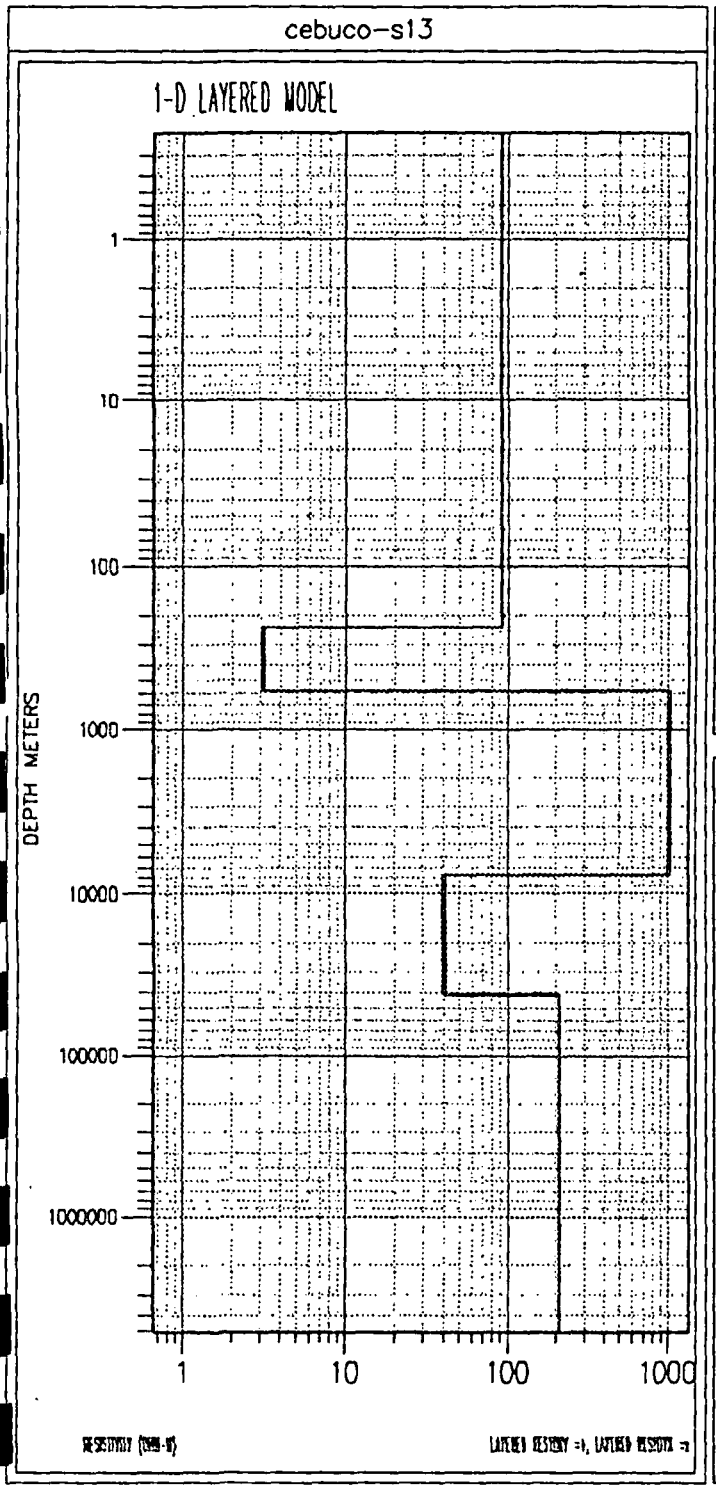
cebuco-s13
1-D LAYERED MODEL
DEPTH METERS
1
10
100
1000
10000
100000
1000000
1
10
100
1000

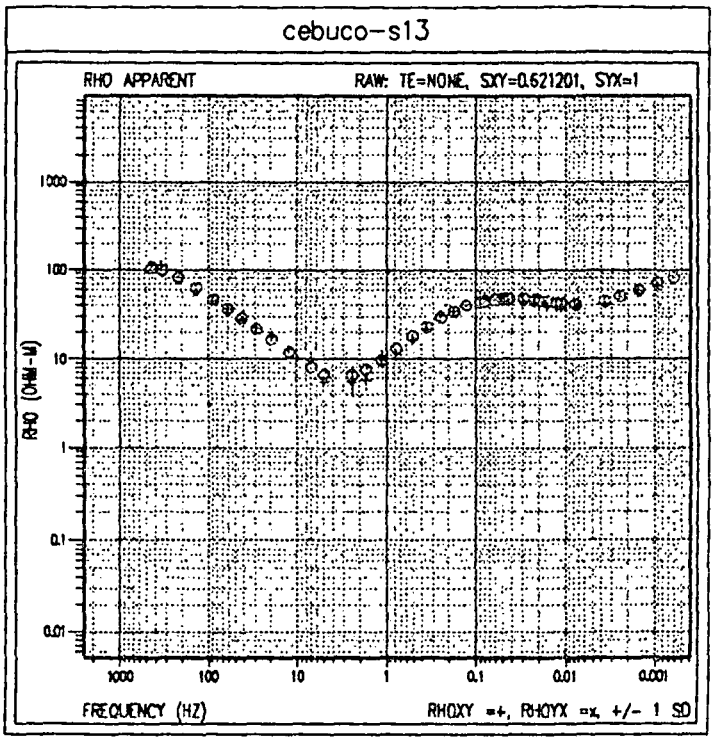
cebuco-s13
RHO APPARENT
RAW: TE=NONE, SXY=0.621201, SYX=1
RHO (OHM-M)
1000
100
10
1
0.1
0.01
1000
100
10
1
0.1
0.01
0.001
FREQUENCY (HZ)
RHOXY =+, RHOYX =x, +/- 1 SD

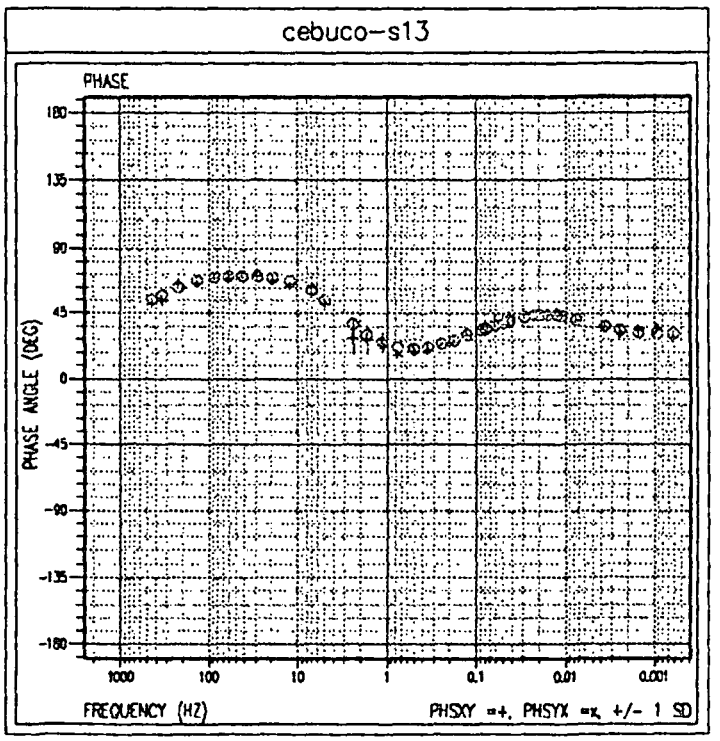
cebuco-s13
PHASE
PHASE ANGLE (DEG)
180
135
90
45
0
-45
-90
-135
-180
1000
100
10
1
0.1
0.01
0.001
FREQUENCY (HZ)
PHSXY =+, PHSYX =x, +/- 1 SD

cebuco-s14

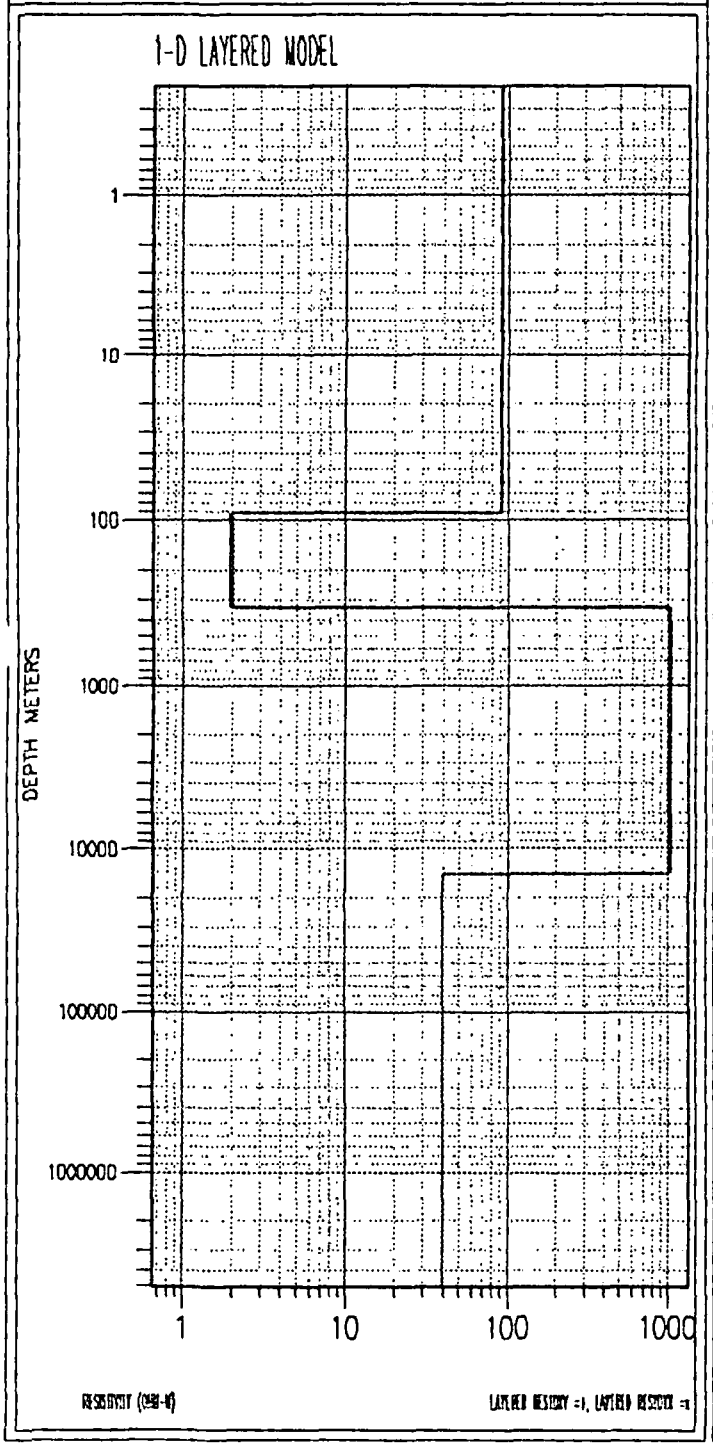


cebuco-s14

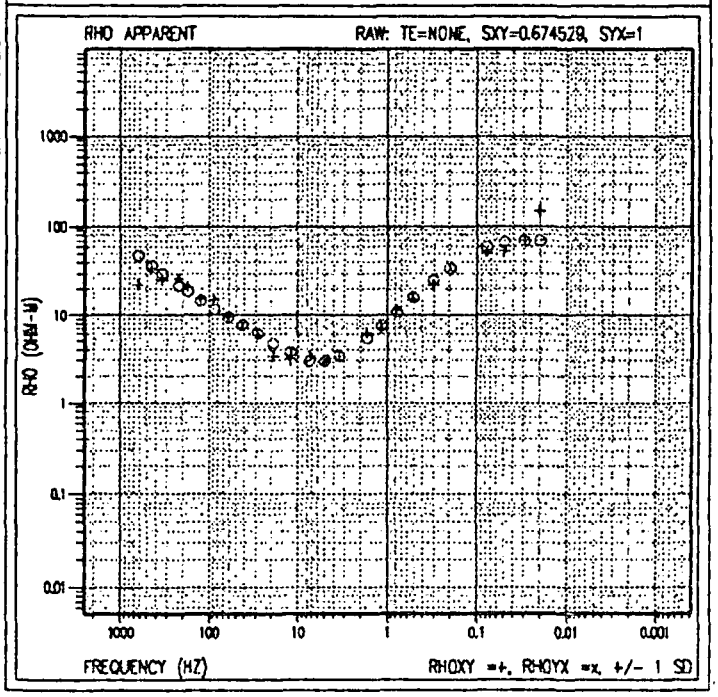


cebuco-s14

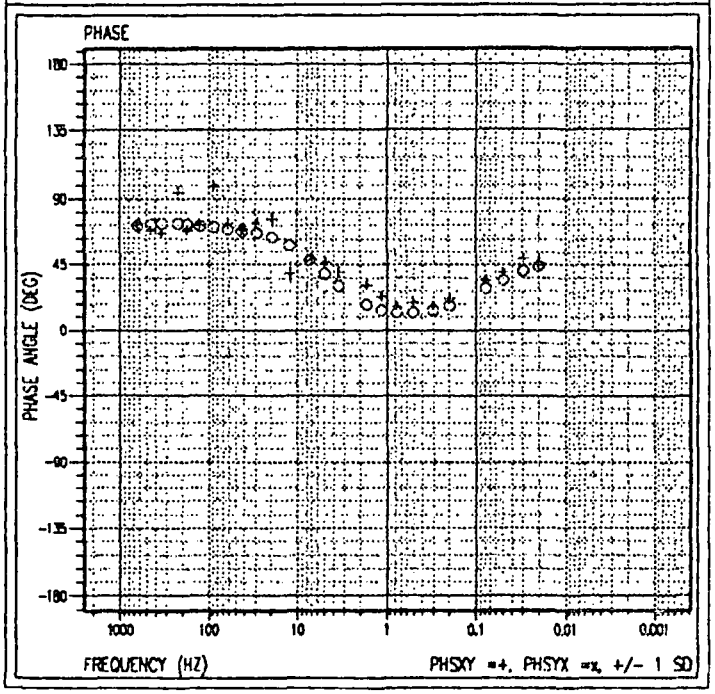

cebuco–s15

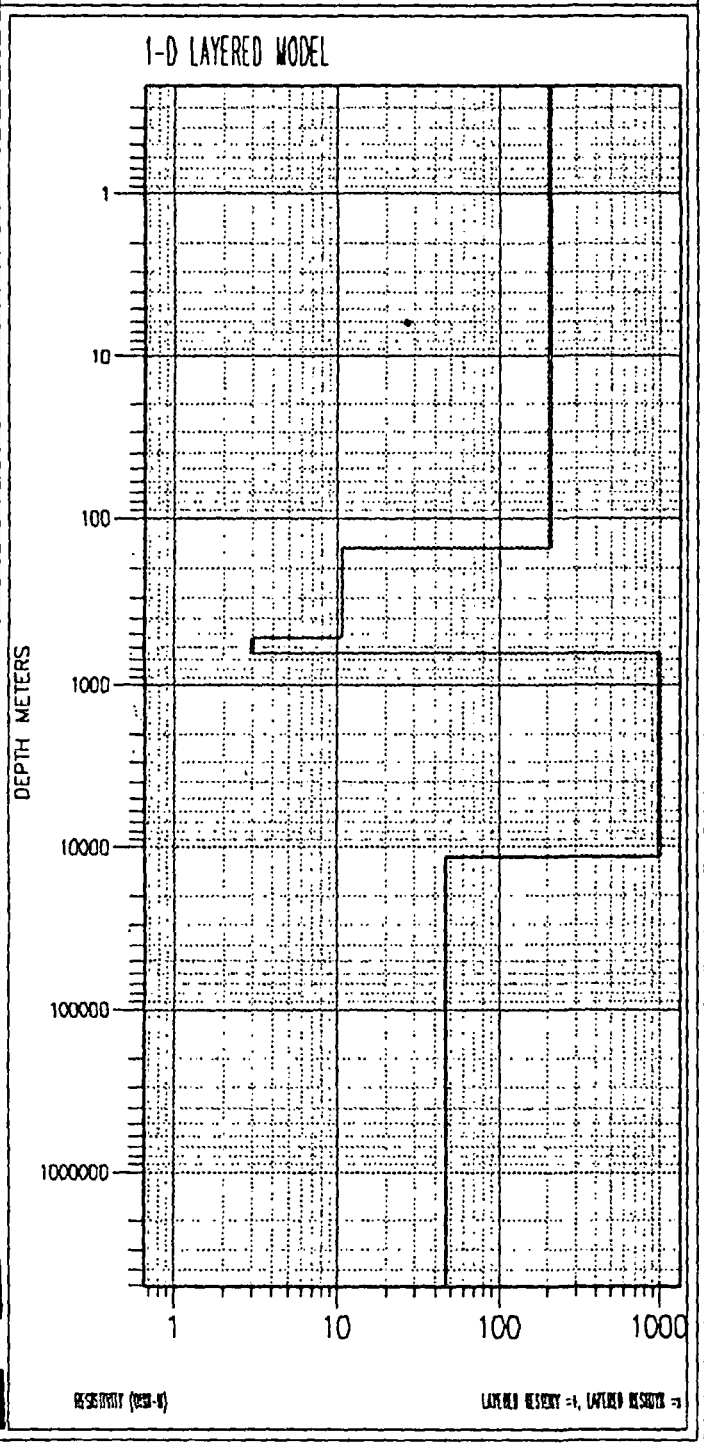


cebuco–s15

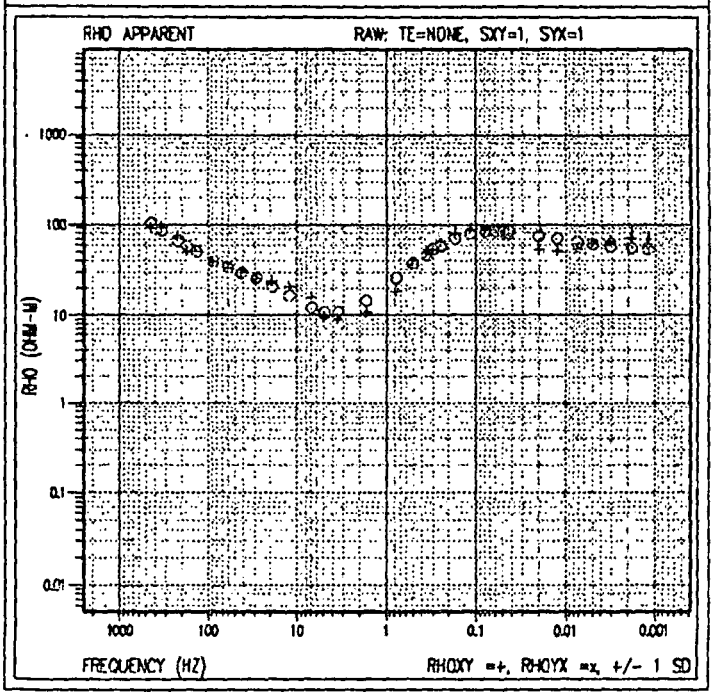


cebuco–s15

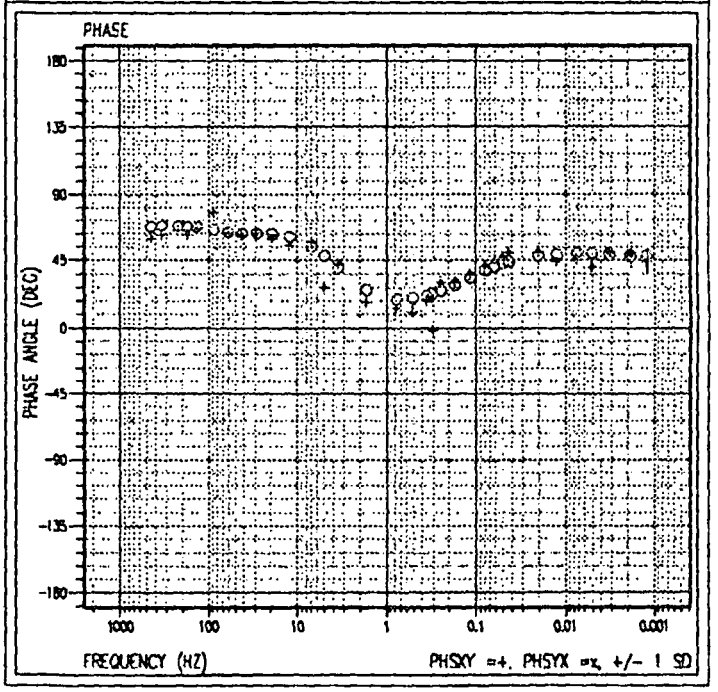

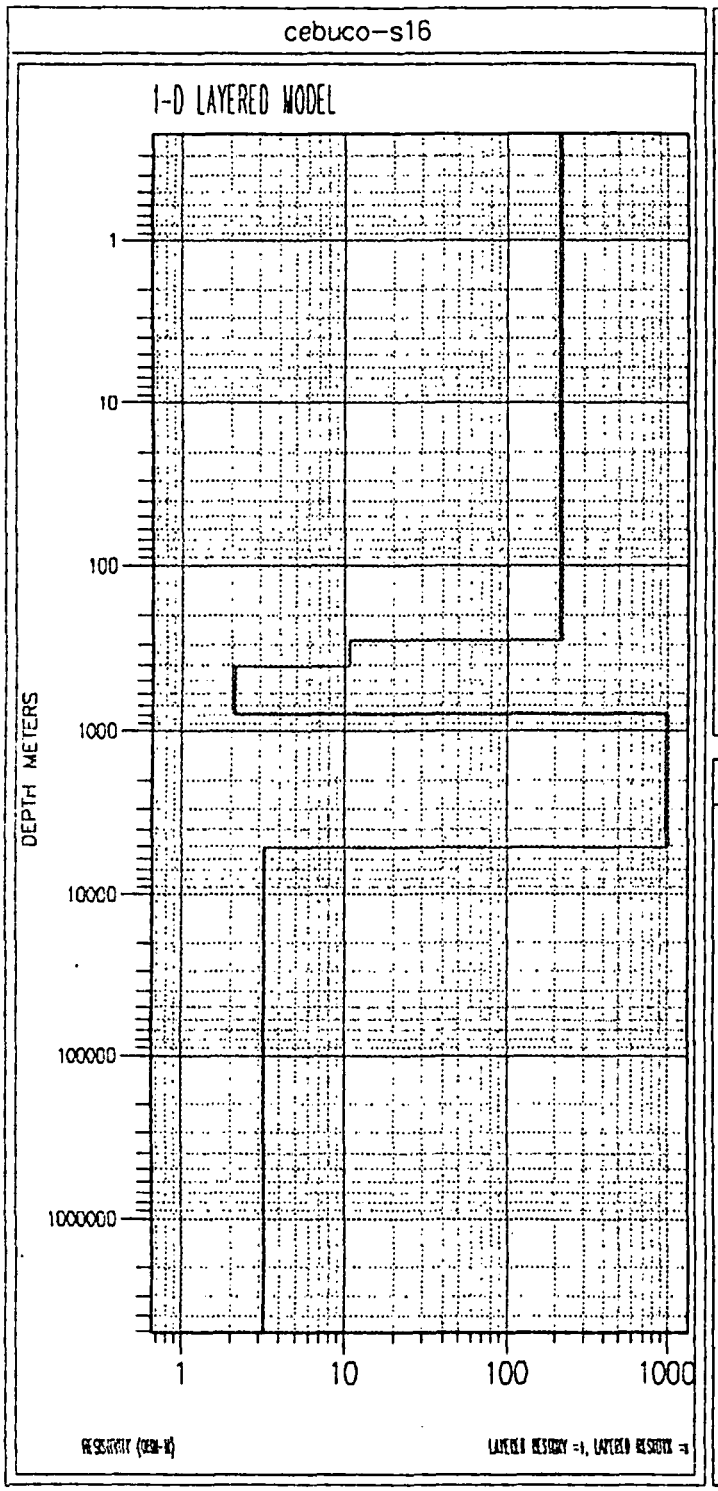
cebuco-s16
1-D LAYERED MODEL
DEPTH METERS
1
10
100
1000
10000
100000
1000000
1
10
100
1000

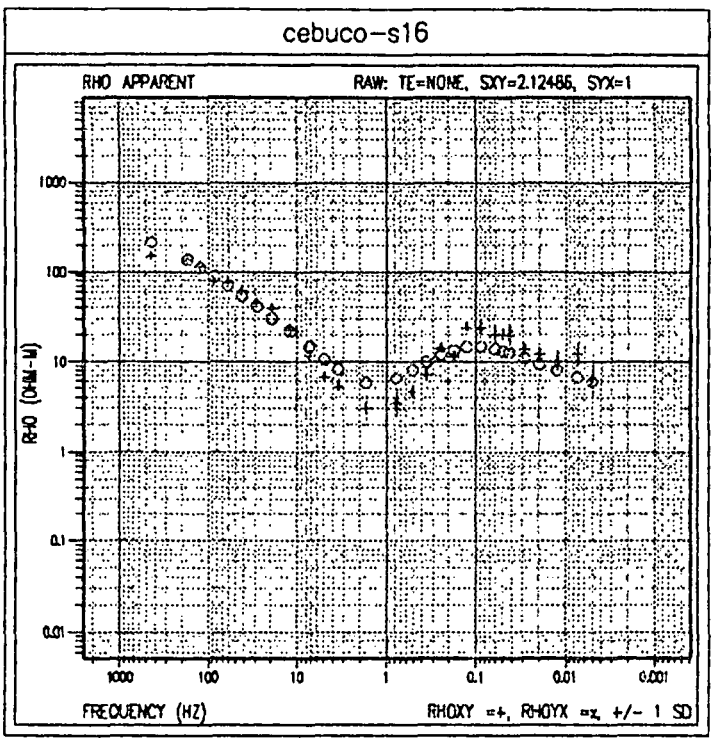
cebuco-s16
RHO APPARENT
RAW: TE=NONE, SXY=2.12486, SYX=1
RHO (OHM-M)
1000
100
10
1
0.1
0.01
1000
100
10
1
0.1
0.01
0.001
FREQUENCY (HZ)
RHOXY =+, RHOYX =x, +/- 1 SD

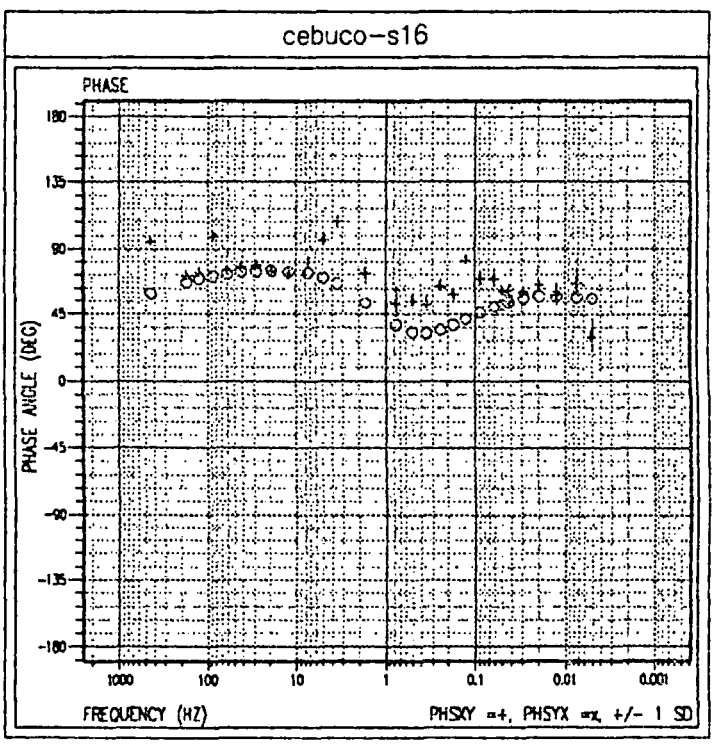
cebuco-s16
PHASE
PHASE ANGLE (DEG)
180
135
90
45
0
-45
-90
-135
-180
1000
100
10
1
0.1
0.01
0.001
FREQUENCY (HZ)
PHSXY =+, PHSYX =x, +/- 1 SD

cebuco-s17

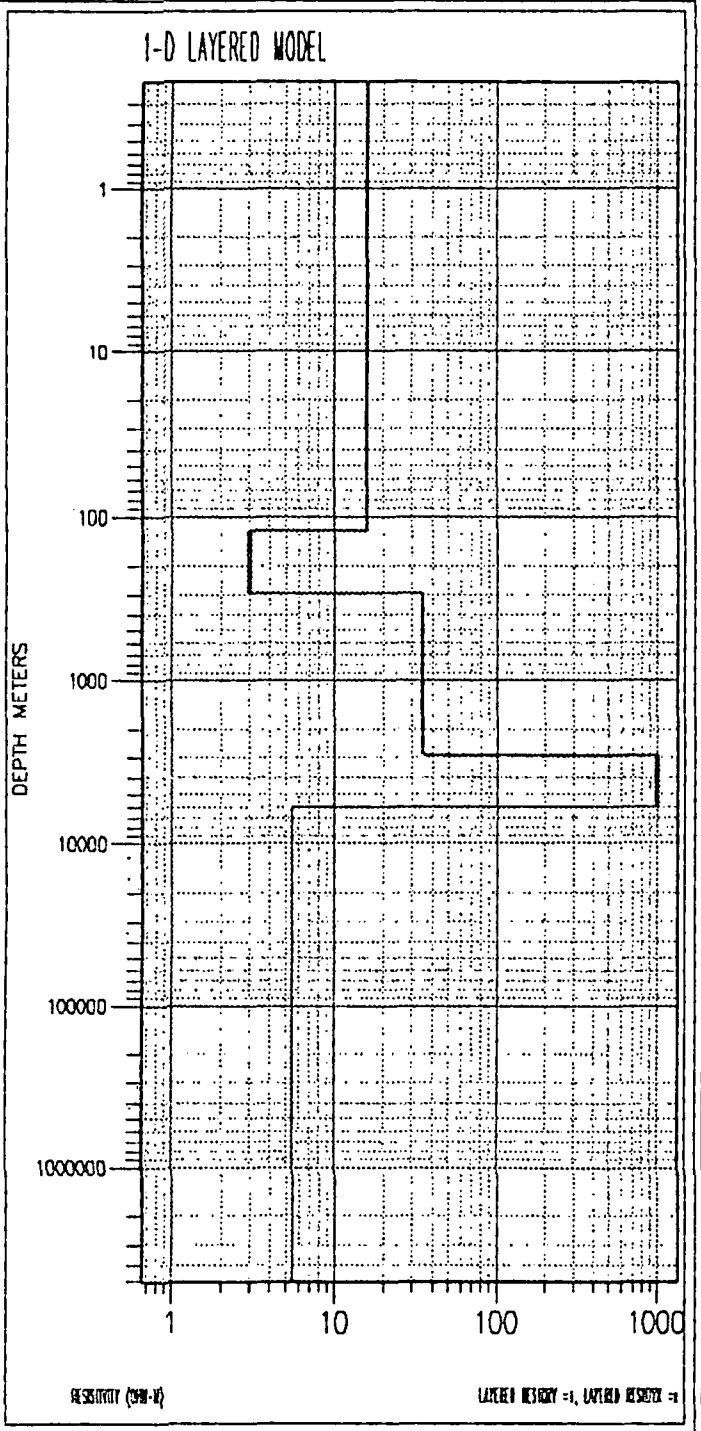


cebuco-s17

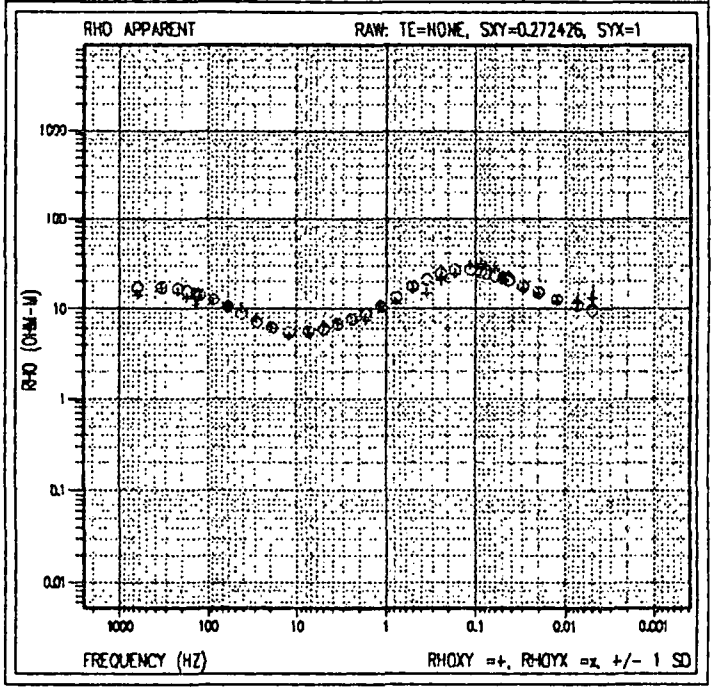


cebuco-s17

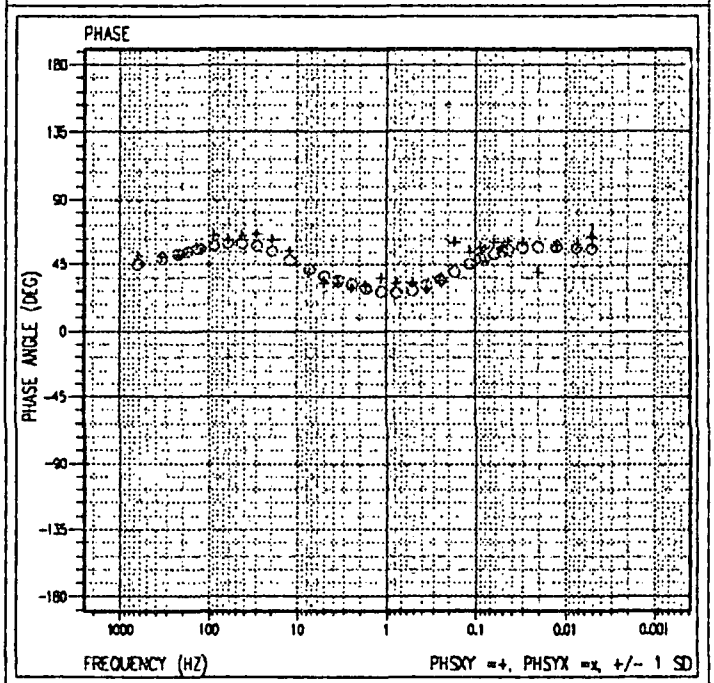

cebuco-s18

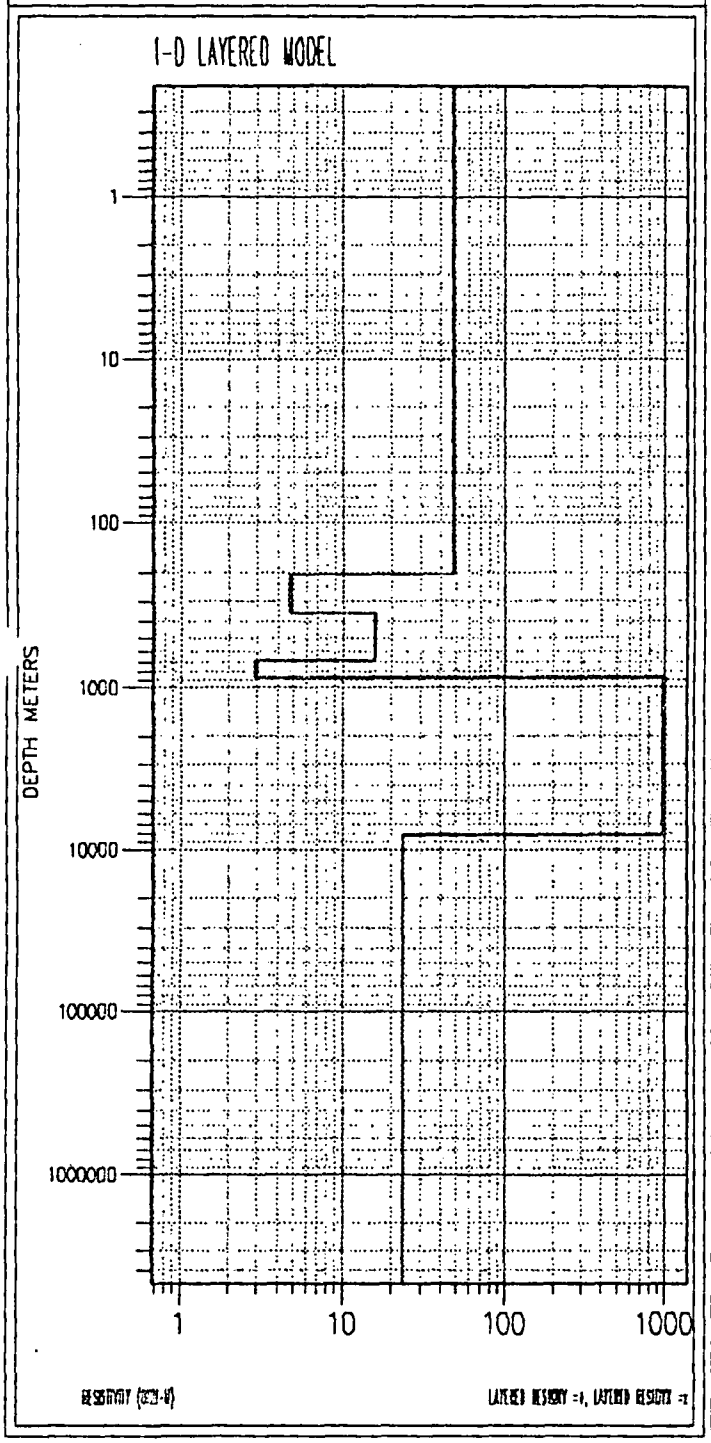


cebuco-s18

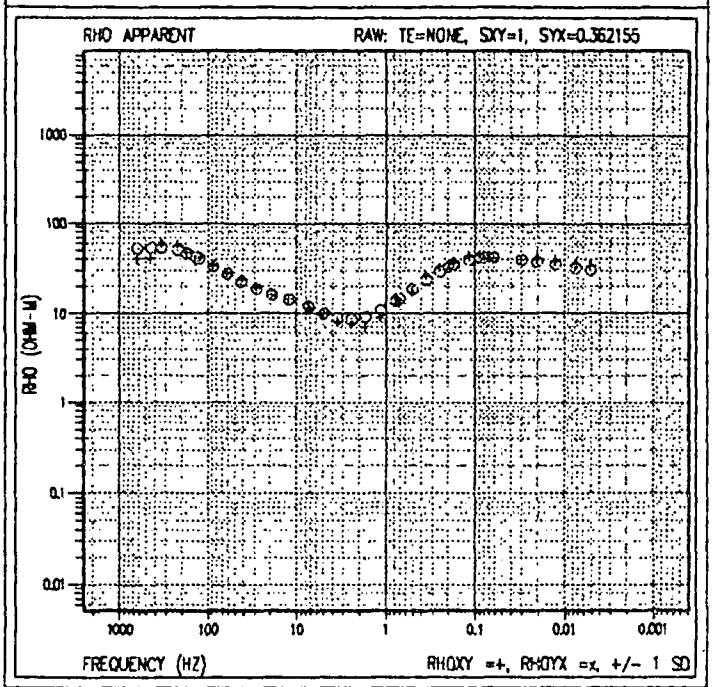


cebuco-s18

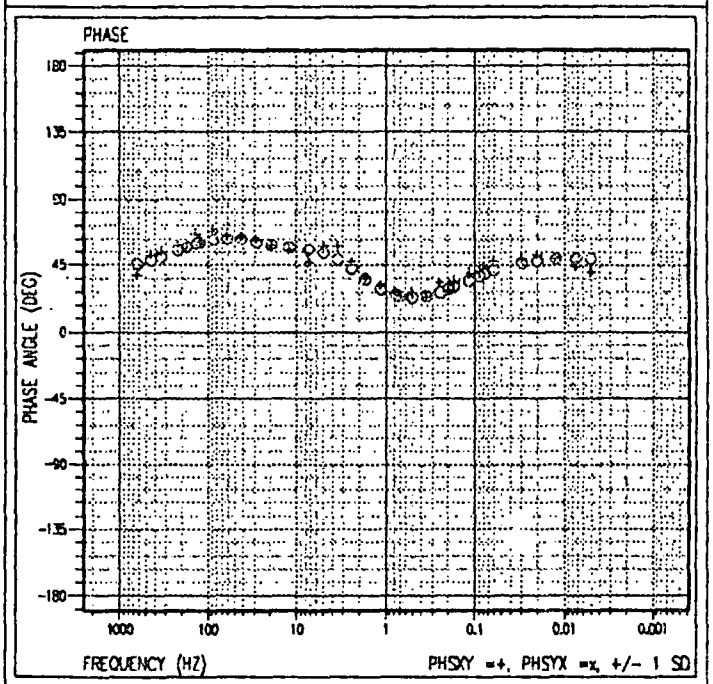

cebuco-s19

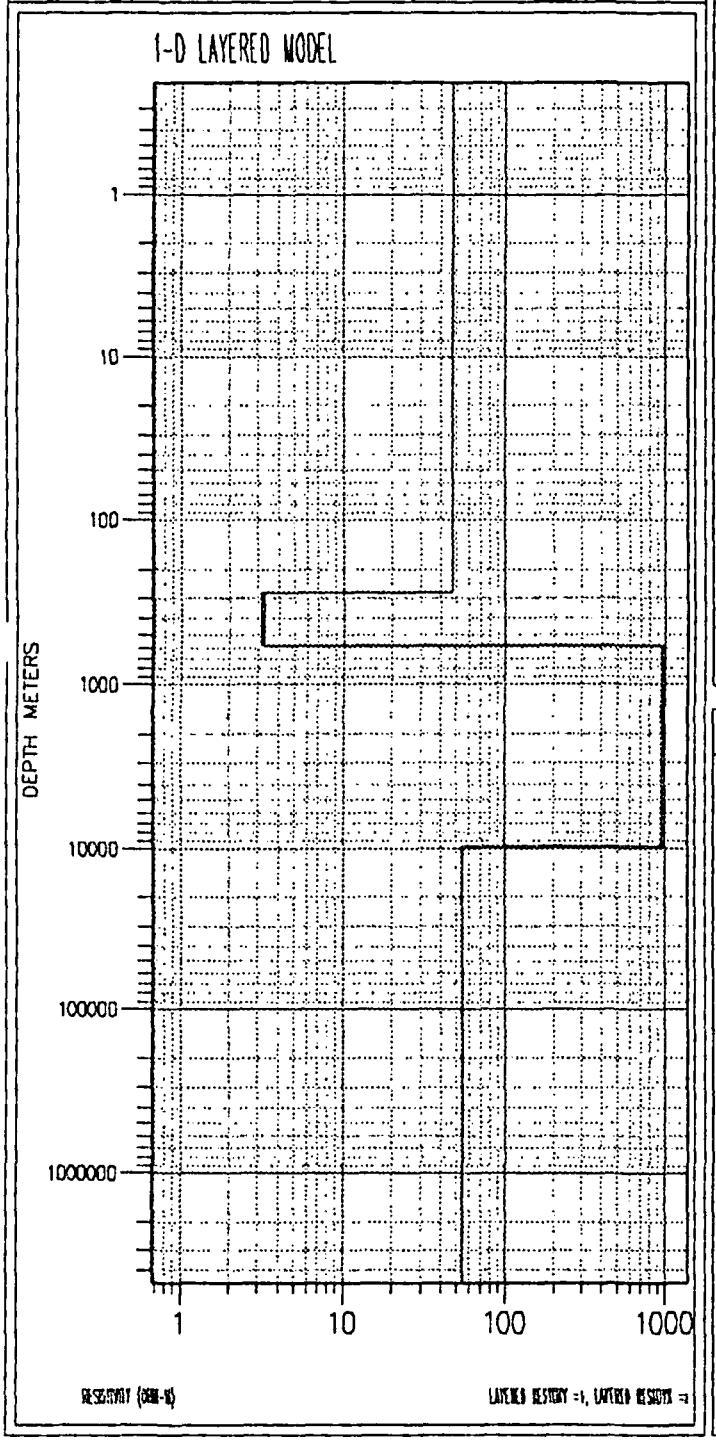


cebuco-s19

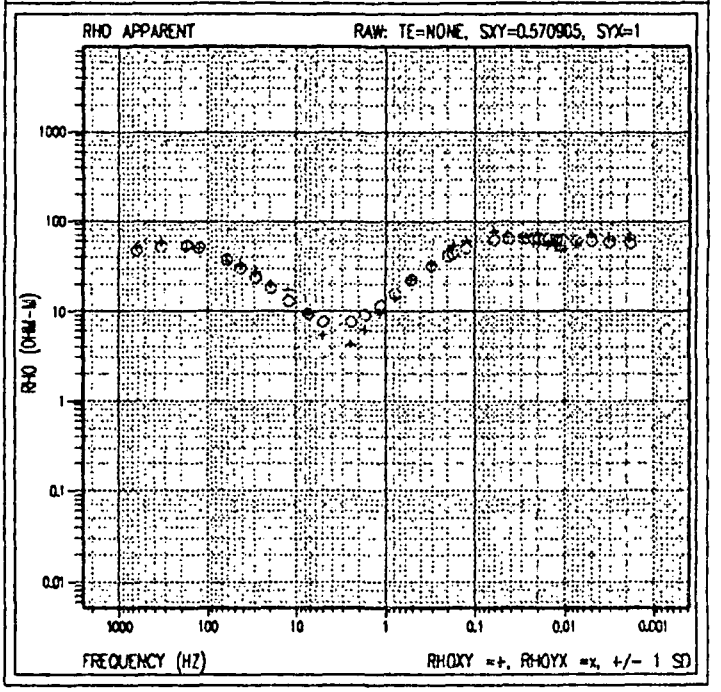


cebuco-s19

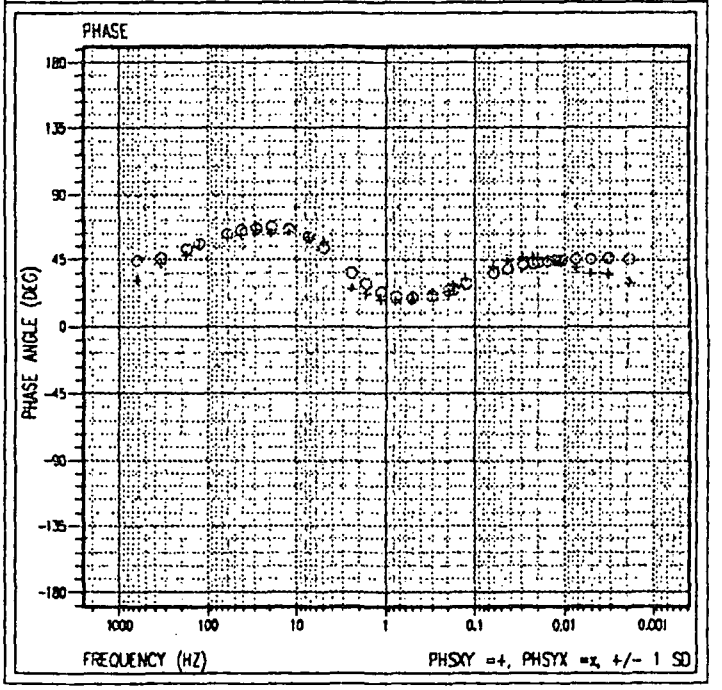

cebuco-s20

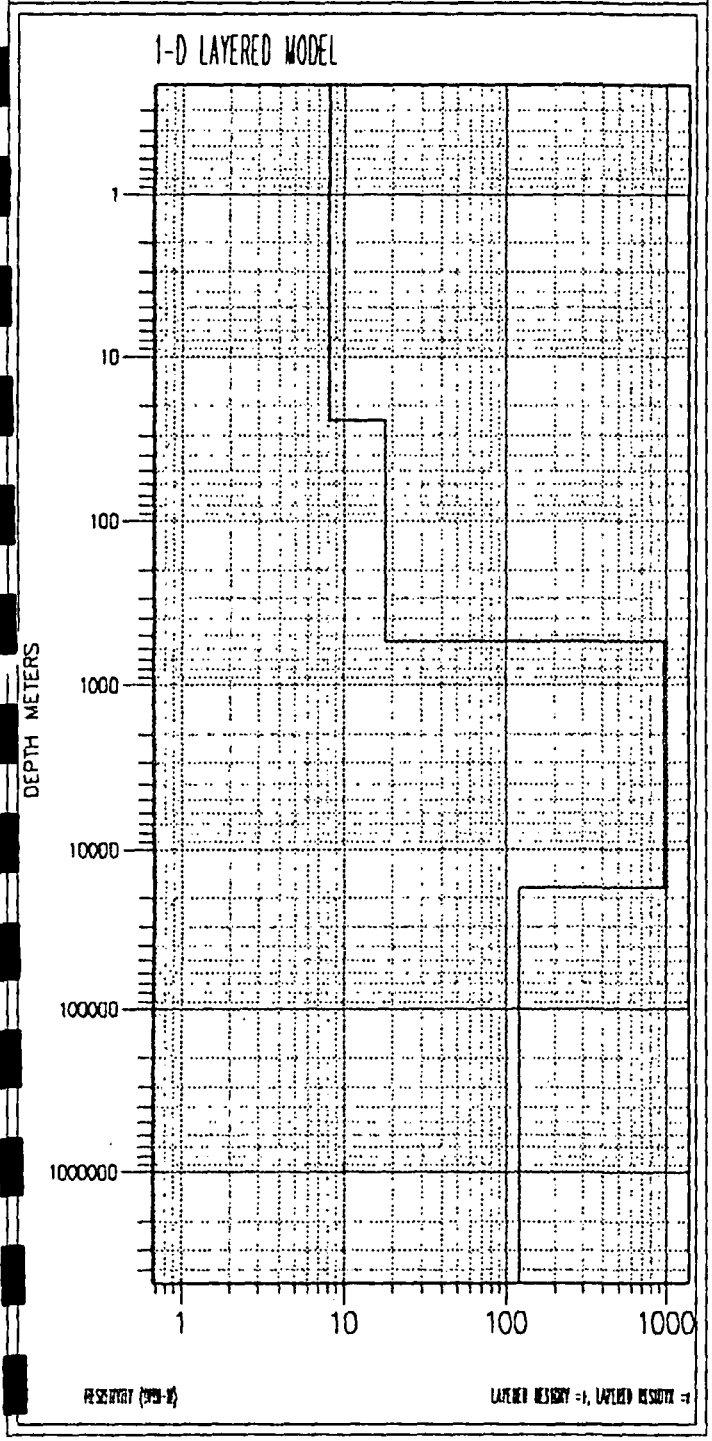


cebuco-s20

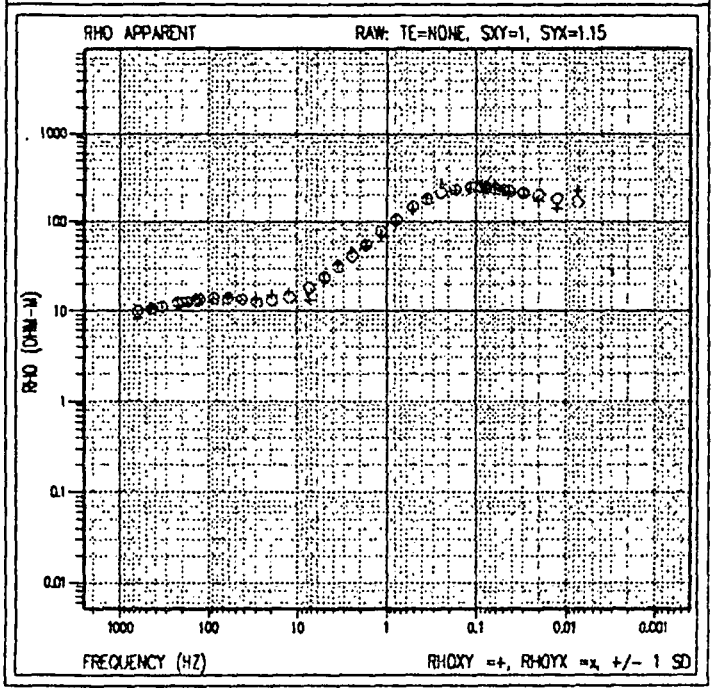


cebuco-s20

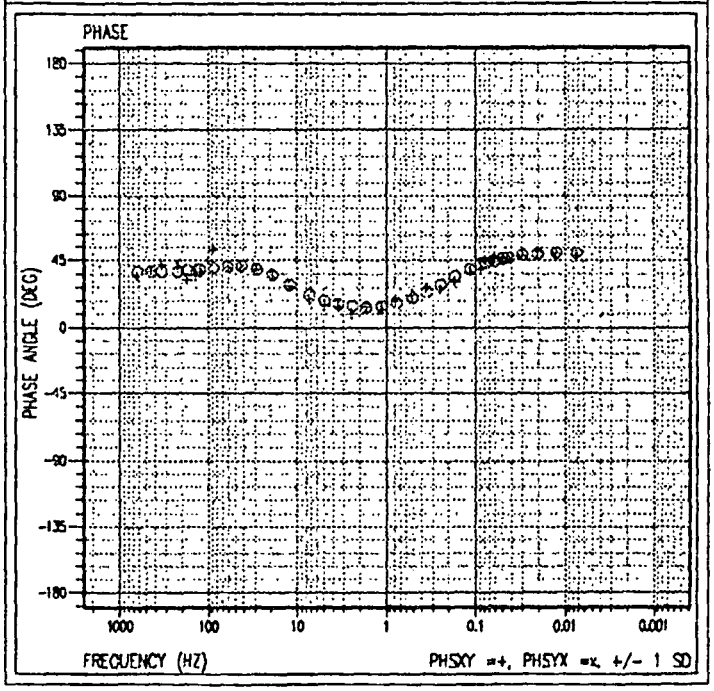

cebuco–s21

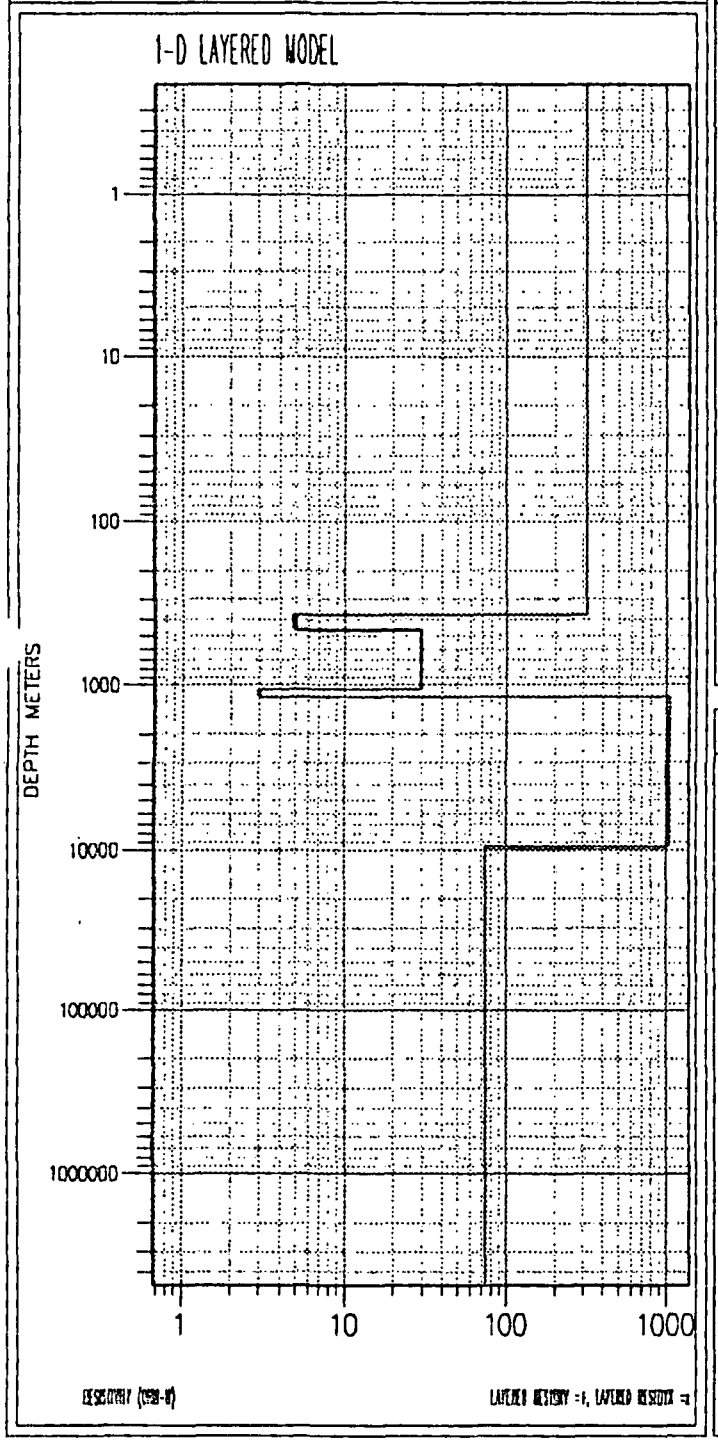


cebuco–s21

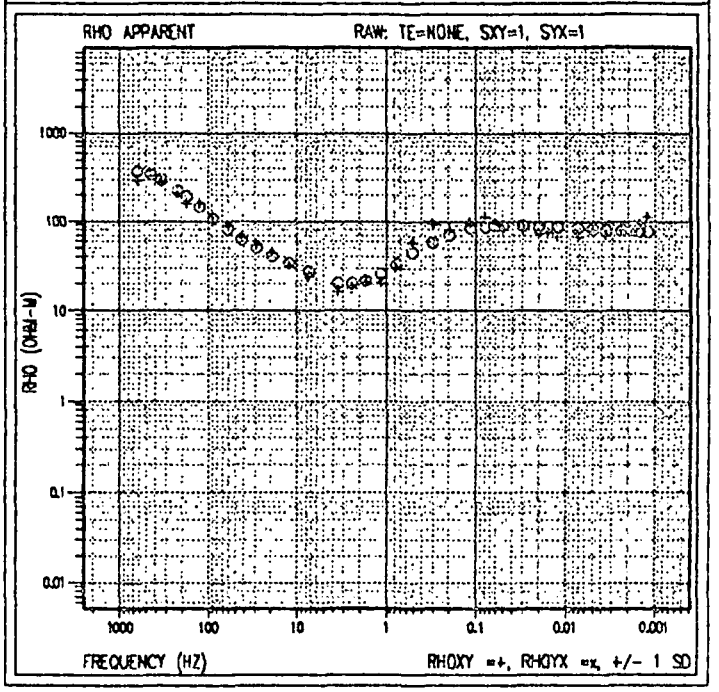


cebuco–s21

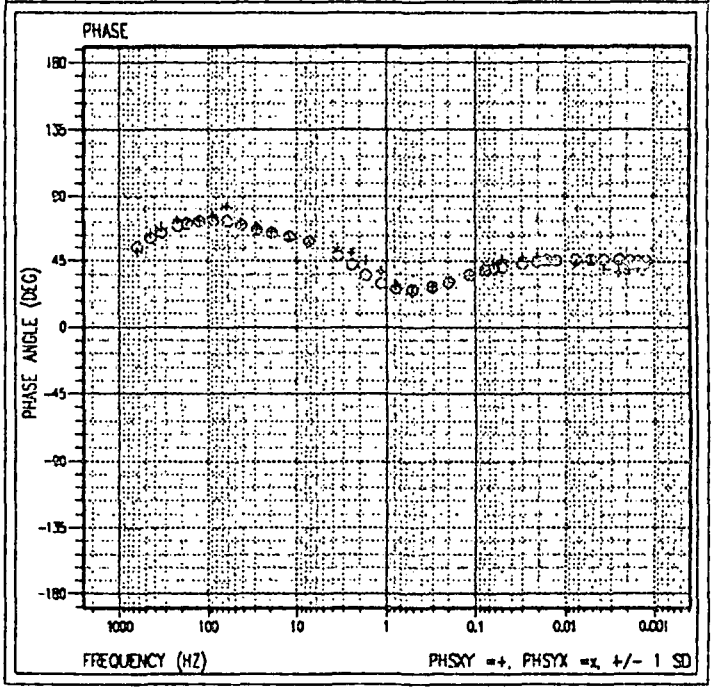

cebuco–s22

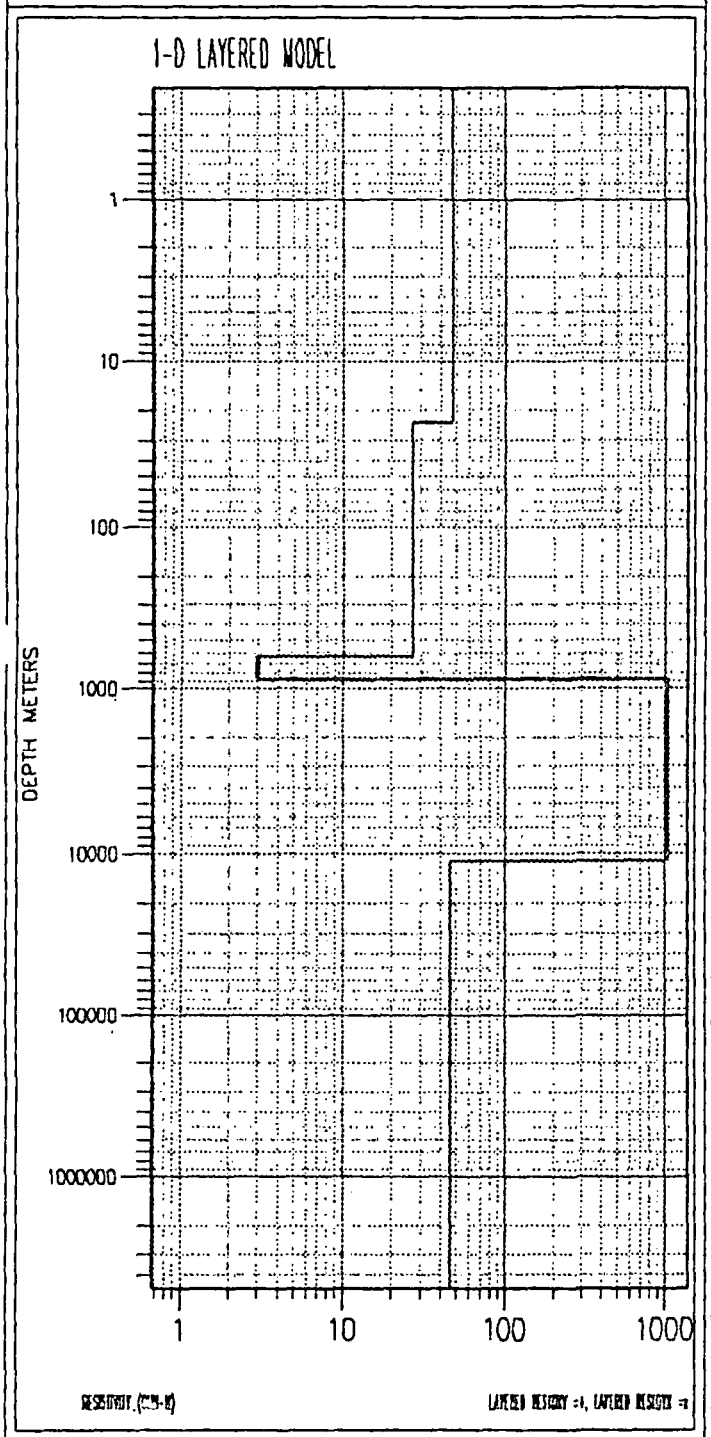


cebuco–s22

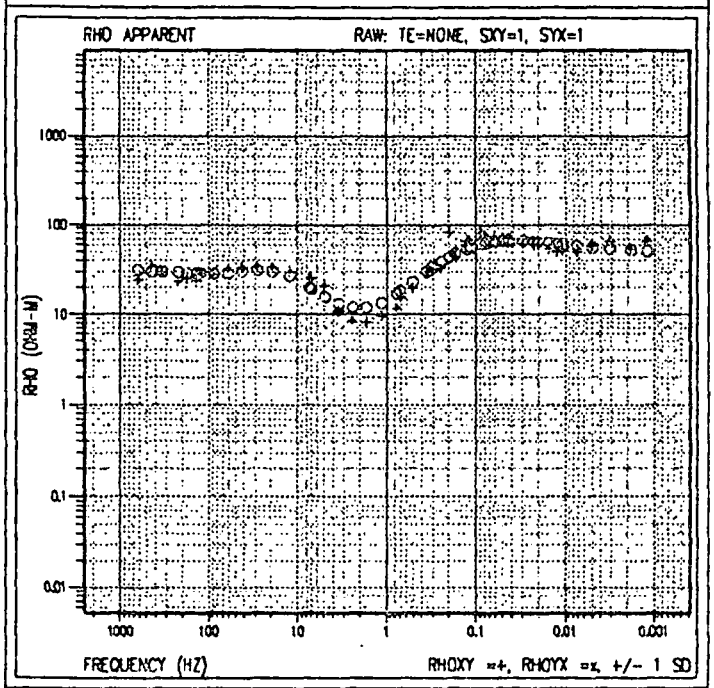


cebuco–s22

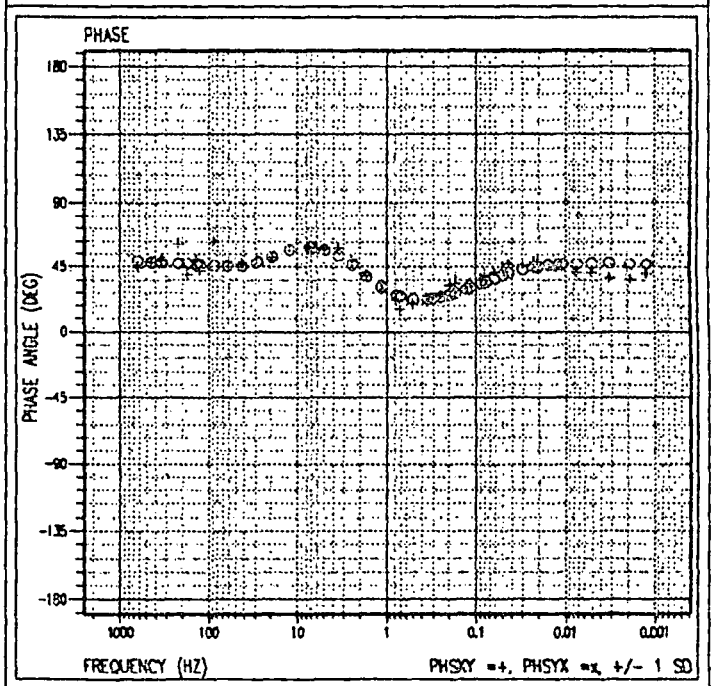

cebuco–s23

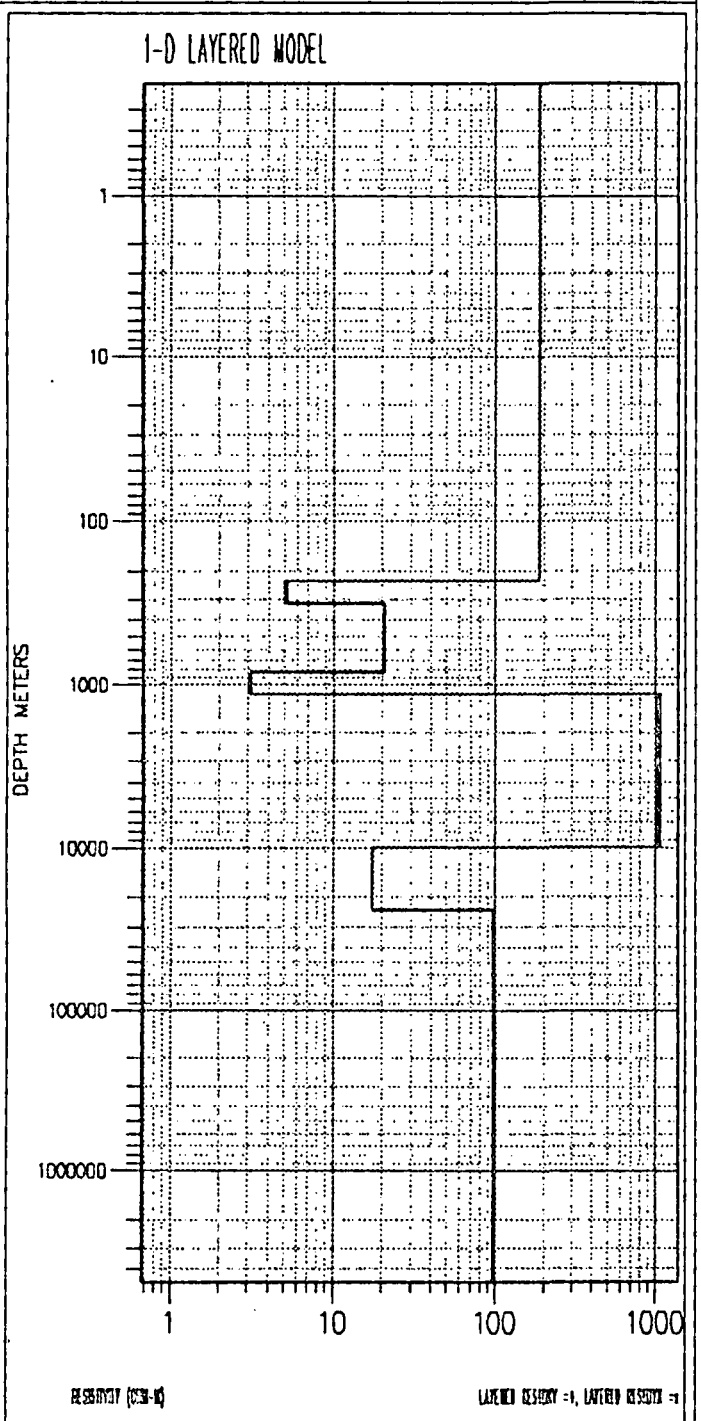


cebuco–s23

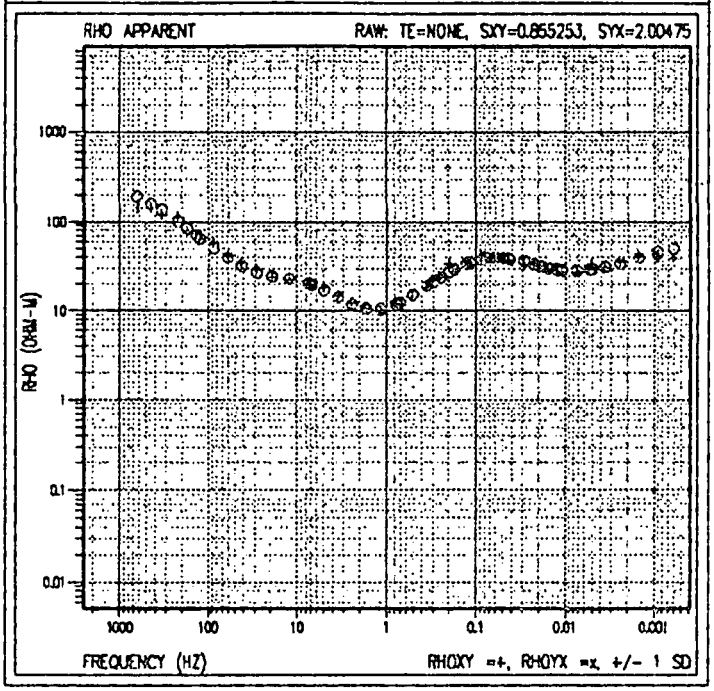


cebuco–s23

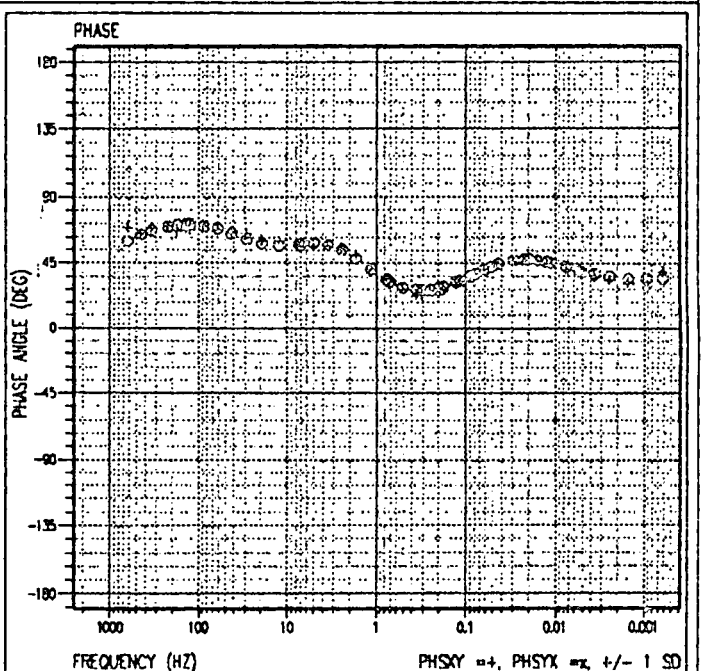

cebuco–s25

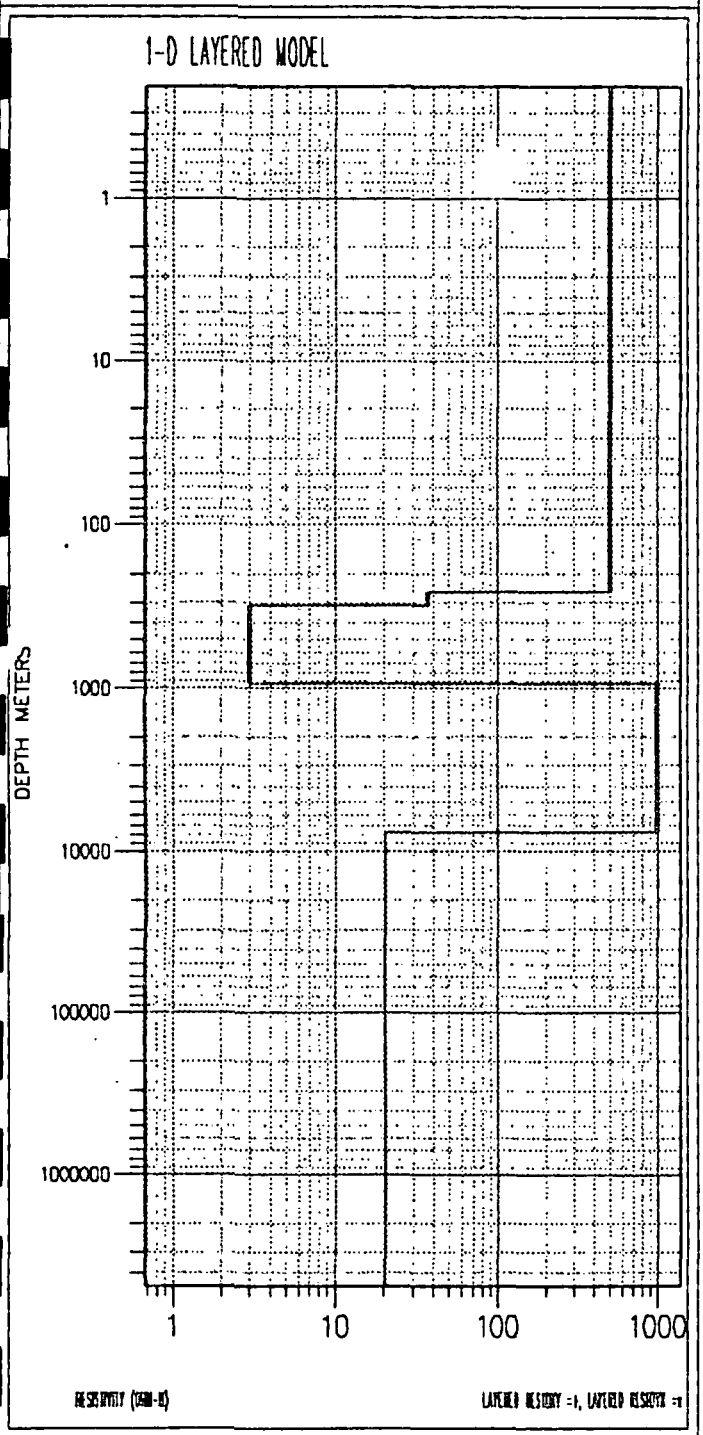


cebuco–s25

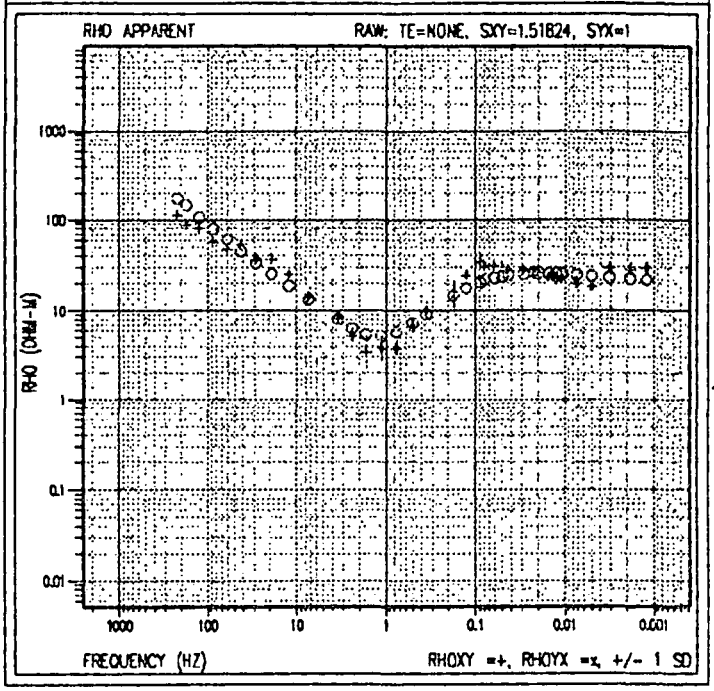


cebuco–s25

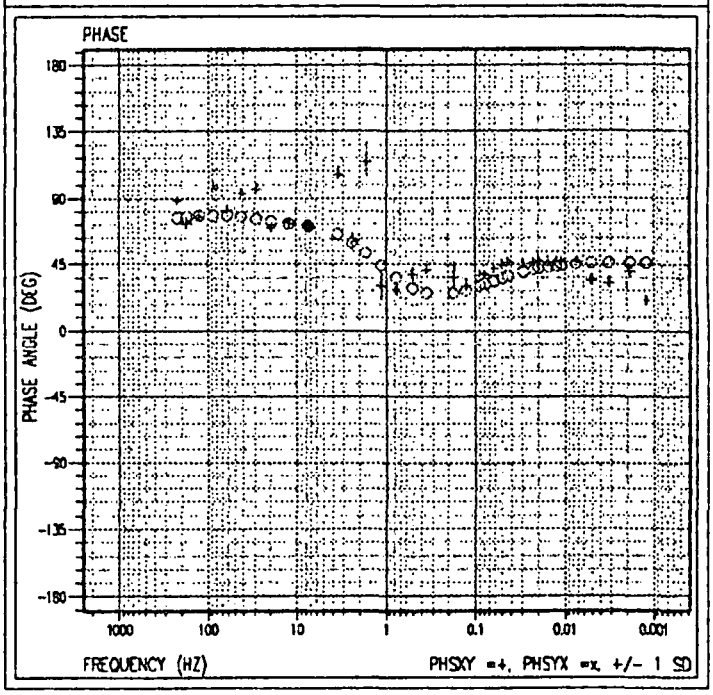

cebuco-s26

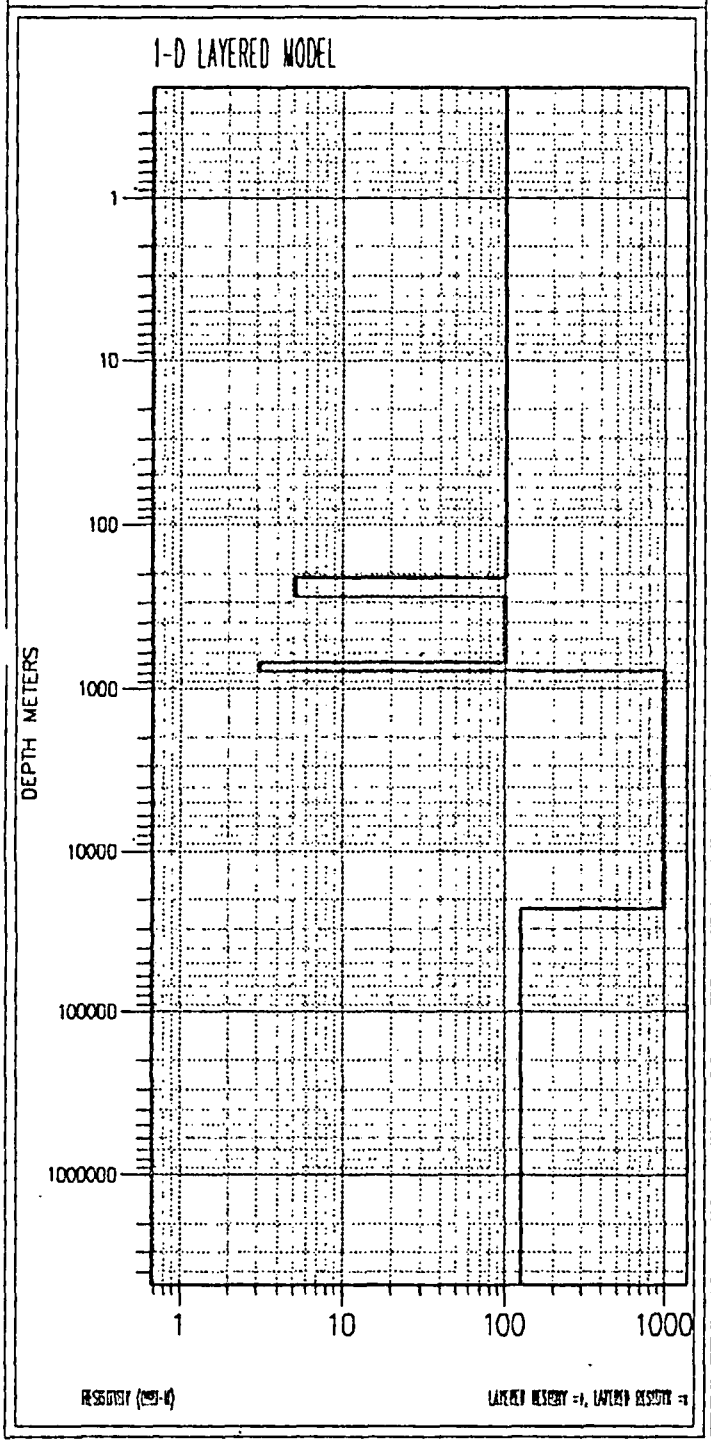


cebuco-s26

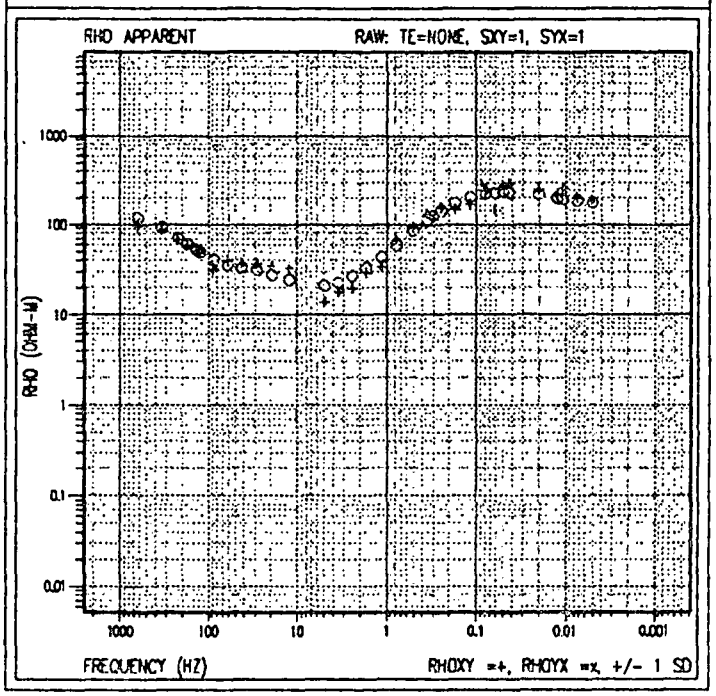


cebuco-s26

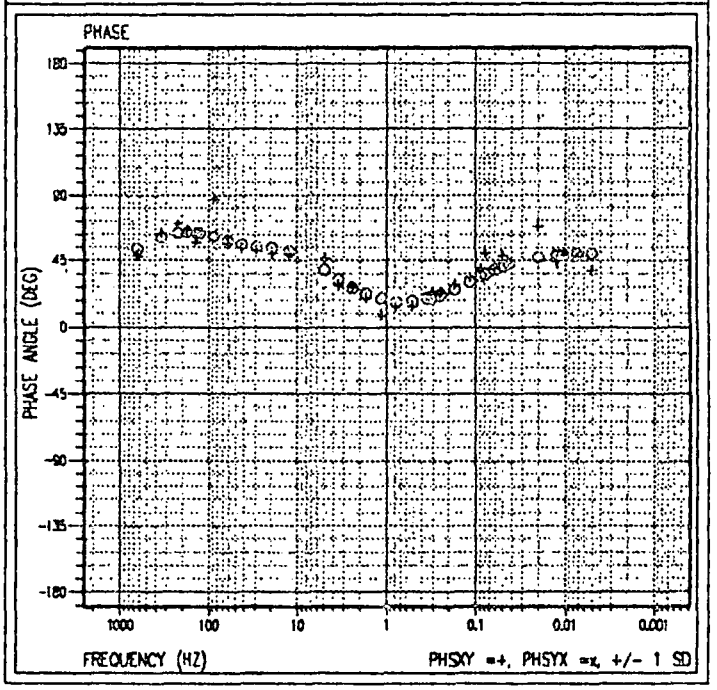

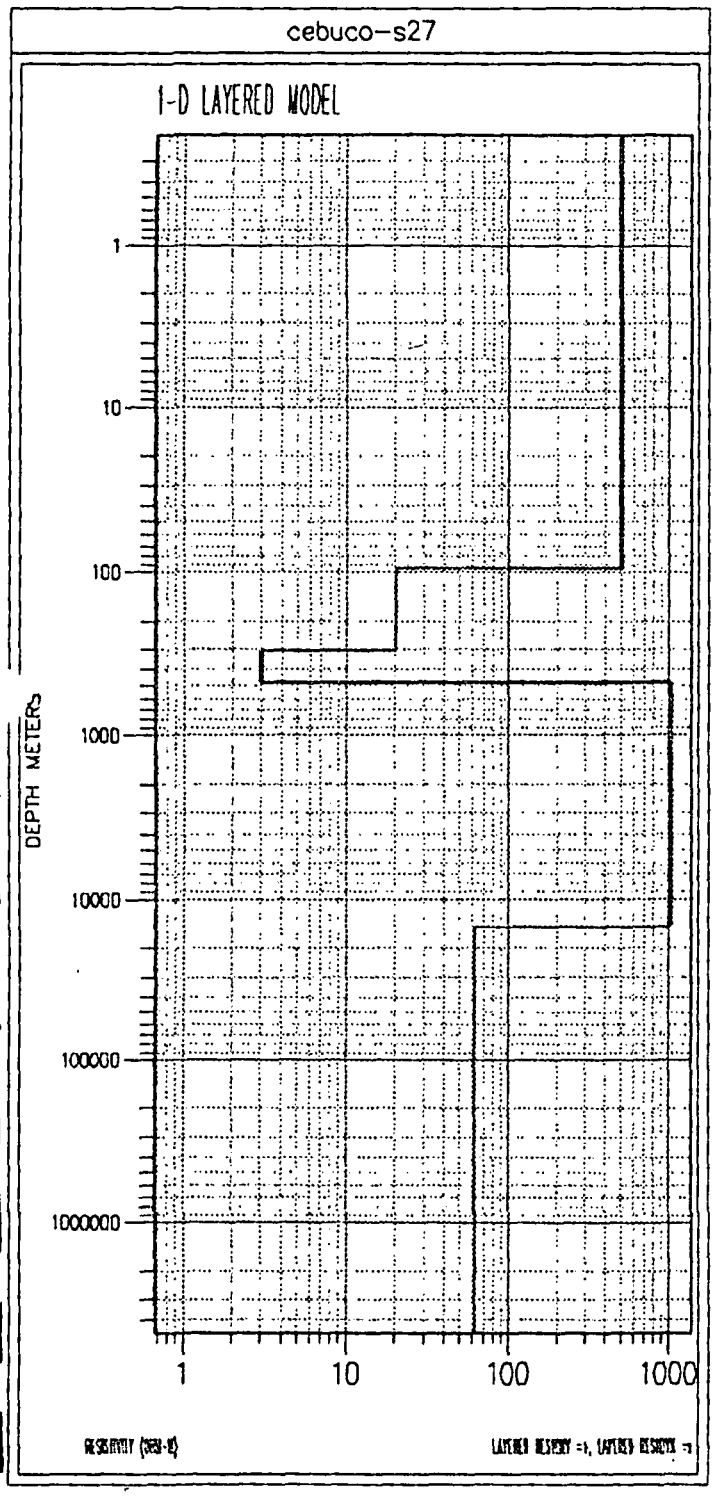
cebuco-s27
1-D LAYERED MODEL
DEPTH METERS
1
10
100
1000
10000
100000
1000000
1
10
100
1000

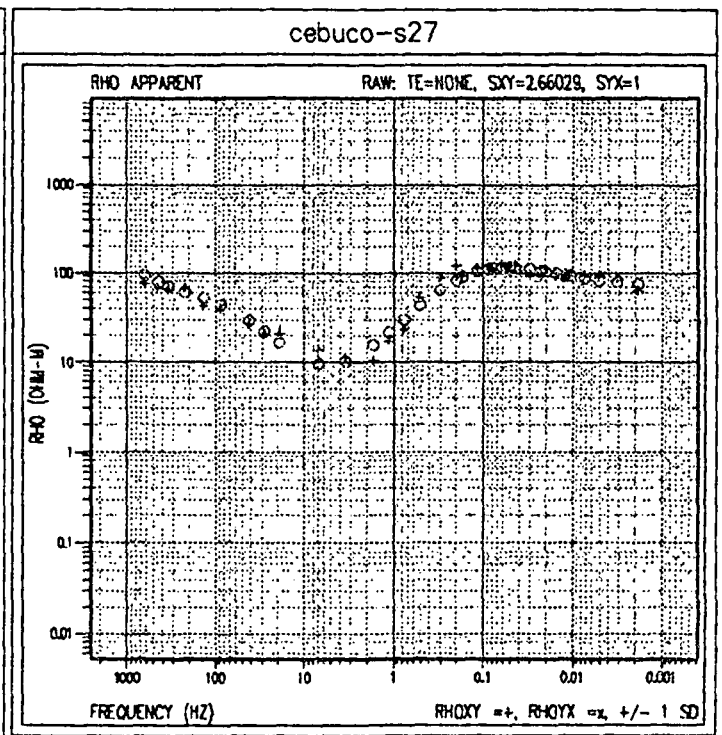
cebuco-s27
RHO APPARENT
RAW: TE=NONE, SXY=2.66029, SYX=1
RHO (OHM-M)
1000
100
10
1
0.1
0.01
1000
100
10
1
0.1
0.01
0.001
FREQUENCY (HZ)
RHOXY =+, RHOYX =x, +/- 1 SD

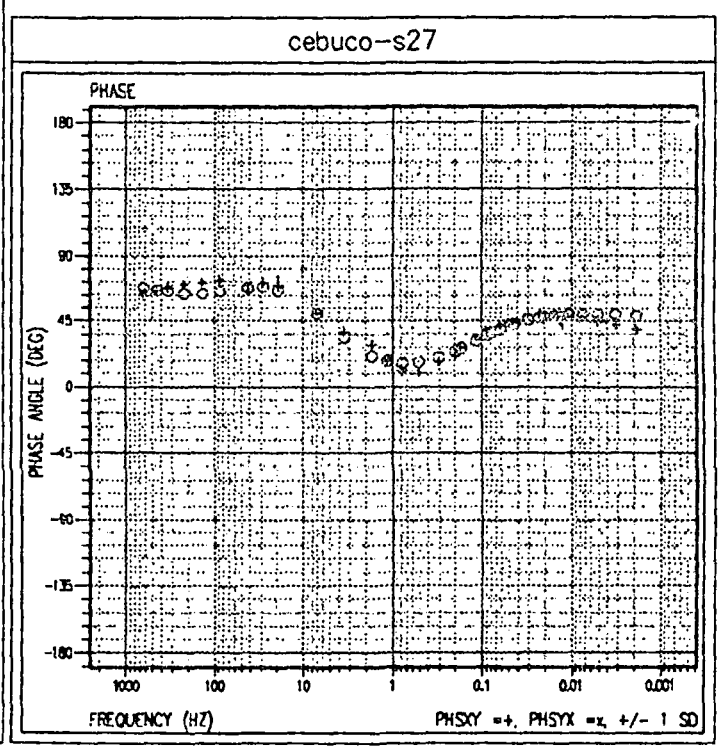
cebuco-s27
PHASE
PHASE ANGLE (DEG)
180
135
90
45
0
-45
-90
-135
-180
1000
100
10
1
0.1
0.01
0.001
FREQUENCY (HZ)
PHSXY =+, PHSYX =x, +/- 1 SD

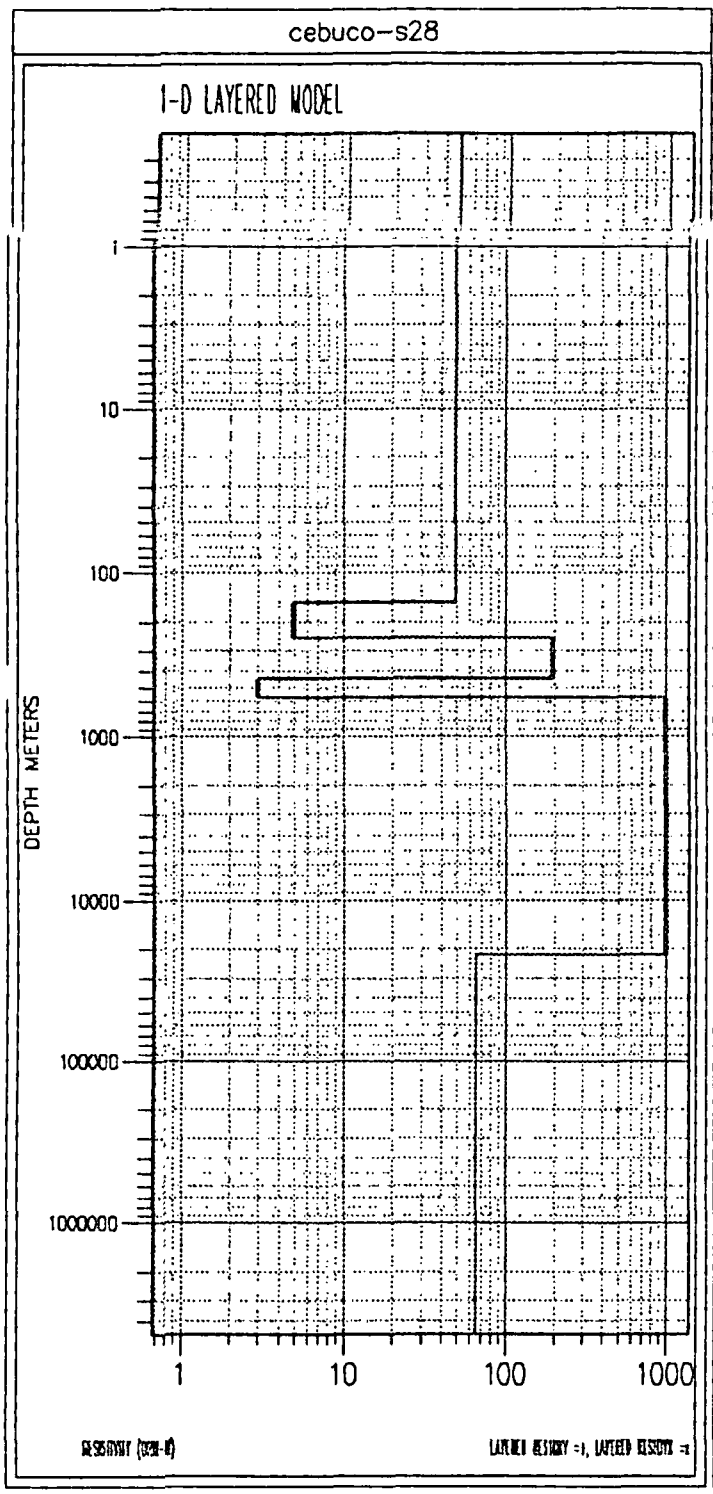
cebuco–s28
1-D LAYERED MODEL
DEPTH METERS
1
10
100
1000
10000
100000
1000000
1
10
100
1000

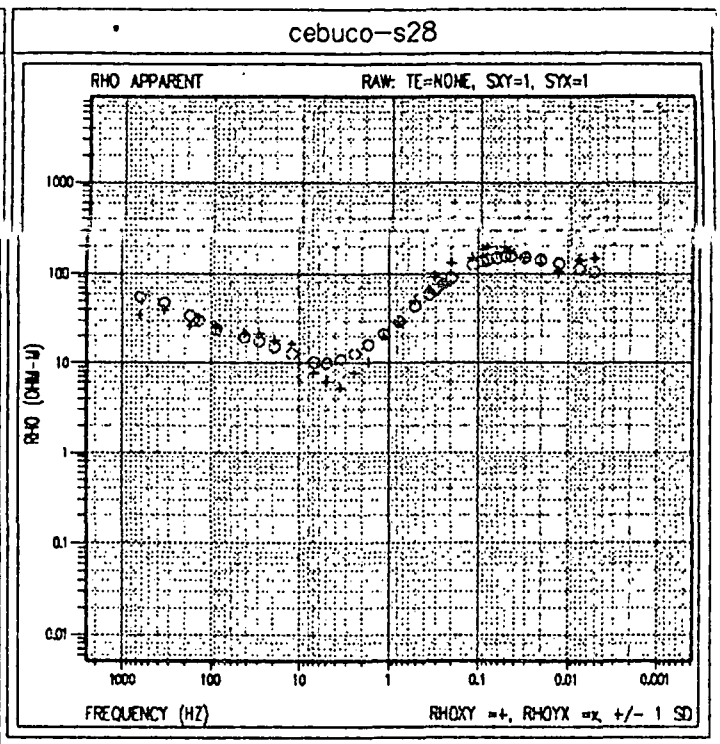
cebuco–s28
RHO APPARENT
RAW: TE=NONE, SXY=1, SYX=1
RHO (OHM-M)
1000
100
10
1
0.1
0.01
1000
100
10
1
0.1
0.01
0.001
FREQUENCY (HZ)
RHOXY =+, RHOYX =x, +/- 1 SD

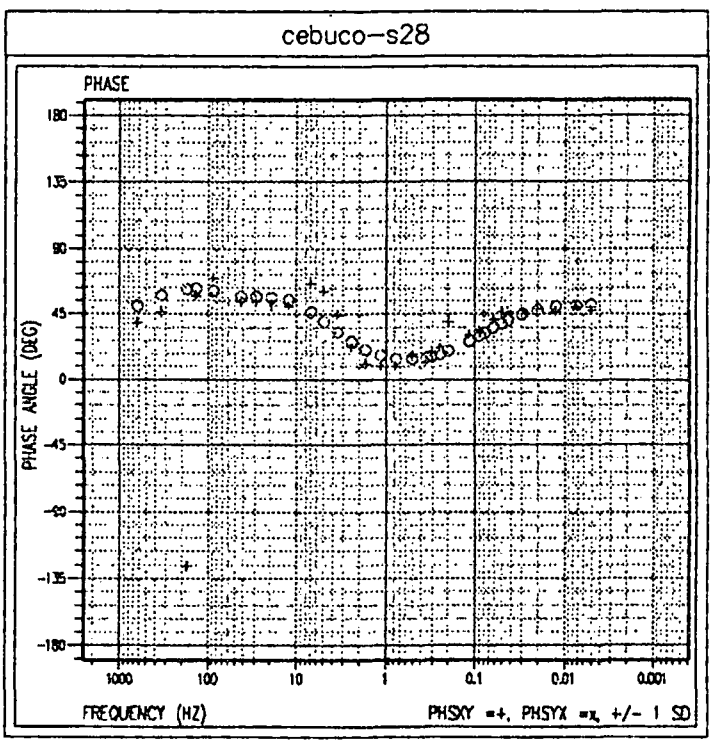
cebuco–s28
PHASE
PHASE ANGLE (DEG)
180
135
90
45
0
-45
-90
-135
-180
1000
100
10
1
0.1
0.01
0.001
FREQUENCY (HZ)
PHSXY =+, PHSYX =x, +/- 1 SD

cebuco–s30

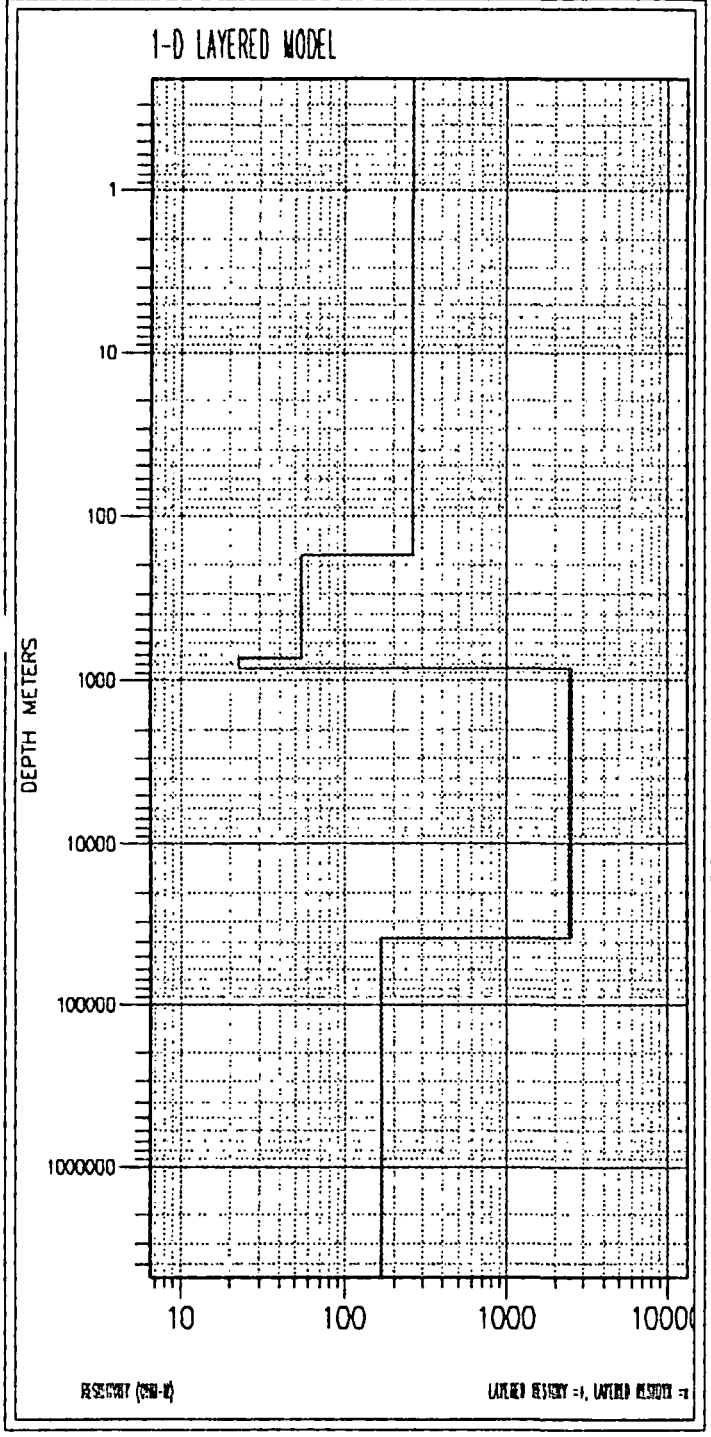


cebuco–s30

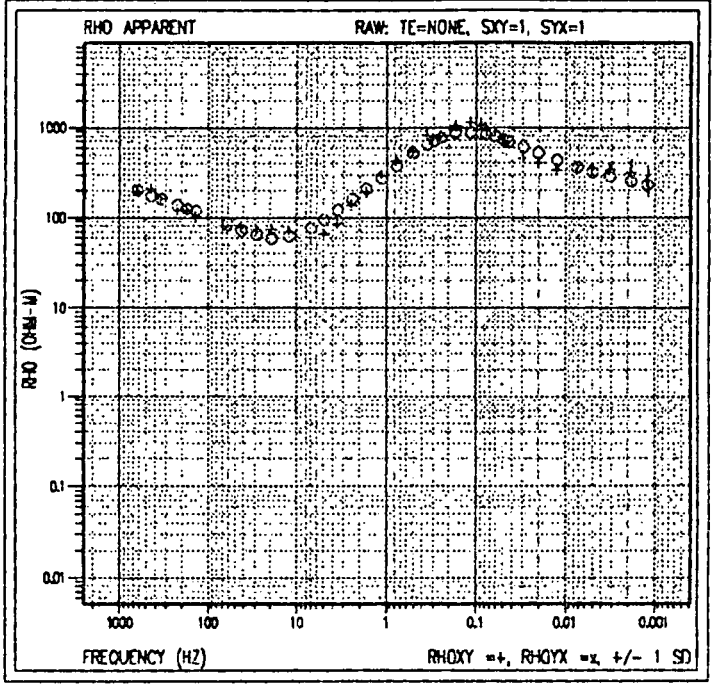


cebuco–s30

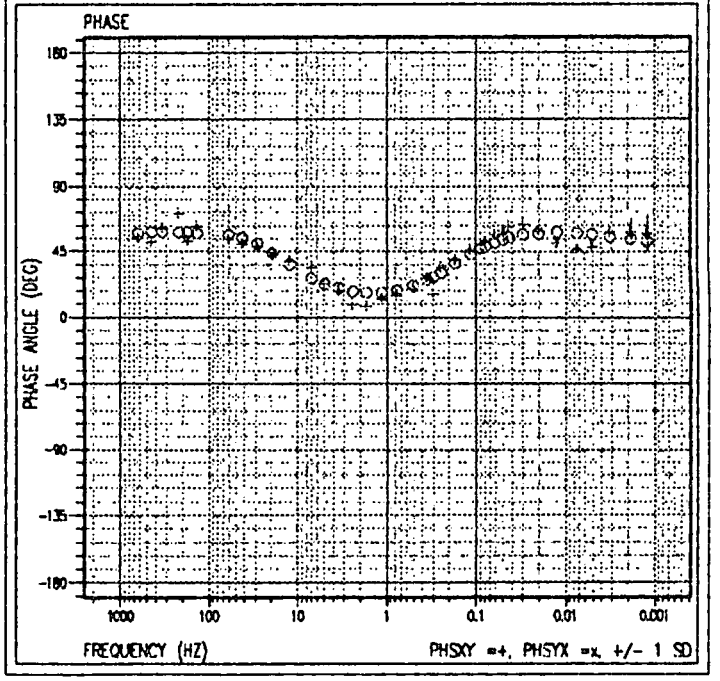

cebuco–s31

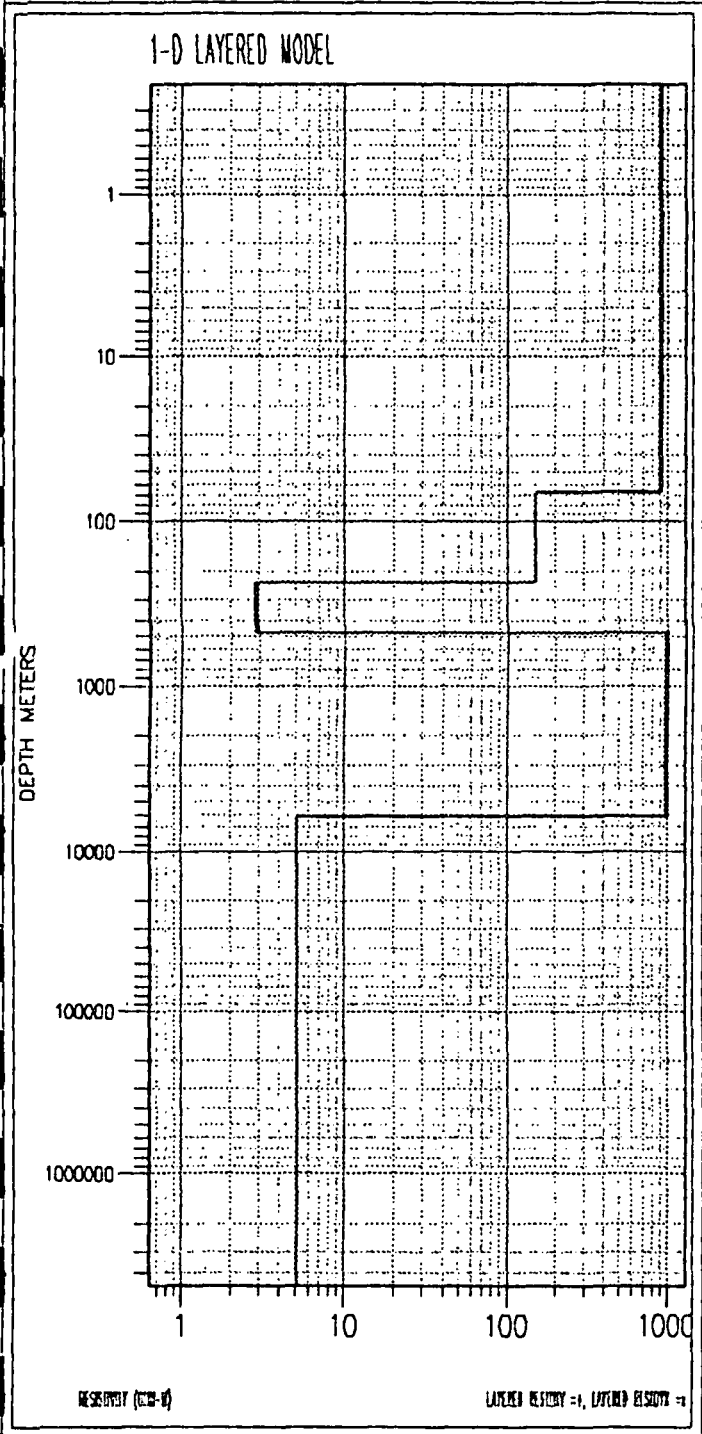


cebuco–s31

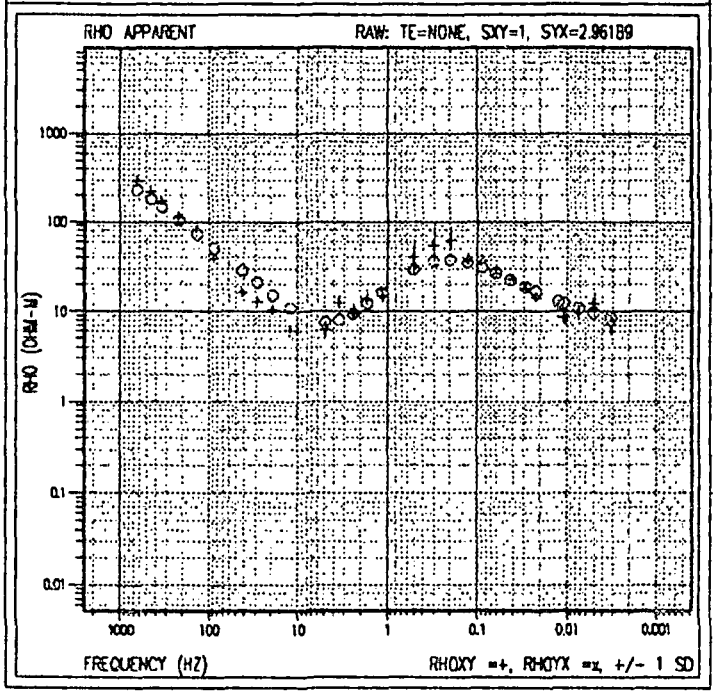


cebuco–s31

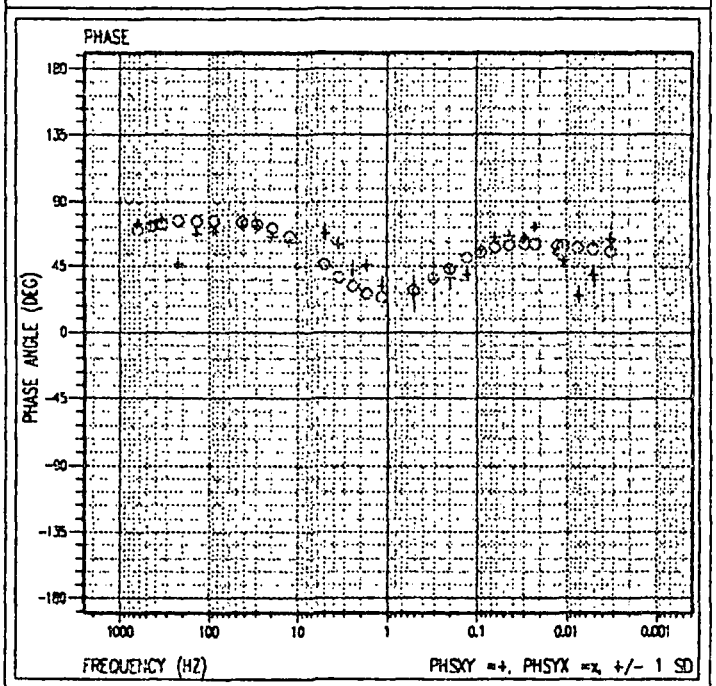

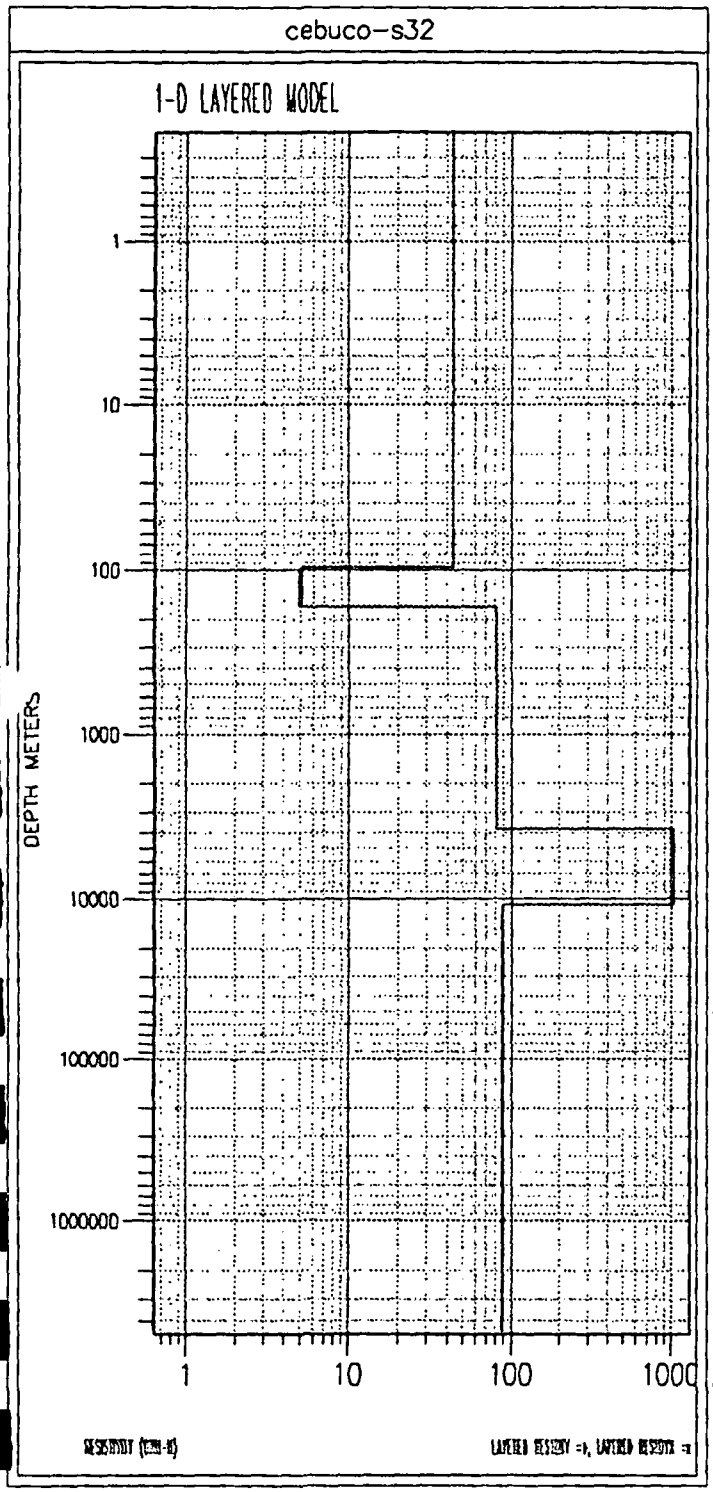
cebuco-s32
1-D LAYERED MODEL
DEPTH METERS
1
10
100
1000
10000
100000
1000000
1
10
100
1000

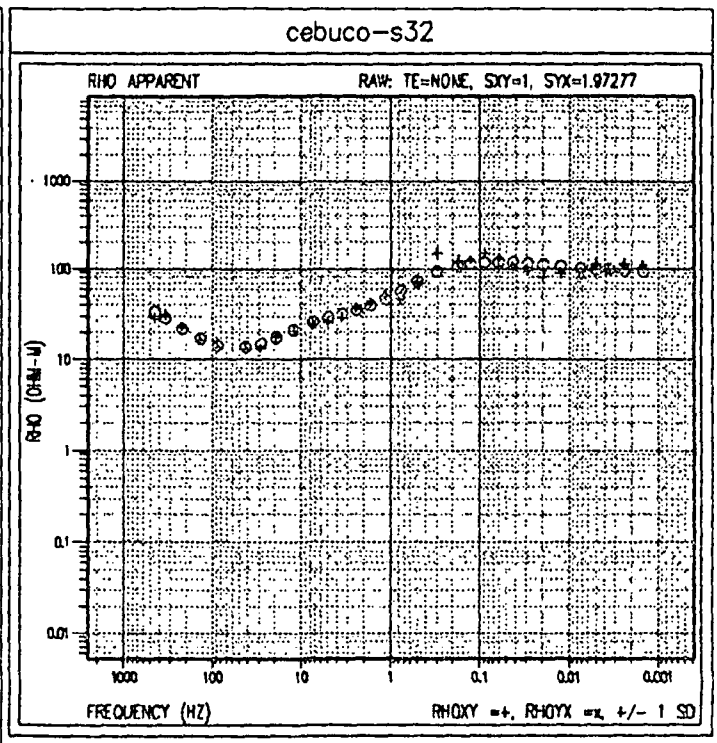
cebuco-s32
RHO APPARENT
RAW: TE=NONE, SXY=1, SYX=1.97277
RHO (OHM-M)
1000
100
10
1
0.1
0.01
1000
100
10
1
0.1
0.01
0.001
FREQUENCY (HZ)
RHOXY =+, RHOYX =x, +/- 1 SD

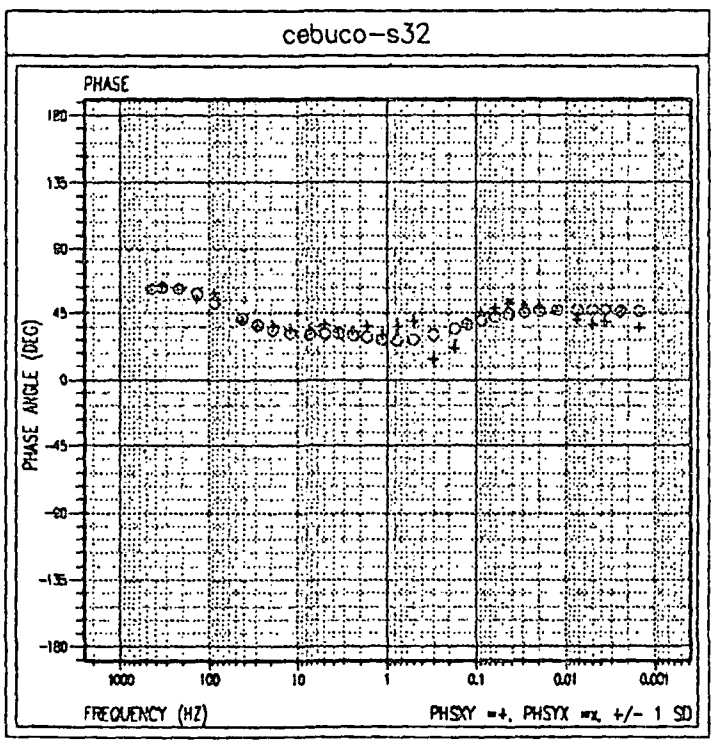
cebuco-s32
PHASE
PHASE ANGLE (DEG)
135
90
45
0
-45
-90
-135
-180
1000
100
10
1
0.1
0.01
0.001
FREQUENCY (HZ)
PHSXY =+, PHSYX =x, +/- 1 SD

cebuco-s33

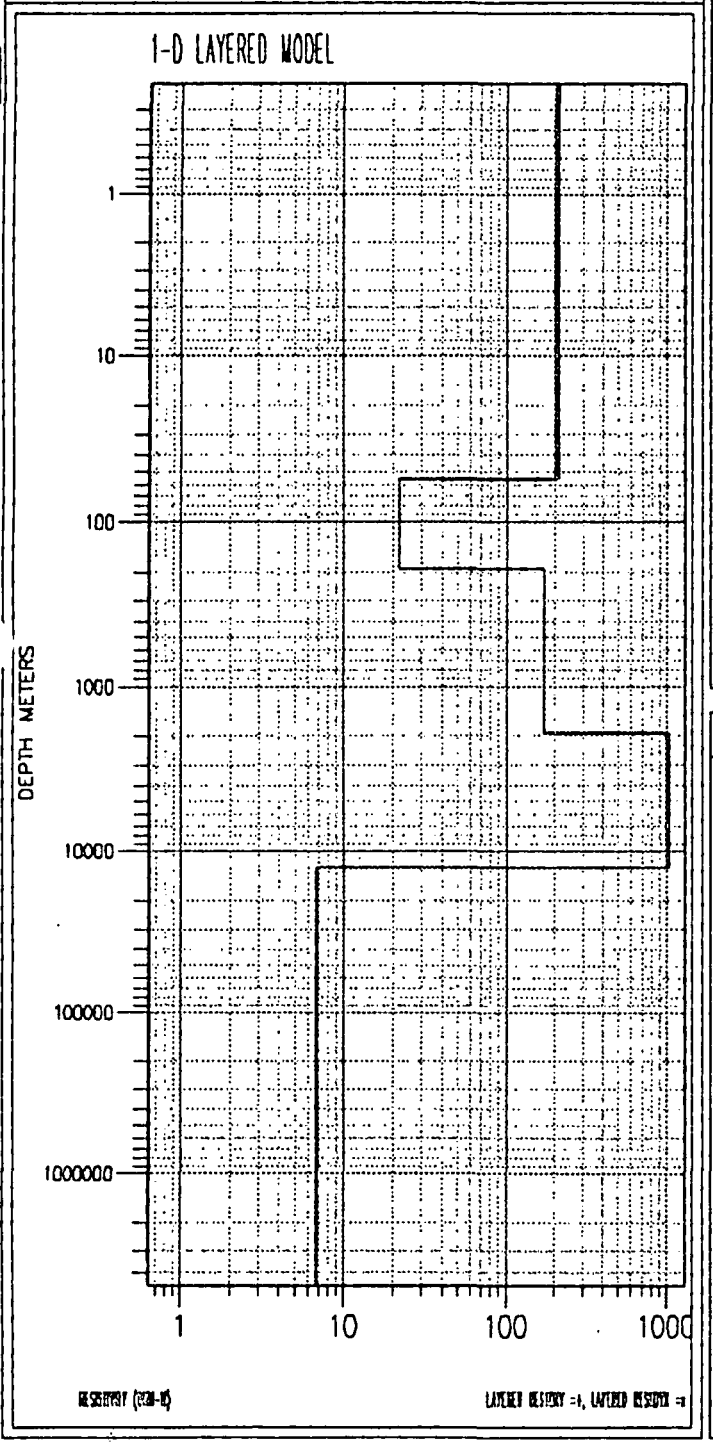


cebuco-s33

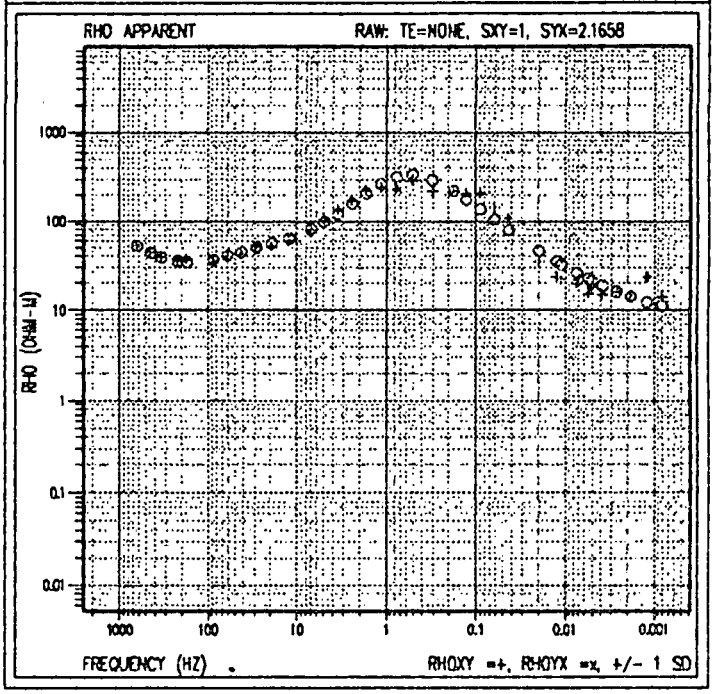


cebuco-s33

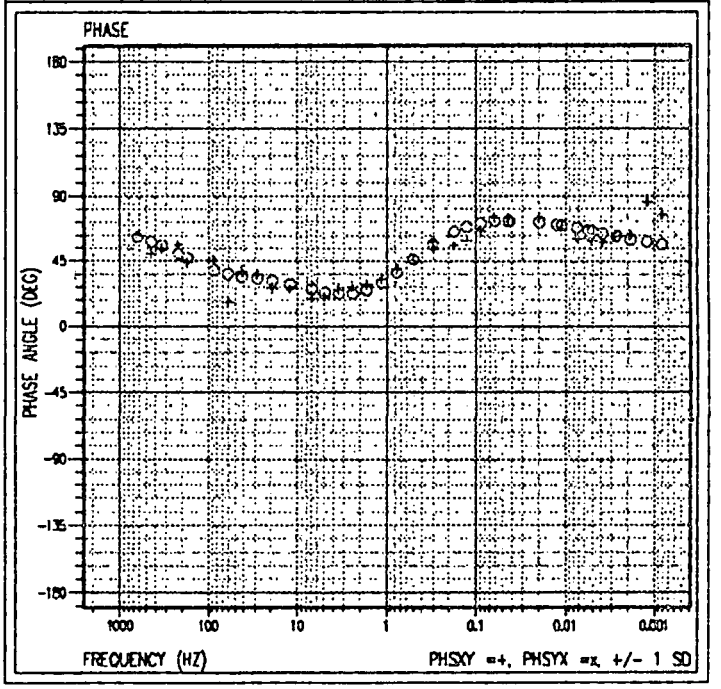

cebuco-s34

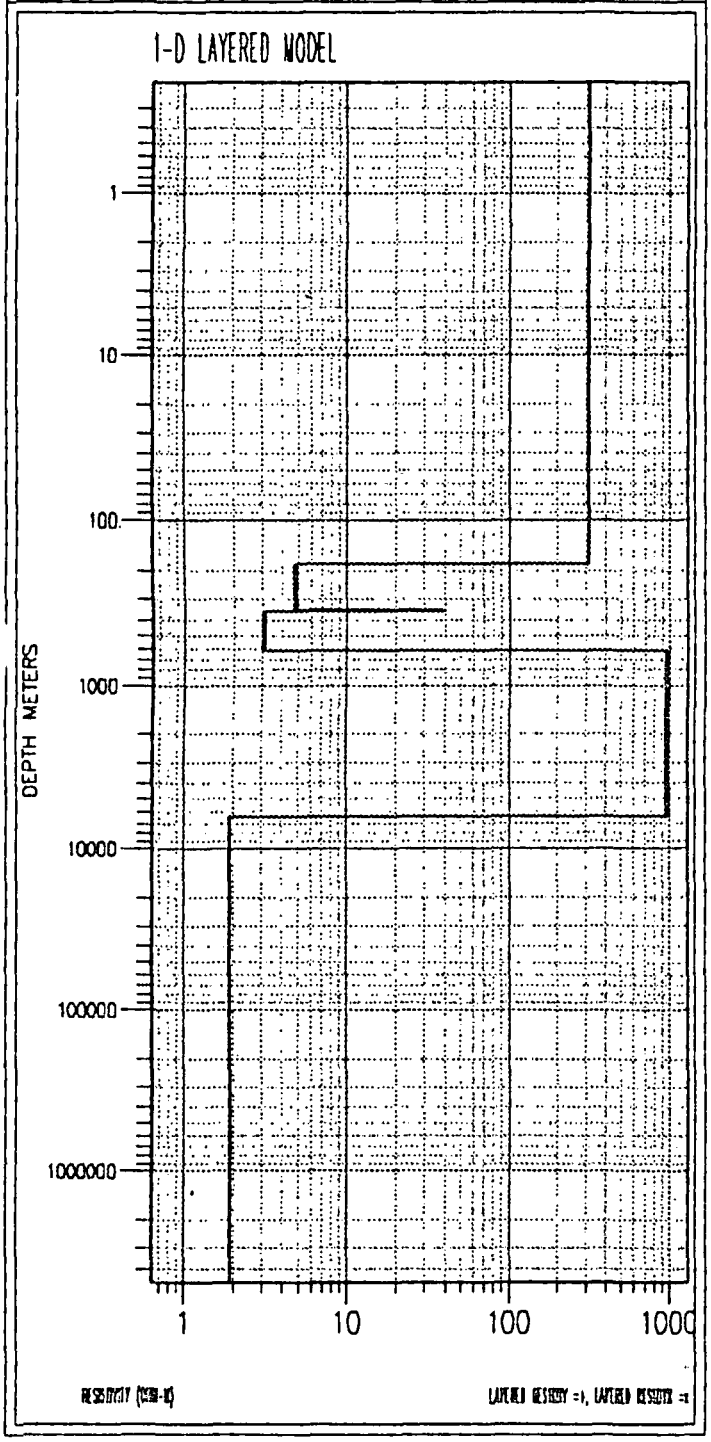


cebuco-s34

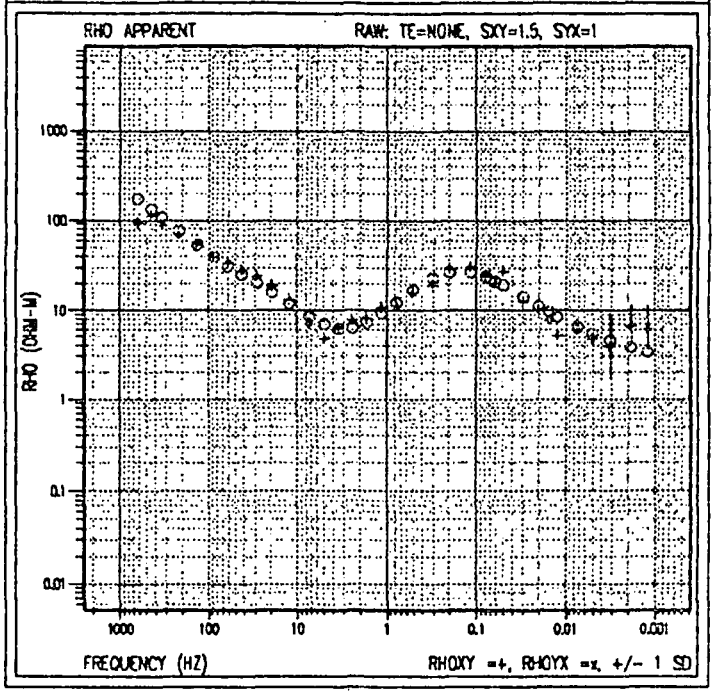


cebuco-s34

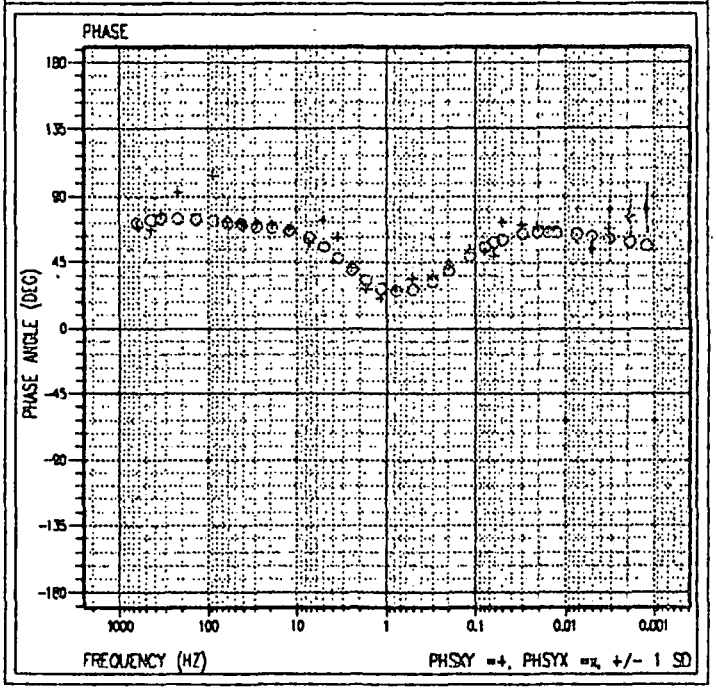

cebuco–s36

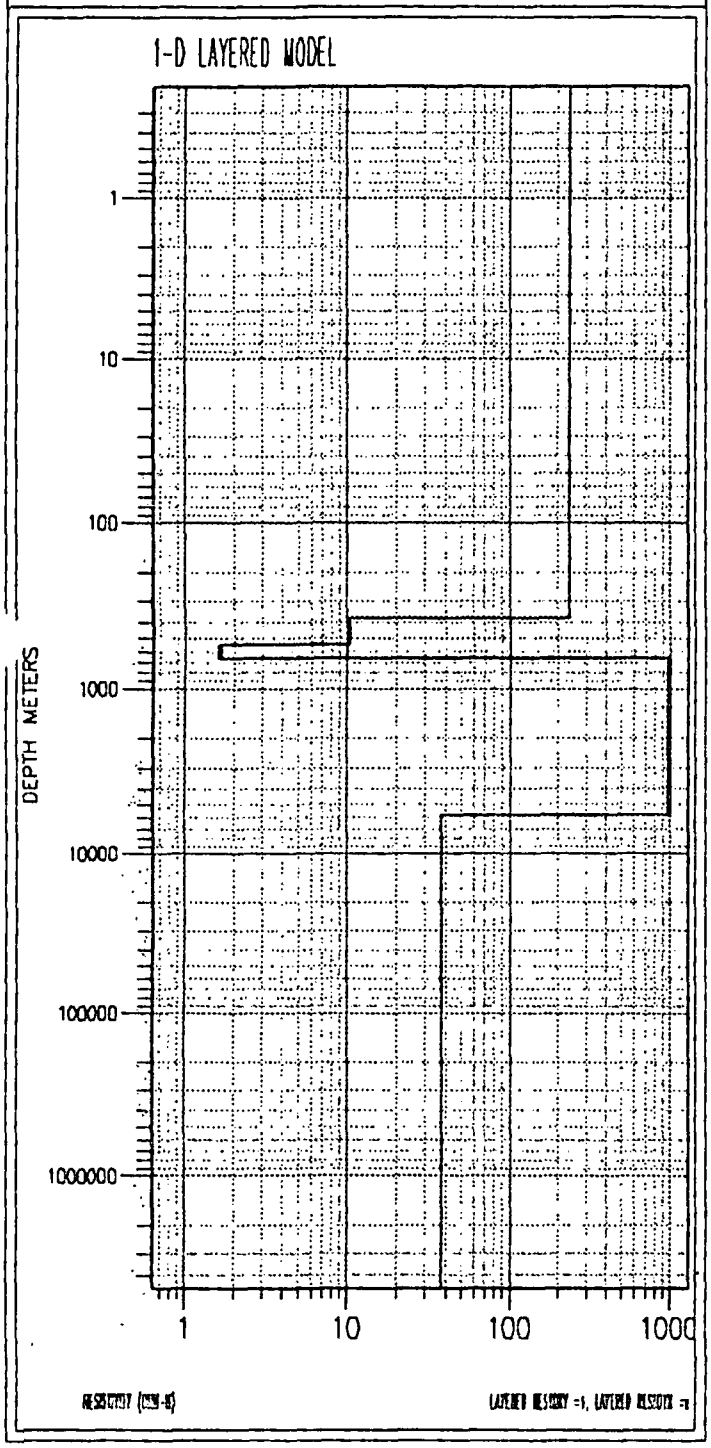


cebuco–s36

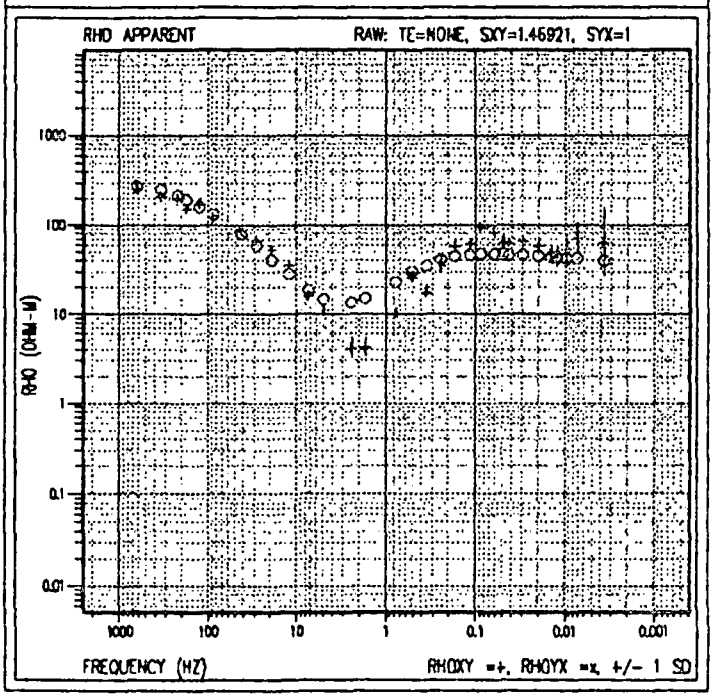


cebuco–s36

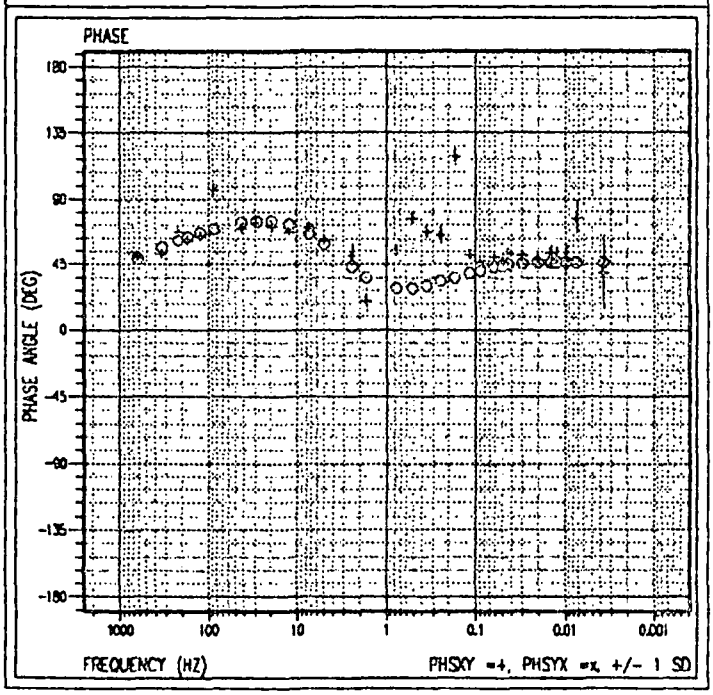

cebuco–s37

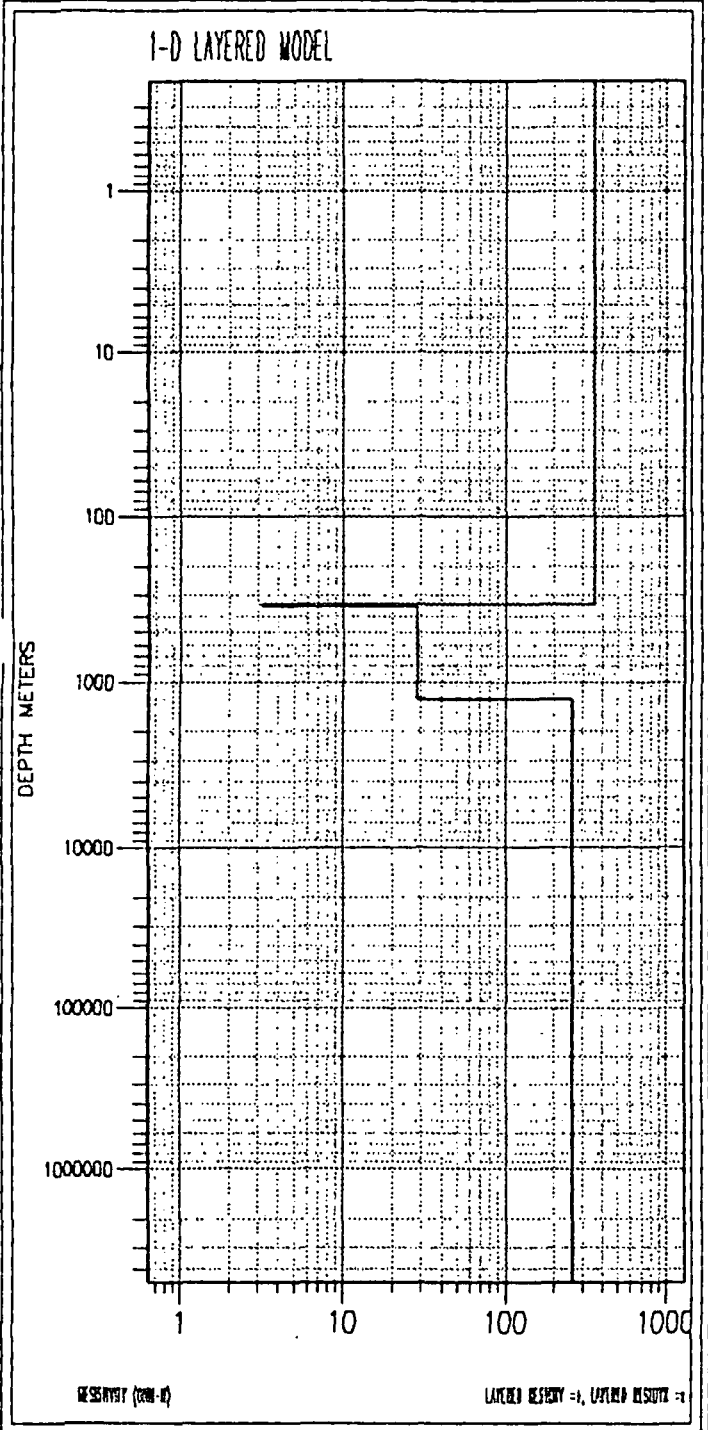


cebuco–s37

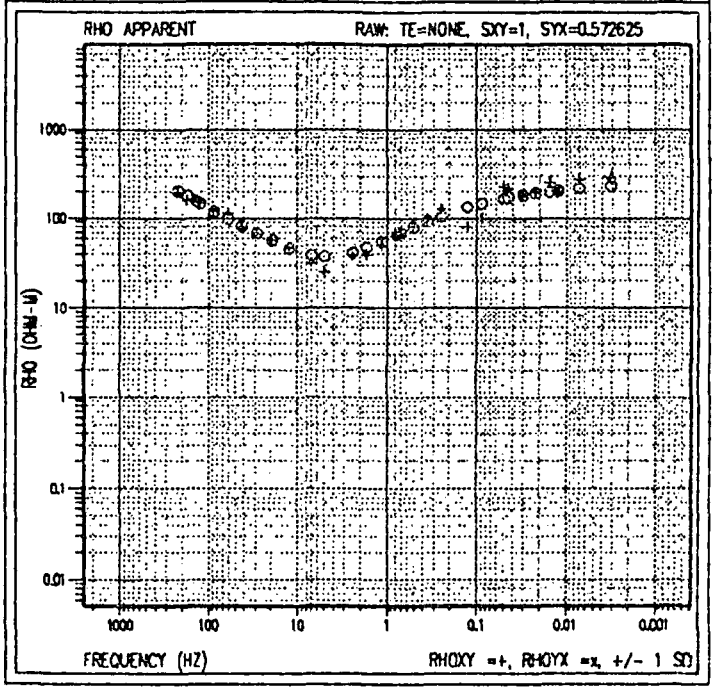


cebuco–s37

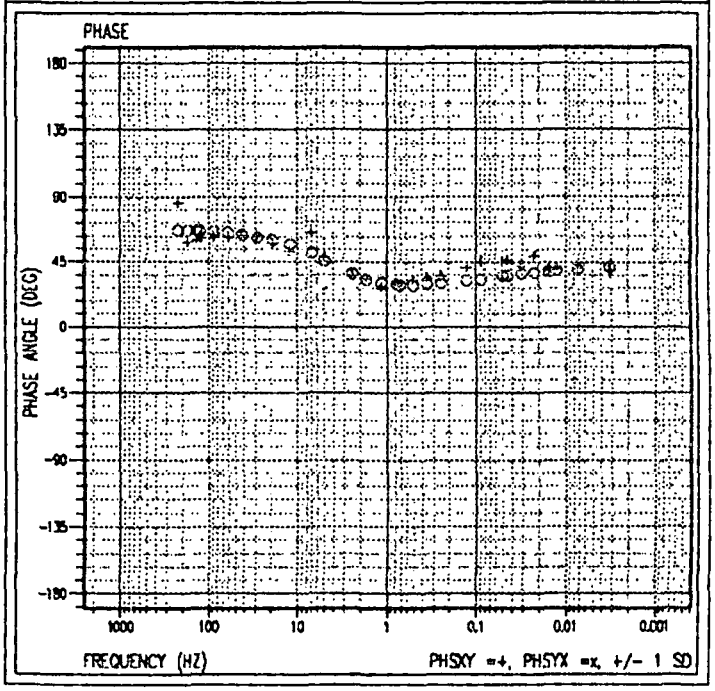

cebuco–s38

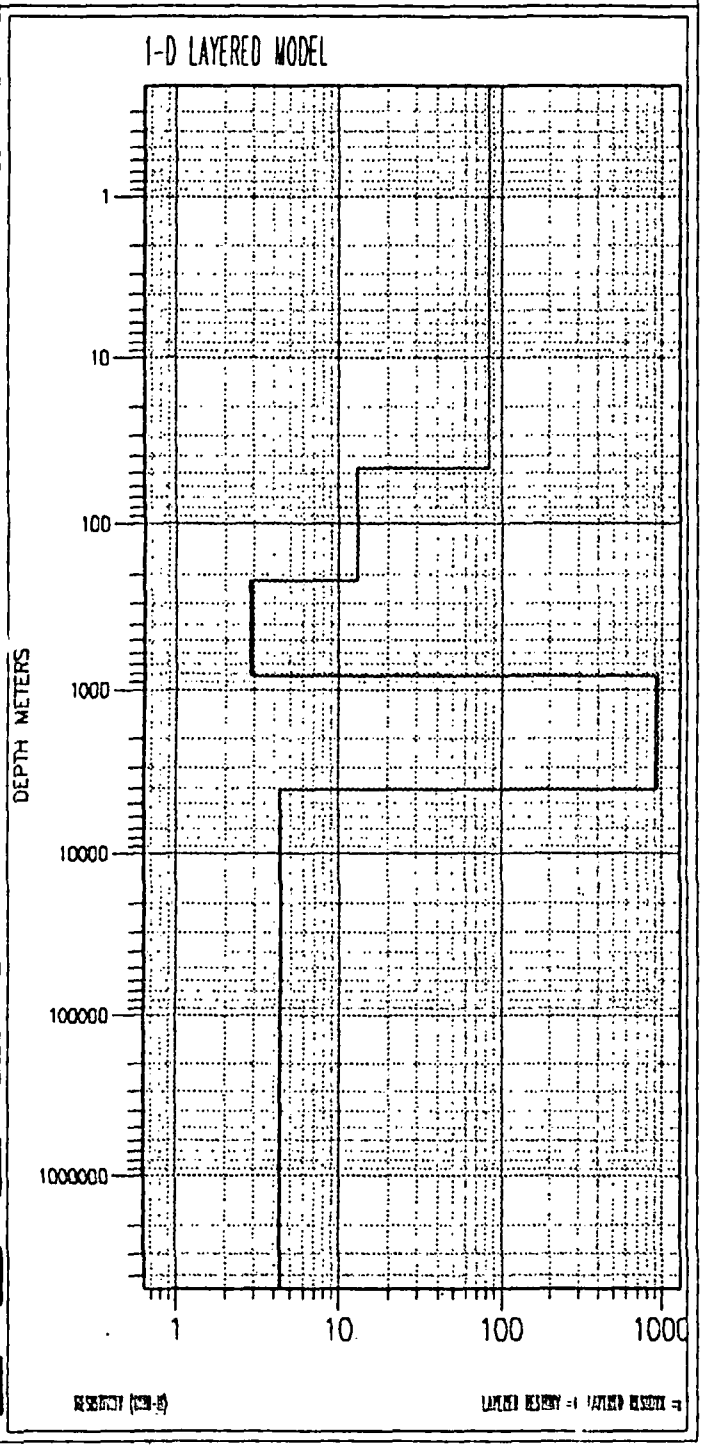


cebuco–s38

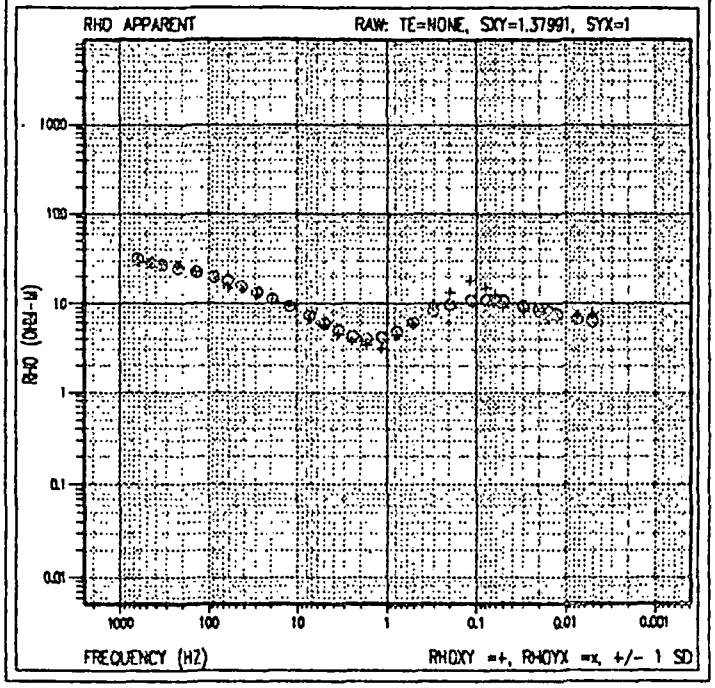


cebuco–s38

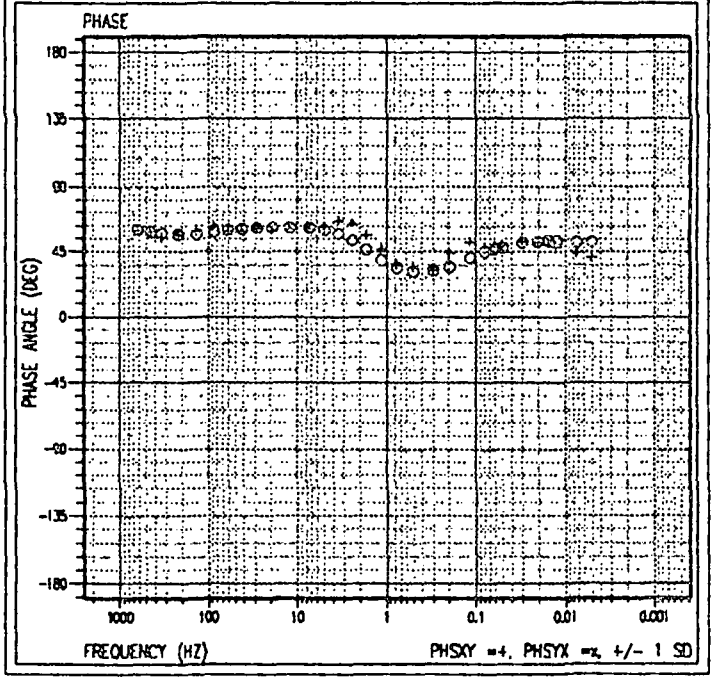

cebuco–s39

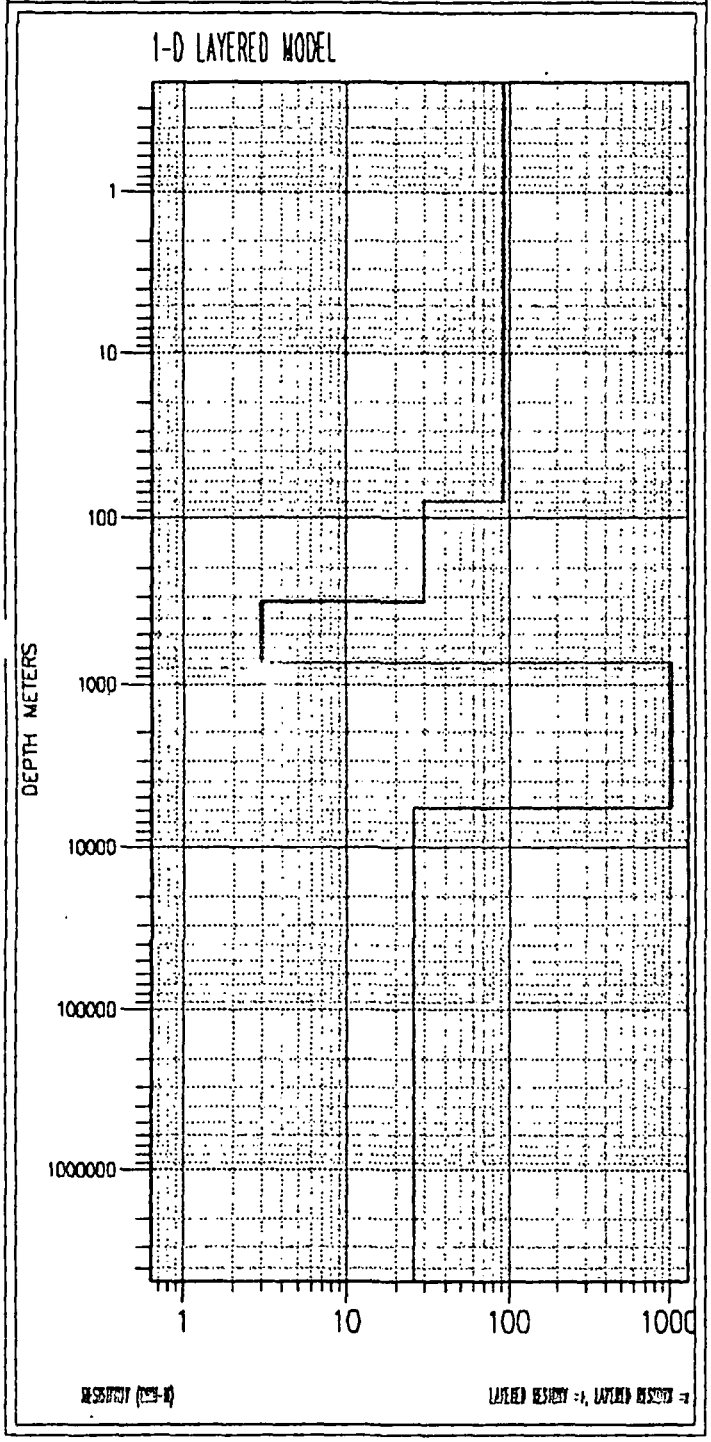


cebuco–s39

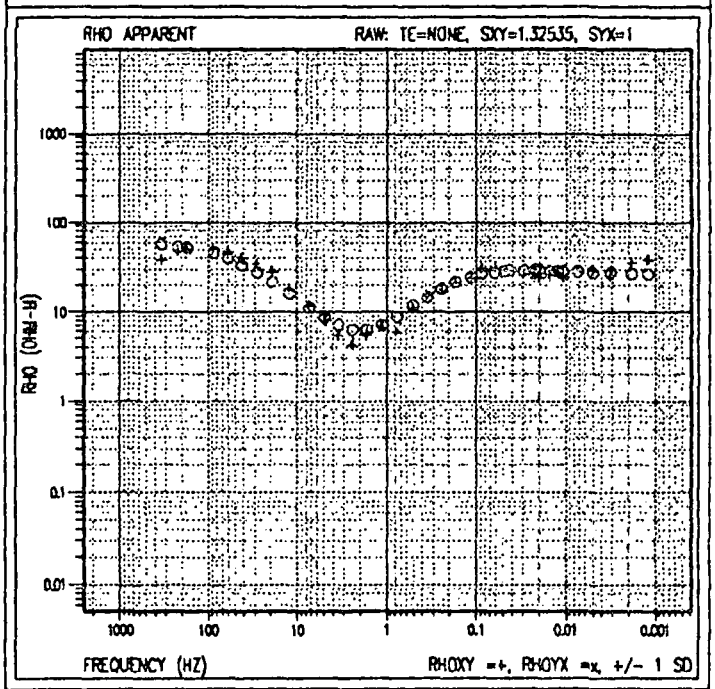


cebuco–s39

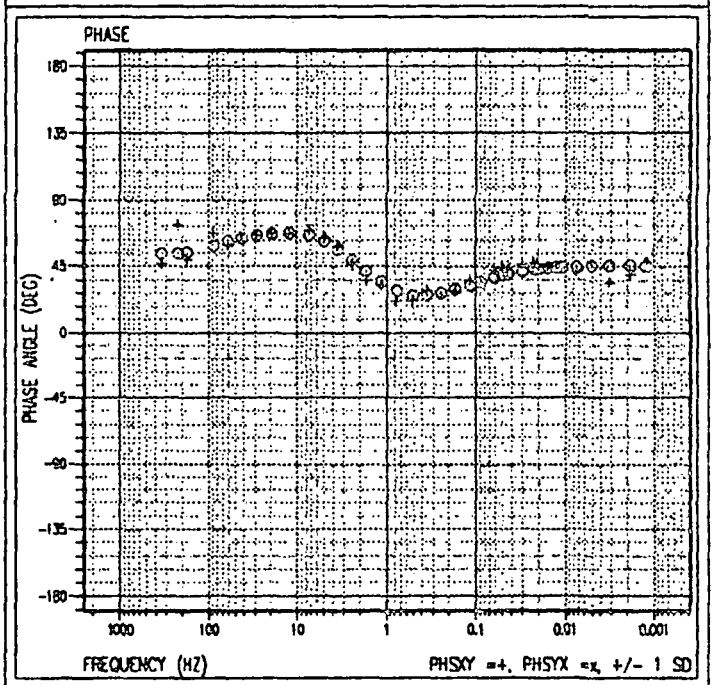

cebuco-s40

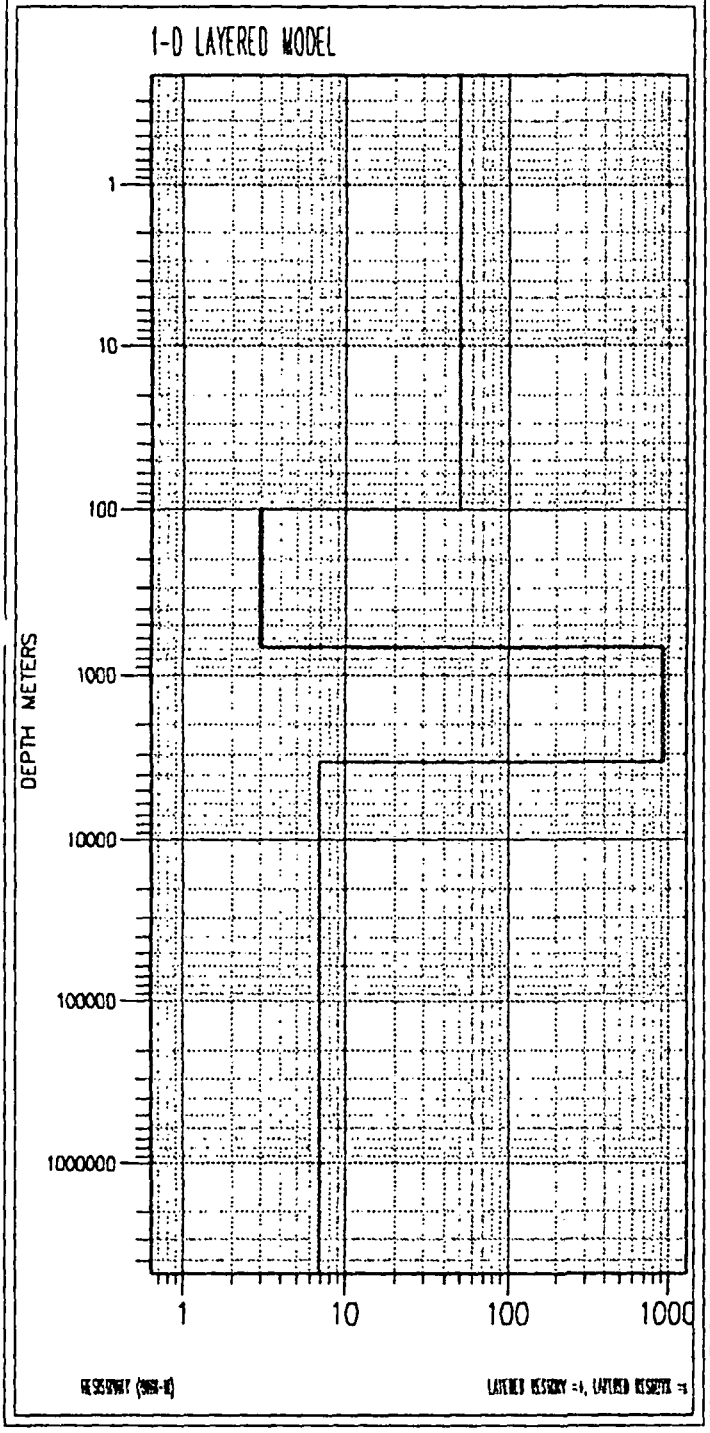


cebuco-s40

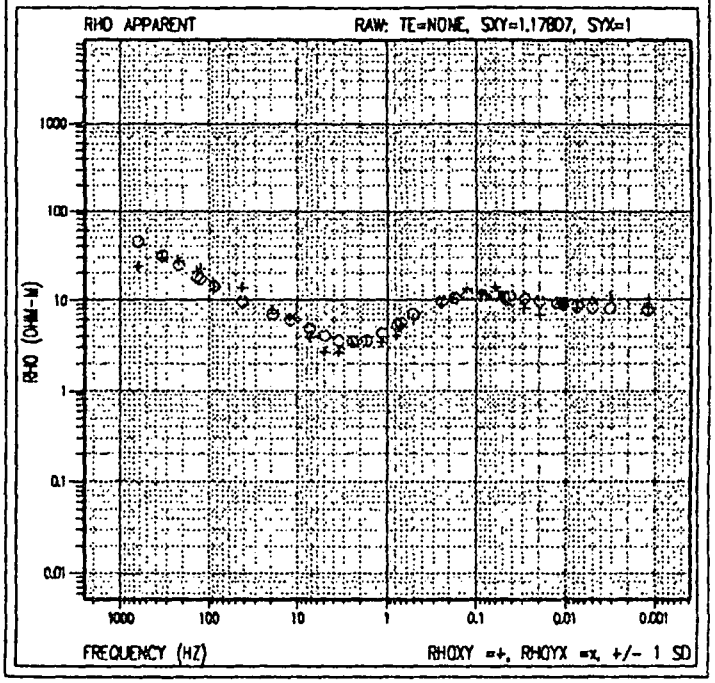


cebuco-s40

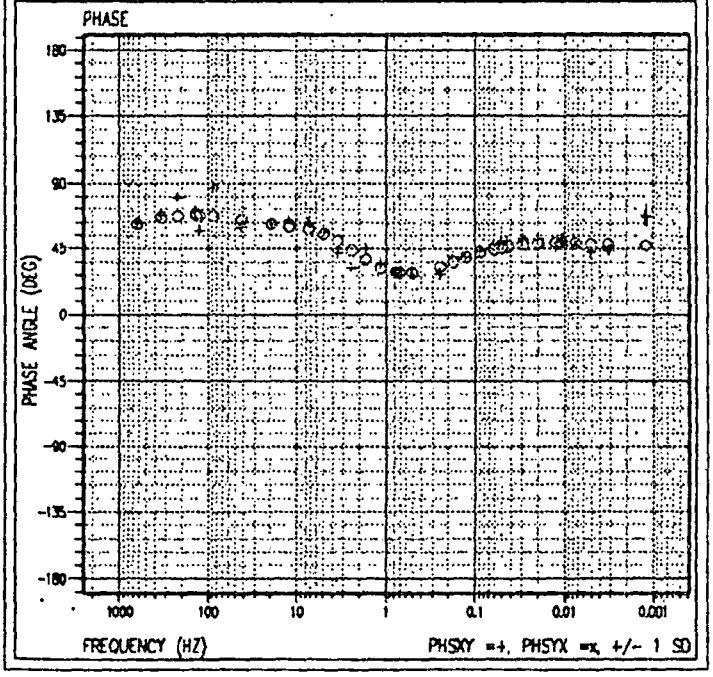

cebuco–s41

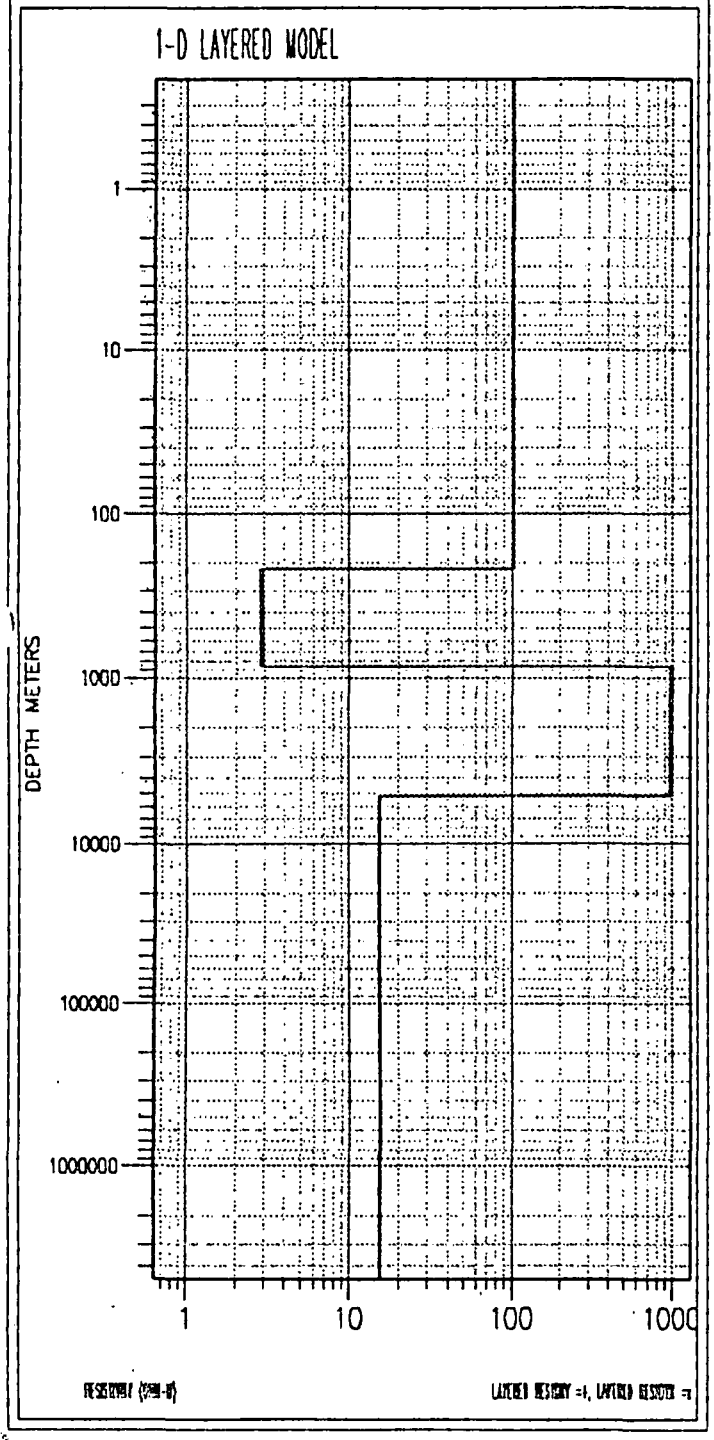


cebuco–s41

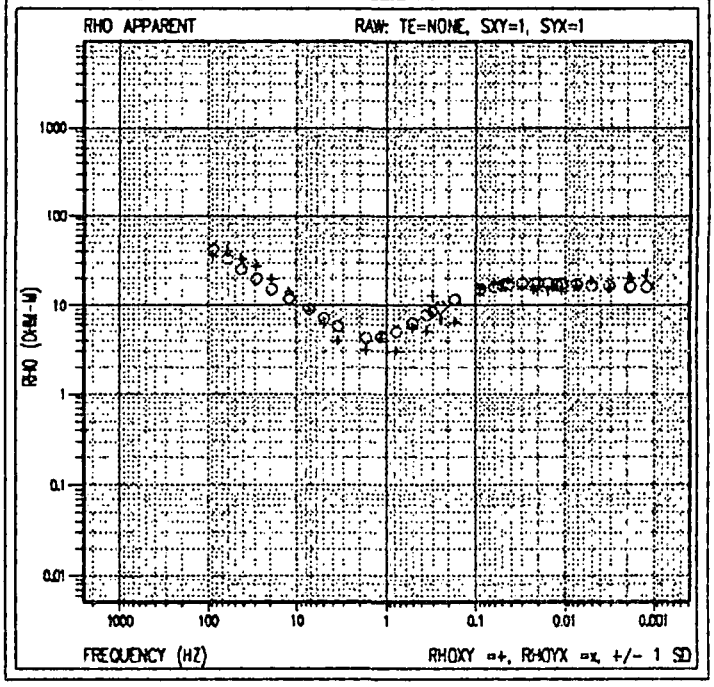


cebuco–s41

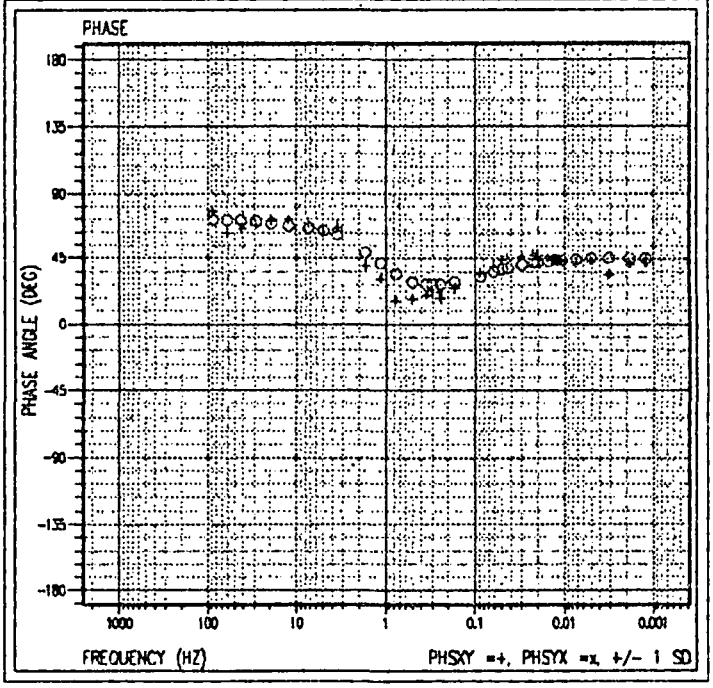

cebuco–s42

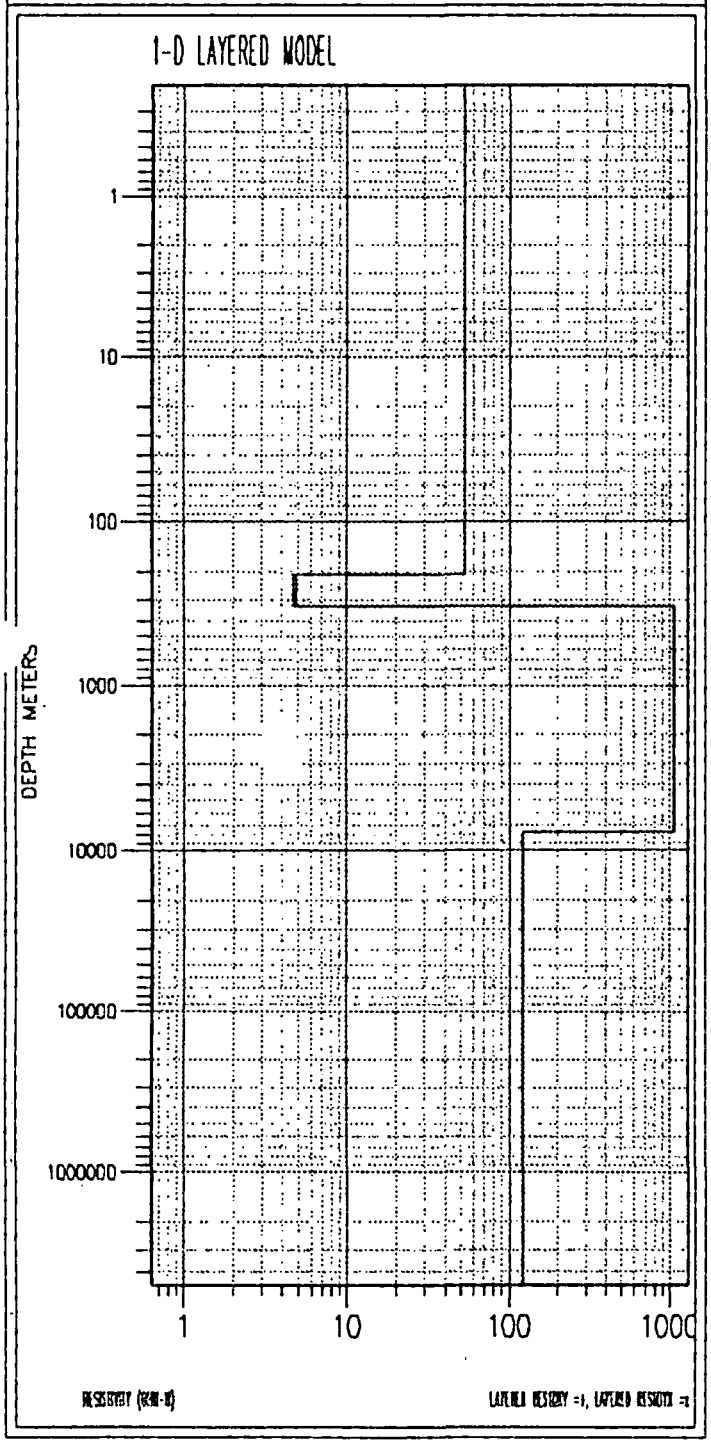


cebuco–s42

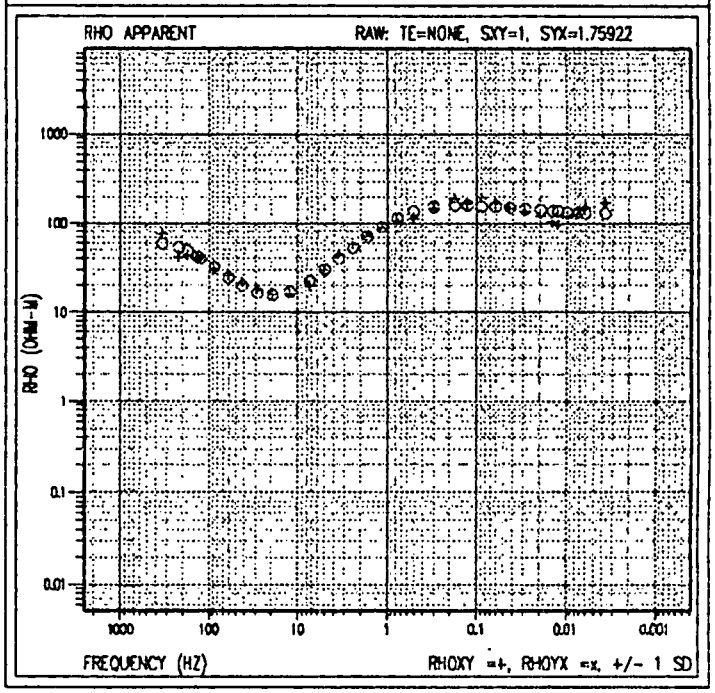


cebuco–s42

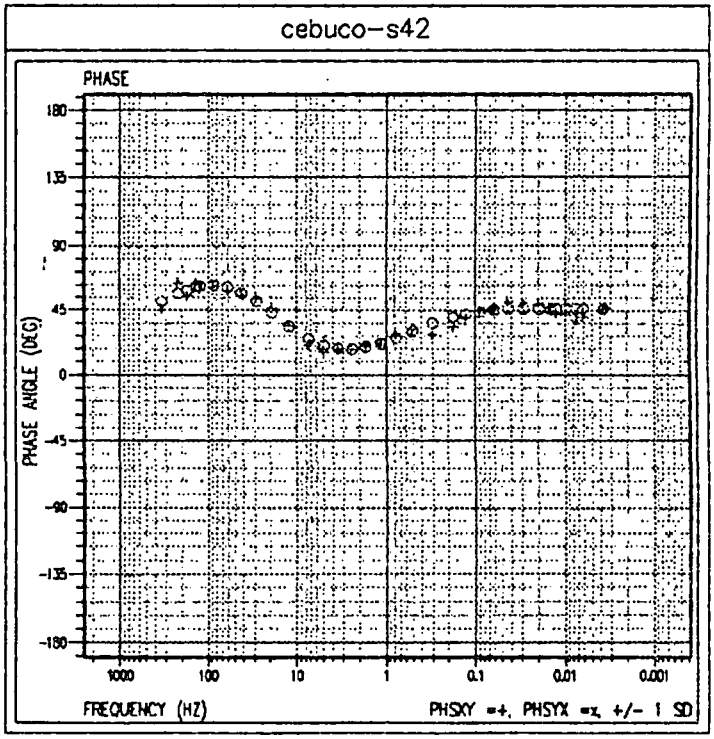

cebuco-s43

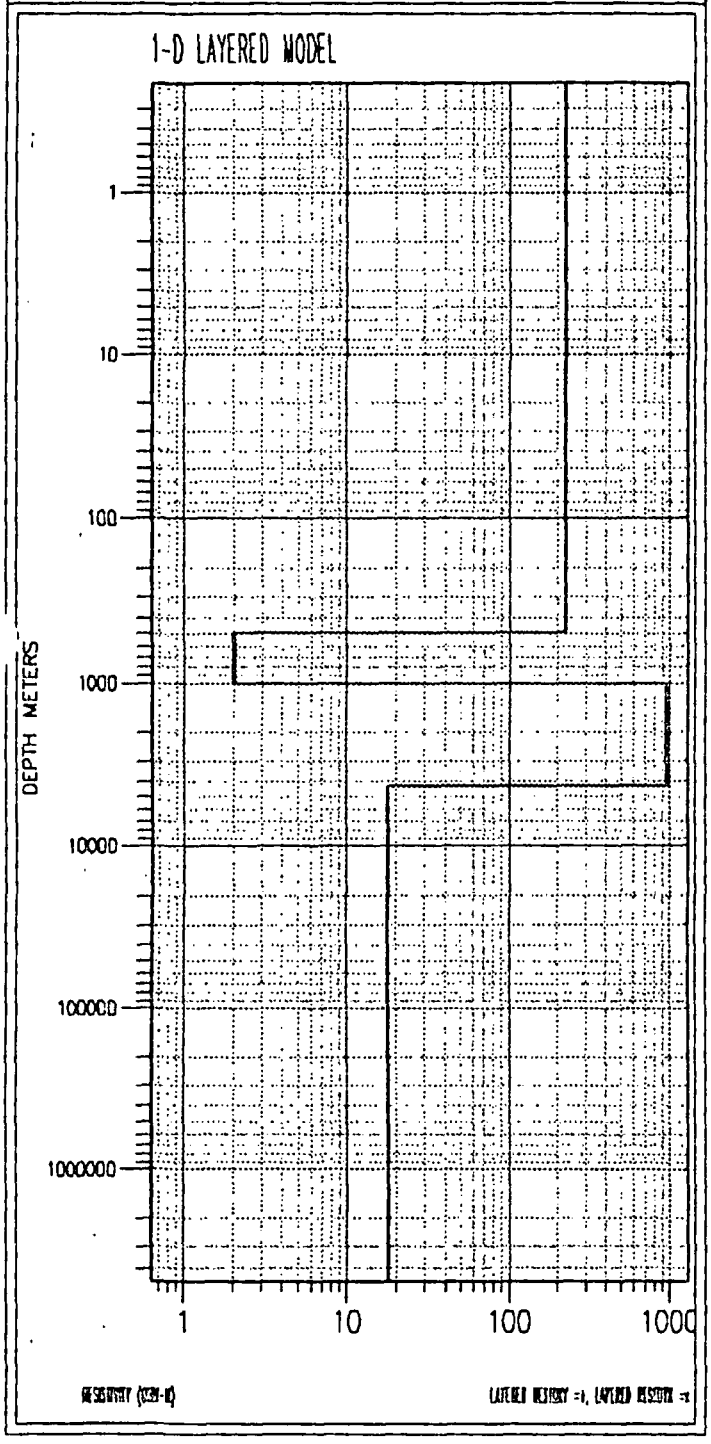


cebuco-s43

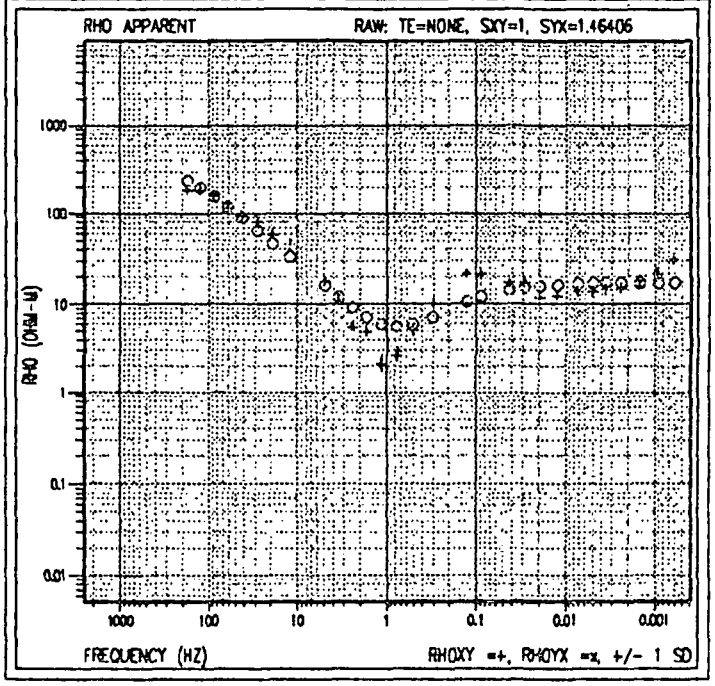


cebuco-s43

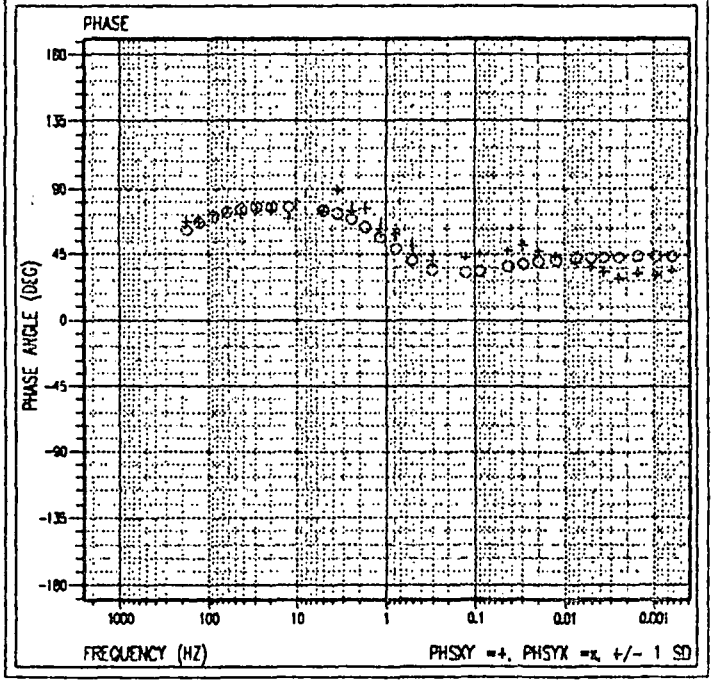

cebuco–s44

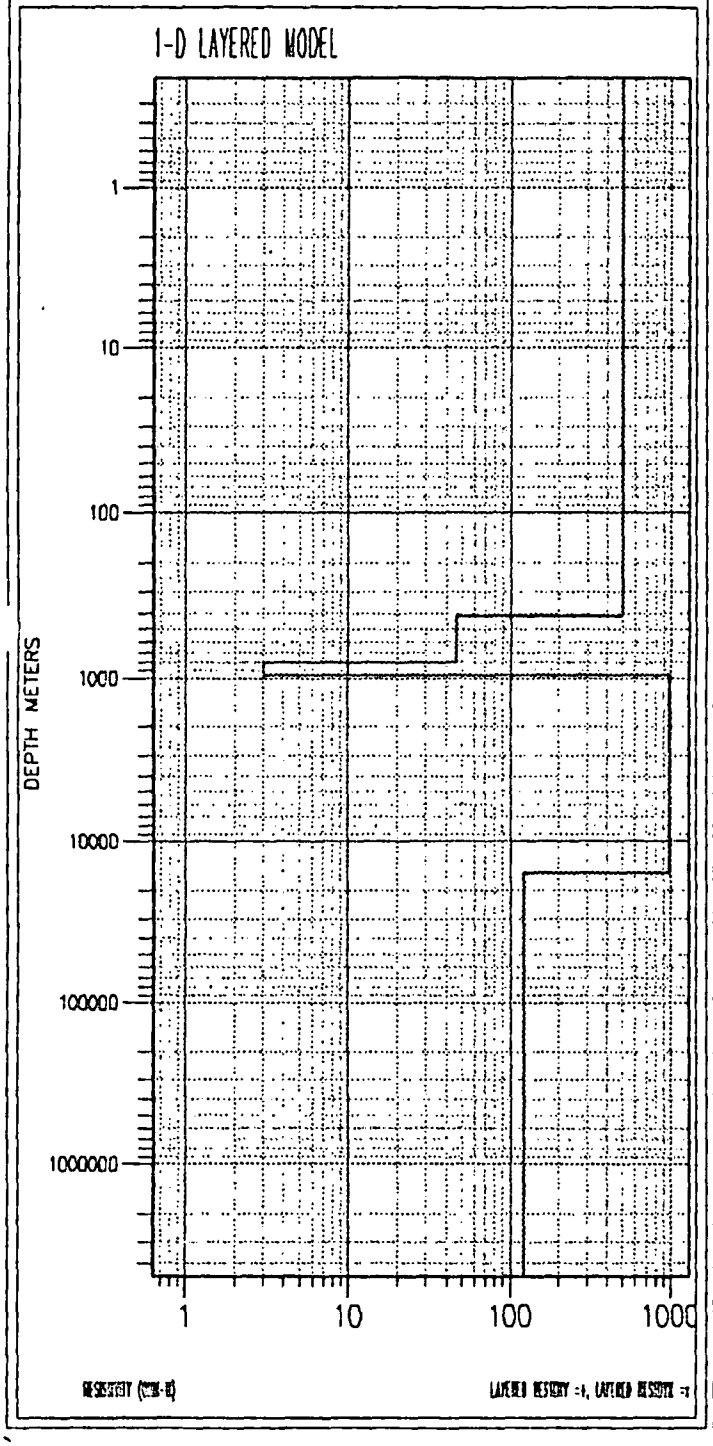


cebuco–s44

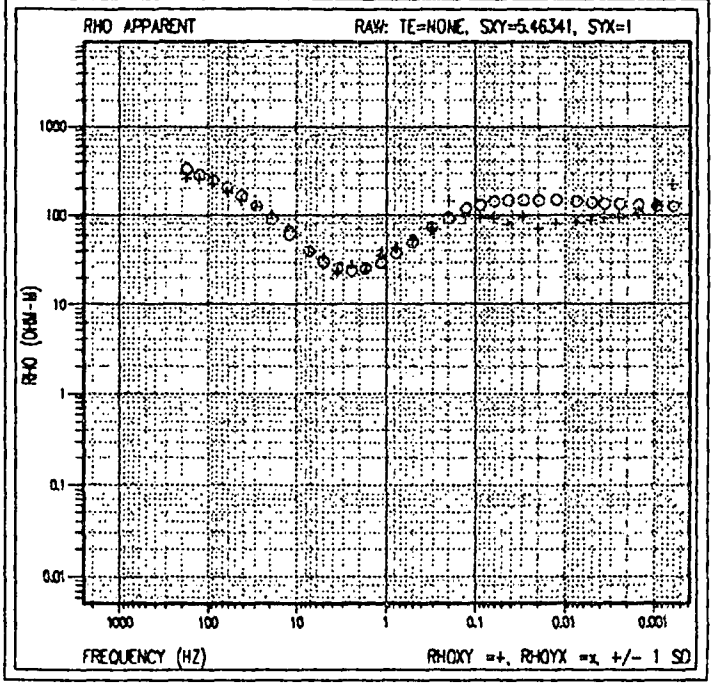


cebuco–s44

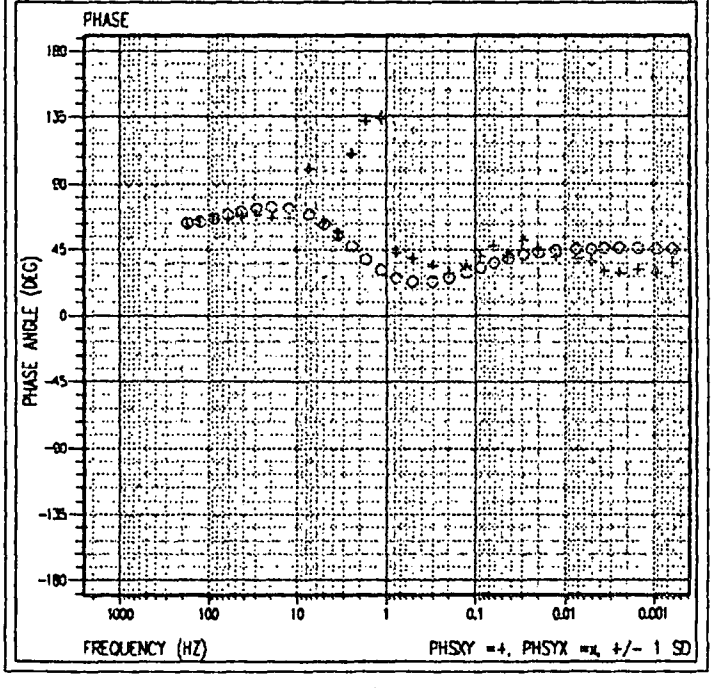

cebuco–s45

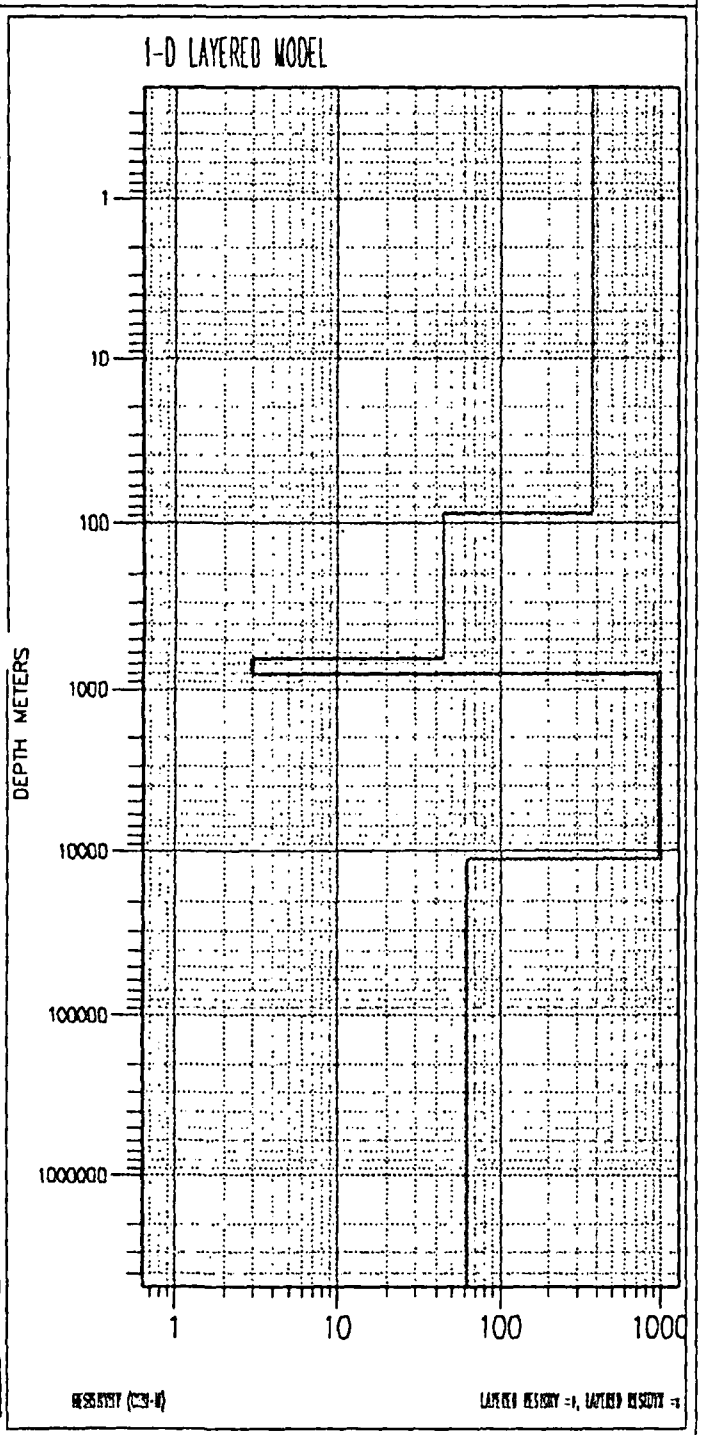


cebuco–s45

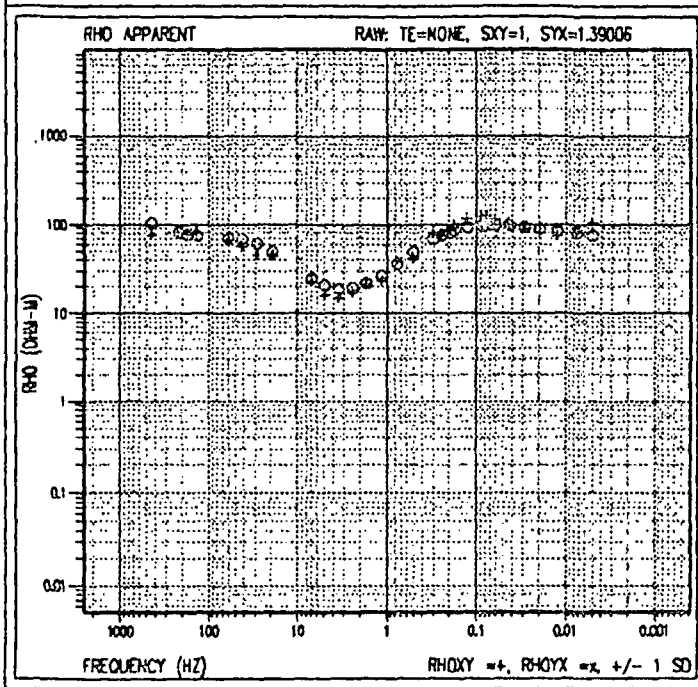


cebuco–s45

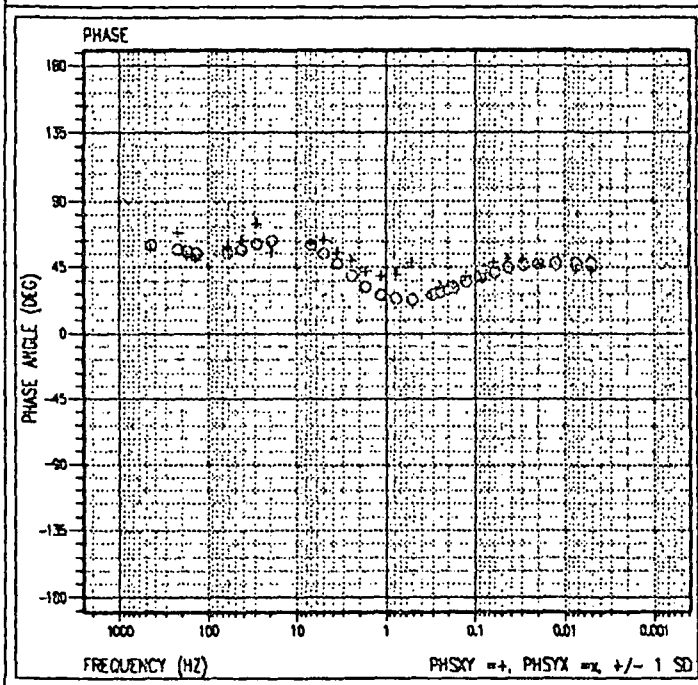

cebuco–s46

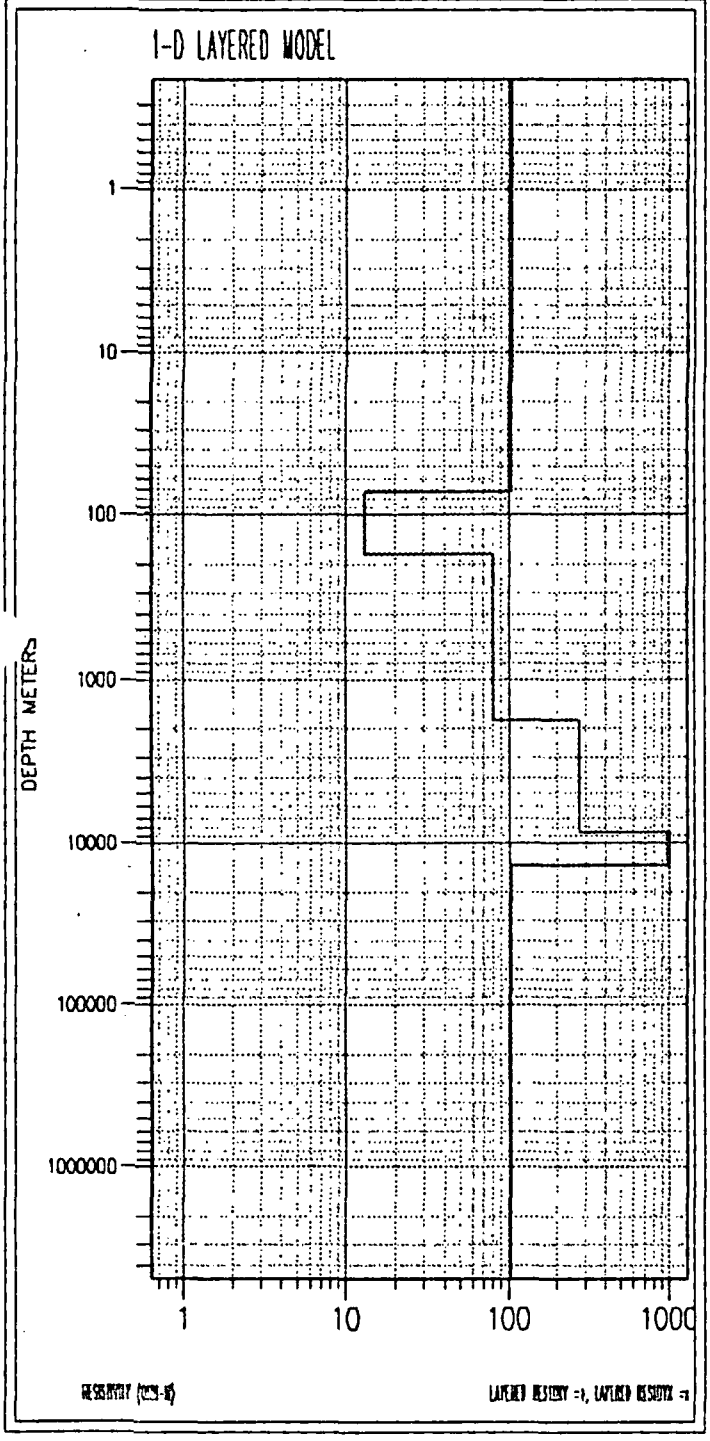


cebuco–s46

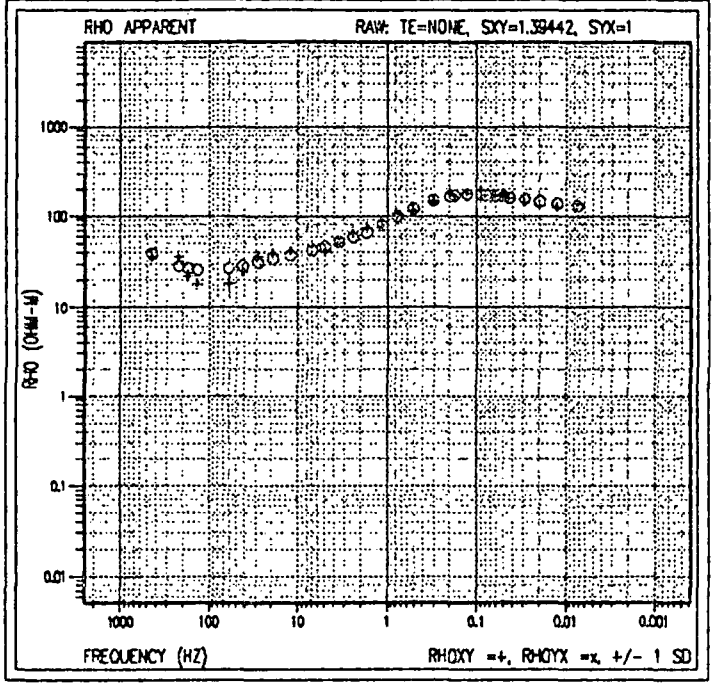


cebuco–s46

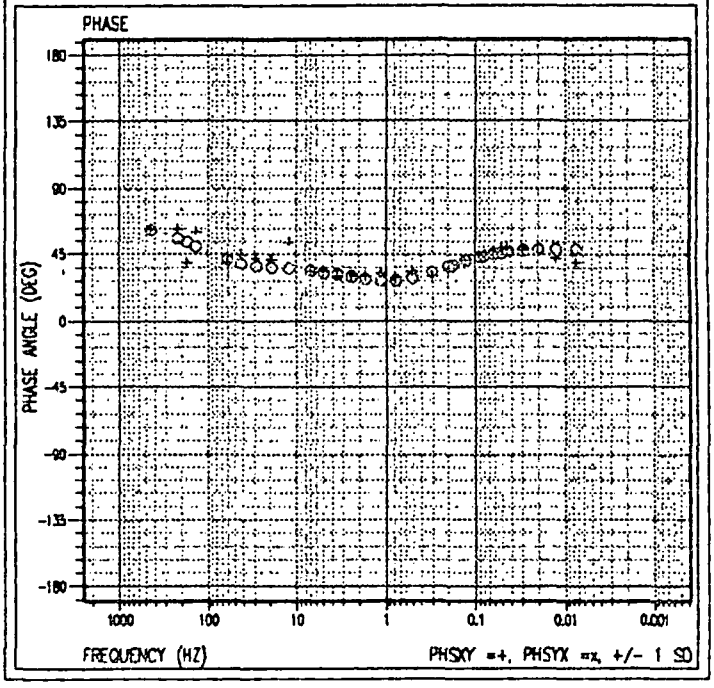

cebuco-s47

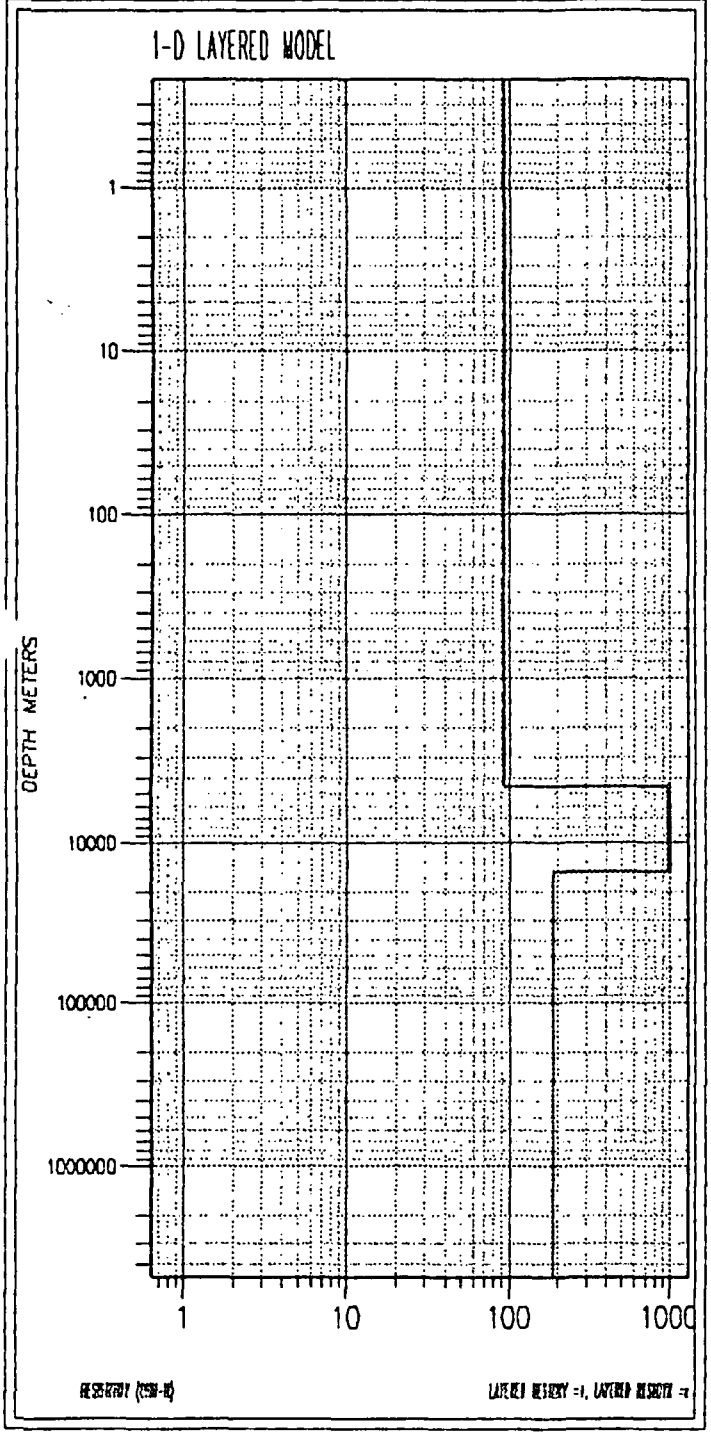


cebuco-s47

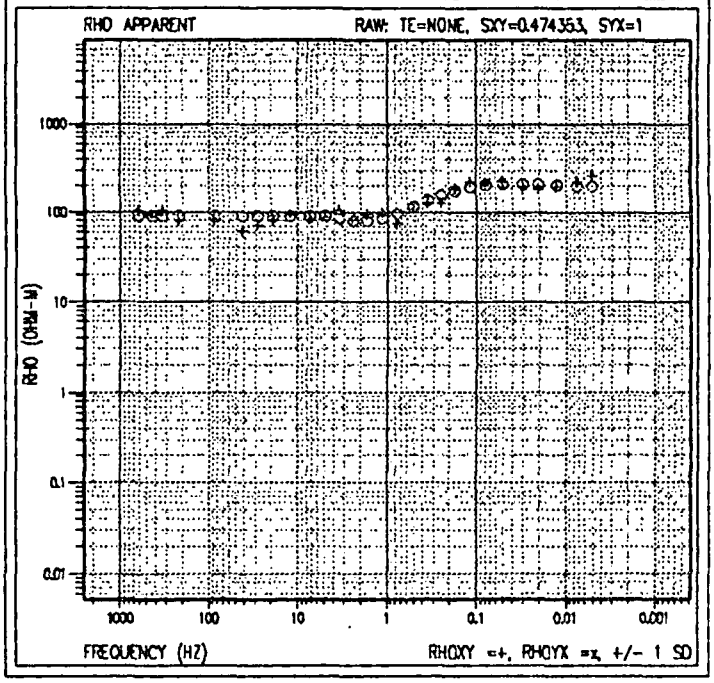


cebuco-s47

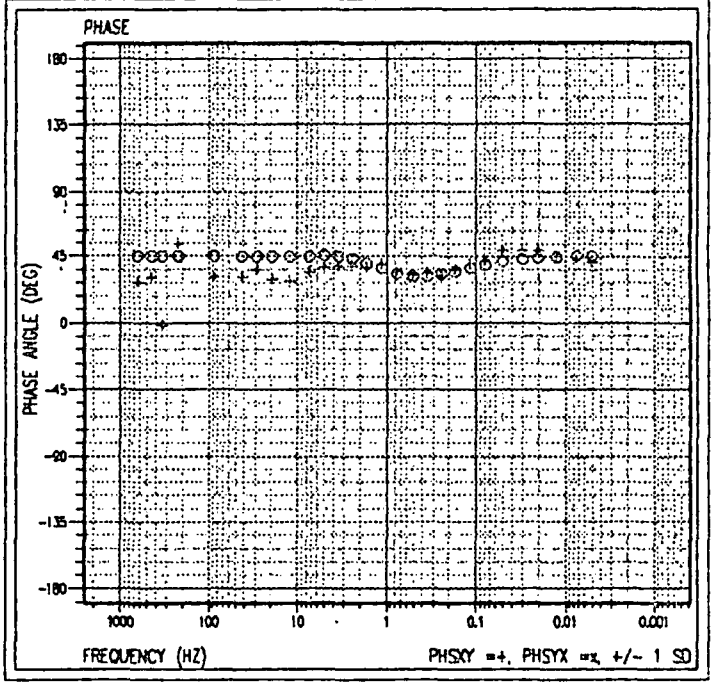

cebuco-s48

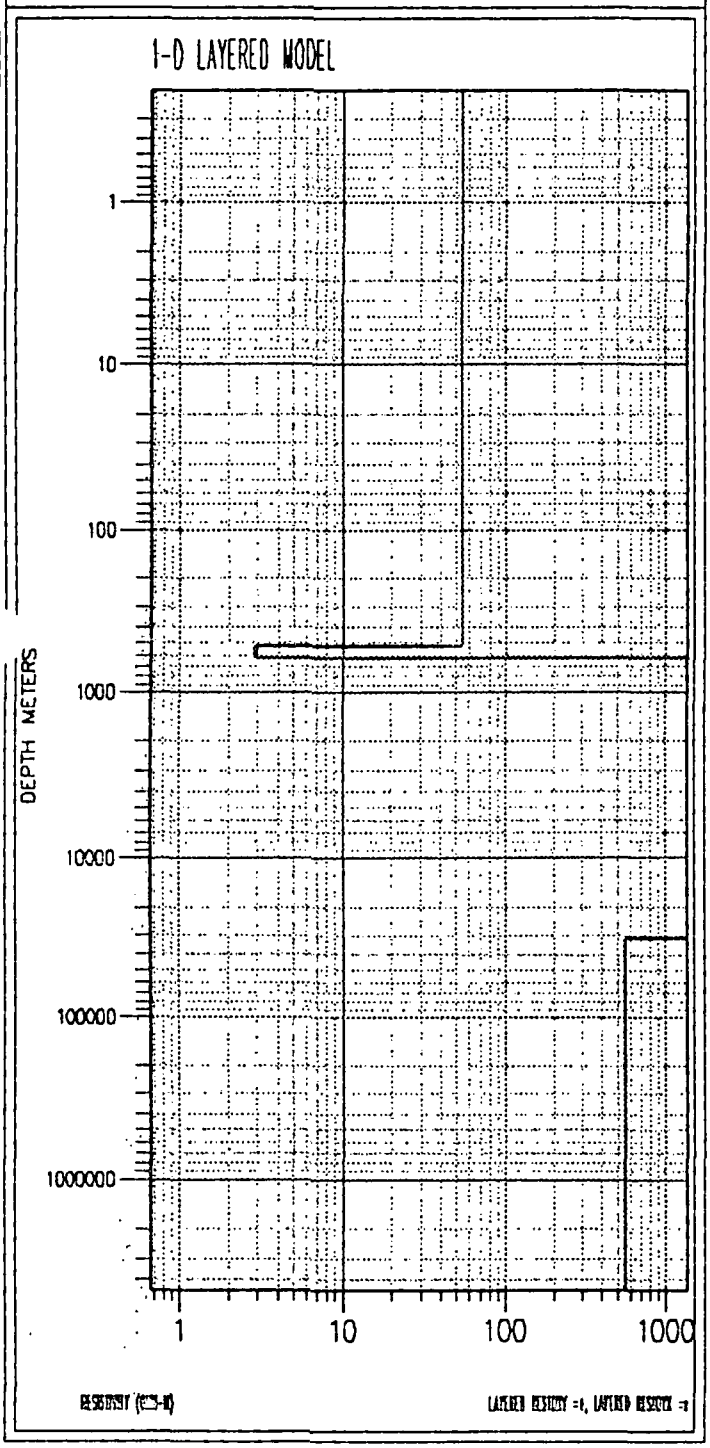


cebuco-s48

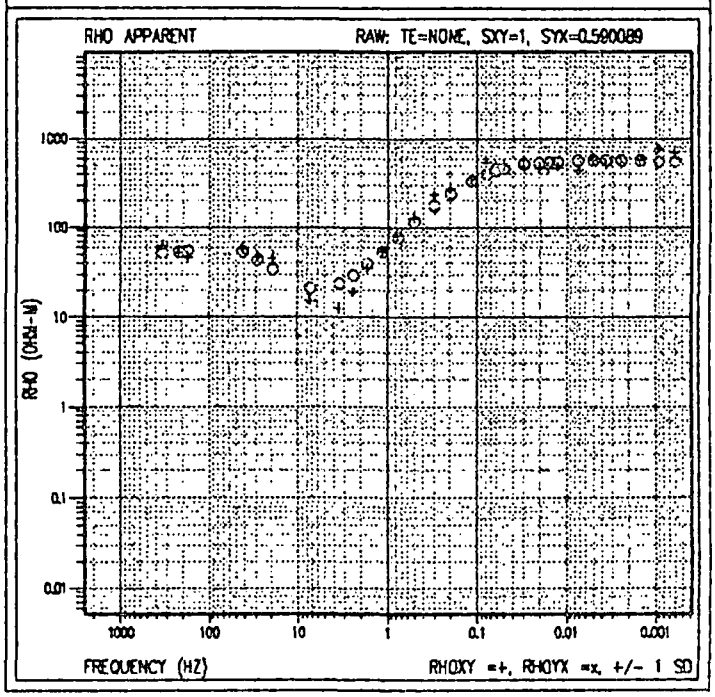


cebuco-s48

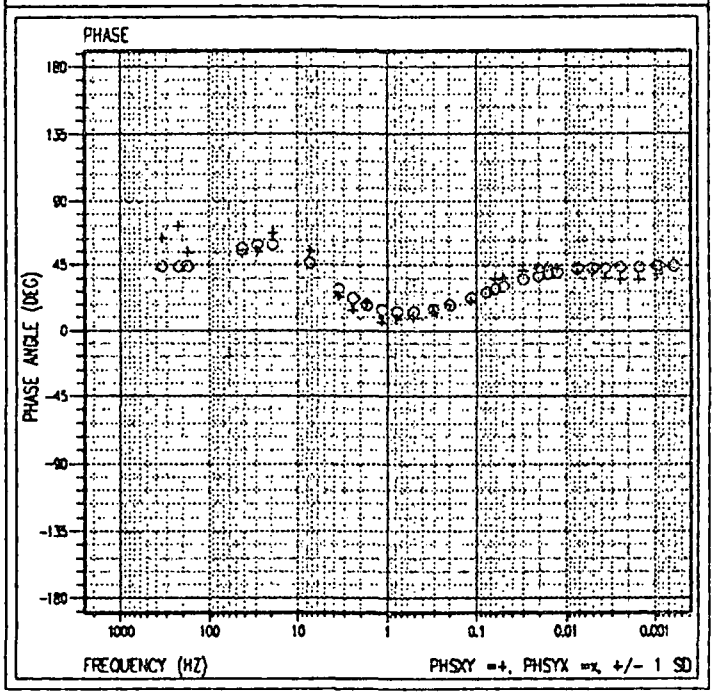

cebuco–s49

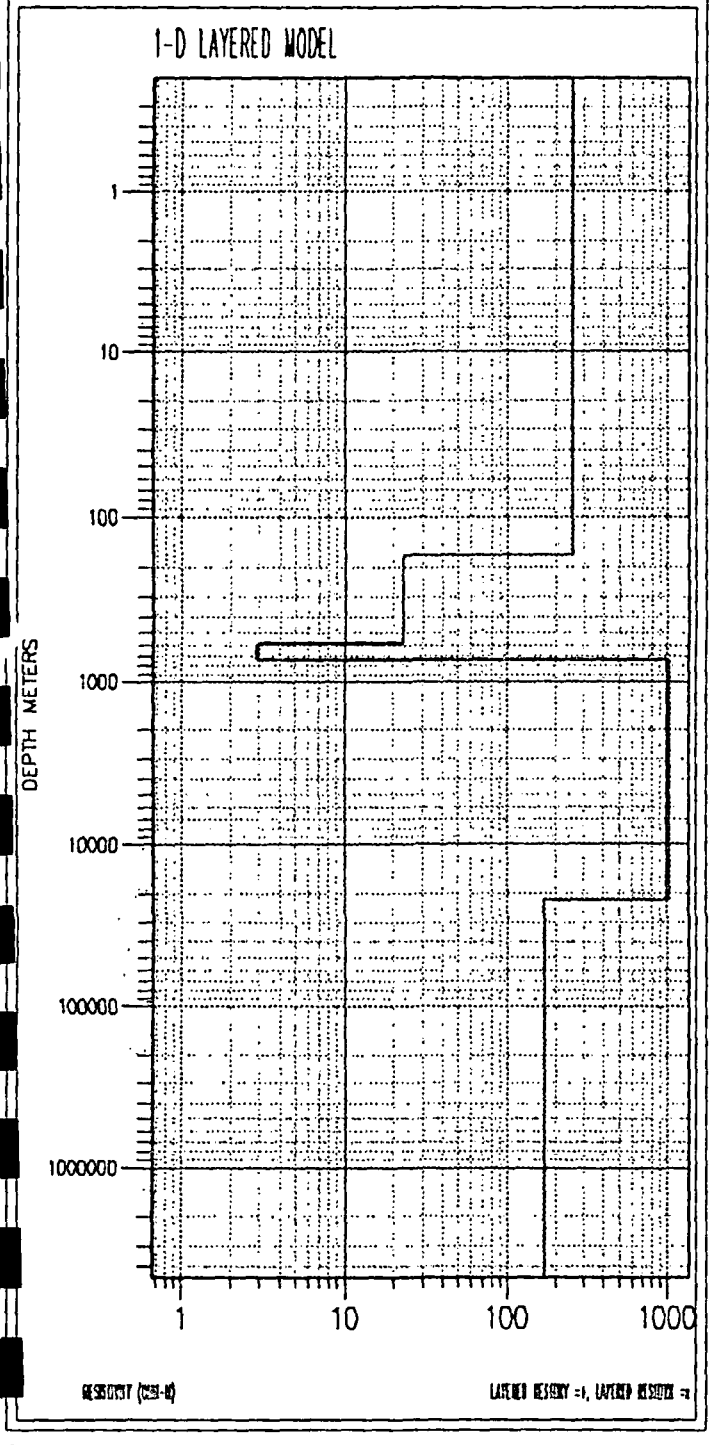


cebuco–s49

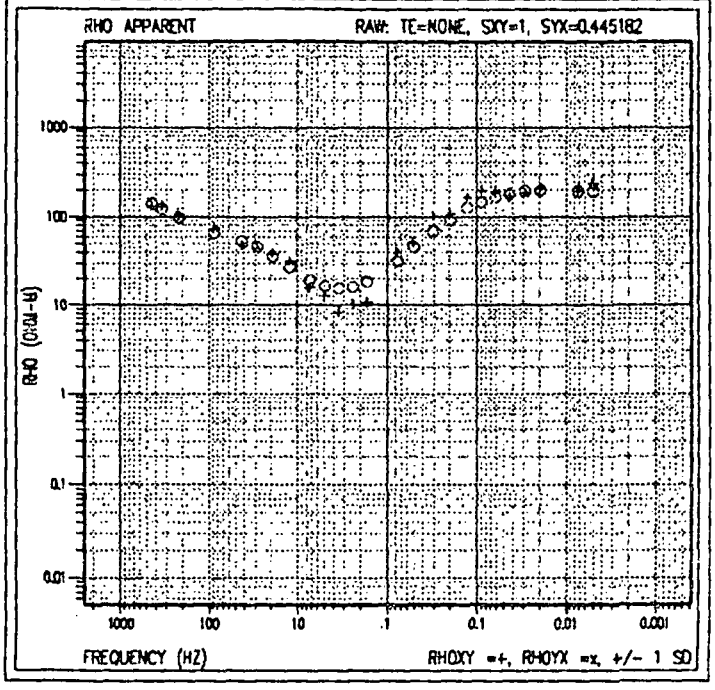


cebuco–s49

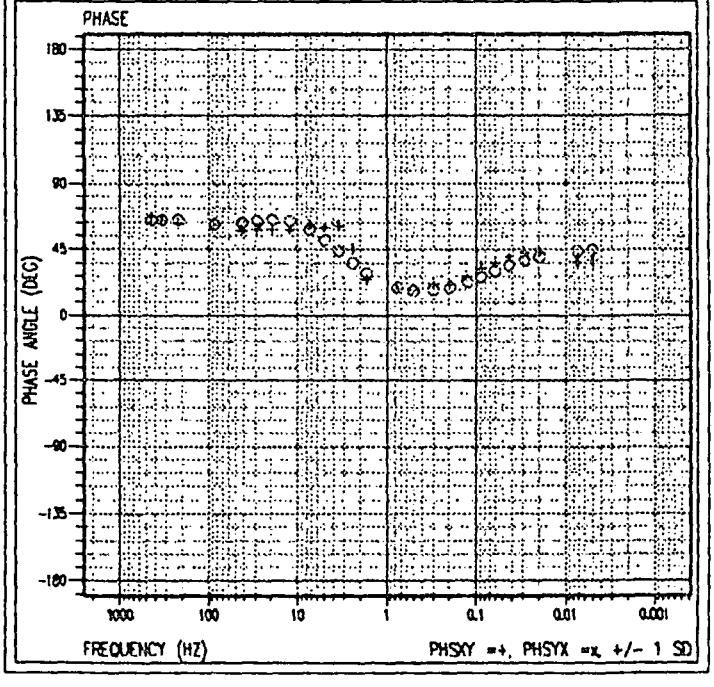

cebuco-s50

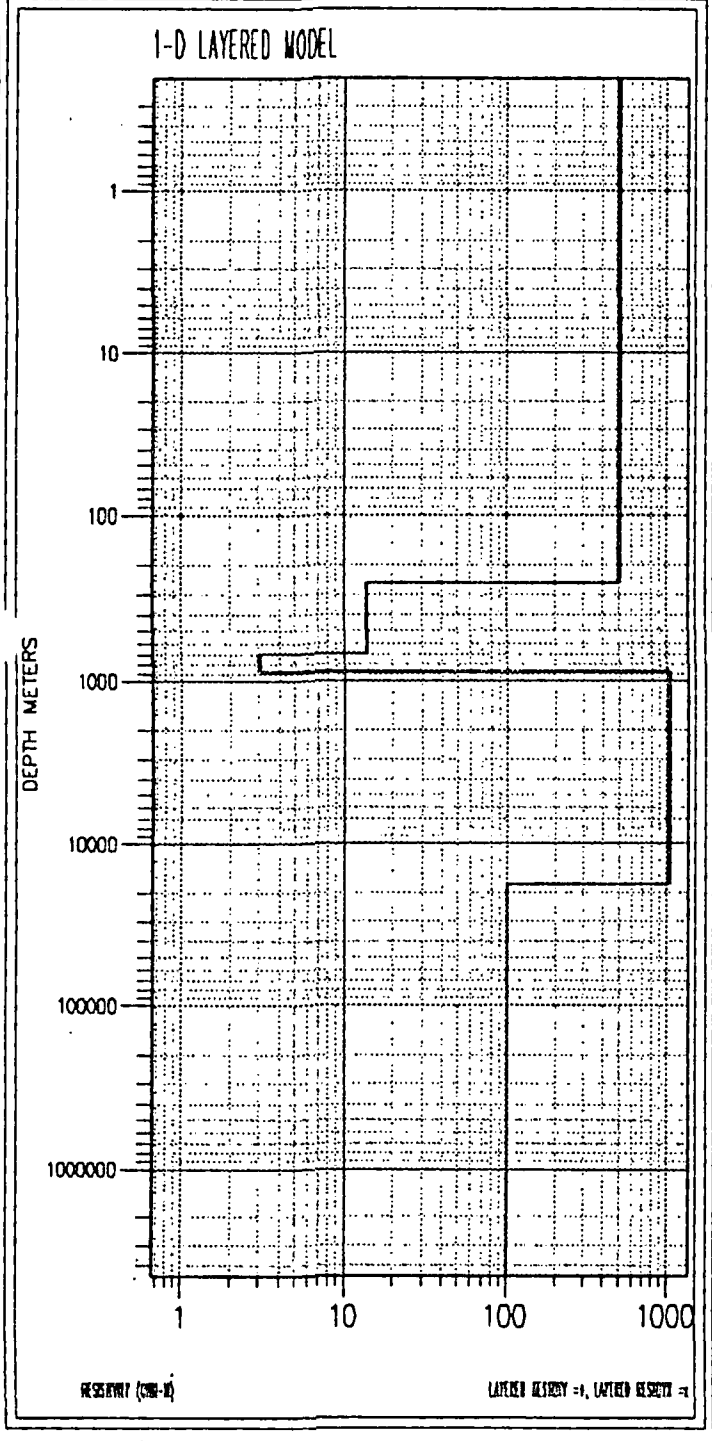


cebuco-s50

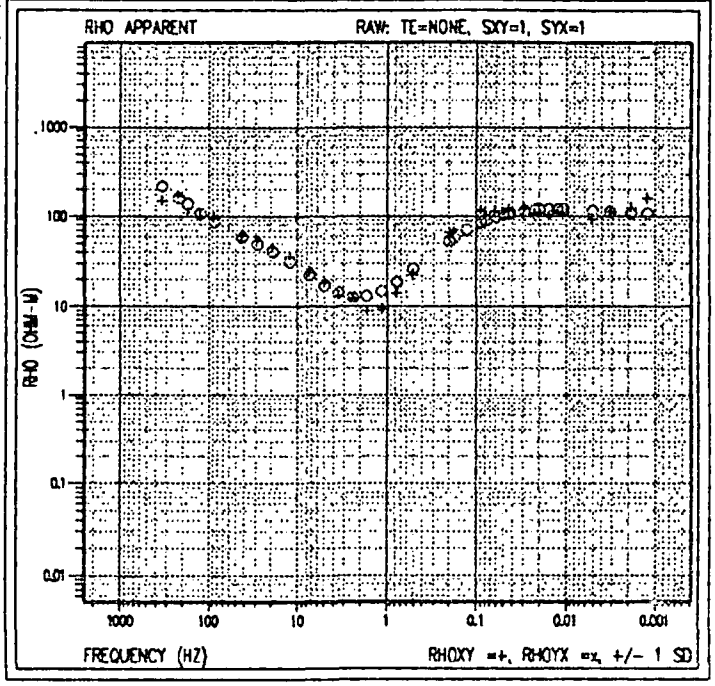


cebuco-s50

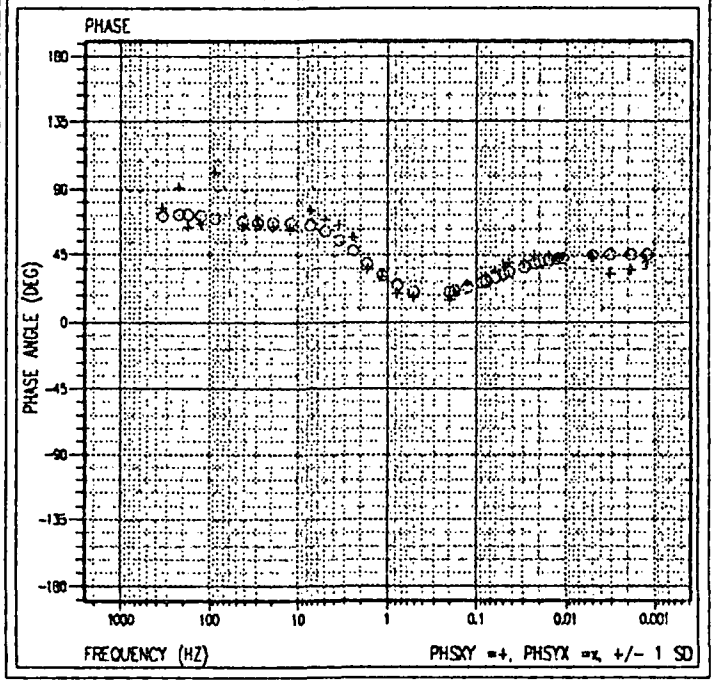

cebuco-s54

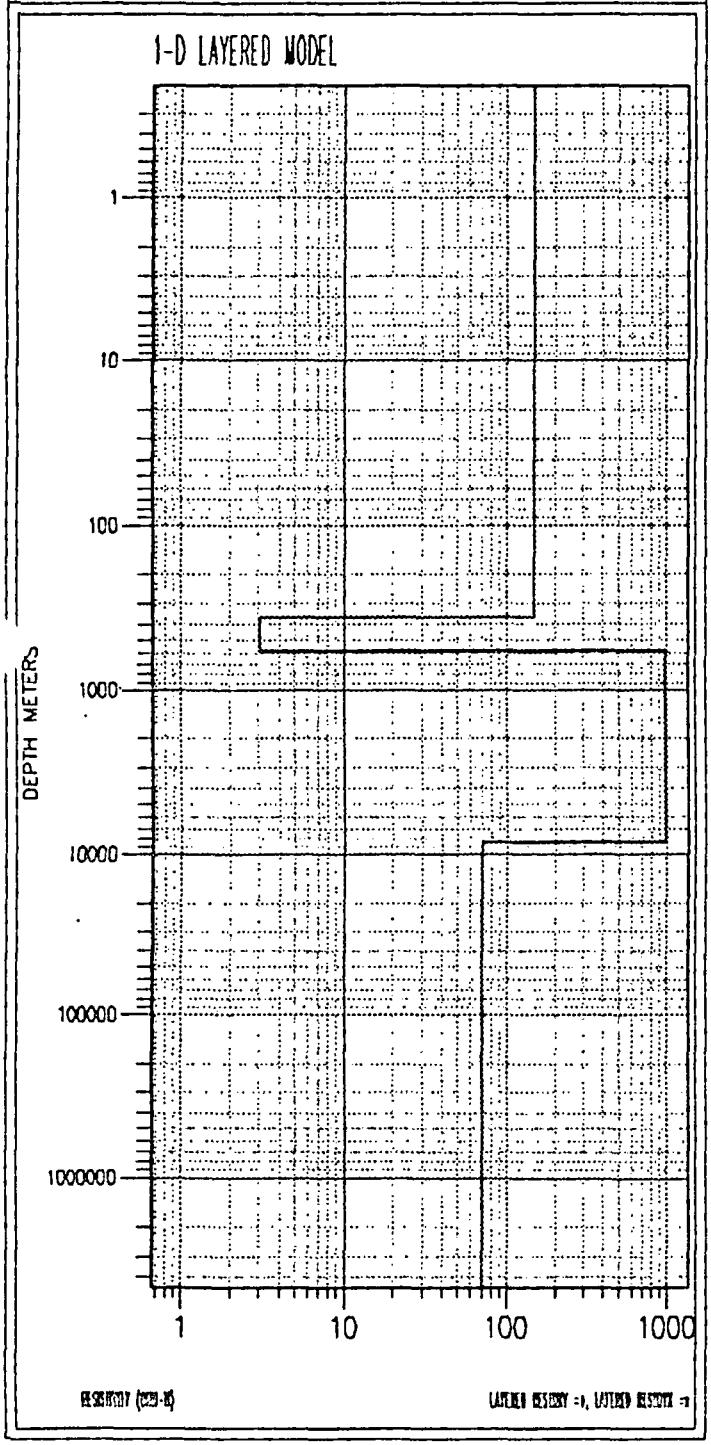


cebuco-s54

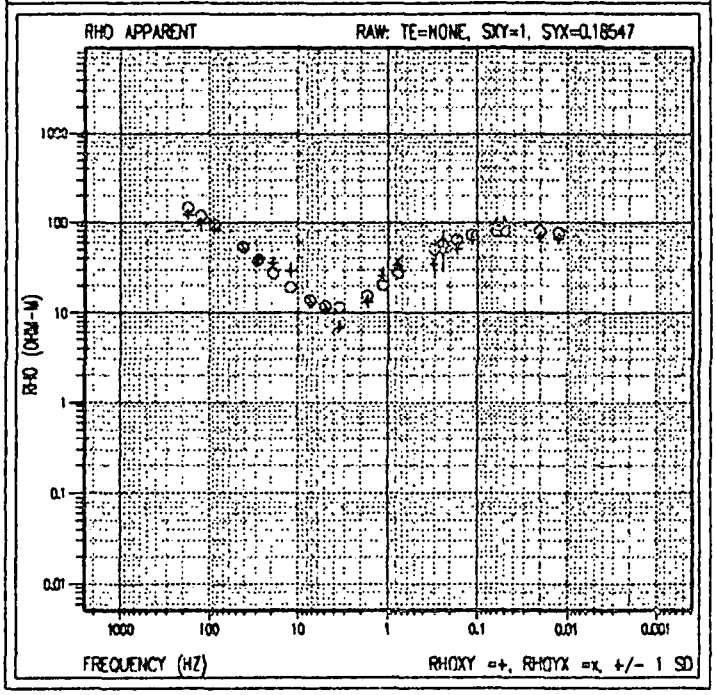


cebuco-s54

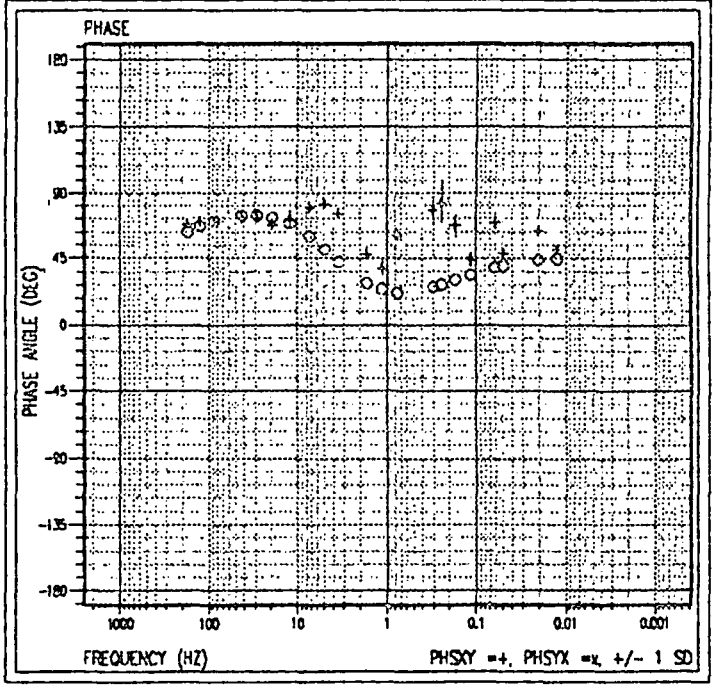

cebuco-s55

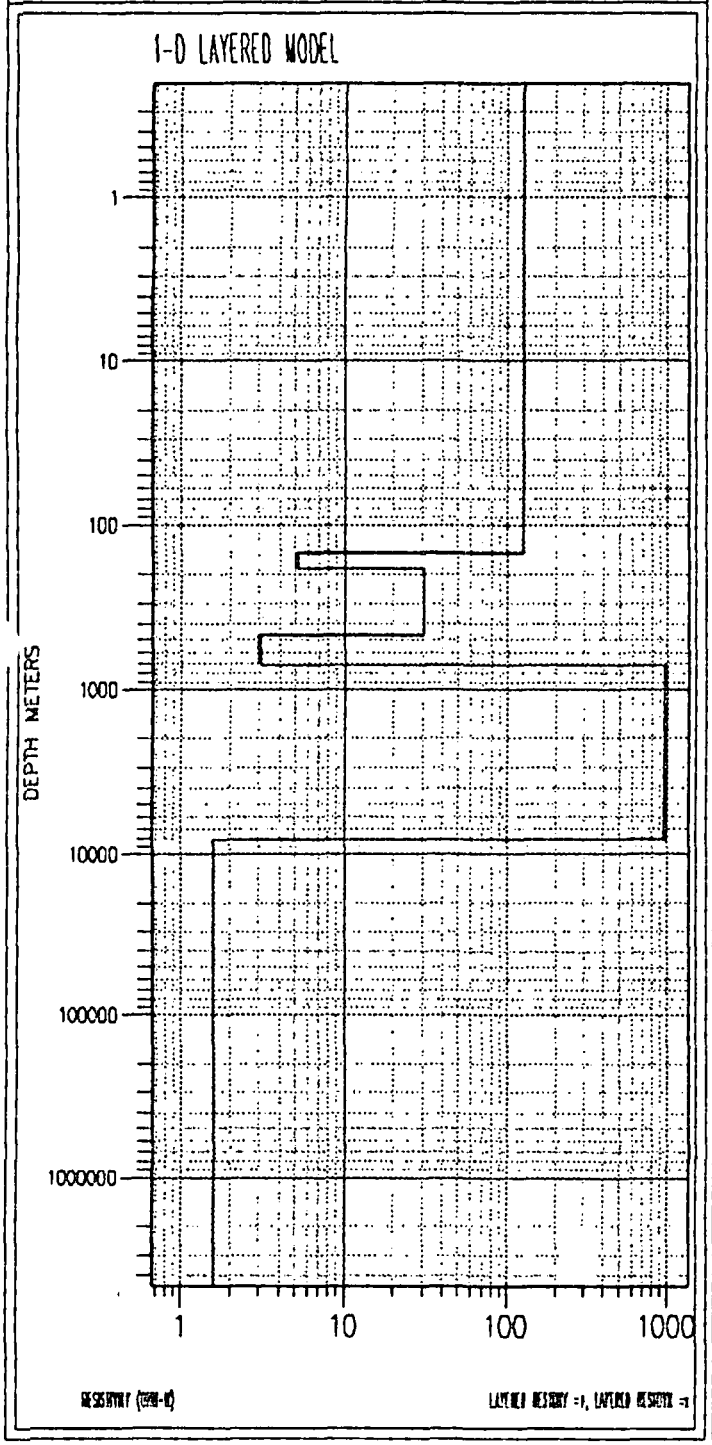


cebuco-s55

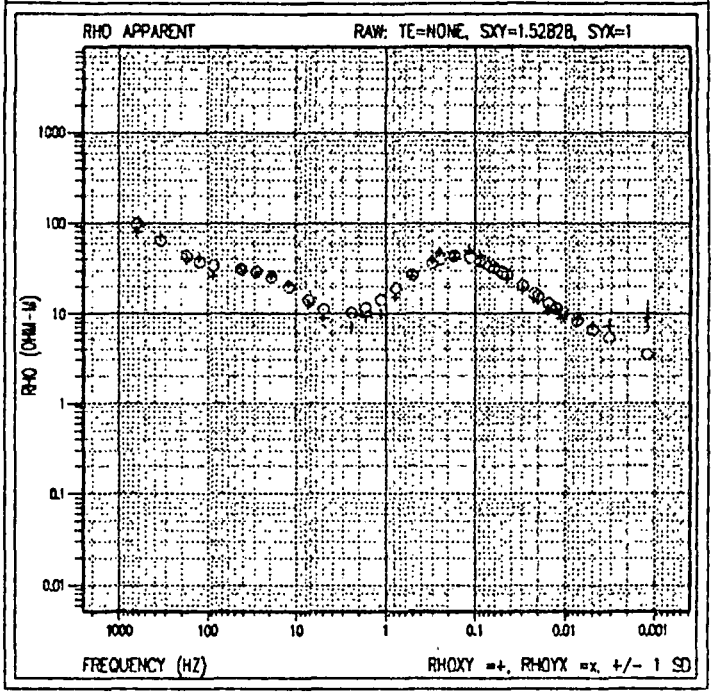


cebuco-s55

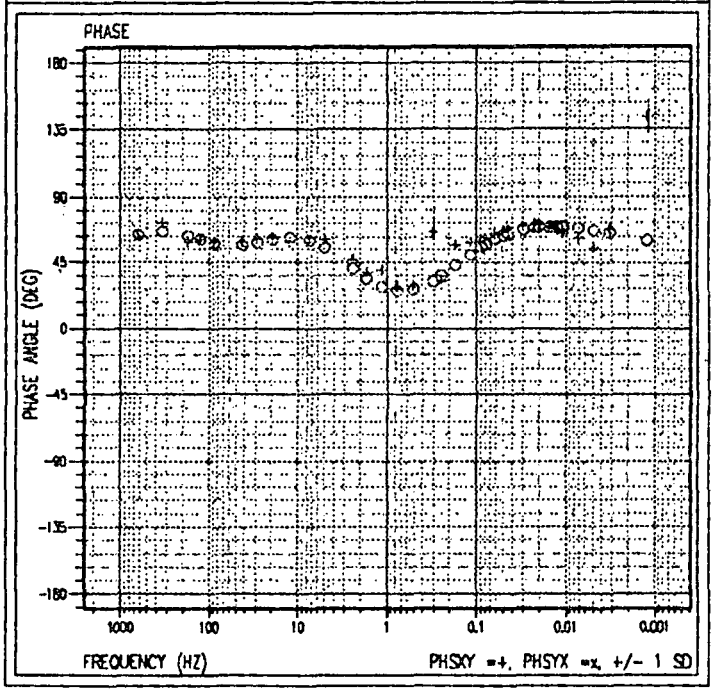

cebuco–s56

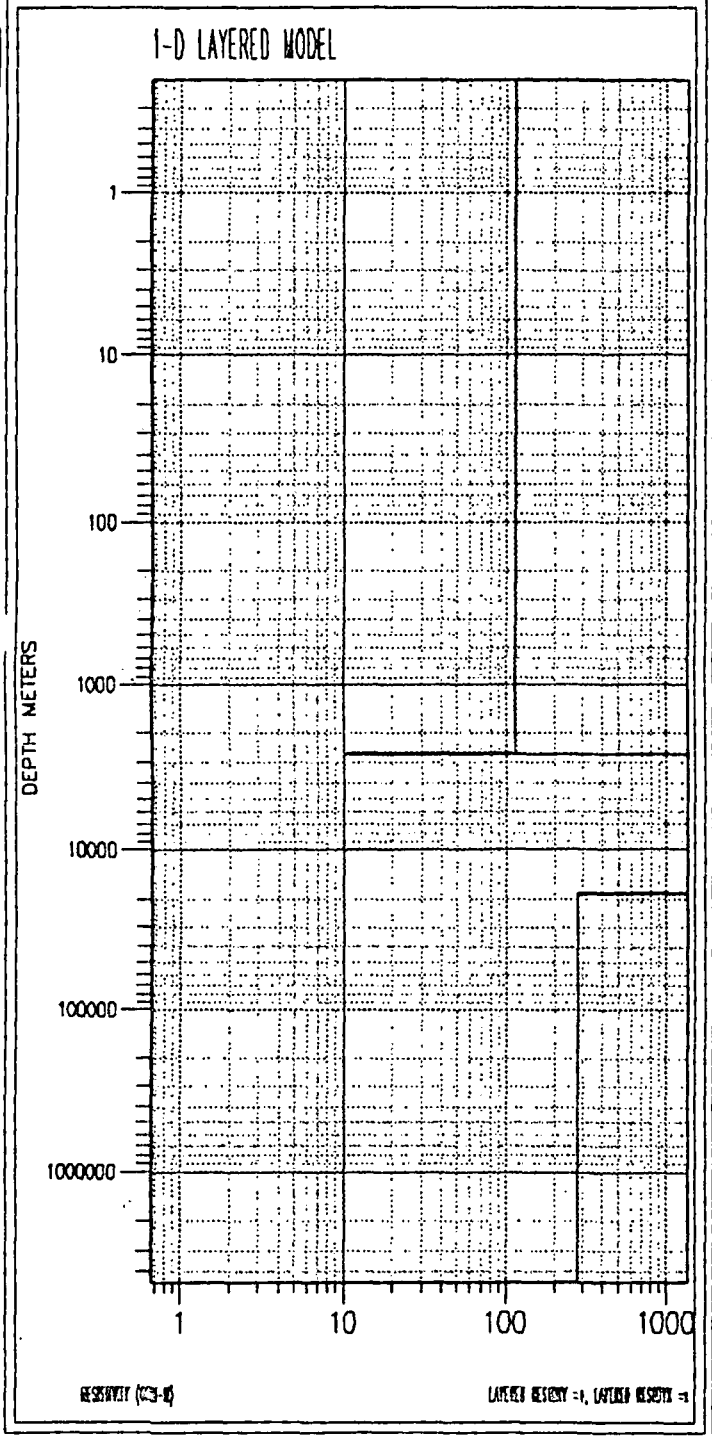


cebuco–s56

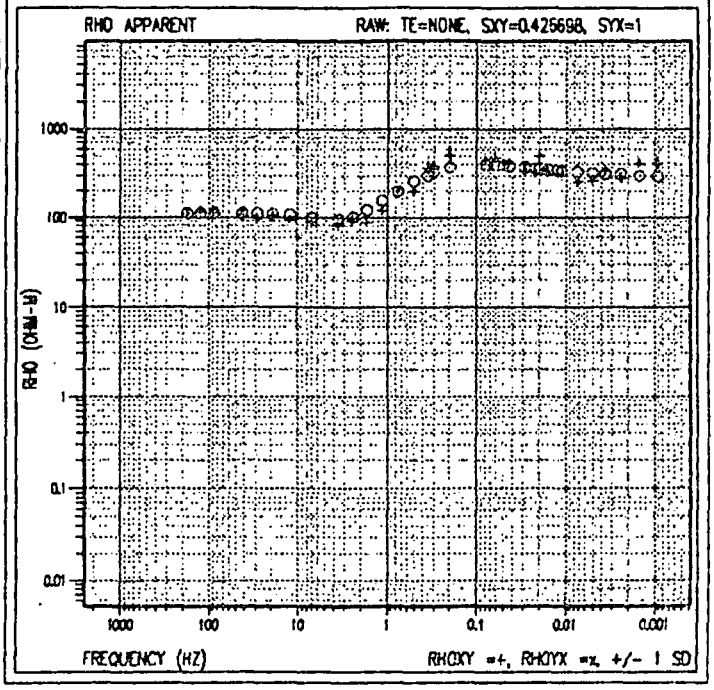


cebuco–s56

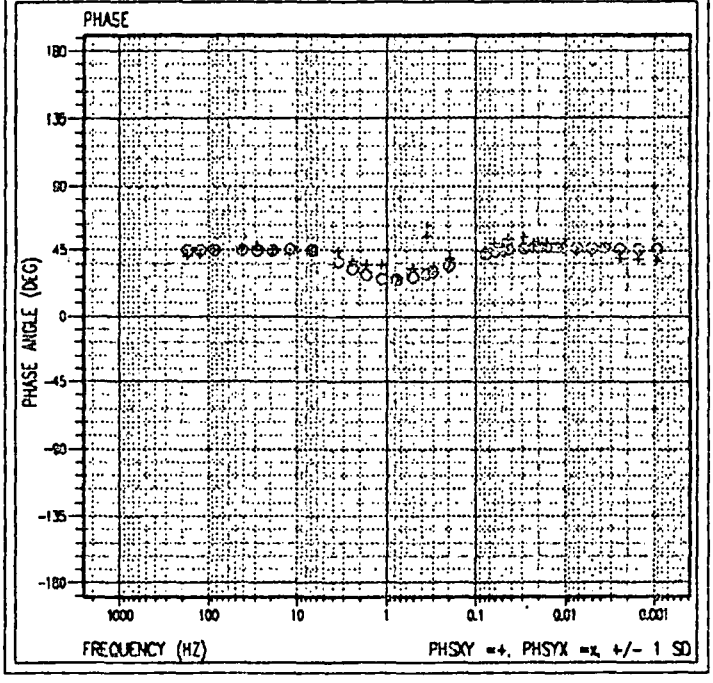

cebuco-s57

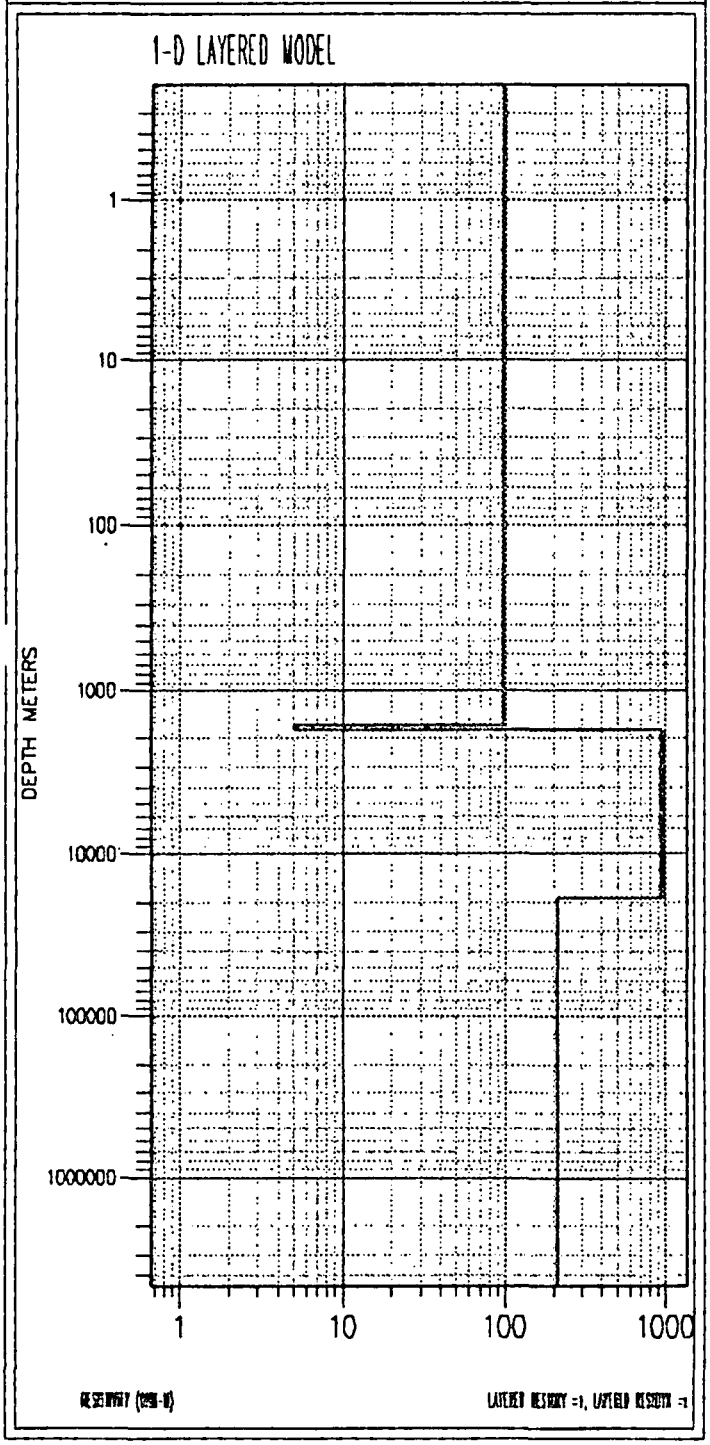


cebuco-s57

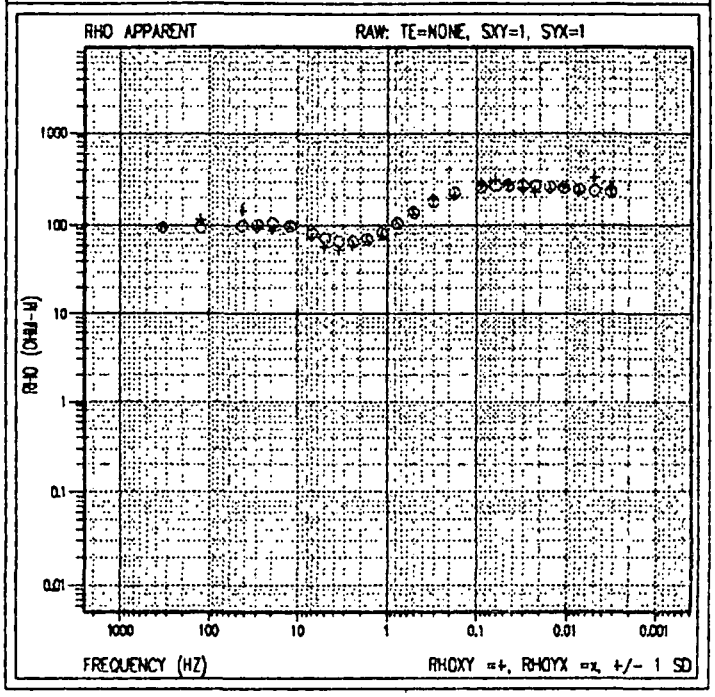


cebuco-s57

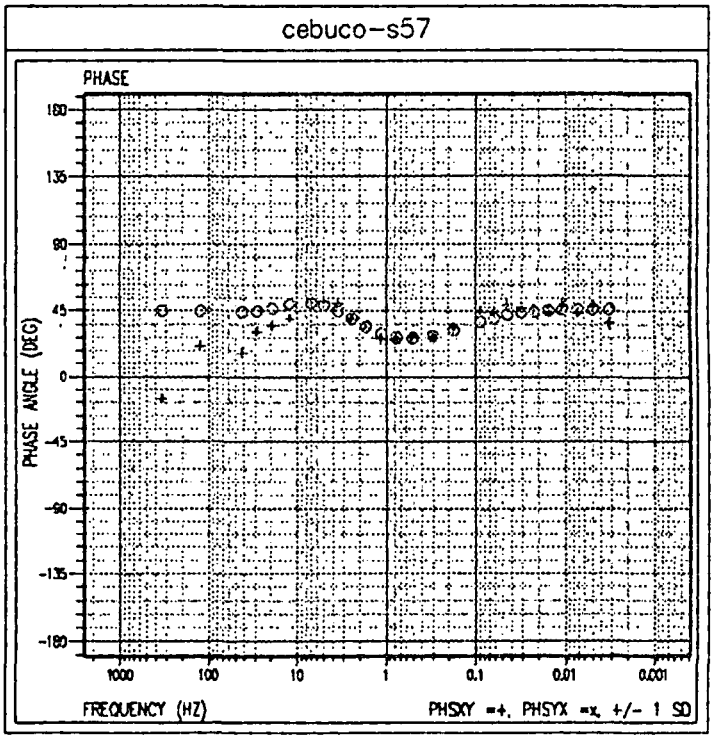

cebuco–s58

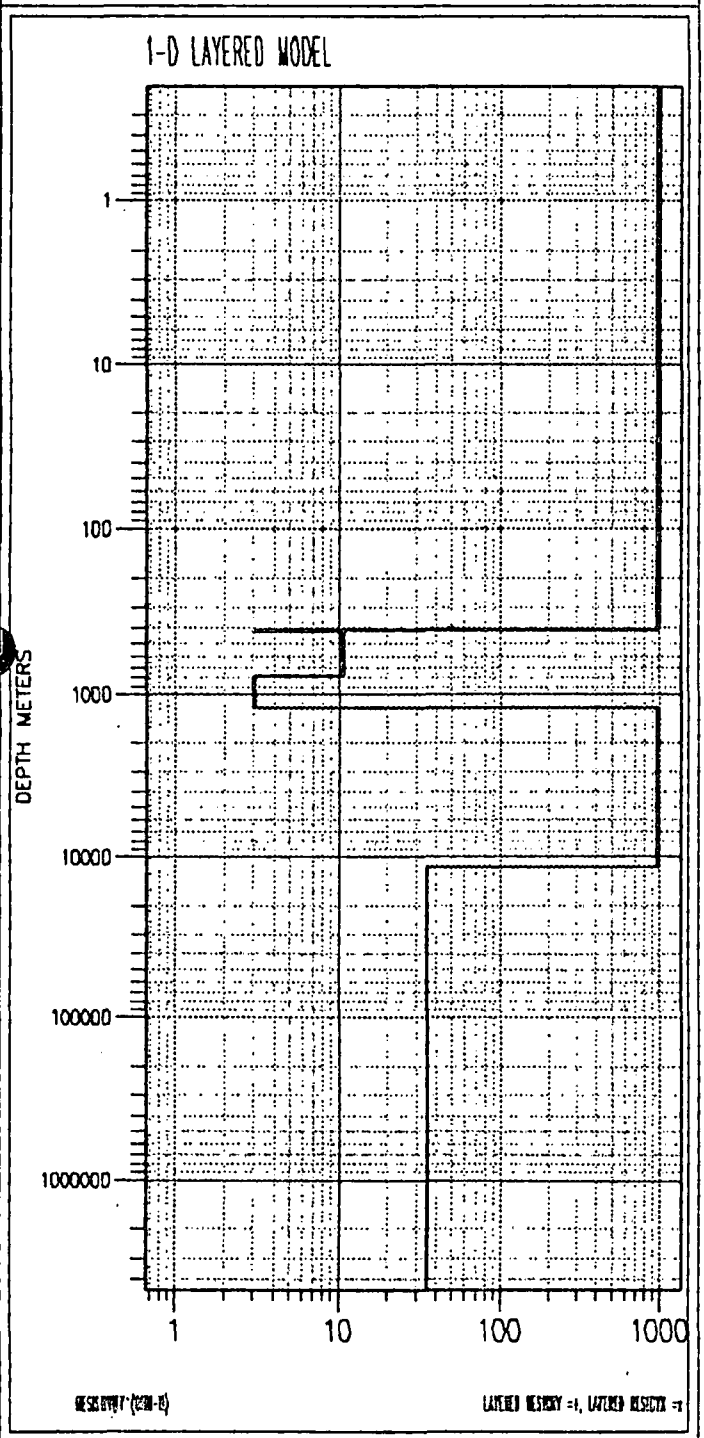


cebuco–s58

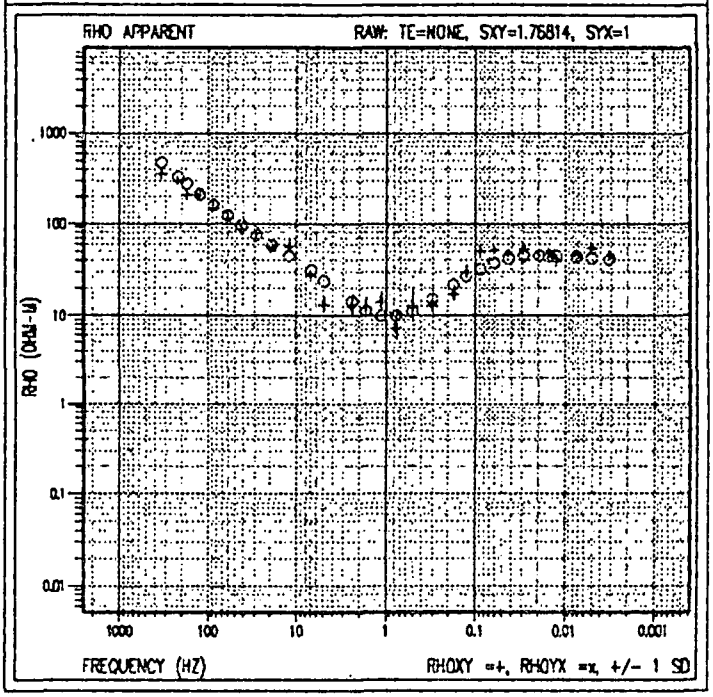


cebuco–s58

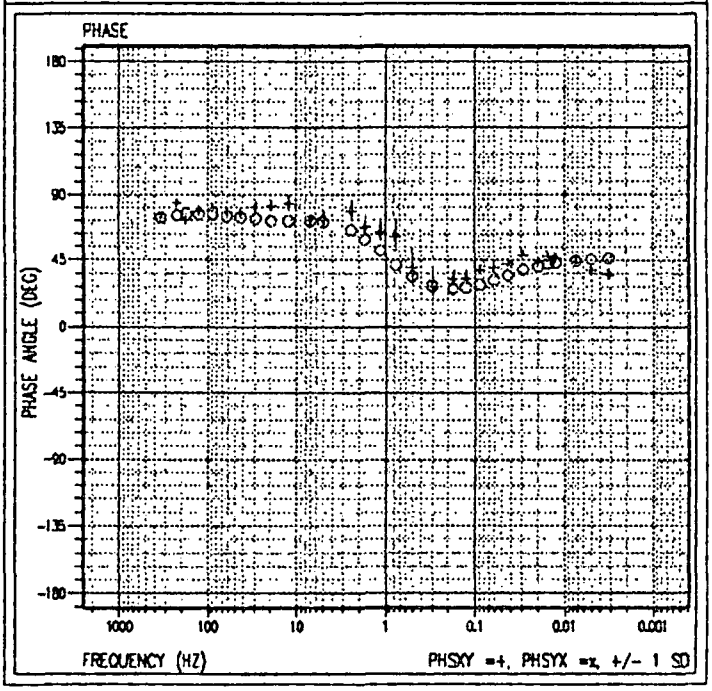

cebuco-s59

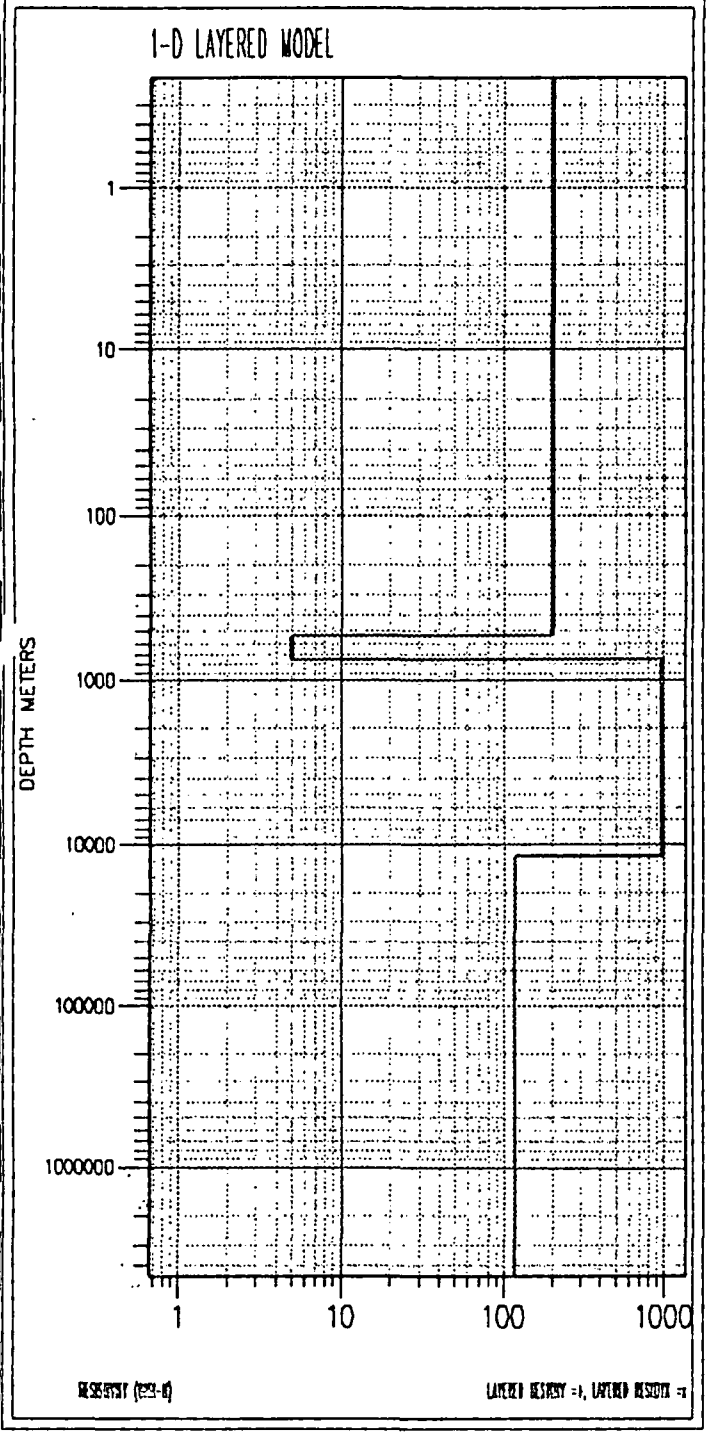


cebuco-s59

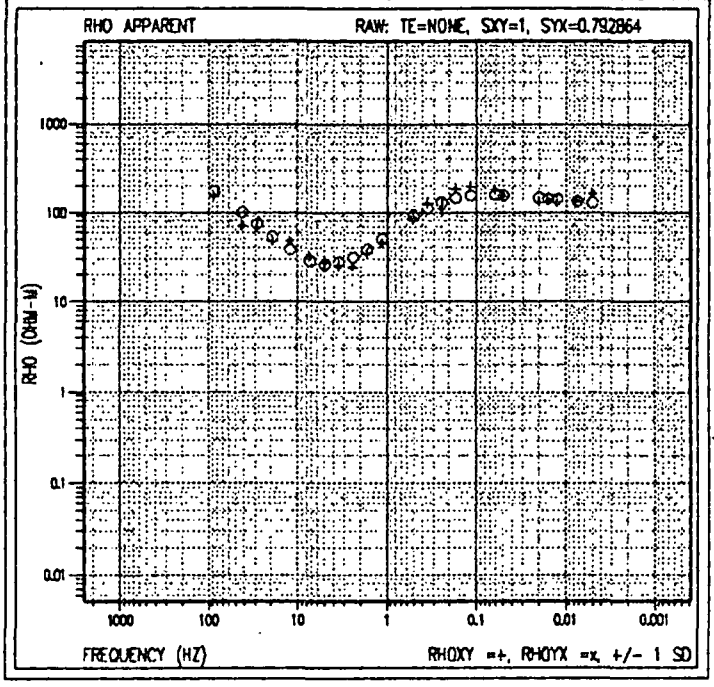


cebuco-s59

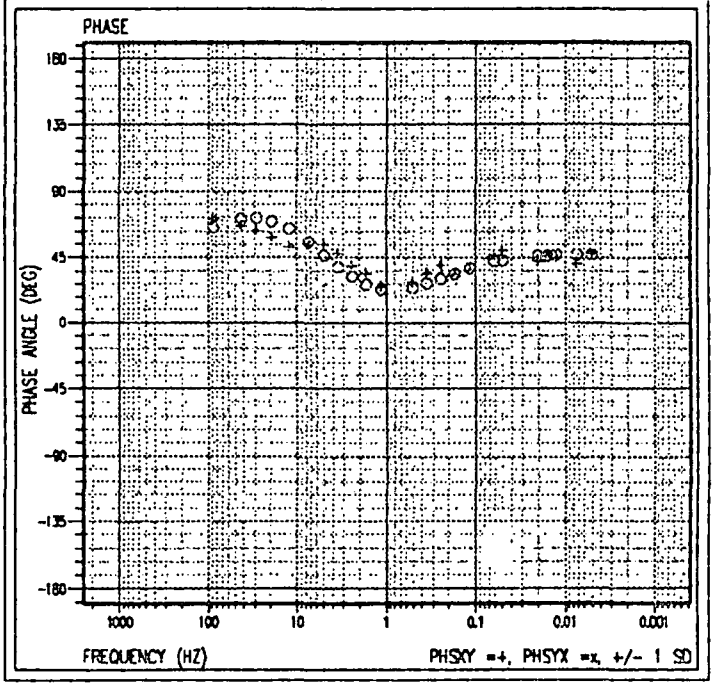

cebuco–s60

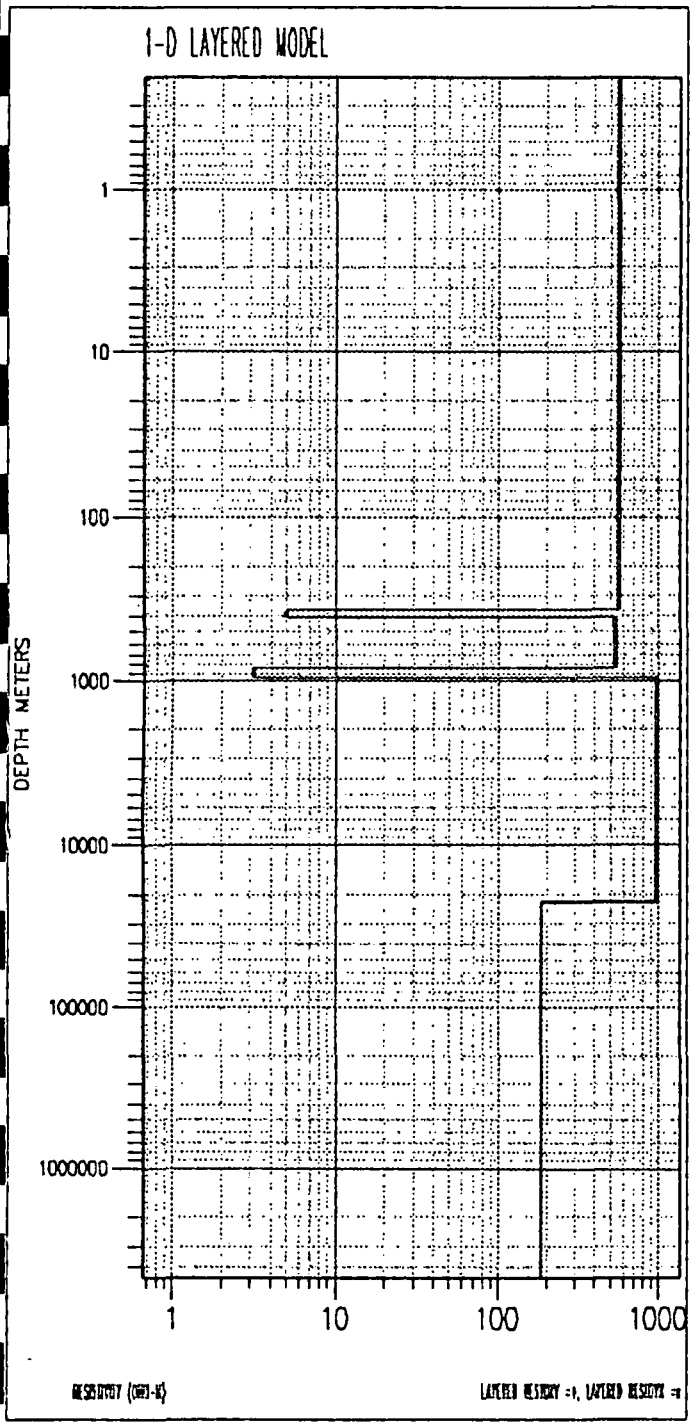


cebuco–s60

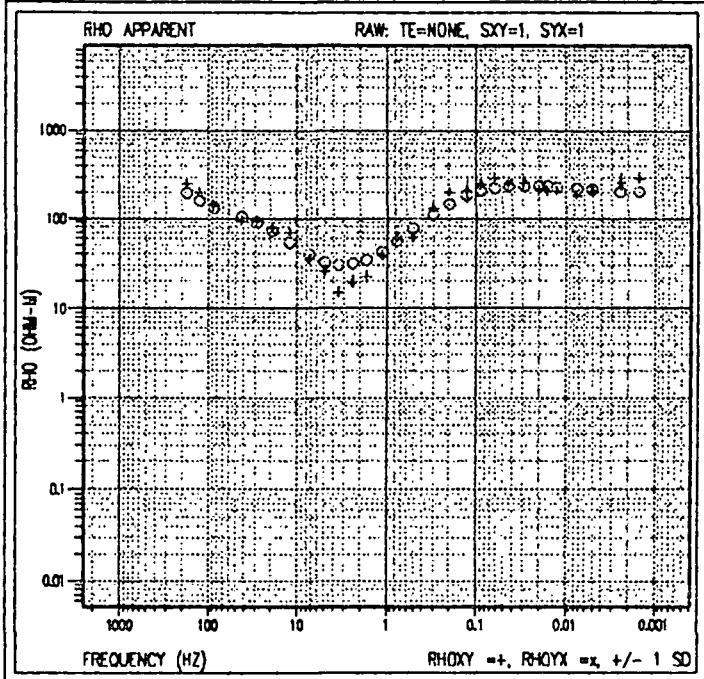


cebuco–s60

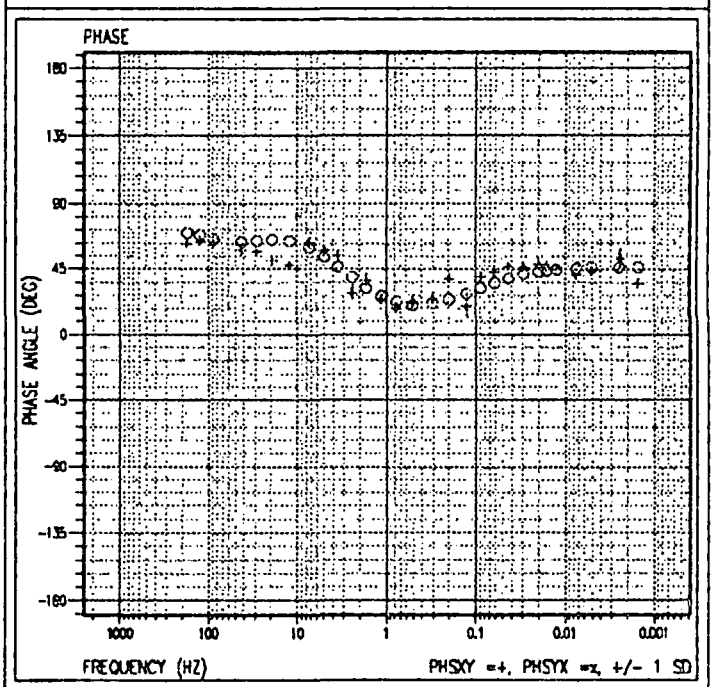

cebuco–s61

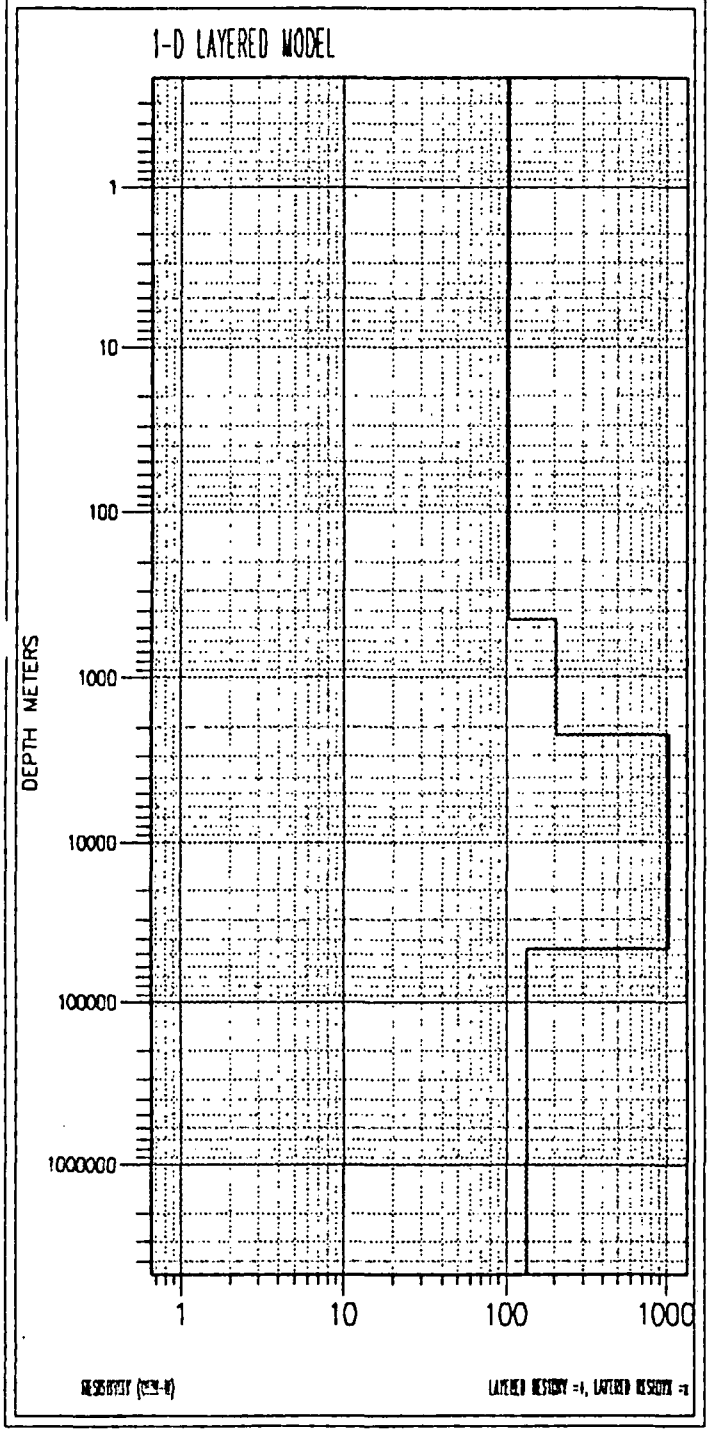


cebuco–s61

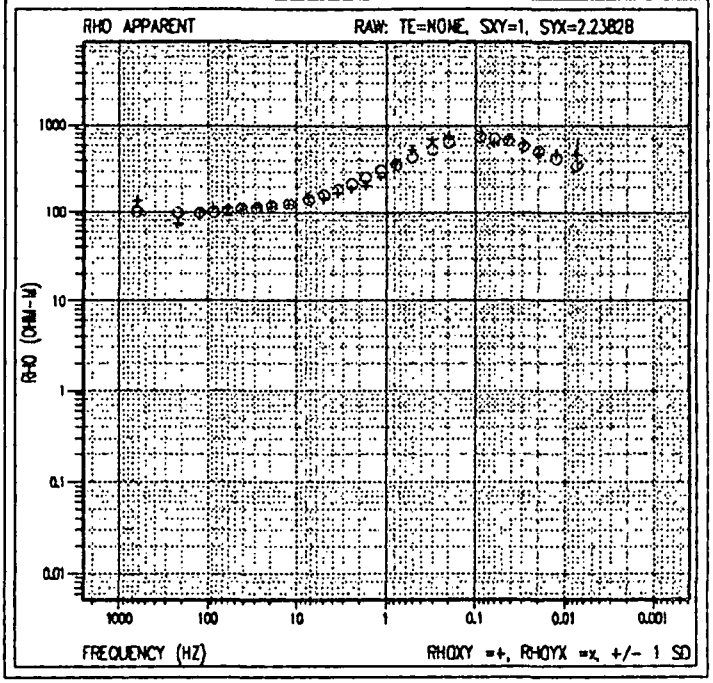


cebuco–s61

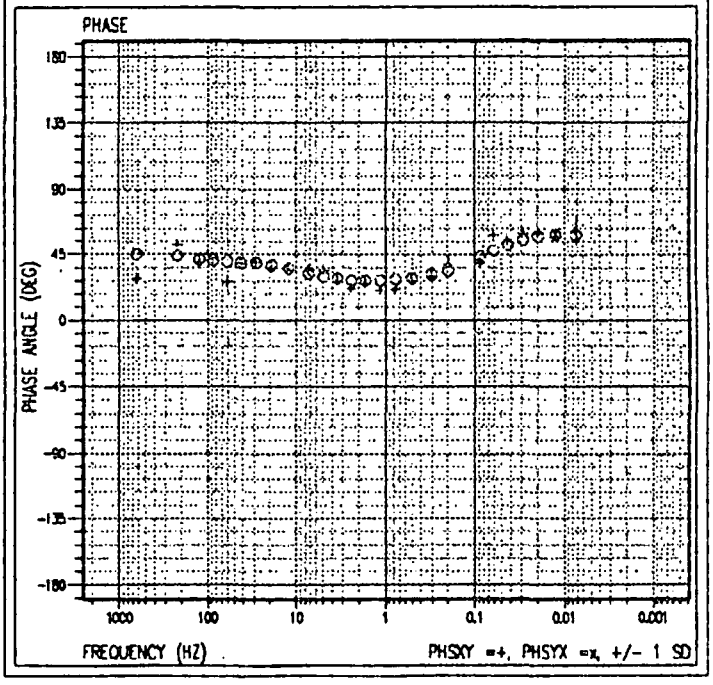

cebuco–s63

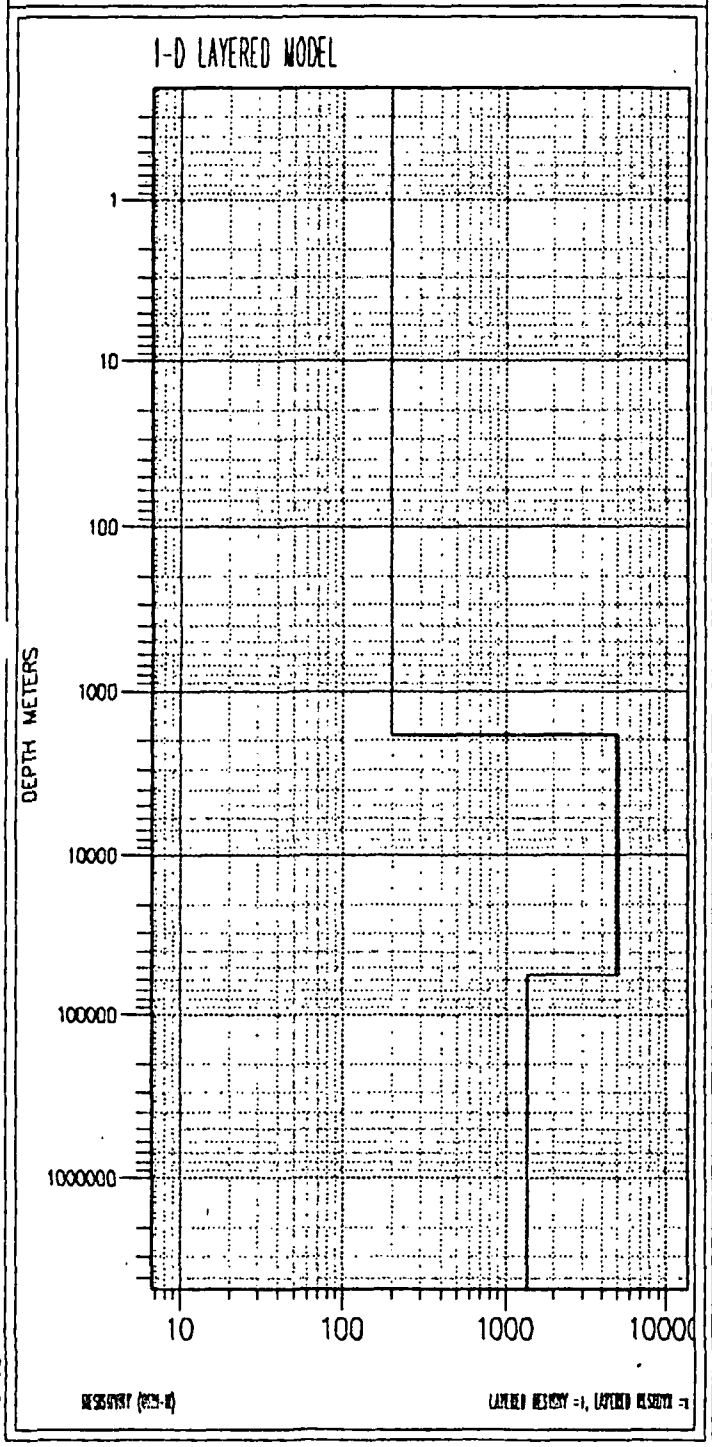


cebuco–s63

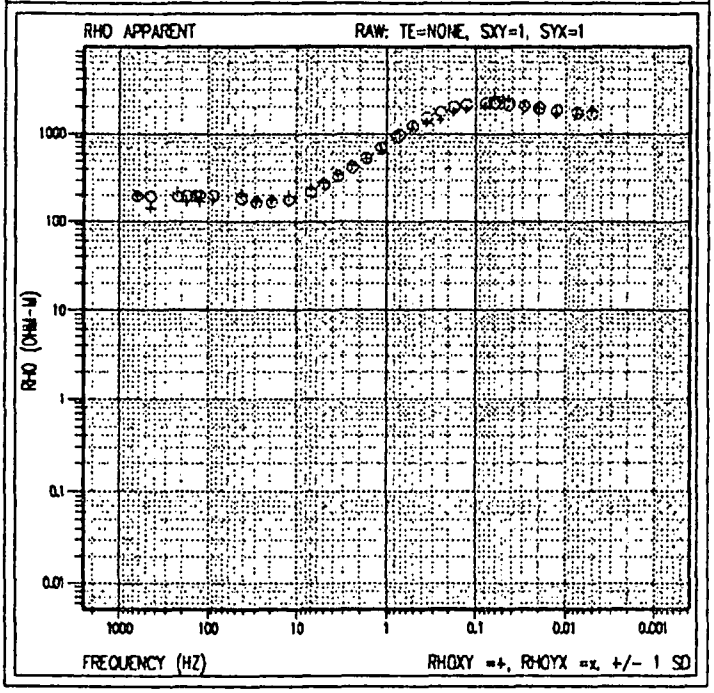


cebuco–s63

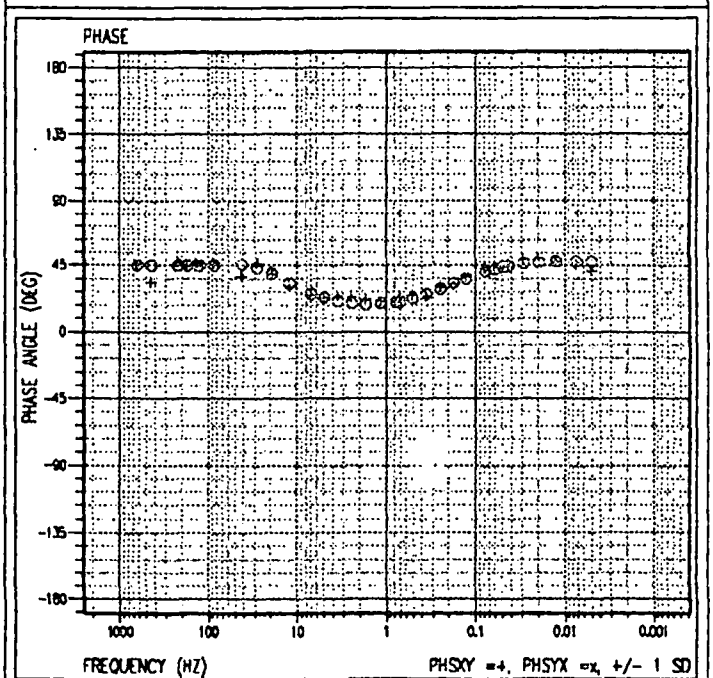

cebuco–s64

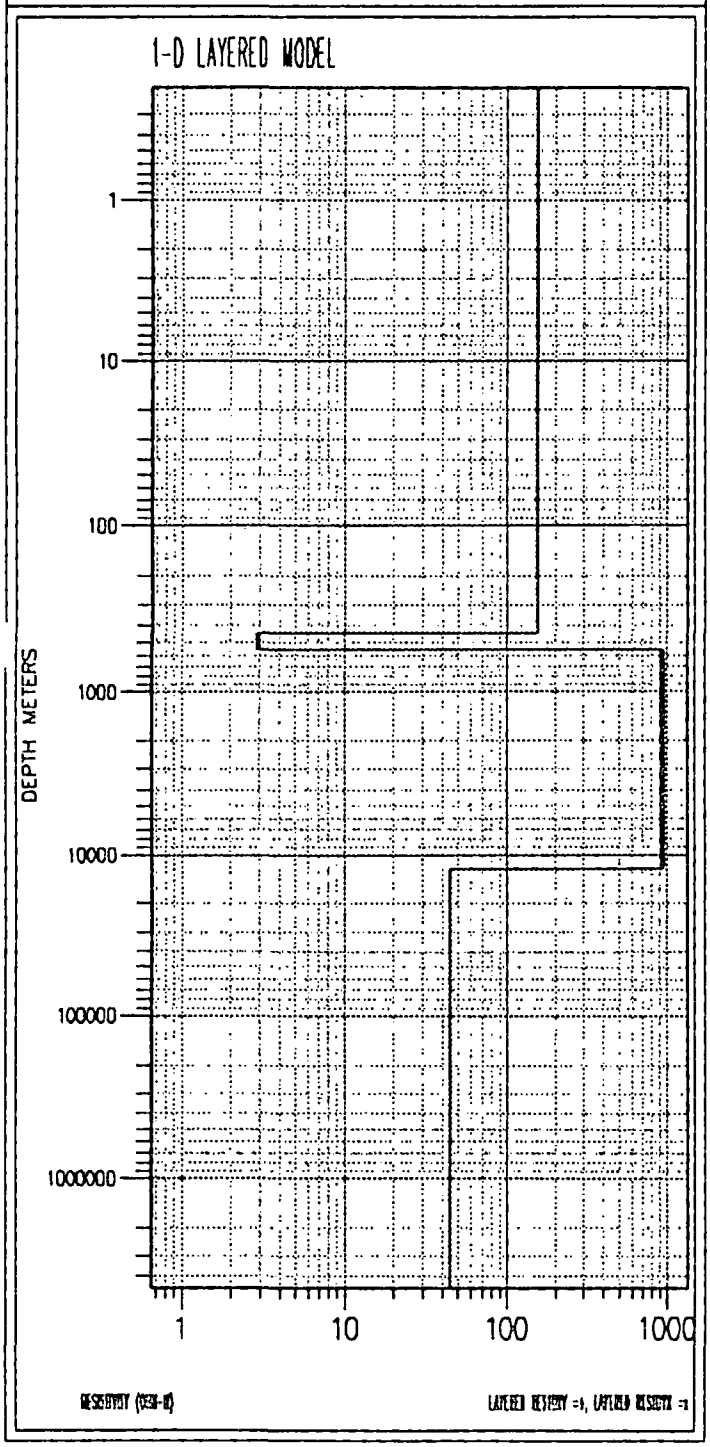


cebuco–s64

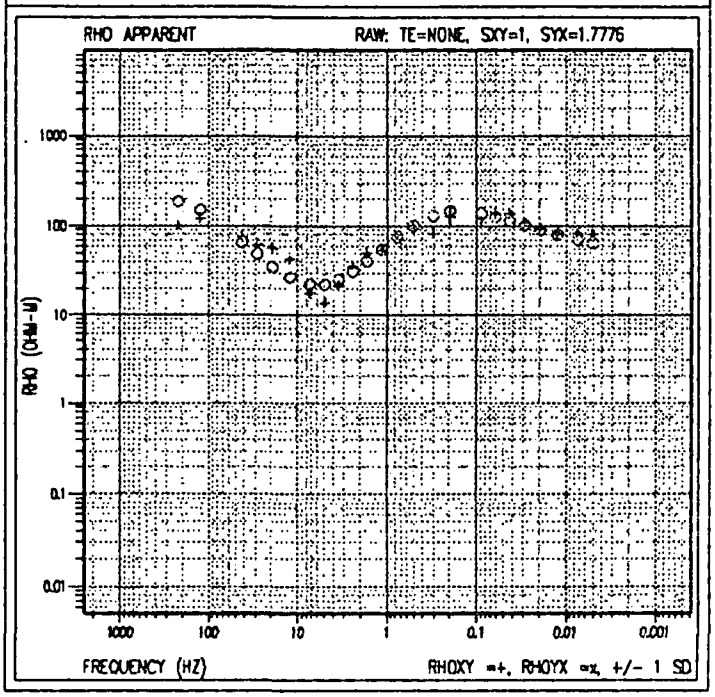


cebuco–s64

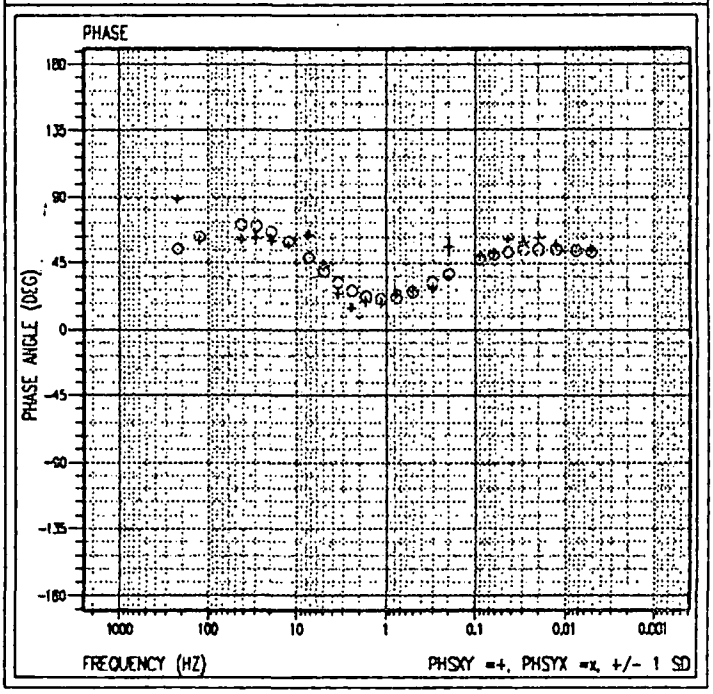

cebuco–s65

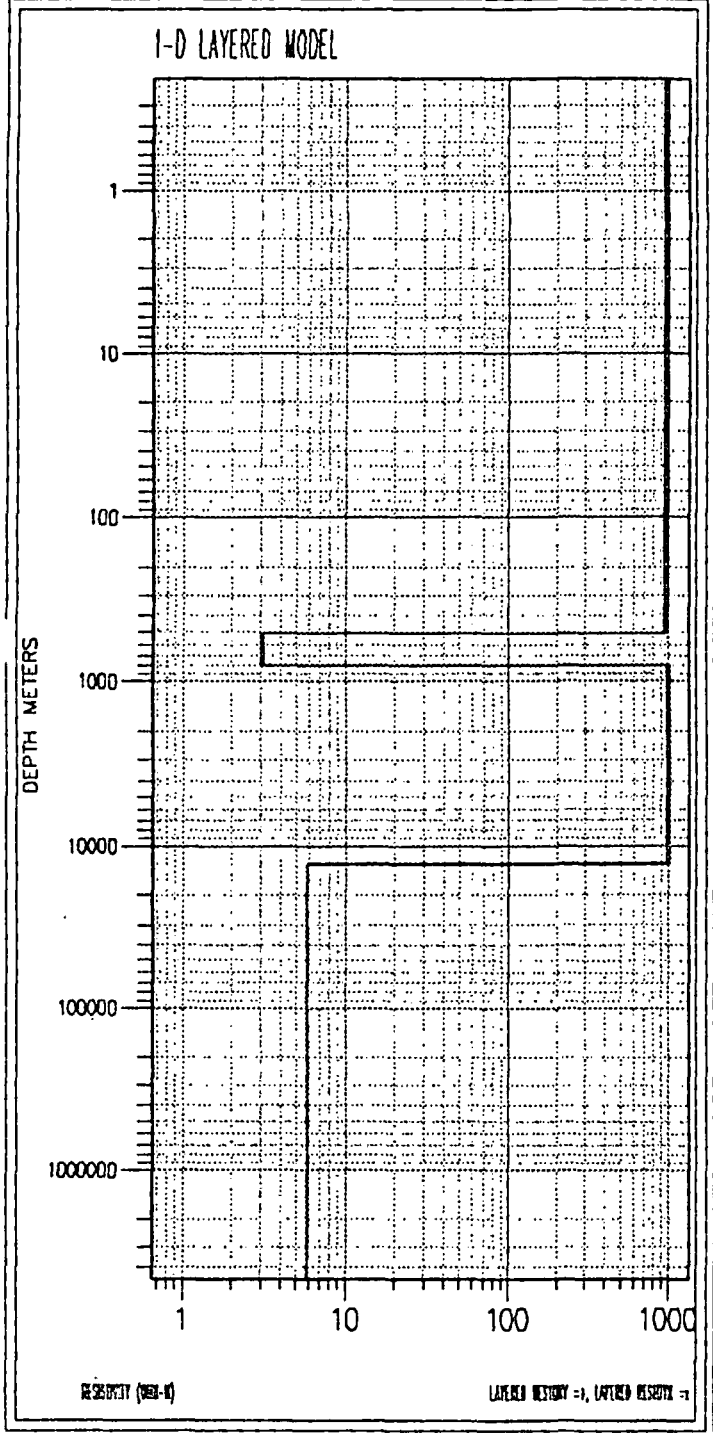


cebuco–s65

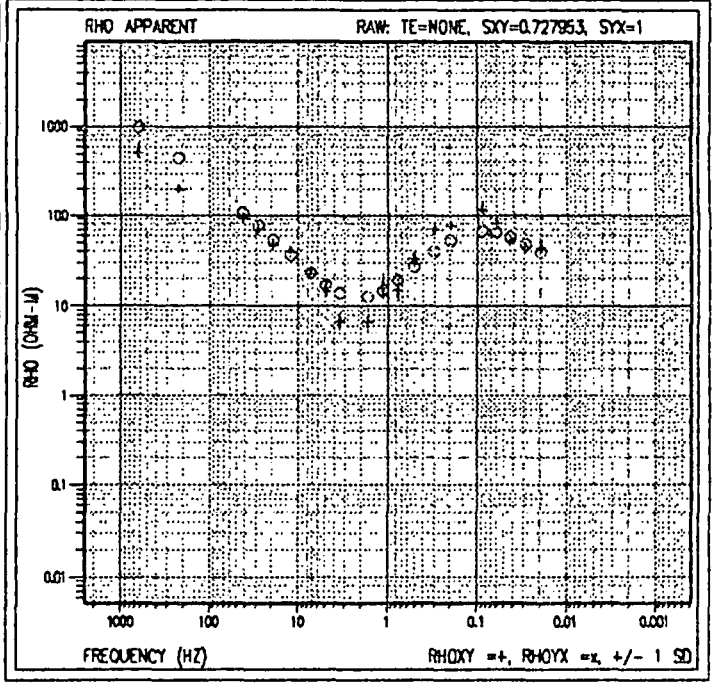


cebuco–s65

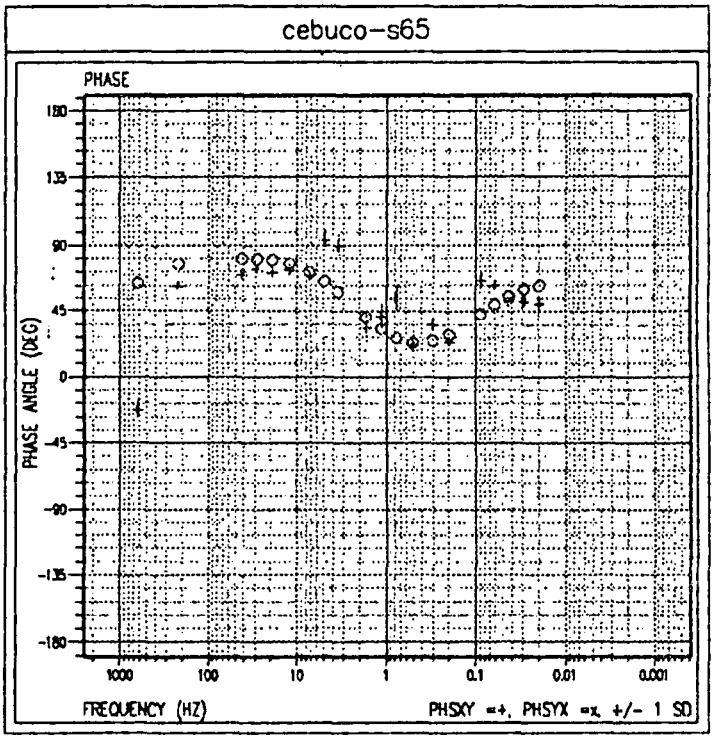

cebuco–s66

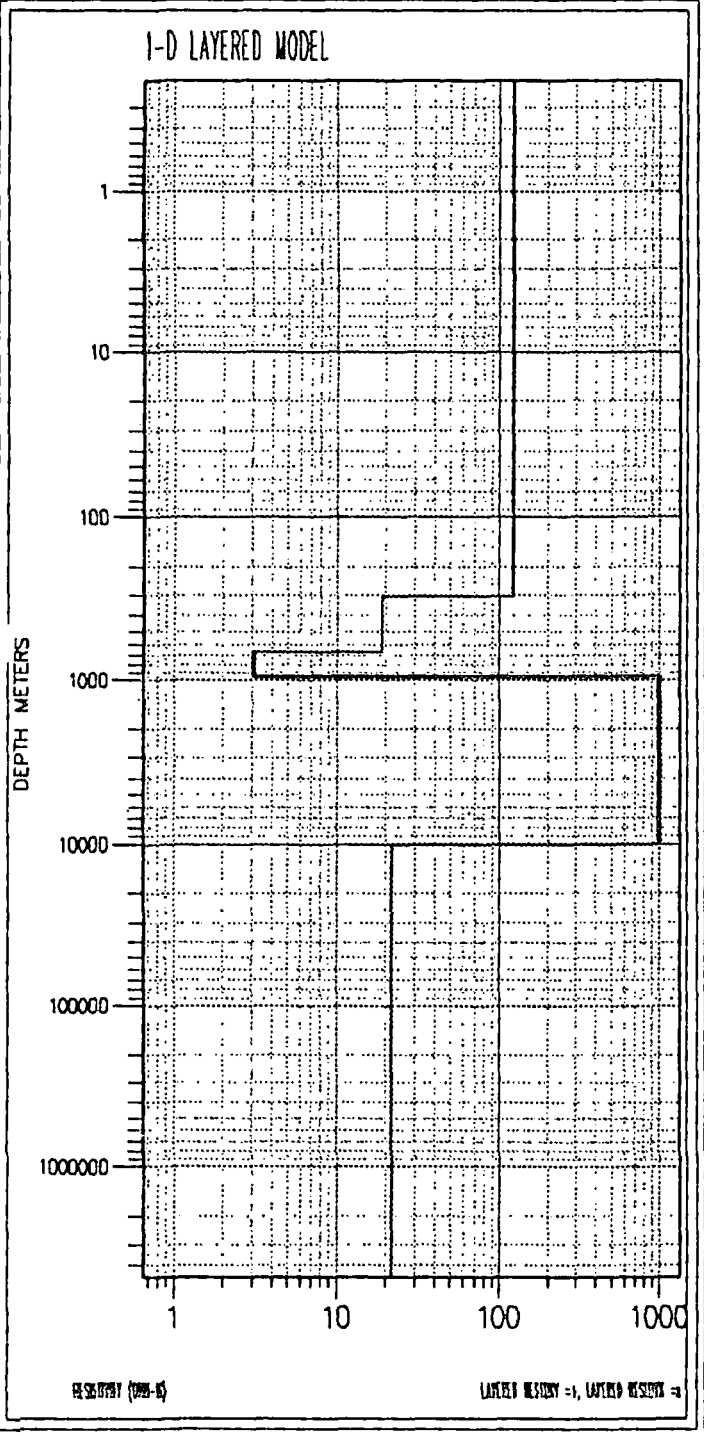


cebuco–s66

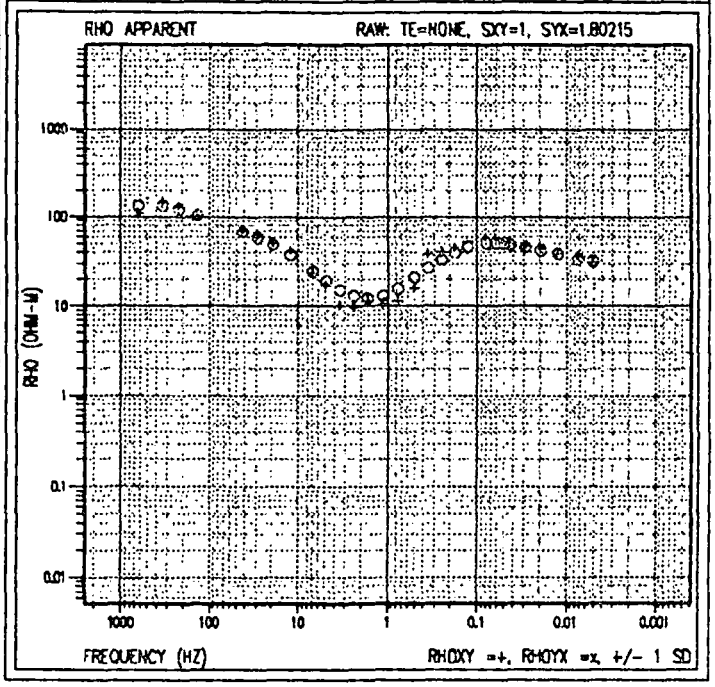


cebuco–s66

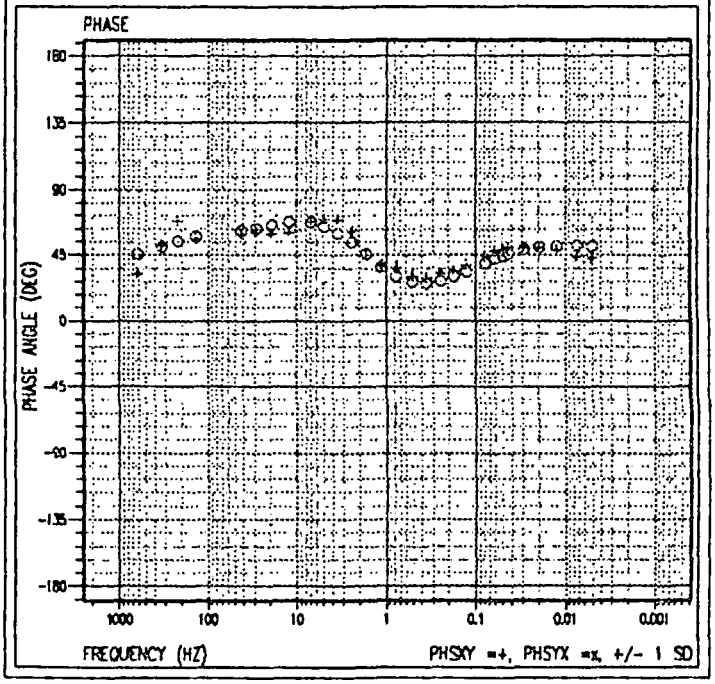

cebuco-s67

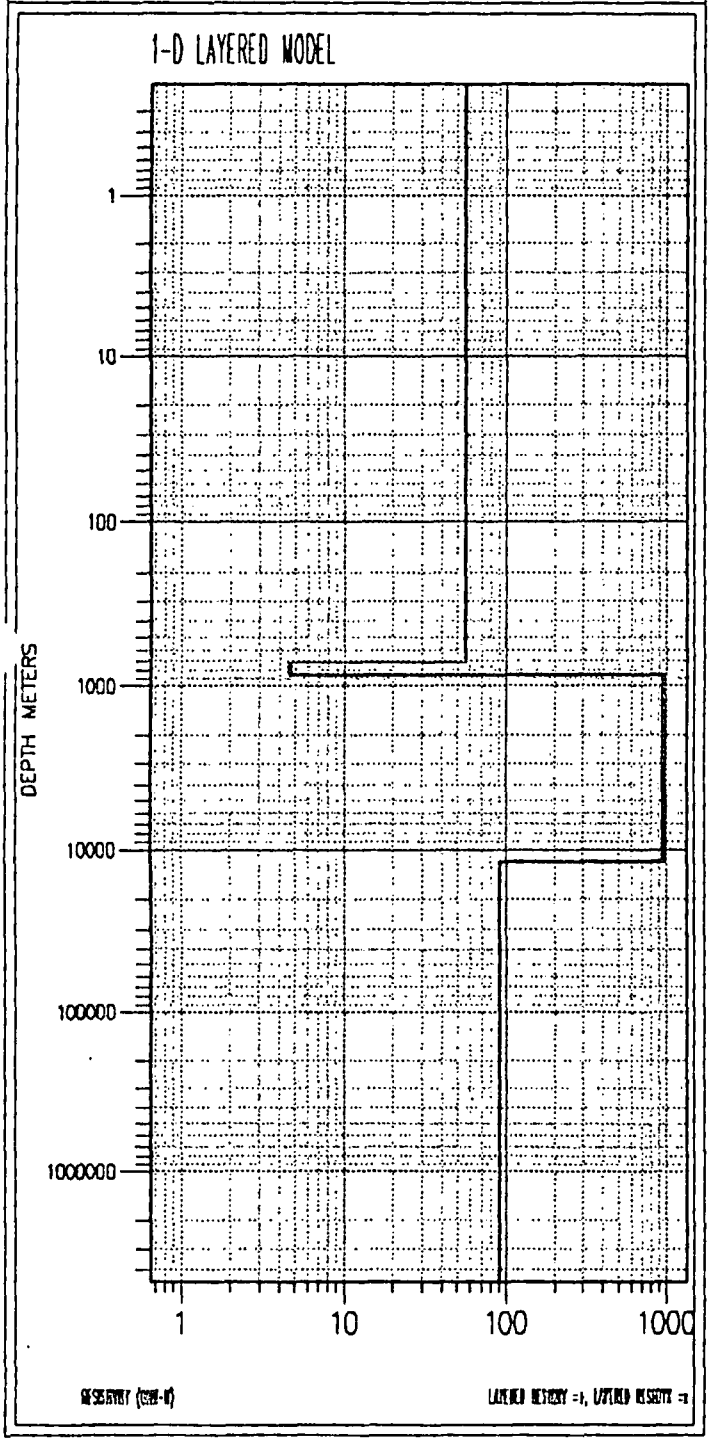


cebuco-s67

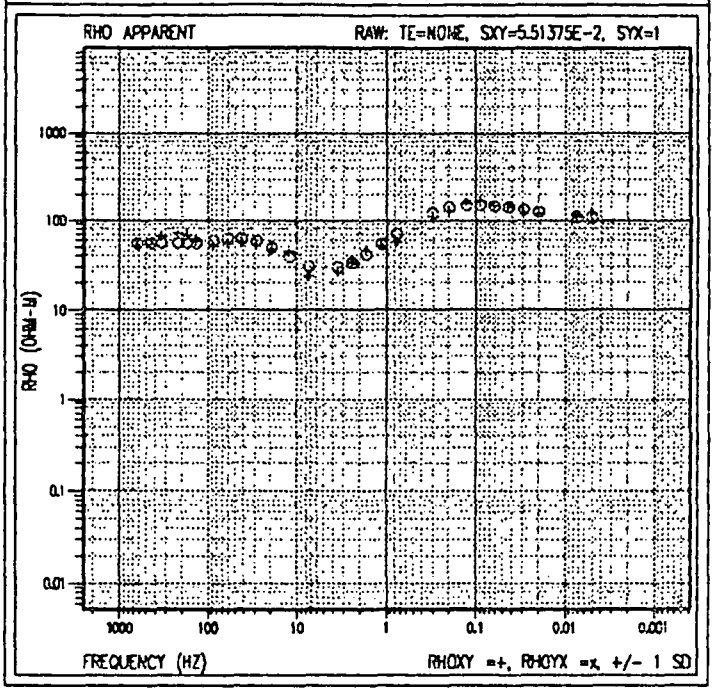


cebuco-s67

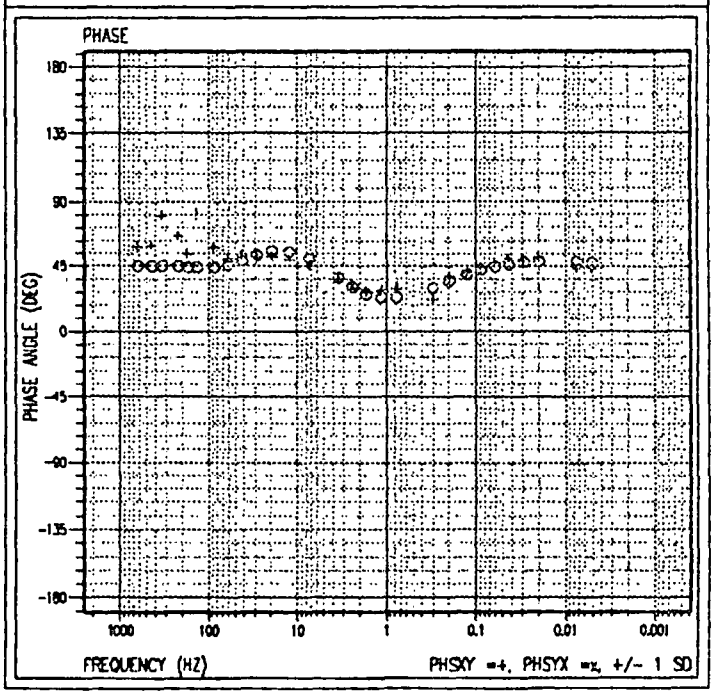

cebuco–s68

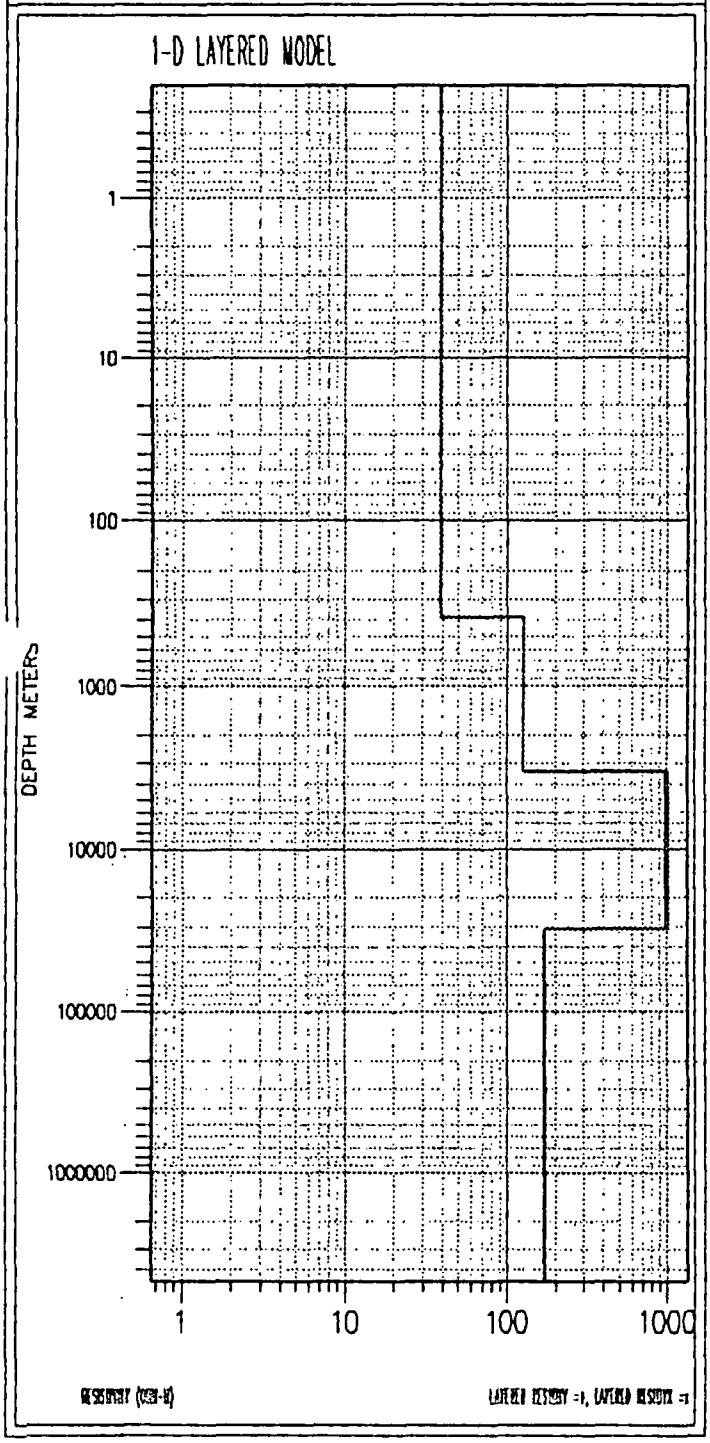


cebuco–s68

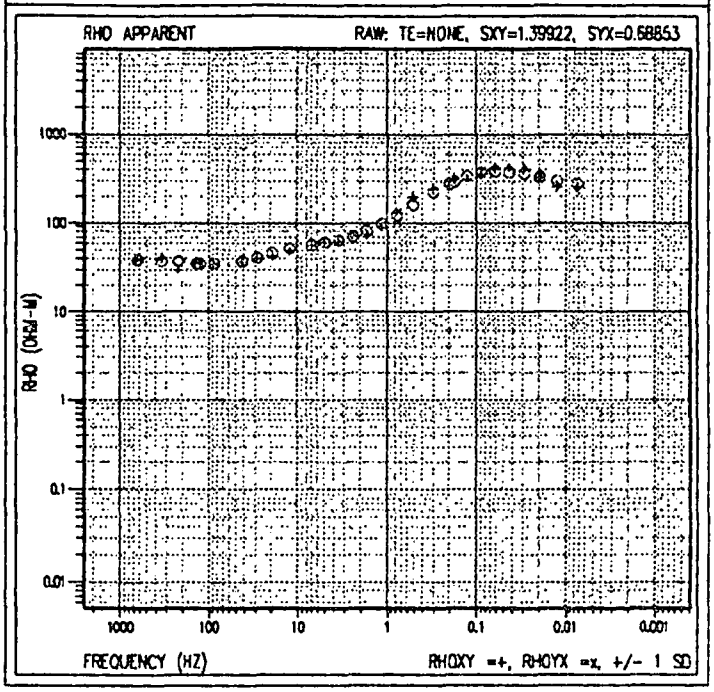


cebuco–s68

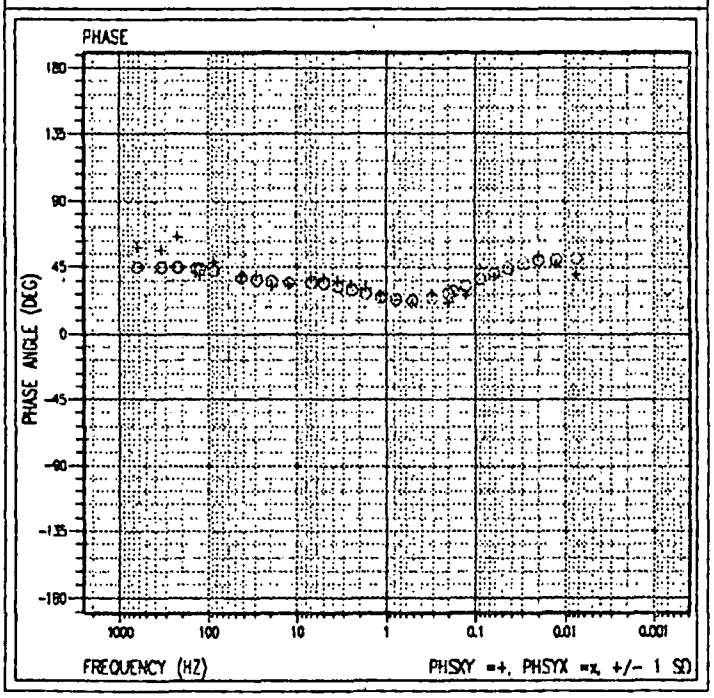

cebuco–s69

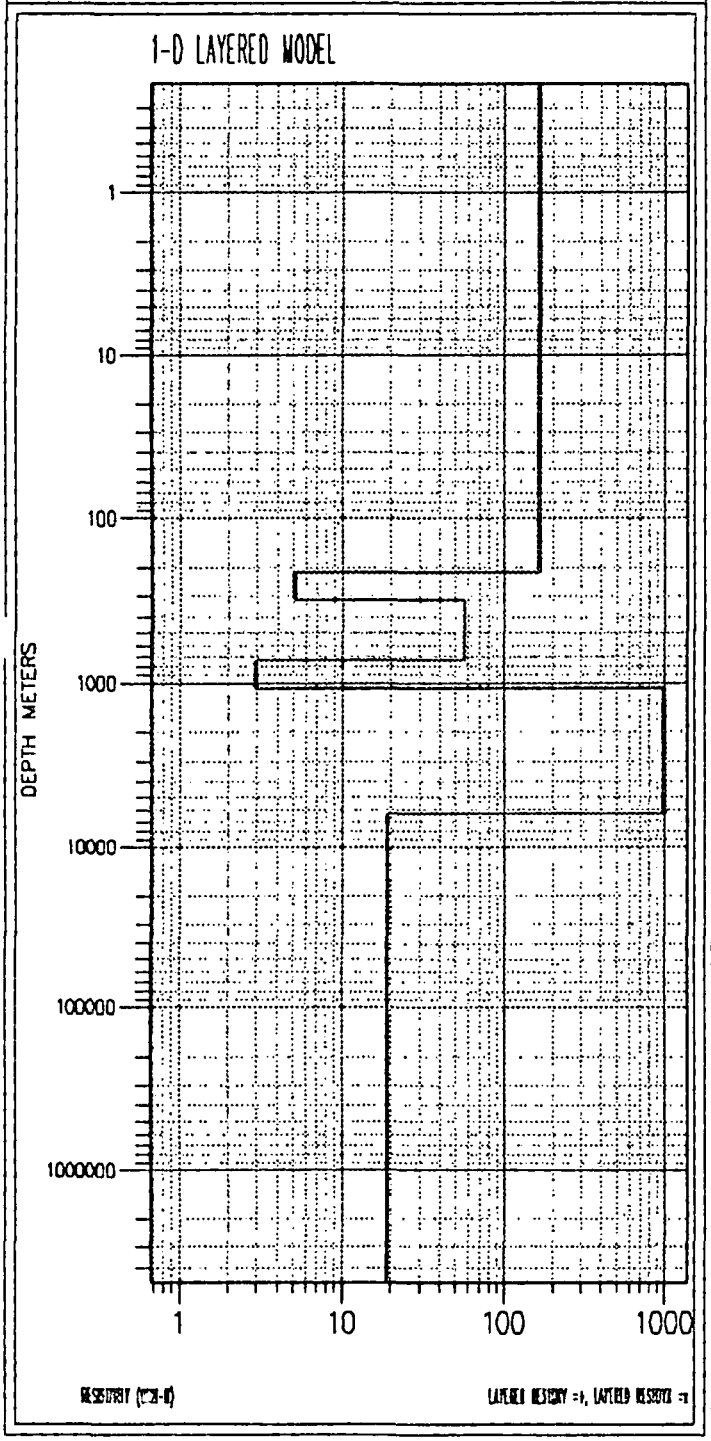


cebuco–s69

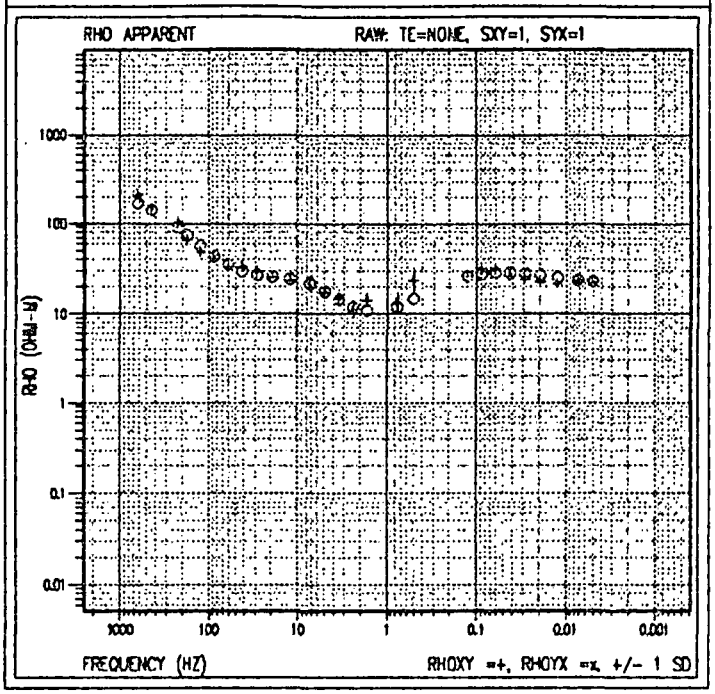


cebuco–s69

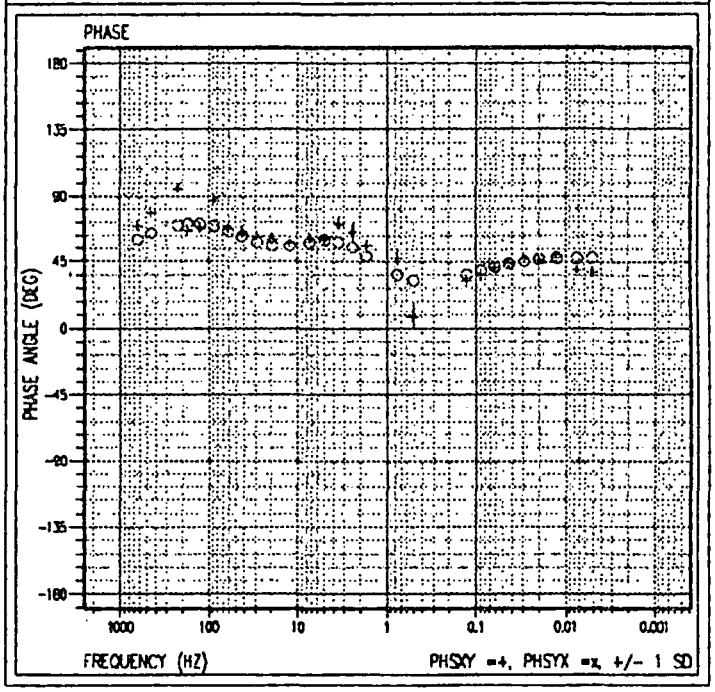

cebuco-s72

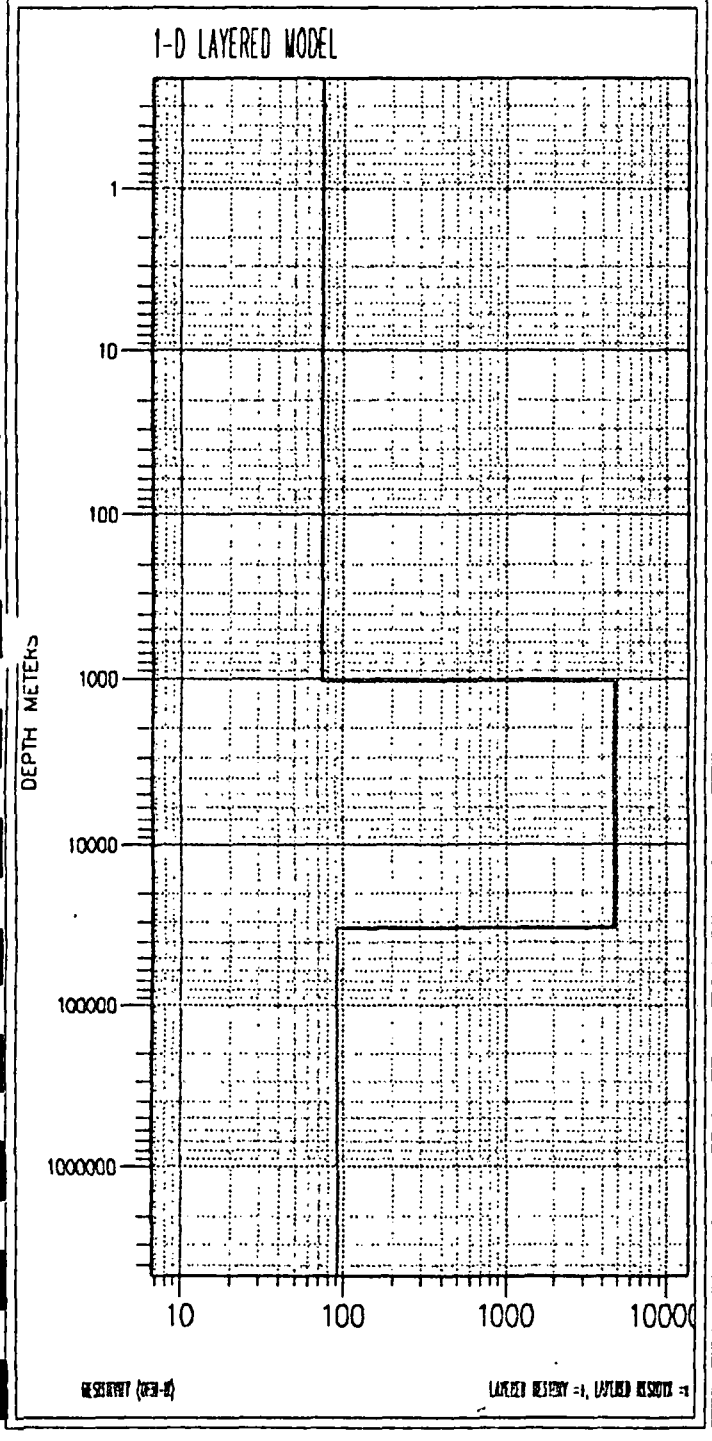


cebuco-s72

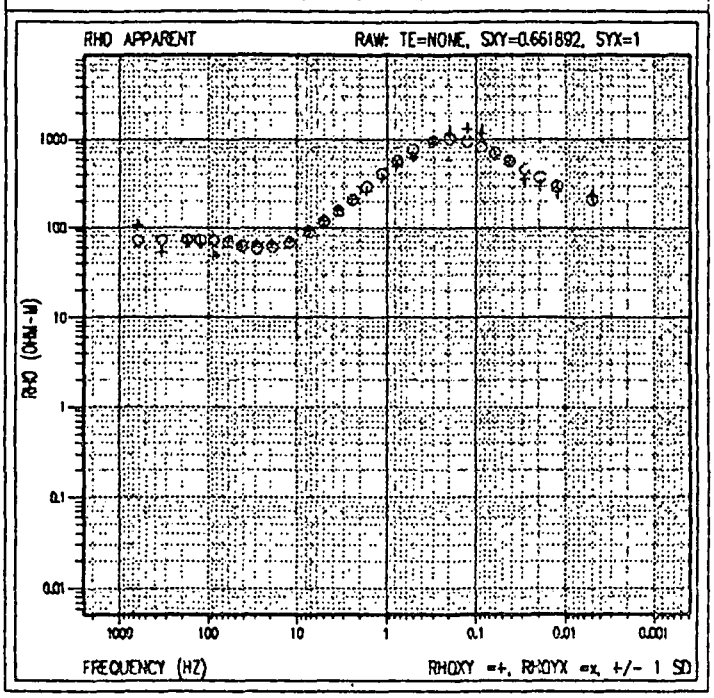


cebuco-s72

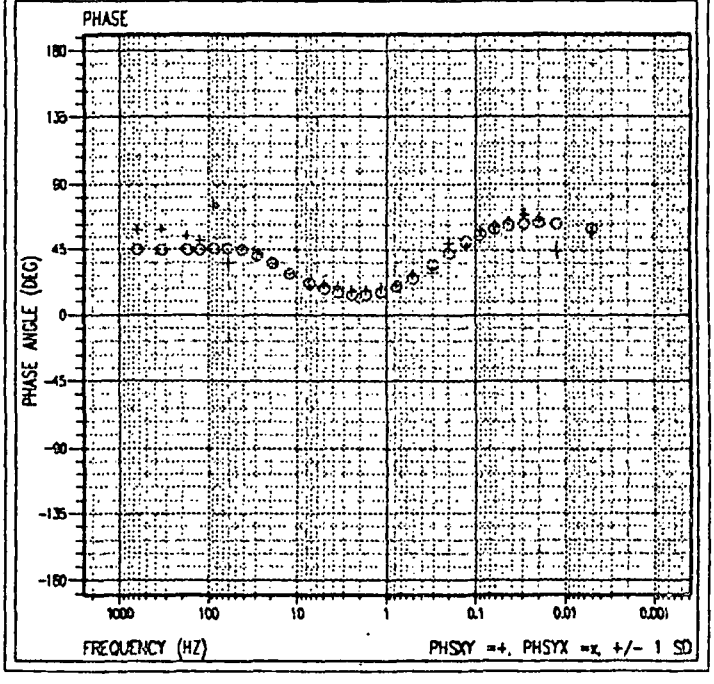

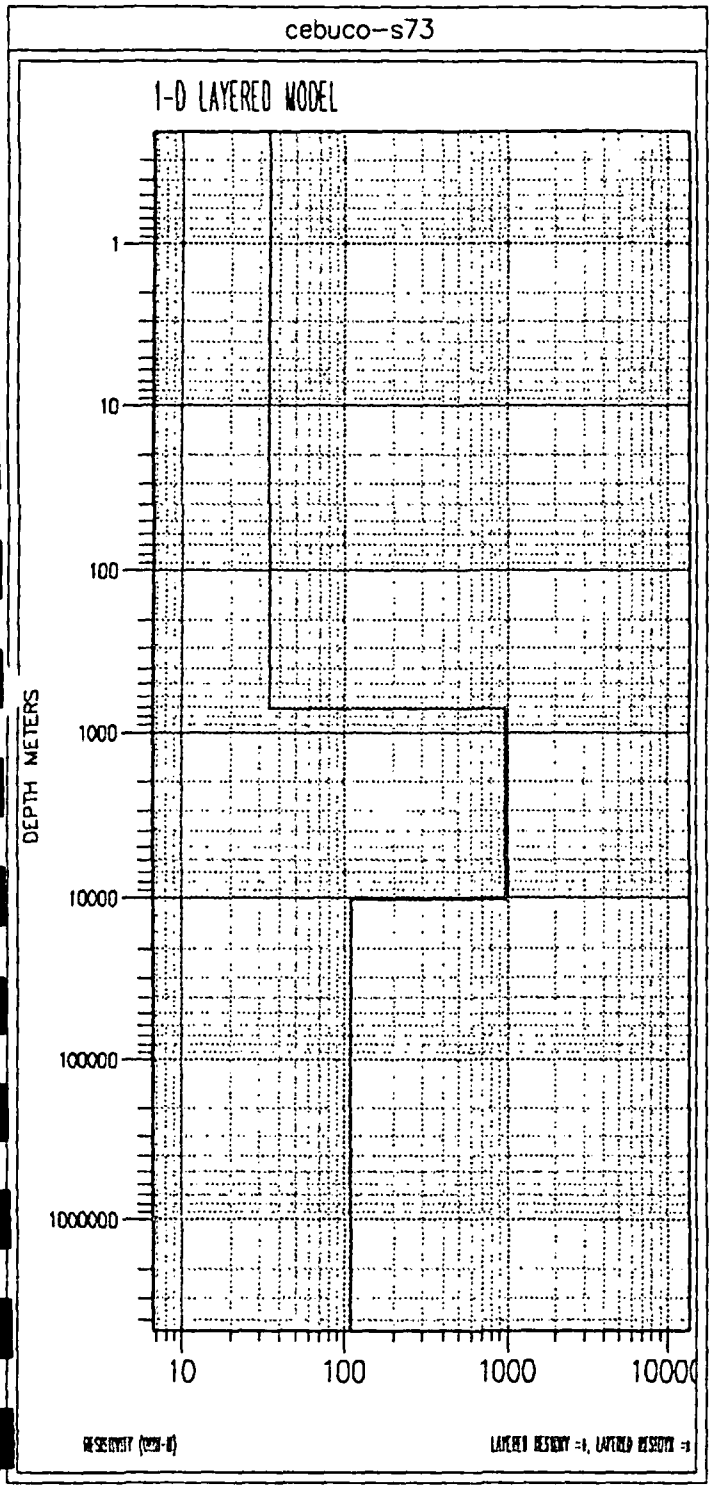
cebuco-s73
1-D LAYERED MODEL
DEPTH METERS
1
10
100
1000
10000
100000
1000000
10
100
1000
10000

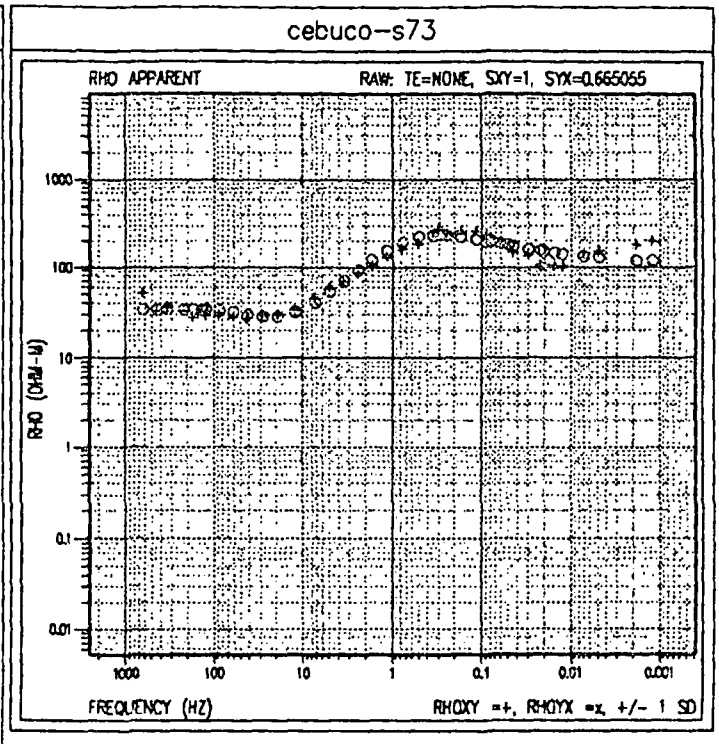
cebuco-s73
RHO APPARENT
RAW: TE=NONE, SXY=1, SYX=0.665055
RHO (OHM-M)
1000
100
10
1
0.1
0.01
1000
100
10
1
0.1
0.01
0.001
FREQUENCY (HZ)
RHOXY =+, RHOYX =x, +/- 1 SD

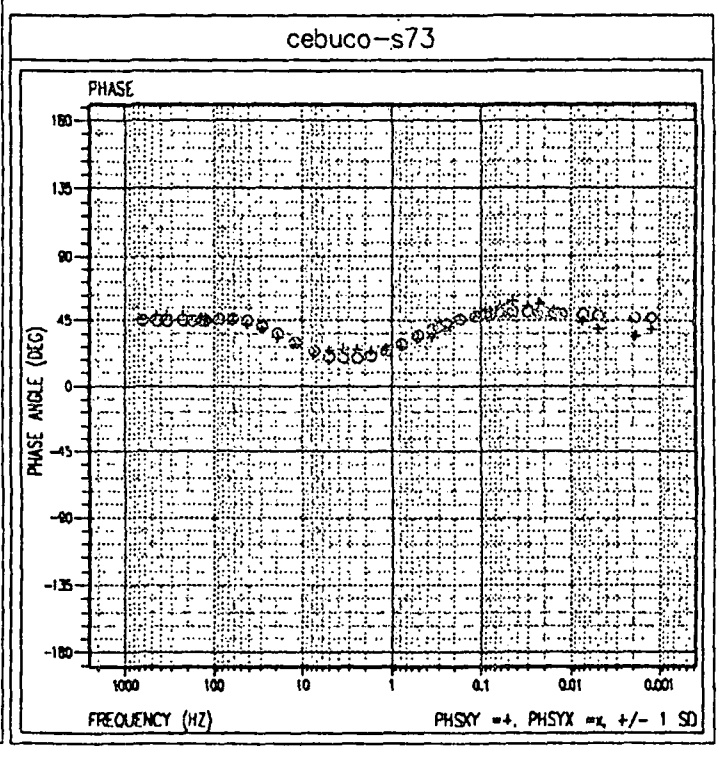
cebuco-s73
PHASE
PHASE ANGLE (DEG)
180
135
90
45
0
-45
-90
-135
-180
1000
100
10
1
0.1
0.01
0.001
FREQUENCY (HZ)
PHSXY =+, PHSYX =x, +/- 1 SD

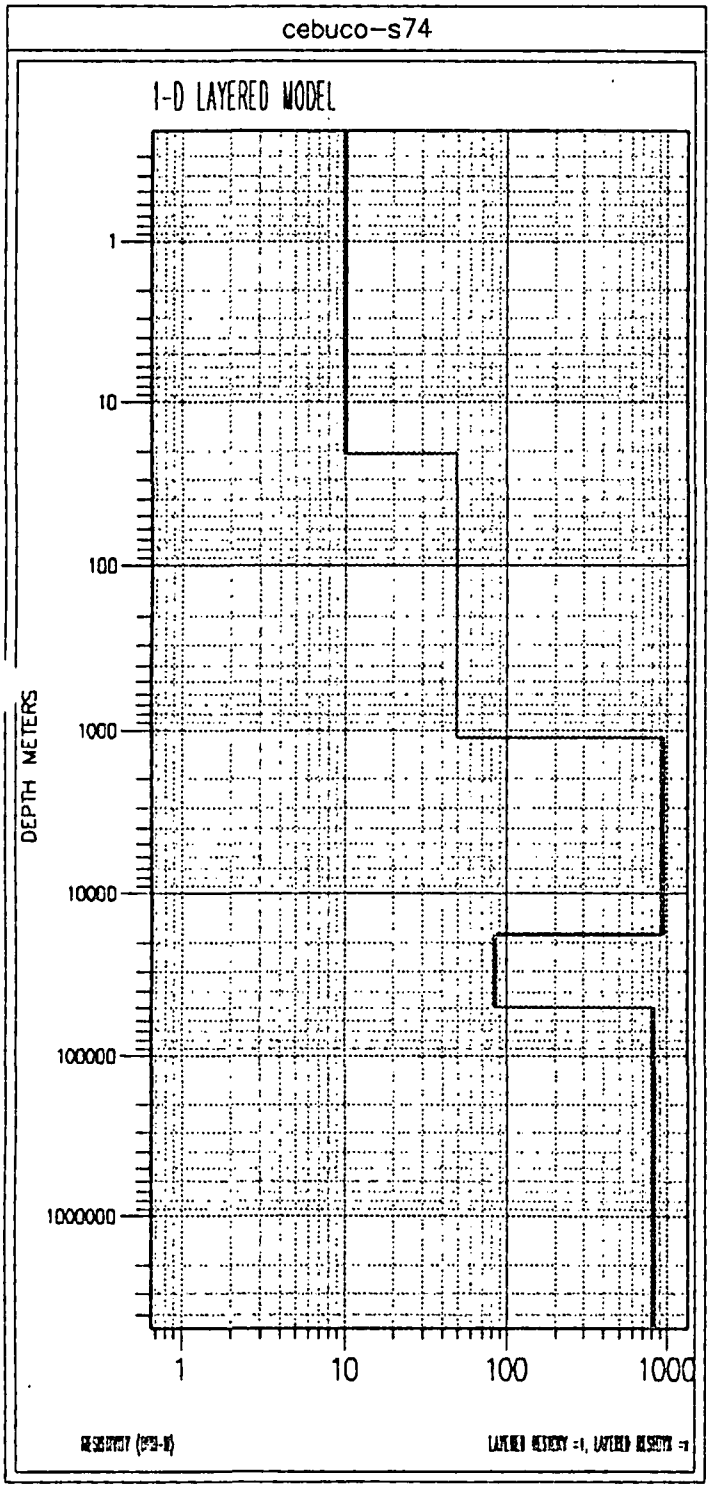
cebuco-s74
1-D LAYERED MODEL
DEPTH METERS
1
10
100
1000
10000
100000
1000000
1
10
100
1000

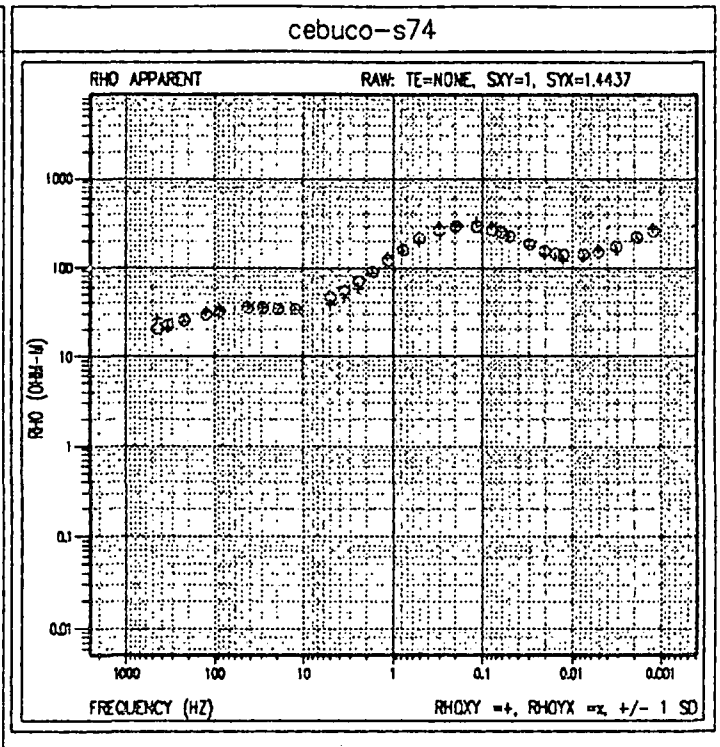
cebuco-s74
RHO APPARENT
RAW: TE=NONE, SXY=1, SYX=1.4437
RHO (OHM-M)
1000
100
10
1
0.1
0.01
1000
100
10
1
0.1
0.01
0.001
FREQUENCY (HZ)
RHOXY =+, RHOYX =x, +/- 1 SD

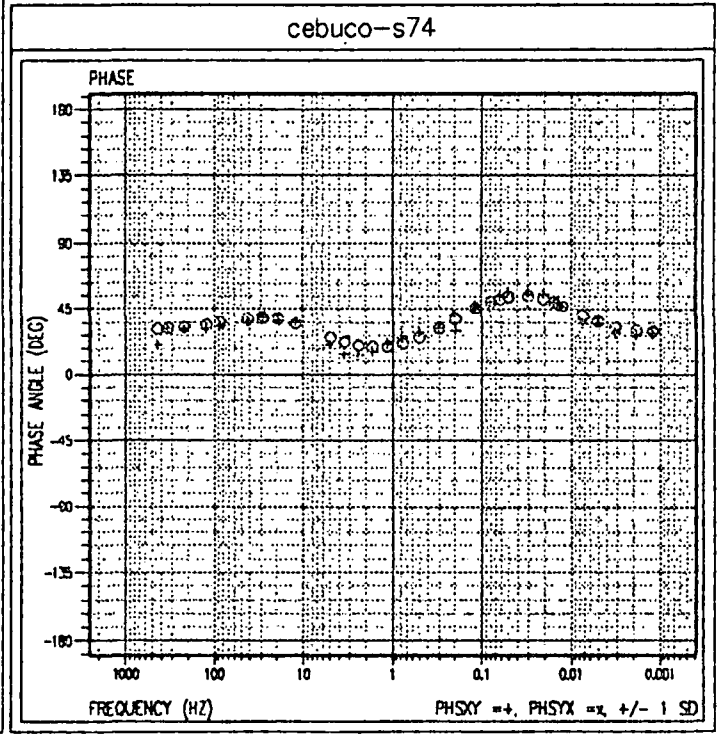
cebuco-s74
PHASE
PHASE ANGLE (DEG)
180
135
90
45
0
-45
-90
-135
-180
1000
100
10
1
0.1
0.01
0.001
FREQUENCY (HZ)
PHSXY =+, PHSYX =x, +/- 1 SD

cebuco-s75

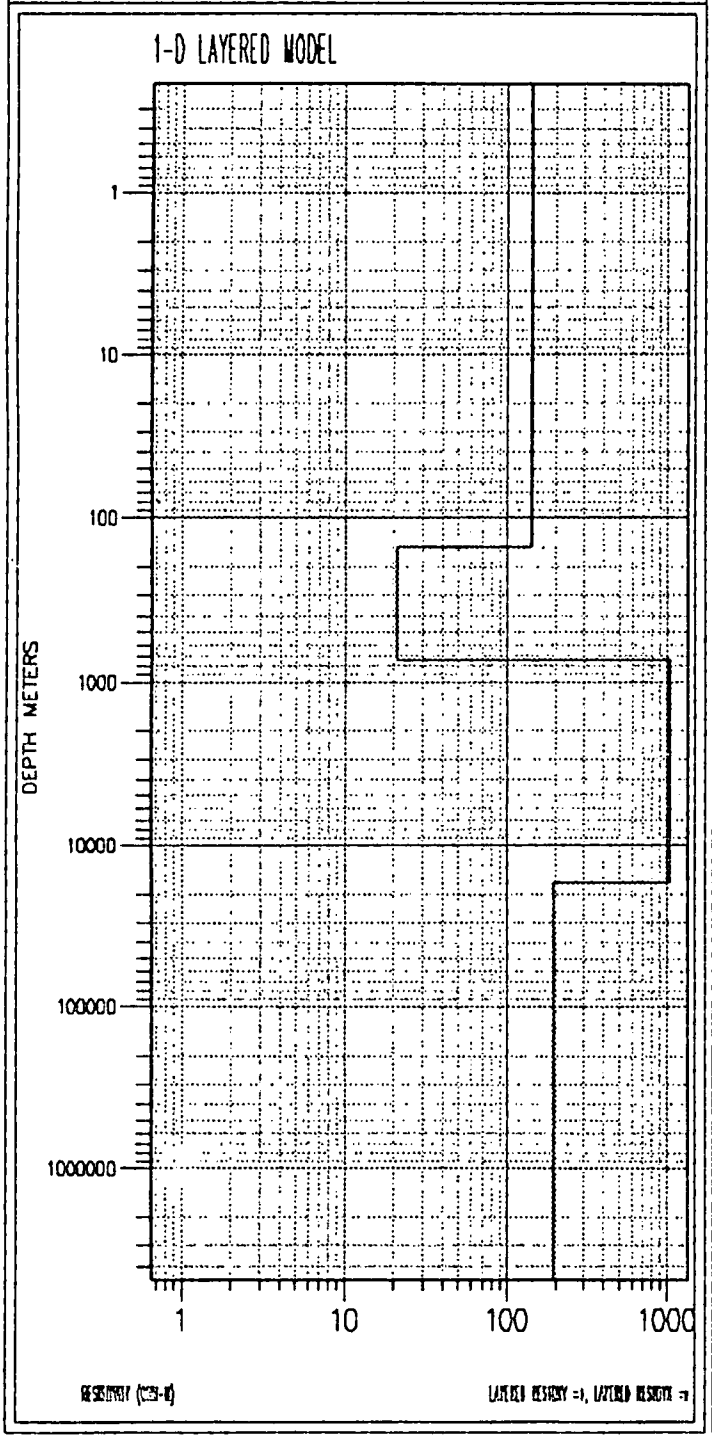


cebuco-s75

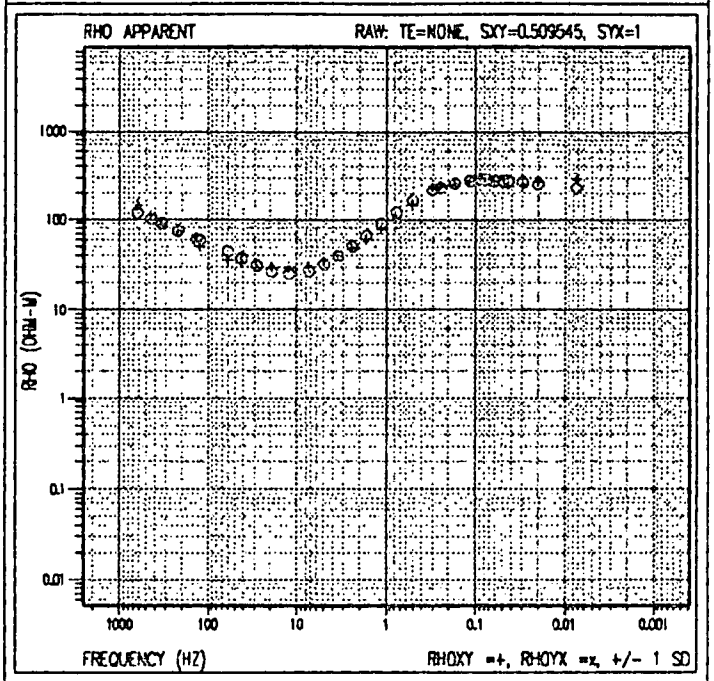


cebuco-s75

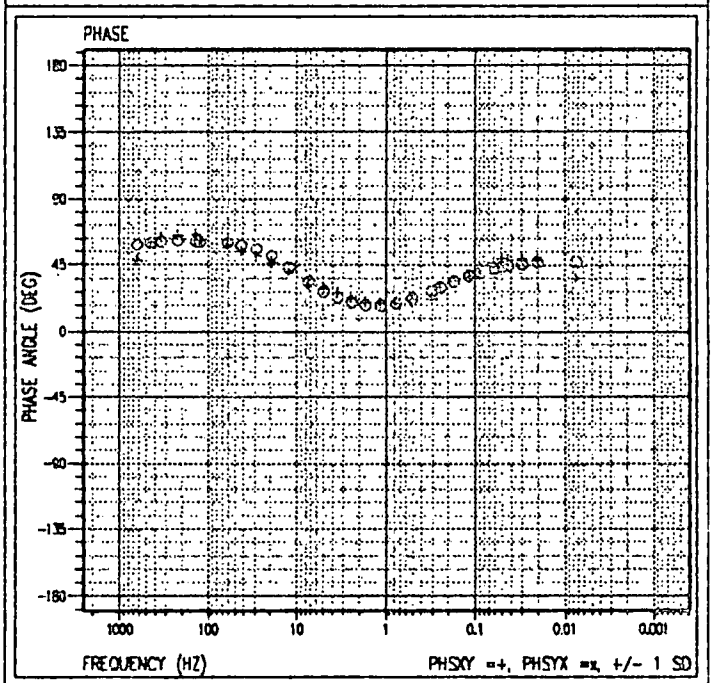

cebuco–s76

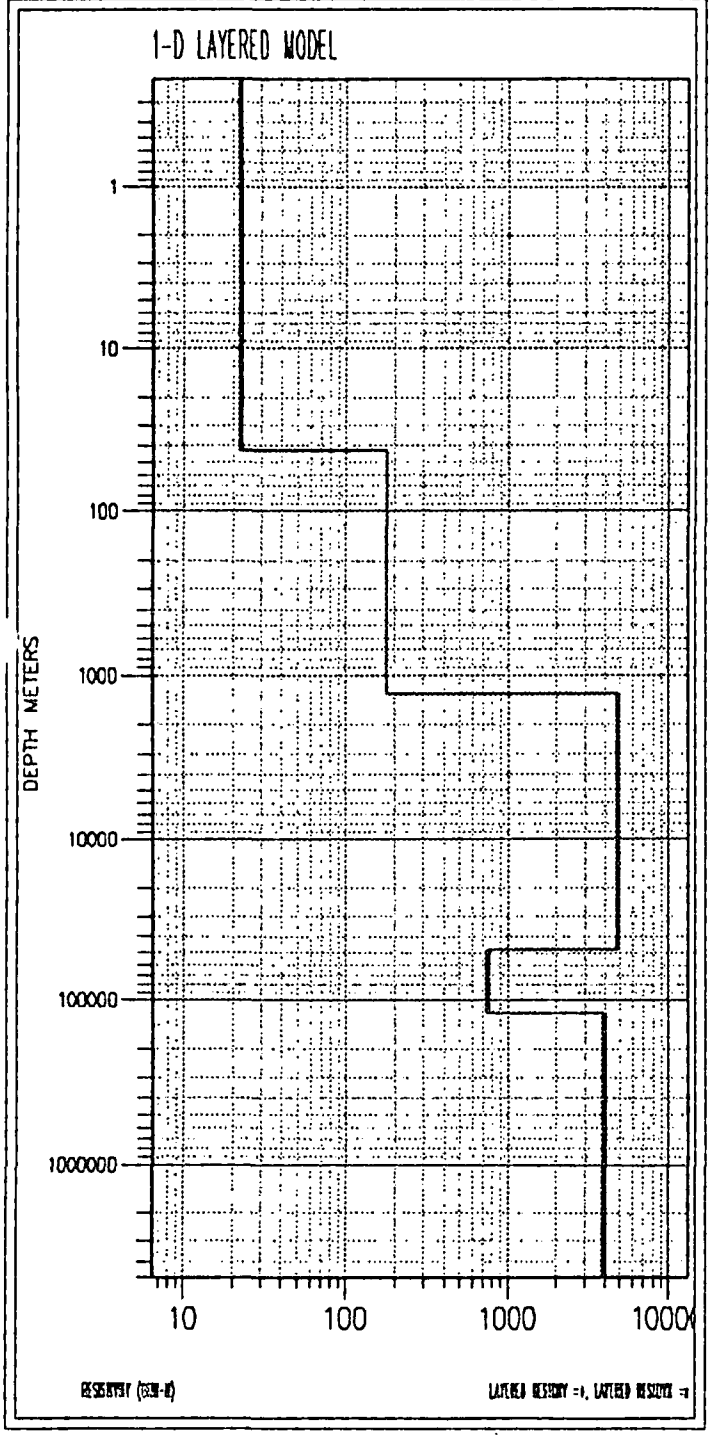


cebuco–s76

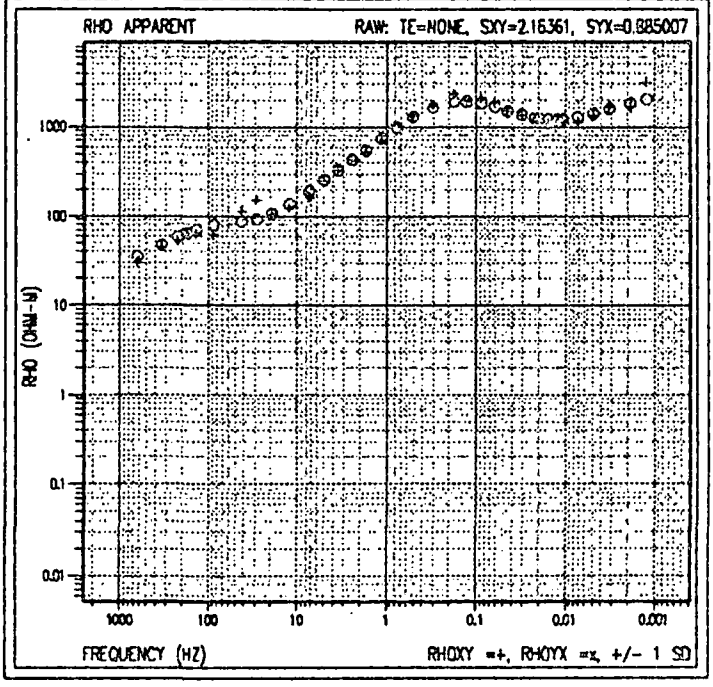


cebuco–s76

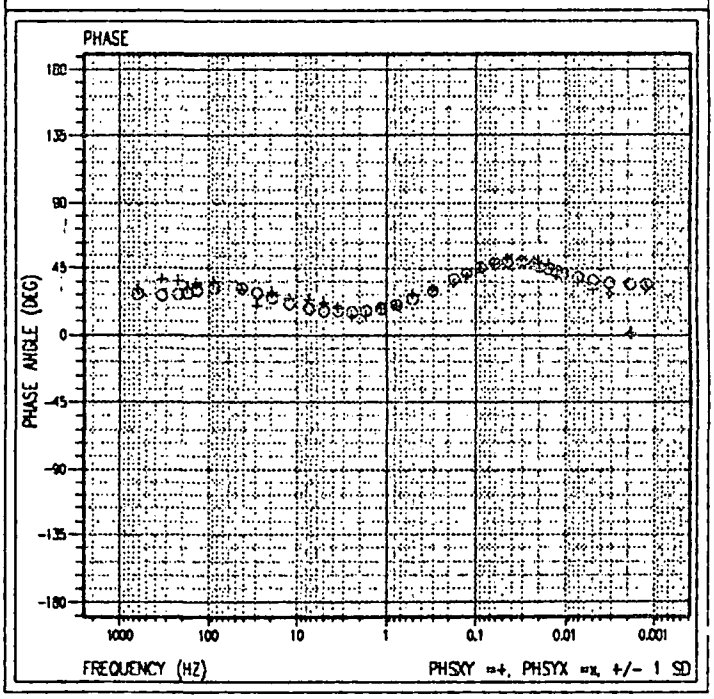

cebuco–s77

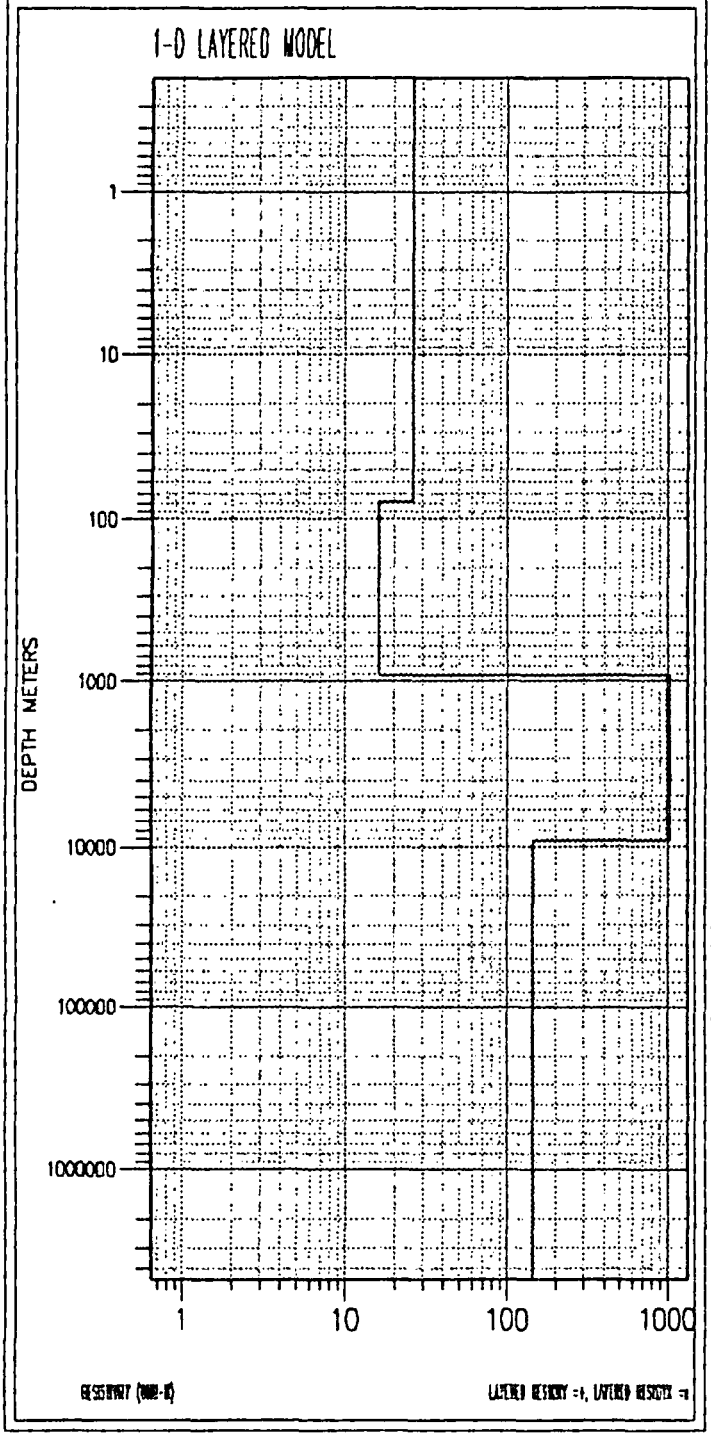


cebuco–s77

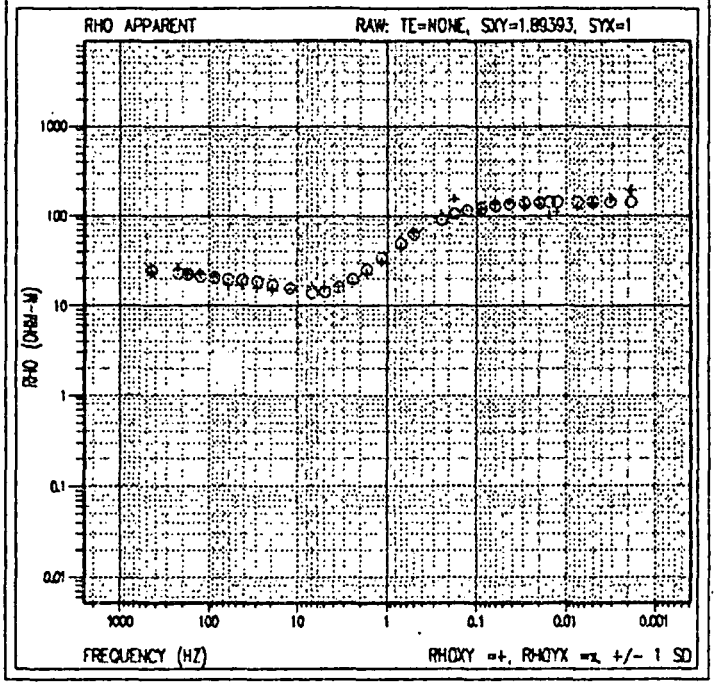


cebuco–s77

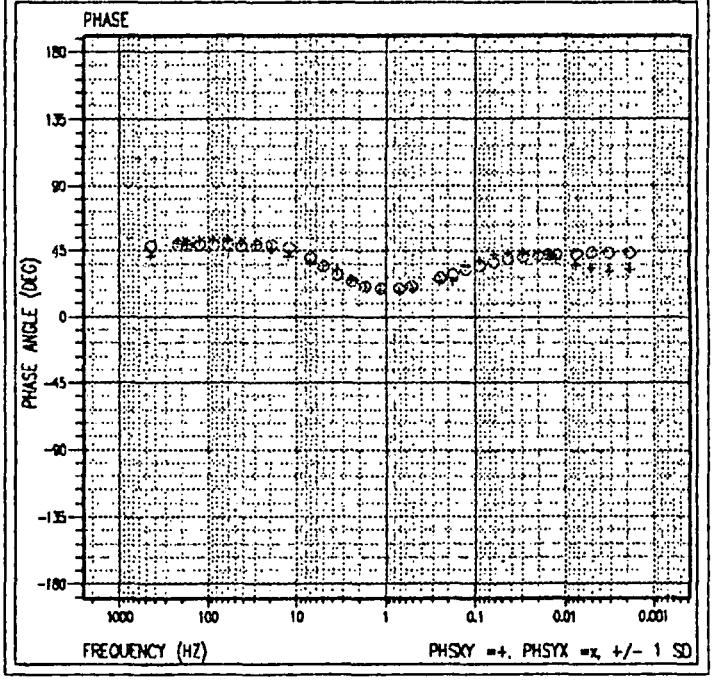

cebuco–s78

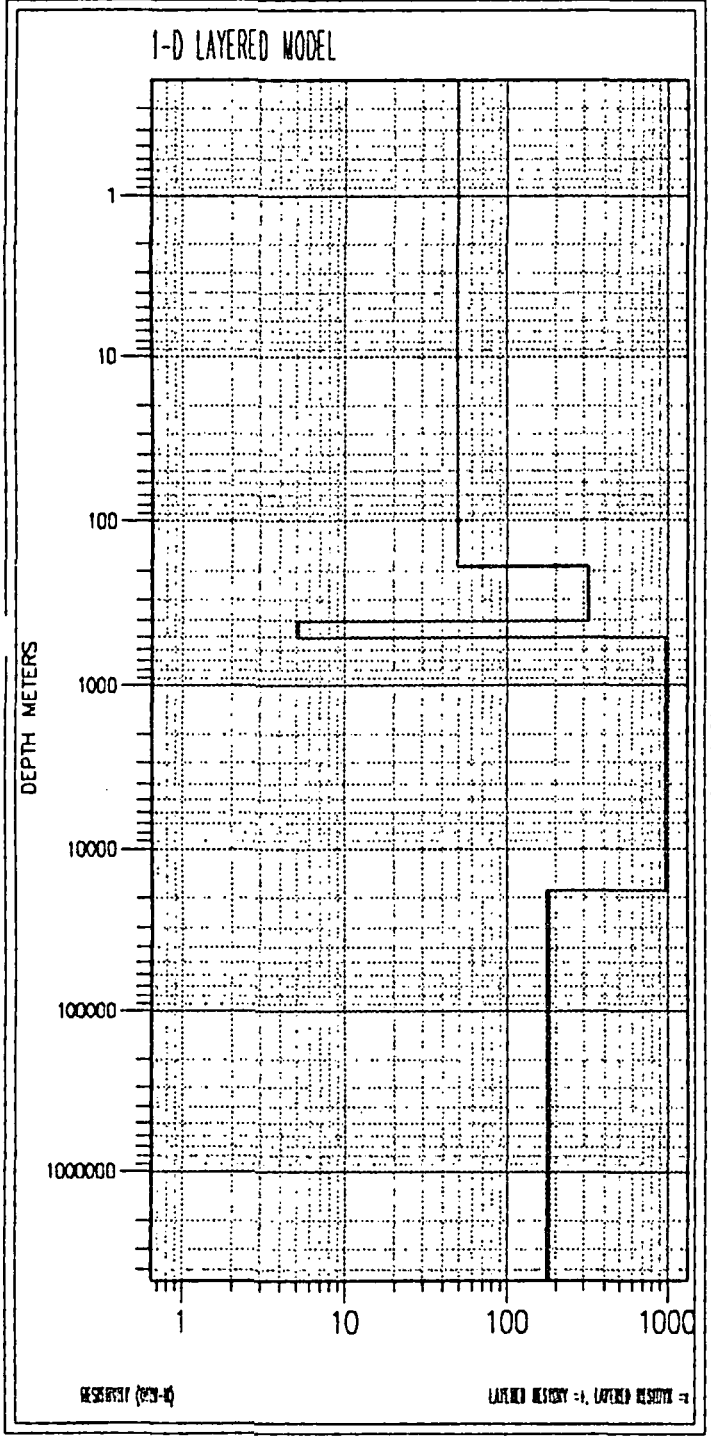


cebuco–s78

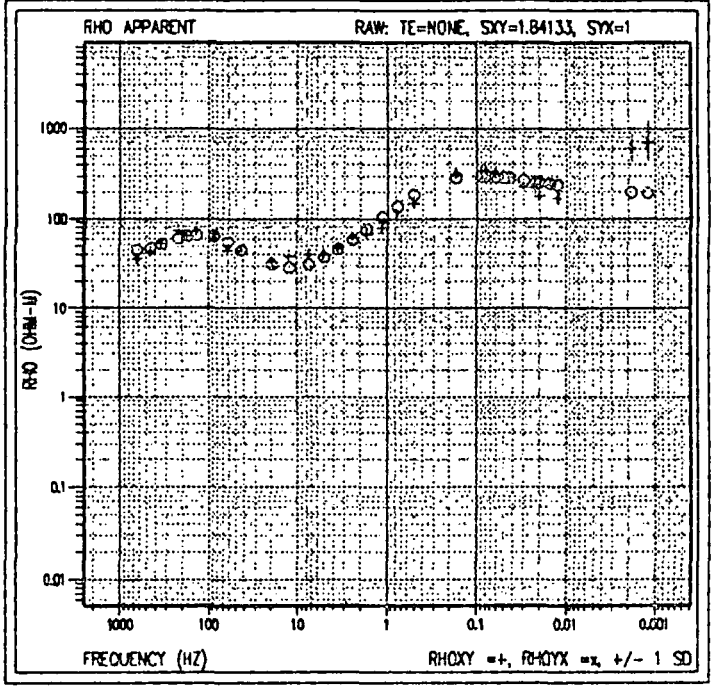


cebuco–s78

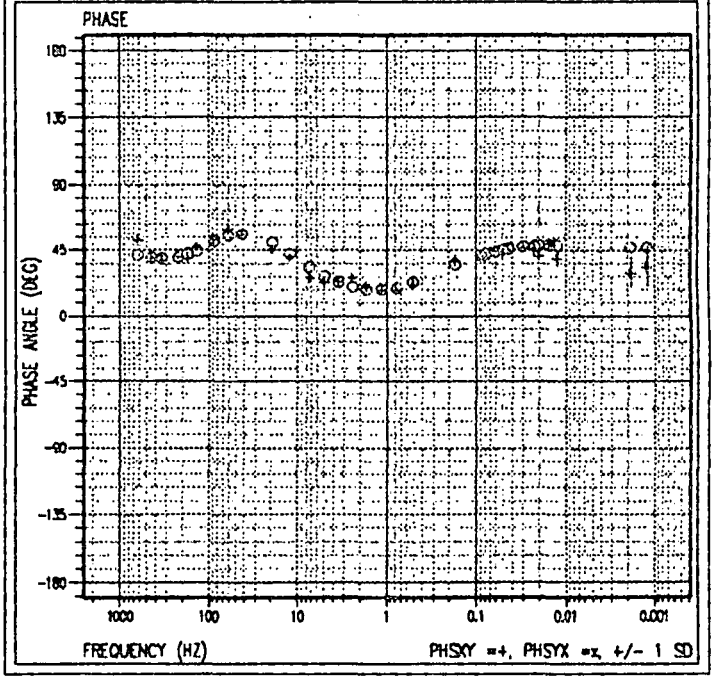

cebuco–s79

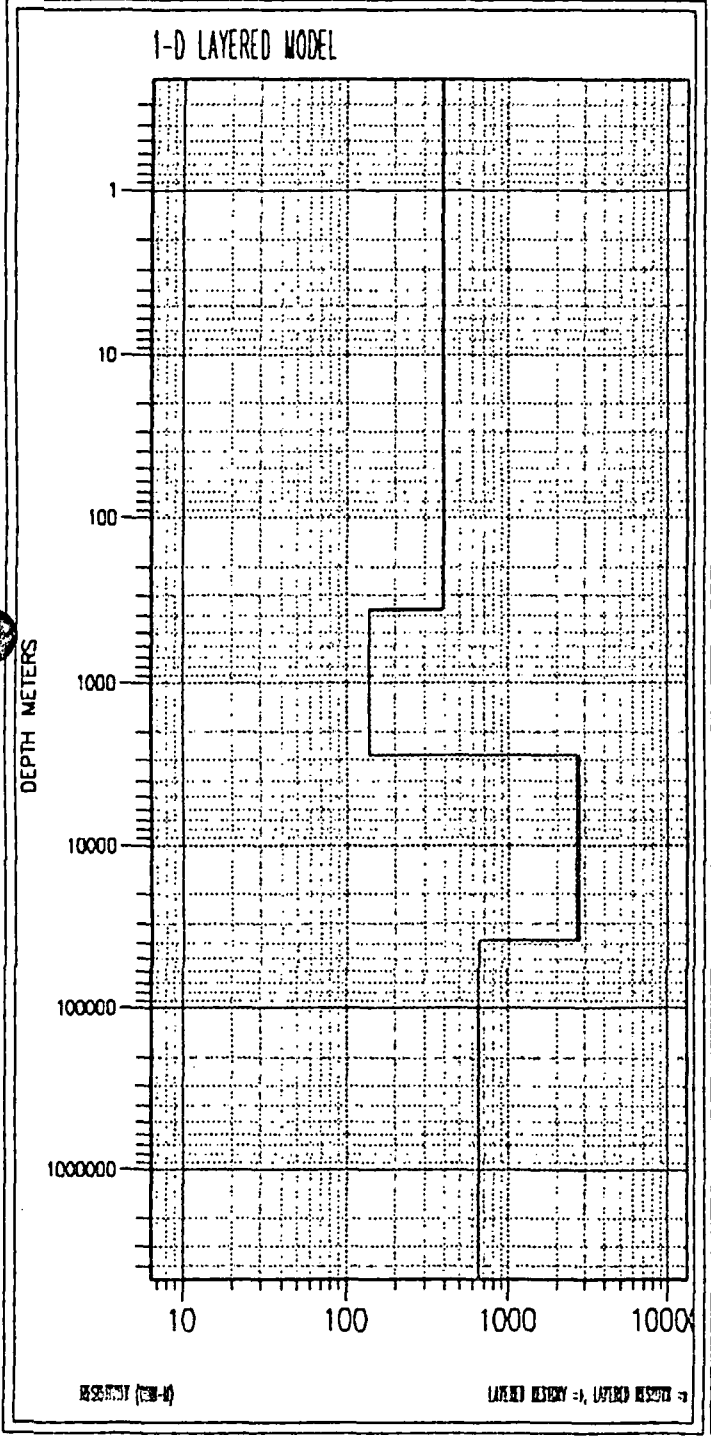


cebuco–s79

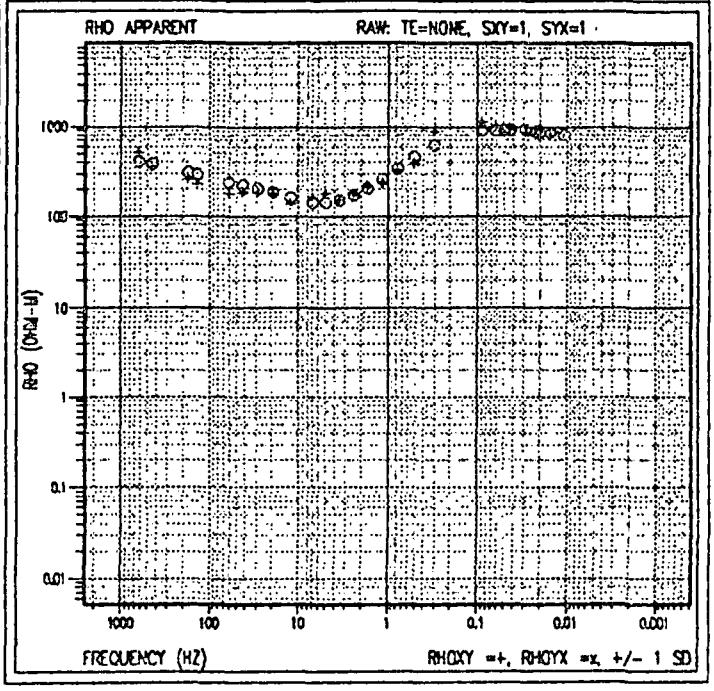


cebuco–s79

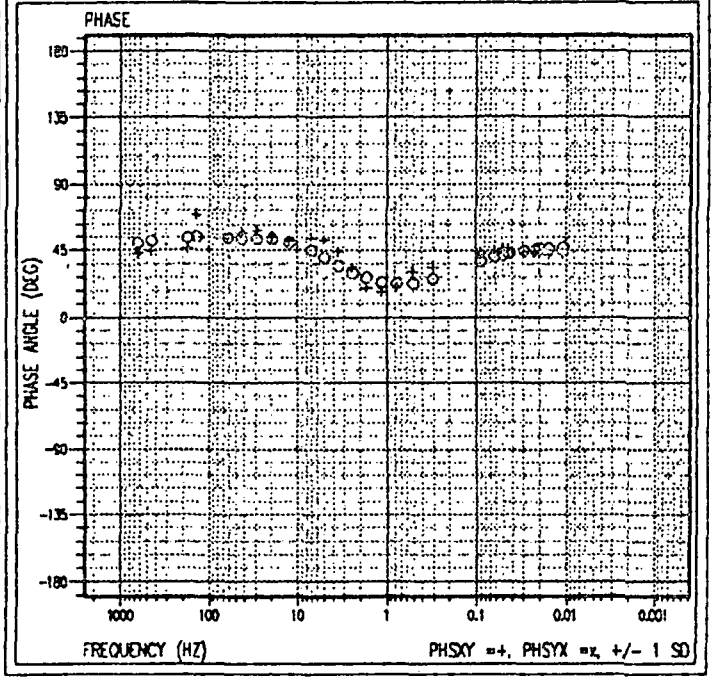

cebuco–s80

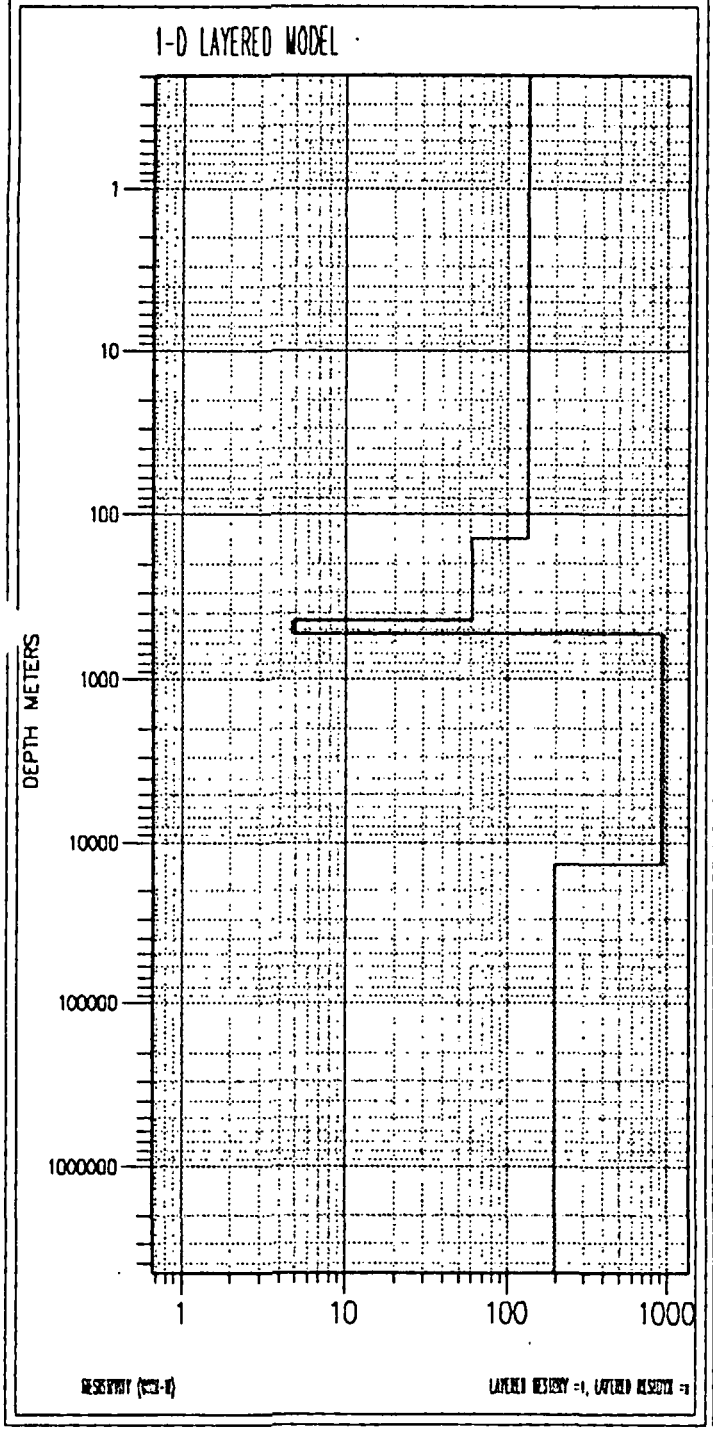


cebuco–s80

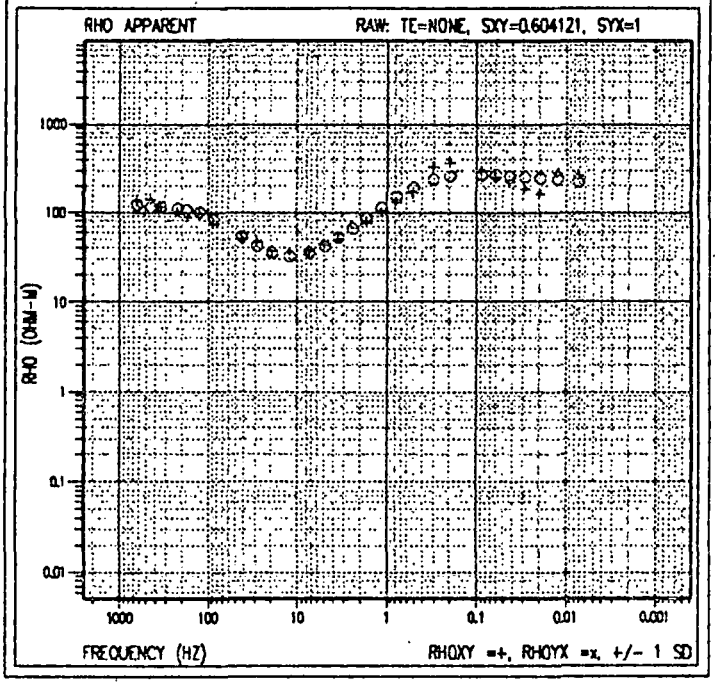


cebuco–s80

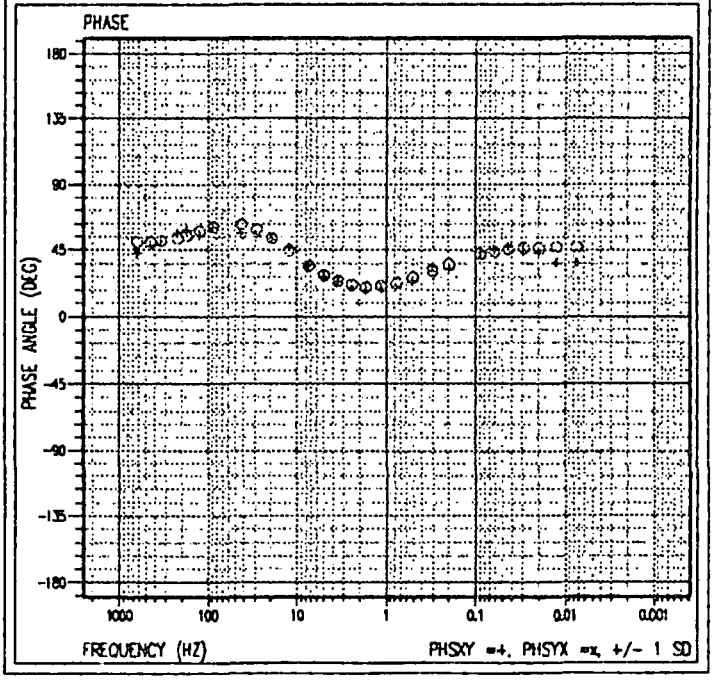

cebuco–s81

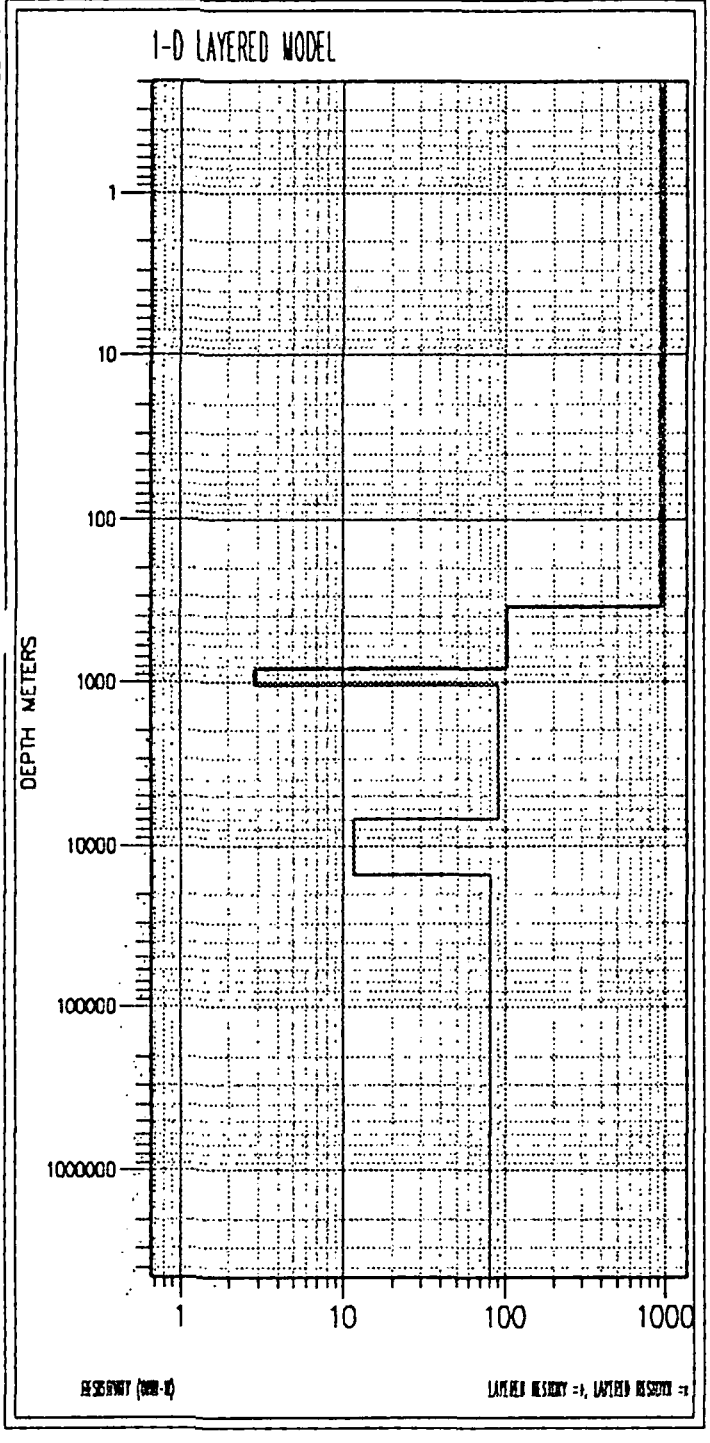


cebuco–s81

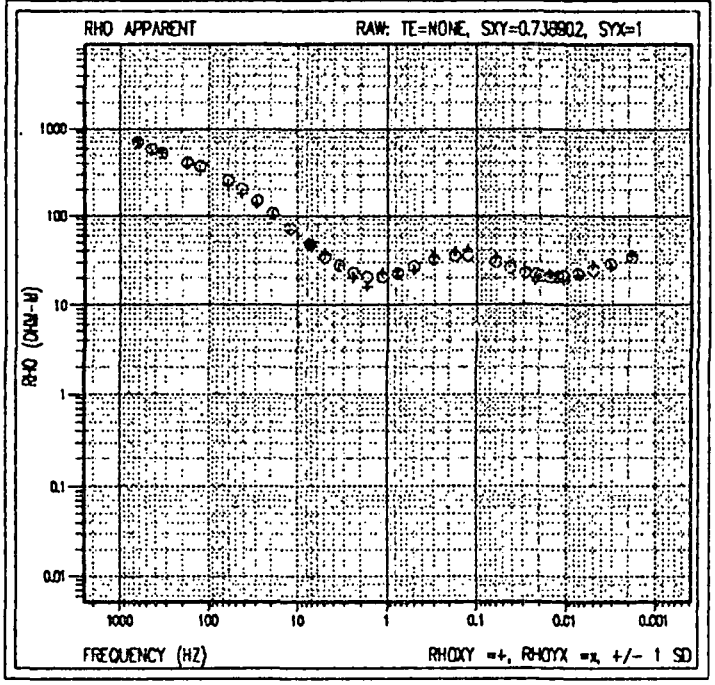


cebuco–s81

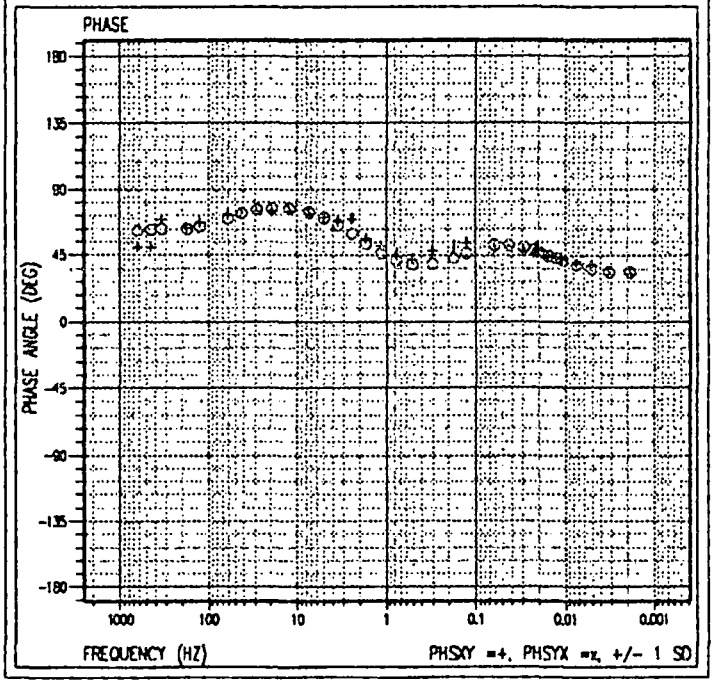

cebuco–s82

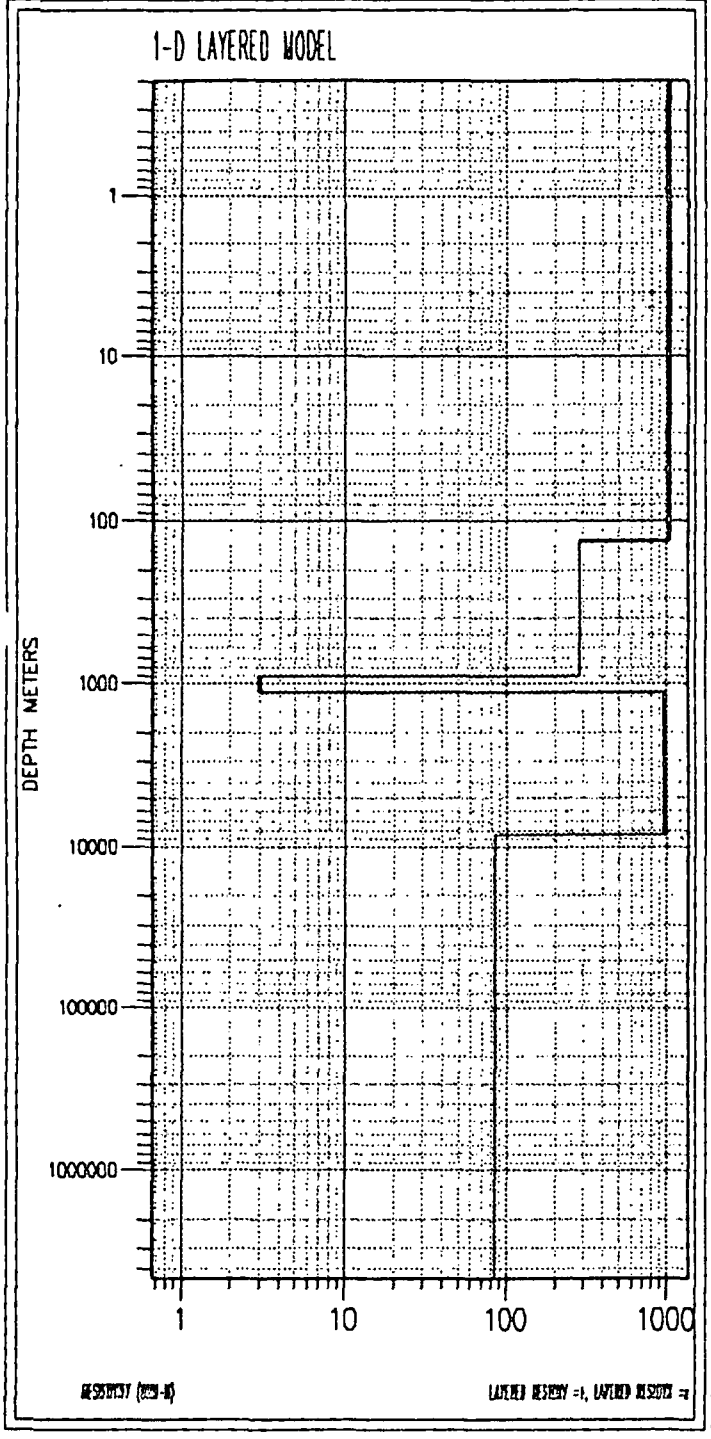


cebuco–s82

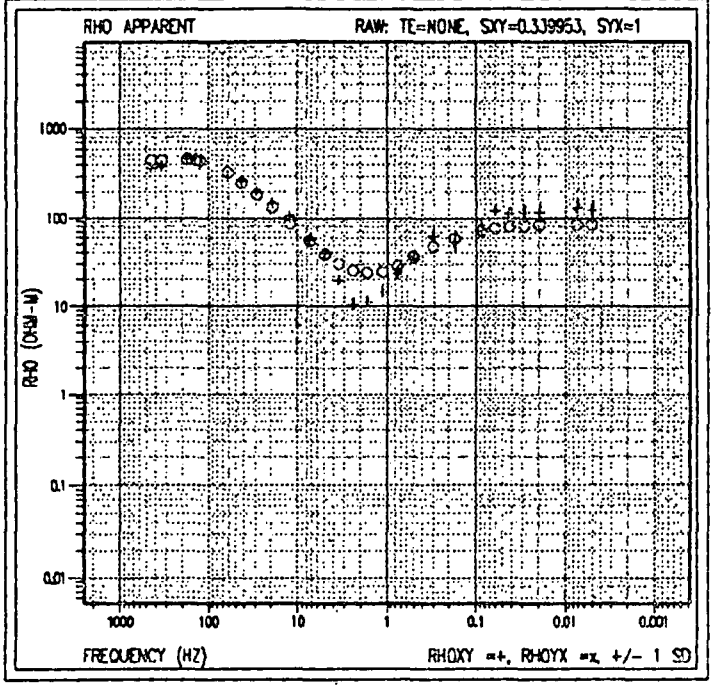


cebuco–s82

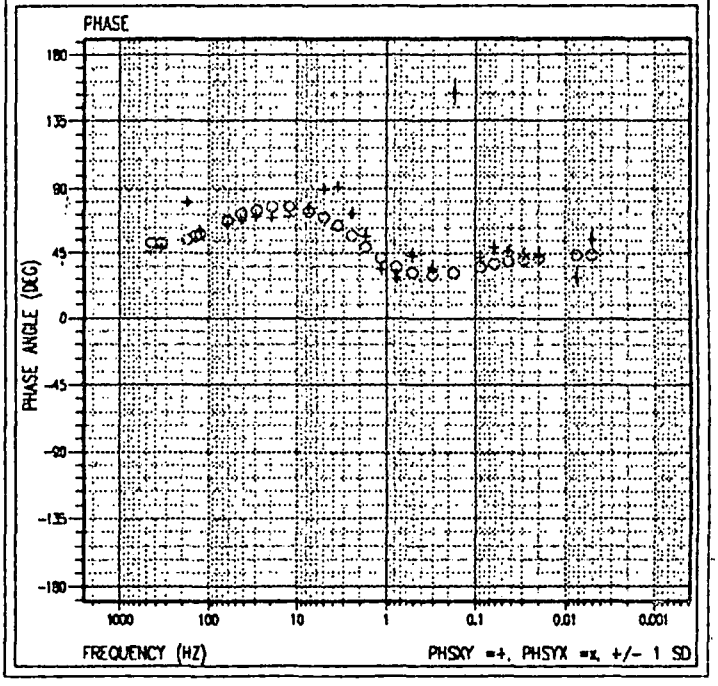

cebuco–s85

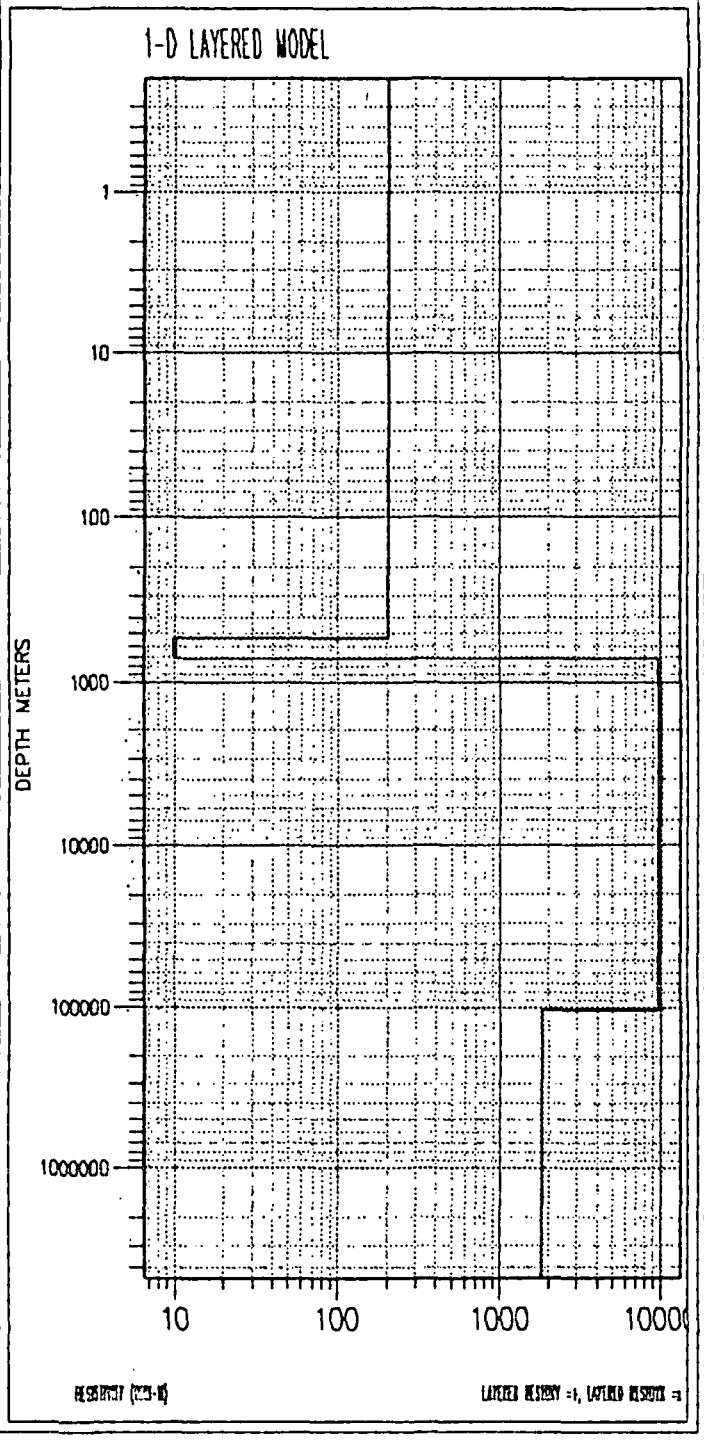


cebuco–s85

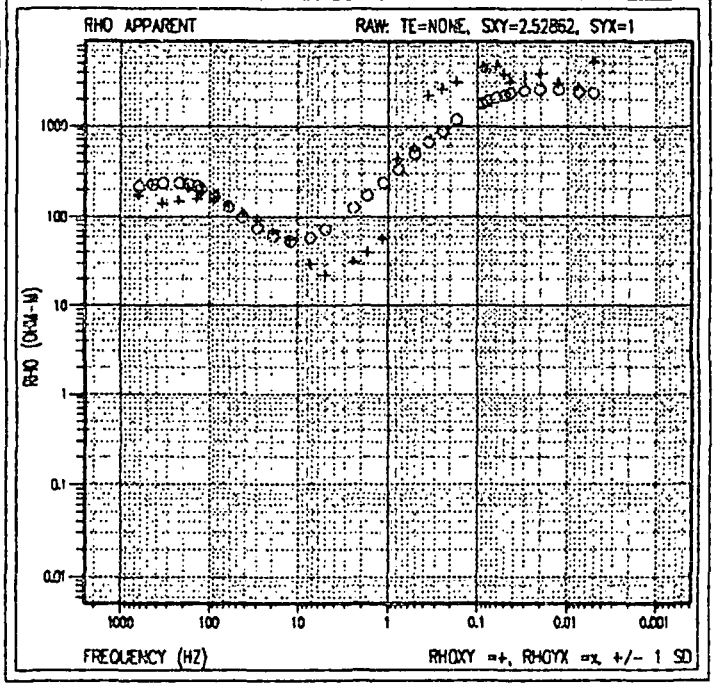


cebuco–s85

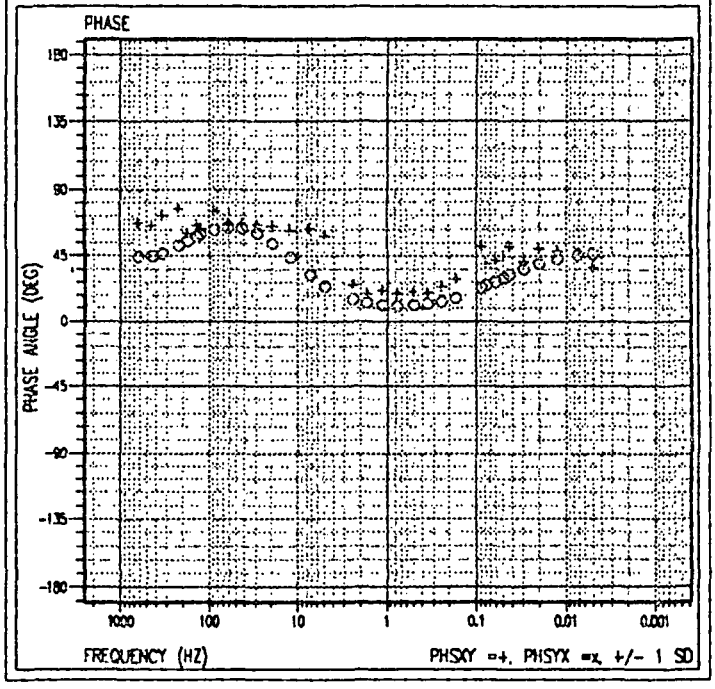

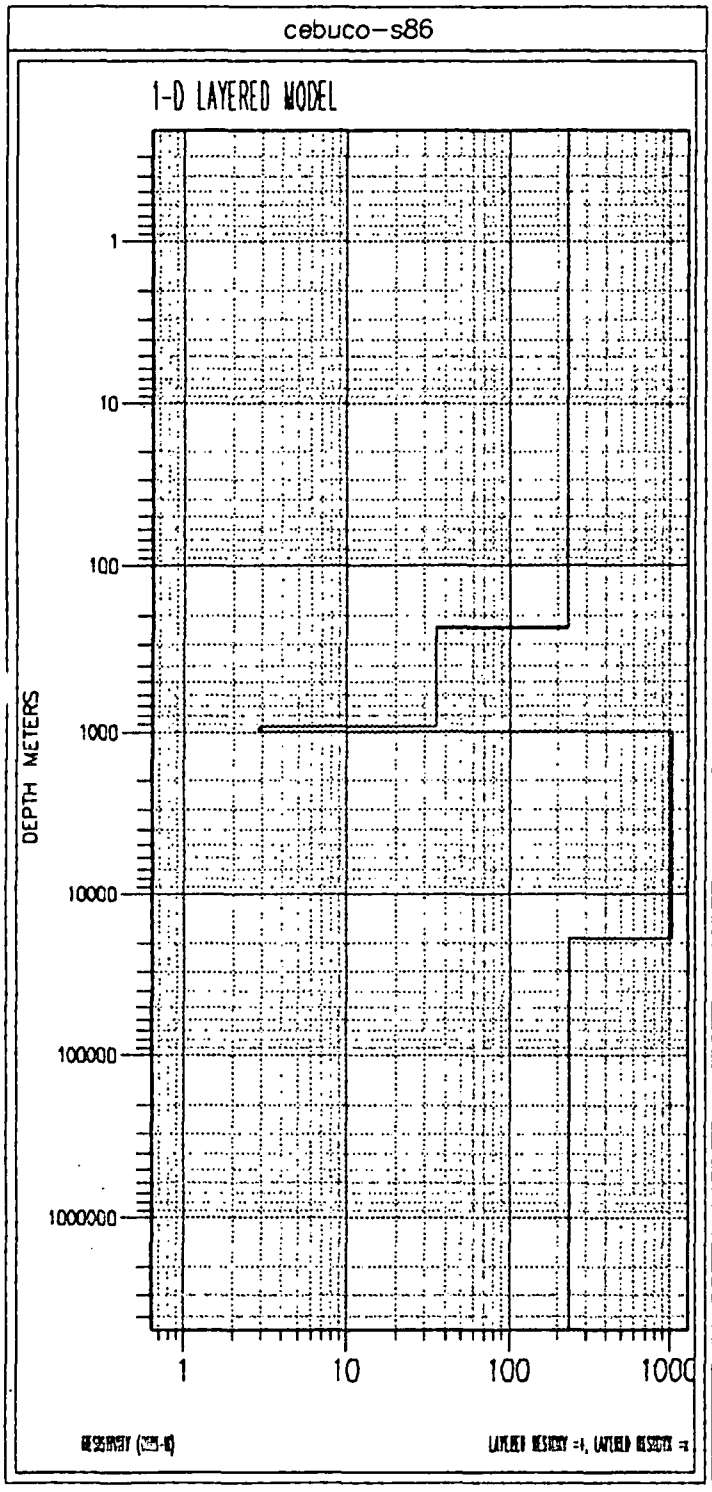
cebuco–s86
1-D LAYERED MODEL
DEPTH METERS
1
10
100
1000
10000
100000
1000000
1
10
100
1000

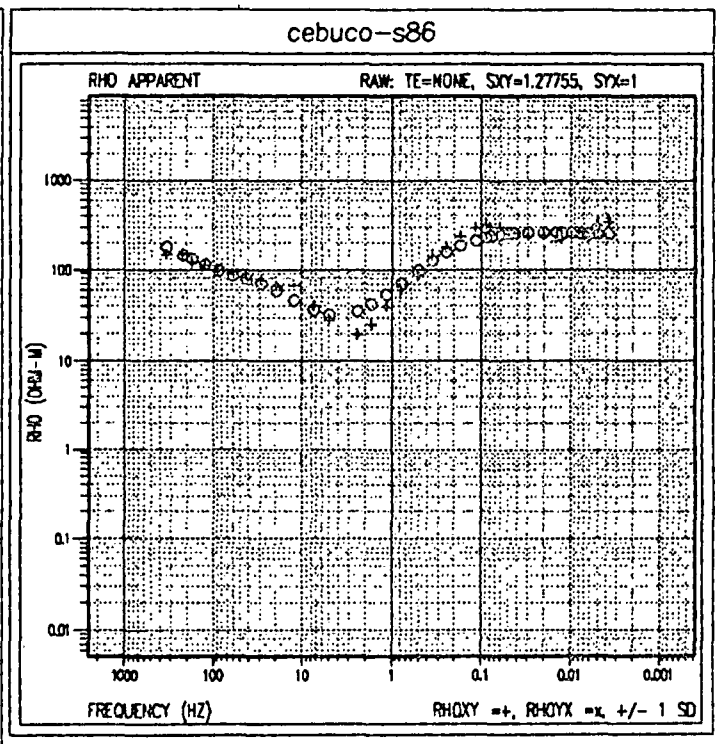
cebuco–s86
RHO APPARENT
RAW: TE=NONE, SXY=1.27755, SYX=1
RHO (OHM-M)
1000
100
10
1
0.1
0.01
1000
100
10
1
0.1
0.01
0.001
FREQUENCY (HZ)
RHOXY =+, RHOYX =x, +/- 1 SD

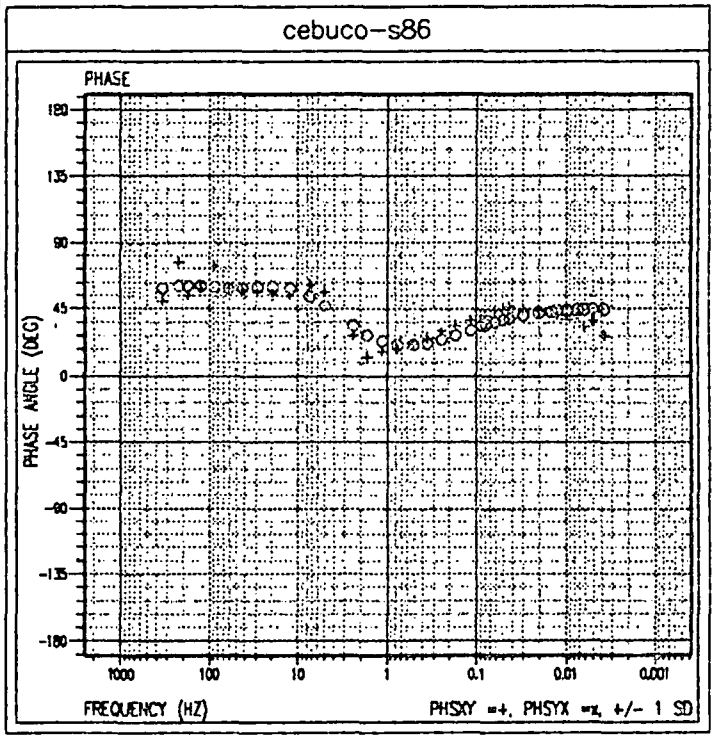
cebuco–s86
PHASE
PHASE ANGLE (DEG)
180
135
90
45
0
-45
-90
-135
-180
1000
100
10
1
0.1
0.01
0.001
FREQUENCY (HZ)
PHSXY =+, PHSYX =x, +/- 1 SD

cebuco-s87

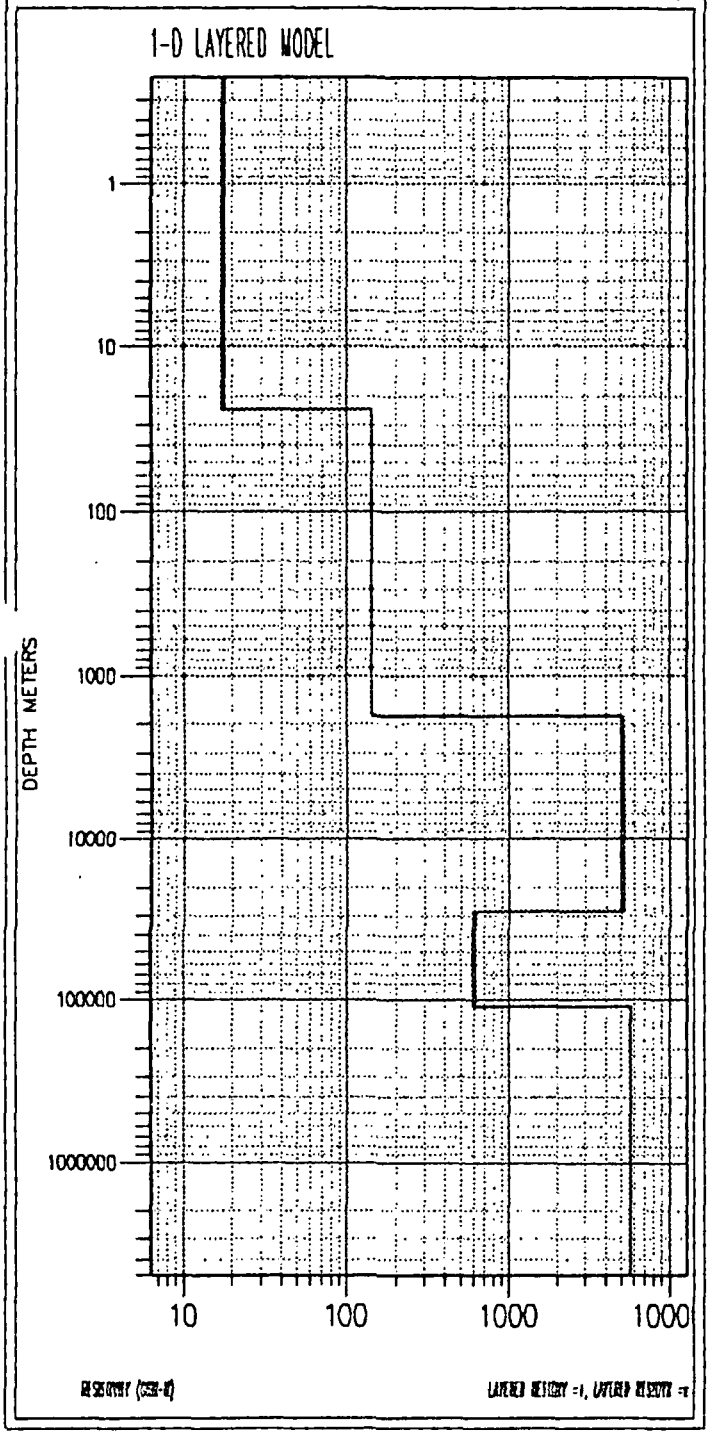


cebuco-s87

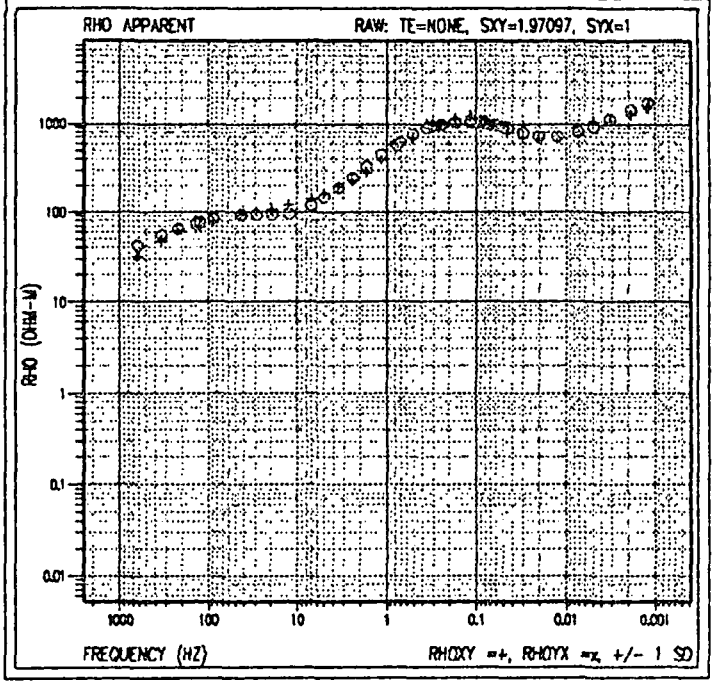


cebuco-s87

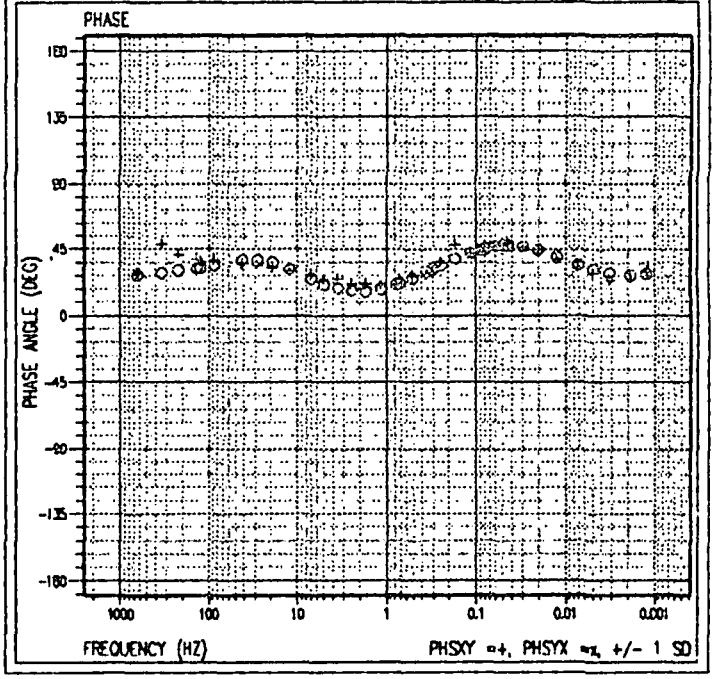

cebuco–s88

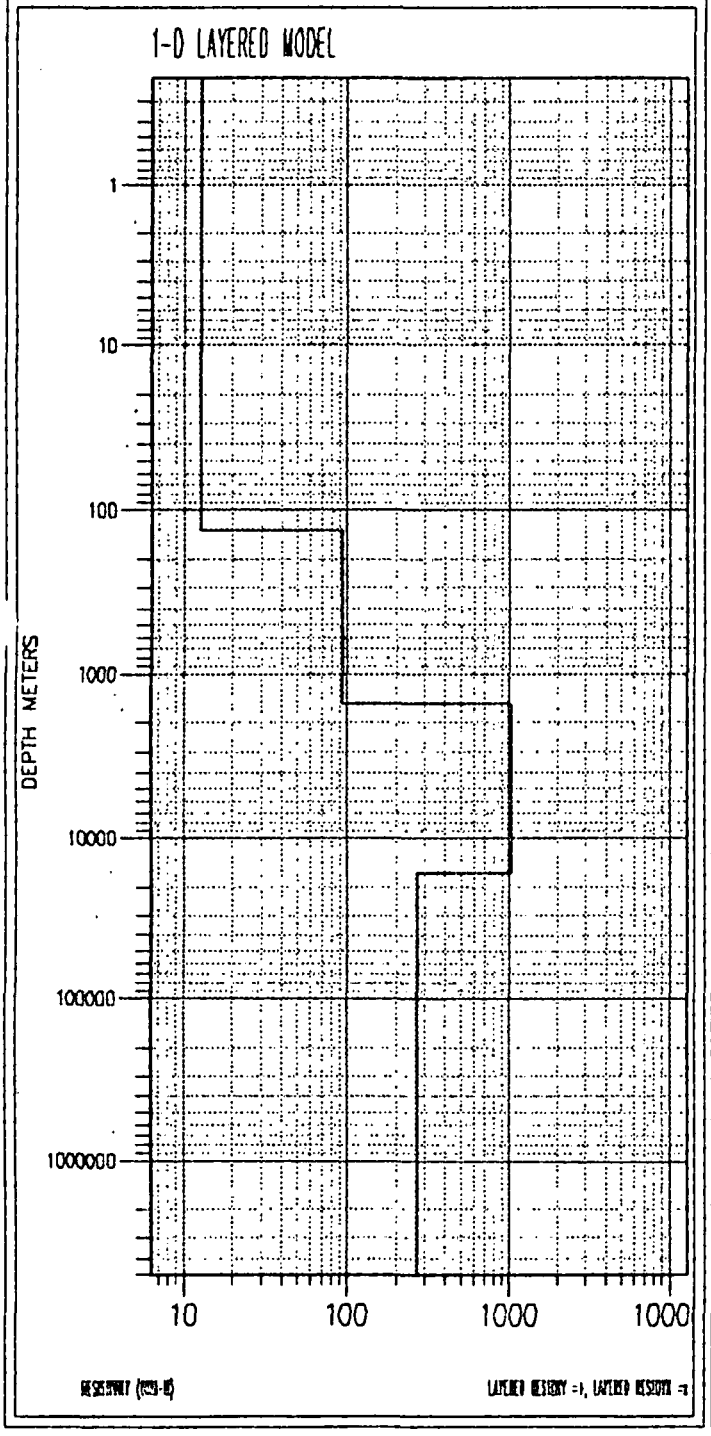


cebuco–s88

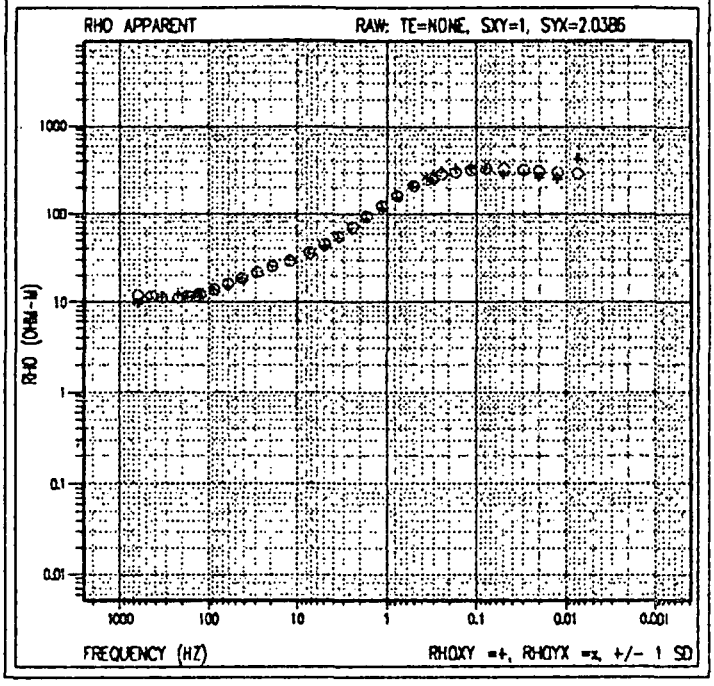


cebuco–s88

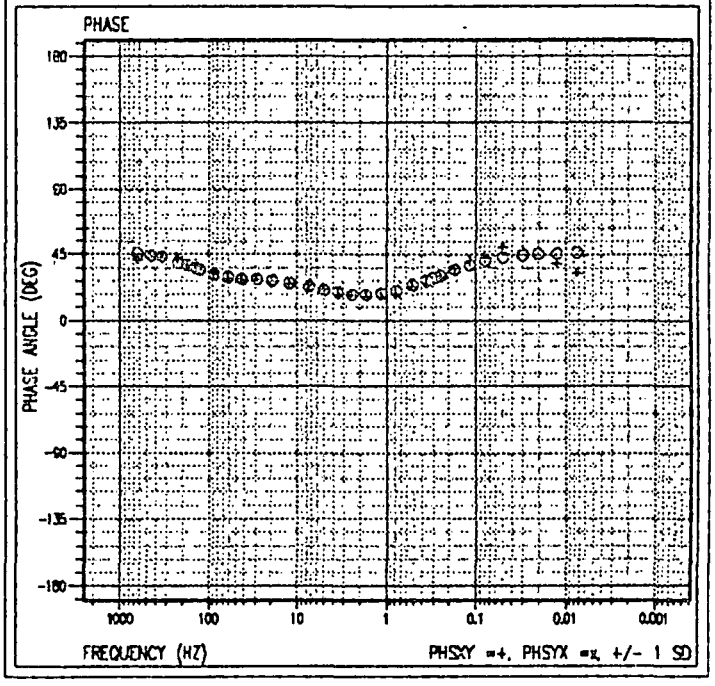

cebuco-s89

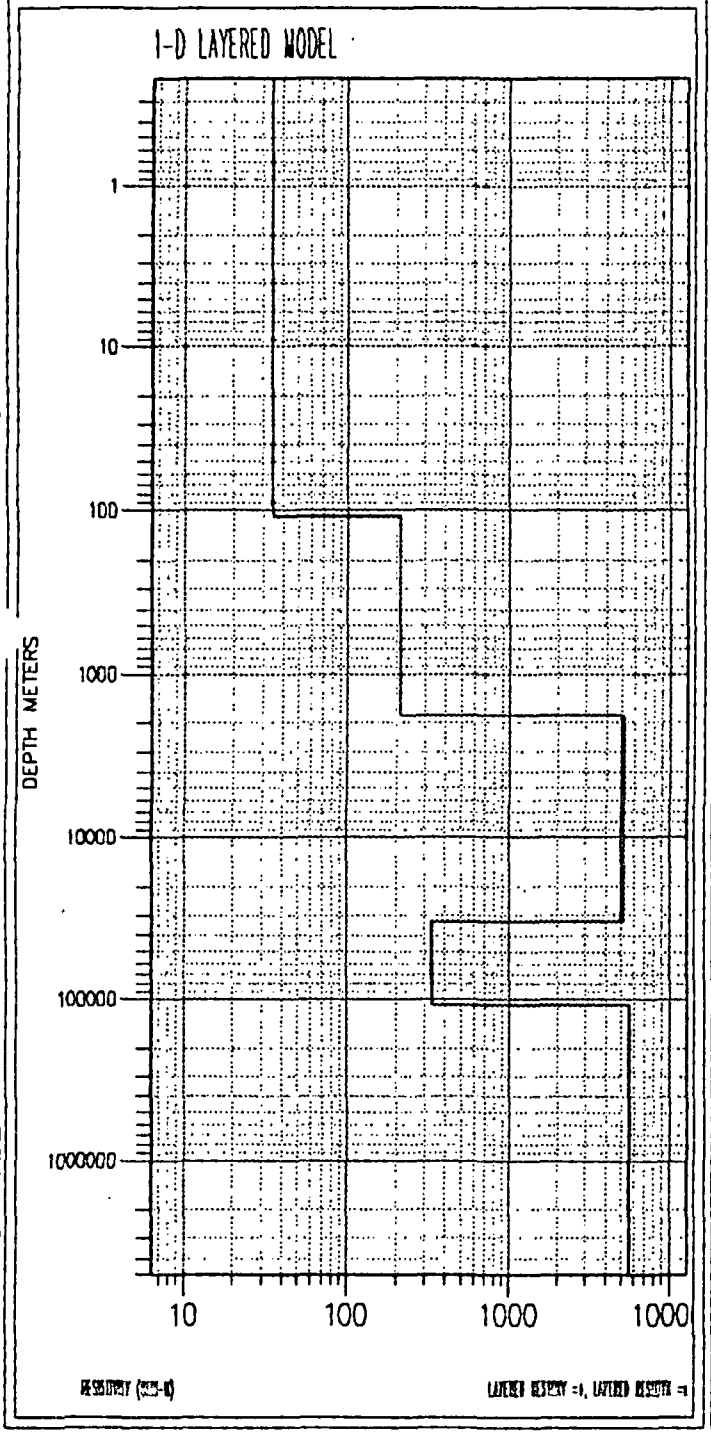


cebuco-s89

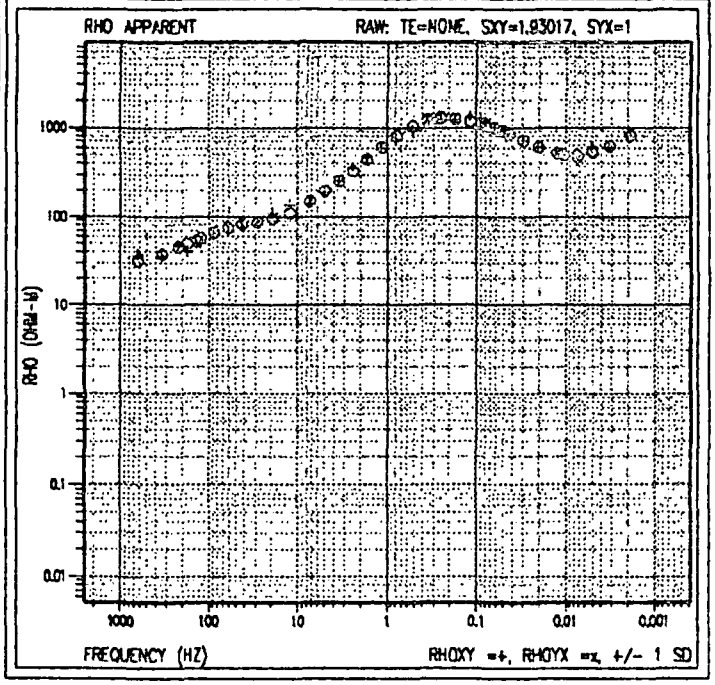


cebuco-s89

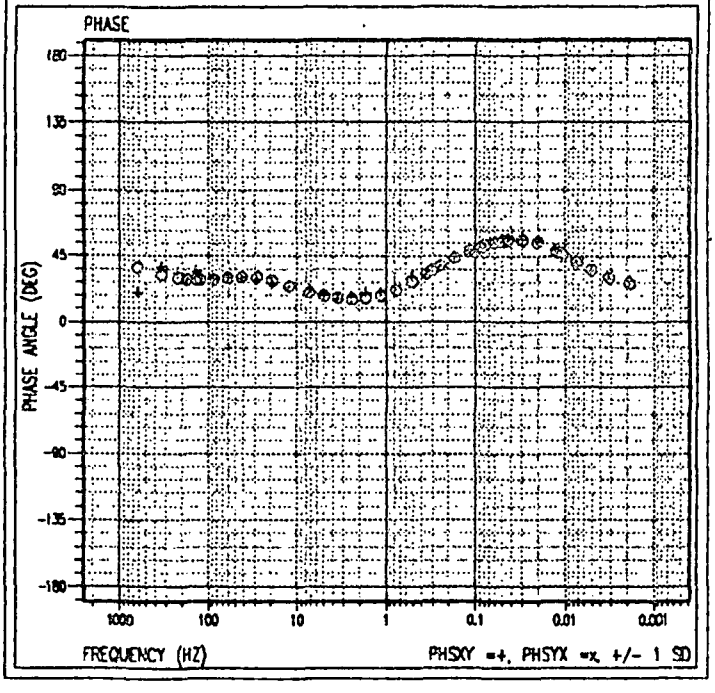

cebuco-s90

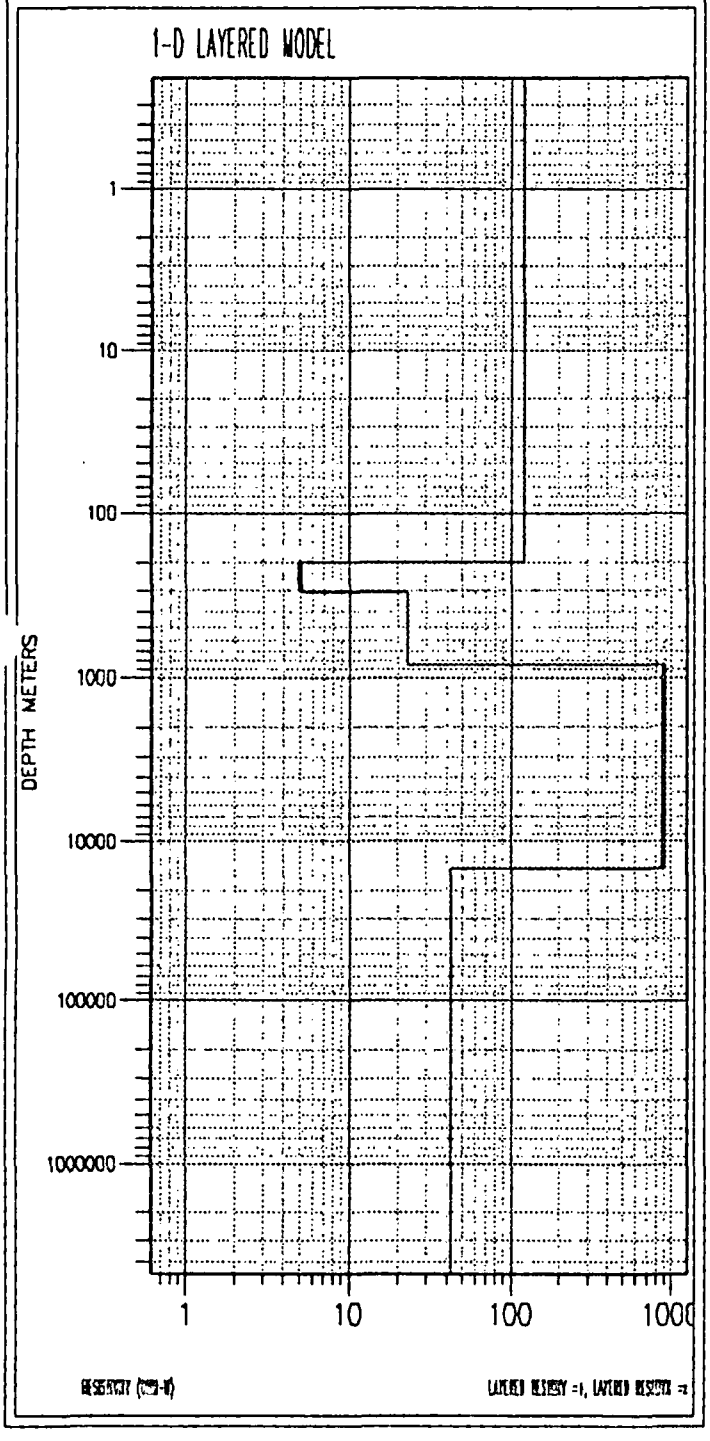


cebuco-s90

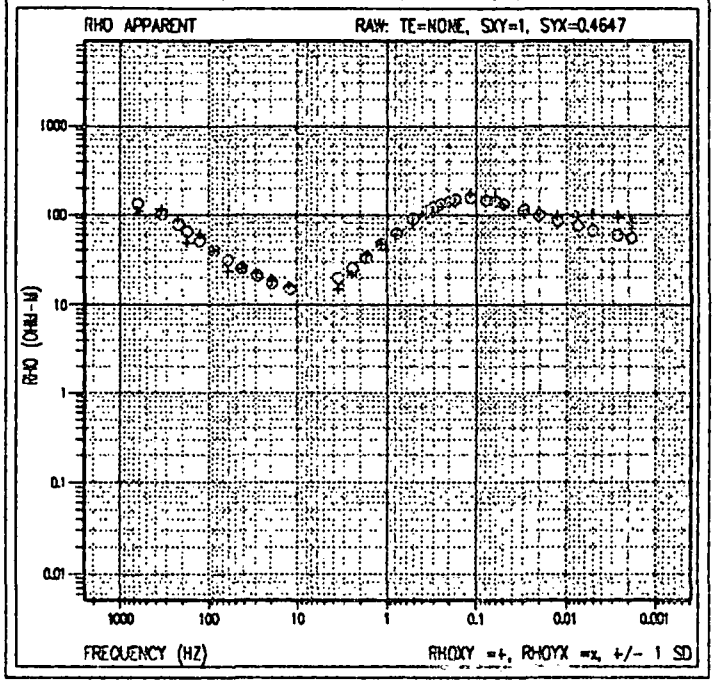


cebuco-s90

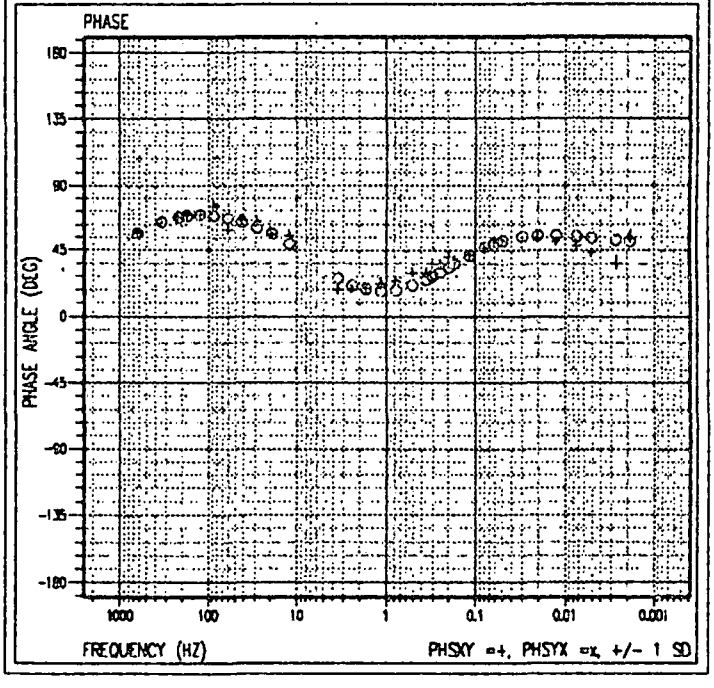

cebuco–s91

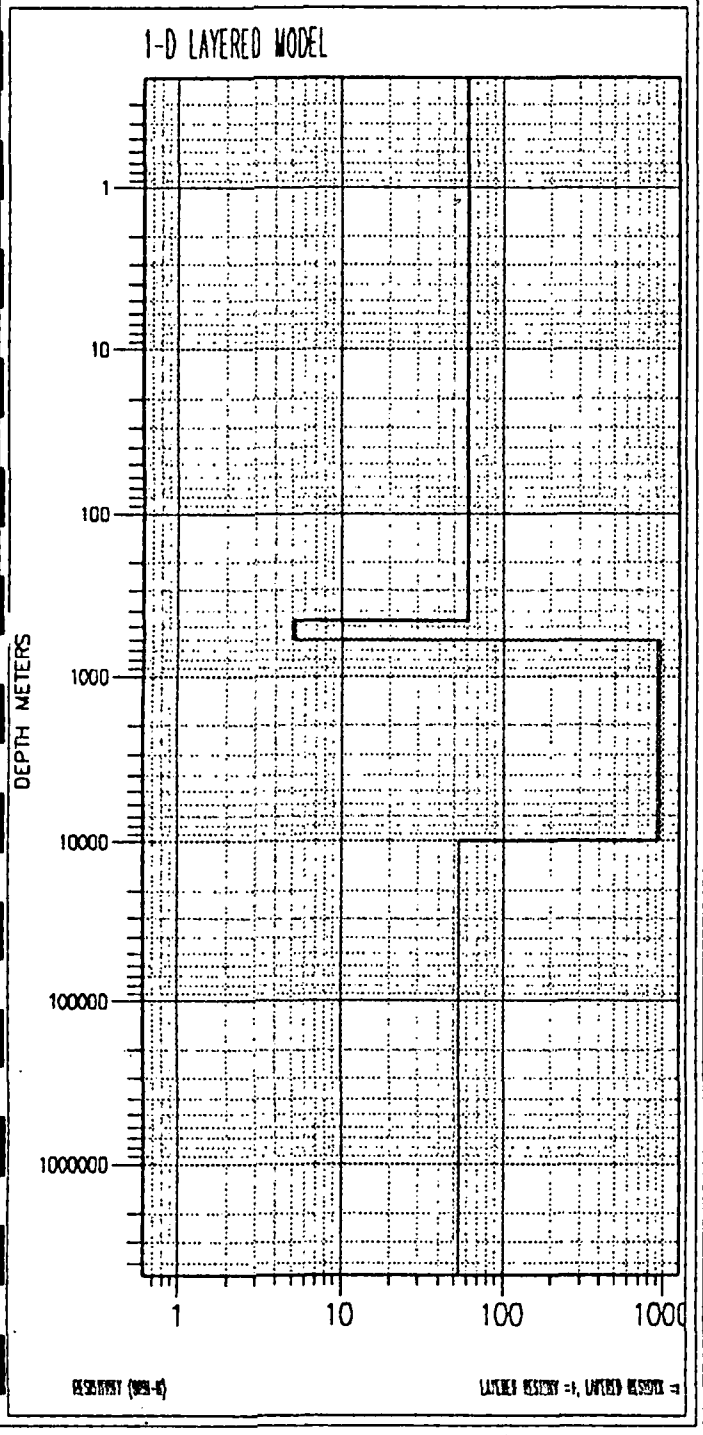


cebuco–s91

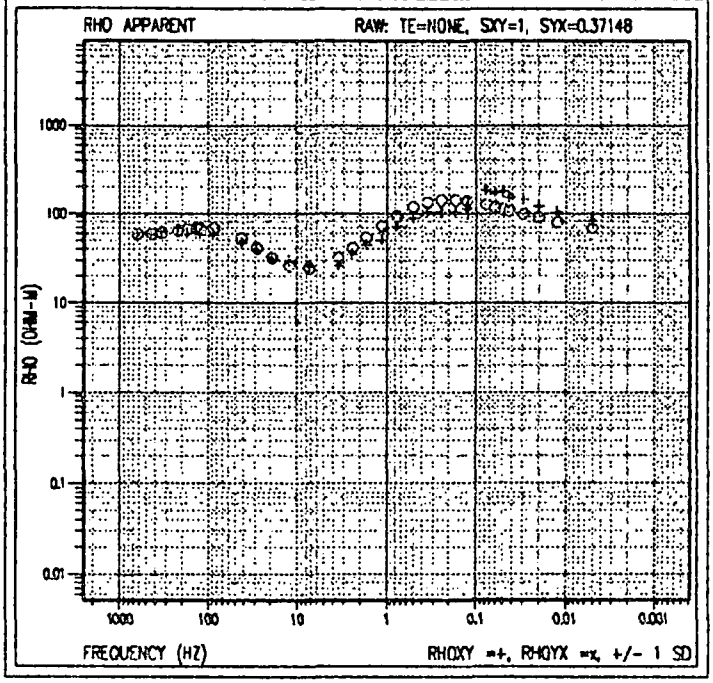


cebuco–s91

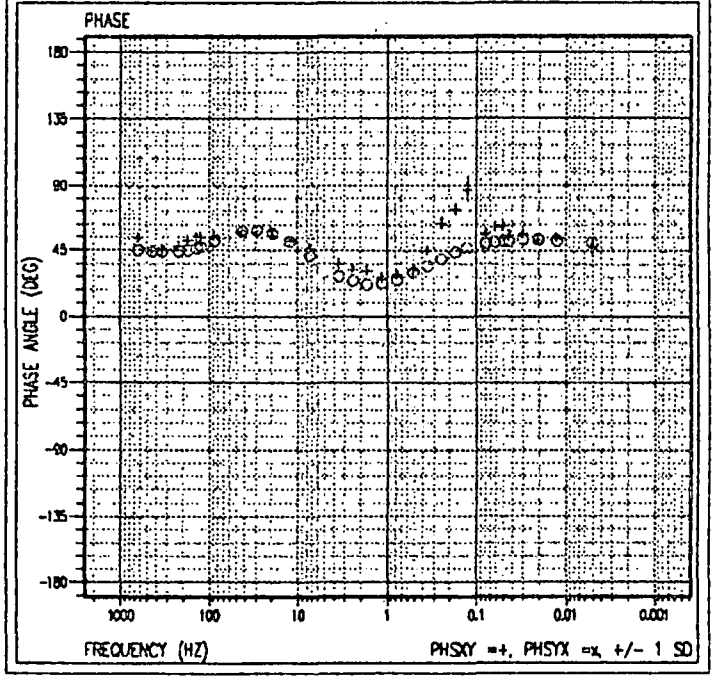

cebuco–s92

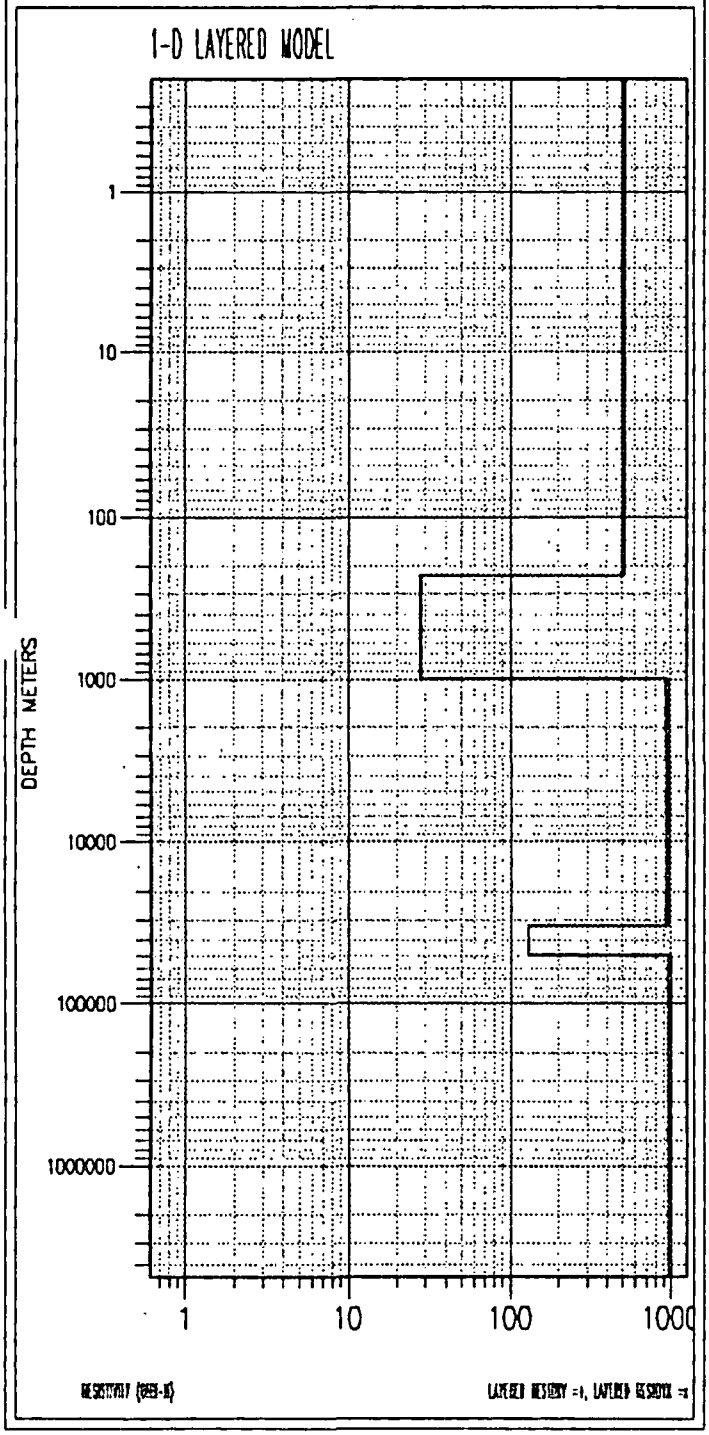


cebuco–s92

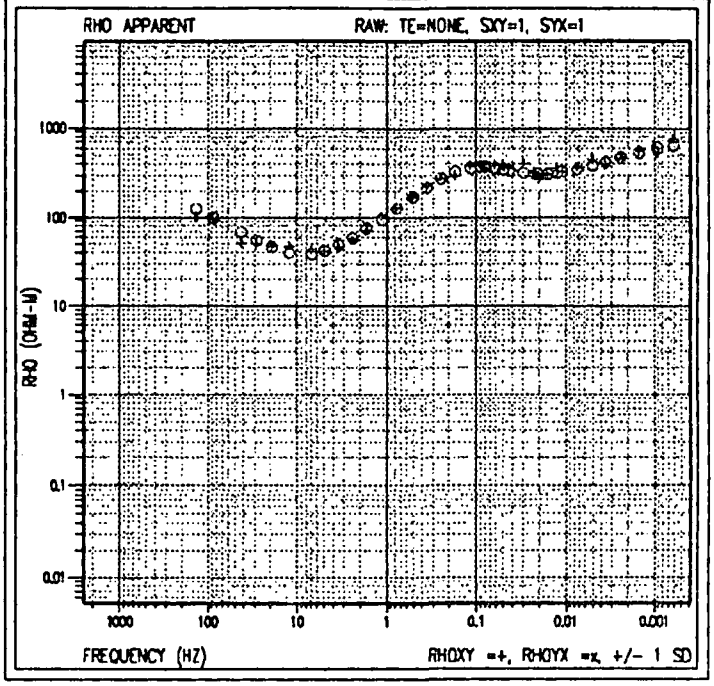


cebuco–s92